UNIVERSIDAD DE CANTABRIA

FACULTAD DE MEDICINA

DEPARTAMENTO DE BIOLOGÍA MOLECULAR

INSTITUTO DE BIOMEDICINA Y BIOTECNOLOGÍA DE CANTABRIA

NUEVOS MECANISMOS TRANSFORMANTES DE MYC: INDUCCIÓN DE SKP2 Y DEGRADACIÓN DE p27

Tesis Doctoral presentada por

Gabriel Bretones Sánchez para optar

al Grado de Doctor por la Universidad de Cantabria

Enero 2014

El Dr. Javier León Serrano, Catedrático de Bioquímica y Biología Molecular de la Facultad de Medicina de la Universidad de Cantabria

CERTIFICA: que el Ldo. D. Gabriel Bretones Sánchez ha realizado bajo su dirección el presente trabajo titulado "**NUEVOS MECANISMOS TRANSFORMANTES DE MYC: INDUCCIÓN DE SKP2 Y DEGRADACIÓN DE p27" (NEW MYC TRANSFORMING MECHANISMS: INDUCTION OF SKP2 AND DEGRADATION OF p27)** en el Departamento de Biología Molecular de la Universidad de Cantabria.

Considero que este trabajo reúne los requisitos de originalidad y calidad científica necesarios para su presentación como Memoria de Doctorado por el interesado, al objeto de poder optar al grado de Doctor por la Universidad de Cantabria.

Y para que conste y surta los efectos oportunos, firmo el presente certificado.

Santander, a 20 de Enero de 2014

Fdo. Javier León Serrano

Esta Tesis ha sido realizada en el Instituto de Biomedicina y Biotecnología de Cantabria (IBBTEC) y el Departamento de Biología Molecular de la Facultad de Medicina de la Universidad de Cantabria (Santander).

La financiación necesaria para la realización de esta Tesis doctoral ha sido aportada por el Ministerio de Educación y Ciencia (SAF2008-01581 y SAF2011-23796) del Instituto Carlos III (RD06/0020/0017).

Parte de los experimentos presentados en la Memoria de Doctorado fueron realizados por el Ldo. Gabriel Bretones Sánchez en el laboratorio del Dr. Oriol Bachs en el Departamento de Biología Celular de la Facultad de Medicina de Barcelona (Barcelona) durante una estancia de cuatro meses financiada por el Ministerio de Educación y Ciencia a través de su programa de ayudas para estancias cortas en otros centros de investigación.

El autor de esta Tesis ha disfrutado de una beca predoctoral de Formación de Personal Investigador (FPI) (BES-2006-12120) (2006-2010) concedida por el Ministerio de Educación y Ciencia y de un contrato de nueve meses por la Universidad de Cantabria.

AGRADECIMIENTOS GENERALES

Esta Tesis no solo es el resultado de muchos años de esfuerzo y sacrificio personal, también es el resultado del trabajo generoso y desinteresado y del apoyo prestado por muchas otras personas que merecen todo mi respeto y mi más sincero agradecimiento.

Por ello, quiero dar las gracias en primer lugar a mi director de Tesis, por su dedicación inagotable a este trabajo, por confiar en mí y darme la oportunidad de formar parte de su grupo. Por ser tan cercano y por su infinita paciencia. Por todas esas horas de discusión que tanto me han aportado, algo impensable con cualquier otro director. En definitiva, por enseñarme todo lo que se de esta profesión. Por todo y por mucho más, mereces toda mi admiración y mi más sincera gratitud.

También quiero dar las gracias al director y resto de catedráticos y profesores del Departamento de Biología Molecular que han participado en mi formación como doctorando e investigador, sin olvidarme del personal de administración y mantenimiento que, a pesar de intentar pasar inadvertidos, siempre han estado ahí para facilitar nuestro trabajo.

Por supuesto a todas las personas que han ido pasando por el laboratorio de Bioquímica durante todo este tiempo. Muy especialmente a los que han sido compañeros de poyata y de fatigas, con los que he compartido realmente el día a día, que me acogieron en su comedor social y me consideraron como un compañero de piso más. Ha sido todo un placer conoceros y recorrer este camino juntos. Gracias por vuestra amistad. También quiero dar las gracias a aquellos que nos transmitieron sus conocimientos y su buen hacer, de los cuales aprendimos a trabajar en el laboratorio y que hoy se encuentran desperdigados por medio mundo. Gracias también a las que han sido nuestras otras manos en el laboratorio, por su constante ayuda y por hacer más fácil nuestro trabajo, pero también, por sus consejos personales y por ejercer de madres en más de una ocasión. Por supuesto a las nuevas becarias, por vuestra simpatía, por vuestra paciencia y por vuestras ganas de aprender, porque espero que os vaya tan bien como nos ha ido a nosotros. Y como no, gracias al otro jefe y a la otra jefa del laboratorio, por su calidad científica y humana, por tener siempre la puerta abierta para resolvernos cualquier problema, pero también, por enseñarnos donde están las líneas que no debemos sobrepasar.

Por supuesto a toda la familia de becarios y becarias (hoy ya doctores, porque creo que soy el último de esta generación) del Departamento de Biología Molecular y resto de departamentos de la Facultad. Gracias por vuestras innumerables opiniones y consejos en lo personal y en lo laboral. Gracias por vuestro apoyo y por estar siempre disponibles para echar una mano. Por hacer que este trabajo haya sido más ameno y por haber ayudado a despejar cuerpo y mente compartiendo deportes acuáticos y esas tardes de fútbol y vóley que tanto se echan de menos. Gracias también por los momentos televisivos, futboleros y videoconsoleros. Gracias por tantos momentos buenos. Gracias por todo.

No voy a olvidarme del resto de compañeros de los laboratorios de Genética, Microbiología e Inmunología. En definitiva, gracias a toda la gente del Departamento de Biología Molecular, sin

olvidarme de la gente de los Departamentos de Anatomía, Fisiología y Farmacología y de los nuevos grupos del IBBTEC.

También agradecer al grupo de señalización celular y dianas terapéuticas en cáncer del IFIMAV, especialmente a su director, por acogerme temporalmente y por darme la oportunidad de participar en su trabajo. También a la gente de los nuevos grupos del IFIMAV, especialmente a aquellos con los que compartimos laboratorio y amistad.

A toda la gente del departamento de Biología Celular de la Facultad de Biología en la Universidad de León, porque allí fue realmente donde comencé esta andadura y porque, aunque pase el tiempo, uno nunca se olvida de sus comienzos.

A mis dos compañeros de carrera, aunque ya sabéis que os considero mucho más que eso, por lo que valéis, porque espero que algún día lleguemos a trabajar juntos.

A mis amigos del pueblo, porque siempre sois los últimos con los que cuento pero siempre sois los primeros en estar ahí a pesar del tiempo y la distancia.

Por último quisiera dedicar unas líneas a toda mi familia, empezando por mis abuelos (a la que aún resiste al paso de los años y a los que ya no están) pasando por mis tíos y primos, y como no, mis sobrinos, porque junto a vosotros uno se siente importante y desaparecen todos los males. Gracias a mis suegros, mi otra familia en esta tierra adoptiva. Pero en especial, gracias a mis padres y a mis hermanos, por vuestro cariño y por enseñarme los verdaderos valores de la vida. Por inculcarme el respeto a los demás y por enseñarme que las cosas se consiguen poco a poco, con paciencia y mucho trabajo.

Y por supuesto, gracias a la persona con la que he compartido estos últimos años y sin la cual no hubiese podido terminar este trabajo. Gracias por tu apoyo incondicional y por confiar ciegamente en mí. Gracias por enseñarme esos valores que no conocía y que me ayudan día a día a ser mejor persona. Pero sobre todo, gracias por hacerme feliz.

Para finalizar, pediros disculpas a todos por no mencionar vuestros nombres. Sois demasiados y era la única forma de no dejar a nadie atrás y de intentar expresaros mi gratitud por igual. Todos habéis participado de una u otra forma en este trabajo y a todos os debo de estar infinitamente agradecido. Deciros que a lo largo de este tiempo he conocido a personas excelentes y que espero que a todos os vaya genial porque es los que merecéis.

AGRADECIMIENTOS A COLABORADORES

Me gustaría agradecer por último, a todos aquellos investigadores e instituciones que me han proporcionado materiales, aparatos, técnicas y financiación, sin las cuales no hubiera sido posible el desarrollo de esta Tesis doctoral.

Al Dr. Ignacio Arechaga y la Dra. Elena Cabezón del Departamento de Biología Molecular en la Facultad de Medicina de la Universidad de Cantabria por introducirme en el mundo de la purificación de proteínas recombinantes y por su asesoramiento en la técnica de cromatografía de exclusión molecular, pero también por todo lo que he aprendido de vosotros.

Al Dr. Oriol Bachs y a su grupo en el Departamento de Biología Celular, Inmunología y Neurociencias de la Facultad de Medicina de la Universidad de Barcelona por acogerme como uno más y por hacerme sentir como en casa. Por haber puesto a mi disposición todos los conocimientos y herramientas de su laboratorio sobre el ciclo celular, y por enseñarme las técnicas de cromatografía de afinidad y FRET.

Al Dr. Mariano Barbacid y al Dr. David Santamaría del Centro Nacional de Investigaciones Oncológicas (Madrid) por darme la oportunidad de conocer y de trabajar en un centro de referencia internacional en investigación en cáncer. Por poner a mi disposición material de trabajo que no tiene precio, que sé que es el resultado de muchos años de trabajo.

A Marta Albajar del Servicio de Hematología del Hospital Universitario Marqués de Valdecilla (Santander) y a la Dra. Teresa Gómez Casares del Servicio de Hematología del Hospital Dr. Negrín (Las Palmas de Gran Canaria) por el suministro de las muestras clínicas de leucemia mieloide crónica. Por supuesto, a todos los pacientes que a pesar de las dificultades han decido aportar su granito de arena a la ciencia para que otros puedan vivir mejor.

Al Dr. Germán Rivas y al Dr. Carlos Alfonso del Centro de Investigaciones Biológicas (Madrid) por los experimentos de ultracentrifugación analítica.

Al Dr. Juan Carlos Acosta por la línea celular Kp27MER entorno a la cual he basado gran parte de esta Tesis. También al Dr. John Sedivy por las células HO15.19 (*Myc*$^{-/-}$), al Dr. Marcos Malumbres por las células *Cdk2*$^{-/-}$ y al Dr. Piort Sicinski por las células ciclina E1$^{-/-}$/E2$^{-/-}$.

Al Dr. Richard Kriwacki por los complejos ciclina E/CDK2 y por sus comentarios y sugerencias sobre proteínas intrínsecamente desestructuradas.

Al Dr. Ignacio Pérez Roger por el anticuerpo anti-SKP2 y por el plásmido shSKP2. Al Dr. Wen-Chun Hung por el plásmido reportero del promotor de *SKP2* (-1148-SKP2-Luc) y al Dr. Jesús Gil por el plásmido shMYC.

A Mar Rodríguez por su asistencia técnica y ayuda con los experimentos de xenotransplante en ratones desnudos.

A Rosa Blanco y Pilar Frade por su asistencia técnica y por su ayuda en numerosas técnicas y cultivos celulares.

A todos aquellos que han prestado plásmidos, anticuerpos y líneas celulares desinteresadamente.

UNIVERSIDAD DE CANTABRIA

FACULTAD DE MEDICINA

DEPARTAMENTO DE BIOLOGÍA MOLECULAR

INSTITUTO DE BIOMEDICINA Y BIOTECNOLOGÍA DE CANTABRIA

NEW MYC TRANSFORMING MECHANISMS: INDUCTION OF SKP2 AND DEGRADATION OF p27

Gabriel Bretones Sánchez

i. ABBREVIATIONS

ABBREVIATIONS

Ø	Diameter
4HT	4-Hydroxytamoxifen
A_{260nm}	Absorbance at 260 nm
aa	Amino acid
AML	Acute Myeloid Leukemia
APC/C	Anaphase promoting complex / cyclosome
ARF	Alternative reading frame protein
ATCC	American Type Culture Collection
ATP	Adenosine triphosphate
BSA	Bovine serum albumin
bp	Base pairs
CAK	CDK-activating kinase
CDK	Cyclin-dependent kinase
cDNA	Complementary DNA
ChIP	Chromatin Immunoprecipitation
CHX	Cycloheximide
CKI	CDK inhibitor
CML	Chronic Myeloid Leukemia
CMR	Complete Molecular Response
CMV	Cytomegalovirus
Ct	Cycle threshold
CTD	Carboxy-terminal domain of RNA Polymerase II
Ctrol	Control
d	Day/s
DAPI	4´,6´-diamino-2 phenylindole dihydrochloride
DLR	Dual-Luciferase Reporter
DMEM	Dulbecco's Modified Eagle Medium
DMSO	Dimethyl sulphoxide
DNA	Deoxyribonucleic acid
DNMT	DNA-methyltransferase
dNTP	Deoxyribonucleoside Triphosphate
Doxy	Doxycycline
DTT	Dithiothreitol
EDTA	Ethylenediaminetetracetic acid
EGTA	Ethyleneglycoltetraacetic acid
FCS	Foetal calf serum
FITC	Fluorescein isothiocyanate

g	Gravitational constant
GEFs	Guanine-nucleotide Exchange Factors
GFP	Green Fluorescent Protein
GST	Glutathione S-transferase
h	Hour/s
HAT	Histone Acetyltransferase
HDAC	Histone deacetylase
HLH	Helix-loop-helix
IB	Immunoblot
IF	Immunofluorescence
IgG	Immunoglobulin G
Inr	Initiator element
IP	Immunoprecipitation
IPTG	Isopropyl β-D-1-thiogalactopyranoside
IRES	Internal ribosome entry site
KAP	CDK-associated phosphatase
KAT	K (lysine) Acetyltransferase
kb	Kilobase
kDa	Kilodalton
KDM	K (lysine) Demethylase
KID	CDK-inhibitory domain
KMT	K (lysine) Methyltransferase
KO	Knockout
LB	Luria Broth
LiCl	Lithium chloride
LRR	Leucine-rich repeats
Lv	Lentiviral
LZ	Leucine zipper
M	Molar
mAU	Milli-Absorbance units
MB	MYC box
MEFs	Mouse embryonic fibroblasts
miRNA (miR)	Micro-RNA
MW	Molecular weight
MYST	MOZ, YBF2/Sas3, Sas2, TIP60
Na-DOC	Sodium-deoxycholate
NES	Nuclear export signal
NLS	Nuclear Localization Signal
NP40	Nonidet-P40 or octyl phenoxylpolyethoxylethanol
NRTK	Non-receptor tyrosine kinase

PAGE	Polyacrylamide Gel Electrophoresis
PBS	Phosphate Buffer Saline
PcG	Polycomb group proteins
PCR	Polymerase Chain Reaction
PMSF	Phenylmethylsulfonyl fluoride
Pol	Polymerase
qPCR	Quantitative polymerase chain reaction
R10F	RPMI-10 %-FCS
RNA	Ribonucleic Acid
rpm	Revolutions per minute
RPMI	Roswell Park Memorial Institute medium
RT-qPCR	Reverse transcription and quantitative polymerase chain reaction
rRNA	Ribosomal Ribonucleic Acid
SAGE	Serial analysis of gene expression
SCF	SKP1-Cullin-F-box protein complex
SDS	Sodium Dodecyl Sulfate
SDS-PAGE	SDS polyacrylamide gel electrophoresis
seq	Sequencing
shRNA	Short (small) hairpin RNA
SNP	Single-nucleotide polymorphism
TAE	Tris-acetate-EDTA buffer
TBS-T	Tris buffer saline – Tween 20
TE	Tris-EDTA buffer
TPA	Phorbol-12-myristate-13-acetate
TSS	Transcription Start Sites
UTR (3´ and 5´)	Untranslated regions
UV	Ultraviolet light
V	Volt/s
Vol	Volume
wt	Wild-type

ii. INDEX

INDEX

1. INTRODUCTION

1. INTRODUCTION

1.1. MOLECULAR CONTROL OF CELL CYCLE

1.1.1. Overview of cell cycle

The cell cycle is the process by which a eukaryotic cell duplicates exactly its genetic content and then divided into two daughter cells genetically identical to the parent cell. To achieve this, the cell also need to double the cell mass and duplicate all the organelles. Therefore, the cell cycle is therefore a complex set of nuclear and cytoplasmic processes that must be coordinated. The eukaryotic cell cycle commonly consists of four well-defined and sequential phases (Figure 1.1): G1, S (for DNA **S**ynthesis), G2 and M (for **M**itosis). Arguably, the two major cell cycle events required for cell division are S and M-phase. During S-phase the cell replicates the entire genome and the centrosome to produce copies for both daughter cells whereas during mitosis the cell divides the duplicated genetic content into two identical cells. Mitosis constitutes the shortest phase of the cycle and, in cells growing in culture, occupies only about 10% of the entire process which takes about 24 hours on average. The M and S-phases are separated by two "**G**ap" stages, the G1 and G2 phases. G1 follows on from mitosis and is a time when the cell is sensitive to negative or positive cues from growth signalling networks. During G2, the cell assesses that the genome and other cellular organelles are correctly duplicated; the cell doubles its size and prepares to undergo mitosis (Morgan, 2007).

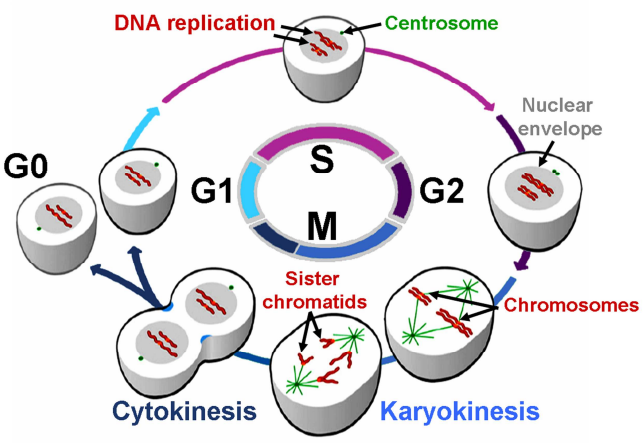

Figure 1.1. The eukaryotic cell cycle phases. The eukaryotic cell cycle consists of four sequential phases: G1, S, G2 and M. During S-phase the cell replicates its DNA and the centrosome. Mitosis is accompanied by breakdown of the nuclear envelope, chromosome condensation, segregation of the sister chromatids into two new nuclei (karyokinesis) and cell division into two genetically identical daughter cells (cytokinesis). After mitosis the new cells either continue through another division cycle or enter in a resting state (G0).

After passing through mitosis and into a new G1-phase, the new cell either continues through another division cycle or ceases to divide, entering a resting state (G0) that may last hours, days, or the whole lifetime of the cell (Figure 1.1). In most cultured cell lines, G0 represents a state when cells have reversibly withdrawn from the cell cycle in response to high cell density or growth factors deprivation. Stimulation by mitogens causes these quiescent cells to re-enter the cell cycle through G1 phase and undergo a new cell division cycle. Alternatively, cells may irreversibly withdraw from the cell cycle into terminally differentiated or senescent out-of-cycle state. Most functional cells in the human body reside in this differentiated state. They have

acquired their specialized form and function and are not cycling. Only minorities of cells are actively proliferating and these are located mainly in the stem-transit amplifying compartments of self-renewing tissues such as epithelia and bone marrow (Morgan, 2007).

In addition, the transition from one phase to the next are monitored by sensor mechanisms, called checkpoints, which exist to ensure the correct order of events (Hartwell and Weinert, 1989). Initiation of each phase is dependent on the proper progression and completion of the previous one. The primary checkpoint acts late in G1 and is known as the "restriction point" (Figure 1.2). Once cells have passed this point, they normally are committed to a round of cell division. Apart from the restriction point, other checkpoints exist at S-phase and G2/M transition to ensure that cells have fully and correctly replicated their DNA or during mitosis to ensure that conditions remain suitable to complete cell division (Morgan, 2007).

1.1.2. The cell cycle machinery. CDKs and cyclins

Eukaryotic cell division represents an evolutionarily conserved process involving temporally ordered and discrete steps. This implied a tightly controlled series of molecular events and different rate-limiting proteins to regulate specific cell cycle phase transitions (Hartwell*, et al.*, 1974; Nurse, 1975; Evans*, et al.*, 1983). These concepts gave birth to the idea of the cell cycle machinery that both drives and controls progression through the division cycle (Murray and Hunt, 1993). For the discoveries that led to the identification of the key elements in cell cycle researchers Leland Hartwell, Paul Nurse, and Tim Hunt received the Nobel Prize for Physiology and Medicine in 2001.

Progression through the cell cycle is under the strict control of a family of serine/threonine protein kinases, which act at precisely timed intervals, phosphorylating proteins involved in cell cycle progression and modulating their activities (Murray, 2004). Some of these substrates include for example nuclear lamins, histone H1 or myosin whose phosphorylation respectively promotes breakdown of the nuclear envelope, mitotic chromosome condensation or inactivation of the contractile machinery after cytokinesis (Morgan, 2007). These kinases are heterodimers consisting of a regulatory subunit, the cyclin, and a catalytic subunit, the cyclin-dependent protein kinase (CDK). As its name indicates, the catalytic activity of the CDK depends on the binding of the regulatory cyclin subunit (Figure 1.3). The number of CDKs has increased considerably during evolution. According to the latest versions of the human and mouse genomes, there are 21 genes encoding CDKs and 5 other genes encoding CDK-like proteins with conserved primary structure (Malumbres*, et al.*, 2009). Of these 21 CDKs, CDK1-11 are the best-characterized members. CDK1, 2, 3, 4 and 6 are thought to be the major regulators of "the core cell cycle", CDK5 functions in neuronal development and CDK7-11 function mainly as transcriptional regulators, although CDK7 and 11 have additional cell cycle functions (Satyanarayana and Kaldis, 2009). The physiological role of the rest of CDKs remains essentially unknown (Malumbres*, et al.*, 2009).

The expression of the majority of core cell-cycle CDKs remains relatively constant throughout the cell cycle. In contrast, the activating partners are synthesized and destroyed in a

cyclical fashion during each phase of cell cycle and thus they were originally designated “cyclins” (Evans*, et al.*, 1983). Nowadays, the analysis of the human genome has revealed up to 29 genes sharing a conserved domain of approximately 150-amino acids involved in the binding to CDKs and termed the “cyclin box” (Malumbres and Barbacid, 2005). Similarly to CDKs, of all cyclins identified, only a few have been reported to regulate the core cell cycle, such as D, E, A and B-type cyclins. Cyclins C, H and T are involved in regulation of the RNA polymerase II transcription (Loyer*, et al.*, 2005). Moreover, as we will see below, every cyclin determines the substrate specificity of selected CDKs and generally confers them of spatial and temporal activity at defined points in the cell cycle (Morgan, 1997; Miller and Cross, 2001).

1.1.3. Cell cycle regulation

The basic regulation of the cell cycle was established by pioneering studies in yeasts. In these organisms, cell cycle progression is controlled by a single CDK (Cdc28 in *S. cerevisiae* and Cdc2 in *S. pombe*) that binds to specific cyclins at different stages of the cycle. In contrast, in mammalian cells, cell cycle progression is regulated by specific cyclin/CDK complexes at defined phases in a sequential and orderly fashion (Morgan, 1997).

According to the “classical” cell cycle model (Figure 1.2), at early G1 phase, mitogenic signals such as growth factors and cytokines are first sensed and integrated by expression of the D-type cyclins (D1, D2 and D3) (Matsushime*, et al.*, 1991; Won*, et al.*, 1992; Sherr, 1995) that preferentially bind to and activate CDK4 and CDK6 (Matsushime*, et al.*, 1992). These complexes initiate phosphorylation of retinoblastoma (RB) protein family members (RB, p107 and p130) whose phosphorylation status plays a major role in controlling E2F transcriptional activity (Harbour*, et al.*, 1999). Unphosphorylated RB binds to and inhibits the transcription factor E2F. Thus, activation of CDK4/6 leads to the partial inactivation of RB and the release of active E2F transcription factors which results in the transcriptional activation of E2F responsive genes (Weinberg, 1995; Dyson, 1998). These genes include E-type (E1 and E2) cyclins (Botz*, et al.*, 1996; Geng*, et al.*, 1996) as well as genes necessary for DNA synthesis such as the DNA polymerase-α, among others (DeGregori*, et al.*, 1995). This allows the activation of CDK2 by binding to E-type cyclins in the late G1 phase (Sherr and Roberts, 1999,2004). Cyclin E/CDK2 complexes complete the phosphorylation and inactivation of pocket proteins (Lundberg and Weinberg, 1998; Harbour*, et al.*, 1999) leading to passage through the restriction point at the boundary of the G1/S phase (Figure 1.2), which commits the cell to S-phase entry and to complete a round of cell division (Planas-Silva and Weinberg, 1997). Later CDK2 plays an important role in S-phase progression by complexing with A-type (A1 and A2) cyclins (Pines and Hunter, 1990; Tsai*, et al.*, 1991), which are expressed throughout the S and G2 phases and are required for DNA replication (Girard*, et al.*, 1991; Geley*, et al.*, 2001). A-type cyclins also activate CDK1 at G2/M transition (Tsai*, et al.*, 1991; Murphy*, et al.*, 1997) to facilitate the onset of mitosis (Furuno*, et al.*, 1999) and they are rapidly degraded upon entry into mitosis by the anaphase promoting complex (APC) (Geley*, et al.*, 2001). Finally, B-type cyclins synthesis that begins at the

end of S-phase (Pines and Hunter, 1989), facilitates the formation of the cyclin B/CDK1 complexes responsible for driving cells through mitosis (Riabowol, *et al.*, 1989). Degradation of B cyclins also by the APC complex is required to the output of mitosis (Geley, *et al.*, 2001; Harper, *et al.*, 2002).

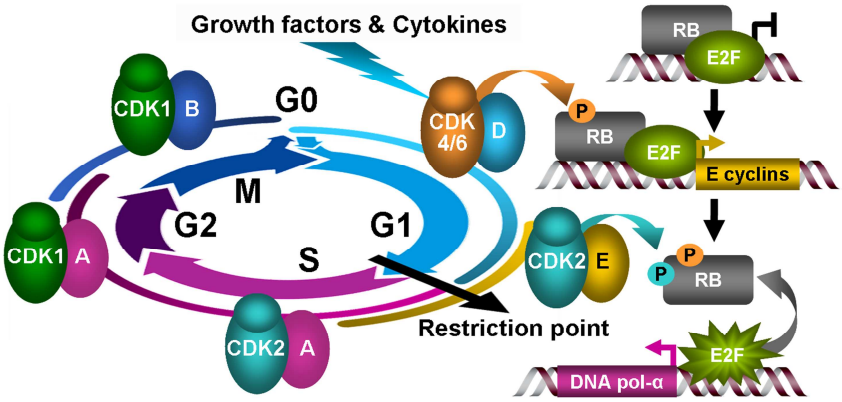

Figure 1.2. Regulation of the cell cycle progression through the different phases by cyclin/CDK complexes. Cyclin D/CDK4-6 first and then cyclin E/CDK2 trigger the transition from G1 to S phase (Restriction point) by phosphorylating RB protein family members among other proteins and activating E2F transcription factors. Progression into S and G2 phases requires the activity of cyclin A bound to CDK2 and CDK1 respectively. Finally, the activity of cyclin B/CDK1 is required for mitosis ("M").

However, the basic concept put forward in which each phase of the cycle is driven by specific cyclin/CDK complexes, has recently challenged by genetic studies in mice. Systematic knockout of CDK loci in the mouse germline has shown that CDK2 (Berthet, *et al.*, 2003; Ortega, *et al.*, 2003), CDK4 (Rane, *et al.*, 1999; Tsutsui, *et al.*, 1999) and CDK6 (Malumbres, *et al.*, 2004) are not essential for cell cycle progression of most cell types, although loss of each of these CDKs results in particular developmental defects. Furthermore, concomitant loss of multiple interphase CDKs (CDK2,4,6) enhances the scope of these developmental defects but does not result in a general disturbance of the cell cycle in most cell types (Malumbres, *et al.*, 2004; Berthet, *et al.*, 2006; Barriere, *et al.*, 2007). This may be due to compensatory activities among mitotic kinase CDK1 and these CDKs (Aleem, *et al.*, 2005). Altogether, the mouse knockout studies have shown that CDK1 alone is sufficient to drive cell cycle progression, compensating for the loss of CDK2, 3, 4 and 6. In this sense, triple knockout (TKO) mouse embryos lacking all interphase CDKs develop normally until mid-gestation (Santamaria, *et al.*, 2007).

Interestingly, there are no compensatory activities between interphase CDKs and CDK1. The ablation of *Cdk1* leads to embryonic development arrest, preventing embryos from developing beyond the blastocyst stage (Diril, *et al.*, 2012) or even the two-cell stage (Santamaria, *et al.*, 2007) in spite of carrying all interphase CDKs. *Cdk1* replacement by *Cdk2* using homologous recombination also results in early embryonic lethality, indicating that CDK1 cannot be compensated by CDK2, despite being expressed from the *Cdk1* locus (Satyanarayana, *et al.*, 2008). The conditional *in vivo* ablation of *Cdk1* in MEFs results in DNA re-replication because of an increase in cyclin A2/CDK2 activity (Diril, *et al.*, 2012). The fact that CDK1 alone

can drive the cell cycle in most mammalian cells suggests that animal cells and yeasts share the basic control mechanism of the cell cycle.

There are also compensatory activities among cyclins. Ablation of the genes encoding individual D-type cyclins only leads to specific developmental defects in mice (Ciemerych and Sicinski, 2005). However, concomitant ablation of the three D-type cyclins results in embryonic lethality owing to haematopoietic defects. Nevertheless, $D1^{-/-}/D2^{-/-}/D3^{-/-}$ mouse fibroblasts proliferate normally although they require increased mitogenic stimulation for cell cycle re-entry (Kozar*, et al.*, 2004).

Ablation of the genes encoding cyclin E1 and cyclin E2 also results in embryonic lethality owing to placental defects. However, E-type cyclins are largely dispensable for embryonic development when the placental defects are rescued and therefore for cell cycle progression of most embryonic cells (Geng*, et al.*, 2003; Parisi*, et al.*, 2003). Interestingly, expression of cyclin E1 within the cyclin D1 locus rescues most phenotypes observed in cyclin $D1^{-/-}$ mice, revealing a functional overlap between different classes of cyclins (Geng*, et al.*, 1999).

Cyclin A1 is expressed almost exclusively during meiosis of male germline cells in the testes (Sweeney*, et al.*, 1996; Yang*, et al.*, 1997). Accordingly, male cyclin $A1^{-/-}$ mice are completely viable but sterile because of a meiotic arrest during spermatogenesis (Liu*, et al.*, 1998; van der Meer*, et al.*, 2004). In contrast, cyclin $A2^{-/-}$ mouse embryos die shortly after implantation (Murphy*, et al.*, 1997; Kalaszczynska*, et al.*, 2009). Conditional ablation of both cyclin A1 and A2 in mouse fibroblasts leads to prolonged expression of cyclin E1 across the cell cycle without affecting cell cycle progression. Nevertheless, they are essential for cell-cycle progression of hematopoietic and embryonic stem cells. Only when all A- and E-type cyclins are deleted, the cell division is arrested, suggesting that cyclins A and E play redundant roles in cell cycle progression (Kalaszczynska*, et al.*, 2009).

Finally, studies in cyclin B1- and cyclin B2-null mice have confirmed that cyclin B2 is non-essential for normal growth and development. Cyclin B1 appears to compensate for the loss of cyclin B2 in $B2^{-/-}$ mice. In contrast, loss of cyclin B1 results in early embryonic lethality (Brandeis*, et al.*, 1998). It is unclear whether cyclin $B1^{-/-}$ MEFs do proliferate or not.

In summary, from all the different cyclin members that regulate the canonical cell cycle, cyclin A2 and B1 appear to be the most non redundant cyclins, as their deletion led to early embryonic lethality. Altogether, the information available to date leads to the current model where cyclins A and B and CDK1 represent absolutely the basic ‘‘core’’ elements of the cell-cycle machinery (Murphy*, et al.*, 1997; Hochegger*, et al.*, 2008).

1.2. MOLECULAR REGULATION OF CDKs ACTIVITY

As indicated above, CDKs play pivotal roles in cell cycle control. Their regulation ensures the correct timing of kinase activity during cell cycle. Apart from binding to cyclins, CDKs activity is regulated by two others mechanisms including phosphorylation of critical residues in the CDKs and binding of cyclin dependent kinase inhibitors (CKIs). CDK activity can also be modulated by

its subcellular localization and/or its accessibility to substrates, although these regulatory mechanisms are less well characterized (Morgan, 1995; Murray, 2004).

1.2.1. Cyclin binding to CDKs

Most of the current information on the structure and activity of CDKs is based on crystal structures of human CDK2 (De Bondt*, et al.*, 1993) and cyclin A/CDK2 complex (Jeffrey*, et al.*, 1995; Russo*, et al.*, 1996b). Essentially, it can be translated to others CDKs although each cyclin induces specific conformation changes on its bound CDK. Roughly, the structure of monomeric CDK2 consists of a small N-terminal lobe (N-lobe) rich in β-sheets and a larger C-terminal lobe (C-lobe) rich in α-helices (Figure 1.3). The ATP-binding site lies in a deep cleft between the two lobes of the kinase. Monomeric CDK2 differs from the cyclin-bound structure basically in two regulatory regions: an α-helix which contains a conserved PSTAIRE amino acid sequence exclusive of CDKs and a flexible loop called the activation loop or "T-loop" which contains a phosphorylatable residue (Thr160). The PSTAIRE helix also contains a conserved catalytic residue (Glu51) which is involved in ATP binding. In absence of the cyclin, the PSTAIRE helix is outwards and the T-loop is positioned in front of the catalytic cleft entrance, blocking the access of the ATP. CDK2 association with cyclin A causes significant conformational changes in the kinase that serves to configure the catalytic site for ATP binding (Figure 1.3). The PSTAIRE helix domain moves inwards, bringing the Glu51 inside the catalytic cleft, where together with others conserved residues (Lys33 and Asp145) and a magnesium ion (Mg^{2+}) coordinates the ATP phosphate atoms and correctly orients them for catalysis. Meanwhile, the T-loop moves away from the catalytic cleft entrance and exposes the phosphorylatable Thr160, setting the stage for the full activation of the kinase (Pavletich, 1999).

1.2.2. CDKs regulation by phosphorylation

Apart from cyclin binding, the complete activation of cyclin A/CDK2 complex requires several phosphorylation and dephosphorylation events at different residues in the protein.

First, Thr160 phosphorylation on the T-loop promotes an additional conformational change in CDK2 and completes the reorganization of the substrate binding site that was started by the cyclin (Figure 1.3) (Russo*, et al.*, 1996b). The phosphate group at Thr160 acts as an organizing center in the substrate binding site and allows the CDK to interact more effectively with substrates, optimizing the phosphoryl transfer and increasing the catalytic activity of cyclin/CDK complex (Jeffrey*, et al.*, 1995; Russo*, et al.*, 1996b; Brown*, et al.*, 1999). This Thr160 phosphorylation event is catalyzed by the CDK activating kinase (CAK), which is composed of three subunits: CDK7, cyclin H and MAT1 (ménage a trois) (Fesquet*, et al.*, 1993; Fisher and Morgan, 1994; Makela*, et al.*, 1994; Devault*, et al.*, 1995). The CAK is also responsible for the activating phosphorylation of Thr161 in CDK1, Thr172 in CDK4 and Thr177 in CDK6 which are structurally equivalent to Thr160 in CDK2 (Lolli and Johnson, 2005).

CDK phosphorylation by CAK is antagonized by a specific phosphatase called KAP (CDK-associated phosphatase). KAP dephosphorylates Thr160 in human CDK2 when the cyclin subunit is degraded or dissociates, and prevents CDK2 kinase activity upon subsequent association with cyclin A (Hannon, *et al.*, 1994; Poon and Hunter, 1995).

Second, cyclin/CDK complexes can also be inactivated via inhibitory phosphorylation of two conserved residues near the N-terminus (Thr14 and Tyr15 in human CDK1 and 2; Tyr17 and Thr19 in CDK4 and Tyr13 in CDK6) located within the ATP-binding site of the kinase. The negatively charged phosphate group on Thr14 prevents ATP binding, while that on Tyr15 interferes with phosphate transfer to the substrate (Gould and Nurse, 1989; Atherton-Fessler, *et al.*, 1993; Morgan, 1995). These inhibitory phosphorylation events are carried out by Wee1, a kinase conserved in all eukaryotes and Myt1. Nuclear Wee1 specifically phosphorylates Tyr15, whereas cytoplasmic Myt1 phosphorylates both Tyr15 and Thr14, with a stronger affinity for Thr14 (Featherstone and Russell, 1991; Parker and Piwnica-Worms, 1992; Mueller, *et al.*, 1995). Unlike activating phosphorylation, CDK inhibitory phosphorylations are essential for cell cycle regulation and particularly at mitosis for the control of CDK1 activation (Solomon, *et al.*, 1990; Krek and Nigg, 1991). Dephosphorylation of both residues accompanies entry into mitosis and this is carried out by dual specific phosphatases of the CDC25 family (Dunphy and Kumagai, 1991; Strausfeld, *et al.*, 1991). In vertebrates, CDC25 family has three isoforms: CDC25A, CDC25B and CDC25C. Inhibition of CDC25 phosphatases in response to DNA damage or other stress conditions, decreases CDK activity and leads to cell cycle arrest (Boutros, *et al.*, 2006).

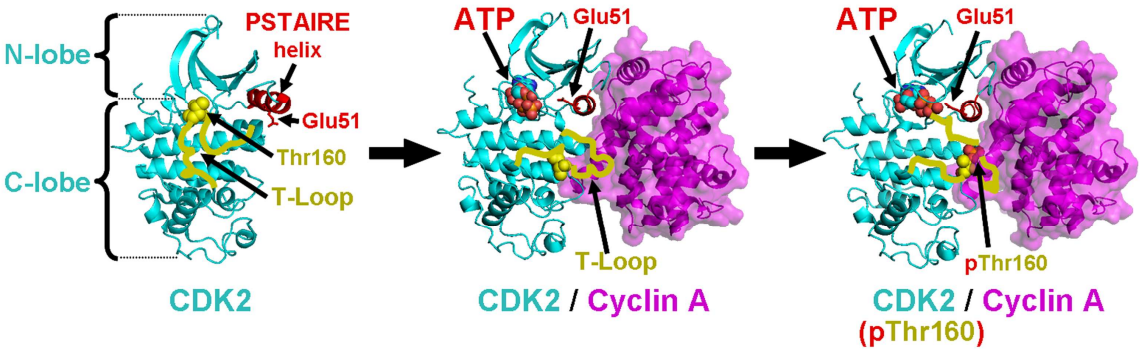

Figure 1.3. CDK activation by cyclin binding and CAK phosphorylation at Thr160. CDK structures corresponding to non-activated (monomeric CDK2), partially active (cyclin A/CDK2 complex) and fully active (phosphorylated cyclin A/CDK2 complex) states. In CDK2, the PSTAIRE helix is highlighted in red, the T-loop in yellow and the Thr160 is indicated by yellow spheres. The phosphate groups of ATP and phosphorylated Thr160 are indicated by red spheres. Adapted from (Pavletich, 1999).

1.2.3. Cell cycle inhibitors: INK and CIP/KIP protein families

The interaction of cyclin/CDK complexes with CDK inhibitors or CKIs is one of the most important mechanisms regulating CDK activity and therefore the cell cycle progression (Morgan, 1997). Negative CDK regulation by CKIs is an important step linking anti-mitogenic signals to cell cycle arrest in response to normal as well as extreme conditions, such as stress or DNA damage

(Satyanarayana and Kaldis, 2009). Based on their sequence homology, structure and CDKs specificities, CKIs are divided into two distinct families: The INK4 (Inhibitors of CDK4) and the CIP/KIP (CDK Interacting Protein/Kinase Inhibitory Protein) protein families (Pavletich, 1999; Sherr and Roberts, 1999).

The INK4 family comprises $p16^{INK4A}$, $p15^{INK4B}$, $p18^{INK4C}$ and $p19^{INK4D}$. These inhibitors bind to free CDK4/6 and inhibit their kinase activity interfering with their association to D-type cyclins and distorting the ATP binding site that leads to reduced affinity for ATP. Its ectopic expression arrests the cell cycle in G1-phase (Pavletich, 1999; Sherr and Roberts, 1999) and functional Rb seems to be required for this process (Bruce*, et al.*, 2000).

The CIP/KIP family consists of three members, $p21^{CIP1/Waf1}$ (CDK Interacting Protein 1), $p27^{KIP1}$ (Kinase Inhibitory Protein 1) and $p57^{KIP2}$ (Kinase Inhibitory Protein 2). This family is characterized to contain a conserved N-terminal domain that mediates binding to a broader spectrum of cyclin/CDK complexes already formed, inhibiting their activities. These complexes include cyclin A-E/CDK2, cyclin D/CDK4-6 and cyclin A-B/CDK1 heterodimers and therefore they are able to inhibit progression at every cell cycle phase (Sherr and Roberts, 1999). Among these CKIs, $p27^{KIP1}$ is specifically relevant because reduced $p27^{KIP1}$ levels are frequently observed in human cancers in association with tumor aggressiveness and poor patient outcome as described below.

1.2.4. The CDK inhibitor $p27^{KIP1}$

$p27^{KIP1}$ (p27 hereafter) was first identified by affinity chromatography as a 27 kDa protein (hence its name) that bound to cyclin E/CDK2 complexes and inhibited their activity in response to the proliferation arrest induced by TGF-β and cell-cell contact in lung epithelial cells (Polyak*, et al.*, 1994a; Slingerland*, et al.*, 1994). Soon after, the p27 cDNA was cloned from mink, mouse, and human cDNA libraries by two different screening approaches: identifying proteins that interacted with mouse cyclin D1 and CDK4 in a yeast "two-hybrid" interaction assay (Toyoshima and Hunter, 1994) and by peptide micro-sequencing of purified p27 protein isolated from Mv1Lu cells arrested in G1 by contact inhibition (Polyak*, et al.*, 1994b).

1.2.4.1. Structure of p27 gene and protein

In humans, p27 is encoded by the *CDKN1B* (Cyclin-Dependent Kinase Inhibitor 1B) gene (Figure 1.4) and maps to the locus 12p13.1-p12 (Pietenpol*, et al.*, 1995; Ponce-Castaneda*, et al.*, 1995). It contains two coding and one non-coding exons. In agreement with the NCBI RNA reference sequence collection (RefSeq), this gene is transcribed into a single mRNA of 2413 base pairs which encodes a protein of 198 amino acids. As we previously mentioned, it contains a conserved N-terminal kinase inhibitory domain (KID) (aa 25-93) which is homologous to the KID domains of $p21^{CIP1}$ and $p57^{KIP2}$ (38% and 44% identity respectively) (Russo*, et al.*, 1996a). The crystal structure of p27KID domain bound to cyclin A/CDK2 complex has been resolved and shows that it binds the complex interacting with both cyclin A and CDK2 in an extended but

ordered conformation, comprising two α-helices and a β-structure (Figure 1.5). Binding of p27 to CDK2 is accompanied by extensive structural changes in the N-lobe and the catalytic cleft of CDK2. This domain also contains a small 3_{10} helix that inserts into the catalytic cleft of CDK2, mimicking ATP and inhibiting its kinase activity (Russo*, et al.*, 1996a).

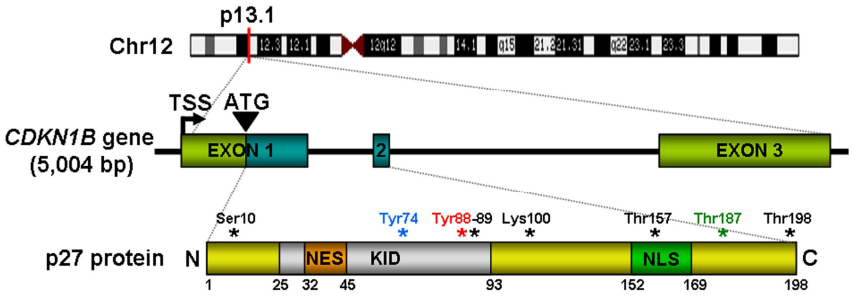

Figure 1.4. *CDKN1B* gene structure and localization in the human genome and major features p27 protein. Chr (Chromosome); TSS (Transcription start site); KID (Kinase inhibitory domain); NES (Nuclear export signal); NLS (Nuclear localization signal); posttraductional modifiable amino acids (*) and bp (base pairs).

In contrast, p27 C-terminal domain is extended and flexible when p27 is bound to cyclin A/CDK2 complex (Figure 1.5) according to results obtained from NMR studies (Galea*, et al.*, 2008a). This flexibility provides a molecular basis for the sequential signal transduction conduit that regulates p27 degradation. The C-terminal domain also contains a classical bipartite nuclear localization signal (NLS), consisting of two clusters of basic residues separated from each other by ten amino acids (aa 152/154-165/169) (Reynisdottir and Massague, 1997) of which Lys153, Arg154, Lys165 and especially Arg166, play a critical role in the nuclear localization of p27 (Zeng*, et al.*, 2000). In addition, p27 also contains a putative nuclear export signal (NES) identified between amino acids 32 and 45 (Muller*, et al.*, 2000; Connor*, et al.*, 2003).

Moreover, p27 presents several phosphorylatable residues (Ser10, Tyr74, Tyr88, Tyr89, Thr157, Thr187 and Thr198) which are involved in regulation of p27 activity, localization and stability, that we will be discussed below (Chu*, et al.*, 2008). In addition, it has been shown that p27 can be acetylated at Lys100 by the acetyltransferase PCAF (P300/CBP-Associated Factor) inducing its degradation via proteasome (Perez-Luna*, et al.*, 2012).

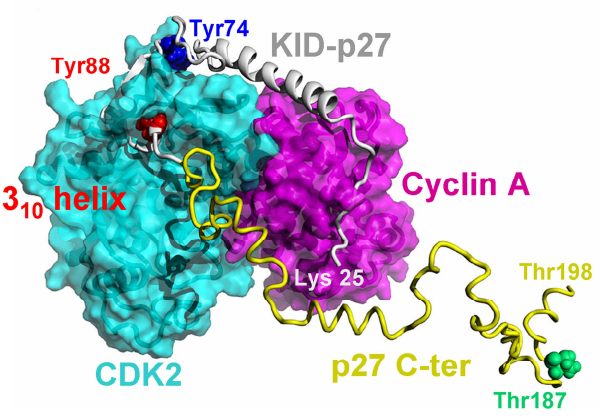

Figure 1.5. Structure of the p27/cyclin A/CDK2 complex. Schematic view of p27 (25-198 aa) illustrated as ribbons, bound to cyclin A/CDK2 complex illustrated as solvent accessible surface (magenta and cyan, respectively). The KID domain (grey) contains two critical phosphorylatable residues, Tyr74 and TyrY88 (blue and red spheres, respectively) and the 3_{10} helix subdomain which is inserted into the ATP binding pocket of CDK2. The C-terminal domain of p27 (yellow tube), which contains Thr187 (green spheres), is intrinsically unstructured and highly dynamic. Adapted from (Galea*, et al.*, 2008a).

Finally, p27 belongs to the growing family of “natively unfolded”, “intrinsically disordered” or “unstructured” proteins. The disordered protein regions lack of secondary structure and present a large number of possible conformations that, after the substrate binding, converge to a well-defined structure with high affinity for the substrate. In this sense, p27 binds cyclin/CDK complexes through a sequential mechanism involving binding-induced protein folding. The absence of a pre-existing folding strongly facilitates p27 interaction with a number of targets (Bienkiewicz*, et al.*, 2002; Lacy*, et al.*, 2004).

1.2.4.2. Regulation of p27

Expression of p27 is controlled at different levels including transcription, translation and ubiquitin mediated degradation. In addition, p27 activity can be modulated at the same time by its subcellular localization or by complexing into different cyclin/CDK complexes. Furthermore, p27 degradation and its subcellular localization are governed in turn by its phosphorylation status (Chu*, et al.*, 2008). Therefore, p27 regulation is complex, although it is largely accepted that p27 is mainly regulated at protein stability level.

Regulation of p27 gene transcription

Although p27 levels are largely controlled at the post-transcriptional level, several transcription factors have been shown to bind and regulate the *CDKN1B* promoter. For instance, E2F1, which is itself activated by cyclin/CDK complexes (through RB phosphorylation), activates the p27 promoter leading to a negative feedback loop (Wang*, et al.*, 2005a). SP1, NF-Y and the vitamin D3 receptor (VDR) might also up-regulate p27 expression during cell differentiation in response to vitamin D3 stimulation (Inoue*, et al.*, 1999; Huang*, et al.*, 2004). STAT3 also binds to murine p27 promoter and induces p27 expression, mediating differentiation of myeloid murine cells in response to granulocyte colony-stimulating factor (G-CSF) (de Koning*, et al.*, 2000). Menin, the protein encoded by the *MEN1* (multiple endocrine neoplasia) tumour suppressor gene, recruits MLL histone methyltransferase complex to the first exon of *CDKN1B*, activating the p27 expression (Milne*, et al.*, 2005). However, *CDKN1B* regulation is carried out mainly by transcription factors of the Forkhead box class O family, such as FoxO3a (also called FKHR-L1) and FoxO4 (also called AFX). These transcription factors integrate signals from cytokines, PI3K/AKT(PKB) and RAS signaling pathways to modulate p27 gene transcription (Dijkers*, et al.*, 2000; Medema*, et al.*, 2000; Trotman*, et al.*, 2006). For example, AKT phosphorylates and inactivates FoxO4, suppressing FoxO4-mediated p27 gene transcription in LNCaP human prostate carcinoma cell line (Graff*, et al.*, 2000).

On the other hand, the transcription factor MYC represses the *CDKN1B* promoter in several immune system cell lines through a putative Inr element at the transcription start site (TSS) (Yang*, et al.*, 2001; Chandramohan*, et al.*, 2004).

Regulation of p27 mRNA translation

p27 mRNA translation is maximal in quiescence and early G1 and decreases after mitogen stimulation as cells progress toward S-phase (Hengst and Reed, 1996; Millard*, et al.*, 1997). Cell cycle-dependent translation of p27 is mainly controlled by the 5' untranslated region of p27 mRNA (5′ UTR), which contains an internal ribosome entry site (IRES). The IRES is a specialized RNA structure that recruits ribosomes to the mRNA in a cap-independent manner and maintains efficient p27 mRNA translation during quiescence when most cellular cap-dependent translation is reduced (Miskimins*, et al.*, 2001; Kullmann*, et al.*, 2002). Several proteins, such as PTBP1 (also known as hnRNP I) or ELAVL1 and ELAVL4 (also known as Hu-R and Hu-D, respectively) have been described to bind to the p27 IRES and to modulate p27 mRNA translation (Millard*, et al.*, 2000; Kullmann*, et al.*, 2002; Cho*, et al.*, 2005). Finally, miR-221 and miR-222 bind to the 3′UTR of p27 mRNA and inhibit its translation. Down-regulation of miR-221/222 in different tumour cells increased p27 expression and inhibited cell proliferation (le Sage*, et al.*, 2007).

Regulation of p27 protein stability

However, the best known mechanism regulating p27 protein levels in the cell is post-translational and controls the protein degradation through the ubiquitin-proteasome pathway (Pagano*, et al.*, 1995). In quiescent cells, p27 accumulates in the nucleus where it binds to cyclin/CDK complexes to block cell cycle progression (Sherr and Roberts, 1999). To re-enter the cell cycle upon mitogenic stimulation, the cell need to down-regulate p27 levels rapidly. In fact, p27 half-life falls five-to eightfold during G1/S transition. For it, p27 undergoes a rapid ubiquitin-proteasome-mediated proteolysis following two main pathways, dependent or independent of p27-Thr187 phosphorylation (Nakayama and Nakayama, 2006; Chu*, et al.*, 2008).

p27 proteolysis dependent on Thr187-phosphorylation

The best characterized degradation pathway takes place in the nucleus at G1/S transition and is mediated by the SCF^{SKP2} (SKP1/CUL1/F-Box protein: SKP2) ubiquitin ligase complex (Figure 1.6 and 1.7) (Carrano*, et al.*, 1999; Sutterluty*, et al.*, 1999; Tsvetkov*, et al.*, 1999) which will be discussed in more detail below. The SCF^{SKP2} complex consists of the RING-finger protein RBX1, CUL1, SKP1, the F-box protein SKP2 and the accessory protein CKS1 (Nakayama and Nakayama, 2006). Efficient p27 ubiquitination by SCF^{SKP2} complex requires prior p27 phosphorylation at Thr187 which is mediated by active cyclin E-A/CDK2 complexes (Muller*, et al.*, 1997; Sheaff*, et al.*, 1997; Vlach*, et al.*, 1997; Montagnoli*, et al.*, 1999). The phosphate group at Thr187 is recognized by the phosphate binding pocket of CKS1, and promotes the binding of p27 to the CKS1/SKP2 interface (Hao*, et al.*, 2005) (Figure 1.11). Thus, CKS1 deficiency prevents SKP2 binding to p27, leading to p27 up-regulation (Ganoth*, et al.*, 2001; Spruck*, et al.*, 2001). In addition, p27 ubiquitination also requires its stable binding to a cyclinA/CDK2 complex (Montagnoli*, et al.*, 1999; Zhu*, et al.*, 2004b) because cyclin A binds SKP2 (Zhang*, et al.*, 1995; Ji*, et al.*, 2006) and CDK2 binds CKS1 (Bourne*, et al.*, 1996). Therefore, cyclin A/CDK2 complex

phosphorylates and stimulates p27 recruitment to the SCF^{SKP2} ubiquitin ligase complex which induces p27 polyubiquitination and subsequent degradation by the proteasome (Nakayama and Nakayama, 2006).

Nevertheless, p27 binds to and inhibits cyclin A-E/CDK2 catalytic activity at G0/G1 phases (Pavletich, 1999) preventing p27-Thr187 phosphorylation. Therefore, active trimeric complexes are required to efficiently phosphorylate p27 at Thr187. To solve this conflict p27 contains several phosphorylatable tyrosines within its KID domain (Tyr74, Tyr88 and Tyr89). Tyr88 is highly conserved among CKIs of CIP/KIP family and it is part of the 3_{10}-helix that inserts into the catalytic cleft of CDK2 displacing the ATP (Russo*, et al.*, 1996a). Tyr88 phosphorylation by non-receptor tyrosine kinases (NRTKs), such as ABL and SRC family members or Janus kinase 2 (JAK2) (Galea*, et al.*, 2008b; Jakel*, et al.*, 2011), promotes 3_{10}-helix ejection from the catalytic cleft, opening up the ATP binding pocket and allowing p27-Thr187 phosphorylation by the own CDK2 in the trimeric complex (Figure 1.6). Thus, p27 phosphorylation at Tyr88 initiates the passage from a cyclin E/CDK2 inhibitor at G0 to a cyclin E-A/CDK2 substrate at the G1/S transition (Chu*, et al.*, 2007; Grimmler*, et al.*, 2007).

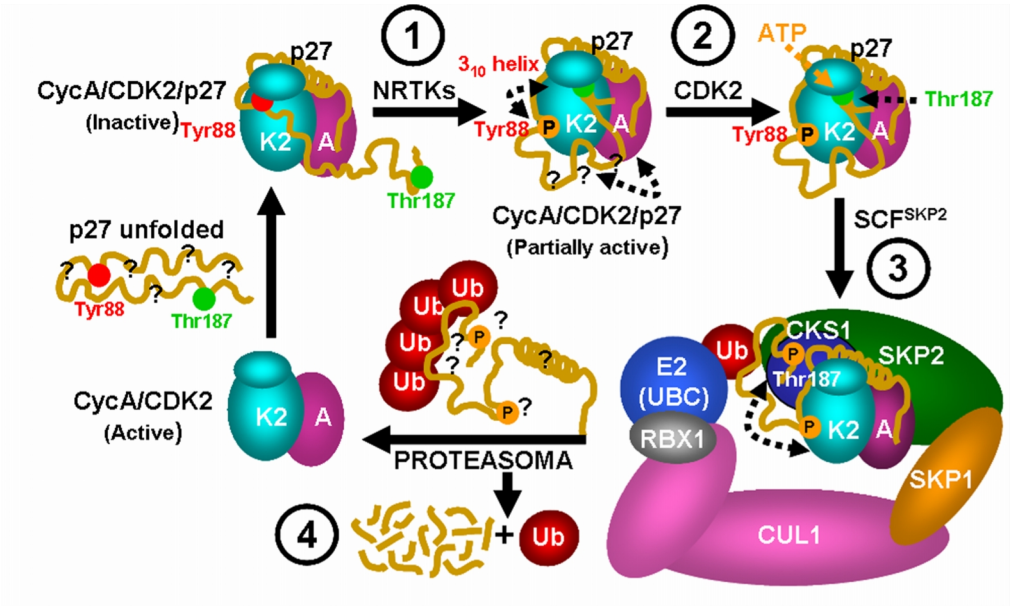

Figure 1.6. Scheme illustrating the phosphorylation mechanism involving Tyr88 and Thr187 which triggers p27 ubiquitination and 26S proteasomal degradation in both normal and cancer cells. Phosphorylation of Tyr88 (1), (and possibly Tyr74) by non-receptor tyrosine kinases (NRTKs), ejects subdomain 3_{10} from the ATP binding pocket of CDK2 allowing Thr187 within the flexible C-terminal domain to encounter the CDK2 active site and to be phosphorylated by CDK2 (2). P-Thr187-p27 is recognized by SCF^{SKP2} ubiquitin ligase which ubiquinates p27 (3) targeting it for proteasomal degradation and releasing active cyclin A/CDK2 complexes (4).

p27 proteolysis independent on Thr187-phosphorylation

Although SCF^{SKP2} mediates probably the most potent degradation pathway of nuclear p27 at G1/S transition, p27 proteasome-mediated degradation can also occur by SCF^{SKP2} and Thr187-independent pathways (Hara*, et al.*, 2001; Malek*, et al.*, 2001). The second main degradation pathway is carried out by the KIP1 ubiquitination-promoting complex (KPC) and takes place in the

cytoplasm in early G1 (Kamura*, et al.*, 2004) (Figure 1.7). The KPC ubiquitin ligase consists of two subunits, the RING finger protein KPC1 and KPC2. KPC1 binds to free cytoplasmic p27 whereas KPC2 interacts with the 26S proteasome (Hara*, et al.*, 2005; Kotoshiba*, et al.*, 2005). Recently, a third E3 ubiquitin ligase, Seven in Absentia Homolog 1 (SIAH1) together with its adaptor protein SIAH-interacting protein (SIP), has been also shown to ubiquitinate p27 in the cytoplasm, in response to glucose depletion (Nagano*, et al.*, 2011). Finally, it has been reported other ubiquitin ligases involved in the ubiquitination and proteasomal degradation of p27 such as the transcription factor and HECT domain family ubiquitin ligase UBE3A/E6-AP, the p53-inducible protein with a RING-H2 domain Pirh2 or CUL4A/B-based E3 ligases, but their mechanisms of action are less well characterized (Chu*, et al.*, 2008; Lu and Hunter, 2010).

Regulation by the subcellular localization of p27

The subcellular localization of p27 plays an important role by rendering the protein available to the different degradation pathways, as mentioned, but also by regulating cell cycle-independent functions such as cell motility.

To perform its function as cell-cycle inhibitor, p27 needs to be imported into the nucleus during the G1-phase. For that, the C-terminal region of p27 contains a NLS (aa 152–169) that guides p27 into the cell nucleus (Reynisdottir and Massague, 1997; Zeng*, et al.*, 2000). Importins-α3 and α5 recognize p27-NLS and importin-β mediates p27-importin-α association with the nuclear pore complex (Sekimoto*, et al.*, 2004). In this transport also participates the nuclear pore complex-associated protein mNPAP60 (Muller*, et al.*, 2000).

However, in early G1, p27 can also be detected in cytoplasm. p27 phosphorylation on Ser10 increases p27 binding to exportin 1 (also known as CRM1) through the NES and promotes nuclear export of p27 (Figure 1.7) (Rodier*, et al.*, 2001; Ishida*, et al.*, 2002; Connor*, et al.*, 2003). In this process also participates the core component of COP9/signalosoma Jab1/CSN5 which functions as an adaptor between p27 and CRM1 (Tomoda*, et al.*, 1999; Tomoda*, et al.*, 2002). Ser10 is one of the major phosphorylation sites of p27. It is estimated that 75% of p27 phosphate incorporation occurs on this residue (Borriello*, et al.*, 2007). Ser10 can be phosphorylated by multiple kinases including MIRK (also known as DYRK 1B), CDK5, KIS, AKT/PKB, TM4SF5 or the CaM kinase II (Jakel*, et al.*, 2012). Nevertheless, there are discrepancies about the role of Ser10 phosphorylation in the nuclear export of p27 at the G0/G1 transition, because this export occurs normally in knock-in $p27^{S10A}$ MEFs, indicating that it is not essential for this process (Kotake*, et al.*, 2005).

In the cytoplasm, p27 phosphorylation on Thr157 and Thr198 delays nuclear import of p27 (Larrea*, et al.*, 2009b). Thr157 is located within the NLS and phosphorylation of this residue promotes p27 association to 14-3-3 protein which suppresses importin α/β-dependent nuclear localization, leading to p27 cytoplasmic retention (Figure 1.7) (Sekimoto*, et al.*, 2004). Several protein kinases can phosphorylate Thr157 including SGK1 (Hong*, et al.*, 2008), AKT/PKB (Liang*, et al.*, 2002; Shin*, et al.*, 2002; Viglietto*, et al.*, 2002) and all Pim family members (Pim1, Pim2, and Pim3) (Morishita*, et al.*, 2008). Pim and AKT kinases also phosphorylate p27 on Thr198

promoting p27 binding to 14-3-3 proteins and preventing p27 re-entry into cell nucleus (Fujita, *et al.*, 2002; Morishita, *et al.*, 2008). In addition, Thr198 phosphorylation by RSK1 which is an effector of both Ras/MAPK and PI3K/PDK1 pathways or AMP-activated protein kinase (AMPK), also stabilizes p27 at G1-phase, preventing ubiquitin-dependent degradation of free p27 (Kossatz, *et al.*, 2006; Liang, *et al.*, 2007; Larrea, *et al.*, 2009a).

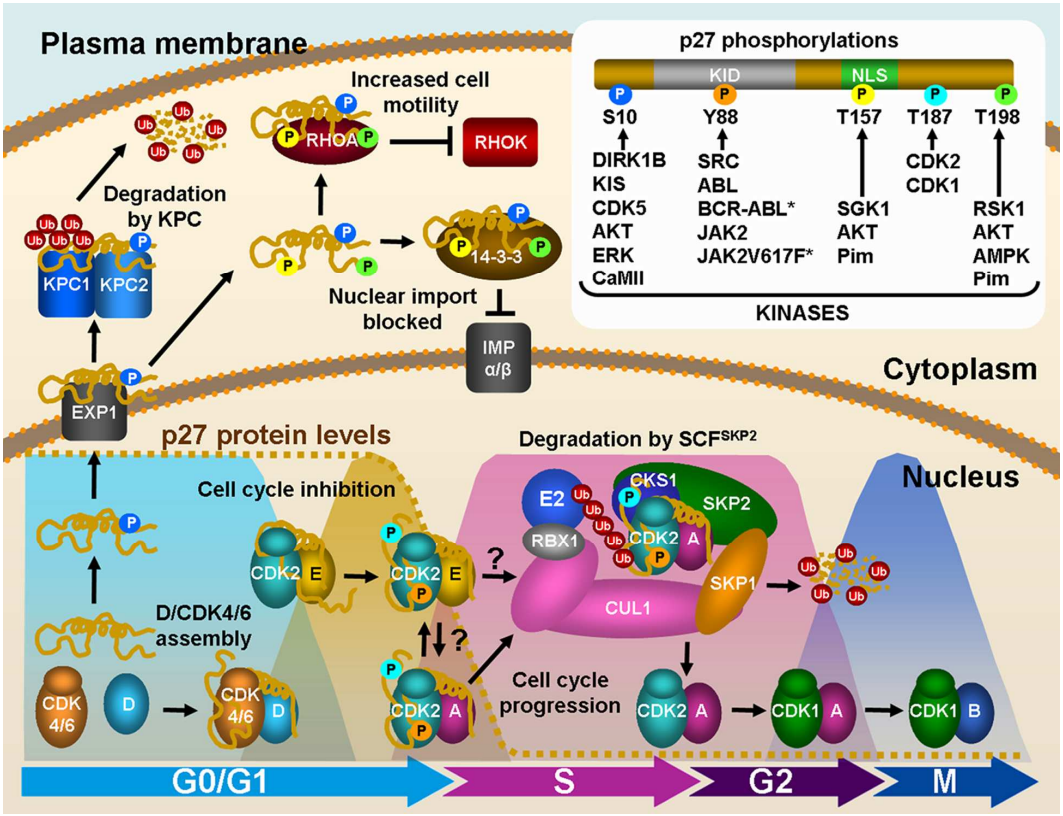

Figure 1.7. Role of phosphorylation events in modulating p27 function, activity and stability related to its subcellular localization during cell cycle. In early G1, p27 phosphorylation at Ser10 promotes EXP1-dependent nuclear export to the cytoplasm where p27 interacts with the KPC ubiquitin ligase complex that promotes p27 ubiquitination and degradation by the proteasome. However, phosphorylation at Thr157 and Thr198 lead to p27 cytoplasmic retention bound to 14-3-3 proteins, stabilizing p27, suppressing importin α/β-dependent nuclear localization and promoting increased cell motility via inhibition of RhoA-ROCK activity. While in the nucleus, p27 promotes cyclin D/CDK4-6 complexes assembly. In mid-G1, p27 inhibits cyclin E/CDK2 complexes, preventing G1/S transition. Upon mitogenic stimulation, p27-Tyr88 phosphorylation contributes to cyclin E/CDK2 activation and Thr187 phosphorylation, allowing p27 ubiquitination through SCF^{SKP2}, proteolysis by the proteasome and cell cycle progression through S-phase. **(Inset at the upper right) Protein kinases involved in p27 phosphorylation.** Schematic representation of p27 showing the regulatory phosphorylation residues and the protein kinases involved in every phosphorylation event. For more details, see the text.

Regulation of p27 by sequestration in complexes with D-cyclins

As previously mentioned, the cyclin A-E/CDK2 complexes are the main p27 targets at G1/S transition. However, p27 also binds to cyclin D/CDK4-6 complexes when cells pass through G1-phase of cell cycle. This reduces the p27 levels available for inhibition of cyclin A-E/CDK2 complexes, allowing CDK2 activity and driving cells through G1/S phase transition. However, p27

is redistributed from cyclin D/CDK4-6 to cyclin A-E/CDK2 complexes when cells are arrested by growth factor deprivation, drug treatment or UV irradiation (Poon*, et al.*, 1995). Therefore, it has been suggested that cyclin D/CDK4-6 complexes can function as a reservoir for p27, regulating p27 activity (Poon*, et al.*, 1995; Soos*, et al.*, 1996). In this line, it has been described that cyclin D1 induction by the MEK/ERK pathway regulates the assembly of cyclin D1/CDK4 complexes which sequester and reduce the effective inhibitory threshold of p27, preventing p27-mediated cell cycle inhibition (Cheng*, et al.*, 1998; Ladha*, et al.*, 1998). In addition, the proto-oncogene *MYC* has been also shown to play an important role in p27 sequestration through modulation of cyclin D and E protein levels (Perez-Roger*, et al.*, 1997; Bouchard*, et al.*, 1999; Perez-Roger*, et al.*, 1999; Obaya*, et al.*, 2002).

1.2.4.3. p27 functions

Although most studies focus on p27 function in cell cycle regulation, it has also been associated to many other biological processes, such as cell differentiation, apoptosis and cell motility, and its subcellular localization appears to play an important role in these functions (Borriello*, et al.*, 2007; Chu*, et al.*, 2008). It is also important to mention that recently it has been described a new function of p27 as a transcriptional regulator of genes involved in different cellular processes as cell cycle, mitochondrial organization and respiration, RNA processing, splicing and translation among others. p27 was found bound to the promoters in association with p130/E2F4 complexes and co-repressors as mSIN3A and HDACs (Pippa*, et al.*, 2011). This work lays the foundation for a new function of p27 unknown to date.

p27 function in cell cycle regulation

As previously mentioned, p27 was initially identified associated to cyclin E/CDK2 complexes in cells that had been growth arrested with TGF-b (Koff*, et al.*, 1993; Polyak*, et al.*, 1994b). Subsequently, p27 was linked to G1-arrest in response to several other antimitogenic signals such as growth factors deprivation, differentiation signals, contact inhibition, loss of cell adhesion to the extracellular matrix, cAMP, rapamycin, lovastatin or anti-IgM treatment (Hengst and Reed, 1998). Nowadays, it is widely accepted that the effect of p27 in cell proliferation is mainly due to the inhibition of cyclin E/CDK2 complexes in G1 and G1/S transition of cell cycle (Figure 1.7 and 1.8). In this sense, a p27 mutant ($p27^{CK-}$) unable to bind cyclin/CDK complexes owing to four point mutations in the KID domain (Arg30, Leu32, Phe62 and Phe64 for Ala substitutions), cannot arrest cell cycle at G1 (Vlach*, et al.*, 1997). Furthermore, its importance in regulating cell proliferation is emphasized by the fact that $p27^{-/-}$ mice are 20-30% larger than *wt* animals and display organomegaly and hyperproliferation of multiple tissues (Fero*, et al.*, 1996; Kiyokawa*, et al.*, 1996; Nakayama*, et al.*, 1996).

On the other hand, p27 binds not only to the cyclin E/CDK2 complex, but also to cyclin A/CDK2, cyclin D/CDK4-6 and cyclin B/CDK1 complexes. Early studies indicated that inhibition of these complexes occurred at greater stoichiometric amounts of p27 than those needed to inhibit cyclin E/CDK2 complexes (Figure 1.8) (Polyak*, et al.*, 1994b; Toyoshima and Hunter, 1994; Blain*,*

et al., 1997; Obaya*, et al.*, 2002). However, structural and biochemical studies suggest that only one CIP/KIP molecule should be able to block the activity of a cyclin/CDK complex (Russo*, et al.*, 1996a; Hengst*, et al.*, 1998). Recently, it has been described that tyrosine phosphorylation in the KID domain (Tyr88 and Tyr89 by ABL kinases (James*, et al.*, 2008; Ray*, et al.*, 2009) or Tyr74 by SRC kinases (Larrea*, et al.*, 2008)), converts p27 from a cyclin D1/CDK4 bound inhibitor to a bound non-inhibitor, in a similar way as occurs in the binding of p27 to cyclin A-E/CDK2 complexes described above (Chu*, et al.*, 2007; Grimmler*, et al.*, 2007).

Finally, although the CIP/KIP family of CKIs were originally described as general inhibitors of CDK activity (Harper*, et al.*, 1993; Xiong*, et al.*, 1993), several studies suggest an active role for both p21 and p27 as assembly factors for the formation of cyclin D/CDK4-6 complexes (Figure 1.7 and 1.8) (LaBaer*, et al.*, 1997). In fact, p27 and p21 deficient cells show defects in the assembly of these complexes (Cheng*, et al.*, 1999a). However, more recent studies show that although cyclin D/CDK4-6 complex formation is favored by p21 or p27 (Bagui*, et al.*, 2000; Obaya*, et al.*, 2002), their presence is not strictly required (Bagui*, et al.*, 2003). Finally, p27 phosphorylations at Thr198 and Thr157 have also been involved in p27 assembly function, increasing cyclin D1/CDK4 assembly in early G1 (Larrea*, et al.*, 2008).

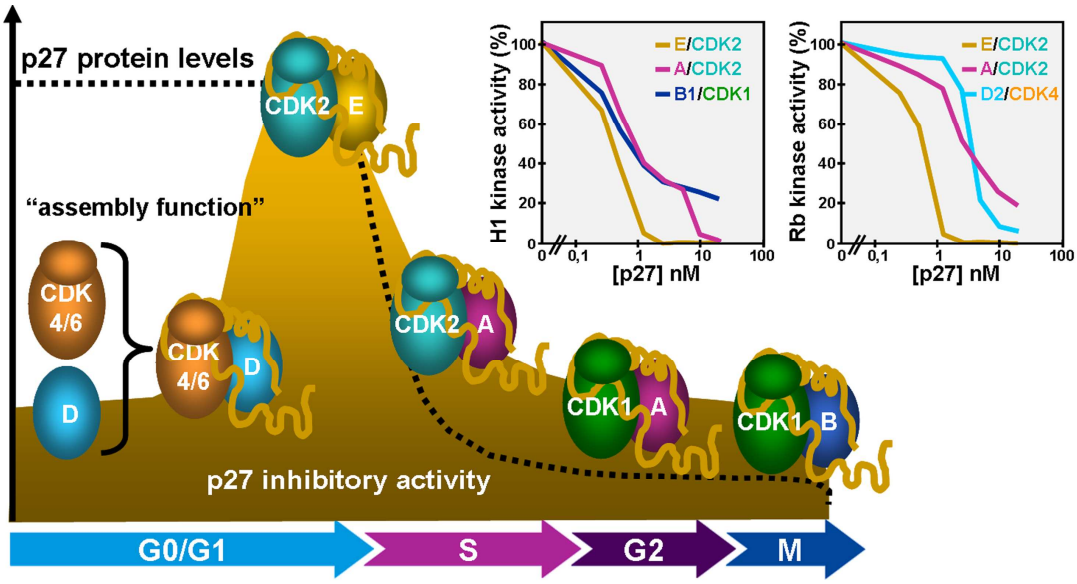

Figure 1.8 Schematic model of p27 levels and activity during cell cycle and the relative sensitivity of cyclin/CDK complexes to inhibition by p27. The p27 protein levels remains maximal at G0 and early G1 and drop rapidly at the G1/S-phase transition. p27 binds to and inhibits a broader spectrum of cyclin/CDK complexes already formed. Graphs were taken and adapted from (Polyak*, et al.*, 1994b). They show baculovirally expressed human cyclin/CDK combinations assayed for *in vitro* histone H1 and RB kinase activity in the presence of different concentrations of pure recombinant C-terminal hexahistidine tagged p27. Relative phosphorylation levels were quantitated and plotted as the percentage of phosphorylation observed in reaction without p27. Cyclin E/CDK2 was inhibited half-maximally at 0.5 nM p27 (Polyak*, et al.*, 1994b). Complete inhibition of cyclin A/CDK2, cyclin B1/CDK1 or cyclin D2/CDK4 required an 8 to 10-fold higher concentration of p27.

Involvement of p27 in cell differentiation processes

With a few exceptions, terminal differentiation involves an irreversible cell cycle exit into a G0 state (Munoz-Alonso and Leon, 2003). This process is usually accompanied by up-regulation of CKIs. For instance, p27 is induced during progression to terminal differentiation of human hematopoietic progenitors (CD34+ blast cells) (Taniguchi*, et al.*, 1999). p27 is also up-regulated during chemically induced differentiation of several hematopoietic cell lines into myeloid, erythroid or megakaryocytic lineages (Steinman, 2002; Munoz-Alonso and Leon, 2003; Gomez-Casares*, et al.*, 2012). Furthermore, p27 overexpression promotes the differentiation of different hematopoietic cell lines toward monocytic (Liu*, et al.*, 1996; Muto*, et al.*, 1999; Rots*, et al.*, 1999), erythroid (Munoz-Alonso*, et al.*, 2005; Acosta*, et al.*, 2008) or megakaryocytic lineages (Matsumura*, et al.*, 1997). However, despite inducing proliferative arrest, p27 cannot induce differentiation in others erythroleukemia cell lines (Matushansky*, et al.*, 2000; Tamir*, et al.*, 2000) and, in contrast to its potential requirement in myelopoiesis, p27 down-modulation is a prerequisite for normal T-cells development (Tsukiyama*, et al.*, 2001).

Finally, studies carried out in $p27^{-/-}$ mice shows that p27 controls the development of the mouse cerebral cortex by regulating differentiation of cortical progenitor cells into neurons by stabilizing the Neurogenin 2 transcription factor (Nguyen*, et al.*, 2006) and that p27 cooperates with $p57^{KIP2}$ regulating the cell cycle exit and differentiation in lens, placenta and pituitary gland (Zhang*, et al.*, 1998; Bilodeau*, et al.*, 2009). However, despite exhibit an expansion of hematopoietic progenitors, $p27^{-/-}$ mice do not display a defect in the ability to differentiate these cells (Fero*, et al.*, 1996).

The role of p27 in apoptosis

The role of p27 in programmed cell death remains ambiguous (Drexler and Pebler, 2003). In a number of cancer cell lines, overexpression of p27 induces a pro-apoptotic effect (Katayose*, et al.*, 1997; Wang*, et al.*, 1997; Dijkers*, et al.*, 2000; Nickeleit*, et al.*, 2008). However, the molecular mechanism by which p27 causes apoptosis is largely unknown although it appears to require the activation of downstream effectors such as caspase-3 (Nickeleit*, et al.*, 2008). On the other hand, p27 protects different carcinoma and leukemic cell lines from chemically-induced apoptosis (Philipp-Staheli*, et al.*, 2001; Drexler and Pebler, 2003) and it also plays an anti-apoptotic role in normal fibroblasts from $p27^{-/-}$ mice cultured in absence of growth factors (Hiromura*, et al.*, 1999).

Involvement of p27 in cell motility

p27 also displays a dual behavior in the regulation of cell motility. On the one hand, cytoplasmic p27 stimulates cell motility through inhibition of RhoA GTPase. p27 binds through its C-terminal domain to RhoA, preventing its activation by Rho–GEFs and disrupting ROCKs activation (Figure 1.7). In keeping with this finding, $p27^{-/-}$ MEFs show increased RhoA-ROCK activity, increased actin stress fibres and focal adhesions, and decreased cell motility (Besson*, et al.*, 2004b). In this manner, p27 controls mouse cerebral cortex development by regulating

migration of neurons to the cortical plate (Nguyen*, et al.*, 2006). In addition, cytoplasmic p27 also stimulates cell migration through action on GTPase RAC (a positive regulator of cell motility) (Nagahara*, et al.*, 1998; McAllister*, et al.*, 2003).

In contrast, p27 negatively regulates migration in several other cell models (Goukassian*, et al.*, 2001; Sun*, et al.*, 2001). In normal MEFs and fibrosarcoma cells, cytoplasmic p27 inhibits migration by binding also through its C-terminal domain to stathmin, a microtubule-destabilizing protein. p27 impairs the tubulin sequestering activity of stathmin, promoting increased microtubule polymerization and inhibition of cell motility (Baldassarre*, et al.*, 2005).

Altogether, these effects of cytoplasmic p27 in cell migration have been associated with p27 oncogenic functions as tumor invasiveness and metastasis (Besson*, et al.*, 2004a; Baldassarre*, et al.*, 2005; Wu*, et al.*, 2006; Denicourt*, et al.*, 2007).

1.2.4.4. p27 and cancer

Given the main key function of p27 as CDK inhibitor and thus as an essential cell cycle regulator, disruption of p27 function was promptly associated to cancer development. Actually, p27 down-regulation has been observed in almost 50% of all human cancers and it usually correlates with their histological aggressiveness and with poor prognosis of the tumor (Slingerland and Pagano, 2000; Philipp-Staheli*, et al.*, 2001; Chu*, et al.*, 2008). Moreover, low p27 expression has been also correlated with high proliferation rate in lymphomas, prostate and liver cancer although not in other cancer types as colon or breast cancer (Slingerland and Pagano, 2000).

With a very few exceptions such as human patients with MEN1 syndrome-like phenotype (Pellegata*, et al.*, 2006; Molatore*, et al.*, 2010), mutations and especially the homozygous deletion of *CDKN1B* gene are extremely rare in cancer (Ponce-Castaneda*, et al.*, 1995; Philipp-Staheli*, et al.*, 2001). Therefore, p27 gene cannot be classified as a "classic" tumor suppressor gene because it does not fulfil the Knudson's double mutation criterion (Fero*, et al.*, 1998). Nevertheless, loss of p27 heterozygosity is frequent in certain human cancers including myeloid and lymphoblastic leukemias (Pietenpol*, et al.*, 1995; Takeuchi*, et al.*, 1995) and ovarian cancer (Hatta*, et al.*, 1997).

The reduction of nuclear p27 protein levels in different human cancers (such as breast and prostate cancer) without apparent changes in the p27 mRNA expression support the hypothesis that p27 down-regulation is mainly due to posttranslational mechanisms (Catzavelos*, et al.*, 1997; Cordon-Cardo*, et al.*, 1998). In keeping with this hypothesis, reduced p27 expression has been associated to SKP2 overexpression and enhanced proteasome-mediated degradation in breast, prostate and colorectal cancer among others (Gstaiger*, et al.*, 2001; Hershko*, et al.*, 2001; Signoretti*, et al.*, 2002; Drobnjak*, et al.*, 2003) (Figure 1.14).

Another mechanism used by the tumor cells to impair the p27-mediated regulation of cell cycle progression is the cytoplasmic sequestration of the protein. p27 retention in the cytoplasm mediated by AKT-dependent Thr157 phosphorylation has been observed in breast cancer (Liang*, et al.*, 2002; Shin*, et al.*, 2002; Viglietto*, et al.*, 2002) and pituitary tumors (Musat*, et al.*, 2005). Interestingly, this aberrant cytoplasmic localization of p27 has been associated with higher

metastatic potential in carcinomas of the breast, esophagus and uterus, as well as in some lymphomas and leukemias (Besson, *et al.*, 2004a) supporting the hypothesis that p27 may also act as pro-oncogenic factor in particular circumstances and supporting way p27 is rarely entirely lost in human malignancies.

Several mouse models confirm the role of p27 in suppressing tumorigenesis. All $p27^{-/-}$ mice develop intermediate lobe pituitary adenomas over the age of 10 weeks. The loss of only one p27 allele ($p27^{+/-}$) reduces the frequency and increases the latency of these tumors at an intermediate level when compared with $p27^{-/-}$ mice (Fero, *et al.*, 1996). Molecular analysis of these tumors showed that the remaining wild type allele is neither mutated nor silenced. Thus, p27 is a dose-dependent tumor suppressor in mice (Fero, *et al.*, 1998). Moreover, p27 deficiency cooperates with other oncogenic events such activation of the TRK-T1 oncogene; PTEN, RB and APC mutation (Min/+) heterozygosity or inhibin-α deletion to promote tumor formation in different mouse organs (Figure 1.9) (Blain, *et al.*, 2003). Interestingly, in Eμ-MYC transgenic mice (in which MYC is overexpressed in B lymphocytes under the control of the immunoglobulin heavy chain promoter), the loss of p27, but not p21, synergizes with MYC in lymphomagenesis, reducing mice survival (Martins and Berns, 2002). However, CDK2 is not required for the effect of p27 in both cell cycle and tumor formation (Martin, *et al.*, 2005).

Finally, homozygous $p27^{CK-/CK-}$ mice and to a lesser extend $p27^{CK-/+}$ mice, are prone to a higher tumor multiplicity than homozygous $p27^{-/-}$ mice indicating the existence of cyclin/CDK-independent pro-oncogenic functions of p27 and that $p27^{CK-}$ mutant behaves as a dominant oncogene *in vivo* (Besson, *et al.*, 2007).

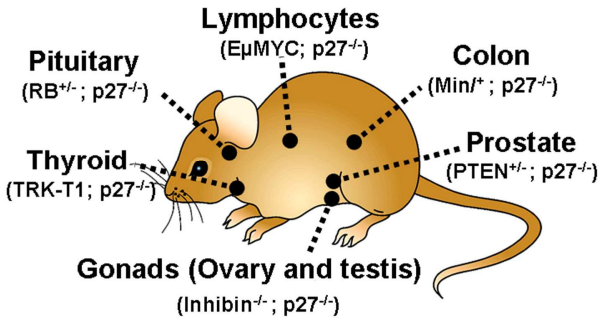

Figure 1.9 Mouse models recapitulate the role of p27 in human cancers. While $p27^{-/-}$ mice only display pituitary tumors, p27 loss enhances the malignancy and frequency of tumor formation in cooperation with different oncogenic stimuli. Adapted from (Blain, *et al.*, 2003).

1.3. CONTROLLED DEGRADATION OF CELL CYCLE REGULATORS

The levels of cyclins, CKIs and many other key regulators oscillate during the cell cycle as a result of periodic proteolysis. The ubiquitin-proteasome system (UPS) is a protein-quality control system responsible for the degradation of most intracellular misfolded proteins, but also has a crucial role in maintaining and regulating cellular homeostasis. This system mediates the degradation up to 90% of such short-lived cell cycle regulatory proteins, controlling accurately their intracellular concentrations and thus the correct timing of cell cycle. Therefore, aberrant activity of UPS is crucial in cancer development (Murray, 2004; Pickart, 2004; Lipkowitz and Weissman, 2011)

1.3.1. The ubiquitin–proteasome system

The ubiquitin–proteasome proteolytic pathway comprises two discrete steps: First, the covalent attachment of multiple ubiquitin molecules to the target protein or Ubiquitination (Pickart, 2001) and second, the degradation of the polyubiquitynated protein by the 26S proteasome complex, the only ATP and ubiquitin-dependent multicatalytic protease that is responsible for most non-lysosomal protein degradation in eukaryotic cells (Finley, 2009) (Figure 1.10).

Ubiquitin is a small (76 aa) highly conserved protein (Goldstein*, et al.*, 1975; Schlesinger and Goldstein, 1975) that has been found ubiquitously in all eukaryotic organisms, hence its name. Ubiquitination is the reaction that results in the formation of a covalent isopeptide bond between the C-terminal glycine residue (Gly76) in the ubiquitin and the epsilon-amino group of a lysine residue in the substrate. This requires the sequential action of at least three enzymes: an ubiquitin-activating enzyme (UBA or E1), an ubiquitin-conjugating enzyme (UBC or E2) and an ubiquitin ligase (E3). The E1 enzyme activates ubiquitin as a thiolester in an ATP-dependent reaction and transfers the activated ubiquitin to the catalytic cysteine residue of an E2. Finally, E3 ligases act as mediators to transfer ubiquitin from E2 to a lysine residue in the substrate protein (Pickart, 2001). Successive conjugation rounds of ubiquitin monomers to lysines of previously attached ubiquitins result in the formation of a poly-ubiquitin chain that ultimately can be recognized by the proteasome, leading to its processing into small peptides and the recycling of ubiquitins (Figure 1.10) (Pickart and Cohen, 2004; Finley, 2009).

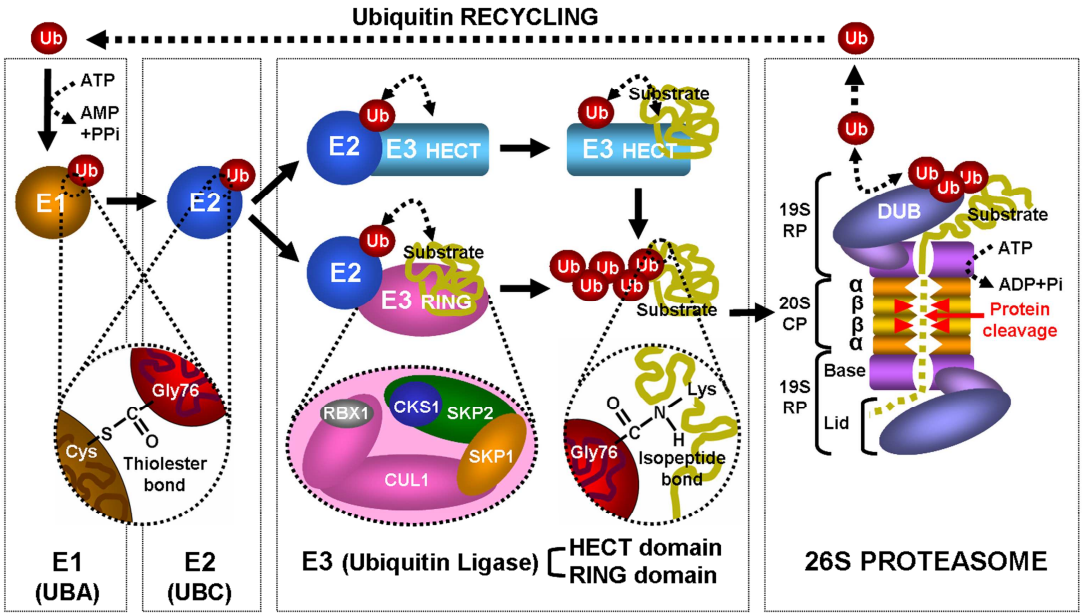

Figure 1.10. Overview of the ubiquitin-proteasome pathway. Ubiquitination involves three enzymes: a ubiquitin-activating enzyme (UBA or E1), a ubiquitin conjugating enzyme (UBC or E2) and a ubiquitin ligase (E3). E3s can themselves form a thiolester bond with ubiquitin (HECT-domain E3s) before substrate attachment, or can function as a bridge between an activated E2 and its target (RING E3s). The ubiquitinated substrate is then recognized by the 26S proteasome which recycle the ubiquitins and destroys the substrate in an ATP-dependent manner. DUB (Deubiquitylating enzyme); PPi (pyrophosphate) and Ub (Ubiquitin). Adapted from (Pickart, 2001; Ravid and Hochstrasser, 2008)

1.3.2. The ubiquitin ligase enzymes (E3s)

However, the specificity and adaptability of ubiquitination is provided by ubiquitin ligases (E3s), which physically interact with target substrates (Nakayama and Nakayama, 2005). In humans, only two E1 enzymes (UBA1 and UBA6) and approximately 40 E2 enzymes have been identified. By contrast, it is estimated that there may be as many as 1000 E3 ligases, each of which has the potential to recognize multiple substrates (Hicke*, et al.*, 2005; Li*, et al.*, 2008).

Based on the sequence homology and structural similarities of their E2-binding domains, E3s can be classified into two major subfamilies (Figure 1.10): the HECT domain family (Homologous to E6-AP C-terminus) and the RING finger domain family (Really Interesting New Gene). They differ in the way they transfer ubiquitin to the substrate. The HECT proteins contain a conserved catalytic cysteine, which acts as an ubiquitin acceptor from E2 enzymes forming an ubiquitin thiolester intermediate. Ubiquitin is then transferred to the substrate from HECT E3 enzyme. In contrast, RING E3s enzymes act as scaffolds by facilitating interaction between E2s and substrates but do not possess catalytic activity per se (Deshaies and Joazeiro, 2009; Rotin and Kumar, 2009; Metzger*, et al.*, 2012).

RING E3s ligases comprise >95% of all predicted E3s and they can function as monomers, dimers or multi-subunit complexes. In the case of multi-subunit RING E3 ligases, the RING protein functions as part of a multi protein complex and substrates are recruited by a separate subunit (Deshaies and Joazeiro, 2009; Metzger*, et al.*, 2012). Multi-subunit RING E3s include the Cullin based RING E3 ligase (CRL) superfamily and several CRL-like E3 ligases as the Anaphase Promoting Complex/ Cyclosome (APC/C). CRLs are defined by a common catalytic core which consists of a RING finger protein (RBX1 or 2) and a Cullin family member (CUL1, 2, 3, 4A, 4B, 5, 7 and 9 (PARC)). In CRLs, the Cullin protein serves as a scaffold to assemble multiple proteins, besides the RING finger protein that recruits the E2 enzyme**,** an adaptor protein which in turn binds to the substrate-recognition proteins often characterized by the presence of F-box, SOCS box or BTB protein-protein interaction domains (Petroski and Deshaies, 2005; Li*, et al.*, 2008).

1.3.3. The SCF ubiquitin ligases and the F-box component

The archetypal CRLs, which contain CUL1 and the RING finger protein RBX1, are commonly known as SCF ubiquitin ligases (from SKP1-CUL1-F-box). Within the SCF complex, CUL1 brings the E2 enzyme through the RBX1 (also known as HRT1 or ROC1), and recruit substrates through the adaptor protein SKP1 (S-phase kinase associated protein 1) and an F-box protein. This latter component confers the SCF complex designation, as SCF^{SKP2}, where SKP2 (S-phase kinase associated protein 2) is the F-box protein (Figure 1.11) (Cardozo and Pagano, 2004; Petroski and Deshaies, 2005). In the SCF complex, the interaction of F-box proteins with the adaptor protein (SKP1) occurs through the F-box domain, a ~40 aa motif that was first identified in human cyclin F, hence its name (Bai*, et al.*, 1996). The F-box proteins are the substrate-recognizing subunits which determine the versatility in substrate specificity of SCF E3

ligase complexes (Jia and Sun, 2011). According to the HUGO Gene Nomenclature Committee, 71 F-box proteins have been identified in humans. They have been classified into three major classes, depending on the types of substrate interaction domains identified in addition to the F-box motif: those with leucine-rich repeats (LRR) known as (FBXLs), those with WD40 domains or (FBXWs) and those with "other" types of protein-protein interaction motifs or no recognizable domains (FBXOs) (Jin, *et al.*, 2004).

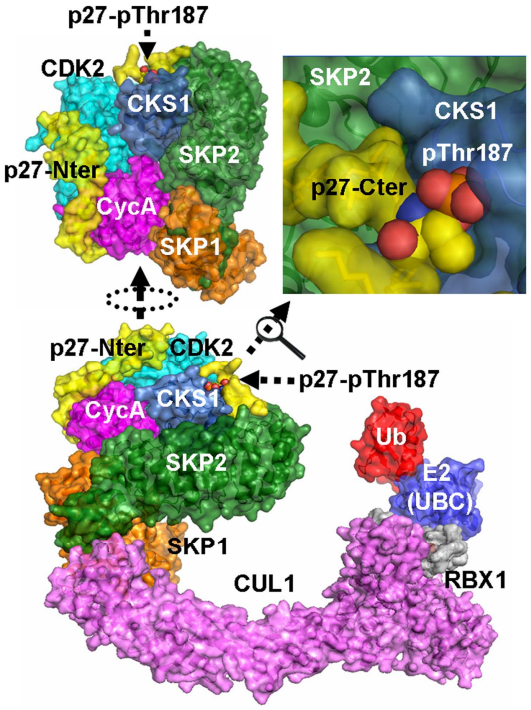

Figure 1.11. Model of the SCF^{SKP2} complex whit their substrate target. CUL1 forms a rigid, bi-lobed structure which acts as a 'molecular scaffold' on which to assemble the SCF^{SKP2} complex. The C-terminal globular domain recruits RBX1, which in turn recruits the E2 enzyme (UBC) and the ubiquitin. In the other hand, the CUL1 N-terminal domain recruits SKP1, which then binds to the SKP2 protein substrate recognition subunit via interactions between its F-box domain and the C-terminus of SKP1. SKP2 also binds to the adaptor protein CKS1 and Cyclin A. For its part, CKS1 binds to CDK2 and recognizes the p27 phosphorylated on Thr187. Adapted from (Schulman, *et al.*, 2000; Zheng, *et al.*, 2002; Hao, *et al.*, 2005). (Protein data bank files: 2AST; 1JSU; 1LDK and 3A33)

A single F-box protein can target multiple substrates even with opposite biological functions, whereas the same substrate can be recognized by different F-box proteins (Skaar, *et al.*, 2009). Moreover, most SCF substrates are recognized and bound by the F-box protein only when they are post-translationally modified, adding an extra level of regulation. Although the most widely reported prior modification is phosphorylation, substrates have also been reported to require acetylation (Hwang, *et al.*, 2010) or glycosylation (Guinez, *et al.*, 2008). For instance and as mentioned above, degradation of p27 by SCF^{SKP2} is triggered only following phosphorylation at Thr187 (Figure 1.11) (Carrano, *et al.*, 1999; Montagnoli, *et al.*, 1999; Sutterluty, *et al.*, 1999; Tsvetkov, *et al.*, 1999). In this thesis, we will focus on FBXL1 (SKP2), the best characterized mammalian F-box protein and the one involved in p27 degradation.

1.3.4. The F-box protein SKP2

The discovery of SKP2 (S-phase Kinase-associated Protein 2) preceded the identification of F-box proteins as components of the SCF ubiquitin ligase complexes. SKP2 belongs to the FBXL class of F-box proteins. It was originally discovered because of its ability to interact with cyclin A/CDK2 complexes in transformed cells together with SKP1 (p19) and CKS1 (p9), (Zhang, *et al.*, 1995). Several important characteristics of SKP2 were described in this early study,

including its overexpression in many transformed cell lines and that its regulation along the cell cycle. Unlike SKP1 and CUL1, SKP2 protein level is low in early G1 phase, while it increases during G1/S transition and is maximal in S and G2 phases of the cell cycle (Zhang*, et al.*, 1995; Kurland and Tansey, 2004; Yung*, et al.*, 2007). Nowadays, It is well known that, through degradation of its target substrates, SKP2 plays a critical role in regulating many cellular processes such as cell cycle progression, inhibition of differentiation, apoptosis or senescence and cell motility all of which are closely related to cancer development (Frescas and Pagano, 2008).

1.3.4.1. Structure of *SKP2* gene and protein

In humans, *SKP2* gene is located in the locus 5p13.2 with a genomic size of 31998 pb according to the UCSC database (hg19 assembly) (Figure 1.14). In agreement with the NCBI RNA reference sequences collection (RefSeq), alternative splicing of this gene generates three transcript variants encoding three different isoforms. The transcript variant 1 represents the longest transcript and encodes for the most studied isoform of 424 aa, SKP2A (SKP2 hereafter). As prototypical FBXL protein, it contains an N-terminal F-box domain (aa 94-140) through which it interacts with SKP1 (Schulman*, et al.*, 2000; Zheng*, et al.*, 2002). Deletion of this domain prevents SKP2 to assemble into a SCF^{SKP2} complex (Schulman*, et al.*, 2000). In addition, the N-terminal domain shows a “destruction box” (D-Box) (aa 3-6) that critically controls SKP2 stability (Bashir*, et al.*, 2004) and two phosphorylatable serines (Ser64 and Ser72) and two acetylatable lysines (Lys68 and Lys71) within a NLS (aa 63-80) which also play an important role in SKP2 stability, localization, and activity (Gao*, et al.*, 2009; Lin*, et al.*, 2009; Inuzuka*, et al.*, 2012). In the other hand, the C-terminal domain contains 10 tandem leucine-rich repeats (LRR) and an unstructured C-tail region responsible for the interaction of SKP2 with CKS1 and their substrates (Figure 1.12) (Wang*, et al.*, 2004).

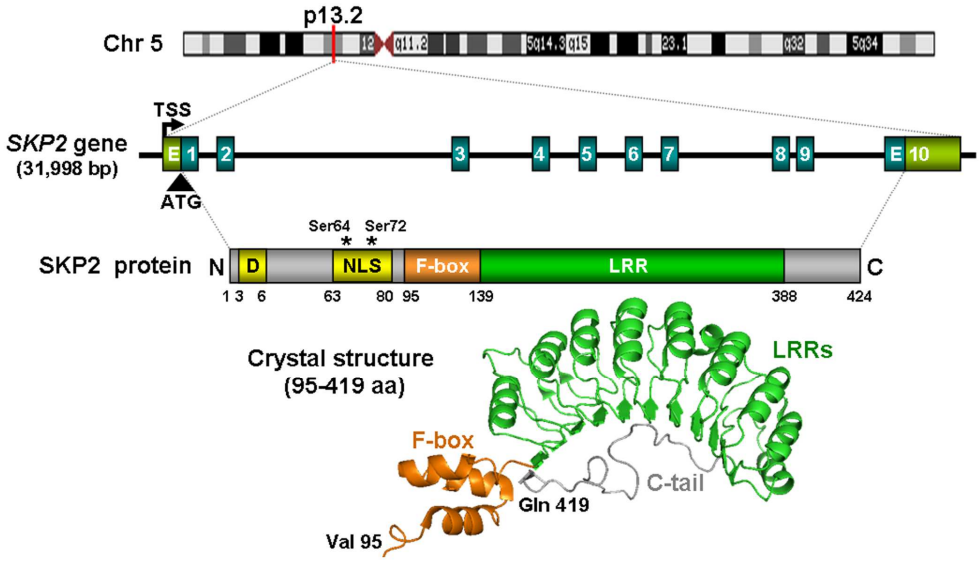

Figure 1.12. *SKP2* gene structure, localization in the human genome and major features of SKP2 protein. Chr (Chromosome); TSS (Transcription start site); D (Destruction box); NLS (Nuclear localization signal); LRR (Leucine-rich repeat) posttraductional modifiable amino acids (*) and bp (base pairs).

The transcript variant 2 presents a different C-terminal domain that is encoded by an alternative tenth exon. The resulting isoform SKP2B is shorter (410 aa). Unlike SKP2A, the SKP2B amino acid sequence changes from aa 355 interrupting the ninth and tenth LRRs and the remaining C-terminal tail. However, they are practically undistinguishable by size using conventional immunoblot and an antibody directed toward the full length of SKP2 (Ganiatsas*, et al.*, 2001).

Finally, the transcript variant 3 lacks the first to five coding exons and presents a new first exon which match within the fourth intron of variant 1, while the sixth forward exons are in-frame. The resulting isoform is shorter (210 aa) at the N-terminus, lacking of the F-box domain compared to SKP2A while maintaining all the LRR and C-terminal domain. According to *Schulman et al.* it could not assemble into SCF complexes (Schulman*, et al.*, 2000).

1.3.4.2. SKP2 regulation

SKP2 gene is periodically expressed throughout the cell cycle (Kurland and Tansey, 2004). Alteration in SKP2 protein levels during cell cycle progression is partly due to changes in gene expression and protein stability. Nevertheless, post-translational modifications such as phosphorylation and acetylation also regulate protein localization, stability, and activity.

Regulation of SKP2 gene expression

Several transcription factors have been found to bind to the *SKP2* promoter (Figure 1.13) and to induce *SKP2* gene expression such as E2F1 (Zhang and Wang, 2006), the GA-binding protein (GABP) which has been found to be dependent on the cell cycle (Imaki*, et al.*, 2003), CBF1 (RBPJ) which is a key effector of the Notch signaling pathway (Sarmento*, et al.*, 2005), FoxM1 (Wang*, et al.*, 2005b), SP1 and Elk-1 (Appleman*, et al.*, 2006) or the orphan nuclear hormone receptor 1 (NOR1) which regulates vascular smooth muscle cells (VSMC) proliferation in response to mitogenic stimulation (Gizard*, et al.*, 2011).

In addition, numerous oncogenic signals such as the overexpression of Janus kinase 2 mutant ($JAK2^{V617F}$) or BCR-ABL, both involved in myeloproliferative disorders, are also known to induce *SKP2* gene expression through the STAT3-5 transcription factors (Furuhata*, et al.*, 2009). BCR-ABL has been also shown to induce *SKP2* gene expression through the PI3K/AKT signalling pathway (Andreu*, et al.*, 2005; Chen*, et al.*, 2009). AKT could trigger *SKP2* gene expression by regulating E2F protein levels (Reichert*, et al.*, 2007). Finally, NF-κB (nuclear factor kappa-light-chain-enhancer of activated B cells) signaling, involved in inflammation and cancer, also regulates *SKP2* gene expression through the binding of p52/RelA or p52/RelB to the *SKP2* promoter (Schneider*, et al.*, 2006; Barre and Perkins, 2007).

On the other hand, the transcriptional repressors for *SKP2* are less well-known (Figure 1.13). Nevertheless, it has been described that STAT1 and Foxp3 (Forkhead box p3) can act as repressors on the *SKP2* promoter. Interestingly, Foxp3 down-regulation has been correlated with SKP2 overexpression in human breast cancer samples (Zuo*, et al.*, 2007; Wang*, et al.*, 2010b).

Lastly, p53 has been also shown to repress *SKP2* gene expression in response to UV-induced DNA damage (Barre and Perkins, 2010).

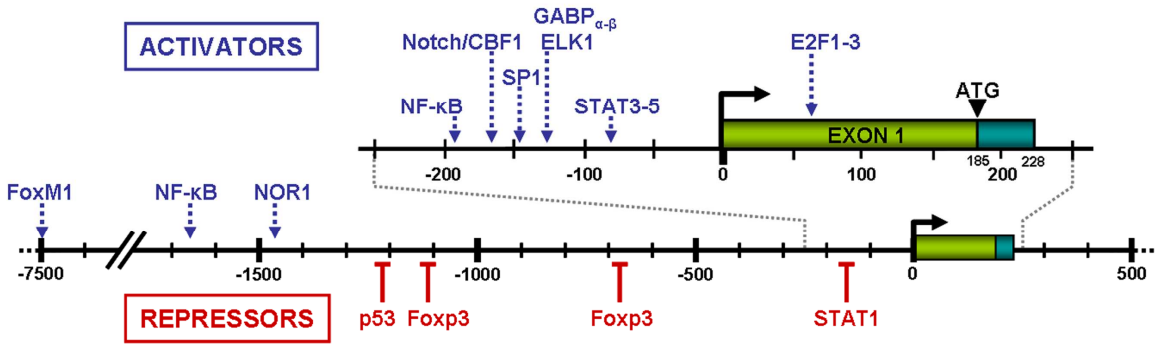

Figure 1.13. Regulation of *SKP2* gene expression. Transcription factor binding site position described on the literature relative to the *SKP2* transcription start site (TSS) from UCSC genome browser. Exon 1 is illustrated by a green box. The relative position to the TSS is indicated along the horizontal axis.

Regulation of SKP2 protein stability

SKP2 levels may also be regulated by post-translational modifications and changes in its rate of protein degradation. In early G1, SKP2 is ubiquitinated and degraded by the ubiquitin ligase APC/C^{Cdh1} (Bashir, *et al.*, 2004; Wei, *et al.*, 2004). However, after mitogenic stimulation SKP2 is highly phosphorylated and up-regulated (Bilodeau, *et al.*, 1999). SKP2 phosphorylation at Ser-64 by CDK2 and, to a lesser extent, Ser-72 by AKT1 contributes to the stabilization of SKP2 by preventing its association with Cdh1 and protecting it from APC/C^{Cdh1}-mediated degradation (Rodier, *et al.*, 2008; Gao, *et al.*, 2009; Lin, *et al.*, 2009). Ser72 phosphorylation by AKT also promotes SKP2 cytosolic relocalization (Gao, *et al.*, 2009; Lin, *et al.*, 2009). Cytosolic SKP2 neither forms a complex with CUL1 and SKP1 and therefore it may not trigger p27 degradation (Lin, *et al.*, 2009). However, SKP2 phosphorylation on Ser64 by CDK2 is dispensable for its subcellular localization and for SKP2 assembly into an active SCF complex (Bashir, *et al.*, 2010; Boutonnet, *et al.*, 2010).

In addition, SKP2 can be acetylated by p300 at Lys-68 and Lys-71 within of the NLS leading also to increased SKP2 stability through impairment of the Cdh1-mediated proteolysis and to its cytoplasmic retention. Moreover, this process can be antagonized by the mitochondrial deacetylase SIRT3 (NAD-dependent deacetylase sirtuin-3). Inactivation of this tumor suppressor leads to elevated SKP2 acetylation and stability (Inuzuka, *et al.*, 2012).

1.3.4.3. Biological functions of SKP2

SKP2 in cell cycle progression and proliferation

The function of SKP2 in cell cycle progression and proliferation is closely linked to its ability to promote degradation of cell cycle regulatory proteins. In fact, a SKP2 mutant (LRR^{SKP2}) lacking the N-terminal and F-box domains and thus defective in SCF^{SKP2} E3 ligase activity (Schulman, *et al.*, 2000) is less efficient at promoting cell cycle progression and proliferation, and primary tumor

formation compared to wild-type SKP2 (Chan*, et al.*, 2010). As previously mentioned, the best-known substrate of SKP2 is p27. This is mainly based on the genetic evidence showing that p27 accumulates at high levels in *Skp2*$^{-/-}$ cells, resulting in a reduced cell proliferation. Accordingly, *Skp2*$^{-/-}$ mice are characterized by a reduced organ size and body weight (Nakayama*, et al.*, 2000). Combined ablation of p27 (*Skp2*$^{-/-}$/p27$^{-/-}$ cells) rescues this phenotype and the cell proliferation defect shown in *Skp2*$^{-/-}$ cells suggesting that p27 is required for their development and that p27 is the main substrate for SKP2 functions (Nakayama*, et al.*, 2004).

However, it has been reported that SKP2 also regulates ubiquitination and degradation of many other substrates involved in cell proliferation including the p27-related CKIs p21^{CIP1} (Yu*, et al.*, 1998) and p57^{KIP2} (Kamura*, et al.*, 2003); and several cell cycle regulators such as p130 (Tedesco*, et al.*, 2002), cyclin A (Nakayama*, et al.*, 2001), cyclin D1 (Yu*, et al.*, 1998) or cyclin E (Nakayama*, et al.*, 2000). Transcription factors such as E2F-1 (Marti*, et al.*, 1999), FOXO1 (Huang*, et al.*, 2005), and MYC (Kim*, et al.*, 2003; von der Lehr*, et al.*, 2003), have also been implicated as potential substrates of SKP2. Some of these proteins such as, cyclin A, cyclin D1 and E2F-1 do not accumulate in *Skp2*$^{-/-}$ cells, suggesting that there exists a certain redundancy for their ubiquitination in the absence of SKP2 (Nakayama*, et al.*, 2000; Nakayama*, et al.*, 2001). Two examples are cyclin E and MYC which can be both targeted by SCF^{SKP2} or by SCF^{FBW7} complexes (Koepp*, et al.*, 2001; Welcker*, et al.*, 2004; Yada*, et al.*, 2004).

Other biological functions of SKP2

In addition to its well-known role in cell cycle progression, targeting one of the most important cell cycle inhibitors, SKP2 has been also involved in additional biological functions such as differentiation, cell survival or cell migration. Generally, SKP2 hinders cell differentiation processes, such as differentiation of human embryonic stem cells (hESc) (Egozi*, et al.*, 2007) or chemically-induced erythroid differentiation of human leukaemia cells (Gomez-Casares*, et al.*, 2012) at least in part, through its ability to down-regulate p27.

In the other hand, SKP2 plays an important role in cell survival through its ability to restraint apoptosis and senescence. *Skp2*$^{-/-}$ MEFs display a higher apoptosis rate compared to *wt* MEFs (Nakayama*, et al.*, 2000). Consistent with this observation, SKP2 silencing induces apoptosis in different lung cancer cell lines (Yokoi*, et al.*, 2003) and potentiates cell apoptosis of HCT116 cells upon stimulation with DNA damage agents in a p53-dependent manner (Kitagawa*, et al.*, 2008). Moreover, human RB1$^{-/-}$ cells also undergo apoptosis after SKP2 knockdown (Wang*, et al.*, 2010a).

With regard to its role in senescence, SKP2 deficiency alone does not induce senescence *per se* but sensitizes cancer-prone cells expressing RAS and E1A oncoproteins to cellular senescence response. Furthermore, genetic SKP2 inactivation in combination with ARF loss or PTEN heterozygosity also triggers senescence response by ARF/p53 and DDR (DNA damage response)-independent pathways (Lin*, et al.*, 2010).

Finally, SKP2 has been also involved in promoting cell motility and migration. SKP2 is primarily localized in the nucleus in normal cells. However, acetylation by p300 (Inuzuka*, et al.*,

2012) or AKT-mediated phosphorylation (Lin*, et al.*, 2009) in the NLS region promotes its cytoplasmic relocalization where SKP2 enhances cellular migration through ubiquitination and destruction of E-cadherin (Inuzuka*, et al.*, 2012). In this sense, *Skp2*$^{-/-}$ cells display a defect in cell migration and invasion whereas restoration of a permanent cytosolic SKP2 mutant (SKP2^{NES}) rescues these defects (Lin*, et al.*, 2009). Furthermore, the expression of RhoA GTPase has been also shown to rescue partially these defects observed in *Skp2*$^{-/-}$ MEFs, indicating that it is an important downstream effector responsible for SKP2-mediated cell migration (Chan*, et al.*, 2010).

SKP2 as a transcriptional regulator

Finally, apart from its function as ubiquitin ligase, SKP2 has been also found to function as a possible transcriptional regulator. It was known that SKP2 appeared to stimulate the transcriptional activity of MYC (Kim*, et al.*, 2003; von der Lehr*, et al.*, 2003) but the underlying mechanism remained elusive. Recently, it has been described that SKP2 cooperates with MYC to induce RhoA transcription by recruiting MIZ1 and the transcriptional coactivator p300 to the RhoA promoter. This interaction seems to be independent of its E3 ligase activity because a SKP2 mutant (LRR^{SKP2}) which lacks of the N-terminal and F-box domains also interacts with MYC, p300, and MIZ1 and cooperates with them in the up-regulation of transcription. Moreover, SKP2 mutants defective in MYC binding fail to activate transcription suggesting that the function of SKP2 in transcriptional regulation is critically dependent on MYC (Chan*, et al.*, 2010).

1.3.4.4. SKP2 and cancer

As previously mentioned, SKP2 is a key player in the control of proliferation and differentiation targeting several cell cycle regulators for degradation. In addition, SKP2 has been involved in many other biological processes such as cell survival, migration, invasion, and metastasis all of which are closely related to cancer development (Frescas and Pagano, 2008). Consistent with this notion, SKP2 overexpression has been detected in most human cancers (Wang*, et al.*, 2012b), frequently associated with reduced p27 levels, high proliferative rates and poor outcome, representing an adverse prognostic marker (Figure 1.14) (Hershko, 2008). Moreover, in certain human cancers, SKP2 overexpression has been associated to cancer progression and metastasis (Wang*, et al.*, 2012a).

The mechanisms involved in SKP2 up-regulation in human cancers are diverse and include gene amplifications and over-activated oncogenic signalling pathways leading to the *SKP2* transcriptional induction or/and the SKP2 protein stabilization. For instance, amplification of the region within chromosome 5 that contains the *SKP2* gene have been reported in selected human tumors such as glioblastoma (Saigusa*, et al.*, 2005) and non-small cell lung cancers (Yokoi*, et al.*, 2004; Zhu*, et al.*, 2004a). However, gene amplification has been associated with advanced stage of tumor progression, but not with early cancers that overexpress SKP2 (Hershko, 2008). On the other hand, a correlation between SKP2 over-expression and elevated AKT activity has been reported in colon and prostate cancer (Lin*, et al.*, 2009) and also in breast cancer metastasis (Chan*, et al.*, 2012). Interestingly, AKT activation has been also correlated with SKP2 cytosolic

accumulation during colon cancer metastasis to lymph nodes (Lin, *et al.*, 2009) and cytoplasmic SKP2 has been also reported in the more aggressive forms of breast and prostate cancers (Inuzuka, *et al.*, 2012).

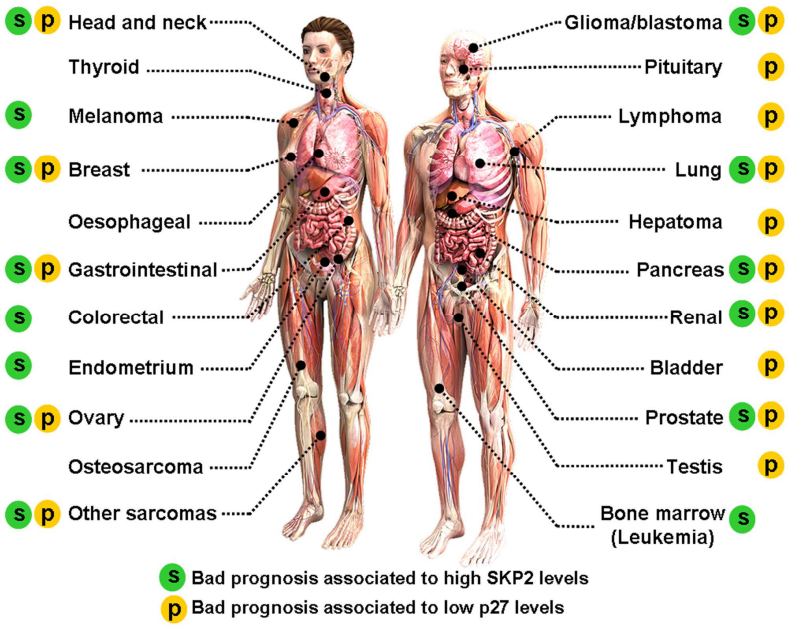

Figure 1.14. Oncogenic role and prognostic significance of SKP2 overexpression in human cancers. SKP2 has been found overexpressed in all listed human cancers, inversely correlated with p27 protein levels. S and P denote bad prognosis of disease associated to high SKP2 or low p27 levels, respectively. Adapted from (Malumbres and Barbacid, 2001; Chu, *et al.*, 2008; Hershko, 2008).

Finally, several mouse models also confirm the oncogenic role of SKP2 in tumorigenesis. Overexpression of SKP2 in the T-cell compartment cooperates with N-Ras to induce T cell lymphomas in mice (Latres, *et al.*, 2001), while prostate specific expression of SKP2 leads to prostatic intraepithelial neoplasia (PIN) (Shim, *et al.*, 2003). Moreover, in agreement with a critical role for SKP2 in tumor progression, *Skp2*$^{-/-}$ mice are resistant to tumor development induced by loss of either p19^{ARF} or the PTEN tumor suppressor proteins (Lin, *et al.*, 2010). Moreover, *Skp2* deficiency delays BCR-ABL–induced leukemogenesis in a bone marrow transplantation model, suggesting that SKP2 plays an important role in this process upon BCR-ABL overexpression (Agarwal, *et al.*, 2008). In contrast, *Skp2* loss has modest effects on MYC-driven lymphomagenesis, despite cancelling MYC's ability to suppress p27 protein levels (Old, *et al.*, 2010). Finally, using a well-established lung metastasis model generated by tail vein injection of breast cancer cells, it has been demonstrated that overexpression of SKP2 or MYC promotes lung metastasis whereas its knockdown reduces it (Chan, *et al.*, 2010). Taken together, these studies clearly establish that SKP2 behaves as a proto-oncogene and that SKP2 overexpression may contribute to the development and progression of human cancers.

1.4. THE TRANSCRIPTION FACTOR MYC

MYC (originally known as c-MYC) was the first oncogenic transcription factor discovered. In the late seventies, the study of the genome of three retroviruses (MC29, MH2 and OK10) that produced a kind of leukemia in birds known as "MYeloCytomatosis", led to the identification of the viral transforming gene *v-Myc* (Duesberg and Vogt, 1979; Hu, *et al.*, 1979; Sheiness and Bishop, 1979). Three years later, chicken MYC (c-MYC), the proto-oncogenic version of *v-Myc* the host genome, was identified by homology (Vennstrom, *et al.*, 1982). Subsequently, *MYC* genes from

human, mouse and rat were cloned and characterized (Crews*, et al.*, 1982; Dalla-Favera*, et al.*, 1982b; Hayashi*, et al.*, 1987). The discovery that *MYC* was consistently altered in Burkitt lymphoma by chromosomal translocation marked it as a bona fide human oncogene (Dalla-Favera*, et al.*, 1982a; Taub*, et al.*, 1982). Nowadays, it is well known that *MYC* is one of the most highly over-activated oncogenes among different human cancers (Beroukhim*, et al.*, 2010).

MYC belongs to a family of transcription factors that includes N-MYC and L-MYC, which are encoded by *MYCN* and *MYCL1* genes respectively (DePinho*, et al.*, 1987). *MYCN* was identified from the discovery of amplified sequences highly homologous to *v-Myc* oncogene in human neuroblastoma cell lines (Kohl*, et al.*, 1983; Schwab*, et al.*, 1983) whereas *MYCL1* was identified in small cell lung cancer, by homology to *MYC* (Nau*, et al.*, 1985). All members of MYC family have a predominantly nuclear localization and a short half-life, and its expression is generally correlated with cell proliferation. However, they have different expression pattern during embryonic development, being MYC the most widely expressed in adult tissues. Both MYC and N-MYC are crucial for proper functioning of Hematopoietic Stem Cell (HSCs) (Laurenti*, et al.*, 2008). *Myc*$^{-/-}$ mice embryos die before E12 due to hematopoietic and placental defects (Dubois*, et al.*, 2008), while *Mycn*$^{-/-}$ embryos die before E11.5 with neuroectodermal and heart defects (Charron*, et al.*, 1992). In contrast, *Mycl*$^{-/-}$ mice show no altered phenotype, making it non-essential for normal murine development (Murphy*, et al.*, 2005). Finally, it has been shown that *Mycn* can replace *Myc in vivo* (Malynn*, et al.*, 2000).

1.4.1. Structure of *MYC* gene and protein

In humans, *MYC* maps in the locus 8q24.21, consisting of 3 exons. Its expression is regulated by four potential promoters, called P0, P1, P2 and P3 (Figure 1.15), although mRNA transcribed from promoters P1 and P2 accounts for approximately 25% and 75% of total *MYC* mRNAs, respectively (Liu and Levens, 2006; Wierstra and Alves, 2008). Depending on the translation start codon, the MYC protein can be translated into three different isoforms, which mainly differ at the N-terminal region of the protein. The predominant isoform (MYC-2) is translated from the canonical AUG located at the start of second exon and possesses 439 amino acids and a molecular weight of 64 kDa (Persson*, et al.*, 1984). A minor MYC protein variant of 454 amino acids and 67 kDa (MYC-1), initiates at a CUG-leucine codon at the 3´-end of the first exon (Hann*, et al.*, 1988). In addition, *MYC* gene also produces a smaller protein called MYC-S (MYC-Short), translated from internal AUG codons and lacking most of the N-terminal region of the protein, in which resides the transcriptional regulatory region. Accordingly, it has been suggested that it could serve as a dominant negative of MYC protein (Spotts*, et al.*, 1997; Xiao*, et al.*, 1998). In most system studied the expression of this protein is much lower than MYC1/2.

MYC belongs to a small group of transcription factors containing basic (b), helix-loop-helix (HLH) leucine zipper (LZ) domains (Figure 1.15) (Landschulz*, et al.*, 1988; Dang*, et al.*, 1989; Murre*, et al.*, 1989; Prendergast and Ziff, 1989). These domains are located in the C-terminal region of the protein and are highly conserved among MYC family members. The basic domain is

responsible for specific sequence recognition and DNA binding whereas the HLH-LZ domains are involved in the formation of heterodimers with the protein MAX (Figure 1.16) (Blackwood and Eisenman, 1991; Amati, *et al.*, 1992; Kato, *et al.*, 1992, Kretzner, 1992 #270).

On the other hand, the MYC protein also contains an unstructured N-terminal transcriptional regulatory region, which includes several highly conserved regions across species and between different MYC family members, termed MYC Boxes (MB). These regions are responsible for most of the biological effects exerted by MYC. To date, four different MYC boxes have been identified, denoted as MBI, MBII, MBIII and MBIV (Figure 1.15).

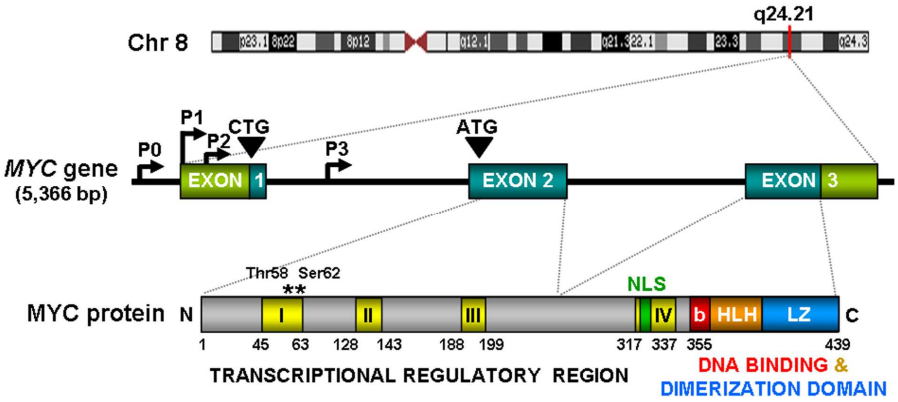

Figure 1.15. *MYC* gene structure, localization in the human genome and major features of MYC protein. Chr (Chromosome); P (Promoter); UTR (Untranslated region); NLS (Nuclear localization signal); I, II, III and IV (MYC Boxes); b (basic)-HLH (helix-loop-helix)-LZ (Leucine zipper) domain; phosphorylatable amino acids (*) and bp (base pairs).

MBI and MBII are located in the region initially described as responsible for the activation of transcription, also known as Transcriptional Activation Domain (TAD) (aa 1-143) (Kato, *et al.*, 1990). MBI contains two major phosphorylation sites of MYC, Thr 58 and Ser 62, and it has been associated with its stability and its transforming capacity (Stone, *et al.*, 1987; Sears, *et al.*, 2000). MBII is the most important region in relation to the transcription. Mutations in this region inhibit the binding of most transcription coactivators recruited by MYC (Freytag, *et al.*, 1990; McMahon, *et al.*, 1998; Oster, *et al.*, 2003). Both regions are needed for MYC induced transformation, blocking differentiation and apoptosis (Stone, *et al.*, 1987; Freytag, *et al.*, 1990; Evan, *et al.*, 1992). On the other hand, MBIII is involved in the repression of transcription (Herbst, *et al.*, 2005; Kurland and Tansey, 2008) while MBIV contains a NLS and it is important for the binding of MYC to DNA despite being located outside of the basic domain (Dang and Lee, 1988; Cowling, *et al.*, 2006).

1.4.2. Regulation of *MYC* expression

MYC expression is tightly regulated by transcriptional, posttranscriptional and posttranslational mechanisms. In the first place *MYC* expression is controlled by many transcriptional regulatory motifs found within its proximal promoter region in which converge multiple signaling pathways that are triggered from diverse extracellular signals (Wierstra and

Alves, 2008; Levens, 2010; Dang, 2012). *MYC* expression remains almost undetectable when cells are at quiescent state and increases rapidly under various mitogenic stimuli. During quiescence, complexes formed by E2F (1, 2 and 4); proteins of the pocket family (Rb, p107, p130) and histone deacetylases (HDACs) bind to the *MYC* promoter preventing its transcription (Albert*, et al.*, 2001). In contrast, MYC is steadily expressed in cells that are in continuous proliferation (Hann*, et al.*, 1985; Rabbitts*, et al.*, 1985; Thompson*, et al.*, 1985). For that, it is very important a sequence located 1.5 kb upstream of the P1 promoter called FUSE (The Far Up-Stream Element), at which constitutively binds the FUSE binding protein (FBP) activating its transcription and allowing continuity in the *MYC* expression (He*, et al.*, 2000). In contrast, the binding of the FIR protein (FBP interacting repressor), which forms a ternary complex with FBP and FUSE, blocks activator-dependent *MYC* transcription (Liu*, et al.*, 2000; Chung and Levens, 2005; Liu*, et al.*, 2006). Moreover, the ability of MYC to negatively regulate their own expression through a negative feedback loop, keeps this expression at moderate levels in the absence of specific activation (Facchini*, et al.*, 1997; Luo*, et al.*, 2004).

MYC levels decay rapidly during cellular differentiation, until its disappearance in terminally differentiated cells. MYC repression during differentiation is usually regulated, directly or indirectly, by transcription factors that control differentiation on each cell type such as GATA-1 (Acosta*, et al.*, 2008), CTCF (Delgado*, et al.*, 1999; Torrano*, et al.*, 2005), C/EBPα (Freytag and Geddes, 1992) or Klf4 and Ovol1 (Nascimento*, et al.*, 2011). In addition, the complexes formed by E2F4/pRb (Iakova*, et al.*, 2003); E2F6, HMTs and PcG proteins (Ogawa*, et al.*, 2002); or BRG1/BAF subunit of the SWI/SNF chromatin remodeling complex (Nagl*, et al.*, 2006) collaborate in the repression of MYC during cell differentiation.

MYC promoter is also target of multiple oncogenic stimuli. For instance, the loss of the tumor suppressor APC results in constitutive nuclear localization of the b-catenin cofactor TCF4, downstream of the WNT pathway, which promotes a constitutive oncogenic MYC expression (Pomerantz*, et al.*, 2009; Tuupanen*, et al.*, 2009; Sotelo*, et al.*, 2010). Recently, BRD4 (Bromodomain-containing protein 4) has been shown to bind to the *MYC* promoter and to play a critical role in *MYC* expression in leukemia and lymphoma cell lines (Delmore*, et al.*, 2011; Mertz*, et al.*, 2011).

Finally, *MYC* expression is regulated not only by an array of transcription factors, but also by non-B DNA structures including single-stranded bubbles, G-quadruplexes or Z-DNA structures in the promoter (Hurley*, et al.*, 2006; Brooks and Hurley, 2010; Levens, 2010). Genome-wide association studies have also identified common SNPs 1Mb upstream *MYC* gene associated with different cancers (breast, prostate and colorectal cancer) that have been involved in *MYC* overexpression (Pomerantz*, et al.*, 2009; Tuupanen*, et al.*, 2009; Ahmadiyeh*, et al.*, 2010; Sotelo*, et al.*, 2010; Wasserman*, et al.*, 2010).

MYC expression is also controlled by posttranslational mechanisms. *MYC* mRNA has a short half-life of about 30 minutes. This feature is related to A-U rich sequences located in the 3'-UTR whose deletion greatly increases the stability of *MYC* mRNA (Jones and Cole, 1987; Brewer and Ross, 1988). In addition, *MYC* mRNA has been also shown to be targeted by several

miRNAs such as let-7, miR-34 or miR-145, affecting also its stability (Kim, *et al.*, 2009; Sachdeva, *et al.*, 2009; Cannell, *et al.*, 2010; Christoffersen, *et al.*, 2010).

Finally, posttranslational modifications also affect the stability of MYC protein, helping to regulate their levels in the cell (Hann, 2006; Vervoorts, *et al.*, 2006). The MYC protein itself is phosphorylated, ubiquitinated, and degraded, with a half-life in the order of 20–30 min (Gregory and Hann, 2000). MYC stability is mainly controlled by phosphorylation at two residues, Thr58 and Ser62 (Figure 1.15). CDK1/2 and/or mitogen-activated kinases activated by RAS, phosphorylate MYC at Ser62 leading to its stabilization. By contrast, phosphorylation at Thr58 by GSK-3β, facilitates dephosphorylation at Ser62 by a complex formed by the PP2A phosphatase, the PIN1 prolyl-isomerase and the scaffold protein Axin1, allowing its recognition by the SCF^{FBW7} E3 ligase. SCF^{FBW7} ubiquitinates MYC and targets it for proteasomal degradation (Sears, 2004; Arnold, *et al.*, 2009; Hydbring, *et al.*, 2010). Nevertheless, MYC binding to the ubiquitin-specific protease USP28 (Popov, *et al.*, 2007) or MYC ubiquitination at N-terminus by $SCF^{\beta\text{-}TrCP}$ (Popov, *et al.*, 2010) antagonizes SCF^{FBW7} mediated turnover, leading to MYC stabilization. In addition, it has been reported that acetylation of MYC by acetyltransferases such as GCN5, PCAF, TIP60 or p300/CBP usually results in an increase in protein stability (Vervoorts, *et al.*, 2003; Patel, *et al.*, 2004a; Faiola, *et al.*, 2005; Nascimento, *et al.*, 2011), although it has been also described that deacetylation by Sirt1 similarly results in increased MYC stability (Menssen, *et al.*, 2012).

All these mechanisms contribute to the regulation of MYC levels in the cell. Tumor-associated alterations affecting any of these mechanisms in general deregulate and enhance MYC expression. Given that MYC proteins function primarily as transcription factors, the consequences of these alterations result in the deregulation of MYC target genes, some of which are in turn oncogenes, contributing to tumorigenesis.

1.4.3. Transcriptional activation by MYC

Activation of transcription by MYC is intimately ligated to the formation of heterodimeric complexes with MAX (MYC-associated factor X) (Figure 1.16) (Blackwood and Eisenman, 1991; Prendergast, *et al.*, 1991; Wenzel, *et al.*, 1991). MAX is a small size protein, of which up to 6 isoforms resulting from alternative splicing processes have been identified according to the UCSC database (provided by RefSeq, August 2012), being MAX(L) with 160 aa (22 kDa) and MAX(S) with 151 aa (21 kDa) the two majority isoforms (Blackwood, *et al.*, 1992; Kato, *et*

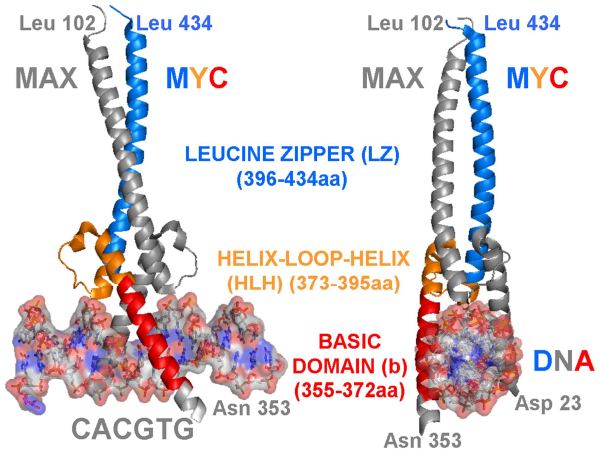

Figure 1.16 Two perspectives of heterodimeric structure of b-HLH-LZ domains of MYC-MAX bound to and E-box sequence of DNA. The colours of the helixes correspond to the coloured domains in the figure 1.15. Adapted from PDB 1NKP deposited by (Nair and Burley, 2003).

al., 1992; Makela*, et al.*, 1992; Zhang*, et al.*, 1997). MAX protein, like MYC, is a member of the b-HLH-LZ family of transcription factors. MYC-MAX heterodimerization through the HLH-LZ domain aligns the adjacent basic regions on each molecule to grip onto specific DNA hexanucleotide sequences termed E-boxes (Nair and Burley, 2003). The canonical E-box CACGTG is the sequence recognized with higher affinity by MYC-MAX heterodimers (Blackwood and Eisenman, 1991; Seitz*, et al.*, 2011), although there are several non-canonical E-boxes which are also recognized with a similar affinity *in vivo* and whose sequence slightly differs from the canonical (Blackwell*, et al.*, 1990; Grandori*, et al.*, 1996).

Activation of gene transcription by MYC requires the recruitment of a number of cofactors which ultimately modify the global chromatin structure (Knoepfler*, et al.*, 2006; Knoepfler, 2007). On the one hand, MYC has been reported to interact through the b-HLH region with the BAF47/SNF5/INI1 subunit of SWI/SNF ATP-dependent chromatin remodeling complex, being this interaction important for its transactivation potential (Cheng*, et al.*, 1999b). This complex provokes ATP-dependent nucleosomal remodeling to make the chromatin more accessible to the basal transcriptional machinery (Reisman*, et al.*, 2009).

On the other hand, MYC has been also shown to recruit to the chromatin different Histone Acetyl-Transferases (HATs) coactivators, or in the more recently proposed nomenclature, KATs [Lysine (K) Acetyl Transferases] (Allis*, et al.*, 2007) (Figure 1.17). They are able to catalyze the transfer of an acetyl group (CH_3CO) from acetyl-CoA to the terminal amine on the side chain of lysine residues on histones but also on many other proteins (Glozak*, et al.*, 2005). Acetylation of histones tails reduces the positive charges and promotes a relaxation of chromatin conformation, usually known as the passage to an "open chromatin", which allows the recruitment of transcription factors and an increase in transcription.

It has been reported that MYC binds GCN5-related HATs (GNATs) such as TFTC and STAGA complexes (McMahon*, et al.*, 2000; Flinn*, et al.*, 2002; Liu*, et al.*, 2003); the MYST-related HATs, TIP60 and HBO1 (Frank*, et al.*, 2003; Martinato*, et al.*, 2008); CBP (CREB binding protein) and p300 (E1A-associated protein 300 kDa) (Vervoorts*, et al.*, 2003; Adhikary*, et al.*, 2005) and the general transcription factor TFIID subunit TAF1 (TBP-associated factor-1) (Hateboer*, et al.*, 1993).

In the GNAT complexes, MYC interacts with TRRAP (Transactivation-Transformation Associated Protein), the largest subunit of these 2 MDa complexes that functions as scaffold for the GCN5 histone acetyltransferase (Figure 1.17). TRRAP is a member of the ATM/PI3K-related serine/threonine kinase (PIKK) family that was originally isolated as a cofactor of MYC and recruited to most MYC target genes after mitogen-mediated activation in a MBII-dependent manner (McMahon*, et al.*, 1998; Frank*, et al.*, 2001). In addition, GNC5 is a MYC target gene and GNC5 knockdown interferes with MYC-induced global histone (H3 and H4) acetylation (Knoepfler*, et al.*, 2006).

TIP60-type HAT complex also contain TRRAP as the largest scaffold subunit together with P400 (EP400) and the ATP-dependent DNA helicases TIP48 (RUVBL2) and TIP49 (RUVBL1) (Figure 1.17) (Frank*, et al.*, 2003). TIP48 and TIP49 have been also found to bind directly to MYC

through the MBII independently of TRRAP, and TIP49 has been found to play an essential role in MYC-dependent transformation (Wood, *et al.*, 2000). Lastly, p300 recruitment to MYC target genes requires MYC polyubiquitination by the E3 ubiquitin ligase HectH9 and this process seems to be required for MYC-induced cell proliferation (Adhikary, *et al.*, 2005). The acetyltransferases GCN5, TIP60, HBO1, CBP, P300 and TAF1 are now known as KAT2A, KAT5, KAT7, KAT3A, KAT3B and KAT4 respectively (Allis, *et al.*, 2007).

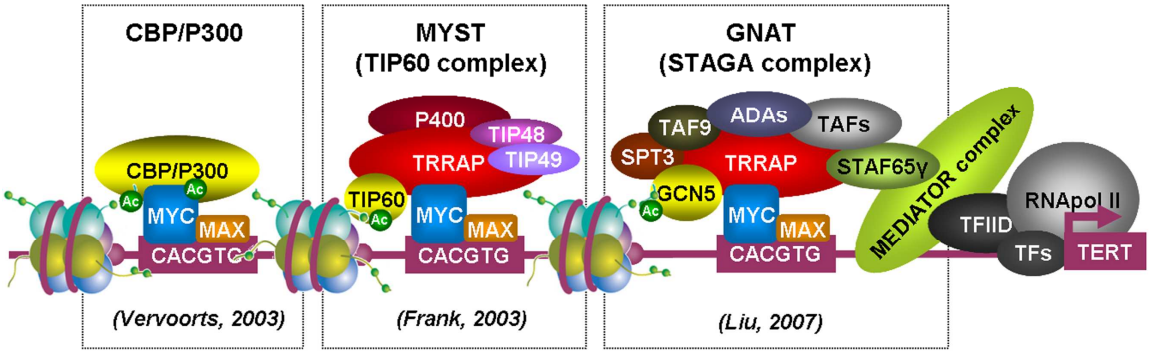

Figure 1.17. MYC is present on the chromatin in association with different Histone acetyltransferase complexes (HATs). HATs recruited by MYC principally acetylate multiple lysines on histones H3 and H4 (such as H3K9 or H3K27), promoting a locally relaxed chromatin conformation which is associated to transcriptionally active genes (Frank, *et al.*, 2003; Vervoorts, *et al.*, 2003; Liu, *et al.*, 2007).

Consistently with its biding to HATs, MYC has been found associated to chromatin regions enriched in acetylated lysines on histone H3 (H3K9ac, H3K14ac, H3K18ac and significantly H3K27ac), histone H4 (H4K5ac, H4K12ac, H4K8ac and H4K91ac) and H2A (H2AK5ac) (Guccione, *et al.*, 2006; Martinato, *et al.*, 2008). For instance, promoter regions of transcriptionally active genes are highly enriched in H3K27ac (Wang, *et al.*, 2008) and there is a good correlation between MYC and H3K27ac on genome positioning in Hela and K562 cells (Shao, *et al.*, 2012). Moreover, it has been shown that MYC interacts with CBP/P300, the only KAT described at the moment which is able to acetylate H3 on Lys27 (H3K27ac) (Tie, *et al.*, 2009; Jin, *et al.*, 2011; Tie, *et al.*, 2012).

It has also been described that promoters occupied by MYC show a strong correlation with H3K4me3 and H3K79me3 (histone H3 lysine trimethylated on lysine 4 and 79); chromatin marks that also have a positive correlation with active genes (Guccione, *et al.*, 2006; Martinato, *et al.*, 2008; Nascimento, *et al.*, 2011). Furthermore, histone methylation seems to be critical for MYC to recognition of its target genes. In this sense, histone methyltransferase SMYD3 (KMT3E) knockdown leads to diminished histone H3K4me3 at the hTERT promoter, resulting in a reduction in MYC occupancy on this promoter (Liu, *et al.*, 2007). In addition, changes in the histone methylation patterns have been also observed upon MYC binding. In *Drosophila*, dMYC binds and inhibits the activity of H3K4me3 demethylases, Rbp2 and Plu1. These proteins are lysine (K) DeMethylases (KDMs) of the Jumanji family. The mammalian orthologs of Rbp2 (JARID1A or

KDM5A) and Plu1 (JARID1B or KDM5B), have been also shown to bind to MYC, indicating that the MYC function regulating demethylase activity is highly conserved (Secombe and Eisenman, 2007; Secombe, *et al.*, 2007).

Moreover, MYC has been also found to directly interact with different components of Mixed (Myeloid/Lymphoid) Lineage Leukemia complex (MLL1) (Figure 1.18) such as Menin, ASH2L, RBBP5, and the own MLL1 (KMT2A). This complex possesses H3K4 trimethylase activity further supporting a role of MYC in controlling H3K4me3 (Steward, *et al.*, 2006; Luscher-Firzlaff, *et al.*, 2008; Bres, *et al.*, 2009). Since the abundance of histone modifications and their combinations has exponentially grown in recent years, the role of MYC in chromatin remodelling is getting more important.

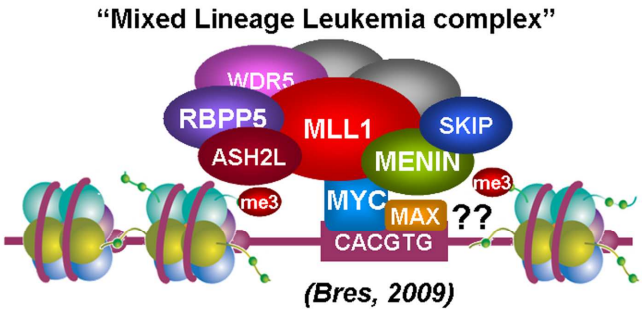

Figure 1.18. MYC interacts with different subunits of MLL1 complex. This complex possesses H3K4 trimethylase activity and is also associated to transcriptionally active genes (Bres, *et al.*, 2009).

Finally, MYC also interacts with different subunits of general transcription factors that make up the RNA polymerase II preinitiation complex (PIC) (Figure 1.19) such as TBP (TATA binding protein), a key component of TFIID (Hateboer, *et al.*, 1993; Maheswaran, *et al.*, 1994; Barrett, *et al.*, 2005); the RAP74 subunit of TFIIF (McEwan, *et al.*, 1996) or the CDK7 subunit of TFIIH. CDK7 recruitment by MYC in an MBII-dependent manner to TSS, increases CAK (cyclin H/CDK7/MAT1) activity and concomitant Ser5 phosphorylation of C-terminal repeat domain (CTD) of RNA Pol II, which in turn is associated to initiation of transcription (Bouchard, *et al.*, 2004; Cowling and Cole, 2007). Furthermore, MYC can promote the mRNA transcriptional elongation by activation of RNA pol II (Figure 1.19) (Price, 2010; Rahl, *et al.*, 2010). Once the RNA pol II has been recruited to the promoter of the target gene, MYC binds through the MBI to the cyclin T1/CDK9 complex, also known as P-TEBb (positive transcription elongation factor b) (Eberhardy and Farnham, 2001,2002; Gargano, *et al.*, 2007). P-TEFb phosphorylates the Ser2 of RNA Pol II CTD ultimately activating mRNA transcriptional elongation. In this interaction of MYC with P-TEFb also participates SKIP/SNW1 (Ski-interacting protein) and Menin (Marshall, *et al.*, 1996; Bres, *et al.*, 2008; Bres, *et al.*, 2009). Recent reports suggest that MYC functions as an amplifier of gene expression, i.e., MYC does not activate silent genes but increases the transcription rate of genes already actives. The mechanism seems to lie on its ability to promote transcriptional elongation (Lin, *et al.*, 2012; Nie, *et al.*, 2012).

In summary, MYC has a triple activity as a transcriptional regulator. On one side, MYC acts as a general chromatin activator. Second, MYC acts as a "classical" transcription factor activating the basal transcription machinery of genes which it binds. Third, MYC is an enhancer of transcription elongation.

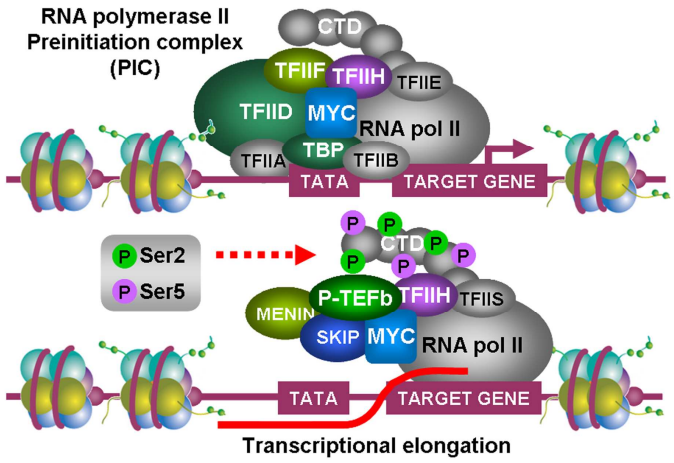

Figure 1.19. MYC interacts with the RNA polymerase II preinitiation complex (PIC) and stimulates mRNA transcriptional elongation. MYC has been found associated to different subunits of TFIID (TBP and TAF1), TFIIF (GTF2F1) and TFIIH (CDK7). In the other hand, MYC functionally cooperates with TFIIH and P-TEFb to phosphorylate the C-terminal domain (CTD) of the RNA polymerase II on Ser5 and Ser2 respectively stimulating transcriptional elongation.

1.4.4. Transcriptional repression by MYC

In addition to its known role in the activation of transcription, MYC also plays an important role as transcriptional repressor and this activity is also important for its transforming potential (Claassen and Hann, 1999). The first evidence supporting a negative role of MYC in transcription came from the observation that ectopic MYC or v-MYC overexpression repressed endogenous MYC protein, resulting in an auto-repression loop (Cleveland, *et al.*, 1988). This negative feedback mechanism is not precisely understood, although it is known the implication of PcG (Polycom) proteins and suggests that it could act as a homeostatic regulator of MYC protein levels *in vivo* (Penn, *et al.*, 1990; Goodliffe, *et al.*, 2005). Currently, Genome-wide analyses have demonstrated that MYC represses at least as many genes as it activates (Dang, *et al.*, 2006).

To repress target genes, MYC does not bind DNA directly instead it physically interacts with other transcriptional activators such as TFII-I, YY1, NF-Y, SMAD, SP1 or MIZ1 that are bound to enhancers or initiator elements (Inr) in the core promoter regions, preventing them from their transactivation function. For it, MYC disrupts their interactions with other coactivators such as p300 or recruits the corepressor DNMT3A. DNA methylation by DNMT3A has a silencing effect on transcription. Examples of genes repressed by MYC through these mechanisms include the CDK inhibitors $p15^{INK4B}$ and $p21^{CIP1}$ (Wanzel, *et al.*, 2003; Kleine-Kohlbrecher, *et al.*, 2006; Herkert and Eilers, 2010).

Finally, another critical but indirect mode for MYC-mediated gene repression is through its ability to induce miRNAs expression (Chang, *et al.*, 2008) such as the miR-17-92 cluster which targets many components of the TGF-b signaling pathway (Dews, *et al.*, 2010), E2F1 (O'Donnell, *et al.*, 2005) or the own MYC (Aguda, *et al.*, 2008).

1.4.5. MYC target genes

Direct targets of MYC are defined as those genes whose expression is directly altered by direct MYC binding to the genes (Dang, *et al.*, 2006). The identification of these genes is difficult because of the abundance of E-boxes and other sequences recognized by MYC in the genome,

as well as the limited transactivation ability of MYC as demonstrated by reporter assays (Barrett, *et al.*, 2005).

The first strategy developed to identify MYC target genes was based on the design of chimeric protein called “MYCER”, fusing the hormone-binding domain of the human estrogen receptor (ER) to the C-terminal domain of MYC (Eilers, *et al.*, 1989; Littlewood, *et al.*, 1995). Upon exposure to estrogens the chimeric protein changes conformation activating transcription. Genes responding to ligand-stimulated MYCER in the presence of a protein synthesis inhibitor such as the cycloheximide, and therefore without requiring newly synthesized transcription factors, are considered direct MYC target genes. This system allowed the identification of α-prothymosin, the first reported MYC target gene (Eilers, *et al.*, 1991). Another strategies used to identify MYC target genes and to differentiate them of those induced indirectly by growth factors were the use of MYCER in serum deprived cells or the absence of gene regulation in serum-stimulated *Myc*$^{-/-}$ rat fibroblasts (Mateyak, *et al.*, 1997; Watson, *et al.*, 2002).

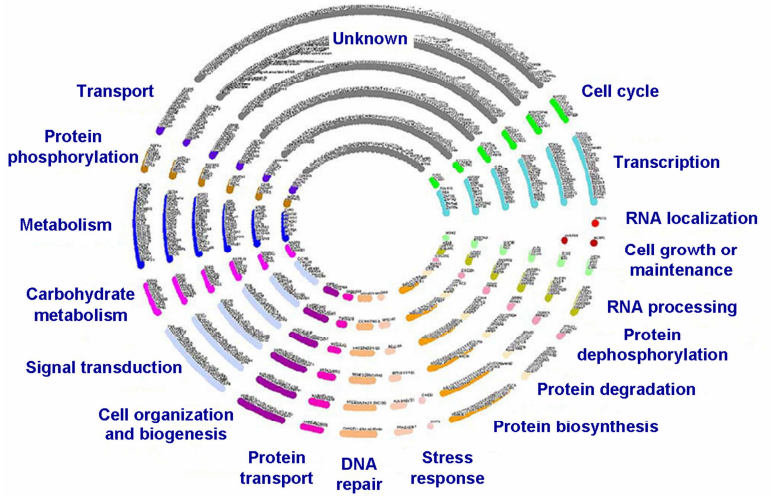

Figure 1.20 Distribution of MYC targets by gene ontology (GO). One thousand five hundred and sixty-one MYC targets from http://www.myccancergene.org are displayed in concentric rings with functional groups colored and labelled. Adapted from (Dang, *et al.*, 2006).

On the other hand, promoter-reporter assays have been extensively used as supporting evidence for direct target genes and to validate the activity of several transcription factors (Kretzner, *et al.*, 1992). However, these artificial constructs are unable to reflect the *in vivo* chromatin context of target genes. Chromatin immunoprecipitation (ChIP) provides direct physical evidence of the association of a transcription factor with a specific target gene *in vivo*. Subsequently, the development of genome-scale techniques (SAGE, microarrays, ChIP-on-chip, ChIP-PET and ChIP-sequencing) has allowed significantly increasing the amount of information available about the genes regulated by MYC. All these techniques have highlighted the global role of MYC in the regulation of transcription. Depending on the study, it is estimated that MYC is able to regulate the expression of over 15% of all human genes (Dang, *et al.*, 2006). Moreover, as discussed above and below, given that MYC controls the three RNA polymerases (I, II and III), the target genes encode all forms of RNAs including mRNA, rRNA, tRNA, miRNA as well as other

non-coding RNAs. Through the regulation of all these genes MYC achieves broad effects on many different cell biology processes such as cell cycle regulation; signal transduction; transcription and RNA processing; protein biosynthesis, transport and degradation; carbohydrate, amino acid and nucleotide metabolism; and cell adhesion and cytoskeleton remodelling among others (Figure 1.20) (Menssen and Hermeking, 2002; Fernandez*, et al.*, 2003; Patel*, et al.*, 2004b; Dang*, et al.*, 2006; Luscher and Vervoorts, 2012).

1.4.6. Biological functions of MYC

In general, the biological functions of MYC depend on its transcriptional activity. The widespread influence of MYC in the regulation of transcription and its many target genes make him a very important regulator of multiple biological functions, among which it should be noted the induction of cell proliferation and cell growth, inhibition of terminal differentiation, induction of apoptosis but suppression of senescence, as well as its role in tumorigenesis and cancer development (Grandori*, et al.*, 2000).

1.4.6.1. MYC function in proliferation and cell cycle regulation

Soon after MYC discovery several studies showed its ability to stimulate cell proliferation (Palmieri*, et al.*, 1983; Hann*, et al.*, 1985). MYC is not expressed in quiescent cells, but it is rapidly induced by growth factors (Kelly*, et al.*, 1983; Armelin*, et al.*, 1984; Campisi*, et al.*, 1984). MYC overexpression or activation produces a shortening of G1 phase and promotes cell cycle progression through S-phase (Karn*, et al.*, 1989; Eilers*, et al.*, 1991; Steiner*, et al.*, 1995). In contrast, disruption of both *MYC* alleles in rat fibroblast (Rat-1 cells) leads to a prolongation of G1 and G2 phases and a delay of S-phase entry (Mateyak*, et al.*, 1997); and conditional MYC ablation in murine fibroblast and/or B lymphocytes reduces their proliferation rate (de Alboran*, et al.*, 2001).

MYC promotes cell proliferation regulating the expression of several genes involved in cell cycle progression. On the one hand, MYC promotes the transcription of positive cell cycle regulators such as D1 and D2 cyclins (Bouchard*, et al.*, 1999; Perez-Roger*, et al.*, 1999), cyclin A2 (Jansen-Durr*, et al.*, 1993; Hoang*, et al.*, 1994; Barrett*, et al.*, 1995), cyclin B1 (Yin*, et al.*, 2001), cyclin E1 (Jansen-Durr*, et al.*, 1993; Perez-Roger*, et al.*, 1997), CDK4 (Hermeking*, et al.*, 2000) and CDK6 (Li*, et al.*, 2003); CDC25A and B (Galaktionov*, et al.*, 1996; Li*, et al.*, 2003) and E2F1 and E2F2 (Sears*, et al.*, 1997; Baudino*, et al.*, 2003). On the other hand, MYC represses the transcription of negative cell cycle regulators as $p15^{INK4B}$ (Seoane*, et al.*, 2001; Staller*, et al.*, 2001) and $p21^{CIP1}$ (Claassen and Hann, 2000; Gartel*, et al.*, 2001; Wu*, et al.*, 2003) or genes implicated in promoting cell cycle arrest under stress conditions such as GADD45 and GADD153 (Chen*, et al.*, 1996; Marhin*, et al.*, 1997).

However, one of the most important targets of MYC in cell proliferation is the CDK inhibitor p27. MYC accelerates cell proliferation rates, at least in part, through its ability to down-regulate p27 protein levels (Vlach*, et al.*, 1996; Keller*, et al.*, 2007). First, MYC can suppress p27

expression at transcriptional level in lymphoid and breast cancer cells (Yang*, et al.*, 2001; Chandramohan*, et al.*, 2004). Second, MYC induces cyclin E transcription directly or through the induction of E2F transcription factors, increasing the levels of cyclin E/CDK2 complexes (Ohtani*, et al.*, 1995; Steiner*, et al.*, 1995; Vlach*, et al.*, 1996; Perez-Roger*, et al.*, 1997). Third, induction of both D cyclins and their catalytic partners CDK4 and 6 by MYC, allows the assembly of cyclin D/CDK4-6 complexes, which sequester p27 and relieve the inhibition of cyclin E/CDK2 complexes (Soos*, et al.*, 1996; Bouchard*, et al.*, 1999; Obaya*, et al.*, 2002). All these effects stimulate cyclin E/CDK2 activity which in turn phosphorylates p27 on Thr-187. P-Thr187-p27 is recognized by the SCF^{SKP2} complex following, ubiquitination and degradation by the proteasome, as previously described. Finally, MYC induces the expression of some of the components of the SCF^{SKP2} complex, including CUL1 (O'Hagan*, et al.*, 2000) and CKS1 (Keller*, et al.*, 2007).

The antagonism between MYC and p27 in proliferation and tumor development has been evidenced in knockout mouse models. Loss of p27 accelerates lymphoma development in *Eμ-MYC* transgenic mice (Martins and Berns, 2002), a mouse model of human Burkitt lymphoma (Adams*, et al.*, 1985). In contrast, loss of *Cks1* in *Eμ-MYC* mice suppresses the MYC ability to down-regulate p27 protein levels, impairs MYC-induced proliferation and delays lymphoma onset tripling the lifespan of these mice (Keller*, et al.*, 2007). Similarly, *Skp2* ablation in *Eμ-MYC* B cells abolishes the suppression of p27 protein, showing these cells slower proliferation rates *ex vivo*. Nevertheless, *Skp2* loss only has modest effects on MYC-induced lymphomagenesis (Old*, et al.*, 2010). By contrast, $Myc^{-/-}$ cells usually show increased p27 protein levels (Mateyak*, et al.*, 1999; de Alboran*, et al.*, 2001). Altogether, these findings make MYC a key regulator of cell cycle and cell proliferation, with particular importance in the G1-S transition, promoting p27 degradation.

1.4.6.2. Role of MYC in differentiation

Inhibition of cell differentiation was one of the first biological effects described for MYC; concretely, the inhibition of chemically-induced erythroid differentiation of the F-MEL murine erythroleukemia cell line (Coppola and Cole, 1986; Dmitrovsky*, et al.*, 1986; Prochownik and Kukowska, 1986). Accordingly, MYC expression usually decreases when cells differentiate (Gonda and Metcalf, 1984; Lachman and Skoultchi, 1984; Grosso and Pitot, 1985) and inhibition of MYC expression has been associated with induction of myeloid differentiation in HL-60 promyelocytic cells (Holt*, et al.*, 1988). Lately, the role of MYC as inhibitor of differentiation is gaining more attention since the discovery that MYC is one of four transcription factors able to reprogram differentiated cells into pluripotent cells (Takahashi and Yamanaka, 2006).

MYC-mediated inhibition of differentiation usually occurs by blocking the up-regulation of "master genes" required to trigger the cell specific differentiation process, such as C/EBP-α during adipocyte differentiation of murine 3T3-L1 cells (Freytag and Geddes, 1992; Tao and Umek, 1999) or GATA1 during erythroid differentiation of K562 leukemia cells (Acosta*, et al.*, 2008). On the other hand, MYC is also able to inhibit differentiation through its ability to induce proliferation insomuch as cell differentiation usually implies a proliferative arrest and cell cycle exit into G0, although not always (Leon*, et al.*, 2009). Finally, it has been described that MYC-Nick, a

cytoplasmic cleavage product of MYC which lacks the NLS and DNA-binding domain, promotes muscle cell differentiation in a transcription independent manner (Conacci-Sorrell*, et al.*, 2010).

Nevertheless, there are certain models such as human epidermal and hematopoietic stem cells or B lymphocytes in which MYC expression is required for differentiation. In these models, MYC promotes differentiation by amplifying the population of precursor or stem cells. (Gandarillas and Watt, 1997; Wilson*, et al.*, 2004; Habib*, et al.*, 2007).

1.4.6.3. MYC functions in cell size

MYC overexpression has been associated with the accumulation of cell mass and the increase in cell size in different models (Langdon*, et al.*, 1986; Iritani and Eisenman, 1999; Johnston*, et al.*, 1999). This increase has been related with the effects of MYC in protein synthesis (Mateyak*, et al.*, 1997; Iritani and Eisenman, 1999) and cell metabolism (Dang, 1999). For instance, MYC stimulates transcription of rRNAs genes involved in ribosome biogenesis through RNA polymerase I and regulates the expression of several proteins involved in rRNA processing and maturation (van Riggelen*, et al.*, 2010). In addition, MYC stimulates transcription of transfer RNAs (tRNAs) and 5S ribosomal RNAs (5S rRNAs), by activating RNA polymerase III (Gomez-Roman*, et al.*, 2003; Kenneth*, et al.*, 2007). On the other hand, MYC regulates the expression of many genes involved in mitochondrial biogenesis (Li*, et al.*, 2005), and nucleotide and glucose metabolism (Shim*, et al.*, 1997; Kim*, et al.*, 2004; Liu*, et al.*, 2008; Wang*, et al.*, 2011a).

1.4.6.4. Role of MYC in apoptosis

High MYC levels induce apoptosis in different cell models in the absence of growth factors or when the cells are placed in suboptimal growth conditions (Askew*, et al.*, 1991; Evan*, et al.*, 1992; Shi*, et al.*, 1992). MYC sensitizes cells to undergo apoptosis by both p53-dependent and p53-independent mechanisms (Sakamuro*, et al.*, 1995). On the one hand, MYC overexpression can activate p53 indirectly through the ARF–MDM2–p53 pathway (Hermeking and Eick, 1994; Wagner*, et al.*, 1994; Zindy*, et al.*, 1998) or through the ATM-p53 pathway in response to DNA-damage (Lindstrom and Wiman, 2003). On the other hand, MYC can mediate apoptosis by altering the balance of pro- and anti-apoptotic factors. In the *Eμ–MYC* mouse model, MYC indirectly suppresses the anti-apoptotic proteins Bcl-2 and Bcl-XL and triggers apoptosis by inducing the pro-apoptotic proteins Bax or Bim (Adhikary and Eilers, 2005; Dansen*, et al.*, 2006). Finally, loss-of-function mutations interfering with apoptosis are strongly selected for MYC-driven tumorigenesis (Eischen*, et al.*, 1999).

1.4.6.5. Role of MYC in senescence

In contrast, MYC expression has been associated to the suppression of oncogene-induced senescence (OIS). For example, MYC suppresses RAS-induced senescence in primary rat embryonic fibroblasts (Hydbring*, et al.*, 2010). For that, MYC represses $p21^{CIP1}$, involved in

promoting senescence (Post*, et al.*, 2010); and stimulates the activity of CDK2 and drives the expression of hTERT and WRN target genes, whose inactivation promotes senescence under the condition of active MYC (Xu*, et al.*, 2001; Grandori*, et al.*, 2003; Campaner*, et al.*, 2010). Finally, conditional MYC inactivation induces senescence even in established tumours including lymphoma, being this an important mechanism to induce tumor regression (Wu*, et al.*, 2007).

1.4.7. Role of MYC in tumorogenesis and cancer

Deregulation of MYC is strongly associated with the emergence of a variety of human cancers and is also able to induce tumorigenesis in several transgenic mice models. *MYC* translocation in Burkitt lymphoma was the first example connecting a specific chromosomal alteration with malignant transformation in human cancer. In this type of B-cell lymphoma, the *MYC* gene is translocated from chromosome 8 to 14, 2 or 22, containing the genes for heavy and light immunoglobulin chains (Dalla-Favera*, et al.*, 1982a; Taub*, et al.*, 1982). Thus, *MYC* expression becomes regulated by the promoters of the immunoglobulin chains, resulting in MYC overexpression. In addition, *MYC* has been also found frequently translocated in multiple myeloma and in diffuse large B-cell lymphoma (DLBCL) (Boxer and Dang, 2001). With or without translocation, MYC levels have been found deregulated in a wide range of human cancers, such as melanoma, lymphoma, multiple myeloma, myeloid leukemia, breast, prostate, lung and gastrointestinal cancers (Nesbit*, et al.*, 1999). The mechanisms by which MYC appears deregulated are very different and they include, in addition to the previously mentioned translocations, gene amplifications, transcriptional activation or retroviral transduction, being this the first mechanism identified in chicken (Sheiness and Bishop, 1979). All these mechanisms result in an increase of the MYC protein in tumor cells. On the other hand, they have also been described several point mutations in the *MYC* coding sequence associated with cancer. These alterations prevent MYC binding to proteins that inhibit its activity, such as p107 (Gu*, et al.*, 1994) or increase the stability of MYC protein as mutations affecting Thr58 or Ser62 which render MYC resistant to degradation by SCF^{FBW7}. These mutations are frequent in Burkitt's lymphoma (Boxer and Dang, 2001) and have been shown to perturb transgenic mammary tumorigenesis (Wang*, et al.*, 2011b).

The involvement of MYC in tumorigenesis is clearly related to its role as activator of cell proliferation, evading growth suppressors and differentiation, as well as its ability to regulate cell metabolism and protein synthesis, all discussed in previous sections. However, there are other processes of great significance in cancer development (Hanahan and Weinberg, 2011) in which MYC has been also involved (Figure 1.21), such as increased genomic instability, immortalization, angiogenesis and changes in morphology and cell adhesion:

i) MYC overexpression has been linked to increased genomic instability and loss of chromosomal organization in tumor cells (Mai*, et al.*, 1996; Felsher and Bishop, 1999; Prochownik, 2008) through different mechanisms as the induction of reactive oxygen species (ROS) which results from increased mitochondrial biogenesis and metabolism (Vafa*, et al.*, 2002)

or by enhancing DNA replication with subsequent DNA damage (Iguchi-Ariga, *et al.*, 1987; Gutierrez, *et al.*, 1988; Dominguez-Sola, *et al.*, 2007). In addition, MYC inhibits the repair of double-strand DNA breaks provoked by gamma irradiation in normal human cells (Karlsson, *et al.*, 2003) and possesses the ability to structurally modify chromosomes through induction of telomeric fusions (Louis, *et al.*, 2005). Finally, overexpression of MYC cooperates with loss of p53 to induce genomic instability, evading the G1 and G2/M checkpoints (Yin, *et al.*, 1999). In our laboratory, it has been shown that MYC contributes to genomic instability during CML progression (Albajar, *et al.*, 2011).

ii) MYC overexpression promotes immortalization of murine cells (Sedivy, 1998), human fibroblasts (Benanti, *et al.*, 2007) or human prostate epithelial cells, at least in part, through its ability to induce hTERT, the catalytic subunit of telomerase (Gil, *et al.*, 2005). hTERT is a well-known MYC target gene and telomerase is critical for cells to avoid senescence and acquire immortality (Wu, *et al.*, 1999; Cerni, 2000).

iii) MYC is essential for vasculogenesis during murine embryonic development through the induction of pro-angiogenic factors such as VEGF (Baudino, *et al.*, 2002; He, *et al.*, 2008). In addition, MYC overexpression stimulates the growth and the expansion of blood and lymphatic vessels during lymphomagenesis in *Eμ-MYC* transgenic mice (Ruddell, *et al.*, 2003; Mezquita, *et al.*, 2005). Finally, MYC possesses the ability to induce neovascularization of tumors by inducing interleukin-1β (Shchors, *et al.*, 2006) or by suppressing the angiogenesis inhibitor thrombospondin-1 (Ngo, *et al.*, 2000; Watnick, *et al.*, 2003) through the induction of mir17-92 microRNA cluster (Dews, *et al.*, 2006).

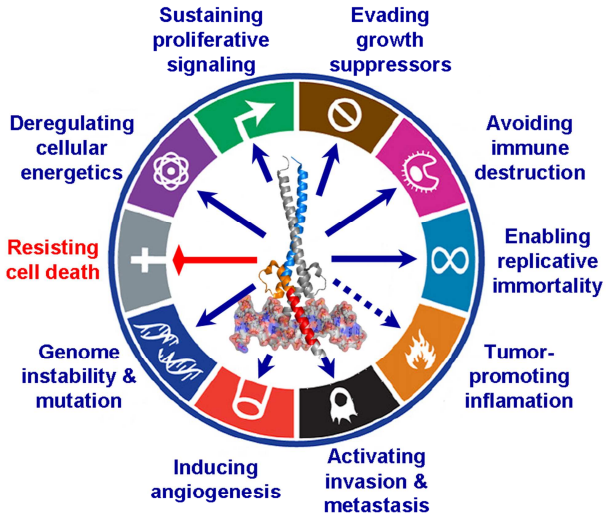

Figure 1.21. MYC has been direct- or indirectly involved in all and every one of the hallmarks of cancer defined in 2011 by Hanahan and Weimberg. (Hanahan and Weinberg, 2011).

iv) MYC promotes cell motility by repressing many genes involved in cell adhesion, cytoskeletal architecture and extracellular matrix such as actin, cdc42, the α3β1 integrin, N-cadherin or several collagens (Inghirami, *et al.*, 1990; Barr, *et al.*, 1998; Coller, *et al.*, 2000; Wilson, *et al.*, 2004) or by inducing the expression of several metalloproteases such as MPP-7, 11 and 13 (Giambernardi, *et al.*, 1998). On the other hand, MYC has been linked to epithelial-mesenchymal transition (EMT) and metastasis via its up-regulation of miR-9, which targets E-cadherin (Ma, *et al.*, 2010), as well as by its ability to transactivate the PcG repressor protein Bmi-1 (Guney, *et al.*, 2006; Song, *et al.*, 2009).

v) Finally, MYC possesses immunosuppressive potential by impairing antigen processing and presentation, and thus preventing T-cells from recognizing tumor cells (Staege*, et al.*, 2002; God and Haque, 2010).

1.5. THE K562 AND THE Kp27MER CELL MODELS

The K562 cell line derives from a patient with chronic myeloid leukemia (CML) in blast crisis (Lozzio and Lozzio, 1975). This has led to an extensive use of this cell line as a model for studying CML and other hematological malignancies. Among the molecular features of this cell line should be noted the expression of BCR-ABL tyrosine kinase resulting from a reciprocal translocation between chromosome 9 and 22 which is intimately related to the pathogenesis of CML (Collins*, et al.*, 1987; Goldman and Melo, 2003). Moreover, this cell line does not express p53 (Law*, et al.*, 1993) and is deficient in the CKIs p15INK4b and p16INK4a (Drexler, 1998). In contrast, it shows a high MYC expression although *MYC* gene is not amplified (Gomez-Casares*, et al.*, 1993). Finally, this cell line is multipotent and it can mature along distinct hematopoietic lineages (Lerga*, et al.*, 1999) making it an excellent model to study the hematopoietic differentiation.

The stable Kp27MER cell line was developed in our laboratory to study the antagonism between MYC and p27 in proliferation and cell differentiation (Acosta*, et al.*, 2008). This cell line derives from the original K562 cell line and it contains an additional p27 gene controlled by the sheep metallothionein promoter which responds to different concentrations of $ZnSO_4$ in the culture medium (ranging between 0-75 µM in non-toxic conditions) and the quimera MYCER protein which can be activated in presence of low doses (100-200 nM) of 4-hydroxy-tamoxifen (4HT) (Littlewood*, et al.*, 1995). Induction of high levels of p27 with 75 µM of $ZnSO_4$ (the maximum allowable dose without affecting their viability) result in a rapid proliferative arrest accompanied by cell accumulation in G1-phase and a moderate erythroid differentiation of these cells. The activation of MYCER by 4HT in these conditions is not able to reverse this growth arrest but inhibits the p27-mediated differentiation repressing several erythroid master genes. However, in presence of moderate p27 levels (50 µM $ZnSO_4$), MYC provokes an increase in the fraction of cells in S-phase and a consistent increase in cell proliferation. This effect of MYC on cell proliferation can be explained, at least in part, by the ability of MYC to induce a reduction in the p27 protein levels (Acosta*, et al.*, 2008).

2. AIMS

2. AIMS

There is a functional antagonism between the CDKs inhibitor p27 and the oncogenic transcription factor MYC in cell proliferation and tumorigenesis. Besides being a positive regulator of cyclins and CDKs, MYC has the ability to down-modulate p27 levels. Several mechanisms have been proposed to explain the inverse relationship between MYC and p27 both at transcriptional and posttranscriptional level. However some of these mechanisms have not been reproduced in other experimental models or no correlation was found in the clinical context. Furthermore, in our laboratory we have observed that this antagonism between MYC and p27 seems to be dependent on p27 expression levels.

In the present study we aim to investigate the molecular mechanisms that may explain the antagonism between MYC and p27 in different experimental contexts. For this purpose we propose the following objectives:

1. To establish the molecular mechanism that determines the antagonism between MYC and p27 in proliferation; to study its functionality in different cell systems, in animal models and in human cancer.

2. To establish why MYC effect on cell proliferation is dependent on the levels of p27.

3. MATERIAL AND METHODS

3. MATERIAL AND METHODS

3.1. CHRONIC MYELOID LEUKEMIA SAMPLES

Bone marrow mononuclear cells from 4 healthy controls, 31 CML patients at diagnosis and 8 patients that achieved the remission of the leukemia after imatinib treatment (Complete Molecular Response) were studied. Patients were diagnosed and evaluated for complete molecular response as described (Baccarani*, et al.*, 2009). The patients were from the Hospital Universitario Marqués de Valdecilla (Santander, Spain) and Hospital Universitario Dr. Negrín (Las Palmas, Spain). The study was according to procedures approved by the ethics committees of both hospitals.

Bone marrow mononuclear cells were prepared by Ficoll-Hypaque density gradient centrifugation method. For this purpose, bone marrow samples (~3.5 ml) were diluted with one volume of PBS (~3.5 ml). Diluted sample was carefully poured over 3 ml of Ficoll-Hypaque solution (Histopaque®-1077, Sigma-Aldrich) avoiding mixing both phases. Tube was then centrifuged at 2,000 rpm for 15 min in a swinging-bucket rotor with no brake. The mononuclear cells located at the interphase between the plasma (upper layer) and the Ficoll-Hypaque (bottom) phases, were transferred to a new tube, washed twice in PBS and pelleted at 1,500 rpm for 5 min. Total RNA and protein extracts from bone marrow mononuclear cells were then extracted as indicated below (Section 3.4.2 and 3.6.1 respectively). *MYC* and *SKP2* mRNA expression correlation was determined with the Pearson´s correlation coefficient. *SKP2* and *MYC* mRNA expression between groups (control, diagnosis and CMR) was compared using the non-parametric Mann–Whitney U test. P-values below 0.05 were considered significant. Statistical analysis was carried out with the GraphPad Prism 4.0 software.

3.2. CELL CULTURE

3.2.1. Cell lines and maintenance

K562 cell line was obtained from American Type Culture Collection (ATCC). K562, K562-derived and non-adherent cell lines were grown in R10F medium, i.e., RPMI 1640 basal medium (Lonza) supplemented with 10% (v/v) foetal calf serum (Lonza), 150 µg/ml gentamycin (Lab. Normon) and 2 µg/ml ciprofloxacin (Sigma-Aldrich). When indicated, R10F medium was also supplemented with specific selective antibiotics [500 µg/ml geneticin (G418), 1 µg/ml puromycin or 100 µg/ml hygromycin B (all from Sigma-Aldrich)] to grow each cell line in particular as indicated in table 3.1. Cells were maintained in a humidified atmosphere at 37ºC and 5% CO_2. Non-adherent cells were kept growing in exponential phase (<10^6 cells/ml) and sub-cultured twice a week at a ratio of 1:3 and 1:6 depending on the confluence.

Table 3.1. Non-adherent cell lines used in this study.

Cell lines	Origin	Culture medium and resistence	References
K562	Human chronic myeloid leukemia (ATCC)	R10F	(Lozzio and Lozzio, 1975)
KMYCJ	K562 cells stably transfected with a *MYC* gene inducible by $ZnSO_4$	R10F supplemented with hygromycin B	(Delgado, *et al.*, 1995)
KMER4	K562 cells stably transfected with a vector expressing the MYCER construct	R10F with puromycin	(Albajar, *et al.*, 2011) (Acosta, *et al.*, 2008)
Kp27-5	K562 cells stably transfected with a p27 gene inducible by $ZnSO_4$.	R10F with G418	(Munoz-Alonso, *et al.*, 2005)
Kp27MER	Kp27-5 cells stably transfected with the MYCER gene	R10F with G418 and puromycin	(Acosta, *et al.*, 2008)
KMYCBp53	KMYCB cells expressing a p53 mutant (Val^{135}) that is activated at 32 °C	R10F with hygromycin B and puromycin	(Ceballos, *et al.*, 2000)
KMERpSR	KMER4 cells infected with retrovirus expressing pSR empty vector	R10F with puromycin	This Thesis
KMERshSKP2	KMER4 cells infected with retrovirus expressing pSR-shSKP2	R10F with puromycin	This Thesis
P493.6	Immortalized human B cells (EREB2-5) expressing a tetracycline-repressible *MYC* gene	R10F with hygromycin B	(Schuhmacher, *et al.*, 1999)

Adherent cell lines were grown in D10F media i.e., Dulbecco's Modified Eagle Medium (DMEM) (Lonza) supplemented with 10% foetal calf serum (Lonza), 150 µg/ml of gentamycin (Lab. Normon) and 2 µg/ml of ciprofloxacin (Sigma-Aldrich). When indicated, D10F medium was also supplemented with specific selection antibiotics: geneticin/G418, puromycin or hygromycin B at the concentrations indicated above. Cells were maintained in a humidified atmosphere at 37ºC and 5% CO_2. Adherent cell lines were sub-cultured twice a week at a ratio of 1:6 and 1:10 and cell densities were kept below 70-80% confluence. For this purpose, cell culture media was aspirated, the cells were washed with 15 ml phosphate buffered saline (PBS). Cells were then detached using 1-3 ml Trypsin-EDTA solution (Sigma-Aldrich). Finally, trypsin activity was neutralized with D10F. Table 3.2 provides a list of the adherent cell lines used in this study and their selection antibiotics.

Table 3.2. Adherent cell lines used in this study.

Cell lines	Origin	Culture medium and resistance	References
TM1	Mv1Lu lung epithelial cell line with a tetracycline-repressible *MYC* gene	D10F with G418 and hygromycin B	(Warner, *et al.*, 1999)
TGR-1	Rat-1 fibroblasts *Hprt*$^-$	D10F	(Prouty, *et al.*, 1993)
HO15.19	*Myc*-null rat fibroblasts generated from TGR1 cells by homologous recombination	D10F with G418	(Mateyak, *et al.*, 1997)
MEFs *Cdk2*$^{-/-}$	Mouse embryonic fibroblasts from *Cdk2*$^{-/-}$ mouse	D10F with G418	(Ortega, *et al.*, 2003)
MEFs *Cdk2*$^{-/-}$ Lv	MEFs *Cdk2*$^{-/-}$ transduced with Lv141-GFP empty vector	D10F with G418	This Thesis
MEFs *Cdk2*$^{-/-}$ LvMYC	MEFs *Cdk2*$^{-/-}$ transduced with Lv141-GFP-MYC vector	D10F with G418	This Thesis
MEFs cyclin E1$^{-/-}$/E2$^{-/-}$	Mouse embryonic fibroblasts from cyclin E1$^{-/-}$/E2$^{-/-}$ mouse	D10F with G418 and puromycin	(Geng, *et al.*, 2003)
MEFs cyclin E1$^{-/-}$/E2$^{-/-}$ Lv	MEFs cyclin E1$^{-/-}$/E2$^{-/-}$ transduced with Lv141-GFP empty vector	D10F with G418 and puromycin	This Thesis
MEFs cyclin E1$^{-/-}$/E2$^{-/-}$ Lv-MYC	MEFs cyclin E1$^{-/-}$/E2$^{-/-}$ transduced with Lv141-GFP-MYC vector	D10F with G418 and puromycin	This Thesis
HEK293T	Human embryonic kidney expressing the T antigen	D10F	(Graham, *et al.*, 1977)
Phoenix-A	HEK293T cells expressing gag-pol and envelope proteins.	D10F	(Pear, *et al.*, 1993)

3.2.2. Cell proliferation analysis

For proliferation assays, cells were plated at a concentration of 2.5 x 10^5 cells/ml on day 0 and cell proliferation was monitored every 24 hours, during 3-4 more days after treatment with the corresponding drug. Cell growth was assayed by cell counting in a hemocytometer. Trypan blue exclusion test was used for assessment of cell viability.

3.2.3. Drug treatments

When indicated, the exponentially growing cells were treated with 50-75 µM $ZnSO_4$, 200 nM 4-hydroxytamoxifen (4HT), 10 nM phorbol-12-myristate-13-acetate (TPA), 10 µg/ml cycloheximide (CHX), 1-2 µg/ml doxycycline (Doxy) (all reagents from Sigma-Aldrich) or 1 µM imatinib mesylate (LC Laboratories, Woburn, MA,USA).

$ZnSO_4$ was used to induce p27 transgene controlled by the metallothionein promoter in Kp27-5 and Kp27MER cells or to induce *MYC* transgene in KMYCJ and KMYCBp53 cells. 4HT was used to activate the MYCER protein in KMER4 and Kp27MER cell lines. The tyrosine-kinase inhibitor Imatinib and the TPA were used to block cell proliferation and to repress endogenous MYC expression in K562 and K562 derived cell lines. Doxycycline was used to repress the tetracycline-responsive *MYC* transgene in P493.6 and TM1 cell lines. CHX was used to inhibit protein synthesis in transcriptional experiments in Kp27MER cells.

75 mM $ZnSO_4$ stock solution was dissolved in distilled water and filtered through 0.22 µm pore size sterile syringe filters (Millipore). 200 µM 4HT, 10 mM TPA, 1 mM Imatinib, 1mg/ml doxycycline and 10 mg/ml CHX stock solutions were dissolved in dimethyl sulfoxide (DMSO) (Sigma-Aldrich). All stock solutions were aliquoted and stored at -20ºC, in the absence of light. Stock solutions were added directly to the culture medium (1µl per ml of culture medium) to obtain the final desired concentration (usually 1:1000 dilutions). An equal volume of drug solvent (distilled water or DMSO) was added to the untreated control cells.

3.2.4. Transfection

Electroporation or nucleofection methods were mainly used for transient transfection of non-adherent cells (K562 or K562 derived cells) whereas methods based in cationic lipids, such the JetPEI transfection reagent, were generally used for transient transfection of adherent cells (HEK293T or Phoenix A cells).

3.2.4.1. Electroporation and nucleofection

Electroporation and nucleofection were used for reporter transfection in luciferase assays or for transient silencing of SKP2 or MYC expression in K562 or K562 derived cells (KMYCJ).

For electroporation, 5 x 10^6 cells were resuspended in 800 µl of serum-free medium RPMI (Lonza) or 800 µl of Mirus Ingenio transfection reagent (Mirus BioLLC) containing 5 µg of total DNA (usually 1 µg of total DNA per 10^6 cells). The mixture was electroporated in a sterile gene pulser cuvette with 0.4 cm gap between electrodes (Bio-Rad) using a Gene Pulser apparatus (Bio-Rad) with the following voltage and capacitance settings: 260 V and 1 mFa. After electroporation, cells were briefly kept on ice for 5 min and then plated in complete medium (R10F) and incubated for the indicated time (24-48 hours).

For nucleofection 1-3 x 10^6 cells were resuspended in 100 µl of cell line nucleofector solution V (Amaxa) or 100 µl of Mirus Ingenio transfection reagent (Mirus BioLLC) containing 1-3 µg of total DNA (1 µg of total DNA per 10^6 cells). The mixture was nucleofected in a nucleofector cuvette of 0.1 cm gap using an Amaxa nucleofector apparatus (Amaxa) following the manufacturer's instructions (T-16 program). After nucleofection, cells were briefly kept on ice for 5 min and then plated in complete medium (R10F) and incubated for the indicated time.

3.2.4.2. Transfection based on cationic lipids: jetPEI (Polyplus)

Cationic lipids-based methods were used for transient transfection of adherent cell lines. JetPEI transfection reagent (Polyplus) was used for Phoenix-A or HEK293T cells transfection for retroviral or lentiviral particles production respectively. For this purpose ~2 x 10^6 Phoenix-A or HEK293T cells were seeded on 100 mm Ø plates one day before transfection to achieve a 70-80% confluence the day of transfection. For a 100 mm Ø plate, 10 µl of jetPEI were resuspended in 240 µl of 150 mM NaCl in a sterile eppendorf tube (usually 2 µl jetPEI per 1 µg DNA). On a different tube, 5 µg of total plasmid DNA were resuspended in 250 µl of 150 mM NaCl. Both tubes were vortexed and incubated separately for 5 min at room temperature. Then, both tubes were mixed, and incubated for 30 min at room temperature. The resultant mixture containing the cationic lipids/DNA complexes was directly added in a drop wise manner onto the plates and gently homogenized with the culture medium (D10F) by swirling. Cells were incubated for 24-48 h after transfection and transfection efficiency was evaluated by GFP expression under a fluorescence microscope.

3.2.5. Retrovirus production and infection

For stable expression of the shSKP2 into KMER cells, the cells were infected with retroviral particles containing a shSKP2 construct under human H1 promoter produced in Phoenix-A amphotropic packaging cells. Phoenix-A cells derive from HEK293T cell line and they constitutively express the gag-pol and the envelope proteins to produce amphotropic (A) retrovirus. Therefore, to produce retroviral particles with this cell line it is only required to transfect the retroviral construct to be packaged. Thus, cells at 70-80% confluence in 100 mm Ø plates were transfected with pSR-shSKP2 (Andreu*, et al.*, 2005) or the empty retroviral vector pSuper-Retro, using jetPEI transfection reagent as previously described (Section 3.2.4.2).

Two days after transfection retrovirus-containing supernatants were harvested, clarified at 3,000 rpm, mixed with 4 µg/ml polybrene (Sigma-Aldrich) and filtered through a 0.45 µm filter (Millipore). Retrovirus-containing filtered supernatants were used for resuspending a KMER cell pellet (~2 x 10^6 cells). 24 hours after infection, supernatants were replaced with fresh medium (R10F) and transduced cells were selected with 1 µg/ml puromycin for 2 weeks.

3.2.6. Lentivirus production and infection

For stable MYC-FLAG expression into *Cdk2*$^{-/-}$ and cyclin E1$^{-/-}$/E2$^{-/-}$ MEFs, the cells were infected with lentiviral particles containing a MYC-FLAG gene construct controlled by the CMV promoter, packaged in HEK293T cells. To produce these lentiviral particles, HEK293T cells at 70-80% confluence in 100 mm Ø plates were transfected with a mix of three constructs composed of 1µg of pCMV-VSV-G (Addgene), 3µg of psPAX2 (Addgene) and 6 µg of LV141-CMV-MYCwt-IRES-GFP (GeneCopoeia) or the corresponding empty vector LV141-CMV-IRES-GFP (GeneCopoeia), using jetPEI transfection reagent (Polyplus) as previously described.

The three plasmids together provide all the elements required for packaging the expression vector into virions. The LV141-CMV-MYCwt-IRES-GFP plasmid provides the packaging signal (Ψ) and the gene construct to be packaged (CMV promoter-MYC-FLAG-IRES-GFP) flanked by the LTRs (Long terminal repeats); whereas the packaging plasmids (pCMV-VSV-G and psPAX2) provide structural and replication proteins *in trans* required to produce the lentiviral particles (Gag, Pol and VsVg proteins).

Two days after HEK293T transfection lentivirus-containing supernatants were harvested, clarified at 3,000 rpm, mixed with 4 µg/ml polybrene (Sigma-Aldrich) and filtered through a 0.45 µm filter (Millipore). Then, the culture medium of knockout MEFs was replaced by lentivirus-containing supernatants and infection was carried out for 24 hours. After transduction, supernatant was replaced again with complete fresh medium D10F and lentiviral infection efficiency was evaluated by GFP expression in a fluorescence microscope. GFP positive colonies were selected and expanded.

3.3. NUDE MICE XENOGRAFTS

Six-week-old female nude (Hsd: Athymic Nude-Foxn1$^{nu/nu}$) mice were provided by Harlan Laboratories (Italy) and animal maintaining was performed at the animal facilities of the University of Cantabria. Mice were housed in sterile filter-capped cages, with a temperature of 22 ± 2°C, 12 h light/dark cycle and provided with sterilized food and water *ad libitum*.

For xenografts, KMERpSR and KMERshSKP2 cells were resuspended in a serum-free culture medium (RPMI 1640) / Geltrex (GIBCO) mixture (1:1 v/v) to a final concentration of 5 x 10^7 cells per ml. Then, each mouse was injected subcutaneously with 200 µl KMERpSR cell suspension (~10^7 cells per injection) into the left rear flank and 200 µl KMERshSKP2 cell suspension (~10^7 cells per injection) into the right rear flank by using G-27 needles. After injections, tumor development was followed by daily monitoring of the mice. Tumor-bearing mice were sacrificed after 21–24 days when the larger tumors reached approximately 1 cm diameter. Mice were photographed and the tumors were excised, weighed and measured by using a caliper. This study was approved by the Cantabria University Institutional Laboratory Animal Care and Use Committee and performed in accordance with the Declaration of Helsinki and the European Communities Council Directive (86/609/EEC).

3.4. DNA AND RNA ANALYSIS

3.4.1. Bacterial transformation and plasmid DNA purification

Plasmid DNA (Table 3.3) was transformed into *E. coli* DH5α competent cells (Invitrogen) for DNA amplification. For this purpose, 50 µl *E. coli* DH5α cells were briefly thawed in hand and mixed with 100 ng of plasmid DNA. The mixture was kept on ice for 30 min, followed by a heat shock for 1 min at 42 °C and then immediately 2 min incubation on ice. Transformed *E. coli* DH5α

cells were then supplemented with 300 µl LB-media containing no antibiotics and incubated in an orbital shaking incubator at 160 rpm for 1 h at 37 °C. After this, the *E. coli* cells were spread on LB-Agar 100 mm Ø plates containing the corresponding selective antibiotic (100 µg/ml ampicillin or 50 µg/ml kanamycin) and incubated overnight at 37ºC.

The next day, a single colony was inoculated into 5 ml LB medium containing the appropriate antibiotic and grown overnight in an orbital shaking incubator at 37°C and 160 rpm. Subsequently, the bacterial culture was harvested by centrifugation at 4,000 rpm for 10 min and plasmid DNA was purified with the NucleoSpin Plasmid Miniprep Kit (Macherey-Nagel) following the manufacturer's instructions and analysed by restriction analysis to verify the identity of purified vector. Plasmid digestions were carried out with two specific restriction endonucleases (Fermentas) following the manufacturer's instructions. Usually, 1 µg of plasmid DNA was digested with 1 µl of every selected restriction endonucleases for 1 h at 37ºC. The restriction DNA-fragments were analysed by agarose gel electrophoresis. For this purpose, the low melting point agarose (Pronadisa) was melted in 1X TAE buffer (90 mM Tris-acetate, 2 mM EDTA) in a conventional microwave. The agarose concentration of the gels varied from 0.8 to 2.0 % (w/v) depending on the size of DNA-fragments to be analysed. Ethidium bromide (0.5 µg/ml) was added before gel casting. Samples were mixed with 1/5 volume of agarose gel loading buffer (0.005 % bromophenol blue (w/v) and 30 % glycerol (v/v), before loading on the gel. "1 Kb DNA ladder" or "100 bp DNA ladder" (Fermentas) were used as DNA size standards. Electrophoresis was carried out in an iMupid Mini gel Electrophoresis system at 50-100V for 60-30 min in 1X TAE buffer. Finally, gels were visualized in an UV-transilluminator and recorded using a Gel Doc EZ Imager (Bio-Rad).

Alternatively, to prepare high amounts of plasmid DNA for transfections, a single colony was inoculated into 5 ml LB medium containing the appropriate antibiotic (100 µg/ml ampicillin or 50 µg/ml kanamycin) and incubated for 8 hours in an orbital shaking incubator at 37 °C and 160 rpm. Then, 200 µl of this starter culture were used to inoculate 200 ml LB medium containing the same selection antibiotic and grown overnight in the same culture conditions (37 °C and 160 rpm).

The following day, the bacterial culture was harvested by centrifugation at 6,000 rpm for 10 min and plasmid DNA was purified using the Plasmid Midi Kit (Qiagen) following the manufacturer's instructions. After DNA elution from the Anion-Exchange column, DNA was desalted and concentrated by isopropanol precipitation and finally, plasmid DNA was resuspended in 200 µl of nuclease free water.

Plasmid DNA concentration was determined by measuring the A_{260nm} using a NanoDrop Spectrophotometer (NanoDrop Technologies, Inc.). For DNA concentration calculations, one Absorbance unit was considered as 50 µg/ml of double-stranded DNA.

Table 3.3. Plasmids used in this study.

Plasmid	Insert	Origin	Reference
pRS	Retroviral empty vector	Jesús Gil and David H. Beach Lab. (London)	-
pRS-shMYC	Short hairpin against human *MYC*	Jesús Gil and David H. Beach Lab. (London)	(Bernard*, et al.*, 2003)
pSR	Retroviral empty vector	Commercial (Oligoengine)	-
pSR-shSKP2	Short hairpin against human *SKP2*	Ignacio Pérez-Roger Lab. (Moncada)	(Andreu*, et al.*, 2005)
Lv141-CMV-IRES-GFP	Lentiviral empty vector	Commercial (Genecopoeia)	-
Lv-CMV-MYCwt-IRES-GFP	Human MYC with FLAG epitope at C-terminal domain	Commercial (Genecopoeia)	-
psPAX2	Gag-Pro-Pol elements for lentiviral particles production	Commercial (Addgene)	Didier Trono Lab. (Lausanne)
pCMV-VSV-G	VsVg envelope protein for lentiviral particles production	Commercial (Addgene)	Robert A. Weinberg Lab. (Cambridge, USA)
pET-28a	Empty vector for His_6-recombinant proteins generation.	Ignacio Arechaga Lab. (Santander)	Commercial (Novagen)
pGEX-KG-GST-p27	Human p27 with GST epitope at N-terminal domain	Oriol Bachs Lab. (Barcelona)	(Taules*, et al.*, 1999)
pET28-His_6-p27	Human p27 with hexahistidine epitope at N-terminal domain (His_6-p27)	Javier Leon Lab. (Santander)	This Thesis.
pGL3-basic	*firefly* reporter with no promoter region (empty vector)	Commercial (Promega)	-
-1148-SKP2-Luc	1148 pb of SKP2 promoter and *firefly* luciferase reporter	Wen-Chun Hung Lab. (Taiwan, China)	(Huang and Hung, 2006)
pGL3-4XEBox-Luc	Synthetic promoter bearing 4 E-boxes and *firefly* luciferase reporter	T. Berg Lab. (Martinsried)	(Kiessling*, et al.*, 2006)
pGL3-4XEBoxMut-Luc	Synthetic promoter bearing 4 mutated E-boxes and *firefly* luciferase reporter	T. Berg Lab. (Martinsried)	(Kiessling*, et al.*, 2006)
pRL-TK	Herpes simplex virus thymidine kinase promoter (HSV-TK) and *Renilla* luciferase reporter	Commercial Promega	-

3.4.2. DNA subcloning

For pET28-His_6-p27 vector construction, the p27 insert from pGEXKG-p27 vector (Taules*, et al.*, 1999) was subcloned into pET-28a vector (Novagen). For this purpose, pGEXKG-p27 and pET-28a vectors (1 µg of each) were both double digested with NdeI and XhoI restriction endonucleases in 1X buffer Orange (Fermentas) for 1 hour at 37ºC. Digested vectors were run in 1% agarose gels and visualized with a UV-transilluminator. The linearized pET-28a vector and the p27 insert were excised from the agarose gel with a scalpel blade and purified with the Wizard SV Gel and PCR Clean-up System Kit (Promega) following the manufacturer's instructions. Then, both fragments were ligated with the T4 DNA ligase (Invitrogen) overnight at 22ºC. The following day, ligation was transformed into *E.coli* DH5α cells (Invitrogen) as previously indicated (Section 3.4.1), plated in LB-agar plates with kanamycin (50 mg/ml) and growth overnight at 37ºC.

Next day, transformed bacterial colonies were selected and their plasmidic DNA purified. PCR screening with T7 promoter (5'-TAATACGACTCACTATAGGG-3') and T7 terminator (5'-GCTAGTTATTGCTCAGCGG-3') primers was performed to identify whether transformants contained the p27 insert (Amplicon with p27 insert = 856 pb; amplicon without insert = 318 pb). The PCR was analyzed using agarose gel electrophoresis. Positive colonies for pET28-His_6-p27 were grown; plasmid was purified with the NucleoSpin plasmid Kit (Macherey-Nagel) and transformed by electroporation into *E.coli* C41 (DE3) strain (Miroux and Walker, 1996) to subsequent protein expression and purification.

3.4.3. RNA extraction and purification

Total mRNA extraction from cell cultures was carried out using the RNeasy® Kit (Qiagen) according to manufacturer's instructions protocol. Briefly, samples (~10^6 cells per extraction) were directly lysed and homogenized by pipetting in the presence of a highly denaturing guanidine-thiocyanate containing buffer (RLT) and then the RNA was selectively bound to a silica membrane contained within the RNeasy mini spin columns in presence of ethanol. After several washes with RWI and RPE washing buffers to eliminate contaminants, RNA was eluted in 50 µl RNase-free water. All steps were carried out in a micro-centrifuge at 10,000 rpm for 1-2 min at room temperature.

On the other hand, total RNA extraction from CML samples was performed using Trizol reagent (Invitrogen). Approximately 5 x 10^6 bone marrow mononuclear cells were lysed directly with 1 ml of Trizol reagent for 5 min at room temperature. Then, 200 µl of chloroform was added to the homogenized sample, vortexed vigorously for 15 seconds and centrifuged at 12,000 rpm for 15 min at 4ºC. After centrifugation, upper aqueous phase containing total RNA was transferred carefully into a fresh tube, mixed with 500 µl of 100% isopropanol and incubated for 10 min at room temperature to precipitate RNA. To improve RNA precipitation, the samples were then centrifuged at 12,000 rpm for 20 min at 4ºC. The RNA pellet was washed once with 1 ml 75% ethanol and re-centrifuged at 7,500 rpm for 5 min at 4ºC. Finally, RNA pellet was briefly allowed

to dry at room temperature to eliminate ethanol residues and resuspended in 50 µl of RNase-free water. RNA concentration was determined by measuring the A_{260nm} using a NanoDrop spectrophotometer. 1 µl RNA sample was subjected to electrophoresis in 1% agarose gels to evaluate RNA integrity and the rest of RNA was stored at -70^{o}C until use.

3.4.4. Reverse Transcription and Polymerase Chain Reaction

For gene mRNA expression analysis 2 µg of total RNA were retro-transcribed to cDNA using the iScript cDNA Synthesis Kit (Bio-Rad), including the iScript reverse transcriptase enzyme, RT buffer, oligo (dT) and random hexamers. The reaction mix (40 µl) was incubated as follows: 5 min at 25ºC, 30 min at 42ºC and 5 min at 85ºC. Complementary DNA (cDNA) was stored at -20ºC until used. For Polymerase Chain Reaction (PCR) 2 µl of cDNA were amplified using specific primers pairs for each gene to be analyzed (Table 3.4). Primers pairs were designed using the Primer 3 software tool (http://frodo.wi.mit.edu, 18-25 bp length; 40-65% GC content; Tm 55-65ºC). For conventional PCR, sample reaction was prepared containing 15 µl of 2X Premix Taq™ (TaKaRa) [including TaKaRa Taq DNA polymerase, 400 nM dNTPs, and PCR buffer 2X (20 mM Tris-HCl pH8.3, 100 mM KCl and 3 mM $MgCl_2$)], 300 nM of specific primers (forward and reverse primers), 2 µl of template cDNA and distilled water to a final volume of 30 µl. Reactions were run using a Thermal Cycler C1000 (Bio-Rad).

For quantitative PCR, sample reaction was prepared containing 15 µl of 2X SYBR® Green PCR Reaction Mix (Bio-Rad) (including antibody–mediated hot-star iTaq DNA polymerase, dNTPs, $MgCl_2$, SYBR Green I dye, fluorescein and PCR buffer 2X), 300 nM of specific primers (forward and reverse), 2 µl of cDNA and distilled water to a final volume of 30 µl. The sample was divided into two aliquots and loaded on a 96 well plate for real-time PCR as duplicate (15 µl per well). Reactions were run using an iQ5 apparatus (Bio-Rad).

The general PCR-amplification protocol was performed as follows:

1) 3 min at 95ºC for cDNA denaturalization and hot-star DNA polymerase activation.

2) 40 repeats including 3 steps for DNA amplification:

-15 seconds at 95ºC (denaturation).

-15 seconds at 55-60ºC (primer annealing)

-15-30 seconds at 72ºC (primer extension)

3) 10 min at 72 ºC (Full-extension of amplicons)

For real time PCR an additional step was added after PCR amplification to determine the amplicon melting curve and consisting of:

4) 81 steps of 10 seconds each one, increasing 0.5ºC each step from 55ºC to 95ºC.

Real-time PCRs were analyzed with the iQ5 Optical system 2.0 software and threshold cycles (Ct) were determined by default at the beginning of the exponential phase of PCR amplification. The relative mRNA expression was normalized to a housekeeping gene, such as

the ribosomal protein *RPS14* for human samples or the β-actin for mouse samples, using the comparative Delta Ct (ΔCt) method according to the next expression:

$$\Delta Ct = 2^{(Ct\ RPS14\ or\ \beta\text{-}actin - Ct\ gene\ of\ interest)}$$

Reactions with distilled water instead of cDNA were used as negative controls to detect possible amplification from contaminating DNA or primer dimers. The identities of the PCR products were verified by agarose gel electrophoresis. Primers sequences and amplicon sizes used in RT-qPCR assays are shown in Table 3.4.

Table 3.4. Primers pairs and amplicons size used for RT-PCR analyses.

Amplified gene	Primers (5´-3´)	Amplicon size
Human B23	5´-AATATGCACTGGCCCTGAAC-3´ 5´-TTGTTGAAGCAGAGGCAATG-3´	158 bp
Human *MYC*	5´-AAGACTCCAGCGCCTTCTCTC-3´ 5´-GTTTTCCAACTCCGGGATCTG-3´	527 bp
Human *SKP1*	5´-CCTGAAAGTTGACCAAGGAAC-3´ 5´-GAAGGTCTTGCGAATCTCCTC-3´	142 bp
Human *RPS14*	5´-TCACCGCCCTACACATCAAACT-3´ 5´-CTGCGAGTGCTGTCAGAGG-3´	157pb
Human *SKP2*	5´-AGCCCGACAGTGAGAACATC-3´ 5´-GAAGGGAGTCCCATGAAACA-3´	168 bp
Mouse *Cdk2*	5´-GTTGACGGGAGAAGTTGTGG-3´ 5´-TCTTGAGGTCCTGGTGCAG-3´	194 bp
Mouse cyclin E1	5´-GCACAGGACTTCTTTGATCG-3´ 5´-GCGCCATCTGTAACATAAGC-3´	155 bp
Mouse cyclin E2	5´-GCATTCTGACCTGGAACCAC-3´ 5´-GGAAGCAATGAACAATGAGG-3´	193 bp
Mouse β-actin	5´-AGACTTCGAGCAGGAGATGG-3´ 5´-AGTTTCATGGATGCCACAGG-3´	169 bp
MYC-FLAG	5´-GTCCGTCCAAGCAGAGGAG-3´ 5´-TCGCTAGCCATAACCACTTTG-3´	162 bp

3.4.5. Chromatin Immunoprecipitation (ChIP)

ChIP assays were performed to analyse MYC occupancy along *SKP2* promoter in K562 cells untreated or treated with 1µM imatinib or 10 nM TPA for 12 h (to down-regulate endogenous MYC). For this end, K562 cells (~25 x 10^6 cells per ChIP) were washed once with PBS and cross-

linked with PBS-1% formaldehyde at room temperature for 10 min with rocking. Then, 2 M Glycine was added to a final concentration of 125 mM and incubated for another 10 min to stop cross-linking. Fixed cells were washed twice with cold PBS-10 mM EDTA and resuspended in 250 µl of ChIP lysis buffer [50 mM Tris-HCl pH8, 1% SDS (w/v), 1mM EDTA, supplemented 1:100 with protease inhibitor cocktail Set I (Calbiochem)]. After this, cells were first roughly homogenized with a syringe by extensive passes (4-5 times) through a G27 needle and then sonicated 6 times for 20 seconds each using a Hielscher UP50H ultrasonic homogenizer (Hielscher Ultrasonics) at the maximum settings (100% amplitude and continuous cycle) in an ice-water bath, leading to chromatin fragments between 250 and 1000 bp length. Afterwards, lysate was cleared of cell debris by centrifugation at 14,000 rpm for 10 min at 10º C and supernatant containing sheared chromatin was collected and diluted 10 fold with dilution buffer [20mM Tris-HCl pH8, 150mM NaCl, 1% Triton X-100 (v/v), 1mM EDTA, supplemented with protease inhibitor cocktail Set I (Calbiochem)]. The diluted chromatin was divided in 2 aliquots (1ml per aliquot) and 100 µl of remaining diluted chromatin were also reserved for *input* DNA.

For chromatin immunoprecipitation, 1 µg of primary antibody anti-MYC (N262, sc-764) was added directly to one aliquot of diluted chromatin and 1 µg of control rabbit IgGs (as control for non-specific immunoprecipitation) was added to another one and both of them were incubated overnight at 4ºC with rotation.

The following day, protein G bound to magnetic beads (Dynabeads®-protein G, Invitrogen) was used to collect immunocomplexes. Protein G has a very high affinity for the Fc region of immunoglobulins, allowing the specific capture of the protein-antibody complexes. For this purpose, Dynabeads-protein G were previously pre-equilibrated with dilution buffer to remove the storage buffer and blocked with salmon sperm DNA (Upstate) for 1hour at 4ºC with rotation. Equilibrated Dynabeads-protein G (25 µl per immunoprecipitation) were added to the samples and incubated for 2 hours at 4ºC with rotation to capture the chromatin-immunocomplexes. After this, Dynabeads-protein G-chromatin immunocomplexes were harvested using a magnet DynaMag™ (Invitrogen) and sequentially washed with 1 ml of low salt wash buffer [20 mM Tris-HCl pH8, 150 mM NaCl, 1% Triton X-100 (v/v), 1mM EDTA], 1 ml of high salt wash buffer [20 mM Tris-HCl pH8, 500 mM NaCl, 1% Triton X-100 (v/v), 1mM EDTA], 1 ml of LiCl wash buffer [20 mM Tris-HCl pH8, 250 mM LiCl, 1% NP-40 (v/v), 0,1% Na-DOC (w/v), 1 mM EDTA] and 1 ml of TE buffer (10 mM Tris-HCl pH8, 1 mM EDTA). Between washes, the tube was separated from the magnet and beads were resuspended by gently pipetting in the respective new wash buffer. Finally protein-DNA complexes where separated from the magnetic beads-protein G with 100 µl of elution buffer [20 mM Tris-HCl pH8, 1% SDS (w/v), 150mM NaCl, 1 mM EDTA]. To reverse protein-DNA formaldehyde cross-linking, immunoprecipitated DNA and *inputs* were incubated at 65ºC overnight.

The next day, samples (Immunoprecipitated DNA and *inputs*) were treated with 1 µg proteinase K for 3 hours at 45ºC; the magnetic beads were removed using the magnet and DNA was purified with the Wizard SV PCR Clean-Up system (Promega) following the manufacturer instructions and using 100 µl of nuclease free water for elution.

Immunoprecipitated DNA was analyzed by quantitative real time-PCR using an iQ5 Real-Time PCR Detection System (Bio-Rad) as previously described (Section 3.4.4). All qPCR were carried out in duplicate with 2 µl of immunoprecipitated DNA at the same annealing temperature (56ºC).

Human *SKP2* gene and promoter genomic DNA sequences (and annotated details) were obtained from UCSC genome browser database (http://genome.ucsc.edu) GRCh37/hg19 assembly (February 2009). The primer pairs were designed with the Primer 3 software tool (http://frodo.wi.mit.edu/primer3/). Lactate dehydrogenase A (*LDHA*) E-box amplicon was used as positive control of MYC binding (Kim*, et al.*, 2004). The sequences of primers pairs used in ChIP assays are listed in Table 3.4. The results are expressed as relative DNA fold enrichment with anti-MYC antibody with respect to the DNA enrichment with anti-rabbit IgG and normalized to the signal of the *input* chromatin for each amplicon.

Table 3.4. Primers pairs and amplicon size used for ChIP analyses. The coordinates are referred to the *SKP2* or *LDHA* transcription initiation sites respectively (as in UCSC genome browser) and are indicated in brackets.

Amplified gene	Primers (5´→3´)	Amplicon size
LDHA (-85/+19)	5´-TCCTGACTCAGGCTCATGGC-3´ 5´-AGACAACCGACCGGCAGA-3´	103 bp
SKP2-A (-2522/-2397)	5´-CAGCAGGATGGAGAAACAAAG-3´ 5´-AGATGATCCACCCACCTCAG-3´	126 bp
SKP2-B (-988/-870)	5´-CACGCTCCCTACTCTTACTGC-3´ 5´-ATTTGGTTGCTTGCTGTCG-3´	119 bp
SKP2-C (-784/-661)	5´-AGACCTGTCAAGGCTGCAAG-3´ 5´-ACGCACAACAGCTAAACACG-3´	124pb
SKP2-D (-507/-366)	5´-ACCACTCAGCAGCCAAGGAC-3´ 5´-ATCGGACGGTGAGCCTAAG-3´	142 bp
SKP2-E (-212/-81)	5´-CATTTCCCAGTCAGCCGTAG-3´ 5´-GCCCTTACTTCCTTCCCTTG-3´	132 bp
SKP2-F (703/854)	5´-TCCAGACCTGAGTAGCAACG-3´ 5´-CCAGGTTTGAGAGCAGTTCC-3´	152 bp
SKP2-G (14366/14505)	5´-ATGTTGTTGAGGGCTTCCAG-3´ 5´-CAACCGACCAGTCACATCC-3´	140 bp

3.5. LUCIFERASE REPORTER ASSAYS

These assays were performed with the Dual-Luciferase Reporter (DLR) System (Promega) which uses the *firefly* luciferase as experimental reporter (pGL3 derived vectors) to evaluate the promoter activity and the *renilla* luciferase (provided by pRL derived vectors such as pRL-TK) as "control" reporter for experimental data normalization. In this manner, the variability caused by differences in transfection efficiency or cell viability is minimized. Both luciferases (*firefly* and *renilla*) use different substrates in their luminescent reaction allowing independent luminescence measurements.

To evaluate the MYC ability to induce the SKP2 promoter, KMYCJ cells (4 x 10^6 cells) were transfected with 4 µg of the -1148-SKP2-Luc, containing 1148 pb of SKP2 promoter region cloned into the pGL3 vector (Huang and Hung, 2006) or the corresponding empty vector (pGL3 basic). Additionally, as positive control to evaluate the trans-activating capacity of MYC in KMYCJ cells after Zn^{2+} addition, KMYCJ cells were transfected with 4 µg of an artificial promoter bearing four E-box elements cloned into the pGL3 promoter vector (4xEbox-Luc) or the same artificial promoter bearing four mutated E-boxes (4xEboxMut-Luc) (Kiessling*, et al.*, 2006). In addition, to monitorize the transfection efficiency, KMYCJ cells were also co-transfected with 400 ng of pRL-TK reporter vector (Promega) containing the *renilla* luciferase as reporter. 12 hours after transfection, the KMYCJ cells were divided in four small plates and every plate was then treated with 75 µM $ZnSO_4$ (to induce exogenous *MYC*) and/or 10 nM TPA (to down-regulate endogenous *MYC*) for another 24 hours.

On the other hand, to analyze the SKP2 effect on MYC transactivation activity, K562 cells (3 x 10^6 cells) were transfected with 1.5 µg of pSR-shSKP2 to down-regulate SKP2 expression or the corresponding empty vector (pSuper-Retro), together with 1.5 µg of 4xEbox-Luc or the MYC-unresponsive 4xEboxMut-Luc reporter constructs (Kiessling*, et al.*, 2006) and 300 ng of pRL-TK *renilla* luciferase reporter vector (Promega). All transfections for luciferase assays were carried out by electroporation with an Amaxa nucleofector apparatus and Mirus Ingenio transfection reagent (Mirus Bio LLC) as previously described (Section 3.2.4.1).

Luciferase activities were assessed 24 hours (for K562 cells) or 36 hours (for KMYCJ cells) after transfections with DLR assay System reagents (Promega) according to the manufacturer's instructions. The luminescence signal was measured in a Turner TD-20/20 luminometer (Turner Designs).

Briefly, the cells were washed once with PBS and centrifuged at 1,500 rpm for 5 min. Cell pellets were resuspended in 100 µl of 1X passive lysis buffer (PLB) and frozen at -80ºC to improve cell lysis. Then, the lysates were clarified by centrifugation at 10,000 rpm for 5 min and supernatants (10 µl) were directly used for bioluminescence reaction. To measure firefly luciferase, 50 µl of Luciferase Assay Reagent II (LAR II) containing the luciferin substrate of the *firefly* luciferase were mixed with 10 µl of supernatant in a luminometer tube and luminescence was immediately quantified. For *renilla* luciferase activity, 50 µl of the Stop & Glow reagent were added to the sample and luminescence was immediately quantified. The Stop & Glo reagent quenches *firefly* luminescence and provides the coelenterazine substrate for *renill*a luciferase.

Luminescence readings were taken in duplicate with a 3 seconds delay and 10 seconds acquisition time at room temperature. The *firefly* data were normalized to *renilla* luciferase values and results were expressed as relative luciferase light units (RLUs) of reporter constructs (-1148-SKP2-Luc or 4xEbox-Luc) with respect to empty vectors (pGL3-basic or 4xEboxMut-Luc respectively).

3.6. PROTEIN ANALYSIS

3.6.1. SDS-PAGE and immunoblot

For protein analysis by immunoblot, cells (~10^6 cells per immunoblot) were harvested by centrifugation at 1,500 rpm for 5 min; washed once with 1ml of cold PBS; resuspended in 100 µl of NP40 lysis buffer [50 mM Tris-HCl pH8, 1 % NP40 (v/v), 150 mM NaCl, 1 mM EDTA, 10 mM NaF, supplemented with protease inhibitor cocktail Set I (1:100; Calbiochem)] and incubated on ice for 30 min. For CML samples lysis, 0.5% SDS (w/v) was added to the NP40 lysis buffer and cell lysate was additionally sonicated for 15 seconds using a Hielscher UP50H ultrasonic homogenizer at the maximum settings (100% amplitude and continuous cycle) in an ice-water bat. The protein lysate was then clarified by centrifugation at 14,000 rpm for 20 min at 4ºC and supernatant containing soluble proteins was stored at -80ºC until used. Protein concentration was determined using the colorimetric Bio-Rad protein assay (Bio-Rad) based on the Bradford method (Bradford, 1976) and by measuring the A_{595nm} in a micro-plate reader spectrophotometer Bio-Tek EL340 (Bio-tek Instruments, Inc. Vermont, USA). The protein concentration of unknown sample was estimated from a standard curve performed with known concentrations of BSA (Bovine Serum Albumin) by extrapolating the A_{595nm} readings.

Protein samples (40-60 µg of protein lysate) were mixed with 1/5 volume of 5X SDS-PAGE loading buffer [100 mM Tris-HCl pH6.8, 5% β-mercaptoethanol (v/v), 5% SDS (w/v), 0.1% bromophenol blue (w/v), 50% glycerol (v/v)] and samples were heated at 95º C for 5 min. Then, the protein samples were fractionated according to their molecular weight (MW) by Sodium dodecyl sulphate-polyacrylamide gel electrophoresis (SDS-PAGE). The percentage of acrylamide acrylamide/bis-acrylamide solution (Bio-Rad) used in the gel was dependent on the molecular weight (MW) of the protein to be analyzed, ranging from 8 to 15%. Electrophoresis was carried out in a Mini Protean III cuvette powered by a basic PowerPAC supply (Bio-Rad) at 100-150 V for 2-3 hours, using electrophoresis running buffer [25 mM Trizma pH8.3, 192 mM glycine and 0.1% SDS (w/v)]. Prestained SDS-PAGE standards (Bio-Rad) were used to evaluate protein migration and separation during gel electrophoresis.

Proteins were transferred from acrylamide gel to a nitrocellulose membrane (Schleicher & Schuell) in a Mini-Trans Blot cell (Bio-Rad) at 300-350 mA for 2 h at 4ºC, using transfer buffer [25 mM Tris pH8.3, 192 mM glycine and 10-20% methanol (v/v)]. The membrane containing the proteins was then incubated for 30 min with 10 ml of TBS-T [20 mM Tris-HCl pH7.5, 150 mM NaCl and 0.05 % Tween 20 (v/v)] supplemented with 5% non-fat dry milk (w/v) or with 5% BSA

(w/v) (for phospho-specific antibodies). After blocking, the membrane was briefly washed twice with 10 ml TBS-T buffer and incubated overnight at 4ºC or for 2-3 hours at room temperature with primary antibody diluted in TBS-T solution as indicated in Table 3.5 and supplemented with 1% BSA (w/v).

After primary antibody incubation, the membrane was washed 3 times for 10 min each one with TBS-T solution and incubated for another 45 min with a secondary antibody conjugated to IRDye680 or IRDye800 fluorochromes (Li-Cor Biosciences) diluted 1:10000 in TBS-T 1% BSA (w/v). Finally, the membrane was washed 3 times for 10 min with TBS-T and signals were visualized and recorded with an Odyssey Infrared Imaging Scanner (Li-COR, Biosciences). In some cases, membranes were incubated with secondary antibodies conjugated to horseradish peroxidase (HRP) and the protein was detected by chemiluminescence using ECL detection reagents system (GE healthcare) and followed by exposition to X-ray films (Konica-Minolta). Excluding overnight primary antibody incubation at 4ºC, all washes and membrane incubations steps were performed under agitation on a shaker platform at room temperature.

For protein loading control, the membranes were incubated with anti-Actin or anti-α-tubulin primary antibodies. In addition, the poly-acrylamide gels were stained with Coomassie Brilliant Blue solution [0.025% Coomassie Brilliant Blue R-250 (w/v), 40% methanol (v/v) and 10% glacial acetic acid (v/v)] for 10 min at room temperature and distained overnight with distilled water. Immunoblot quantification and densitometry analysis was carried out using the ImageJ software. The antibodies used for immunoblot analysis are shown in Table 3.5.

3.6.2. Immunoprecipitation and kinase assays

For immunoprecipitation, cells (~10^7 cells per immunoprecipitation) were harvested at 1,500 rpm for 5 min; washed once with 1 ml PBS; resuspended in non-denaturing lysis buffer [50 mM Tris-HCl pH7.5, 150 mM NaCl, 0.5 % NP40 (v/v), 1 mM EDTA, supplemented (1:100) with protease inhibitor cocktail Set I (Calbiochem)] and incubated on ice for 30 min. The cell lysate was then clarified by centrifugation at 14,000 rpm for 20 min. Protein concentration of the supernatant was determined by the Bio-Rad protein assay (Bio-Rad). 500 µg of total protein extract were mixed with 1 µg of the appropriate antibody and incubated overnight at 4ºC with rotation. The next day, Dynabeads®-protein G (Invitrogen) were used to capture the protein-antibody immunocomplexes. Dynabeads-protein G (25 µl per immunoprecipitation) were pre-equilibrated with non-denaturing lysis buffer to remove the storage buffer; added to antibody-protein extract mixture and incubated for 2 hours at 4ºC with rotation. Finally, Dynabeads-protein G-immunocomplexes were collected by using a magnet DynaMag™ (Invitrogen), washed four times with 1 ml of non-denaturing lysis buffer and resuspended in 30 µl 1X SDS-PAGE loading buffer [20 mM Tris-HCl pH6.8, 1% β-mercaptoethanol (v/v), 1% SDS (w/v), 0.02% bromophenol blue (w/v), 10% glycerol (v/v)]. Immunocomplexes were heated at 95ºC for 5 min and subjected to SDS-PAGE and immunoblot analysis as previously described (Section 3.6.1).

Table 3.5. Primary antibodies used in this work. It is indicated the technique (Tech.) in which they have been used: Immunoblot (IB), immunofluorescence (IF), immunoprecipitation (IP) or chromatin immunoprecipitation (ChIP) and the use dilution.

Antibody	Immunogen	Specie & type	Tech. & Use dilution	Reference
Anti-p27 (C-19)	C-terminus of the human p27	Rabbit polyclonal	IB→1:1000 IF→1:100 IP→2µg	Santa Cruz Biotech. (sc-528)
Anti-p27 (BD)	Full-length of mouse p27	Mouse monoclonal	IB→1:1000	BD Transduction Laboratories. (K-25020)
Anti-p-p27 (Thr-187)	Threonine187-phosphorylated p27 peptide derived from the C-terminus of the human p27	Rabbit polyclonal	IB→1:500	Invitrogen (71-7700)
Anti-MYC (N262)	Full-length of human MYC	Rabbit polyclonal	IB→1:1000 ChIP→2µg	Santa Cruz Biotech. (sc-764)
Anti-Actin (I-19)	C-terminus of the human actin	Goat polyclonal	IB→1:1000	Santa Cruz Biotech. (sc-1616)
Anti-SKP2 p45 (H-435)	Full-length of human SKP2	Rabbit polyclonal	IB→1:1000 IF→1:100	Santa Cruz Biotech. (sc-7164)
Anti-SKP1 p19 (H-163)	Full-length of human SKP1	Rabbit polyclonal	IB→1:1000	Santa Cruz Biotech. (sc-7163)
Anti-CUL1 (H-213)	N-terminus (57-269 aa) of the human CUL1	Rabbit polyclonal	IB→1:1000	Santa Cruz Biotech. (sc-11384)
Anti-CKS1 (FL-79)	Full-length of human CKS1	Rabbit polyclonal	IB→1:1000	Santa Cruz Biotech. (sc-6238)
Anti-p53 (FL-393)	Full-length of human p53	Rabbit polyclonal	IB→1:1000	Santa Cruz Biotech. (sc-6243)
Anti-p21^{CIP1}	Amino acids 1-150 of human p21^{CIP1}	Mouse monoclonal	IB→1:1000	BD transduction laboratories. (C-24420)
Anti-CDK2 (M2)	C-terminus of the human CDK2	Rabbit polyclonal	IB→1:1000 IP→2µg	Santa Cruz Biotech. (sc-163)
Anti-CDK1 (Cdc2 p34 19)	Central region (224-230 aa) of human CDK1	Mouse monoclonal	IB→1:500 IP→2µg	Santa Cruz Biotech. (sc-54)
Anti-Cyclin A (H-432)	Full-length of human cyclin A2	Rabbit polyclonal	IB→1:1000 IP→2µg	Santa Cruz Biotech. (sc-751)
Anti-Cyclin E (HE12)	Full-length of human cyclin E1	Mouse monoclonal	IB→1:500	Santa Cruz Biotech. (sc-247)
Anti-His tag (H-15)	Hexahistidine (His_6) tag	Rabbit polyclonal	IB→1:1000	Santa Cruz Biotech. (sc-803)
Anti-α-Tubulin (H-300)	Amino acids 149-448 of human α-tubulin	Rabbit polyclonal	IB→1:1000	Santa Cruz Biotech. (sc-5546)
Anti-γ-Hemoglobin (51-7)	Full-length of human γ-Hemoglobin	Mouse monoclonal	IB→1:500	Santa Cruz Biotech. (sc-21756)

Alternatively, after washing with non-denaturing lysis buffer, Dynabeads-protein G-immunocomplexes were additionally washed twice with 1ml of kinase buffer [50 mM Hepes-NaOH pH7.2, 150 mM NaCl, 10 mM $MgCl_2$, 2.5 mM EGTA, 1 mM EDTA, 1 mM dithiothreitol (DTT), 10% glycerol (v/v), 10 mM β-glycerophosphate and 10 mM NaF] and resuspended in 40 µl of kinase buffer supplemented with 50 µM ATP. 1 µg of recombinant His_6-p27 purified from bacteria (see Section 3.6.5) per immunoprecipitation was used as substrate for kinase assay. The kinase reaction was incubated for 30 min at 30ºC and stopped by addition of 10 µl 5X SDS-PAGE loading buffer to the reaction mixture. Samples were then heated at 95ºC for 5 min and subjected to SDS-PAGE and immunoblot analysis with anti-p-p27(Thr187) (rabbit polyclonal, Invitrogen) first and with anti-p27 (mouse monoclonal, BD Transduction Labs.) later. Immunoblots were scanned in different channels (680 and 700 nm) in an Odyssey scanner. Relative kinase activity was determined by densitometry analysis using the image J software and represented as the percentage of $p27^{p\text{-}Thr187}$ signal with respect to total p27 signal.

3.6.3. Gel filtration chromatography of total protein extracts

To analyze p27 complexes in Kp27MER cells we used gel filtration chromatography of total protein extracts followed by immunoblot analysis of chromatography fractions. For gel filtration chromatography, cells (~10^7 cells per chromatography) were harvested at 1,500 rpm for 5 min; washed once with 1ml PBS; resuspended in 200-300 µl of non-denaturing chromatography lysis buffer [50 mM Hepes-NaOH pH7.2, 150 mM NaCl, 0.5% Triton X-100 (v/v), 10% glycerol (v/v), 1 mM EDTA, 2,5 mM EGTA, 1 mM DTT, 1 mM PMSF, supplemented (1:100) with protease inhibitor cocktail (Calbiochem)] and incubated on ice for 30 min. Then, the cell lysate was clarified by centrifugation at 14,000 rpm for 20 min and protein concentration was determined by the Bradford method using the Bio-Rad protein assay (Bio-Rad). Protein concentration was adjusted to 10 mg/ml with non-denaturing chromatography lysis buffer.

2 mg of total protein extract (~200 µl) were directly applied onto a Superdex 200 10/300 GL column (GE Healthcare) pre-equilibrated with chromatography buffer [50 mM Hepes-NaOH pH7.2, 150 mM NaCl, 0.05% Triton X-100 (v/v), 1 mM EDTA, 2,5 mM EGTA, 1 mM DTT, 10% glycerol (v/v) and 1 mM PMSF] and subjected to fast-performance liquid chromatography in an ÄKTA purifier apparatus (GE Healthcare) with a flow rate of 0.4 ml/min at 4°C. The protein complexes eluting from the column with different volume retentions according to their native molecular size were fractionated in 500 µl fractions. 40 µl of each collected fraction were mixed with 10 µl of 5X SDS-PAGE loading buffer and subjected to SDS-PAGE and immunoblot as previously indicated. Ferritin (443 kDa), catalase (232 kDa), BSA (67 kDa), ovalbumin (45 kDa) and chymotrypsin (25kDa) were used as molecular mass standards for gel filtration.

3.6.4. Immunofluorescence analysis and fluorescence microscopy

For immunofluorescence assays, approximately 5 x 10^4 Kp27MER cells (treated for 24 h with $ZnSO_4$ and/or 4HT) were spun onto slides at 600 rpm for 3 min by using a cytocentrifuge.

Cells were then fixed for 15 min with PBS-3.7% paraformaldehyde (w/v), washed once for 5 min with PBS-100 mM glycine and permeabilized with PBS-0.5% Triton X-100 (v/v)-1% BSA (w/v) for another 30 min at room temperature. Fixed and permeabilized cells were incubated overnight at 4°C in a wet chamber with 50 µl of primary antibodies [rabbit polyclonal anti-SKP2 (sc-7164) and mouse monoclonal anti-p27 antibody (BD Transduction Labs.)] diluted 1:100 in PBS-0.05% Tween 20 (v/v).

The next day, cells were washed 3 times with PBS-1% BSA (w/v) and incubated for an additional hour with 50 µl of 1:100 diluted fluorescent secondary antibodies [rhodamine conjugated anti-mouse or fluorescein isothiocyanate (FITC) conjugated anti-rabbit (Jackson ImmunoResearch Laboratories)] in a wet dark chamber at room temperature. Finally, the slides were washed again with PBS-1% BSA for 3 times and mounted with anti-fading Vectashield mounting medium (Vector Laboratories) with 4',6'-diamidino-2-phenylindole dihydrochloride (DAPI) to stain nuclei. Cells were covered with a coverslip and sealed with nail polish.

The immunostained cell samples were examined using a Zeiss Axio Imager M1 up-right microscope equipped with 20X and 40X Plan-Apochromat objectives, an HBO mercury lamp and different fluorescent filter Sets for DAPI, FITC and Rhodamine fluorescent dyes (Set 49 for DAPI/UV; Set 38 HE for FITC and set 43 for Rhodamine). 20X or 40X images were captured using an AxioCam MRm digital CCD camera and edited with the Zeiss Axio Vision 4.7 software.

3.6.5. Expression and purification of His_6-p27 protein from *E. coli* cells

For His_6-p27 protein purification, *E. coli* C41 bacteria carrying the pET28-His_6-p27 vector were grown in 1 liter of LB medium supplemented with 50 µg/ml kanamycin at 37ºC and 160 rpm in an orbital shaking incubator. When the culture reached mid-log phase (A_{600nm}=~0.8), protein expression was induced with 1 mM Isopropyl β-D-1-thiogalactopyranoside (IPTG) and cells were allowed to grow for another 4 hours following induction. The cells were then harvested by centrifugation at 6,000 rpm for 20 min at 4 °C using an Avanti J-30I centrifuge (Beckman-Coulter), washed once with ice-cold PBS and cell pellet was frozen in dry ice and stored at -70ºC until cell lysis.

For cell lysis, the bacterial cell pellet was resuspended in 20 ml Lysis buffer [50 mM Hepes-NaOH pH7.2, 100 mM NaCl, 0.5 % Triton X-100 (v/v), 0.2 mg/ml lysozime, 5 mM benzamidine, 1 µg/ml pepstatin, 1mM PMSF and protease inhibitor cocktail (Sigma-Aldrich)], incubated on ice for 20 min and then sonicated with a Hielscher UP50H ultrasonic homogenizer at maximum settings (100% amplitude and constant cycle) in an ice-water bath. The cell lysate was cleared of cell debris by centrifugation at 40,000 *g* for 30 min at 4°C using an Optima XL-100K ultracentrifuge (Beckman-Coulter) equipped with a 50Ti rotor.

The His_6-p27 protein was then purified from the soluble protein extract using Nickel affinity chromatography at room temperature. The cleared lysate was loaded in a Protino® Ni^{2+}-TED 2000 Packed Column (Macherey-Nagel), pre-equilibrated with Ni^{2+}-whasing buffer (Ni-W) [50 mM Hepes-NaOH pH7.2, 100 mM NaCl, 0.05 % Triton X-100 (v/v)], and the column was washed three

times with 10 ml of the same buffer (Ni-W). After washing the bound protein was eluted with 8 ml of Ni-elution buffer (Ni-E) [50 mM Hepes-NaOH pH7.2, 100 mM NaCl, 5 mM benzamidine, 1 mM PMSF, containing an imidazole-gradient (10-250 mM imidazole)] and collected in 8 fractions of 1ml each one (Figure 3.1A). The fractions containing the majority of the protein (160-250 mM imidazole) were pooled and diluted with 5 volumes of elution buffer without imidazole and then the protein solution was concentrated using an Amicon Ultra 10K ultrafiltration device (Amicon®, Millipore) to a final volume of 500 µl following the manufacturer's instructions (1hour at 4,000 rpm in a swinging-bucket rotor).

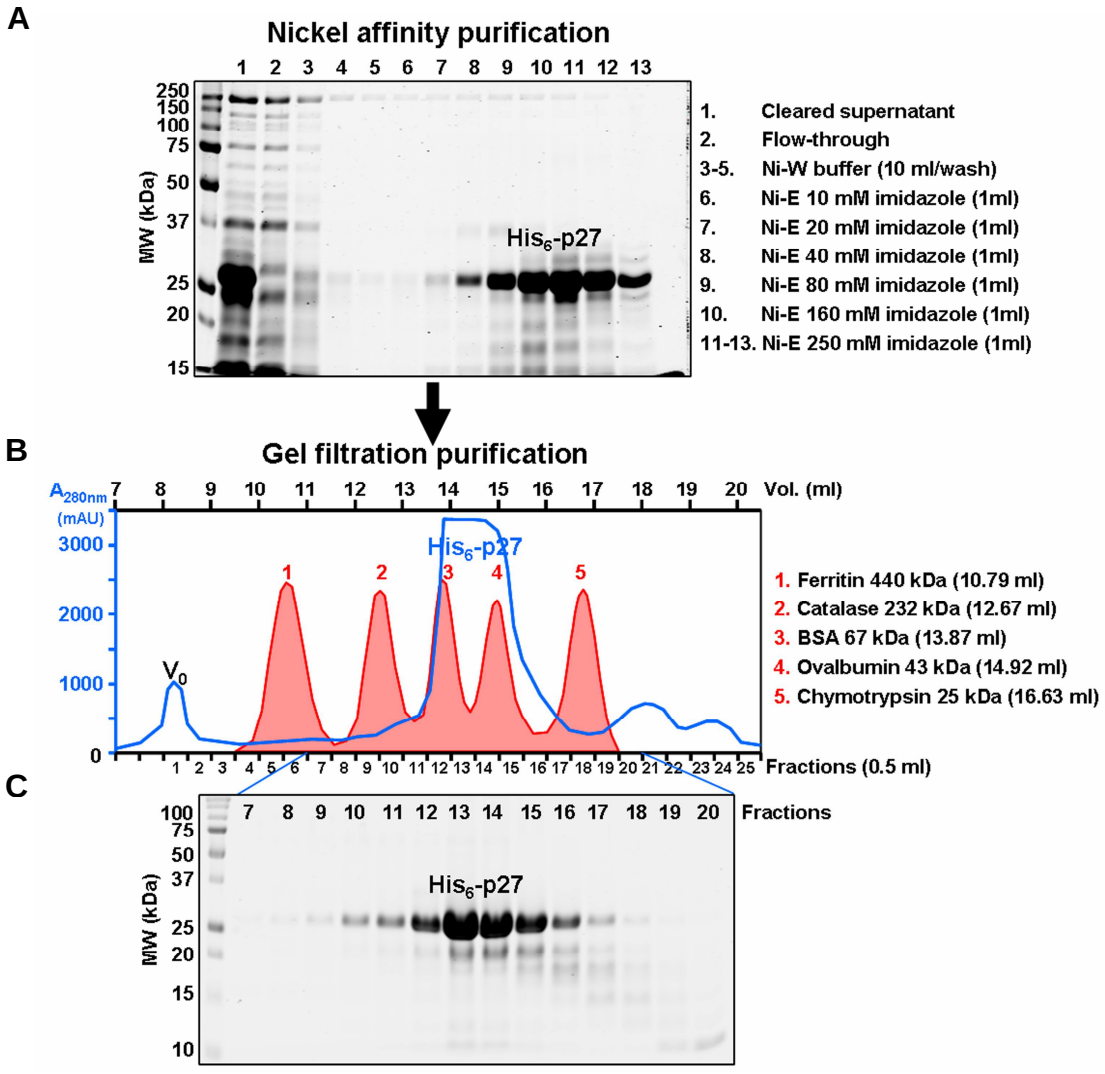

Figure 3.1. Purification process of His_6-p27 protein. A) Nickel affinity purification. B) Gel filtration purification. V_0 = Void Volume (the elution volume of non-retained proteins that are excluded from the gel filtration). C) SDS-PAGE of protein containing fractions. Similar results were achieved for the GST-p27 protein.

Finally, the concentrated protein (500 µl) was loaded on a Superdex 200 10/300 GL column (GE Healthcare, Piscataway, NJ) equilibrated with chromatography buffer [50 mM Hepes-NaOH pH7.2, 100 mM NaCl, 1 mM EDTA, 1 mM DTT, 1 mM PMSF and 10 % glycerol (v/v)] and subjected to Size exclusion chromatography (Figure 3.1B) using an ÄKTA purifier apparatus (GE

Healthcare). The fractions containing the His_6-p27 protein were pooled, supplemented up to 20% glycerol (v/v) and stored at -70°C until use. Protein concentration was determined using the Bio-Rad Protein-Assay (Bio-Rad) as previously described. Every purification step was evaluated by SDS-PAGE to assess the purification process as shown in figure 3.1A and C.

3.6.6. Expression and purification of GST-p27 protein from *E. coli* cells

For GST-p27 protein purification, *E. coli* C41 bacteria containing the pGEXKG-p27 vector (Taules*, et al.*, 1999) were grown in 1 liter of LB medium supplemented with 100 µg/ml ampicillin at 37ºC and 160 rpm in an orbital shaking incubator. When the culture reached mid-log phase (A_{600nm}=~0.8), GST-p27 protein expression was induced with 1 mM IPTG and cells were allowed to grow for another 4 hours. The cells were then harvested by centrifugation at 6,000 rpm for 20 min at 4 °C using an Avanti J-30I centrifuge (Beckman-Coulter), washed once with ice-cold PBS and cell pellet was frozen in dry-ice and stored at -70ºC until cell lysis.

For cell lysis, the cell pellet was resuspended in 20 ml GST Lysis buffer [50 mM Tris-HCl pH8, 100 mM NaCl, 0.5 % Triton X-100 (v/v), 0.2 mg/ml lysozime, 5 mM benzamidine, 1µg/ml pepstatin, 1mM PMSF and protease inhibitor cocktail (Sigma-Aldrich)], incubated on ice for 20 min and then sonicated with a Hielscher UP50H ultrasonic homogenizer at maximum settings (100% amplitude and constant cycle) in an ice-water bath. The cell lysate was cleared of cell debris by centrifugation at 40,000 *g* for 30 min at 4 °C using an Optima XL-100K ultracentrifuge (Beckman-Coulter) equipped with a 50Ti rotor.

The fusion GST-p27 protein was then purified from the soluble protein extract by glutathione-affinity chromatography. For this purpose, the cleared lysate was incubated at 4ºC for 1 hour with 1 ml of pre-equilibrated Glutathione Sepharose 4B resin (GE Healthcare) with rotation. The loaded resin was then packed by gravity force into a Poly-Prep chromatography column (Bio-Rad) and washed three times with 10 ml of GST-washing buffer [50 mM Tris-HCl pH8, 100 mM NaCl, 0.05 % Triton X-100 (v/v)]. After washing step the bound protein was eluted from the column with 8 ml of GST elution buffer (50 mM Tris-HCl pH8, 100 mM NaCl, 20 mM reduced glutathione, 5 mM DTT and 1 mM PMSF) and collected in 8 fractions of 1ml each one. The fractions containing the majority of the protein were pooled and then the protein solution was concentrated using an Amicon Ultra 30K ultrafiltration device (Amicon®, Millipore) to a final volume of 500 µl following the manufacturer's instructions (1hour at 4,000 rpm in a swinging-bucket rotor).

Finally, the concentrated protein (500 µl) was loaded on a Superdex 200 10/300 GL column pre-equilibrated with chromatography buffer and subjected to Size exclusion chromatography using an ÄKTA purifier apparatus (GE Healthcare) in the same conditions as for His_6-p27 purification. The peak fractions containing the GST-p27 protein were pooled; glycerol was added to 20% (v/v) final concentration and stored at -70°C until use. Protein concentration was determined using the Bio-Rad Protein-Assay (Bio-Rad).

4. RESULTS

4. RESULTS

4.1. THE MYC-SKP2 INTERACTION

4.1.1. Induction of MYC is associated to induction of SKP2

We set out to determine the molecular mechanism of p27 down-modulation induced by MYC in the Kp27MER model. In this model, the exogenous p27 expression is induced by activating the metallothionein promoter with zinc (Zn^{2+}). Therefore the model is mainly suited to study the MYC effect on p27 levels by posttranscriptional mechanisms. It had been described that MYC could stimulate proteasome-mediated degradation of p27 through the induction of CUL1 (O'Hagan*, et al.*, 2000) and CKS1 (Keller*, et al.*, 2007), both components of the SCF^{SKP2} complex which targeted p27 for degradation by the ubiquitin-proteasome system. Thus, we decided to analyze CUL1 and CKS1 protein expression by immunoblot in Kp27MER cells treated for 24 hours with 50 μM $ZnSO_4$ and/or 200 nM 4HT. As shown in figure 4.1, we did not found significant changes in CUL1 or CKS1 protein expression 24 hours after MYCER activation in presence of p27. Therefore, none of the mechanisms reported to date could explain the p27 downregulation induced by MYCER activation in the Kp27MER model.

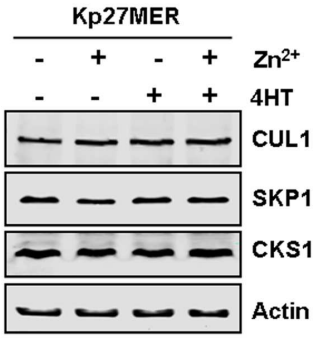

Figure 4.1. MYC has no effect on CUL1 and CKS1 protein expression in Kp27MER cell line. Kp27MER cells were treated for 24 h with 50 μM $ZnSO_4$ and/or 200 nM 4HT and then subjected to immunoblot analysis against CUL1, SKP1, CKS1 and actin (loading control) as indicated.

Previous studies of large-scale gene expression analysis with microarray-based gene profiling in Kp27MER cells showed that MYC blocked the up-regulation of several transcription factors with a pivotal role in erythropoiesis, such as NFE2, JUNB, and GATA1, induced in presence of high levels of p27 (Acosta*, et al.*, 2008). A subsequent analysis of the microarray data revealed that one of the genes up-regulated by MYC in proliferative arrest conditions was *SKP2*. *SKP2* encodes for the F-box component of the SCF^{SKP2} ubiquitin ligase complex which, together with CUL1 and CKS1, mediated p27 degradation by the proteasome system (see “Introduction”, section 1.2.4.2.). Therefore, SKP2 appeared to be a good candidate to explain the p27 down-modulation induced by MYC in Kp27MER cells. Nevertheless, no functional interaction between MYC and SKP2 had been previously reported although they shared the expression pattern during cell cycle. Both proteins showed low expression at G1-phase and were up-regulated when entered in S-phase. To rule out the possibility that SKP2 up-regulation could be due to cell cycle progression induced by MYC, we decided to study anew SKP2 mRNA, but also protein

expression in response to MYC in Kp27MER cells in proliferative arrest conditions. To evaluate the proliferative arrest we determined the growth curves during 3 days by counting viable cells. SKP2 expression was analyzed by RT-qPCR and immunoblot. As shown in figure 4.2, induction of high levels of p27 with 75 µM of $ZnSO_4$ resulted in rapid growth arrest of Kp27MER cells (Figure 4.2A) and it was accompanied of *SKP2* mRNA down-regulation (Figure 4.3B), as predicted. Interestingly, MYC activation (by 4HT treatment) in presence of p27, resulted in a two-fold increase in *SKP2* mRNA expression but did not modify the growth arrest mediated by p27, confirming previous results (Figure 4.2B, black bar). Nonetheless, the activation of MYC alone in Kp27MER cells resulted in a modest *SKP2* mRNA up-regulation. It should be noted that Kp27MER cells already express high levels of endogenous MYC. In contrast to MYCER-expressing cells, 4HT did not modify SKP2 expression in Kp27-5 cells (used here as negative control), in which p27 is induced by Zn^{2+} but do not carry the MYCER allele (Figure 4.2B). This result was also observed at the protein level. MYC activation resulted in a robust up-regulation of SKP2 protein 24 and 48 hours post-induction, as detected by immunoblot (Figure 4.2C, compare lanes 1 vs. 2; 3 vs. 4). The immunoblot also showed down-regulation of endogenous MYC subsequent to ectopic MYCER activation. This well-known effect of ectopic MYC overexpression (Grignani*, et al.*, 1990; Penn*, et al.*, 1990) confirmed MYCER activation by 4HT. These results suggested that MYC was playing a direct role in SKP2 up-regulation in Kp27MER cells independently of the proliferative state of the cells, suggesting that SKP2 up-regulation was not a consequence of MYC-induced proliferation.

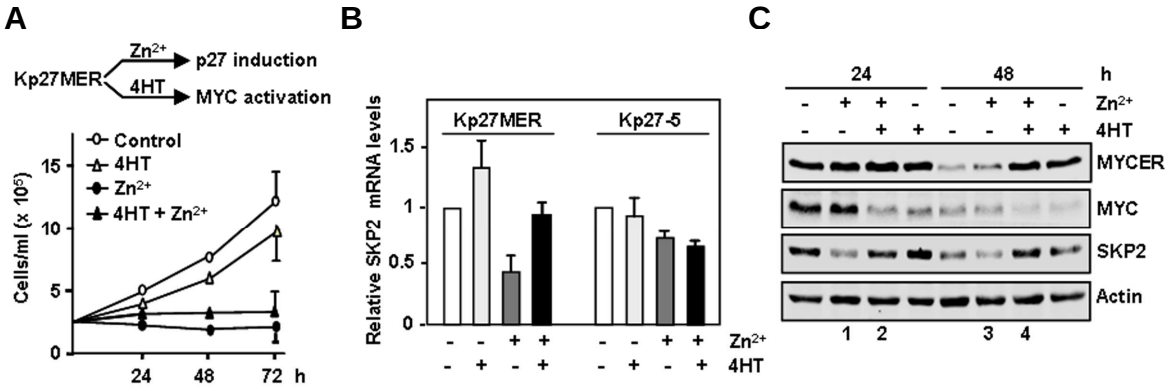

Figure 4.2. SKP2 induction by MYC in Kp27MER cells growth-arrested by p27. A) The Kp27MER cell model is summarized at the top. Proliferation rates of Kp27MER cells treated with 200 nM 4HT and/or 75 µM $ZnSO_4$ were measured by counting viable cells in an hemocytometer over 3 days (bottom panel). B) *SKP2* mRNA expression in Kp27MER and parental Kp27-5 cells. The cells were treated for 12 h with 200 nM 4HT and 50 µM $ZnSO_4$, and mRNA expression was determined by RT-qPCR. C) Immunoblot showing SKP2 up-regulation in response to MYCER in Kp27MER cells treated for 24 and 48 hours with 200 nM 4HT and 50 µM ZnSO4 as indicated. Immunoblot also shows endogenous MYC down-modulation after MYCER activation with 4HT.

To confirm that the effect on SKP2 up-regulation was independent of cell proliferation induced by MYC, we decided to study the MYC-SKP2 relationship in other cell models in which ectopic MYC expression could be also activated or induced in proliferative arrest conditions.

The K562 cell line derived from a chronic myeloid leukemia (CML) patient in blast crisis (Lozzio and Lozzio, 1975) and these cells express the BCR-ABL tyrosine kinase fusion protein. Our group had previously described that K562 cells treated with low concentrations of imatinib (1 μM), a selective BCR-ABL inhibitor, underwent a rapid MYC down-regulation and a reversible proliferative arrest (Gomez-Casares*, et al.*, 2004). Thus, we decided to treat KMER4 cells, another K562 derived cell line carrying only the activatable MYCER protein (Albajar*, et al.*, 2011), with 1 μM imatinib and to test the MYC effect on SKP2 expression. As shown in figure 4.3, imatinib treatment led to down-regulation of endogenous MYC protein, as detected by immunoblot (Figure 4.3C) and resulted in a proliferative arrest of KMER4 cells (Figure 4.3A) as anticipated. In addition, this treatment also led to SKP2 mRNA and protein down-regulation (Figure 4.3B and C respectively). However, MYC activation with 4HT in presence of imatinib did not rescue the proliferation arrest mediated by this drug (Figure 4.3A) but resulted again in a two-fold induction of SKP2 mRNA (Figure 4.3B) and protein (Figure 4.3C, compare lanes 1 vs. 2; 3 vs. 4). It is interesting to mention that, although BCR-ABL was previously reported to induce SKP2 expression (Andreu*, et al.*, 2005; Chen*, et al.*, 2009), ectopic MYC up-regulated SKP2 in arrested cells with inhibited BCR-ABL.

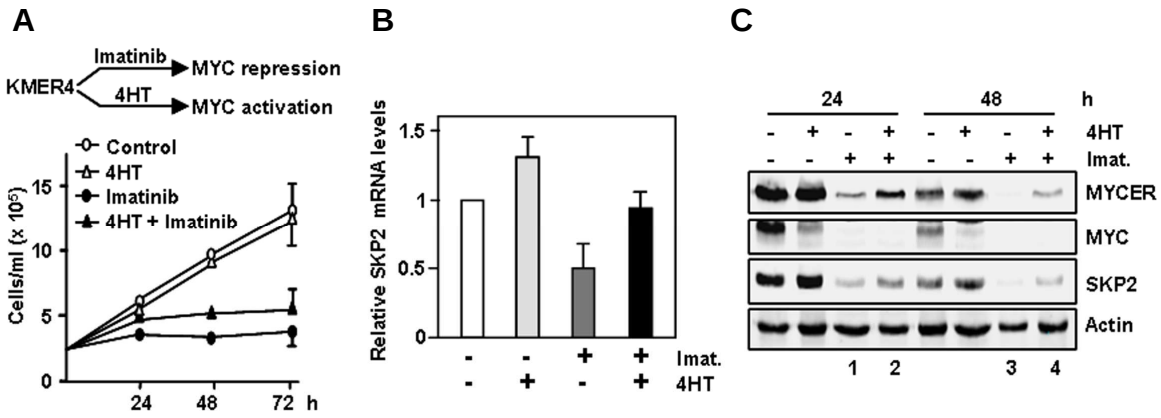

Figure 4.3. SKP2 induction by MYC in KMER4 cells growth-arrested with imatinib. A) The KMER4 cell model is summarized at the top. Proliferation rates of KMER cells treated with 1μM imatinib and 200 nM 4HT over 3 days (bottom panel). B) KMER4 cells were treated with 1μM imatinib and 200 nM 4HT (24 h), and *SKP2* mRNA levels were determined by RT-qPCR. C) KMER4 cells were treated with imatinib and 4HT as indicated, and the levels of SKP2, MYC, MYCER, and actin (loading control) in total cell lysates were assayed by immunoblot.

In a second model, we used a different MYC-inducible K562 cell line (KMYCJ cells) (Delgado*, et al.*, 1995) in presence of 12-0-tetradecanoylphorbol-13-acetate (TPA). The KMYCJ cell line bears a $ZnSO_4$-inducible *MYC* allele controlled by the metallothionein promoter (Grignani*, et al.*, 1990), the same as for p27 in Kp27MER cells. On the other hand, just like imatinib, the phorbol ester TPA also inhibited proliferation of K562 cells (Lerga*, et al.*, 1999) and this was accompanied by MYC downregulation (Delgado*, et al.*, 1995). However, unlike the reversibility of imatinib effect, a just 30 min treatment with 10 nM TPA produced an irreversible proliferative arrest of K562 cells (Lerga*, et al.*, 1999).

As anticipated, treatment of KMYCJ cells with 10 nM TPA resulted in growth arrest (Figure 4.4A) and a patent MYC down-regulation (Figure 4.4C). In addition, TPA also induced a marked down-regulation of SKP2 at mRNA (Figure 4.4B) and protein (Figure 4.4C) levels. However, MYC induction with 75 μM of $ZnSO_4$ in KMYCJ cells pre-treated for 12 h with 10 nM TPA (when the cells contained very low endogenous MYC levels) resulted in a notable increase in SKP2 mRNA, as assessed by RT-qPCR (Figure 4.4D), and protein, as determined in immunoblot (Figure 4.4E). It should be noted again that MYC induction did not rescue cells from TPA-induced growth arrest (Figure 4.4A), confirming previous results (Lerga*, et al.*, 1999). The results were similar when we used a different MYC-inducible K562 clonal cell line (KMYCB) (not shown).

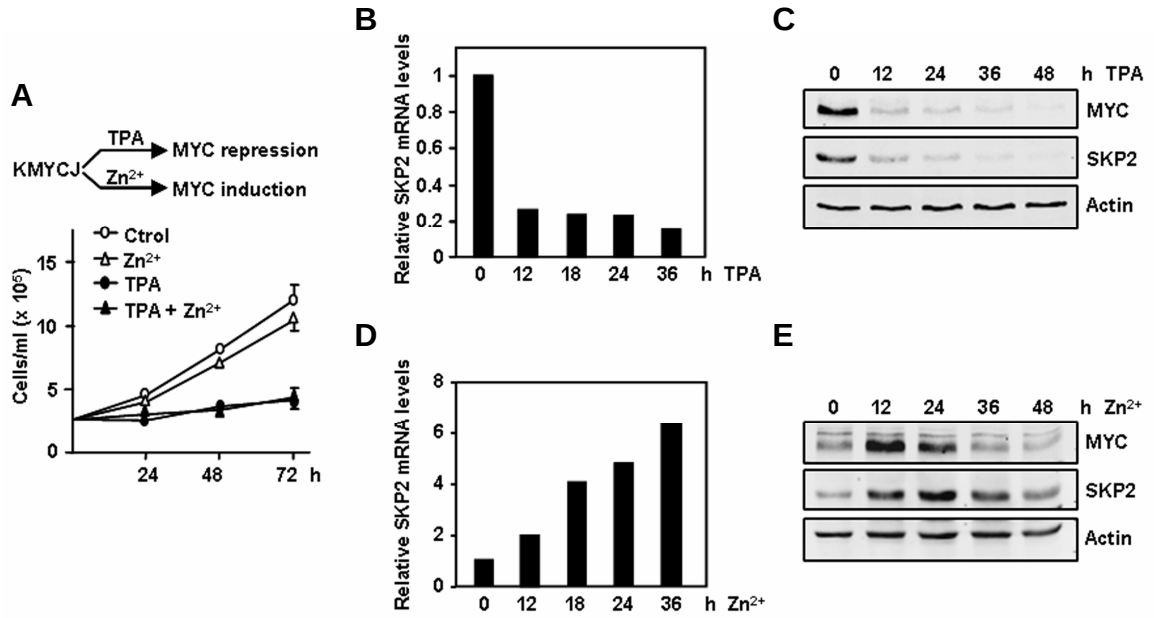

Figure 4.4. SKP2 induction by MYC in KMYCJ cells growth-arrested with TPA. A) The KMYCJ cell model is summarized at the top. Proliferation rates of KMYCJ cells treated with 10nM TPA and/or 75 μM $ZnSO_4$ were measured by counting viable cells in an hemocytometer over 3 days (bottom panel). B) KMYCJ cells were treated with 10 nM TPA for the indicated times and *SKP2* mRNA levels were determined by RT-qPCR. C) KMYCJ cells were treated as in B, and expression of SKP2, endogenous MYC, and actin (loading control) were assayed by immunoblot. D) KMYCJ cells were pre-treated with 10 nM TPA for 12 h and then induced with 75 μM $ZnSO_4$ as indicated. *SKP2* mRNA levels were determined by RT-qPCR. E) KMYCJ cells were pre-treated as in D, and expression of SKP2, exogenous MYC (induced by 75 μM $ZnSO_4$), and actin (loading control) were assayed by immunoblot.

Finally, we assayed SKP2 induction by MYC in the KMYCBp53 cell line (Ceballos*, et al.*, 2000). This cell line had been previously developed in our laboratory to study the functional interaction between MYC and p53. KMYCBp53 cells carried a Zn^{2+}-inducible *MYC* transgene similar to KMYCJ cells. In addition, these cells also carried a constitutively expressed $p53^{Val35}$ mutant which adopted an active conformation at 32ºC but not at normal cell culture conditions of 37ºC. As shown in figure 4.5, p53 activation at 32ºC resulted in an irreversible proliferative arrest (Figure 4.5A), as expected. This was accompanied of endogenous MYC down-regulation as shown by immunoblot (Figure 4.5C). p53 activation also resulted in a down-modulation of SKP2 mRNA and protein (Figure 4.5B and C respectively). Once again, MYC induction with Zn^{2+} did not

antagonize the p53-mediated proliferative arrest (Figure 4.5A), but it provoked a concomitant increase of SKP2 mRNA (Figure 4.5B) and protein (Figure 4.5C). As control of p53 activation, we assayed the p21 expression by immunoblot (Figure 4.5C).

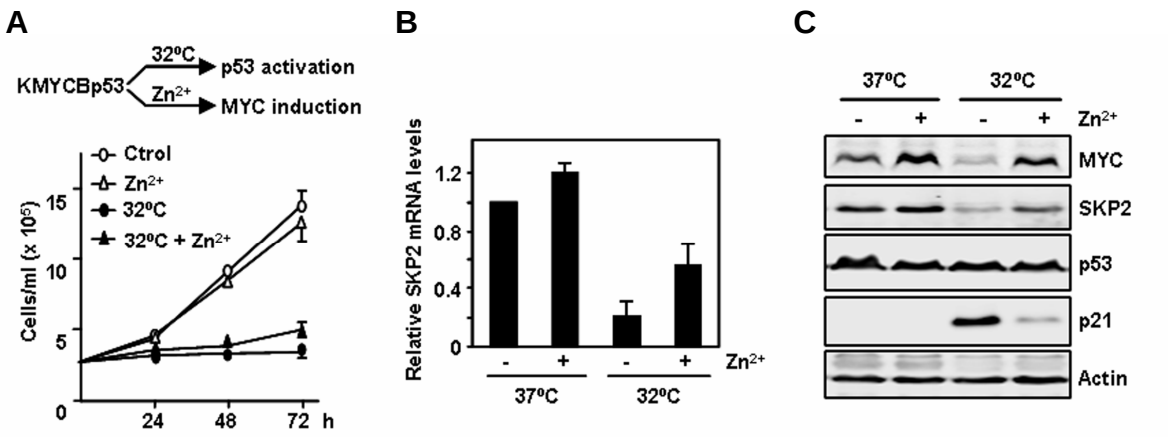

Figure 4.5. SKP2 induction by MYC in KMYCBp53 cells growth-arrested by p53. A) The KMYCBp53 cell model is summarized at the top. Proliferation rates of KMycBp53 cells treated with 75 μM $ZnSO_4$ and incubated at 37 or 32 °C were measured by counting viable cells in an hemocytometer over 3 days (bottom panel). B) KMYCBp53 cells were incubated at 37 or 32 °C, with or without $ZnSO_4$ for 24 h. *SKP2* mRNA levels were determined by RT-qPCR. C) KMYCBp53 cells were treated as in B, and the levels of SKP2, MYC, and actin (loading control) in total cell lysates were assayed by immunoblot.

In summary, in the four models tested, the methods used to inhibit proliferation (p27 induction, imatinib or TPA treatment and p53 activation) promoted the down-regulation of endogenous MYC and SKP2 expression. However, the induction or activation of MYC in these proliferative arrest conditions promoted the up-regulation of SKP2 at mRNA and protein levels. Therefore, we concluded that the induction of SKP2 in the four models studied was independent of the MYC effect on cell proliferation.

4.1.2. SKP2 is down-regulated in response to *MYC* silencing or repression

The above results strongly suggested that *SKP2* could be a MYC target gene as it was induced by MYC in proliferative arrest conditions. To confirm this possibility, next we asked whether SKP2 was down-regulated in response to MYC down-modulation. For this purpose, we used three different experimental models. First, we assessed SKP2 expression after direct *MYC* silencing in K562 cells. K562 cells were nucleofected with a vector (pRSshMYC) codifying a short hairpin directed to the third exon of *MYC* mRNA (Bernard*, et al.*, 2003) or the corresponding empty vector (pRS). *MYC* silencing was confirmed by immunoblot (Figure 4.6A). Interestingly, it was accompanied by SKP2 down-regulation at mRNA and protein levels (Figure 4.6B and A respectively). *MYC* silencing also resulted in down-regulation of B23/nucleophosmin mRNA, a well-known MYC target gene used here as silencing positive control (Zeller*, et al.*, 2001), but not of *SKP1* mRNA, used as negative control (Figure 4.6B). This result suggest that the SKP2 down-

regulation observed in the previously described K562-derived cell models could be due, at least in part, to MYC down-modulation originated by the different treatments.

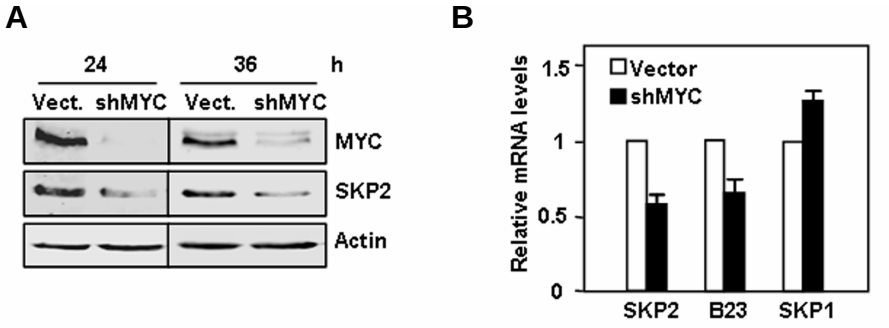

Figure 4.6. SKP2 is down-regulated after *MYC* repression in K562 cells. A) K562 cells were nucleofected with a short hairpin RNA vector for MYC (shMYC) or the empty vector (Vect.), and MYC, SKP2, and actin expression were assayed by immunoblot 24 and 36 h after nucleofection. B) K562 cells were transfected as in A; and 24 h after nucleofection, the levels of *SKP2*, B23/nucleophosmin and *SKP1* mRNA were determined by RT-qPCR.

On the other hand, we had available in the laboratory two different cell lines carrying tetracycline-repressible (tet-off) human *MYC* transgenes: the human lymphoblastoid P493.6 cell line (Pajic*, et al.*, 2000) and the mink lung epithelial TM1 cell line (Warner*, et al.*, 1999). Thus we decided to analyze the SKP2 expression after *MYC* repression with doxycycline in both cell lines. As shown in figure 4.7, doxycycline treatment led to rapid *MYC* down-regulation accompanied by a simultaneous down-regulation of SKP2 at protein level (Figure 4.7A and C) in both cell lines. In P493.6 cells, *SKP2* down-regulation was also tested at mRNA level (Figure 4.7B). Based on these findings, we suggested that the MYC-SKP2 interaction was not specific of the K562 cell model and it could be extended to other human tissues or animal species.

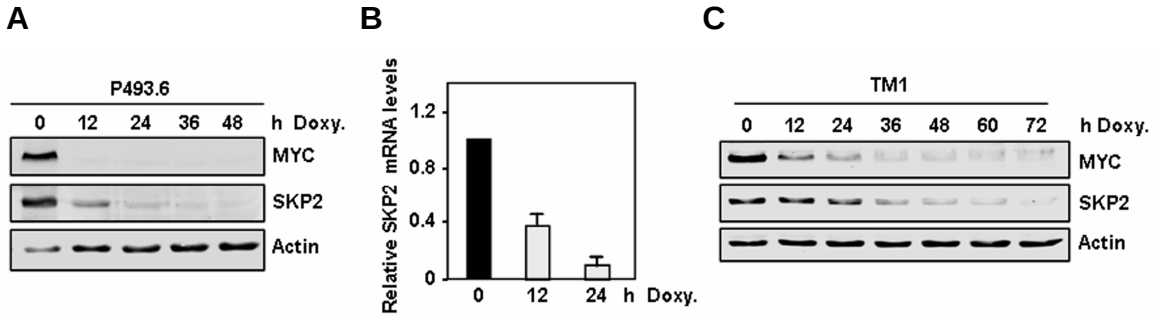

Figure 4.7. SKP2 is down-regulated after MYC repression in lymphoid and epithelial cells. A) Human lymphoid P493.6 cells were treated with 1 µg/ml doxycycline (Doxy.) for the indicated times, and SKP2, MYC, and actin (loading control) expression were assayed by immunoblot. B) P493.6 cells were treated as in A, and *SKP2* mRNA expression was determined by RT-qPCR. C) TM1 cells were treated with 2 µg/ml doxycycline to repress *MYC* for the indicated times, and SKP2, MYC, and actin expression were determined by immunoblot.

Finally, we decided to compare the SKP2 expression between a *Myc*-deficient rat fibroblast cell line (HO15.19 cells) and the corresponding parental cell line (TGR-1 cells) (Mateyak*, et al.*, 1997). As shown in figure 4.8A, SKP2 protein levels were much lower although detectable in *Myc*-null cells. In addition, it had been described that MYC (Dean*, et al.*, 1986) and SKP2 protein expression decreased quickly in cultured fibroblasts after growth factors deprivation (Wirbelauer*,*

et al., 2000; Bashir*, et al.*, 2004; Wei*, et al.*, 2004). Thus, we compared SKP2 expression after serum starvation in HO15.19 (*Myc*-null) and TGR-1 cells to determine whether MYC was essential for SKP2 regulation in absence of growth factors. As anticipated MYC and SKP2 were both down-regulated in response to serum deprivation in parental TGR-1 cells (Figure 4.8B left). In contrast there was not a significant down-regulation of SKP2 protein levels in response to serum deprivation in HO15.19 cells (Figure 4.8B right). This result suggested that in absence of MYC, SKP2 did not respond to growth factors deprivation and therefore that MYC was the main mediator of SKP2 induction in serum response. Taken collectively, all these data suggest that MYC was the major regulator of SKP2 expression in cells from different tissues and species.

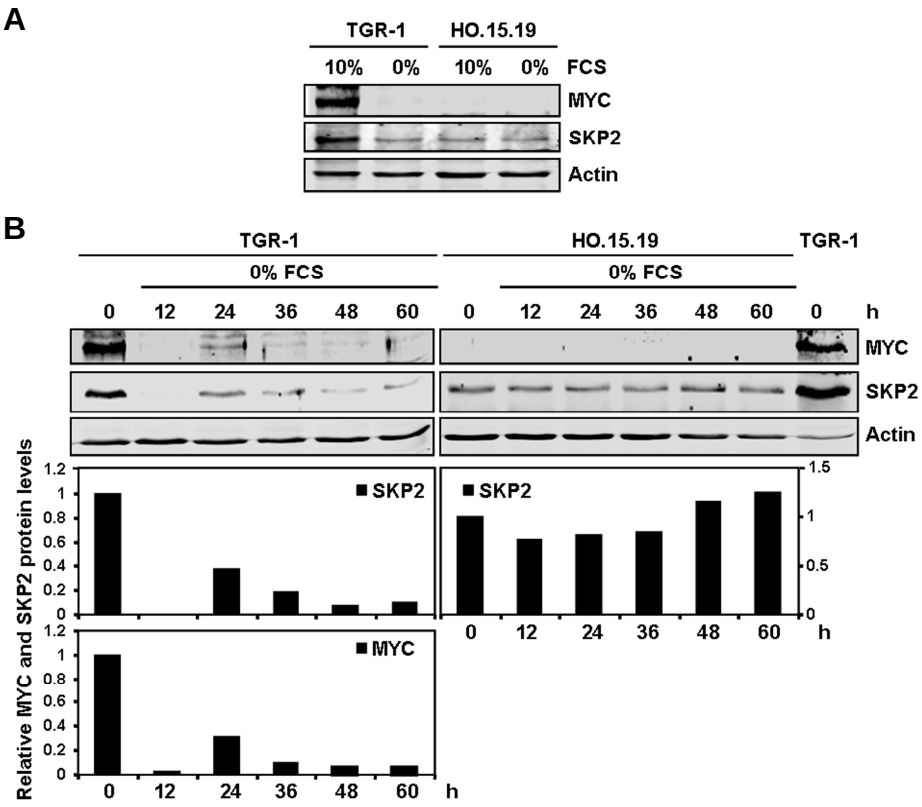

Figure 4.8. SKP2 down-regulation in response to serum deprivation in rat fibroblast but not in *Myc* null cells. A) *Myc*-null HO15.19 and parental TGR-1 rat fibroblasts were analyzed by immunoblot against MYC, SKP2 and actin as loading control. B) TGR1 and *Myc*-null HO15.19 cells were serum-deprived for the indicated times, and SKP2, MYC, and actin expression was analyzed by immunoblot. The bar histograms show the densitometric analysis of SKP2 and MYC immunoblots normalised to the corresponding actin levels using the Image J software.

4.1.3. MYCER induces *SKP2* mRNA expression in the absence of protein synthesis

The previous experiments clearly indicated that MYC was an important regulator of SKP2 expression but they did not confirm that *SKP2* gene was a direct MYC target gene. For this purpose, then we asked whether *SKP2* mRNA was induced by MYC in Kp27MER cells in the presence of cycloheximide (CHX), an eukaryotic protein biosynthesis inhibitor which blocked

translational elongation in the ribosome. In this way we could differentiate whether MYC was directly activating *SKP2* gene transcription or whether *SKP2* expression was indirect and it needed intermediary transcription factors synthesized *de novo*, likely induced by MYC (Watson*, et al.*, 2002). Thus, Kp27MER cells were pre-treated with 10 nM TPA for 12 hours to down-regulate endogenous MYC and then treated with 10 µg/ml CHX together with 75 µM of $ZnSO_4$ (to induce p27) and/or 200 nM 4HT for 6 hours (to activate MYC). CHX effectiveness was confirmed by lack of p27 protein induction in response to Zn^{2+} (Figure 4.9A, compare p27 in lanes 1 and 2 versus lanes 3 and 4 in the absence of 4HT and lanes 5 and 6 versus lanes 7 and 8 in its presence). As predicted, the remaining endogenous MYC protein showed a reduced stability (Figure 4.9A). It had been described that the estimated half-life of MYC was about 30 minutes (Hann and Eisenman, 1984). MYCER was more stable in presence of 4HT (Figure 4.9A, compare MYCER levels in lanes 9 and 10 versus lanes 11 and 12), although the underlying molecular mechanism is unclear. *SKP2* mRNA levels were determined by RT-qPCR (Figure 4.9B). The results showed that activation of MYC with 4HT led to increased *SKP2* mRNA levels even in presence of CHX and thus in the absence protein synthesis. These results strongly suggested that *SKP2* gene was regulated directly by MYC. Both MYC and MYCER protein levels were very low after 6 h of CHX treatment, precluding analysis of *SKP2* mRNA expression at longer treatment times.

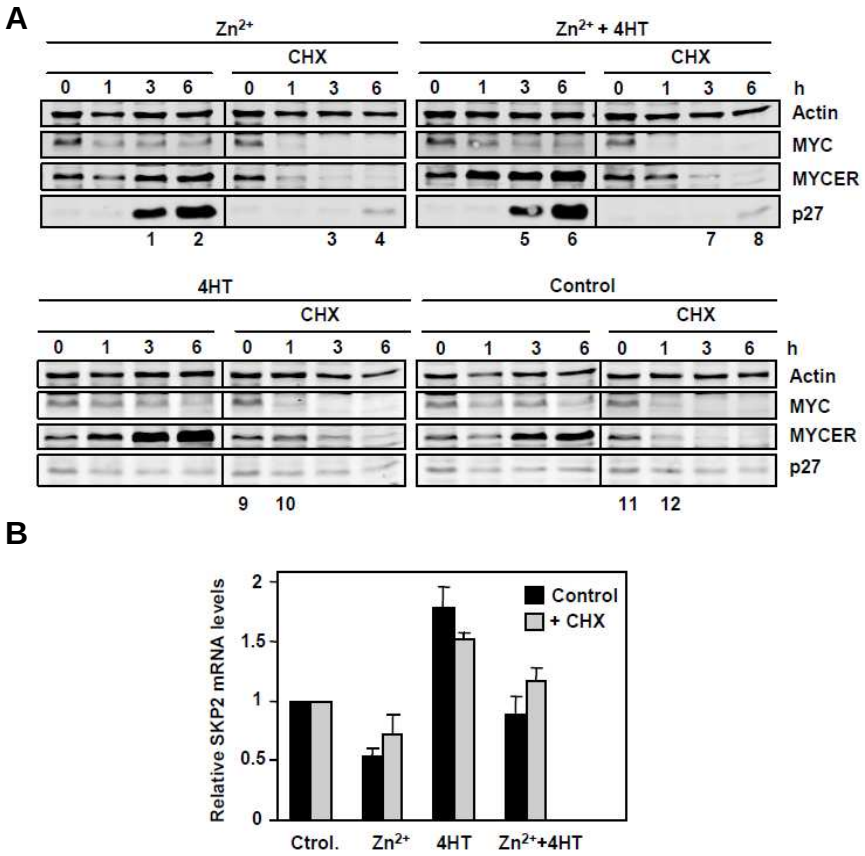

Figure 4.9. MYC induces *SKP2* in the absence of protein synthesis. A) Kp27MER cells were pre-treated for 12 h with 10 nM TPA and then treated with 10 µg/ml cycloheximide (CHX), 4HT, and $ZnSO_4$ for 1–6 h. Expression of p27, MYC, MYCER, and actin were determined by immunoblot. B) *SKP2* mRNA expression was determined by RT-qPCR after 6 h of exposure to CHX, ZnSO4, and 4HT as indicated.

4.1.4. MYC activates and binds to the human *SKP2* promoter

Based on these previous results, it appeared that *SKP2* could be a direct MYC target gene. To confirm this, we carried out two more approaches. First, we tested the ability of MYC to activate the human *SKP2* promoter through promoter-luciferase reporter assays. We transfected KMYCJ cells with a luciferase reporter containing 1148 bp of *SKP2* promoter (Huang and Hung, 2006) or the corresponding empty vector (pGL3-basic) and then we treated these cells for 24 hours with 10 nM TPA to down-regulate endogenous MYC and/or 75 µM of $ZnSO_4$ to induce exogenous MYC expression. The results showed that *SKP2* promoter activity was significantly reduced in TPA-treated cells (Figure 4.10 top panel), consistent with endogenous MYC repression by TPA (Figure 4.4). However, *SKP2* promoter activity was recovered when exogenous MYC was induced by Zn^{2+} (75 µM of $ZnSO_4$) in presence of TPA (Figure 4.10 top panel). As control of the experiment, we used a luciferase reporter bearing four canonical E-boxes (4XEbox-Luc) (Kiessling*, et al.*, 2006), which was also notably activated by MYC (Figure 4.10 bottom panel). The empty luciferase construct and the reporter with four mutated E-boxes (4XEboxMut-Luc) were used for corresponding normalizations. These results clearly showed that the *SKP2* promoter responded to MYC over-expression in K562 cells and strongly suggested that *SKP2* could be a direct MYC target gene.

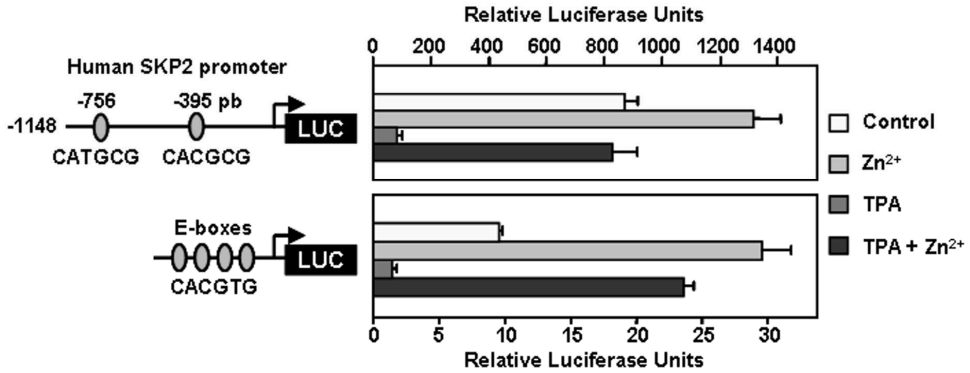

Figure 4.10. MYC activates to the human *SKP2* promoter. KMYCJ cells were electroporated with a luciferase construct containing 1148 bp of *SKP2* promoter (Huang and Hung, 2006) or a 4XE-Box luciferase reporter (Kiessling*, et al.*, 2006) as experimental control. At 12 h post-transfection, the cells were divided into four aliquots and treated with 10 nM TPA to repress endogenous MYC and 75 µM $ZnSO_4$ to induce exogenous MYC. At 36 h post-transfection, the cell lysates were prepared, and *firefly* and *renilla* luciferase activities were determined. SKP2-luciferase data were normalized to the value of cells transfected with the empty vector (pGL3basic-Luc). 4XEbox-Luc data were normalized to the mutated 4XEboxMut-Luc construct. Transfection efficiency was also normalized to *renilla* luciferase activity.

In a second approach we used chromatin immunoprecipitation (ChIP) to analyze *SKP2* promoter occupancy by MYC in K562 cells. To date, ChIP is the only method that provides direct physical evidence of the association of a transcription factor with a specific target gene in the cellular context. Sequence analysis of the human *SKP2* gene revealed two non-canonical E-boxes (CATGCG and CACGCG) in the promoter region (-756 and -395 bp up-stream of the transcription start site respectively) and a canonical E-box (CACGTG) in the second exon (735 pb

down-stream of the TSS). It should be noted that both non-canonical E-boxes have been also described as high affinity sequences for MYC *in vivo* (Grandori*, et al.*, 1996; Kim*, et al.*, 2008). In addition, we also found a conserved CpG island in the *SKP2* promoter. It had been reported an overlapping between these hypomethylated conserved regions and MYC binding sites in the genome (Zeller*, et al.*, 2006). Therefore, we tested several amplicons along *SKP2* gene including these E-boxes and the CpG island to analyze MYC occupancy. The localization of the analyzed amplicons is shown in figure 4.11A.

After cell fixation and DNA sonication (see "Material and Methods", section 3.4.5.) chromatin was immunoprecipitated with a polyclonal antibody against full length MYC protein and then, MYC binding was assessed by qPCR. ChIP demonstrated MYC binding to the promoter region including the two non-canonical E-boxes but not to a canonical E-box located in the second exon (Figure 4.11B left, amplicons C, D and E). MYC binding to the E-box on lactate dehydrogenase A (*LDHA*) promoter (Kim*, et al.*, 2004) was used as ChIP positive control (Figure 4.11B, LDH). As negative controls, we used K562 cells treated with 1 µM imatinib or 10 nM TPA, which inhibit MYC expression as previously described. MYC binding was dramatically reduced after both treatments (Figure 4.11B right). These results definitively confirm that *SKP2* was a new direct MYC target gene.

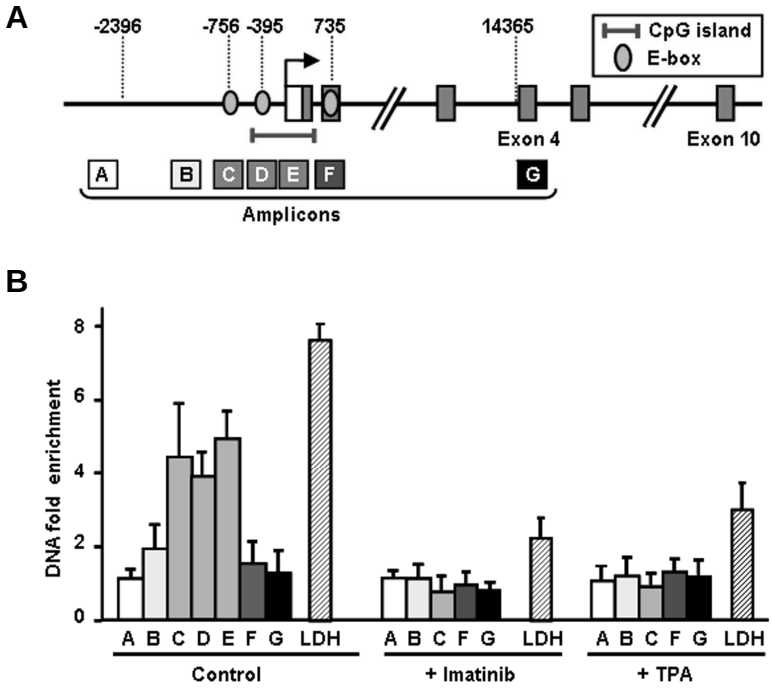

Figure 4.11. MYC binds to the human *SKP2* promoter. A) Scheme of the human *SKP2* gene. Amplicons (boxes A–E) used for ChIP assays are indicated; the E-boxes (ovals) and localization of CpG island are also shown. Coordinates and CpG island are as in the UCSC Genome Browser. B) K562 cells untreated or treated for 12 h with 1 µM imatinib or 10 nM TPA, to down-regulate endogenous MYC, were fixed with 1% formaldehyde and after cell lysis and DNA sonication, chromatin was immunoprecipitated with anti-MYC antibody or rabbit IgG (as negative control of immunoprecipitation). MYC occupancy between amplicons A–E was determined by quantitative PCR. The results are expressed as DNA fold enrichment with anti-MYC antibody with respect to the DNA enrichment with anti-rabbit IgG and normalized to the *input* chromatin signal for each amplicon. Lactate dehydrogenase A (LDH) E-box amplicon was used as positive control (Kim*, et al.*, 2004). The values are the means ±S.E. of three determinations from two (TPA and imatinib) or three (plus control) independent ChIP experiments.

Moreover, while this Thesis was still in progress, the UCSC (The University of California Santa Cruz) Genome Browser (http://genome.ucsc.edu) made public data generated by the ENCODE project (Encyclopedia of DNA Elements) (Dunham*, et al.*, 2012). The data sets included genome-wide ChIP-sequencing data for MYC and several other regulatory elements related to MYC in K562 cells but also in other cell lines. Using these data from Human GRCh37/hg19 assembly and the ChIP-sequencing data sets generated by the Stanford/Yale/USC/Harvard ENCODE study, we corroborated the MYC-binding region to the *SKP2* promoter detected by conventional ChIP in K562 cells but with higher resolution (Figure 4.12). Moreover, the same MYC-binding region was also observed in other cell lines such as NB4 (acute promyelocytic leukemia cells), A549 (Lung carcinoma), HepG2 (Hepatocellular carcinoma cells) and Hela (Cervical carcinoma cells) (not shown). In addition, MAX, the essential dimerization partner of MYC for DNA binding, and the histone acetyl-transferase p300 both immunoprecipitated to the same MYC-binding region in K562 cells (Figure 4.12). These results were consistent with the detection of H3K9ac and H3K27ac (H3 acetylated on Lysine 9 or 27) histone marks on the *SKP2* promoter, both targets of p300 and generally associated with MYC binding regions. These histone ChIP-seq data sets were provided by the Broad Institute. In addition we found that RBBP5, a subunit of MLL1 histone methyltransferase complex, also immunoprecipitated on the *SKP2* promoter correlating with an increase in H3K4me3 histone mark (Figure 4.12).

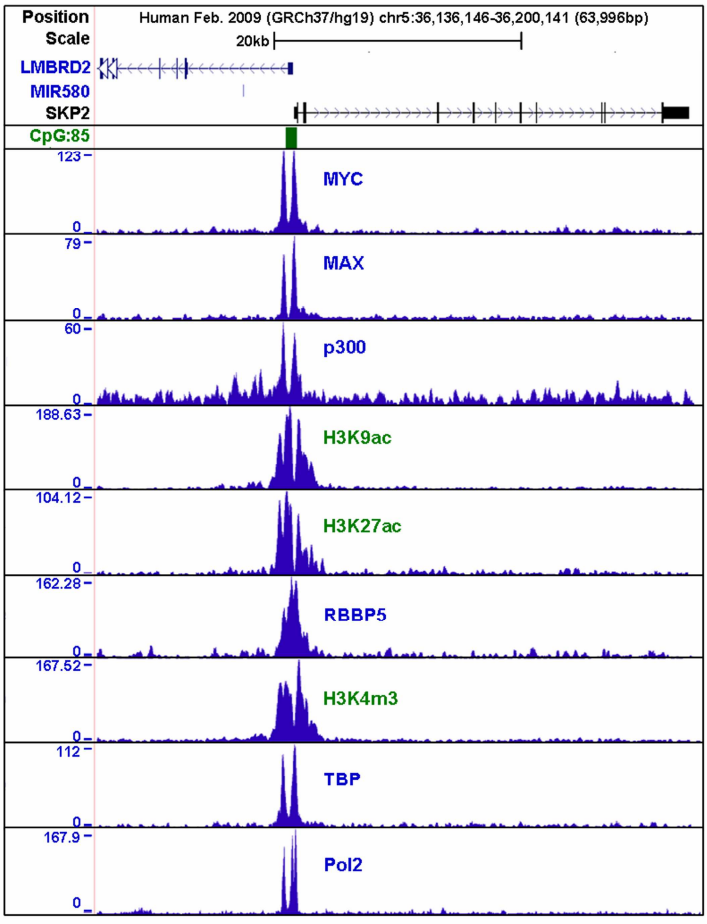

Figure 4.12. MYC binds to the human *SKP2* promoter. ~64 kb genomic window encompassing *SKP2* gene and part of the neighbouring gene *LMBRD2* (chr5:36,136,146-36,200,141) together with ENCODE tracks annotations displayed as shown in the UCSC Genome Browser (Human GRCh37/hg19 assembly, February 2009). The blue density graphs show the signal enrichment based on ChIP-seq processed data for MYC and MAX transcription factors; p300 histone acetyltransferase; RBBP5 subunit of MLL1 histone methyltransferase complex; TATA binding protein (TBP) and RNA polymerase II (Pol2); H3K9ac, H3K27ac and H3K4m3 histone marks on K562 cell line. The two peaks correspond to sequences encompassed by the amplicons C and E of figure 4.11B. Additional details for these annotations are available on (http://genome.ucsc.edu).

Finally, different components of the basal transcriptional machinery such as the TBP, or the RNA polymerase II were also bound *SKP2* promoter with different affinities (Figure 4.12). As we previously mention in the Introduction (Section 1.4.3), all these proteins have been found to interact with MYC in different models and contexts. Taken collectively, these results indicate and suggest that MYC could participate in the recruitment of different complexes with histone acetyl-transferase and histone methyl-transferase activity to the human *SKP2* promoter to coordinate the recruitment of the basal transcriptional machinery to the *SKP2* promoter and to induce its expression, at least in human K562 cells. Moreover these results strongly confirm that *SKP2* is a new direct MYC target gene.

4.1.5. SKP2 has no effects on MYC stability or transcriptional activity

In contrast to our results, previous reports described a positive effect of SKP2 on MYC stability and transcriptional activity (Kim*, et al.*, 2003; von der Lehr*, et al.*, 2003). To assess this possible effect in K562 cell model we decided to analyze MYC protein levels by immunoblot after direct SKP2 silencing. K562 cells were transiently transfected with the pSRshSKP2 vector (Andreu*, et al.*, 2005) codifying a short hairpin directed to the second exon of SKP2 mRNA or the corresponding empty vector (pSR). SKP2 silencing was confirmed by immunoblot (Figure 4.13A). Nonetheless, we found no significant changes in MYC protein levels 24 hours after SKP2 silencing in K562 cells (Figure 4.13A). On the other hand, we also tested MYC transcriptional activity after SKP2 silencing by a luciferase reporter assay using the 4XEbox-Luciferase as MYC activity reporter (Kiessling*, et al.*, 2006). As shown in figure 4.13B, luciferase assays also failed to show a significant SKP2 effect on MYC-dependent transcriptional activity. Thus we ruled out the possible effect of SKP2 on MYC activity and stability at least in the K562 cell model.

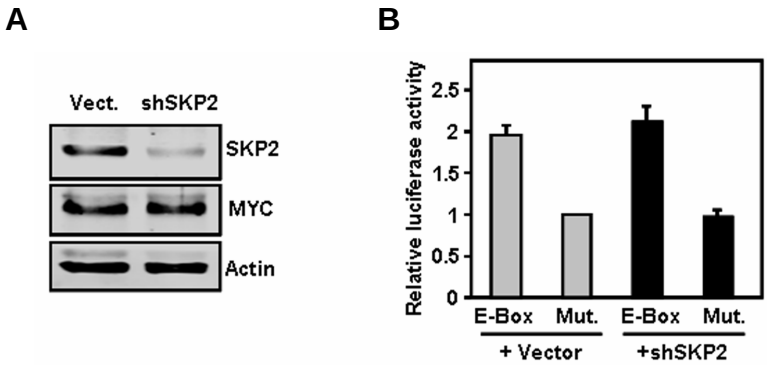

Figure 4.13. SKP2 has no effects on MYC stability or transcriptional activity. A) Immunoblot analysis of transfected cell lysates to assess downregulation of SKP2 protein in cells expressing the shSKP2 vector (Vect.). B) Transactivation of a MYC-responsive reporter in cells with silenced SKP2. K562 cells were cotransfected with the shSKP2 vector (Andreu*, et al.*, 2005) or the corresponding empty vector and the 4XEbox-Luc or 4XE-boxMut-Luc luciferase reporters (Mut.) (Kiessling*, et al.*, 2006). At 36 h post-transfection, the cell lysates were prepared, and luciferase activity was assessed. The data were normalized to *renilla* luciferase activity for transfection efficiency.

4.1.6. MYC and SKP2 expression correlate in different human hematologic tumors

Most of previous results were obtained from K562 or K562-derived cell lines which in turn came from a human CML patient in blast crisis. Thus, we decided to evaluate the MYC-SKP2 correlation in primary tumor samples from real CML patients to see whether this interaction could be translated transferred to a real clinic model. 43 human bone marrow samples, including 4 healthy controls, 31 CML patients at diagnosis and 8 CML patients in complete molecular response [no detection of BCR-ABL transcripts by RT-qPCR after imatinib treatment (Baccarani*, et al.*, 2009; Albajar*, et al.*, 2011)] were provided by both the Hospital Universitario Marques de Valdecilla (Santander) and the Hospital Universitario Dr. Negrín (Las Palmas). *MYC* and *SKP2* mRNA levels were determined by RT-qPCR (Figure 4.14A). Although the cohort was not very large, the correlation between *MYC* and *SKP2* mRNA expression was statistically significant (Figure 4.14B). Next, to determine whether this correlation between *MYC* and *SKP2* at the mRNA level also occurred at the protein level, we analyzed a small cohort of CML protein samples by immunoblot. The results also confirmed the MYC/SKP2 correlation at the protein level in seven of eight patients tested (Figure 4.14C).

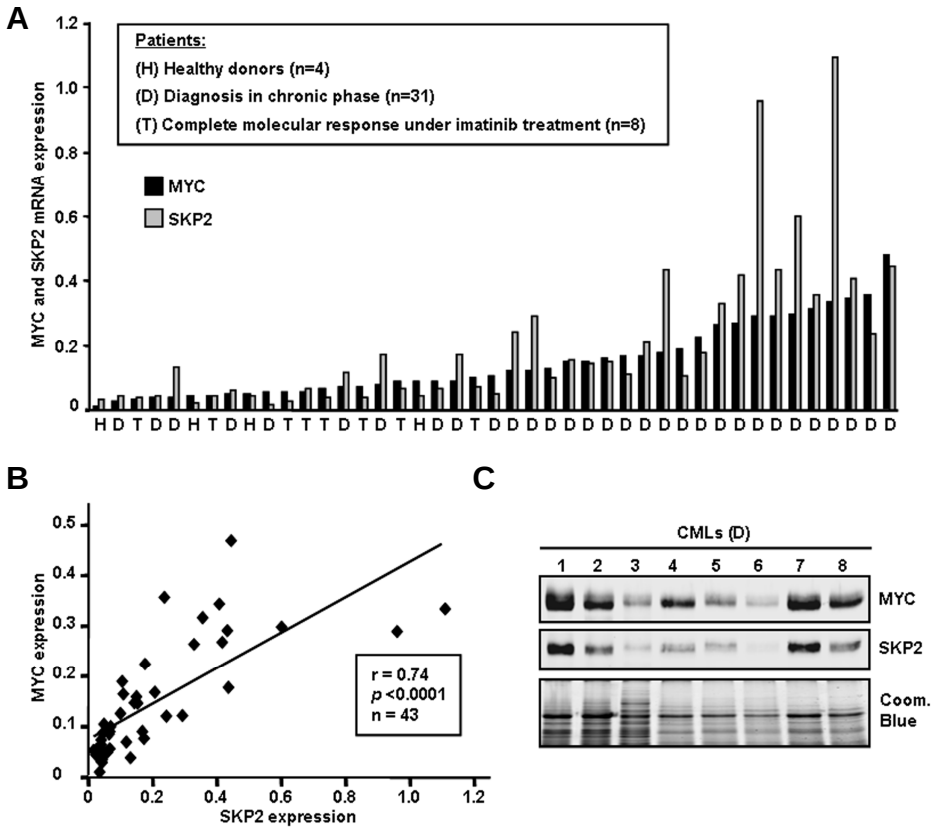

Figure 4.14. *MYC* and *SKP2* expression in CML patients. A) RT-qPCR analysis of *MYC* and *SKP2* mRNA expression in 31 samples from CML patients at diagnosis in chronic phase (D), 8 patients in complete molecular response under imatinib treatment (T), and 4 healthy donors (H). The data are arranged from low to high *MYC* expression. mRNA values were normalized to the levels of ribosomal protein small 14 in each case. B) Correlation between *MYC* and *SKP2* mRNA levels in the 43 bone marrow samples. The *solid line* indicates the linear prediction. The Pearson's *r* and *p* values are indicated. C) Immunoblot showing SKP2 and MYC expression in 8 samples of CML patients at diagnosis. A picture of the gel stained with Coomassie (*Coom*. Blue) is shown to assess protein loading.

We also compared independently the mRNA expression of both *MYC* and *SKP2* between the four control samples, the 31 CMLs at diagnosis and the eight patients that achieved a complete remission under imatinib treatment (essentially cured from their leukemia). The result showed that the mRNA expression of both *MYC* and *SKP2* was significantly lower in the 8 responding patients and similar to healthy controls with respect to CML samples at diagnosis (Figure 4.15). In fact, there were no significant differences between the controls and the CMR (Complete molecular response) samples (Figure 4.15). It should be noted that the treated (T) and healthy controls (H) accumulate in the left part of the graph, as they tend to express less *MYC* and *SKP2*, but still correlate (Figure 4.14A). These data reinforced the conclusion that the expression of *MYC* and *SKP2* correlated in this leukaemia and that imatinib treatment of CML patients down-regulates *MYC* mRNA expression and *SKP2* concomitantly, as in the K562 cell model. Therefore, these results support the idea that MYC could be responsible for the induction of *SKP2* in primary human CML samples.

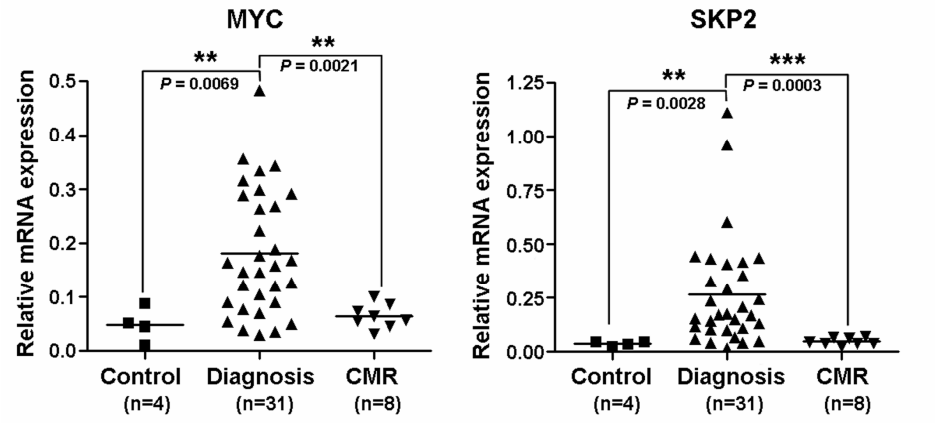

Figure 4.15. Comparative study of *MYC* and *SKP2* mRNA expression between control, diagnosis and CMR samples of CML. *MYC* and *SKP2* mRNA expression was independently analyzed according to the three groups of samples [Control, Diagnosis and patients in Complete Molecular Response (CMR)] and represented by scatter plots. Differential mRNA expression between control patients and patients at diagnosis or between these latter and patients in CMR was compared using the Mann-Whitney test. Horizontal lines represent medians. *P* values are indicated for every *t* tests analysis. The number of samples (n) for every group is indicated under the panels.

On the other hand, we performed an *in silico* approach using the Oncomine database (www.oncomine.org) to examine a possible correlation between *MYC* and *SKP2* mRNA levels in other hematological malignancies. We found a similar distribution of *MYC* and *SKP2* mRNA expression in three independent gene-expression profiling studies carried out to classify human B-cell lymphomas (Figure 4.16) (Basso*, et al.*, 2005; Hummel*, et al.*, 2006; Klapper*, et al.*, 2008). In these three studies, Burkitt´s lymphoma subgroup, in which MYC expression is over-expressed as a consequence of a chromosomal translocation that juxtaposes the *MYC* locus to one of the three immunoglobulin (*IgG*) loci (Delgado and Leon, 2010), also expressed the higher *SKP2* mRNA levels. Nevertheless, it should be noted that *MYC* translocations also occur in other lymphomas such as diffuse large-B-cell lymphoma but they are recurrently associated with non-*IgG* partner loci (Hummel*, et al.*, 2006).

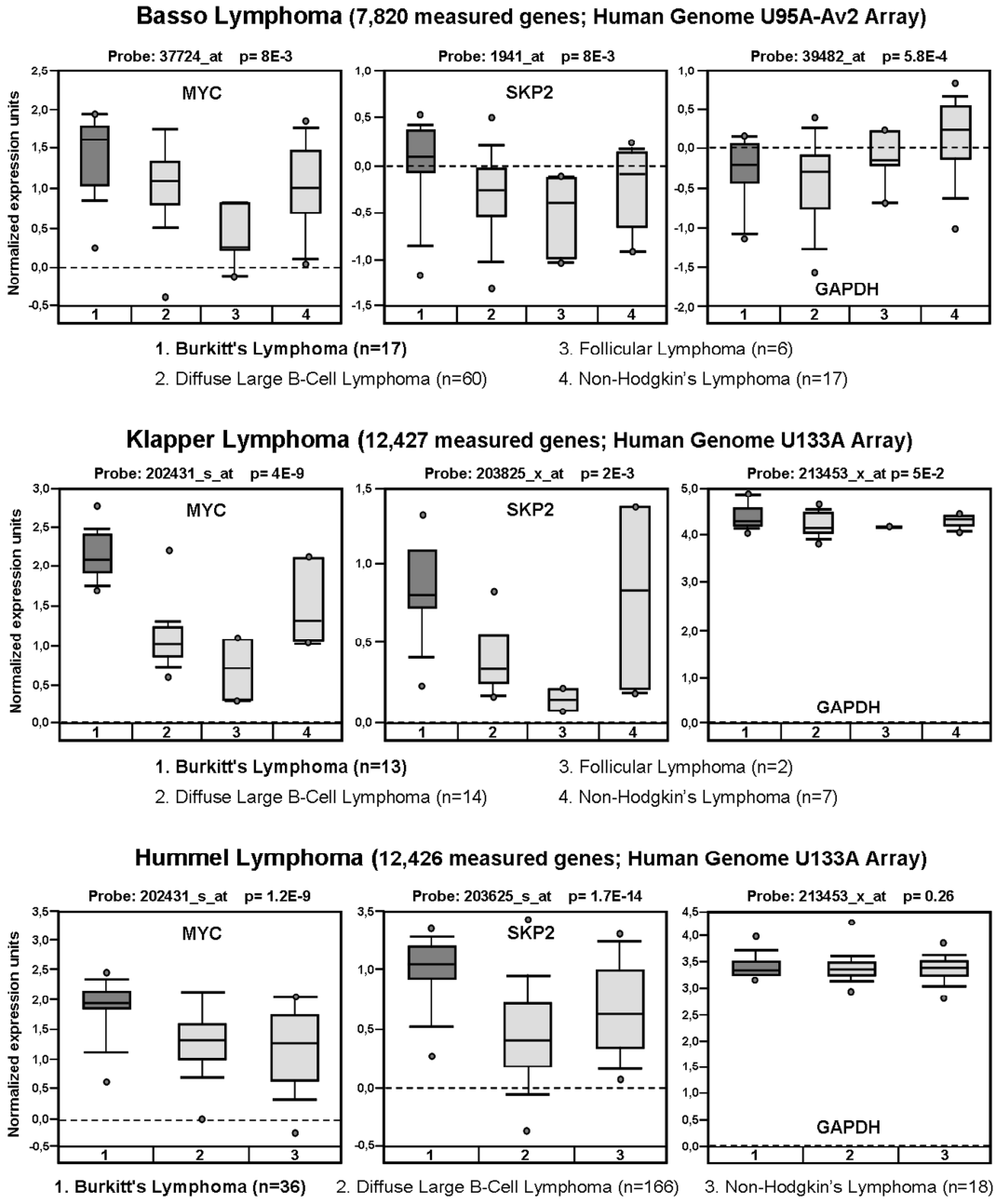

Figure 4.16. Correlation between *MYC* and *SKP2* expression in three independent studies classifying human B-cell lymphomas. Three different microarray-based studies (Affymetrix platform) were collected from the Oncomine database (Oncomine™, Compendia Bioscience, Ann Arbor, MI, https://www.oncomine.org/). The box plots depict the differential expression of *MYC, SKP2* and *GAPDH* (as a housekeeping control gene) between different subgroups of human B-cell lymphomas, as indicated. *P* values from *t* tests, the probes used in each microarray analysis and the study reference are indicated over the panels. The number of samples (n) for every subgroup is indicated under the panels.

Finally, we also queried the correlation between *MYC* and *SKP2* expression in tumor samples with the *in silico* transcriptomics database of the GeneSapiens system (www.genesapiens.org) (Kilpinen*, et al.*, 2008). This database compares the mRNA expression levels of most human genes across 9,783 Affymetrix gene expression array experiments including normal human tissues, different cancer types and other diseases. We found again a positive

correlation between *MYC* and *SKP2* mRNA expression in another human B-cell lymphoma study including 234 patient samples (Figure 4.17A). Moreover, we also found a good *MYC-SKP2* mRNA correlation in acute myeloid leukaemia (AML) (Figure 4.17B) in which MYC has been found frequently overexpressed (Delgado and Leon, 2010; Delgado*, et al.*, 2013) and elevated SKP2 levels represented a poor prognostic factor (Min*, et al.*, 2004).

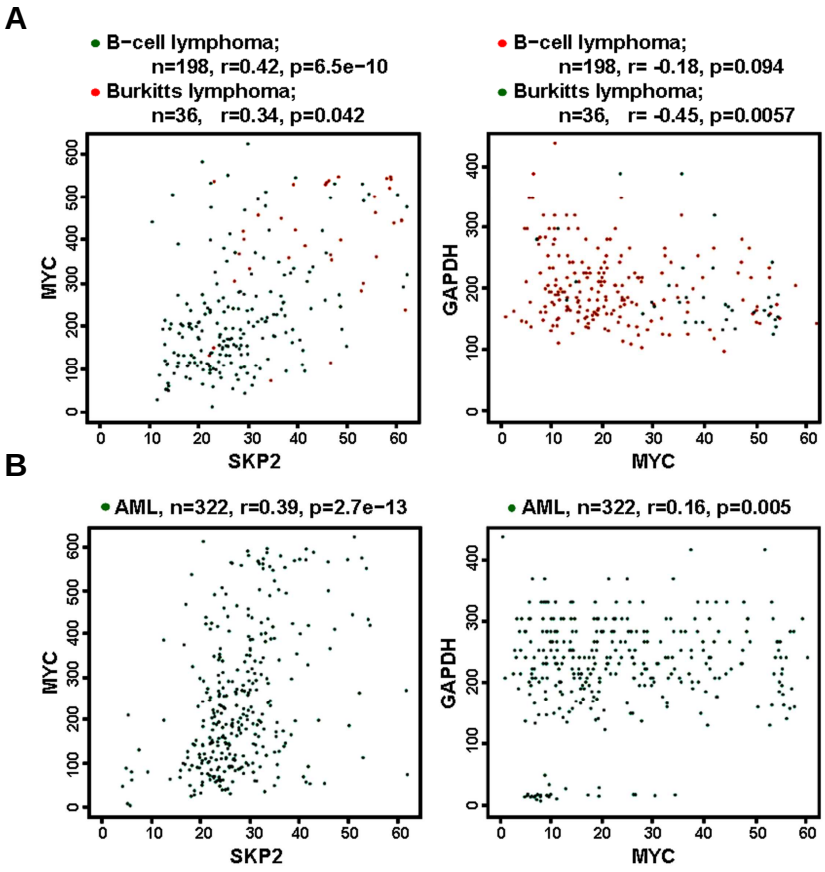

Figure 4.17. Correlation between *MYC* and *SKP2* expression in human B-cell lymphoma and acute myeloid leukemia (AML). Dot plots showing the positive correlation between *MYC* and *SKP2* mRNA expression in individual samples of B-cell lymphoma (A) and AML patients (B). The data were collected from the transcriptomics database of the GeneSapiens system (www.genesapiens.org). As a control, the correlations between *MYC* and the housekeeping gene *GAPDH* are also shown. The number of samples (n), the correlation coefficient (r) and the P values are indicated in each case over the panels.

4.2. THE MYC-SKP2-p27 AXIS

4.2.1. MYC induces p27 phosphorylation on Thr-187

In the first part of this Thesis we have demonstrated that *SKP2* was a MYC target gene in K562 cells, and probably also in other cell models. Moreover, previous reports firmly established that SKP2 was the main F-box protein involved in p27 degradation (Carrano*, et al.*, 1999; Sutterluty*, et al.*, 1999; Tsvetkov*, et al.*, 1999). However, our studies did not demonstrate yet that SKP2 was responsible for p27 down-regulation in our Kp27MER model. Thus we decided to evaluate the MYC-SKP2-p27 axis in Kp27MER cells.

Given that the main target of the SCF^{SKP2} complex is the p27 phosphorylated in Thr187 (Lu and Hunter, 2010), we first studied whether this phosphorylation was taking place in the Kp27MER model. For this purpose, we performed a dose-response study to analyze the fraction of p27 phosphorylated on Thr187 ($p27^{pT187}$). Kp27MER cells were treated with 50 or 75 µM $ZnSO_4$ and 4HT at two different times (12 and 24 hours post-induction) and the levels of p27 total and $p27^{pT187}$ were analyzed by immunoblot. The results showed that MYC activation resulted in a significant increase in the $p27^{pT187}$ fraction at both Zn^{2+} concentrations and 12 hours post-induction (Figure 4.18A). This finding suggests that the kinases involved in this phosphorylation event were not fully inhibited by the high Zn^{2+}-induced p27 levels in presence of active MYC. Then, we performed a kinetic study to determine peak of maximum phosphorylation provoked by MYC activation. We found that it overlapped with the point of maximum p27 overexpression; around 8-12 hours post-induction (Figure 4.18B). At longer treatment times, the phospho-p27 fraction and the total p27 levels were reduced (not shown). Therefore, MYC induced p27 phosphorylation at Thr187, allowing its potential recognition by SCF^{SKP2} complexes.

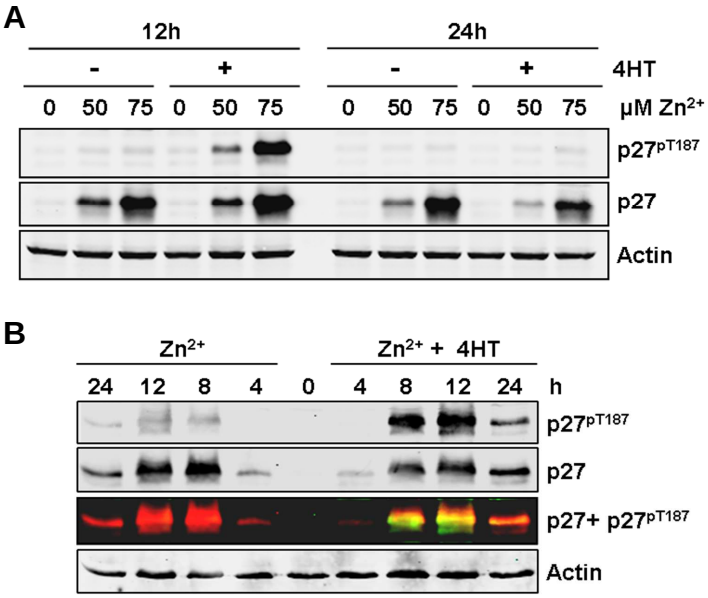

Figure 4.18. MYC induces p27 phosphorylation at Thr187. A) Kp27MER cells were treated for 12 and 24 h with 200 nM 4HT and/or 50 or 75 µM $ZnSO_4$, as indicated. Total p27, p27 phosphorylated on Thr187 ($p27^{pT187}$) and actin (as loading control) were assayed by immunoblot. B) Kp27MER cells were treated for 4–24 h with 75µM $ZnSO_4$ or 200 nM 4HT plus 75 µM $ZnSO_4$. Total p27, p27 phosphorylated on Thr187 ($p27^{pT187}$), and actin (as loading control) were assayed by immunoblot. The yellow signal shows the overlapping between total p27 (red) and $p27^{pT187}$ (green).

4.2.2. MYC induces p27 phosphorylation independently from cyclin E/CDK2 complexes

It had been shown that the cyclin E/CDK2 complexes mediated p27 phosphorylation at Thr-187 at G1/S phase transition (Muller*, et al.*, 1997; Sheaff*, et al.*, 1997; Vlach*, et al.*, 1997). Moreover, it had been also described that MYC induces cyclin E expression activating cyclin E/CDK2 complexes (Jansen-Durr*, et al.*, 1993; Muller*, et al.*, 1997; Perez-Roger*, et al.*, 1997). Thus, to explain the increase in the phosphorylation of p27 in response to MYC we decided to examine whether MYC activation was modifying the cyclin E and CDK2 protein levels in Kp27MER cells. As shown by immunoblot analysis, no changes on their expression were observed after 12 hours of MYC activation (Figure 4.19A, compare -/+ 4HT treatments in cyclin E immunoblot). In contrast, the cyclin E protein levels were increased in cells overexpressing p27, suggesting that p27 was stabilizing cyclin E. This finding is in agreement with previous results showing that p27 inhibited cyclin E ubiquitination and prevented of its degradation by the proteasome (Clurman*, et al.*, 1996).

On the other hand, it has had been described that (i) cyclin A/CDK2 complexes were also able to phosphorylate p27 at Thr-187 *in vitro* (Muller*, et al.*, 1997; Zhu*, et al.*, 2004b) and that (ii) cyclin A was induced by MYC in Rat-1-MYCER fibroblasts (Jansen-Durr*, et al.*, 1993; Hoang*, et al.*, 1994; Muller*, et al.*, 1997). Thus we analyzed cyclin A expression and we found an increase of cyclin A protein levels concomitant to MYC activation in presence of Zn^{2+}-induced p27 (Figure 4.19A, compare lanes 1 and 2). Cyclin A induction by MYC can be explained because MYC-MAX heterodimers also binds to *CCNA2* promoter in K562 cells according to the UCSC genome browser (not shown).

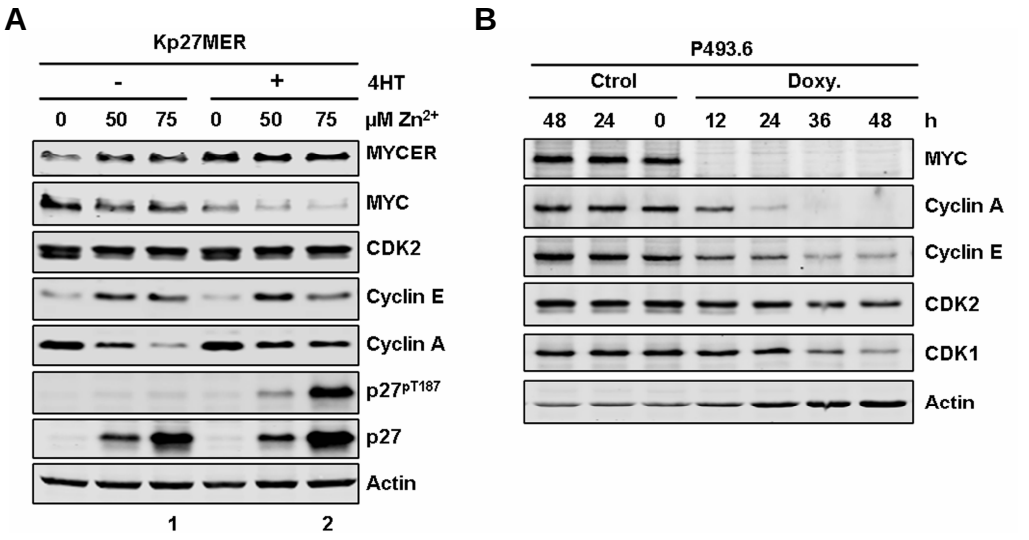

Figure 4.19. MYC induces cyclin A but not cyclin E or CDK2 expression. A) Kp27MER cells were treated for 12 h with 200 nM 4HT and 50 and/or 75 μM $ZnSO_4$, as indicated. MYCER and MYC (as control of MYCER activation); CDK2; cyclin A and E; total p27, p27 phosphorylated on Thr187 ($p27^{pT187}$), and actin (as loading control) were assayed by immunoblot. B) P493.6 cells were treated for the indicated times with 2 μg/ml doxycycline (Doxy.). MYC, cyclin A and E; CDK2, CDK1 and actin were assayed by immunoblot. P493.6 cells do not express p27 (Pajic*, et al.*, 2000).

This result was consistent with an independent observation in P493.6 cells where repression of MYC by doxycycline closely correlated with cyclin A down-regulation (Figure 4.19B). In these cells, *MYC* repression also resulted in cyclin E down-regulation but with a slower kinetics than cyclin A (Figure 4.19B). It should be mentioned that P493.6 cells do not express p27 (Pajic*, et al.*, 2000) so its phosphorylation status could not be tested in this experiment.

Therefore, the induction of cyclin A by MYC could explain the increase in p27-Thr187 phosphorylation in Kp27MER cells. To directly test this, we decided to study the kinase activity associated to cyclin A immunocomplexes on recombinant p27. For this end, we conducted *in vitro* kinase assays using recombinant 6 histidine-tagged p27 (His_6-p27) as substrate and the phosphospecific antibody anti-$p27^{pT187}$ to detect the kinase activity of these cyclin/CDK immunocomplexes by immunoblot, as described in section 3.6.2 of "Material and Methods''.

We confirmed the ability of cyclin A immunocomplexes to phosphorylate recombinant p27 (Figure 4.20A). This kinase activity was strongly inhibited by Zn^{2+}-induced p27 (i.e., endogenous p27) in the absence of activated MYC (Figure 4.20A, Zn^{2+} treatment). However, in presence of activated MYC, cyclin A immunocomplexes phosphorylated efficiently recombinant His_6-p27 even in presence of endogenous p27 (Figure 4.20A, Zn^{2+} + 4HT treatment). These results suggests that the increase in the p27 phosphorylation rate observed in Kp27MER cells in presence of MYC (Figure 4.18) could be due, at least in part, to the kinase activity associated to cyclin A immunocomplexes.

Given that both, CDK2 and CDK1 can be associated to cyclin A (see Introduction, section 1.1.3.), then we decided to analyze the kinase activity of CDK2 and CDK1 immunocomplexes on recombinant His_6-p27. First, we analyzed the kinase activity of CDK2 immunocomplexes and we confirmed the ability of CDK2 to phosphorylate recombinant p27 (Figure 4.20B, no Zn^{2+} treatment). However, the kinase activity of CDK2 was strongly inhibited by Zn^{2+}-induced p27 in the absence but also in the presence of activated MYC, i.e., in the presence of 4HT (Figure 4.20B). Thus, the p27 phosphorylation induced by MYC in the Kp27MER cells (Figure 4.18) is likely not mediated by cyclin A/CDK2 or by cyclin E/CDK2 complexes. Finally, we asked whether cyclin A-associated CDK1 could phosphorylate p27. We confirmed the ability of CDK1 to phosphorylate p27 on Thr187 *in vitro* (Figure 4.20C), as previously shown in a different model (Zhu*, et al.*, 2004b). Moreover, we observed that the Zn^{2+}-induced p27 inhibited much less efficiently the kinase activity associated to CDK1 compared to CDK2 (Figure 4.20, compare Zn^{2+} treatments in B and C upper graphs) confirming previous results during p27 discovery (Polyak*, et al.*, 1994b). Furthermore, we also observed a slightly increase in the levels of $p27^{pThr187}$ in the CDK1 immunoprecipitates in the presence of active MYC (Figure 4.20 C) suggesting that the cyclin A-associated kinase activity was due to cyclinA/CDK1 complexes. As a control, we confirmed the binding of cyclin A to CDK1 and CDK2 by immunoprecipitating cyclin A from Kp27MER lysates and detecting CDK1 and CDK2 in the precipitates (Figure 4.20D). Strikingly, it should be noted that the kinase activity associated to cyclin A, CDK1 and CDK2 was inhibited by Zn^{2+}-induced p27 (i.e., endogenous p27) but not by recombinant His_6-p27. This finding suggests that His_6-p27 requires an intracellular modification to inhibit these immunocomplexes. The lack of

inhibition of CDK1 and CDK2 by recombinant p27 has been previously observed (Zhu, *et al.*, 2004b).

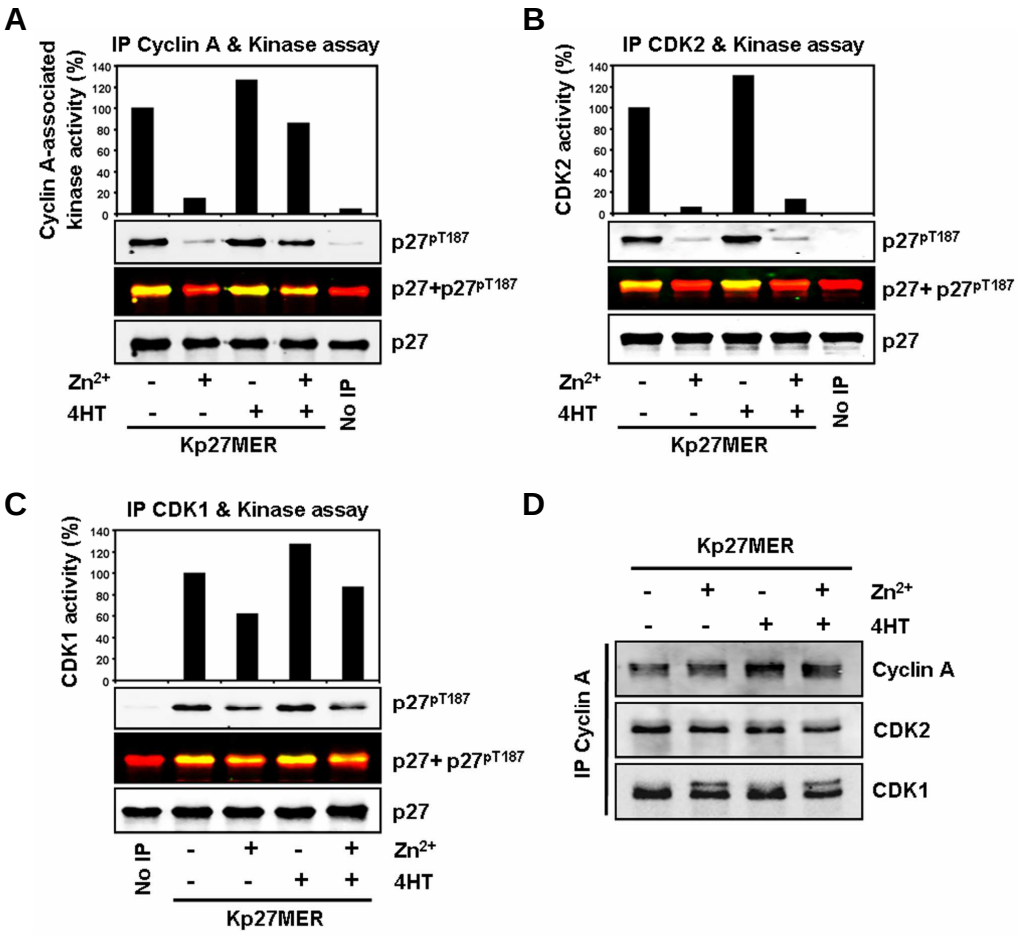

Figure 4.20. MYC induces cyclin A-associated kinase activity in presence of p27 in Kp27MER cells. Kp27MER cells were treated for 12 h with 75 µM $ZnSO_4$ and/or 200 nM 4HT and, as indicated. Cell extracts were immunoprecipitated against A) cyclin A; B) CDK2 and C) CDK1 and immunocomplexes were subjected to *in vitro* p27 phosphorylation assays (see "Material and Methods"). As negative control of phosphorylation assays, beads with no antibody were added to mix reaction (no IP). Total p27 and p27 phosphorylated on Thr187 ($p27^{pT187}$) were assayed by immunoblot. The yellow signal shows the overlapping between total p27 (red) and $p27^{pT187}$ (green). The upper panels show the relative kinase activity of immunocomplexes determined by densitometric analysis of corresponding immunoblots. D) Lysates from Kp27MER cells treated for 12h with 75 µM $ZnSO_4$ and/or 200 nM were immunoprecipitated with anti-cyclin A antibody, and the levels of cyclin A, CDK2 and CDK1 in the immunoprecipitates were determined by immunoblotting.

To better assess the ability of MYC to induce p27 phosphorylation independently of cyclin E/CDK2 complex activity we carried out a parallel study in mouse embryonic fibroblasts deficient for *Cdk2* (Ortega, *et al.*, 2003) and/or E-type cyclins (Geng, *et al.*, 2003) (kindly provided by Marcos Malumbres and Piotr Sicinski, respectively). Gene knockout were confirmed by RT-PCR (Figure 4.21A and B, respectively). MEFs $Cdk2^{-/-}$ and cyclin $E1^{-/-}/E2^{-/-}$ were infected with lentivirus containing the *MYC* gene tagged with FLAG epitope under the control of the CMV promoter. Empty vector (Lv141) was also transduced as a control. Infection was confirmed and scored by GFP expression (not shown). MYC-Flag overexpression was assayed by RT-PCR and

immunoblot (Figure 4.21A, B and C). Cells extracts were immunoprecipitated against cyclin A, CDK1 and CDK2, and immunocomplexes were subjected to *in vitro* p27 phosphorylation assays (Figure 4.21D, E and F respectively).

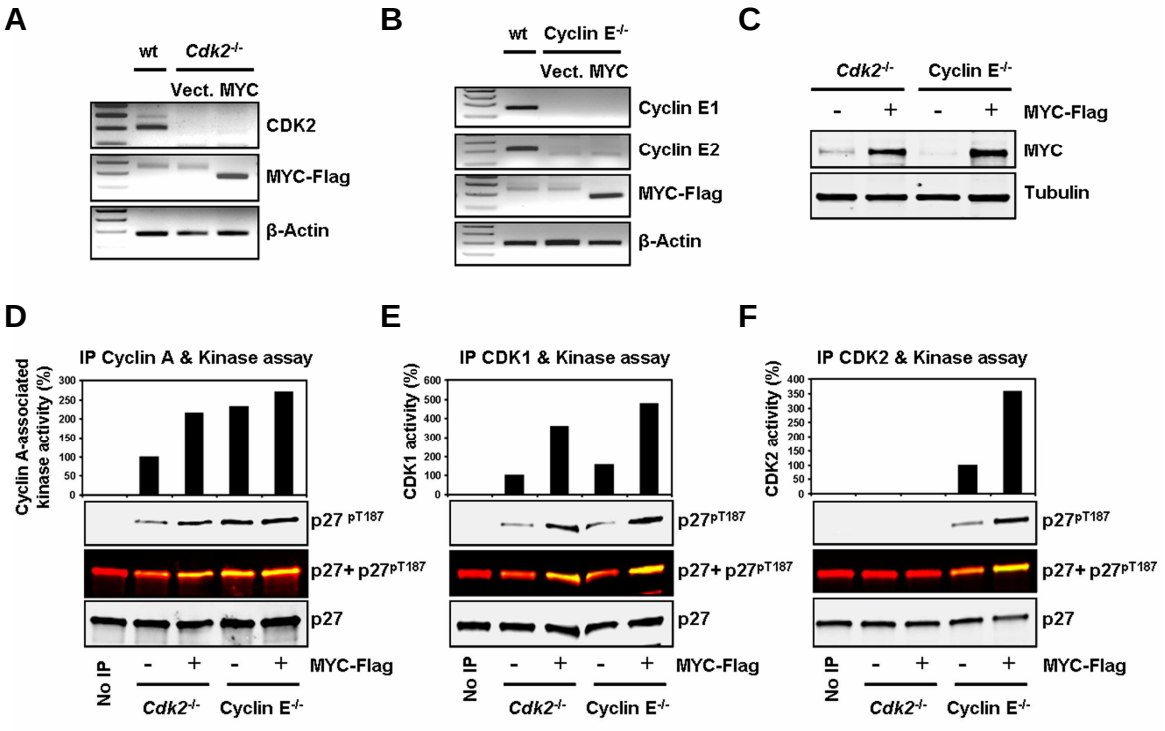

Figure 4.21. MYC induces CDK1 and cyclin A-associated kinase activity in *Cdk2*$^{-/-}$ and cyclin E1$^{-/-}$/E2$^{-/-}$ MEFs. MEFs *Cdk2*$^{-/-}$ and cyclin E1$^{-/-}$/E2$^{-/-}$ were infected with MYC-Flag or the respective empty lentiviral vector Lv141 (vect.). A) *Cdk2* knockdown and MYC-Flag infection were verified by RT-PCR with primers pairs against β-actin (loading control), CDK2 and MYC-Flag. MEFs wt were used as control. B) MEFs cyclin E1$^{-/-}$/E2$^{-/-}$ knockdown and infection were verified by RT-PCR primers pairs against β-actin, cyclin E1, cyclin E2 and MYC-Flag. MEFs wt were used as control. C) MEFs *Cdk2*$^{-/-}$ and cyclin E1$^{-/-}$/E2$^{-/-}$ infected with MYC-Flag or the respective lentiviral empty vector were assayed by immunoblot against MYC and tubulin (as loading control) expression. D) cyclin A, E) CDK1, and F) CDK2 immunocomplexes from *Cdk2*$^{-/-}$ and cyclin E1$^{-/-}$/E2$^{-/-}$ MEFs infected with MYC-Flag or the respective empty vector were subjected to *in vitro* p27 phosphorylation assays (see "Material and Methods"). As negative control of phosphorylation assays, beads with no antibody were added to mix reaction (no IP). Total p27 and p27 phosphorylated on Thr187 (p27^{pT187}) were assayed by immunoblot. The yellow signal shows the overlapping between total p27 (red) and p27^{pT187} (green). The upper panels show the relative kinase activity of immunocomplexes determined by densitometric analysis of respective immunoblots.

We found that cyclin A and CDK1 immunocomplexes from both cyclin E1$^{-/-}$/E2$^{-/-}$ and *Cdk2*$^{-/-}$ MEFs were able to phosphorylate recombinant His$_6$-p27 (Figure 4.21D and E). We also observed that CDK2 immunocomplexes from cyclin E1$^{-/-}$/E2$^{-/-}$ MEFs were also able to phosphorylate recombinant His$_6$-p27 (Figure 4.21F). Altogether, these results suggest that at least in mouse fibroblasts, CDK2 and E-type cyclins are not strictly required for p27-Thr187 phosphorylation and that CDK1 and cyclin A can replace CDK2 and E-type cyclins in this function.

In addition, we found that MYC promoted cyclin A and CDK1 kinase activity on the extracts of both *Cdk2*$^{-/-}$ and cyclin E1$^{-/-}$/E2$^{-/-}$ MEFs infected with MYC (Figure 4.21E). However, the

induction of cyclin A kinase activity by MYC in cyclin $E1^{-/-}/E2^{-/-}$ MEFs was moderate compared to this one in *Cdk2*$^{-/-}$ MEFs. This might be due to a compensatory mechanism to induce cyclin A associated kinase activity in absence of E-type cyclins. In MEFs cyclin $E1^{-/-}/E2^{-/-}$, MYC also promoted kinase activity of CDK2, suggesting that cyclin A was the cyclin responsible of CDK2 activation (Figure 4.21E). Thus, we confirm that MYC is able to induce CDK2 and/or CDK1 kinase activity on p27 associated to cyclin A expression.

4.2.3. MYC reduces p27 protein levels through SKP2 induction

The previous results indicated that MYC promoted p27 phosphorylation at Thr-187 in Kp27MER cells, at least in part, through the induction of cyclin A-associated kinase activity; being this phosphorylation event a prerequisite for p27 recognition by the SCF^{SKP2} ubiquitin ligase complex. Thus, we next asked whether the SKP2-induction mediated by MYC was really responsible for p27 down-regulation. For this purpose, we analyzed the MYC-SKP2-p27 axis by three different approaches.

First, we analyzed the MYC effect on SKP2 and Zn^{2+}-induced p27 protein levels in the Kp27MER model by immunoblot. We treated Kp27MER cells with 50 µM $ZnSO_4$ and/or 200nM 4HT for 24, 36 and 48 hours. Immunoblot analysis showed that MYC activation by 4HT resulted in SKP2 induction and a concomitant significant decrease in p27 levels after p27 overexpression (Figure 4.22A, compare lanes 1 vs. 2; 3 vs. 4 and 5 vs. 6). As we will see later, p27 degradation also occurred at high p27 levels (75 µM $ZnSO_4$) although the p27 accumulation exceeds its degradation rate (Figure 4.27, p27 low exposure).

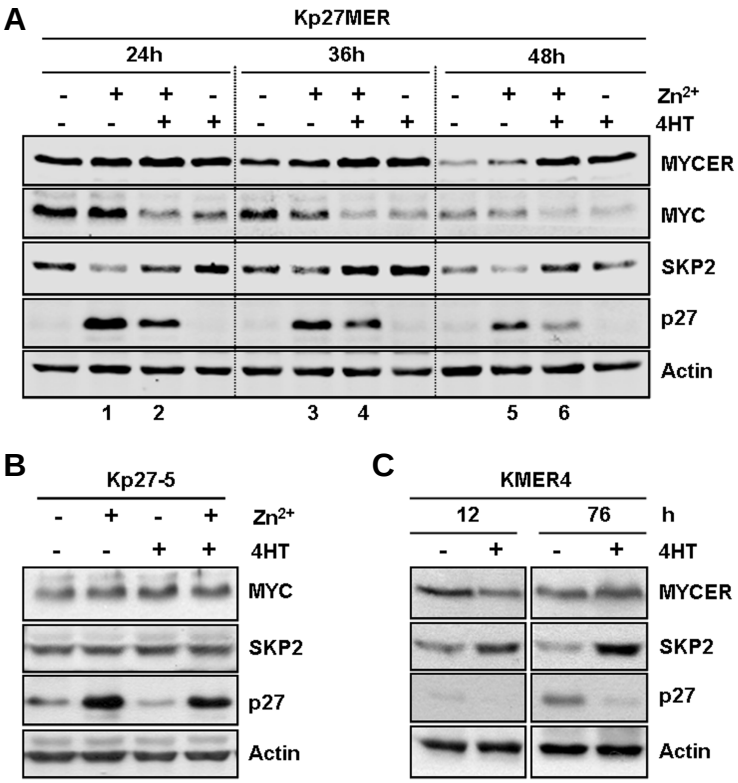

Figure 4.22. MYC-induced SKP2 correlates with p27 down-regulation. A) Expression of p27 in Kp27MER after MYC activation. The cells were treated with 50 µM $ZnSO_4$ and/or 200 nM 4HT for 24, 36 and 48h. MYCER, MYC, SKP2, p27 and actin (loading control) protein levels were determined by immunoblot. B) Kp27-5 cells were treated for 48 h with $ZnSO_4$ and 4HT, and protein levels of MYC, SKP2, p27 and actin (loading control) were determined by immunoblot. C) KMER4 cells were cultured for 76 h to reach quiescence caused by cell density, alone or with 200 nM 4HT to activate MYC. MYCER; SKP2 and p27 protein levels were determined by immunoblot.

As a control that this effect was only due to MYC activation, we performed a similar experiment in parental Kp27-5 cells, which bear a Zn^{2+}-inducible p27 transgene but not the *MYCER* construct. 4HT addition to the culture medium did not modify SKP2 and did not reduce p27 protein levels in these cells (Figure 4.22B). This result partially confirmed that the induction of SKP2 by MYC was responsible for p27 down-regulation in myeloid leukemia cells. Moreover, we also tested the MYCER effect on the endogenous p27 in the KMER4 model. In these cells, as in parental K562 cells, p27 was up-regulated when cells reached quiescence by culture saturation (~1.5 x 10^6 cells/ml after 3 days in culture). Immunoblot analysis showed that SKP2 levels were higher and p27 levels were lower in cells with activated MYC after 72 hours in culture (Figure 4.22C).

As second approach, we tested the SKP2-p27 interaction in Kp27MER cells by immunofluorescence. As shown in figure 4.23 all p27 was predominantly nuclear in Kp27MER cells treated with 75 µM $ZnSO_4$. As expected, MYCER activation promoted SKP2 expression and it was also detected in the cell nucleus. Interestingly, we found no colocalization of p27 and SKP2 in Kp27MER cells treated with Zn^{2+} and 4HT. Instead, p27 and SKP2 expression was mutually exclusive. Cells with high nuclear SKP2 levels showed low p27 levels (Figure 4.23, yellow arrows) and *viceversa* (Figure 4.23, white arrows). This mutually exclusive distribution of SKP2 and p27 has been also reported in other cell models (Lu*, et al.*, 2002). This result also reinforced the result of SKP2 induction by MYC and subsequent SKP2-dependent degradation of p27. Moreover, this result excluded the possibility that the bulk of p27 would be degraded in the cytoplasm by a SKP2-independent pathway (e.g., the KPC ubiquitin ligase).

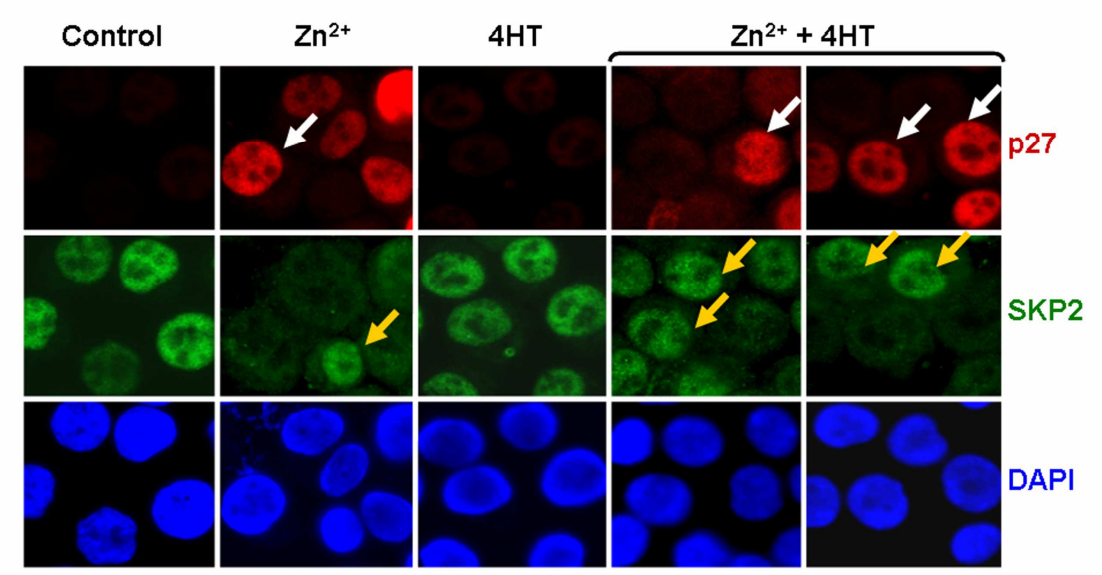

Figure 4.23. SKP2 and p27 localize in the cell nucleus but they are mutually exclusive. Immunofluorescence of p27 and SKP2 proteins in Kp27MER cells exposed to 75 µM $ZnSO_4$ and 4HT for 24 h (as indicated). White arrows indicate cells with high p27 and low SKP2 levels in the nuclei. Yellow arrows indicate cells with high SKP2 and low p27 levels. The nuclei were DAPI-stained.

Third and finally, to really confirm that SKP2 was the main intermediary of p27 degradation induced by MYC in the K562 models, we decided to analyze endogenous p27 levels after *SKP2* silencing. For this purpose, we infected KMER4 cells with retrovirus expressing a short hairpin against *SKP2* mRNA (pSR-shSKP2 vector) (Andreu*, et al.*, 2005) or the corresponding empty vector (pSR vector) and we generated the KMERshSKP2 and KMERpSR sublines. SKP2 silencing in KMER4shSKP2 cells was confirmed by immunoblot, as compared to the KMER4pSR subline (Figure 4.24A). Then we compared p27 levels after 2 and 4 days growing in normal culture conditions by immunoblot. As previously mentioned K562-derived cells reached quiescence by culture saturation (~1.5 x 10^6 cells/ml) after 3-4 days in culture, accumulating p27. As shown also in figure 4.24A, the p27 levels accumulated in the KMERshSKP2 cells were higher than in the KMERpSR cells owing to the lower levels of SKP2 in these cells.

In addition, we also analyzed the effect of *SKP2* silencing on cell proliferation. In agreement with the increased p27 protein levels, shSKP2-expressing cells grew at a reduced rate (Figure 4.24B) and showed cell accumulation in the G1 phase (not shown). This result confirmed the effect of SKP2 on p27 in the K562-derived models and explained, at least in part, the cell cycle activation induced by MYC in the Kp27MER model in presence of low p27 levels (as induced by 50 μM $ZnSO_4$).

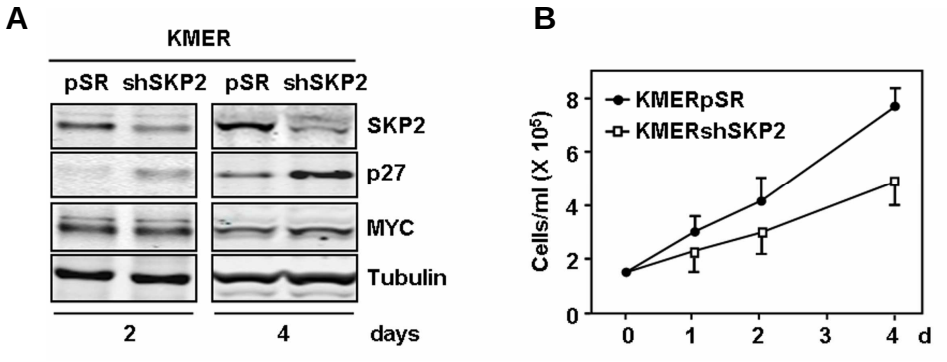

Figure 4.24. *SKP2* silencing results in increased p27 levels and low proliferation rate of K562 cells. A) KMERshSKP2 and KMERpSR cells were cultured for 2 and 4 days, and the protein levels of SKP2, p27, MYC, and α-tubulin (loading control) in cell lysates were assessed by immunoblot. B) Proliferation rates of KMERpSR and KMERshSKP2 cells were measured by counting viable cells in a hemocytometer.

4.2.4. *SKP2* silencing reduces tumor formation from K562 cells in a xenograft model in nude mice

Given the importance of MYC-SKP2-p27 axis in proliferation of K562 cells, as evidenced in the previous section, and that the capacity of these cells to develop subcutaneous tumors in nude mice has been partially attributed to the effects of MYC overexpression (Xie*, et al.*, 2002; Huang*, et al.*, 2012) we evaluated the role of MYC-SKP2-p27 axis in tumorigenesis by comparing the tumorigenic capacity of KMERpSR and KMERshSKP2 sublines in nude mice. For this end, the same amount of KMERpSR and KMERshSKP2 cells (10^7 cells per injection site) were injected

subcutaneously into the left and right flanks respectively of a group of nine female immunocompromised mice *(nu/nu)* and tumor formation and progression was monitored weekly after injections. Three weeks post-injection, the animals were killed and tumours from each mouse were excised, measured and weighed. Figure 4.25A shows two representative nude mice and the respective developed tumors. As shown in figure 4.25B the mean tumor weight produced by KMERshSKP2 cells was significantly reduced as compared to not silenced control cells (KMERpSR). A similar reduction was observed when the volume of the tumours was compared (not shown). Thus we concluded that the SKP2 induction by MYC and the subsequent p27 degradation may account at least in part the tumorigenic capacity of these cells.

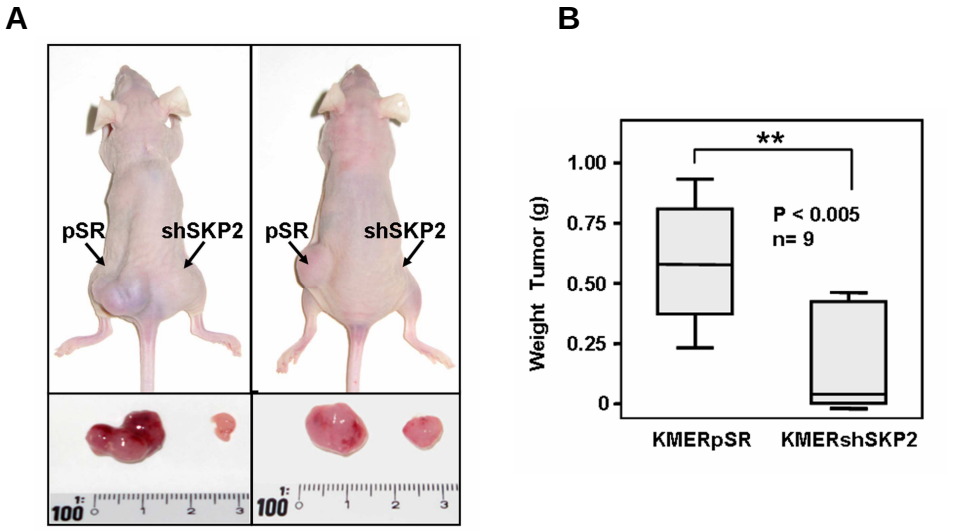

Figure 4.25. *SKP2* silencing reduces the size of tumors produced by K562 cells in nude mice. Approximately 10^7 KMERpSR and KMERshSKP2 cells were subcutaneously injected into the left and right flanks, respectively, of female athymic nude mice as described in ''Materials and Methods''. Tumor-bearing mice were sacrificed after 3 weeks and the mice photographed before excision and weighing of tumors. A) Image showing two representative mice and the respective developed tumors. The scales shown are in centimetres. B) The weight of the tumors generated by KMERpSR and KMERshSKP2 cells respectively was compared using the Mann-Whitney test and represented by box plots (covering from 25 to 75% percentiles). Horizontal lines represent medians. The *P* value and the number of tumors (n) are indicated.

4.2.5. The MYC-SKP2-p27 axis in other cell models

Finally, we studied the MYC-SKP2-p27 axis in some of the initially described models. We observed that KMYCJ cells pre-treated with 10 nM TPA for 12 hours accumulated p27 concomitantly to MYC and SKP2 down-regulation (Figure 4.26A). However, the overexpression of MYC with 75 µM $ZnSO_4$ in TPA pre-treated cells promoted a SKP2 up-regulation and a concomitant p27 down-regulation 24 and 48 hours post-induction (Figure 4.26A). A similar result was also observed in KMYCJ treated with 1 µM imatinib. Endogenous MYC and SKP2 were down-modulated in presence of imatinib in these cells as previously described in the KMER model. This decrease in SKP2 levels was accompanied by a p27 and γ-globin accumulation 24

and 48 hours post-treatment (Figure 4.26B) which resulted in a moderate erythroid differentiation of these cells (Gomez-Casares*, et al.*, 2012). However, the overexpression of exogenous MYC with 75 μM $ZnSO_4$ in presence of imatinib resulted again in SKP2 induction and a concomitant p27 degradation and inhibition of differentiation of these cells (Figure 4.26B).

On the other hand, in the TGR1 cell model in which MYC and SKP2 were down-regulated after serum deprivation we observed a concomitant p27 accumulation as shown by immunoblot in figure 4.26C. This result was also appreciated in the K562 cell model in which the glutamine and the serum starvation also resulted in a progressive MYC and SKP2 down-modulation followed by p27 stabilization (Figure 4.26D).

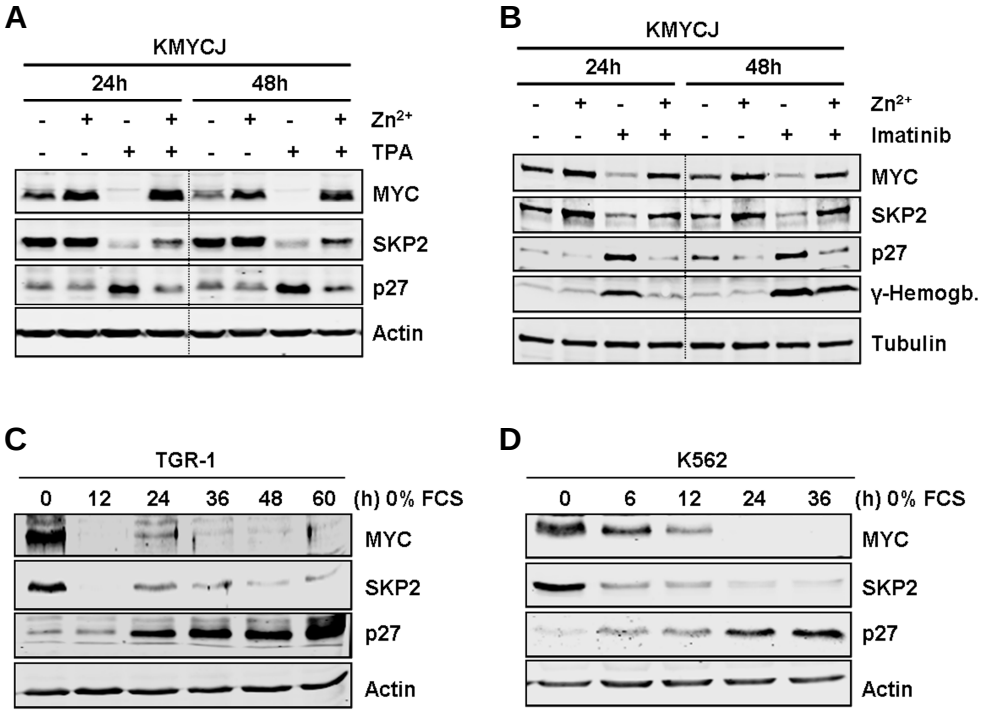

Figure 4.26. The MYC-SKP2-p27 axis in other cell models. A) KMYCJ cells were pre-treated with 10 nM TPA for 12 hours and then MYC was induced with 75 μM $ZnSO_4$ for 24 and 48 hours as indicated. MYC, SKP2, p27 and actin (as loading control) protein levels in total cell lysates were determined by immunoblot. B) KMYCJ cells were treated with 1μM imatinib and/or 75 μM $ZnSO_4$ for 24 and 48 hours as indicated, and the levels MYC, SKP2, p27, γ-Hemoglobin (as an erythroid differentiation marker) and α-tubulin (as loading control) were assayed by immunoblot. C) TGR1 cells were serum-deprived for the indicated times, and MYC, SKP2, p27 and actin were analyzed by immunoblot. D) K562 cells were glutamine and serum-deprived for the indicated times, and MYC, SKP2, p27 and actin protein expression was analyzed by immunoblot.

4.3. MYC EFFECTS ON p27-CONTAINING COMPLEXES AND ITS RELATIONSHIP WITH PROLIFERATION

4.3.1. Characterization of p27-containing complexes in Kp27MER cells by gel filtration

The mechanism previously described of SKP2-induction by MYC explained the p27 down-modulation and the increase in cell proliferation observed upon MYC activation at low p27 levels (with 50 µM $ZnSO_4$) in Kp27MER cells. However, it did not explain the inability of MYC to counteract p27-induced proliferative arrest at high p27 levels (i.e., with 75 µM $ZnSO_4$) (Acosta*, et al.*, 2008) given that p27 degradation was also occurring in these conditions (Figure 4.27 low exposure).

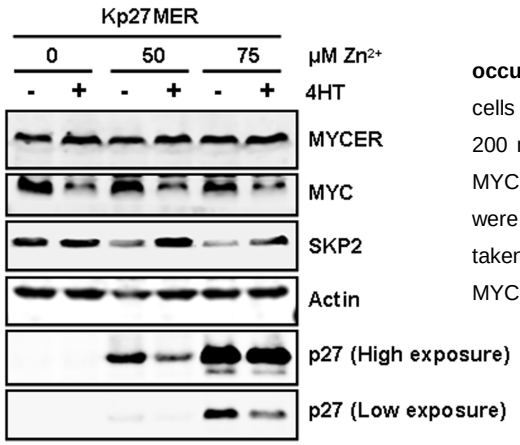

Figure 4.27. MYC-induced degradation of p27 also occurred at high p27 levels (Low exposure). Kp27MER cells were treated for 24 h with 50 or 75 µM $ZnSO_4$, and/or 200 nM 4HT, as indicated. MYCER and MYC (as control of MYCER activation); SKP2; p27 and actin (as loading control) were assayed by immunoblot. A low exposure of p27 was taken to reveal p27 down-modulation in presence of active MYC (plus 4HT) at 75 µM $ZnSO_4$.

It is possible that at these Zn^{2+} doses p27 could be expressing at such high levels that MYC cannot antagonize the p27-mediated proliferative arrest, despite promoting its degradation. To explore this point we decided to analyze the p27 distribution at macromolecular level by gel filtration chromatographic fractionation of protein extracts followed by immunoblot analysis. This technique offered a simple and relatively quick method to analyze the macromolecular distribution of p27 and CDKs between different complexes in native conditions. We used a Superdex-200 HR column which allowed a very high resolution of native protein complexes in a molecular mass range lower than 600 kDa.

We first analyzed protein extracts of Kp27MER cells treated whit 75 µM $ZnSO_4$ to know the p27 distribution in these cells expressing the top p27 protein levels. After the chromatographic separation, aliquots of each fraction were analyzed by immunoblotting against p27, CDK2 and cyclin E content. Figure 4.28A shows a typical result of a chromatographic fractionation. p27 was mainly distributed between two types of complexes: one high molecular weight complex which eluted in a wide peak around ~200 kDa and another complex with a lower molecular weight of about ~50 kDa. It should be mentioned that the resolution of the column at high molecular weights is lower. Therefore, the molecular weight estimation of a protein or protein complex using this

technique is better at low molecular weights. The two peaks were completely resolved, and no additional signals were evident in other fractions of the chromatographic analysis or in the flow-through of the column (~600 kDa aprox.). Interestingly and despite its overexpression, no p27 was observed eluting in the range 20-30 kDa, around the estimated molecular weight of free-eluting p27 protein.

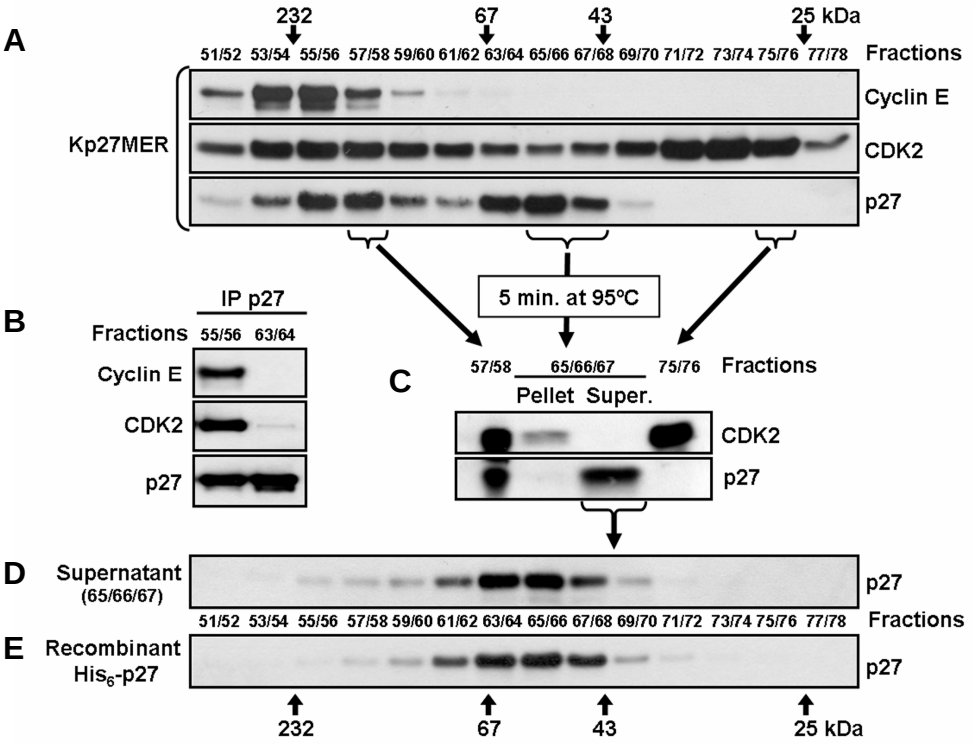

Figure 4.28. Distribution of p27 in Kp27MER cell extracts by gel filtration. A) Kp27MER cells treated with 75 µM $ZnSO_4$ for 24h were lysed softly in nondenaturing conditions and 3 mg of the protein extract was fractionated by gel filtration chromatography on Superdex-200 HR column. Equal aliquots of the indicated fractions (on the top of the panel), were analysed by immunoblotting against p27, cyclin E and CDK2. B) The indicated fractions were immunoprecipitated against p27 and the presence of CDK2, cyclin E and p27 in the immunoprecipitates was assessed by immunoblot. C) Fractions 65/66/67 were heated for 5 min at 100°C and insoluble denatured material (pellet) was separated by centrifugation at 20000 rpm for 20 min. Pellet and supernatant were subjected to immunoblot against p27 and CDK2 to verify p27 release from cyclin/CDK complexes (Hengst*, et al.*, 1994; Polyak*, et al.*, 1994a). Fractions 58/59 and 76/77 were used as immunoblot control. D) The supematant (Super.) was then subjected to gel filtration column and the fractions were immunoblotted again with anti-p27 antibody. E) His_6-p27 was expressed in bacteria and purified as described in "Materials and Methods" (section 3.6.5). The purified His_6-p27 was loaded onto a gel filtration column and the fractions were immunoblotted with anti-p27 antibody. Fraction numbers and the fraction elution of protein standards are shown at the top and the bottom of the figure.

In the ~200 kDa complex, p27 coeluted with CDK2 and cyclin E (Figure 4.28A). Importantly, a part of CDK2 was also found eluting in a peak around 30 kDa corresponding to the molecular weight of its free form (~33 kDa). Given that the cyclin E only appeared in the ~200 kDa complex, this suggested that CDK2 was in excess and that cyclin E was rate limiting when it was complexed with CDK2. In order to confirm the interaction between CDK2, cyclin E and p27 protein in these high molecular weight complexes, the relevant fractions were immunoprecipitated with

anti-p27 antibody and then, the immunocomplexes were analyzed by immunoblot using antibodies against CDK2 and cyclin E. The results showed that p27 was effectively bound to CDK2 and cyclin E in the ~200 kDa complex (Figure 4.28B). Moreover, it has been also shown in our laboratory that in the Kp27MER model, p27 coimmunoprecipitated with D-type cyclins and CDK4/6 in the high molecular weight complex (J. C. Acosta personal communication). Furthermore, it has been also reported that cyclin A is also present in this high molecular weight complex although in other cell models as Swiss 3T3 MEFs (Poon*, et al.*, 1995).

With regard to the p27 eluting at ~50 kDa, p27 did not coimmunoprecipitated with CDK2 or cyclin E (Figure 4.28B). Thus, we decided to study whether p27 eluting at ~50 kDa was associated to another unknown protein. It had been previously described that p27 was heat resistant (Hengst*, et al.*, 1994; Polyak*, et al.*, 1994a). Thus, we treated for 5 min at 100 ºC the fractions containing the low molecular weight p27 to denature the possible associated proteins and to release free p27 (Figure 4.28C). As expected, p27 was heat-resistant but not the co-eluting CDK2 which was denatured and precipitated after heat treatment (Figure 4.28C). Then we re-chromatographed the supernatant under the same conditions to see whether the mobility of p27 was affected. As shown in figure 4.28D, heat-treated p27 was eluting again with the same molecular weight of ~50 kDa. This result suggested that the p27 found in the ~50 kDa was in the form of free protein. Finally, to confirm it, we decided to compare the mobility in gel filtration with a recombinant p27 hexahistidine-tagged (His_6-p27) purified from bacteria. We found again that the His_6-p27 showed the same mobility as the low molecular weight complex (~50 kDa) (Figure 4.28E). This result confirmed that p27 eluting at ~50 kDa was in free form.

Given that free p27 eluted as a 50 kDa protein, it was possible that p27 was behaving as a dimer in native conditions. To explore this possibility we decided to carry out an *in vitro* experiment which consisted in mixing equimolar amounts of His_6-p27 and a bacterially expressed p27 fused with the Glutathione S-transferase at its N-terminus (GST-p27) (Taules*, et al.*, 1999) in order to observe intermediate molecular weight complexes GSTp27-His_6p27. It should be noted that GST-p27 fusion protein has a molecular weight of ~50 kDa in denaturing conditions (Figure 4.29B, SDS-PAGE). Moreover, it had been described that the GST dimerized *in vitro* (Parker*, et al.*, 1990; Maru*, et al.*, 1996). Gel filtration of GST-p27 showed that it eluted as a single peak of around ~300 kDa (Figure 4.29). This finding was consistent with the hypothesis of a dimeric conformation of p27 and the expected tetrameric conformation of GST-p27.

Then we performed the mixing experiment. The mixture His_6-p27 + GST-p27 was incubated for 3 hours at 37ºC in the chromatography buffer and then subjected to gel-filtration chromatography followed by SDS-PAGE and coomassie blue staining. The results did not show any intermediate molecular weight complex (Figure 4.29A, *blue graph* and B). This finding indicated that the low molecular weight complex of p27 was not properly a dimer but monomeric free p27 which migrated anomalously in gel filtration probably owing to its intrinsically unstructured nature (Sivakolundu*, et al.*, 2005). Finally, analytical ultracentrifugation studies confirmed that His_6-p27 presented an elongated shape conformation and it behaved as a monomer in native conditions (German Rivas personal communication).

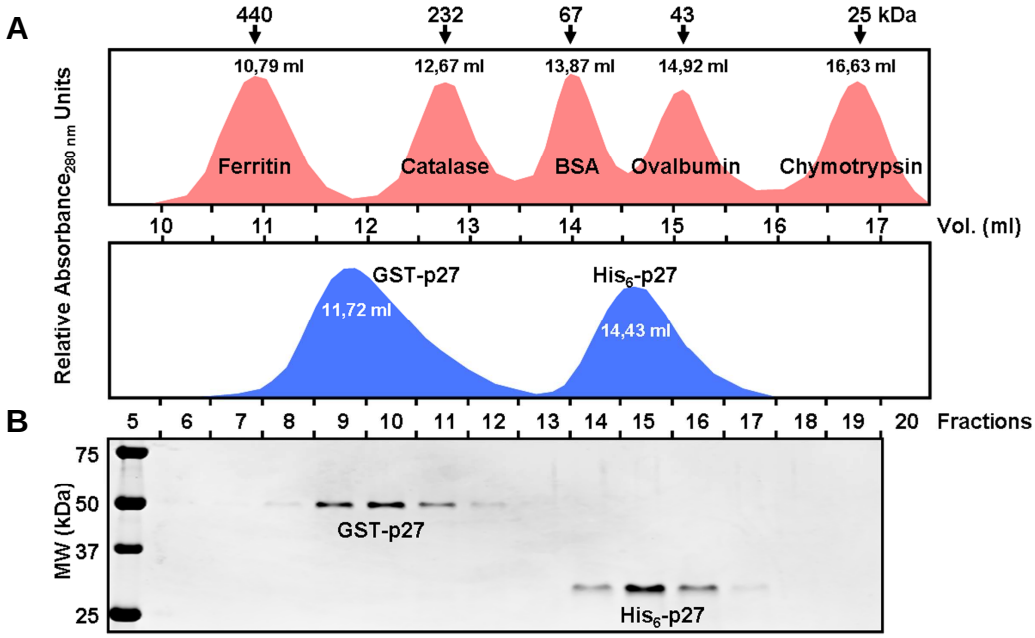

Figure 4.29. GST-p27 and His_6-p27 do not form heterodimers. An equimolar mixture (1:1) of recombinant GST-p27 and His_6-p27 was incubated for 3hours at 37ºC in chromatography buffer and then subjected to gel filtration chromatography on Superdex-200 HR column. A) The exact elution volumes (Vol.) were determined by absorbance a 280 nm using an AKTA purifier apparatus and the UNICORN software (blue graph). The exact molecular weights of recombinants GST-p27 and His_6-p27 in native or non-denaturing conditions were determined by comparing their respective elution volumes with those of known protein standards (red graph). B) Equal aliquots of the indicated fractions were analyzed by SDS-PAGE and Coomassie staining to verify protein distribution and denatured molecular weight of every protein (bottom panel). On the top of the panels, the arrows indicate the elution volume and the molecular weight of protein standards.

4.3.2. p27 accumulation as free form correlates with the complete cell proliferation block observed at high Zn^{2+} doses in presence of active MYC

The p27 accumulation as free form within Kp27MER cells exposed to high Zn^{2+} doses (75 µM $ZnSO_4$) suggested that p27 could be exceeding the requirements to bind and inhibit all available cyclin/CDK complexes. This would explain why MYC could not counteract the cell cycle arrest of Kp27MER cells upon treatment by high Zn^{2+} concentration. To investigate this possibility, we decided to compare by gel filtration chromatography the p27 distribution over time (6,12 and 24 hours) at the two Zn^{2+} concentrations (50 and 75 µM $ZnSO_4$) and in presence or absence of active MYC (4HT) in Kp27MER cells. As shown in figure 4.30, we found that at short periods of time of p27 induction (6 hours) with 75 µM Zn^{2+} all p27 was only present in high molecular weight complexes (~200 kDa) and thus bound to cyclin/CDKs. However at 12 and 24 hours post-induction and coinciding with the top of p27 expression, apart from high molecular weight complexes, we observed that p27 also eluted as free form, even in presence of active MYC. Interestingly, not free form elution was observed at lower Zn^{2+} doses in presence or absence of active MYC (Figure 4.30, 50 µM Zn^{2+} treatments).

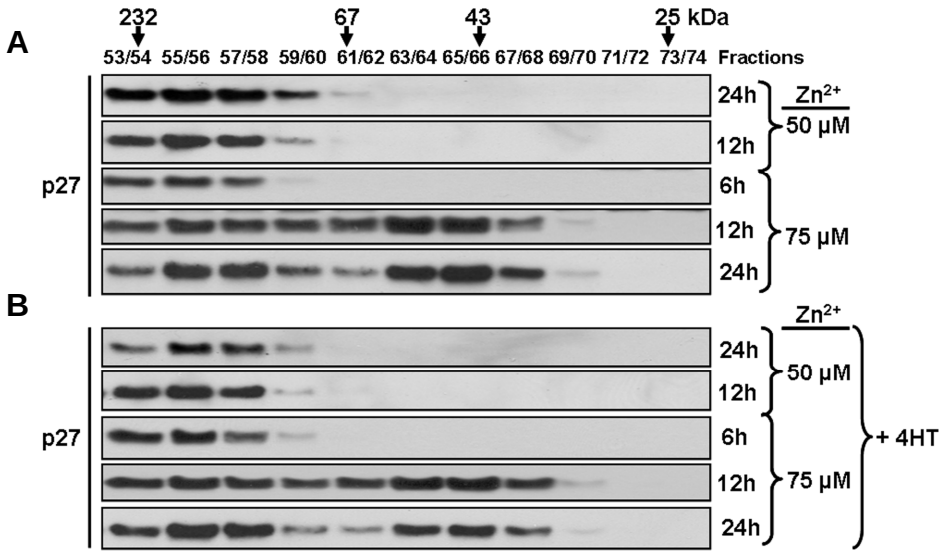

Figure 4.30. p27 accumulates in free form after 12 hours post-induction with high Zn^{2+} doses in Kp27MER cell extracts. Kp27MER cells treated with 50 or 75 µM $ZnSO_4$ in presence (A) or absence (B) of 200 nM 4HT for 6, 12 or 24 hours respectively (as indicated) were lysed softly in nondenaturing conditions and 3mg of every protein extract was fractionated by gel filtration chromatography on Superdex-200 HR column. Equal aliquots of the indicated fractions (on the top of the panel), were analysed by immunoblotting against p27. Fraction numbers and the fraction elution of protein standards are shown at the top of the figure. No appreciable p27 signal was found at 6 hours post-induction and low Zn^{2+} doses (50 µM Zn^{2+}) (not shown).

These findings suggested that at high Zn^{2+} doses (with 75 µM $ZnSO_4$), p27 first bound all available cyclin/CDK complexes and then, the excess of p27 overexpressed, accumulated in free form. Moreover these results also indicated that p27 bound only to cyclin/CDK complexes and not to monomeric CDKs (Figure 4.28A). Based on these findings and the results obtained by J.C Acosta *et al.* (Acosta*, et al.*, 2008) we conclude that the G1-S transition block occurs at this point when p27 begin to accumulate as free form.

4.3.3. MYC promotes free-p27 displacement toward high molecular weight complexes where it co-elutes with SKP2

However, as previously described in this Thesis, p27 degradation also occurs at high p27 levels. Thus we decided to analyze in more detail the effect of MYC in the p27 distribution. The densitometry quantification of chromatograms from cells Kp27MER cells treated whit 75 µM $ZnSO_4$ (Zn^{2+}) at 24h post-induction in the presence and absence of active MYC (Figure 4.30) revealed that MYC activation promoted a subtle redistribution of p27 free form to high molecular weight complexes (Figure 4.31). This redistribution could be explained, at least in part, through the induction of cyclin A (Section 4.2.2.), cyclin D2 or CDK4 among others (Acosta*, et al.*, 2008) by MYC and thus the generation of new cyclin/CDK complexes which could be sequestering free p27.

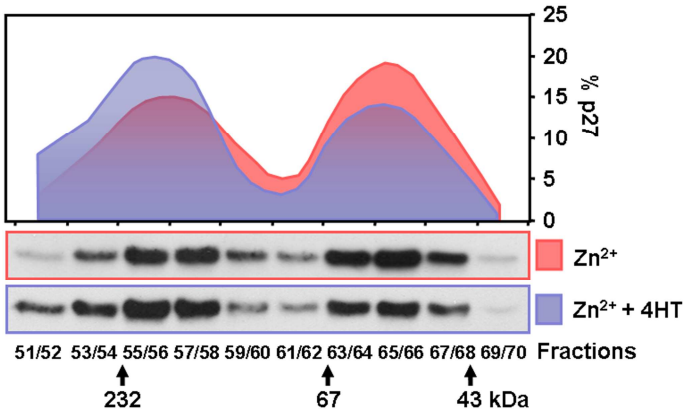

Figure 4.31. MYC promotes p27 free redistribution to high molecular weight complexes. Relative distribution of free and cyclin/CDK bound p27 determined by immunoblot densitometry analysis of Kp27MER cells treated for 24 hours with 75 µM $ZnSO_4$ in presence (blue) or absence (red) of 4HT. The Image J software was used to densitometry quantification analysis. p27 amounts are expressed as % relative to the total p27 in all fractions. Fraction numbers and the fraction elution of protein standards are shown at the bottom of the figure.

Moreover, at lower Zn^{2+} doses (50 µM $ZnSO_4$) and 24h post-induction the total p27 levels decreased from high molecular weight complexes in presence of active MYC (Figure 4.30, compare 50 µM Zn^{2+} treatments +/- 4HT at 24 hours). This decrease from the high molecular weight p27 complexes suggested that the cyclin/CDK/p27 complexes were the main targets for p27 degradation by de SCF^{SKP2} complex, as it has been previously reported (Zhu*, et al.*, 2004b). Given that the estimated average molecular weight of a cyclin/CDK/p27 complex was about ~100 kDa and the high molecular weight complexes had a molecular mass of about ~200 kDa, this also suggested the possible presence of proteins other than cyclins, CDKs and the CDK inhibitor which could participate in its degradation such as proteins of the SCF^{SKP2} complex. In addition, it had been reported that the *in vitro* reconstituted SCF^{SKP2} bound to cyclin A/CDK2/p27 complex migrated with an apparent molecular weight of ~230 kDa (calculated MW 251.6 kDa) in gel filtration chromatography on a Superdex-200 HR column (Hao*, et al.*, 2005). Thus, we decided to study the possible presence of SKP2 in the high molecular weight complex. In cells treated with 50 µM Zn^{2+} and 4HT we found that SKP2 coeluted with p27 complex (Figure 4.32, lower panel) suggesting furthermore the presence of other components of SCF^{SKP2} complex and giving an explanation for degradation of p27 from this complex. However, further studies are required to confirm the presence of SCF^{SKP2} elements in these high molecular weight complexes.

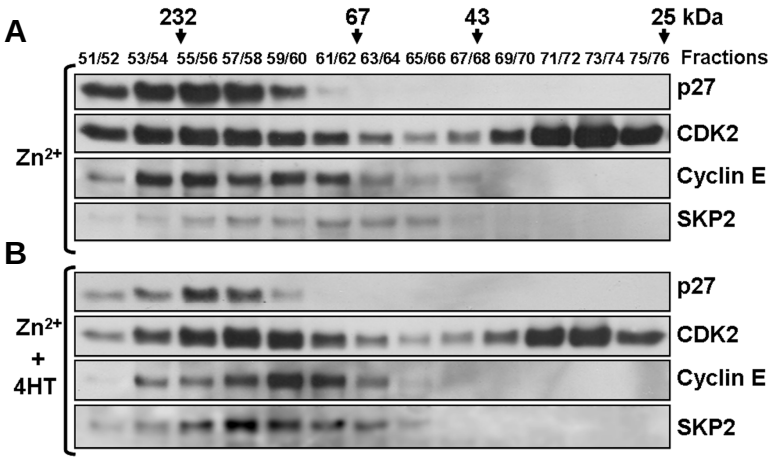

Figure 4.32. SKP2 coelutes with high molecular weight p27 complexes. Immunoblotting analysis against p27, CDK2, cyclin E and SKP2 of protein extracts from Kp27MER cells treated for 24 hours with 50 µM $ZnSO_4$ in presence (A) or absence (B) of 200 nM 4HT, fractionated by gel filltration chromatography on Superdex-200 HR column. Fraction numbers and the fraction elution of protein standards are shown at the top of the figure.

5. DISCUSSION

5. DISCUSSION

It is widely accepted that the function of the oncogenic transcription factor MYC in cell proliferation is ligated to its effects on the cell cycle inhibitor p27 (see “Introduction”, section 1.4.6.1.). Previously in our laboratory it was engineered a K562 derived cell line with conditional expression of p27 and MYC (Kp27MER) to study the antagonism between these two proteins in proliferation and differentiation (Acosta*, et al.*, 2008). The levels of p27 in these cells can be modulated by increasing the concentration of inducer (Zn^{2+}) in the culture media. The effect of MYC in proliferation of these cells was clearly dependent on the levels of p27 protein. At high p27 levels, MYC was not able to counteract the inhibitory effect of p27 on proliferation, but at lower p27 levels MYC was able to promote an increase in cell proliferation of otherwise arrested cells. This was due, at least in part, to a moderate down-modulation of p27 levels induced by MYC (Acosta*, et al.*, 2008). In this work we have used this cell model as a tool to study the mechanism involved in p27 down-modulation mediated by MYC.

5.1. THE MYC-SKP2 INTERACTION

In the first part of this Thesis we have identified SKP2 as a novel MYC target gene in K562 cells. SKP2 is the F-box protein of the SCF^{SKP2} ubiquitin ligase complex and thus the protein involved in the recognition of substrates to be ubiquitinated by this E3 complex, having p27 as main target. Moreover, we have found that SKP2 regulation by MYC is not only specific of K562 cells but can be observed in several others cell models from different origins or even in primary tumor samples (CML).

5.1.1. MYC regulates SKP2 expression independently of its effects on cell proliferation

Several mechanisms have been previously proposed to explain the MYC effect on p27 down-modulation, including transcriptional repression (Yang*, et al.*, 2001; Chandramohan*, et al.*, 2004) or induction of CUL1 (O'Hagan*, et al.*, 2000) and CKS1 (Keller*, et al.*, 2007). CUL1 and CKS1 are also components of the SCF^{SKP2} ubiquitin ligase complex. However, none of the previously mentioned mechanism seems to work in the Kp27MER model. The transcriptional repression p27 has been directly discarded because, in these cells, the exogenous p27 expression is controlled by the sheep metallothionein promoter which only responded to heavy metals. On the other hand, we have not found changes in CUL1 or CKS1 protein expression in Kp27MER cells after MYC activation in presence or absence of p27. This could be due to differences in the origin of cell models used in every experiment. CUL1 induction was observed in primary human fibroblast derived from fetal lung tissue (IMR90 cells) transduced with the MYCER protein (O'Hagan*, et al.*, 2000), whereas CKS1 induction was observed in B cells from Eμ-MYC transgenic mice and MEFs transduced with the MYCER construct (Keller*, et al.*, 2007). All this

has led us to look for an alternative mechanism to explain p27 down-modulation after MYC activation in Kp27MER cells.

Using a large-scale gene expression analysis of Kp27MER cells performed in our laboratory (Acosta*, et al.*, 2008) we identified SKP2 as a possible transcriptional target of MYC. The involvement of SKP2 in p27 degradation is widely accepted and has been confirmed in studies with knockout mice. Indeed, *Skp2*$^{-/-}$ mice accumulate high p27 protein levels in all tissues and they are smaller compared to wild type animals (Nakayama*, et al.*, 2000). Nonetheless, the elimination of p27 gene in *Skp2*$^{-/-}$ mice is able to rescue this phenotype (Nakayama*, et al.*, 2004), demonstrating that SKP2 is the major F-box protein involved in p27 degradation. Given that the induction of SKP2 by MYC could be relevant to explain the p27 degradation observed in Kp27MER cells, we decided to study whether SKP2 up-regulation was an indirect effect of MYC activity or it was a direct effect, i.e., whether *SKP2* was a MYC target gene. Nevertheless, since SKP2 is a protein associated to cell cycle progression (actually, SKP2 stands for “S phase kinase-associated protein 2”) (Zhang*, et al.*, 1995) and MYC stimulates proliferation, it was conceivably that SKP2 induction could be an indirect effect of MYC-induced cell proliferation. In fact, SKP2 expression had been already used as an independent marker of MYC-induced cell proliferation in prostate cancer cells (LNcaP) (Bernard*, et al.*, 2003).

To rule out this possibility we have analyzed SKP2 expression in four K562-derived cell models, in which we could induce or activate MYC in conditions of proliferative arrest. The proliferative arrest was achieved by different approaches: ectopic p27 overexpression, TPA and imatinib treatments, and p53 activation. In all cases, we have found that MYC induces SKP2 at mRNA and protein levels in proliferative arrest conditions. Thus we have concluded that the induction of SKP2 by MYC was not an indirect consequence of a MYC-mediated induction of proliferation but it is directly induced by MYC.

It is worthy to mention that some approaches used here to inhibit cell proliferation have previously been described to affect SKP2 expression in greater or lesser extent. For instance, it had been described that the transcription factor p53 repressed *SKP2* after DNA damage (Barre and Perkins, 2010). Accordingly, we have observed that SKP2 is down-modulated after p53 activation in KMYCBp53 cells. However, we found that MYC is able to counteract the SKP2 down-modulation mediated by p53.

On the other side, K562 cells derive from chronic myeloid leukemia and thus express the tyrosine kinase BCR-ABL. It has been described that BCR-ABL up-regulates MYC expression (Xie*, et al.*, 2002; Gomez-Casares*, et al.*, 2004; Samanta*, et al.*, 2006), but also that BCR-ABL induces SKP2 expression (Andreu*, et al.*, 2005; Chen*, et al.*, 2009). Accordingly, we have observed that inhibition of BCR-ABL by imatinib promotes SKP2 down-regulation in KMER4 cells. However, we have found that ectopic MYC up-regulates SKP2 in presence of imatinib, i.e., with inhibited BCR-ABL. This suggests that the effect of MYC is dominant over the effect of BCR-ABL on SKP2. A likely explanation is that MYC could be acting downstream of BCR-ABL to induce SKP2. Therefore, we propose that BCR-ABL induces MYC and, in turn, MYC induces *SKP2* expression.

5.1.2. SKP2 is a MYC target gene

However, the concomitant SKP2 expression after MYC induction or activation in arrested cells, does not demonstrate yet that SKP2 is a direct MYC target gene. The demonstration is based on four additional observations:

First, we have found that SKP2 was down-modulated after MYC silencing in K562 cells or after *MYC* repression in p493.6 and TM1 cells. In agreement with ours findings, *SKP2* was one of the genes down-regulated in a genome-wide transcriptional study upon *MYC* silencing in human breast carcinoma cells (Cappellen*, et al.*, 2007). In addition, we have observed that *MYC* null rat fibroblast (HO15.19 cells) express lower SKP2 protein levels than parental cells (TGR-1 rat fibroblast). Furthermore, unlike TGR-1 cells, SKP2 is not down-regulated after serum deprivation in *MYC* null cells suggesting that MYC is essential for SKP2 up-regulation in response to growth factors stimulation. However, the presence of SKP2 in *MYC*$^{-/-}$ cells although in small amounts, indicates that MYC is not absolutely required for *SKP2* gene transcription. Thus, SKP2 expression cannot be expected to correlate to MYC in all cell types and tumors. Lastly, it should be noted that all these experiments have been carried out with cell models from different tissues and species, suggesting that the SKP2 regulation by MYC is a general feature in animal cells.

Second, there was the possibility that MYC might stimulate SKP2 expression through the induction of additional transcription factors which in turn would directly bind and activate *SKP2* promoter. For instance, It has been described that MYC induces E2F1 (Berns*, et al.*, 2000) and that *SKP2* was transcriptional target of E2F1 in human tumor cell lines (Zhang and Wang, 2006; Reichert*, et al.*, 2007) and mouse fibroblasts cells (Yung*, et al.*, 2007). Furthermore, it has been reported that E2F1 was required for MYC-mediated down-modulation of p27 in *Eμ-MYC* B cells (Baudino*, et al.*, 2003). However, we have shown that MYC induces SKP2 mRNA expression in presence of cycloheximide and thus in absence of *de novo* protein synthesis. This finding strongly suggests that MYC induces *SKP2* directly and that additional intermediary transcription factors such as E2F1 are not strictly required to induce *SKP2*. In accordance with this last suggestion, it has been reported that *SKP2* expression is induced by MYC in absence of E2F1 (Old*, et al.*, 2010). However, in contrast to our results, Keller and collaborators have shown that MYC regulates *SKP2* indirectly because *SKP2* is not induced after MYCER activation in presence of CHX in primary early-passage MEFs (Keller*, et al.*, 2007). The discrepancy with our results could lie in the time to study *SKP2* mRNA expression after cycloheximide treatment. We have analyzed *SKP2* mRNA expression 6 hours after CHX treatment because MYCER half-life was approximately of 3 hours in Kp27MER (see figure 4.9A). In contrast, Keller *et al.* studied *SKP2* mRNA expression after 24 hours of cycloheximide treatment. Given the short half-life of MYCER, it is likely that 24 hours could be too long period of treatment to detect MYC effects in the experimental setting reported by Keller *et al*.

Third, we have shown that MYC transactivates a reporter construct containing 1148 pb of human *SKP2* promoter. It should be noted that K562 derived cell lines with conditional expression of MYC (KMYCJ, KMYCBp53, KMER4 or Kp27MER cells) express already high levels of endogenous MYC protein in basal conditions. TPA treatment provokes the down-modulation of endogenous MYC and allows us to independently analyse the effect of the induced MYC protein in KMYCJ cells treated with Zn^{2+}. Therefore, we have concluded that MYC induces the *SKP2* promoter and that the exogenous Zn^{2+}-induced MYC is able to revert the effect of TPA on *SKP2* promoter. This result is also in agreement and complements our previous finding showing SKP2 mRNA and protein expression after MYC induction in KMYCJ cells exposed to TPA (Figure 4.5). Finally, TPA could be replaced by imatinib with similar results given that it has been shown that SKP2 promoter is also down-regulated after imatinib treatment in K562 cells (Chen*, et al.*, 2009).

Fourth, we have demonstrated by ChIP experiments that MYC binds to the human *SKP2* promoter in K562 cells growing in normal conditions but not in cells with depleted Myc (i.e., treated with TPA or Imatinib). Specifically, we have found that MYC binds to a ~400 bp long region containing two non-canonical E-boxes (CACGCG and CATGCG) upstream of transcription start site but not to the canonical E-box (CACGTG) found in the second exon. Our results are in agreement with previous findings showing that MYC has more affinity for these two non-canonical E-boxes than for the canonical E-box (Grandori*, et al.*, 1996). Moreover, recent studies of high-throughput sequencing of ChIP DNA (ChIP-PET) have demonstrated that a significant fraction of the loci occupied by MYC lacks obvious DNA element that resemble canonical E-boxes (Zeller*, et al.*, 2006; McMahon, 2010). In this sense, it is interesting to mention that the absence of canonical E-boxes (CACGTG or CACATG) in mouse *Skp2* promoter was used by Old and coworkers to argue that MYC regulated SKP2 expression in an indirect fashion (Old*, et al.*, 2010). Nevertheless, MYC binding to *Skp2* promoter has been recently reported in a ChIP-sequencing study in mouse embryonic stem cells despite the absence of canonical E-boxes (Kim*, et al.*, 2010).

Finally and in consistency with our ChIP results we have corroborated the MYC binding to *SKP2* promoter using ChIP-sequencing datasets generated by the ENCODE consortium and available in the UCSC genome browser. It should be noted that the independent ChIP-sequencing provided by the ENCODE consortium was also developed in K562 cells using the same antibody that we have used in this Thesis. Moreover, besides reinforcing our results, these data have given us the confidence to use this database to *in silico* analyze the *SKP2* promoter looking for additional elements which could be regulating it. In this way, we have found that in K562 cells growing in normal conditions, the *SKP2* promoter presents several histone marks associated to active chromatin such as H3K9ac, H3K27ac and H3K4me3, indicating that this promoter is relatively active. In addition, we have found that it concentrates several proteins including MAX (the MYC dimerization partner); the histone acetyl-transferase p300 and the RBPP5 subunit of the histone methyltransferase complex MLL1 (involved in the acetylation or methylation respectively of these histones) or elements of basal transcription machinery such as

TBP or RNA polymerase II. All these elements have been found to interact with MYC in a greater or lesser extent in other cell models, on other loci or in different experimental conditions (see Introduction, section 1.4.3.). Furthermore, this database shows that MYC binding to *SKP2* promoter is not exclusive of K562 cells but also occurs in several other human cell lines including NB4, HepG2, Hela and A549. These results confirmed that *SKP2* regulation by MYC also occurs in other human tissues, although ChIP-seq data from other species are not available yet.

Taken collectively all these findings we conclude that *SKP2* is a new MYC target gene. Moreover, based on our results and the data of UCSC database we hypothesized the next model by which MYC/MAX heterodimers recognize and bind to both non-canonical E-boxes on *SKP2* promoter, recruiting the histone acetyltransferase CBP/p300 and the histone methyltransferase complex MLL1 and allowing, in turn, the association of the basal transcription machinery (TBP and RNA polymerase II among other subunits) to activate and maintain *SKP2* expression in K562 cells (Figure 5.1).

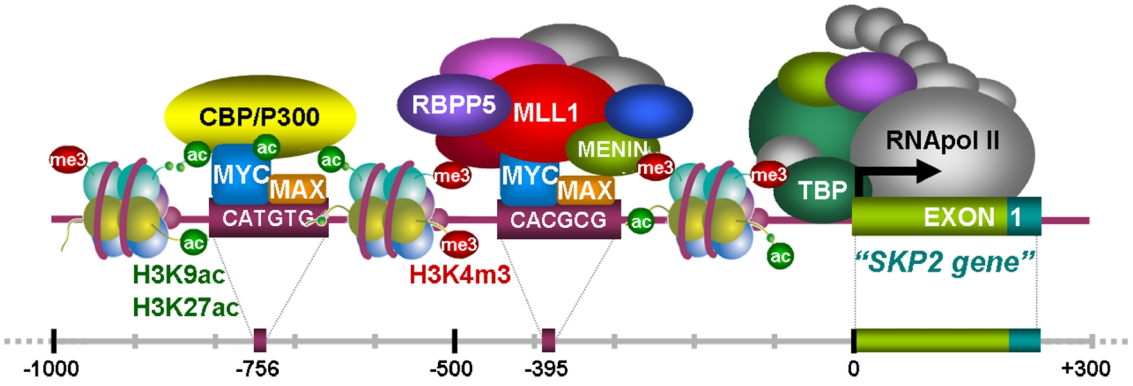

Figure 5.1. MYC binds to the *SKP2* promoter and recruits CBP/p300 and MLL1 complex to activate and maintain its expression in K562 cells. MYC-MAX heterodimers recognize the two non-canonical E-boxes located on the *SKP2* promoter (CATGTG and CACGCG, 756 and 395 pb upstream of transcription start site, respectively) and recruit the CBP/p300 histone acetyltransferase which acetylates histone H3 at lysine 27 and the MLL1 histone methyltransferase complex which trimethylates the histone H3 at lysine 4 on *SKP2* promoter allowing an environment of active chromatin**.** This allows the recruitment of different elements of basal transcription machinery such as TBP and RNA polymerase II which in turn are responsible of *SKP2* transcription.

5.1.3. SKP2 has no effect on MYC expression or transactivation

We have found that *SKP2* is a MYC target gene and therefore that *SKP2* expression is dependent on MYC activity. In addition, it has been reported that SKP2 binds to MYC to activate its transcriptional activity but at the same time to promote its ubiquitination and degradation by the proteasome, (Kim*, et al.*, 2003; von der Lehr*, et al.*, 2003). This has led us to explore whether MYC stability and transcriptional capacity was affected in turn by SKP2 in the K562 model. However, we have not detected any effect of SKP2 on MYC protein stability (as assessed by immunoblot) or transcriptional activity (as assessed by luciferase assays) at least in this model. This discrepancy could be due to differences in cell models used in these studies. We have used

K562 cells, which express high basal MYC levels compared with other human cell lines (Delgado*, et al.*, 1999). Therefore it could be expected exhaustion of the SKP2-dependent degradation machinery for MYC in K562 cells. Nevertheless, our results are in agreement with those of Old and co-workers showing that *Skp2* loss does not led to increased levels of MYC protein and does not affect the expression of MYC targets genes in B-cells from *Eμ-MYC* mice (Old*, et al.*, 2010). Also, most of the recent literature suggest that the major complexes responsible of MYC ubiquitination and degradation are the HECT domain-containing E3 enzyme, HectH9 (Adhikary*, et al.*, 2005) and the F-box protein FBW7 (Welcker*, et al.*, 2004; Yada*, et al.*, 2004). In fact, a recent report has showed that MYC degradation in hematopoietic cells is only dependent on FBW7 ubiquitin ligase and not on SKP2 (Reavie*, et al.*, 2010).

5.1.4. MYC and SKP2 expression correlates in hematologic tumors

Given that the K562 cell model derived from a CML patient in blast crisis, we have studied the interaction between MYC and SKP2 in primary bone marrow samples from CML patients at diagnosis and in a small cohort of imatinib treated patients. As well as in K562 derived cell models, we have found a positive correlation between MYC and SKP2 expression at mRNA and protein level in CML patients. Moreover, we have found that *MYC* and *SKP2* mRNA levels are generally up-regulated at diagnosis and that they are down-regulated in imatinib-treated patients. Accordingly, elevated levels of *MYC* expression in CML patients at diagnosis and its down-modulation after imatinib treatment have been previously reported (Albajar*, et al.*, 2011), although its correlation with *SKP2* expression had never been studied before. The importance of *SKP2* induction by MYC in CML samples is highlighted by previous results showing that SKP2 is a mediator of BCR-ABL-induced myeloid leukemia in mice (Agarwal*, et al.*, 2008). Based on our results we suggest that MYC could be responsible for the induction of *SKP2* in primary human CML samples and that the axis BCR-ABL→MYC→SKP2 could play a key role in the pathogenesis of CML.

On the other hand, using cancer gene expression databases such as Oncomine and GeneSapiens we have also found a MYC-SKP2 correlation in human B cell lymphomas and in acute myeloid leukemia (AML). Remarkably, Burkitt lymphomas express high levels of *SKP2* mRNA. This lymphoma is characterized by the deregulation of *MYC* gene due to a translocation. In addition, *SKP2* mRNA and protein levels have been also found to be markedly elevated in lymphomas that arise in *Eμ-MYC* mice (Keller*, et al.*, 2007). Meanwhile, the importance of *SKP2* correlation with *MYC* in AML samples is enhanced because *MYC* has been found overexpressed in AML (Delgado and Leon, 2010; Delgado*, et al.*, 2013) and elevated SKP2 levels represent a poor prognostic factor in this malignancy (Min*, et al.*, 2004). Finally, recent results in our laboratory show a strong correlation between MYC and SKP2 in chronic lymphocytic leukemia (CLL) (J.M. Caraballo PhD dissertation). Our findings strongly suggest that MYC is the main regulator of SKP2 expression in all these hematologic malignancies but probably in several others human cancers overexpressing SKP2.

5.2. THE MYC-SKP2-p27 AXIS

In the second part of this Thesis we have demonstrated that p27 down-modulation previously observed in Kp27MER cells was due to the induction of SKP2 by MYC. Moreover, and conversely to the idea previously established in the literature, we have identified cyclin A/CDK1 complexes instead of cyclin E/CDK2 complexes as principal mediators of p27 phosphorylation at Thr187 after MYC activation, being this phosphorylation event a prerequisite for p27 targeting by the SCF^{SKP2} ubiquitin ligase complex. Finally, we have shown that SKP2 is an important mediator for MYC mediated tumorigenesis using a xenograft model in nude mice.

5.2.1. MYC promotes p27 phosphorylation by cyclin A induction

Previous studies indicated that p27 needed to be phosphorylated at Thr187 to be recognized by the SCF^{SKP2} ubiquitin ligase complex, and thus to be efficiently ubiquitinated and targeted by the proteasome system (Hao*, et al.*, 2005). We have found that MYC promotes $p27^{Thr187}$ phosphorylation 8-12 hours after MYC activation in cells expressing the MYCER chimera (Figure 4.18B). Moreover we have observed that the phosphorylation was independent of p27 protein level (Figure 4.18A) suggesting that the kinase involved in this event was not inhibited by p27. Induction of $p27^{pThr187}$ by MYC had been previously reported by *in vitro* phosphorylation assays, using protein extracts from MYC-expressing cells (Muller*, et al.*, 1997) although it was never demonstrated *in vivo* in cells with induced expression of MYC.

The induction of $p27^{Thr187}$ phosphorylation by MYC led us to investigate the kinase responsible for this effect. It had been described that MYC induced cyclin E expression (Jansen-Durr*, et al.*, 1993; Perez-Roger*, et al.*, 1997) and that cyclin E/CDK2 complexes mediated p27 phosphorylation at Thr187 at G1/S phase transition (Muller*, et al.*, 1997; Sheaff*, et al.*, 1997; Vlach*, et al.*, 1997; Montagnoli*, et al.*, 1999). However, our findings suggest that, not only cyclin E/CDK2 but also cyclin A/CDK1 complexes play an important role in this phosphorylation event induced by MYC. This conclusion is based on several observations:

First, we have found no correlation between cyclin E protein levels and $p27^{Thr187}$ phosphorylation. By contrast, we have observed cyclin E protein stabilization in presence of Zn^{2+}-induced p27 (Figure 4.19). This effect of p27 on cyclin E stability has been previously reported. It appears that p27 inhibits the ubiquitination and degradation of cyclin E (Clurman*, et al.*, 1996). On the other hand, we have found cyclin A expression concomitant to MYC activation even in presence of Zn^{2+}-induced p27, correlating with $p27^{Thr187}$ phosphorylation. Induction of cyclin A by MYC has been also previously described in several other cell models (Jansen-Durr*, et al.*, 1993; Barrett*, et al.*, 1995; Muller*, et al.*, 1997; Qi*, et al.*, 2007).

Second, the kinase activity of CDK2 on recombinant His_6-p27 was completely inhibited by endogenous p27 in presence of active MYC, after p27 induction by Zn^{2+} (Figure 4.20B). Accordingly, complete inhibition of CDK2 kinase activity by p27 using recombinant RB as

substrate has been previously reported by our group (Acosta*, et al.*, 2008). The complete inhibition of CDK2 by high levels of endogenous p27, in presence of active MYC also rules out a possible mechanism of CDK2 activation by another NRTK (Chu*, et al.*, 2007; Grimmler*, et al.*, 2007) likely induced or activated by MYC. In contrast, besides cyclin A induction by MYC, we have found kinase activity associated to cyclin A immunocomplexes on recombinant His_6-p27 when we activated MYC in presence of endogenous Zn^{2+}-induced p27 (Figure 4.20A).

Third, we have shown by co-immunoprecipitation assays that cyclin A not only binds CDK2 but also binds to CDK1 in Kp27MER cells (Figure 4.20D) and by kinase assays that CDK1 immunocomplexes are also able to phosphorylate recombinant His_6-p27, even in the presence of Zn^{2+}-induced p27 (Figure 4.20C). The ability of CDK1 to bind cyclin A (Tsai*, et al.*, 1991) and to phosphorylate $p27^{Thr187}$ has been previously reported (Montagnoli*, et al.*, 1999; Zhu*, et al.*, 2004b). Moreover, unlike CDK2 immunocomplexes, we have found that CDK1 immunocomplexes are not efficiently inhibited by induced p27. Accordingly, it has been reported that p27 has higher inhibitory potential on CDK2 than on CDK1 complexes (Polyak*, et al.*, 1994b; Toyoshima and Hunter, 1994).

And fourth, through *in vitro* phosphorylation assays using cyclin A and CDK1 immunocomplexes prepared from *Cdk2*$^{-/-}$ and Cyclin $E1^{-/-}/E2^{-/-}$ MEFs overexpressing MYC, we have demonstrated that: i) CDK2 is not necessary for MYC-mediated $p27^{Thr187}$ phosphorylation (Figure 4.21); ii) MYC induces CDK1 and CDK2 kinase activity in absence of E-type cyclins suggesting that cyclin A (and probably also cyclin B, in the case of CDK1) is responsible for this increased kinase activity; and iii) MYC induces the kinase activity associated to cyclin A in absence of CDK2, suggesting that CDK1 is the responsible kinase for this activity. In agreement with ours results, it has been reported the presence of phosphorylated $p27^{Thr187}$ in different tissues from *Cdk2*$^{-/-}$ mice (Berthet*, et al.*, 2003), arguing that CDK1-mediated phosphorylation of $p27^{Thr187}$ also occurs *in vivo*.

In summary, based on these results we propose that MYC promotes $p27^{Thr187}$ phosphorylation through the induction of cyclin A expression and cyclin A-associated kinase activity (Figure 5.2). Cyclin A can form complexes with CDK2 and CDK1, being the cyclin A/CDK1 the complexes which efficiently phosphorylate p27 at Thr187 when cyclin E-A/CDK2 complexes remain completely inhibited by the own p27. This function of CDK1 phosphorylating $p27^{Thr187}$ owing to MYC-induced cyclin A expression might be surprising given that CDK1 activity has been generally associated to G2-M phases and p27 activity to G0-G1 phases (see Introduction). However, the ability of CDK1 alone to drive not only G1-S transition (Aleem*, et al.*, 2005) but the complete mammalian cell cycle has been previously reported (Santamaria*, et al.*, 2007). Moreover, it should be noted that CDK1 and CDK2 shared a 60-65% of sequence identity with an 84% similarity (McGrath*, et al.*, 2005) and thus it is conceivably that they could also share the majority of substrates when complexed with the same cyclin. Lastly and independently of cyclin A

role in p27 phosphorylation, it should be mentioned that the binding of p27 to cyclin A/CDK2 complex but not to cyclin E/CDK2 complex is required for efficient p27 ubiquitination by SCF^{SKP2} (Zhu, *et al.*, 2004b) highlighting the importance of cyclin A in p27 targeting for degradation.

Finally, it might be interesting to study why the kinase activity associated to CDK2, cyclin A and to a lesser extend CDK1 was inhibited by the endogenous Zn^{2+}-induced p27 but not by recombinant His_6-p27 added to the experiment *in vitro*. The inability of bacterially produced p27 to inhibit CDK1 and CDK2 has been already observed (Zhu, *et al.*, 2004b) but no explanation has been proposed yet. The biochemical comparison between recombinant and cellular p27 could shed light on the posttranslational modifications that likely explain this difference.

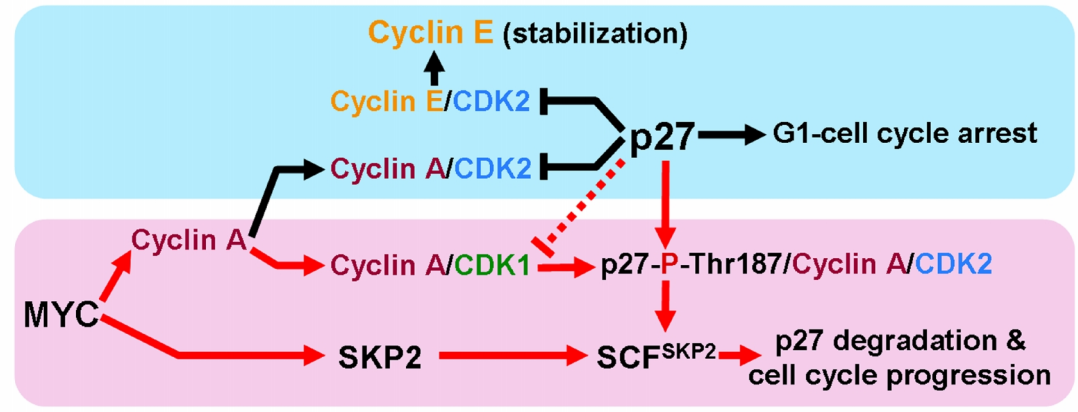

Figure 5.2. MYC promotes p27 phosphorylation trough cyclin A induction and cyclin A kinase associated activity. p27 blocks CDK2 kinase activity which is usually associated to cyclin E and A. MYC induces cyclin A which binds to CDK2 and CDK1. Cyclin A/CDK1 complexes are not inhibited efficiently by p27. In turn, p27 is phosphorylated at Thr187 by cyclin A/CDK1 complexes, promoting its recognition by the SCF^{SKP2} ubiquitin ligase complex and thus its degradation via proteasome.

5.2.2. MYC down-regulates p27 through SKP2 expression and SKP2 mediates tumor growth in nude mice

Apart from inducing $p27^{Thr187}$ phosphorylation, we have demonstrated that MYC-induced SKP2 is responsible for p27 down-regulation in K562-derived cell models (Figure 5.2). This conclusion is based in three findings:

First, we have shown by immunoblot that p27 protein levels inversely correlates with MYC-induced SKP2 expression in K562-derived cell models, including Kp27MER cells (Figure 4.22A), KMER cells growth-arrested by high cell density in culture (Figure 4.22C), KMYCJ cells arrested by TPA or Imatinib (Figure 4.26A and B) and serum deprived K562 cells (Figure 4.26D). We have observed the same result in serum deprived TGR-1 cell line (Figure 4.26C).

Second, we have shown by immunofluorescence assays that p27 and SKP2 localize in the nuclei of Kp27MER cells but they are mutually exclusive (Figure 4.23). Accordingly, it has been reported that SKP2-dependent ubiquitination of p27 only takes place in the cell nucleus (Nakayama and Nakayama, 2006). Moreover, the absence of p27 staining in the cytoplasm excludes the possibility of p27 degradation by ubiquitin ligases other than SKP2, such as KPC or SIAH1/SIP which only operate in the cytoplasm (Kamura*, et al.*, 2004; Nagano*, et al.*, 2011).

Finally, we have found that p27 accumulates in K562 cells after shRNA-mediated SKP2 silencing (Figure 4.24A). This finding confirms that SKP2 is the main mediator of p27 down-modulation in K562 cells but surely also in other K562-derived cell lines as Kp27MER cells.

Moreover, the reduced proliferation rate of the cells with silenced SKP2 compared to control cells (Figure 4.24B) also confirms that the MYC-SKP2-p27 axis is an important effector of cell proliferation mediated by MYC in leukemia cells. In this line, it has been recently reported that SKP2 is critical for *in vivo* MYC-driven keratinocyte (Sistrunk*, et al.*, 2011) and lymphocyte hyper-proliferation (Old*, et al.*, 2010).

We have also confirmed the functionality of the MYC-SKP2-p27 axis in vivo comparing the growth of tumor xenografts induced upon subcutaneous injection of K562 cells with silenced SKP2 expression versus control cells. We found that the tumors developed by KMERshSKP2 subline are smaller than these ones developed by control cells suggesting that SKP2 is an important mediator of the tumor growth. The result is consistent with the reduced proliferation rate of these cells in culture (Figure 4.24B) owing to the accumulation of p27 in absence of SKP2 (Figure 4.24A). However, reportedly SKP2 loss only has a modest effect in MYC-mediated lymphomagenesis in *Eμ-MYC* transgenic mice although lymphoid cell proliferation is impaired (Old*, et al.*, 2010). Similarly, *Skp2* deficiency does not affect the development of spontaneous tumors within the oral cavity in *K5-MYC*-transgenic mice (Sistrunk*, et al.*, 2011), a result that could be explained if cell proliferation in this tissue is less dependent on p27 inhibition.

5.3. THE MYC EFFECTS ON CELL CYCLE DEPENDS ON p27 PROTEIN LEVELS

In the last part of the Thesis we have found that p27 accumulates in free form in Kp27MER cells when high p27 levels were induced (i.e., with high Zn^{2+} doses as 75 μM $ZnSO_4$), even in presence of active MYC. This suggests that the induction rate of p27 is greater than the degradation rate mediated by the MYC-SKP2 axis and offers a possible explanation for the incapacity of MYC to promote proliferation of Kp27MER cells at high p27 concentrations.

5.3.1. p27 accumulation as free form leads to cell proliferation arrest even in presence of active MYC

In Kp27MER cells MYC counteracts the effect of p27 in cell proliferation at low p27 levels (i.e., cells treated with 50 µM $ZnSO_4$) but not at high p27 levels (i.e., cells treated with 75 µM $ZnSO_4$) (Acosta*, et al.*, 2008). However, we have found that p27-Thr187 phosphorylation and p27 down-modulation by the SCF^{SKP2} ubiquitin ligase complex also occurs at high Zn^{2+}-induced p27 levels (Figure 4.27). All these findings led us to consider the possibility that there was a threshold concentration of p27 which determined the complete proliferative arrest and which should be counteracted by MYC-SKP2 axis to result in cell proliferation.

Using gel filtration chromatography of protein extracts followed by immunoblot analysis we have found that in Kp27MER cells overexpressing high p27 protein levels (i.e. in cells treated with 75 µM $ZnSO_4$), all p27 distributed between two complexes: a high molecular weight complex (~200 kDa), in which p27 was found associated to cyclin/CDK complexes, including cyclin E/CDK2 (Figure 4.28B), but also cyclin D/CDK4-6 (J.C. Acosta PhD dissertation) and a low molecular weight elution form of around ~50 kDa. We have demonstrated that the low molecular weight elution form was free p27 by comparing the elution volume of p27 after heat treatment of the corresponding fractions and that of purified recombinant His_6-p27 (Figure 4.28C, D and E). Moreover, the migration of free p27 as a protein of ~50 kDa in gel filtration initially led us to believe that p27 behaved as a dimer in native conditions. This has been also suggested by Bouchard and collaborators (Bouchard*, et al.*, 1999). However, using a mixing experiment with the two recombinant p27 proteins (His_6-p27+GSTp27) we demonstrated that these proteins do not form heterodimers. Thus we conclude that free p27 [His_6-p27 or GSTp27, but also GFPp27 (not shown)] migrates anomalously in gel filtration. This anomalous elution of p27 in gel filtration chromatography has been also mentioned in the literature (Poon*, et al.*, 1995; Borriello*, et al.*, 2000). It should be noted that p27 is an intrinsically unstructured protein (Bienkiewicz*, et al.*, 2002) and thus p27 does not folds into a globular structure as the protein standards used in gel filtration calibration. The monomeric nature of bacterially produced His_6-p27 was confirmed by analytical ultracentrifugation experiments done in collaboration with the laboratory of German Rivas (Centro de Investigaciones Biológicas, CSIC, Madrid).

In addition, the comparative analysis of p27 distribution in Kp27MER cells treated with different Zn^{2+} dosages, in presence or absence of active MYC and at different times by gel filtration (Figure 4.30) revealed that:

i) The presence of p27 free form depends on Zn^{2+} concentration used and thus on the induced p27 protein levels, with p27 free form only appearing after induction with high Zn^{2+} doses (75 µM $ZnSO_4$), and independently of MYC activation.

ii) At short periods of time of p27 induction (~6 hours post-induction), not free p27 was observed (Figure 4.18B). This suggests that newly translated p27 associates immediately to cyclin/CDK complexes but does not remain as free form. All this suggests that p27 “accumulates” as free form into the cells when it is in excess over cyclin/CDK complexes. It must be noted that

the cyclins determine the amount of these complexes given that CDKs can be also found as free form in Kp27MER extracts and that free p27 does not bind to free CDKs but to CDK-cyclin dimers (Figure 4.28). Accordingly, not free form was observed at low p27 levels (50 µM $ZnSO_4$) at any moment.

Therefore, we propose that p27 reaches the threshold concentration which determines the complete proliferative arrest when p27 saturates all available cyclin/CDK complexes and it begins to accumulate as free form. It should be noted that the saturation of all cyclin/CDK complexes does not imply the complete inhibition of all such complexes, as we have previously demonstrated (Figure 4.18), but at least the complexes involved in G1-S transition and cell cycle progression such as cyclin D/CDK4-6 (Acosta*, et al.*, 2008) and cyclin A-E/CDK2 complexes (Section 4.2.2).

5.3.2. MYC promotes the p27 displacement from free form into high molecular weight complexes containing SKP2

The densitometric analysis of gel filtration cromatographies revealed that MYC promoted the displacement of free p27 into high molecular weight complexes containing cyclin/CDKs (Figure 4.31). This could be explained, at least in part, because MYC induces the expression of cyclin A (Section 4.4.2), cyclin D2 or cyclin B1 (Acosta*, et al.*, 2008) and thus MYC induces the assembly of new cyclin/CDK complexes (as CDKs are in excess) allowing that free p27 would bind to these new complexes. Furthermore, given that at low p27 levels we only observed high molecular weight complexes, SKP2-mediated p27 down-modulation only could be taking place from these complexes, and this led us to look for SKP2 distribution on them. Thereby, we found that SKP2 was also co-eluting with the high molecular weight complexes in presence of active MYC (Figure 4.32).

Thus, we hypothesize that SKP2 is bound to cyclin/CDK/p27 complexes. Although we did not formally demonstrated this through co-immunoprecipitation assays, it must be mentioned that SKP2 was originally discovered associated to cyclin A/CDK2 complexes (Zhang*, et al.*, 1995). This might explain the elevated molecular weight of these complexes (~200 kDa) whereas the estimated average molecular weight of a cyclin/CDK/p27 complex was just about ~100 kDa. In agreement with this suggestion, it has been described that the recombinant SCF^{SKP2} complex bound to cyclin/CDK/p27 complex presents an elution volume of ~230 kDa (Hao*, et al.*, 2005) in a gel filtration system similar to the one that we have used in this Thesis (Superdex-200). Moreover, our hypothesis would be also in agreement with previous reports showing that p27 needs the interaction with cyclin E-A/CDK2 complex to be targeted by the SCF^{SKP2} ubiquitin ligase complex (Montagnoli*, et al.*, 1999; Zhu*, et al.*, 2004b)..

In summary, we concluded that the effect of MYC on proliferation of K562 cells (and likely in many other cell types) depends on the p27 protein levels. At moderate p27 levels, the MYC-SKP2 axis is able to counteract the effect of p27 as cell cycle inhibitor thus resulting in cell proliferation. In this scenario, no free p27 is found, as all available p27 is bound and inhibiting cyclin/CDK complexes. However, a fraction of active cyclin/CDK complexes with no p27 bound is still present

in the cell. In contrast, at high p27 levels, there is a saturation of all cyclin/CDK complexes and thus an accumulation of p27 as free form. This p27 free acts as a reservoir to inhibit new cyclin/CDK complexes induced by MYC, but at the same time counteracts the p27 down-modulation from cyclin/CDK/p27 complexes by the MYC-SKP2 axis. As a result, the proliferation continues arrested despite SKP2-mediated p27 degradation (Figure 5.3).

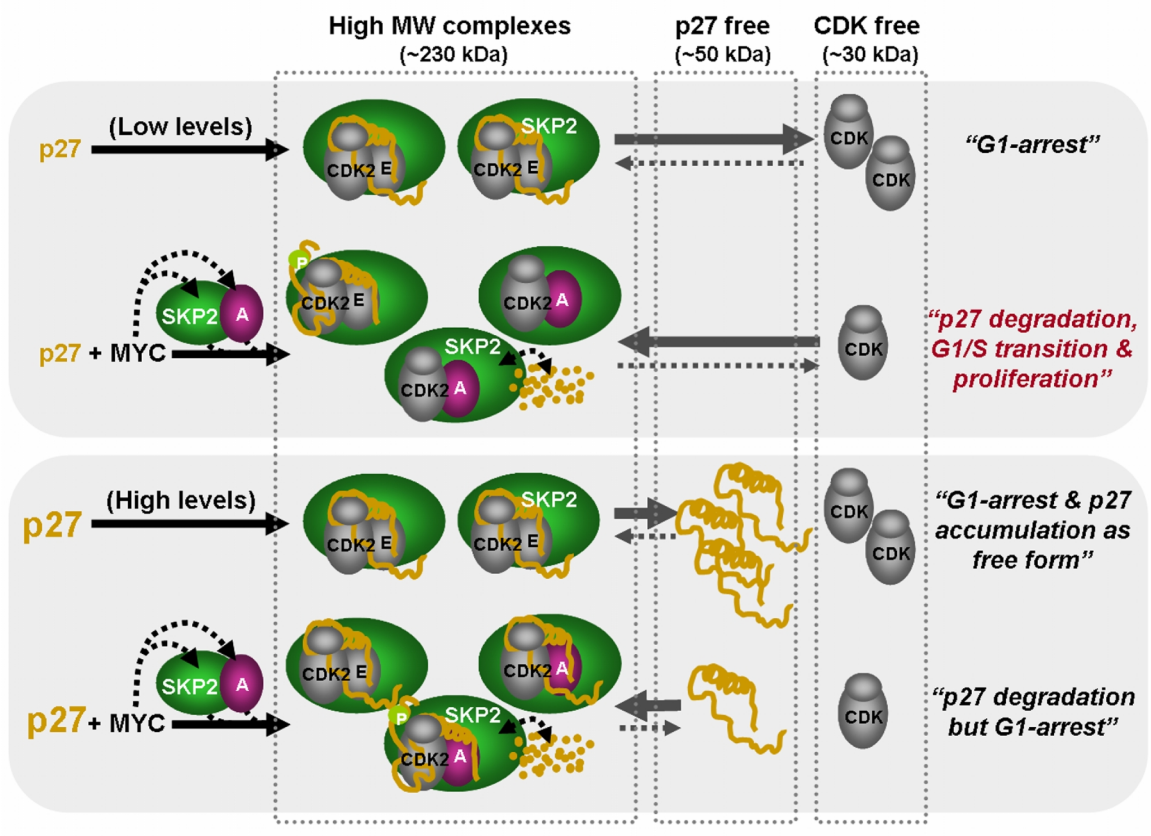

Figure 5.3. The effect of MYC on proliferation of Kp27MER cells depends on the balance between the p27 induction rate and the p27 degradation rate by the MYC-SKP2 axis. At low p27 levels (50 µM $ZnSO_4$) the MYC-SKP2 axis is able to counteract the effect of p27 as cell cycle inhibitor. However at high p27 levels (75 µM $ZnSO_4$), p27 accumulates as free form and it serves as reservoir to counteract the p27 degradation promoted by the MYC-SKP2 axis maintaining the complete cell cycle arrest.

6. CONCLUSIONS

6. CONCLUSIONS

1. MYC up-regulates the expression of SKP2 in several cell lines from different species, and appears to be the primary mediator of the induction of SKP2 in response to serum. This SKP2 up-regulation does not depend on MYC-induced cell proliferation.

2. MYC binds to *SKP2* promoter region and activates their expression in the absence of protein synthesis confirming that *SKP2* is a new target gene MYC.

3. SKP2 does not affect the stability and the activity of MYC in K562 cells.

4. MYC and SKP2 expression correlate in several hematological malignancies including acute and chronic myeloid leukemia, and Burkitt's lymphoma.

5. In K562 cells, MYC promotes p27 phosphorylation at threonine 187 through the induction of cyclin A and the kinase activity associated to this cyclin, a phosphorylation required for p27 recognition by the SCF^{SKP2} ubiquitin ligase complex. In addition, MYC is able to promoting such phosphorylation in mouse cells independently of CDK2 or E-type cyclins.

6. SKP2 induction by MYC in K562 cells correlates with decreased p27 levels, leads to an increase in the proliferative rate and, at least in part, it is responsible for their tumorigenic capacity in xenographs in nude mice.

7. When p27 is expressed at moderate levels in K562 cells, it is found in high molecular weight complex together with cyclin/CDK and possibly with SCF^{SKP2}. At high levels, p27 can also found in free form, which is associated with a total proliferation block. MYC promotes free p27 displacement towards high molecular weight complexes by induction of cyclins and CDKs. The disappearance of p27 as free form correlates with MYC-mediated proliferative stimulus.

7. BIBLIOGRAPHY

7. BIBLIOGRAPHY

Acosta, J.C., Ferrandiz, N., Bretones, G., Torrano, V., Blanco, R., Richard, C., O'Connell, B., Sedivy, J., Delgado, M.D. and Leon, J. Myc inhibits p27-induced erythroid differentiation of leukemia cells by repressing erythroid master genes without reversing p27-mediated cell cycle arrest. *Mol Cell Biol* 28, 7286-7295 (2008).

Adams, J.M., Harris, A.W., Pinkert, C.A., Corcoran, L.M., Alexander, W.S., Cory, S., Palmiter, R.D. and Brinster, R.L. The c-myc oncogene driven by immunoglobulin enhancers induces lymphoid malignancy in transgenic mice. *Nature* 318, 533-538 (1985).

Adhikary, S. and Eilers, M. Transcriptional regulation and transformation by Myc proteins. *Nat Rev Mol Cell Biol* 6, 635-645 (2005).

Adhikary, S., Marinoni, F., Hock, A., Hulleman, E., Popov, N., Beier, R., Bernard, S., Quarto, M., Capra, M., Goettig, S.*, et al.* The ubiquitin ligase HectH9 regulates transcriptional activation by Myc and is essential for tumor cell proliferation. *Cell* 123, 409-421 (2005).

Agarwal, A., Bumm, T.G., Corbin, A.S., O'Hare, T., Loriaux, M., VanDyke, J., Willis, S.G., Deininger, J., Nakayama, K.I., Druker, B.J.*, et al.* Absence of SKP2 expression attenuates BCR-ABL-induced myeloproliferative disease. *Blood* 112, 1960-1970 (2008).

Aguda, B.D., Kim, Y., Piper-Hunter, M.G., Friedman, A. and Marsh, C.B. MicroRNA regulation of a cancer network: consequences of the feedback loops involving miR-17-92, E2F, and Myc. *Proc Natl Acad Sci U S A* 105, 19678-19683 (2008).

Ahmadiyeh, N., Pomerantz, M.M., Grisanzio, C., Herman, P., Jia, L., Almendro, V., He, H.H., Brown, M., Liu, X.S., Davis, M.*, et al.* 8q24 prostate, breast, and colon cancer risk loci show tissue-specific long-range interaction with MYC. *Proc Natl Acad Sci U S A* 107, 9742-9746 (2010).

Albajar, M., Gomez-Casares, M.T., Llorca, J., Mauleon, I., Vaque, J.P., Acosta, J.C., Bermudez, A., Donato, N., Delgado, M.D. and Leon, J. MYC in chronic myeloid leukemia: induction of aberrant DNA synthesis and association with poor response to imatinib. *Mol Cancer Res* 9, 564-576 (2011).

Albert, T., Wells, J., Funk, J.O., Pullner, A., Raschke, E.E., Stelzer, G., Meisterernst, M., Farnham, P.J. and Eick, D. The chromatin structure of the dual c-myc promoter P1/P2 is regulated by separate elements. *J Biol Chem* 276, 20482-20490 (2001).

Aleem, E., Kiyokawa, H. and Kaldis, P. Cdc2-cyclin E complexes regulate the G1/S phase transition. *Nat Cell Biol* 7, 831-836 (2005).

Allis, C.D., Berger, S.L., Cote, J., Dent, S., Jenuwien, T., Kouzarides, T., Pillus, L., Reinberg, D., Shi, Y., Shiekhattar, R.*, et al.* New nomenclature for chromatin-modifying enzymes. *Cell* 131, 633-636 (2007).

Amati, B., Dalton, S., Brooks, M.W., Littlewood, T.D., Evan, G.I. and Land, H. Transcriptional activation by the human c-Myc oncoprotein in yeast requires interaction with Max. *Nature* 359, 423-426 (1992).

Andreu, E.J., Lledo, E., Poch, E., Ivorra, C., Albero, M.P., Martinez-Climent, J.A., Montiel-Duarte, C., Rifon, J., Perez-Calvo, J., Arbona, C.*, et al.* BCR-ABL induces the expression of Skp2 through the PI3K pathway to promote p27Kip1 degradation and proliferation of chronic myelogenous leukemia cells. *Cancer Res* 65, 3264-3272 (2005).

Appleman, L.J., Chernova, I., Li, L. and Boussiotis, V.A. CD28 costimulation mediates transcription of SKP2 and CKS1, the substrate recognition components of SCFSkp2 ubiquitin ligase that leads p27kip1 to degradation. *Cell Cycle* 5, 2123-2129 (2006).

Armelin, H.A., Armelin, M.C., Kelly, K., Stewart, T., Leder, P., Cochran, B.H. and Stiles, C.D. Functional role for c-myc in mitogenic response to platelet-derived growth factor. *Nature* 310, 655-660 (1984).

Arnold, H.K., Zhang, X., Daniel, C.J., Tibbitts, D., Escamilla-Powers, J., Farrell, A., Tokarz, S., Morgan, C. and Sears, R.C. The Axin1 scaffold protein promotes formation of a degradation complex for c-Myc. *Embo J* 28, 500-512 (2009).

Askew, D.S., Ashmun, R.A., Simmons, B.C. and Cleveland, J.L. Constitutive c-myc expression in an IL-3-dependent myeloid cell line suppresses cell cycle arrest and accelerates apoptosis. *Oncogene* 6, 1915-1922 (1991).

Atherton-Fessler, S., Parker, L.L., Geahlen, R.L. and Piwnica-Worms, H. Mechanisms of p34cdc2 regulation. *Mol Cell Biol* 13, 1675-1685 (1993).

Baccarani, M., Cortes, J., Pane, F., Niederwieser, D., Saglio, G., Apperley, J., Cervantes, F., Deininger, M., Gratwohl, A., Guilhot, F.*, et al.* Chronic myeloid leukemia: an update of concepts and management recommendations of European LeukemiaNet. *J Clin Oncol* 27, 6041-6051 (2009).

Bagui, T.K., Jackson, R.J., Agrawal, D. and Pledger, W.J. Analysis of cyclin D3-cdk4 complexes in fibroblasts expressing and lacking p27(kip1) and p21(cip1). *Mol Cell Biol* 20, 8748-8757 (2000).

Bagui, T.K., Mohapatra, S., Haura, E. and Pledger, W.J. P27Kip1 and p21Cip1 are not required for the formation of active D cyclin-cdk4 complexes. *Mol Cell Biol* 23, 7285-7290 (2003).

Bai, C., Sen, P., Hofmann, K., Ma, L., Goebl, M., Harper, J.W. and Elledge, S.J. SKP1 connects cell cycle regulators to the ubiquitin proteolysis machinery through a novel motif, the F-box. *Cell* 86, 263-274 (1996).

Baldassarre, G., Belletti, B., Nicoloso, M.S., Schiappacassi, M., Vecchione, A., Spessotto, P., Morrione, A., Canzonieri, V. and Colombatti, A. p27(Kip1)-stathmin interaction influences sarcoma cell migration and invasion. *Cancer Cell* 7, 51-63 (2005).

Barr, L.F., Campbell, S.E., Bochner, B.S. and Dang, C.V. Association of the decreased expression of alpha3beta1 integrin with the altered cell: environmental interactions and enhanced soft agar cloning ability of c-myc-overexpressing small cell lung cancer cells. *Cancer Res* 58, 5537-5545 (1998).

Barre, B. and Perkins, N.D. A cell cycle regulatory network controlling NF-kappaB subunit activity and function. *Embo J* 26, 4841-4855 (2007).

Barre, B. and Perkins, N.D. The Skp2 promoter integrates signaling through the NF-kappaB, p53, and Akt/GSK3beta pathways to regulate autophagy and apoptosis. *Mol Cell* 38, 524-538 (2010).

Barrett, J.F., Lee, L.A. and Dang, C.V. Stimulation of Myc transactivation by the TATA binding protein in promoter-reporter assays. *BMC Biochem* 6, 7 (2005).

Barrett, J.F., Lewis, B.C., Hoang, A.T., Alvarez, R.J., Jr. and Dang, C.V. Cyclin A links c-Myc to adhesion-independent cell proliferation. *J Biol Chem* 270, 15923-15925 (1995).

Barriere, C., Santamaria, D., Cerqueira, A., Galan, J., Martin, A., Ortega, S., Malumbres, M., Dubus, P. and Barbacid, M. Mice thrive without Cdk4 and Cdk2. *Mol Oncol* 1, 72-83 (2007).

Bashir, T., Dorrello, N.V., Amador, V., Guardavaccaro, D. and Pagano, M. Control of the SCF(Skp2-Cks1) ubiquitin ligase by the APC/C(Cdh1) ubiquitin ligase. *Nature* 428, 190-193 (2004).

Bashir, T., Pagan, J.K., Busino, L. and Pagano, M. Phosphorylation of Ser72 is dispensable for Skp2 assembly into an active SCF ubiquitin ligase and its subcellular localization. *Cell Cycle* 9, 971-974 (2010).

Basso, K., Margolin, A.A., Stolovitzky, G., Klein, U., Dalla-Favera, R. and Califano, A. Reverse engineering of regulatory networks in human B cells. *Nat Genet* 37, 382-390 (2005).

Baudino, T.A., Maclean, K.H., Brennan, J., Parganas, E., Yang, C., Aslanian, A., Lees, J.A., Sherr, C.J., Roussel, M.F. and Cleveland, J.L. Myc-mediated proliferation and lymphomagenesis, but not apoptosis, are compromised by E2f1 loss. *Mol Cell* 11, 905-914 (2003).

Baudino, T.A., McKay, C., Pendeville-Samain, H., Nilsson, J.A., Maclean, K.H., White, E.L., Davis, A.C., Ihle, J.N. and Cleveland, J.L. c-Myc is essential for vasculogenesis and angiogenesis during development and tumor progression. *Genes Dev* 16, 2530-2543 (2002).

Benanti, J.A., Wang, M.L., Myers, H.E., Robinson, K.L., Grandori, C. and Galloway, D.A. Epigenetic down-regulation of ARF expression is a selection step in immortalization of human fibroblasts by c-Myc. *Mol Cancer Res* 5, 1181-1189 (2007).

Bernard, D., Pourtier-Manzanedo, A., Gil, J. and Beach, D.H. Myc confers androgen-independent prostate cancer cell growth. *J Clin Invest* 112, 1724-1731 (2003).

Berns, K., Hijmans, E.M., Koh, E., Daley, G.Q. and Bernards, R. A genetic screen to identify genes that rescue the slow growth phenotype of c-myc null fibroblasts. *Oncogene* 19, 3330-3334 (2000).

Beroukhim, R., Mermel, C.H., Porter, D., Wei, G., Raychaudhuri, S., Donovan, J., Barretina, J., Boehm, J.S., Dobson, J., Urashima, M.*, et al.* The landscape of somatic copy-number alteration across human cancers. *Nature* 463, 899-905 (2010).

Berthet, C., Aleem, E., Coppola, V., Tessarollo, L. and Kaldis, P. Cdk2 knockout mice are viable. *Curr Biol* 13, 1775-1785 (2003).

Berthet, C., Klarmann, K.D., Hilton, M.B., Suh, H.C., Keller, J.R., Kiyokawa, H. and Kaldis, P. Combined loss of Cdk2 and Cdk4 results in embryonic lethality and Rb hypophosphorylation. *Dev Cell* 10, 563-573 (2006).

Besson, A., Assoian, R.K. and Roberts, J.M. Regulation of the cytoskeleton: an oncogenic function for CDK inhibitors? *Nat Rev Cancer* 4, 948-955 (2004a).

Besson, A., Gurian-West, M., Schmidt, A., Hall, A. and Roberts, J.M. p27Kip1 modulates cell migration through the regulation of RhoA activation. *Genes Dev* 18, 862-876 (2004b).

Besson, A., Hwang, H.C., Cicero, S., Donovan, S.L., Gurian-West, M., Johnson, D., Clurman, B.E., Dyer, M.A. and Roberts, J.M. Discovery of an oncogenic activity in p27Kip1 that causes stem cell expansion and a multiple tumor phenotype. *Genes Dev* 21, 1731-1746 (2007).

Bienkiewicz, E.A., Adkins, J.N. and Lumb, K.J. Functional consequences of preorganized helical structure in the intrinsically disordered cell-cycle inhibitor p27(Kip1). *Biochemistry* 41, 752-759 (2002).

Bilodeau, M., Talarmin, H., Ilyin, G., Rescan, C., Glaise, D., Cariou, S., Loyer, P., Guguen-Guillouzo, C. and Baffet, G. Skp2 induction and phosphorylation is associated with the late G1 phase of proliferating rat hepatocytes. *FEBS Lett* 452, 247-253 (1999).

Bilodeau, S., Roussel-Gervais, A. and Drouin, J. Distinct developmental roles of cell cycle inhibitors p57Kip2 and p27Kip1 distinguish pituitary progenitor cell cycle exit from cell cycle reentry of differentiated cells. *Mol Cell Biol* 29, 1895-1908 (2009).

Blackwell, T.K., Kretzner, L., Blackwood, E.M., Eisenman, R.N. and Weintraub, H. in Science, Vol. 250 1149-11511990).

Blackwood, E.M. and Eisenman, R.N. Max: a helix-loop-helix zipper protein that forms a sequence-specific DNA-binding complex with Myc. *Science* 251, 1211-1217. (1991).

Blackwood, E.M., Luscher, B. and Eisenman, R.N. Myc and Max associate in vivo. *Genes Dev* 6, 71-80 (1992).

Blain, S.W., Montalvo, E. and Massague, J. Differential interaction of the cyclin-dependent kinase (Cdk) inhibitor p27Kip1 with cyclin A-Cdk2 and cyclin D2-Cdk4. *J Biol Chem* 272, 25863-25872 (1997).

Blain, S.W., Scher, H.I., Cordon-Cardo, C. and Koff, A. p27 as a target for cancer therapeutics. *Cancer Cell* 3, 111-115 (2003).

Borriello, A., Cucciolla, V., Oliva, A., Zappia, V. and Della Ragione, F. p27Kip1 metabolism: a fascinating labyrinth. *Cell Cycle* 6, 1053-1061 (2007).

Borriello, A., Pietra, V.D., Criscuolo, M., Oliva, A., Tonini, G.P., Iolascon, A., Zappia, V. and Ragione, F.D. p27Kip1 accumulation is associated with retinoic-induced neuroblastoma differentiation: evidence of a decreased proteasome-dependent degradation. *Oncogene* 19, 51-60 (2000).

Botz, J., Zerfass-Thome, K., Spitkovsky, D., Delius, H., Vogt, B., Eilers, M., Hatzigeorgiou, A. and Jansen-Durr, P. Cell cycle regulation of the murine cyclin E gene depends on an E2F binding site in the promoter. *Mol Cell Biol* 16, 3401-3409 (1996).

Bouchard, C., Marquardt, J., Bras, A., Medema, R.H. and Eilers, M. Myc-induced proliferation and transformation require Akt-mediated phosphorylation of FoxO proteins. *Embo J* 23, 2830-2840 (2004).

Bouchard, C., Thieke, K., Maier, A., Saffrich, R., Hanley-Hyde, J., Ansorge, W., Reed, S., Sicinski, P., Bartek, J. and Eilers, M. Direct induction of cyclin D2 by Myc contributes to cell cycle progression and sequestration of p27. *Embo J* 18, 5321-5333 (1999).

Bourne, Y., Watson, M.H., Hickey, M.J., Holmes, W., Rocque, W., Reed, S.I. and Tainer, J.A. Crystal structure and mutational analysis of the human CDK2 kinase complex with cell cycle-regulatory protein CksHs1. *Cell* 84, 863-874 (1996).

Boutonnet, C., Tanguay, P.L., Julien, C., Rodier, G., Coulombe, P. and Meloche, S. Phosphorylation of Ser72 does not regulate the ubiquitin ligase activity and subcellular localization of Skp2. *Cell Cycle* 9, 975-979 (2010).

Boutros, R., Dozier, C. and Ducommun, B. The when and wheres of CDC25 phosphatases. *Curr Opin Cell Biol* 18, 185-191 (2006).

Boxer, L.M. and Dang, C.V. Translocations involving c-myc and c-myc function. *Oncogene* 20, 5595-5610 (2001).

Bradford, M.M. A rapid and sensitive method for the quantitation of microgram quantities of protein utilizing the principle of protein-dye binding. *Anal Biochem* 72, 248-254 (1976).

Brandeis, M., Rosewell, I., Carrington, M., Crompton, T., Jacobs, M.A., Kirk, J., Gannon, J. and Hunt, T. Cyclin B2-null mice develop normally and are fertile whereas cyclin B1-null mice die in utero. *Proc Natl Acad Sci U S A* 95, 4344-4349 (1998).

Bres, V., Yoh, S.M. and Jones, K.A. The multi-tasking P-TEFb complex. *Curr Opin Cell Biol* 20, 334-340 (2008).

Bres, V., Yoshida, T., Pickle, L. and Jones, K.A. SKIP interacts with c-Myc and Menin to promote HIV-1 Tat transactivation. *Mol Cell* 36, 75-87 (2009).

Brewer, G. and Ross, J. Poly(A) shortening and degradation of the 3' A+U-rich sequences of human c-myc mRNA in a cell-free system. *Mol Cell Biol* 8, 1697-1708 (1988).

Brooks, T.A. and Hurley, L.H. Targeting MYC Expression through G-Quadruplexes. *Genes Cancer* 1, 641-649 (2010).

Brown, N.R., Noble, M.E., Lawrie, A.M., Morris, M.C., Tunnah, P., Divita, G., Johnson, L.N. and Endicott, J.A. Effects of phosphorylation of threonine 160 on cyclin-dependent kinase 2 structure and activity. *J Biol Chem* 274, 8746-8756 (1999).

Bruce, J.L., Hurford, R.K., Jr., Classon, M., Koh, J. and Dyson, N. Requirements for cell cycle arrest by p16INK4a. *Mol Cell* 6, 737-742 (2000).

Campaner, S., Doni, M., Hydbring, P., Verrecchia, A., Bianchi, L., Sardella, D., Schleker, T., Perna, D., Tronnersjo, S., Murga, M.*, et al.* Cdk2 suppresses cellular senescence induced by the c-myc oncogene. *Nat Cell Biol* 12, 54-59; sup pp 51-14 (2010).

Campisi, J., Gray, H.E., Pardee, A.B., Dean, M. and Sonenshein, G.E. Cell-cycle control of c-myc but not c-ras expression is lost following chemical transformation. *Cell* 36, 241-247 (1984).

Cannell, I.G., Kong, Y.W., Johnston, S.J., Chen, M.L., Collins, H.M., Dobbyn, H.C., Elia, A., Kress, T.R., Dickens, M., Clemens, M.J.*, et al.* p38 MAPK/MK2-mediated induction of miR-34c following DNA damage prevents Myc-dependent DNA replication. *Proc Natl Acad Sci U S A* 107, 5375-5380 (2010).

Cappellen, D., Schlange, T., Bauer, M., Maurer, F. and Hynes, N.E. Novel c-MYC target genes mediate differential effects on cell proliferation and migration. *EMBO Rep* 8, 70-76 (2007).

Cardozo, T. and Pagano, M. The SCF ubiquitin ligase: insights into a molecular machine. *Nat Rev Mol Cell Biol* 5, 739-751 (2004).

Carrano, A.C., Eytan, E., Hershko, A. and Pagano, M. SKP2 is required for ubiquitin-mediated degradation of the CDK inhibitor p27. *Nat Cell Biol* 1, 193-199 (1999).

Catzavelos, C., Bhattacharya, N., Ung, Y.C., Wilson, J.A., Roncari, L., Sandhu, C., Shaw, P., Yeger, H., Morava-Protzner, I., Kapusta, L.*, et al.* Decreased levels of the cell-cycle inhibitor p27Kip1 protein: prognostic implications in primary breast cancer. *Nat Med* 3, 227-230 (1997).

Ceballos, E., Delgado, M.D., Gutierrez, P., Richard, C., Muller, D., Eilers, M., Ehinger, M., Gullberg, U. and Leon, J. c-Myc antagonizes the effect of p53 on apoptosis and p21WAF1 transactivation in K562 leukemia cells. *Oncogene* 19, 2194-2204 (2000).

Cerni, C. Telomeres, telomerase, and myc. An update. *Mutat Res* 462, 31-47 (2000).

Ciemerych, M.A. and Sicinski, P. Cell cycle in mouse development. *Oncogene* 24, 2877-2898 (2005).

Claassen, G.F. and Hann, S.R. Myc-mediated transformation: the repression connection. *Oncogene* 18, 2925-2933 (1999).

Claassen, G.F. and Hann, S.R. A role for transcriptional repression of p21CIP1 by c-Myc in overcoming transforming growth factor beta -induced cell-cycle arrest. *Proc Natl Acad Sci U S A* 97, 9498-9503 (2000).

Cleveland, J.L., Huleihel, M., Bressler, P., Siebenlist, U., Akiyama, L., Eisenman, R.N. and Rapp, U.R. Negative regulation of c-myc transcription involves myc family proteins. *Oncogene Res* 3, 357-375 (1988).

Clurman, B.E., Sheaff, R.J., Thress, K., Groudine, M. and Roberts, J.M. Turnover of cyclin E by the ubiquitin-proteasome pathway is regulated by cdk2 binding and cyclin phosphorylation. *Genes Dev* 10, 1979-1990 (1996).

Coller, H.A., Grandori, C., Tamayo, P., Colbert, T., Lander, E.S., Eisenman, R.N. and Golub, T.R. Expression analysis with oligonucleotide microarrays reveals that MYC regulates genes involved in growth, cell cycle, signaling, and adhesion. *Proc Natl Acad Sci U S A* 97, 3260-3265 (2000).

Collins, S., Coleman, H. and Groudine, M. Expression of bcr and bcr-abl fusion transcripts in normal and leukemic cells. *Mol Cell Biol* 7, 2870-2876 (1987).

Conacci-Sorrell, M., Ngouenet, C. and Eisenman, R.N. Myc-nick: a cytoplasmic cleavage product of Myc that promotes alpha-tubulin acetylation and cell differentiation. *Cell* 142, 480-493 (2010).

Connor, M.K., Kotchetkov, R., Cariou, S., Resch, A., Lupetti, R., Beniston, R.G., Melchior, F., Hengst, L. and Slingerland, J.M. CRM1/Ran-mediated nuclear export of p27(Kip1) involves a nuclear export signal and links p27 export and proteolysis. *Mol Biol Cell* 14, 201-213 (2003).

Coppola, J.A. and Cole, M.D. Constitutive c-myc oncogene expression blocks mouse erythroleukaemia cell differentiation but not commitment. *Nature* 320, 760-763 (1986).

Cordon-Cardo, C., Koff, A., Drobnjak, M., Capodieci, P., Osman, I., Millard, S.S., Gaudin, P.B., Fazzari, M., Zhang, Z.F., Massague, J.*, et al.* Distinct altered patterns of p27KIP1 gene expression in benign prostatic hyperplasia and prostatic carcinoma. *J Natl Cancer Inst* 90, 1284-1291 (1998).

Cowling, V.H. and Cole, M.D. The Myc transactivation domain promotes global phosphorylation of the RNA polymerase II carboxy-terminal domain independently of direct DNA binding. *Mol Cell Biol* 27, 2059-2073 (2007).

Cowling, V.H., Chandriani, S., Whitfield, M.L. and Cole, M.D. A conserved Myc protein domain, MBIV, regulates DNA binding, apoptosis, transformation, and G2 arrest. *Mol Cell Biol* 26, 4226-4239 (2006).

Crews, S., Barth, R., Hood, L., Prehn, J. and Calame, K. Mouse c-myc oncogene is located on chromosome 15 and translocated to chromosome 12 in plasmacytomas. *Science* 218, 1319-1321 (1982).

Chan, C.H., Lee, S.W., Li, C.F., Wang, J., Yang, W.L., Wu, C.Y., Wu, J., Nakayama, K.I., Kang, H.Y., Huang, H.Y.*, et al.* Deciphering the transcriptional complex critical for RhoA gene expression and cancer metastasis. *Nat Cell Biol* 12, 457-467 (2010).

Chan, C.H., Li, C.F., Yang, W.L., Gao, Y., Lee, S.W., Feng, Z., Huang, H.Y., Tsai, K.K., Flores, L.G., Shao, Y.*, et al.* The Skp2-SCF E3 ligase regulates Akt ubiquitination, glycolysis, herceptin sensitivity, and tumorigenesis. *Cell* 149, 1098-1111 (2012).

Chandramohan, V., Jeay, S., Pianetti, S. and Sonenshein, G.E. Reciprocal control of Forkhead box O 3a and c-Myc via the phosphatidylinositol 3-kinase pathway coordinately regulates p27Kip1 levels. *J Immunol* 172, 5522-5527 (2004).

Chang, T.C., Yu, D., Lee, Y.S., Wentzel, E.A., Arking, D.E., West, K.M., Dang, C.V., Thomas-Tikhonenko, A. and Mendell, J.T. Widespread microRNA repression by Myc contributes to tumorigenesis. *Nat Genet* 40, 43-50 (2008).

Charron, J., Malynn, B.A., Fisher, P., Stewart, V., Jeannotte, L., Goff, S.P., Robertson, E.J. and Alt, F.W. Embryonic lethality in mice homozygous for a targeted disruption of the N-myc gene. *Genes Dev* 6, 2248-2257 (1992).

Chen, C., Nussenzweig, A., Guo, M., Kim, D., Li, G.C. and Ling, C.C. Down-regulation of gadd153 by c-myc in rat fibroblasts and its effect on cell growth and radiation-induced apoptosis. *Oncogene* 13, 1659-1665 (1996).

Chen, J.Y., Wang, M.C. and Hung, W.C. Transcriptional activation of Skp2 by BCR-ABL in K562 chronic myeloid leukemia cells. *Leuk Res* 33, 1520-1524 (2009).

Cheng, M., Olivier, P., Diehl, J.A., Fero, M., Roussel, M.F., Roberts, J.M. and Sherr, C.J. The p21(Cip1) and p27(Kip1) CDK 'inhibitors' are essential activators of cyclin D-dependent kinases in murine fibroblasts. *Embo J* 18, 1571-1583 (1999a).

Cheng, M., Sexl, V., Sherr, C.J. and Roussel, M.F. Assembly of cyclin D-dependent kinase and titration of p27Kip1 regulated by mitogen-activated protein kinase kinase (MEK1). *Proc Natl Acad Sci U S A* 95, 1091-1096 (1998).

Cheng, S.W., Davies, K.P., Yung, E., Beltran, R.J., Yu, J. and Kalpana, G.V. c-MYC interacts with INI1/hSNF5 and requires the SWI/SNF complex for transactivation function. *Nat Genet* 22, 102-105 (1999b).

Cho, S., Kim, J.H., Back, S.H. and Jang, S.K. Polypyrimidine tract-binding protein enhances the internal ribosomal entry site-dependent translation of p27Kip1 mRNA and modulates transition from G1 to S phase. *Mol Cell Biol* 25, 1283-1297 (2005).

Christoffersen, N.R., Shalgi, R., Frankel, L.B., Leucci, E., Lees, M., Klausen, M., Pilpel, Y., Nielsen, F.C., Oren, M. and Lund, A.H. p53-independent upregulation of miR-34a during oncogene-induced senescence represses MYC. *Cell Death Differ* 17, 236-245 (2010).

Chu, I., Sun, J., Arnaout, A., Kahn, H., Hanna, W., Narod, S., Sun, P., Tan, C.K., Hengst, L. and Slingerland, J. p27 phosphorylation by Src regulates inhibition of cyclin E-Cdk2. *Cell* 128, 281-294 (2007).

Chu, I.M., Hengst, L. and Slingerland, J.M. The Cdk inhibitor p27 in human cancer: prognostic potential and relevance to anticancer therapy. *Nat Rev Cancer* 8, 253-267 (2008).

Chung, H.J. and Levens, D. c-myc expression: keep the noise down! *Mol Cells* 20, 157-166 (2005).

Dalla-Favera, R., Bregni, M., Erikson, J., Patterson, D., Gallo, R.C. and Croce, C.M. Human c-myc onc gene is located on the region of chromosome 8 that is translocated in Burkitt lymphoma cells. *Proc Natl Acad Sci U S A* 79, 7824-7827 (1982a).

Dalla-Favera, R., Gelmann, E.P., Martinotti, S., Franchini, G., Papas, T.S., Gallo, R.C. and Wong-Staal, F. Cloning and characterization of different human sequences related to the onc gene (v-myc) of avian myelocytomatosis virus (MC29). *Proc Natl Acad Sci U S A* 79, 6497-6501 (1982b).

Dang, C.V. c-Myc target genes involved in cell growth, apoptosis, and metabolism. *Mol Cell Biol* 19, 1-11 (1999).

Dang, C.V. MYC on the Path to Cancer. *Cell* 149, 22-35 (2012).

Dang, C.V. and Lee, W.M. Identification of the human c-myc protein nuclear translocation signal. *Mol Cell Biol* 8, 4048-4054 (1988).

Dang, C.V., McGuire, M., Buckmire, M. and Lee, W.M. Involvement of the 'leucine zipper' region in the oligomerization and transforming activity of human c-myc protein. *Nature* 337, 664-666 (1989).

Dang, C.V., O'Donnell, K.A., Zeller, K.I., Nguyen, T., Osthus, R.C. and Li, F. The c-Myc target gene network. *Semin Cancer Biol* 16, 253-264 (2006).

Dansen, T.B., Whitfield, J., Rostker, F., Brown-Swigart, L. and Evan, G.I. Specific requirement for Bax, not Bak, in Myc-induced apoptosis and tumor suppression in vivo. *J Biol Chem* 281, 10890-10895 (2006).

de Alboran, I.M., O'Hagan, R.C., Gartner, F., Malynn, B., Davidson, L., Rickert, R., Rajewsky, K., DePinho, R.A. and Alt, F.W. Analysis of C-MYC function in normal cells via conditional gene-targeted mutation. *Immunity* 14, 45-55 (2001).

De Bondt, H.L., Rosenblatt, J., Jancarik, J., Jones, H.D., Morgan, D.O. and Kim, S.H. Crystal structure of cyclin-dependent kinase 2. *Nature* 363, 595-602 (1993).

de Koning, J.P., Soede-Bobok, A.A., Ward, A.C., Schelen, A.M., Antonissen, C., van Leeuwen, D., Lowenberg, B. and Touw, I.P. STAT3-mediated differentiation and survival and of myeloid cells in response to granulocyte colony-stimulating factor: role for the cyclin-dependent kinase inhibitor p27(Kip1). *Oncogene* 19, 3290-3298 (2000).

Dean, M., Levine, R.A., Ran, W., Kindy, M.S., Sonenshein, G.E. and Campisi, J. Regulation of c-myc transcription and mRNA abundance by serum growth factors and cell contact. *J Biol Chem* 261, 9161-9166 (1986).

DeGregori, J., Kowalik, T. and Nevins, J.R. Cellular targets for activation by the E2F1 transcription factor include DNA synthesis- and G1/S-regulatory genes. *Mol Cell Biol* 15, 4215-4224 (1995).

Delgado, M.D., Albajar, M., Gomez-Casares, M.T., Batlle, A. and Leon, J. MYC oncogene in myeloid neoplasias. *Clin Transl Oncol* (2013).

Delgado, M.D., Chernukhin, I.V., Bigas, A., Klenova, E.M. and Leon, J. Differential expression and phosphorylation of CTCF, a c-myc transcriptional regulator, during differentiation of human myeloid cells. *FEBS Lett* 444, 5-10 (1999).

Delgado, M.D. and Leon, J. Myc roles in hematopoiesis and leukemia. *Genes Cancer* 1, 605-616 (2010).

Delgado, M.D., Lerga, A., Canelles, M., Gomez-Casares, M.T. and Leon, J. Differential regulation of Max and role of c-Myc during erythroid and myelomonocytic differentiation of K562 cells. *Oncogene* 10, 1659-1665 (1995).

Delmore, J.E., Issa, G.C., Lemieux, M.E., Rahl, P.B., Shi, J., Jacobs, H.M., Kastritis, E., Gilpatrick, T., Paranal, R.M., Qi, J.*, et al.* BET bromodomain inhibition as a therapeutic strategy to target c-Myc. *Cell* 146, 904-917 (2011).

Denicourt, C., Saenz, C.C., Datnow, B., Cui, X.S. and Dowdy, S.F. Relocalized p27Kip1 tumor suppressor functions as a cytoplasmic metastatic oncogene in melanoma. *Cancer Res* 67, 9238-9243 (2007).

DePinho, R., Mitsock, L., Hatton, K., Ferrier, P., Zimmerman, K., Legouy, E., Tesfaye, A., Collum, R., Yancopoulos, G., Nisen, P.*, et al.* Myc family of cellular oncogenes. *J Cell Biochem* 33, 257-266 (1987).

Deshaies, R.J. and Joazeiro, C.A. RING domain E3 ubiquitin ligases. *Annu Rev Biochem* 78, 399-434 (2009).

Devault, A., Martinez, A.M., Fesquet, D., Labbe, J.C., Morin, N., Tassan, J.P., Nigg, E.A., Cavadore, J.C. and Doree, M. MAT1 ('menage a trois') a new RING finger protein subunit stabilizing cyclin H-cdk7 complexes in starfish and Xenopus CAK. *Embo J* 14, 5027-5036 (1995).

Dews, M., Fox, J.L., Hultine, S., Sundaram, P., Wang, W., Liu, Y.Y., Furth, E., Enders, G.H., El-Deiry, W., Schelter, J.M.*, et al.* The myc-miR-17~92 axis blunts TGF{beta} signaling and production of multiple TGF{beta}-dependent antiangiogenic factors. *Cancer Res* 70, 8233-8246 (2010).

Dews, M., Homayouni, A., Yu, D., Murphy, D., Sevignani, C., Wentzel, E., Furth, E.E., Lee, W.M., Enders, G.H., Mendell, J.T.*, et al.* Augmentation of tumor angiogenesis by a Myc-activated microRNA cluster. *Nat Genet* 38, 1060-1065 (2006).

Dijkers, P.F., Medema, R.H., Pals, C., Banerji, L., Thomas, N.S., Lam, E.W., Burgering, B.M., Raaijmakers, J.A., Lammers, J.W., Koenderman, L.*, et al.* Forkhead transcription factor FKHR-L1 modulates cytokine-dependent transcriptional regulation of p27(KIP1). *Mol Cell Biol* 20, 9138-9148 (2000).

Diril, M.K., Ratnacaram, C.K., Padmakumar, V.C., Du, T., Wasser, M., Coppola, V., Tessarollo, L. and Kaldis, P. Cyclin-dependent kinase 1 (Cdk1) is essential for cell division and suppression of DNA re-replication but not for liver regeneration. *Proc Natl Acad Sci U S A* (2012).

Dmitrovsky, E., Kuehl, W.M., Hollis, G.F., Kirsch, I.R., Bender, T.P. and Segal, S. Expression of a transfected human c-myc oncogene inhibits differentiation of a mouse erythroleukaemia cell line. *Nature* 322, 748-750 (1986).

Dominguez-Sola, D., Ying, C.Y., Grandori, C., Ruggiero, L., Chen, B., Li, M., Galloway, D.A., Gu, W., Gautier, J. and Dalla-Favera, R. Non-transcriptional control of DNA replication by c-Myc. *Nature* 448, 445-451 (2007).

Drexler, H.C. and Pebler, S. Inducible p27(Kip1) expression inhibits proliferation of K562 cells and protects against apoptosis induction by proteasome inhibitors. *Cell Death Differ* 10, 290-301 (2003).

Drexler, H.G. Review of alterations of the cyclin-dependent kinase inhibitor INK4 family genes p15, p16, p18 and p19 in human leukemia-lymphoma cells. *Leukemia* 12, 845-859 (1998).

Drobnjak, M., Melamed, J., Taneja, S., Melzer, K., Wieczorek, R., Levinson, B., Zeleniuch-Jacquotte, A., Polsky, D., Ferrara, J., Perez-Soler, R.*, et al.* Altered expression of p27 and Skp2 proteins in prostate cancer of African-American patients. *Clin Cancer Res* 9, 2613-2619 (2003).

Dubois, N.C., Adolphe, C., Ehninger, A., Wang, R.A., Robertson, E.J. and Trumpp, A. Placental rescue reveals a sole requirement for c-Myc in embryonic erythroblast survival and hematopoietic stem cell function. *Development* 135, 2455-2465 (2008).

Duesberg, P.H. and Vogt, P.K. Avian acute leukemia viruses MC29 and MH2 share specific RNA sequences: evidence for a second class of transforming genes. *Proc Natl Acad Sci U S A* 76, 1633-1637 (1979).

Dunham, I., Kundaje, A., Aldred, S.F., Collins, P.J., Davis, C.A., Doyle, F., Epstein, C.B., Frietze, S., Harrow, J., Kaul, R.*, et al.* An integrated encyclopedia of DNA elements in the human genome. *Nature* 489, 57-74 (2012).

Dunphy, W.G. and Kumagai, A. The cdc25 protein contains an intrinsic phosphatase activity. *Cell* 67, 189-196 (1991).

Dyson, N. The regulation of E2F by pRB-family proteins. *Genes Dev* 12, 2245-2262 (1998).

Eberhardy, S.R. and Farnham, P.J. c-Myc mediates activation of the cad promoter via a post-RNA polymerase II recruitment mechanism. *J Biol Chem* 276, 48562-48571 (2001).

Eberhardy, S.R. and Farnham, P.J. Myc recruits P-TEFb to mediate the final step in the transcriptional activation of the cad promoter. *J Biol Chem* 277, 40156-40162 (2002).

Egozi, D., Shapira, M., Paor, G., Ben-Izhak, O., Skorecki, K. and Hershko, D.D. Regulation of the cell cycle inhibitor p27 and its ubiquitin ligase Skp2 in differentiation of human embryonic stem cells. *Faseb J* 21, 2807-2817 (2007).

Eilers, M., Picard, D., Yamamoto, K.R. and Bishop, J.M. Chimaeras of myc oncoprotein and steroid receptors cause hormone-dependent transformation of cells. *Nature* 340, 66-68 (1989).

Eilers, M., Schirm, S. and Bishop, J.M. The MYC protein activates transcription of the alpha-prothymosin gene. *Embo J* 10, 133-141 (1991).

Eischen, C.M., Weber, J.D., Roussel, M.F., Sherr, C.J. and Cleveland, J.L. Disruption of the ARF-Mdm2-p53 tumor suppressor pathway in Myc-induced lymphomagenesis. *Genes Dev* 13, 2658-2669 (1999).

Evan, G.I., Wyllie, A.H., Gilbert, C.S., Littlewood, T.D., Land, H., Brooks, M., Waters, C.M., Penn, L.Z. and Hancock, D.C. Induction of apoptosis in fibroblasts by c-myc protein. *Cell* 69, 119-128 (1992).

Evans, T., Rosenthal, E.T., Youngblom, J., Distel, D. and Hunt, T. Cyclin: a protein specified by maternal mRNA in sea urchin eggs that is destroyed at each cleavage division. *Cell* 33, 389-396 (1983).

Facchini, L.M., Chen, S., Marhin, W.W., Lear, J.N. and Penn, L.Z. The Myc negative autoregulation mechanism requires Myc-Max association and involves the c-myc P2 minimal promoter. *Mol Cell Biol* 17, 100-114 (1997).

Faiola, F., Liu, X., Lo, S., Pan, S., Zhang, K., Lymar, E., Farina, A. and Martinez, E. Dual regulation of c-Myc by p300 via acetylation-dependent control of Myc protein turnover and coactivation of Myc-induced transcription. *Mol Cell Biol* 25, 10220-10234 (2005).

Featherstone, C. and Russell, P. Fission yeast p107wee1 mitotic inhibitor is a tyrosine/serine kinase. *Nature* 349, 808-811 (1991).

Felsher, D.W. and Bishop, J.M. Transient excess of MYC activity can elicit genomic instability and tumorigenesis. *Proc Natl Acad Sci U S A* 96, 3940-3944 (1999).

Fernandez, P.C., Frank, S.R., Wang, L., Schroeder, M., Liu, S., Greene, J., Cocito, A. and Amati, B. Genomic targets of the human c-Myc protein. *Genes Dev* 17, 1115-1129 (2003).

Fero, M.L., Randel, E., Gurley, K.E., Roberts, J.M. and Kemp, C.J. The murine gene p27Kip1 is haplo-insufficient for tumour suppression. *Nature* 396, 177-180 (1998).

Fero, M.L., Rivkin, M., Tasch, M., Porter, P., Carow, C.E., Firpo, E., Polyak, K., Tsai, L.H., Broudy, V., Perlmutter, R.M.*, et al.* A syndrome of multiorgan hyperplasia with features of gigantism, tumorigenesis, and female sterility in p27(Kip1)-deficient mice. *Cell* 85, 733-744 (1996).

Fesquet, D., Labbe, J.C., Derancourt, J., Capony, J.P., Galas, S., Girard, F., Lorca, T., Shuttleworth, J., Doree, M. and Cavadore, J.C. The MO15 gene encodes the catalytic subunit of a protein kinase that activates cdc2 and other cyclin-dependent kinases (CDKs) through phosphorylation of Thr161 and its homologues. *Embo J* 12, 3111-3121 (1993).

Finley, D. Recognition and processing of ubiquitin-protein conjugates by the proteasome. *Annu Rev Biochem* 78, 477-513 (2009).

Fisher, R.P. and Morgan, D.O. A novel cyclin associates with MO15/CDK7 to form the CDK-activating kinase. *Cell* 78, 713-724 (1994).

Flinn, E.M., Wallberg, A.E., Hermann, S., Grant, P.A., Workman, J.L. and Wright, A.P. Recruitment of Gcn5-containing complexes during c-Myc-dependent gene activation. Structure and function aspects. *J Biol Chem* 277, 23399-23406 (2002).

Frank, S.R., Parisi, T., Taubert, S., Fernandez, P., Fuchs, M., Chan, H.M., Livingston, D.M. and Amati, B. MYC recruits the TIP60 histone acetyltransferase complex to chromatin. *EMBO Rep* 4, 575-580 (2003).

Frank, S.R., Schroeder, M., Fernandez, P., Taubert, S. and Amati, B. Binding of c-Myc to chromatin mediates mitogen-induced acetylation of histone H4 and gene activation. *Genes Dev* 15, 2069-2082 (2001).

Frescas, D. and Pagano, M. Deregulated proteolysis by the F-box proteins SKP2 and beta-TrCP: tipping the scales of cancer. *Nat Rev Cancer* 8, 438-449 (2008).

Freytag, S.O., Dang, C.V. and Lee, W.M. Definition of the activities and properties of c-myc required to inhibit cell differentiation. *Cell Growth Differ* 1, 339-343 (1990).

Freytag, S.O. and Geddes, T.J. Reciprocal regulation of adipogenesis by Myc and C/EBP alpha. *Science* 256, 379-382 (1992).

Fujita, N., Sato, S., Katayama, K. and Tsuruo, T. Akt-dependent phosphorylation of p27Kip1 promotes binding to 14-3-3 and cytoplasmic localization. *J Biol Chem* 277, 28706-28713 (2002).

Furuhata, A., Kimura, A., Shide, K., Shimoda, K., Murakami, M., Ito, H., Gao, S., Yoshida, K., Tagawa, Y., Hagiwara, K.*, et al.* p27 deregulation by Skp2 overexpression induced by the JAK2V617 mutation. *Biochem Biophys Res Commun* 383, 411-416 (2009).

Furuno, N., den Elzen, N. and Pines, J. Human cyclin A is required for mitosis until mid prophase. *J Cell Biol* 147, 295-306 (1999).

Galaktionov, K., Chen, X. and Beach, D. Cdc25 cell-cycle phosphatase as a target of c-myc. *Nature* 382, 511-517 (1996).

Galea, C.A., Nourse, A., Wang, Y., Sivakolundu, S.G., Heller, W.T. and Kriwacki, R.W. Role of intrinsic flexibility in signal transduction mediated by the cell cycle regulator, p27 Kip1. *J Mol Biol* 376, 827-838 (2008a).

Galea, C.A., Wang, Y., Sivakolundu, S.G. and Kriwacki, R.W. Regulation of cell division by intrinsically unstructured proteins: intrinsic flexibility, modularity, and signaling conduits. *Biochemistry* 47, 7598-7609 (2008b).

Gandarillas, A. and Watt, F.M. c-Myc promotes differentiation of human epidermal stem cells. *Genes Dev* 11, 2869-2882 (1997).

Ganiatsas, S., Dow, R., Thompson, A., Schulman, B. and Germain, D. A splice variant of Skp2 is retained in the cytoplasm and fails to direct cyclin D1 ubiquitination in the uterine cancer cell line SK-UT. *Oncogene* 20, 3641-3650 (2001).

Ganoth, D., Bornstein, G., Ko, T.K., Larsen, B., Tyers, M., Pagano, M. and Hershko, A. The cell-cycle regulatory protein Cks1 is required for SCF(Skp2)-mediated ubiquitinylation of p27. *Nat Cell Biol* 3, 321-324 (2001).

Gao, D., Inuzuka, H., Tseng, A., Chin, R.Y., Toker, A. and Wei, W. Phosphorylation by Akt1 promotes cytoplasmic localization of Skp2 and impairs APCCdh1-mediated Skp2 destruction. *Nat Cell Biol* 11, 397-408 (2009).

Gargano, B., Amente, S., Majello, B. and Lania, L. P-TEFb is a crucial co-factor for Myc transactivation. *Cell Cycle* 6, 2031-2037 (2007).

Gartel, A.L., Ye, X., Goufman, E., Shianov, P., Hay, N., Najmabadi, F. and Tyner, A.L. Myc represses the p21(WAF1/CIP1) promoter and interacts with Sp1/Sp3. *Proc Natl Acad Sci U S A* 98, 4510-4515 (2001).

Geley, S., Kramer, E., Gieffers, C., Gannon, J., Peters, J.M. and Hunt, T. Anaphase-promoting complex/cyclosome-dependent proteolysis of human cyclin A starts at the beginning of mitosis and is not subject to the spindle assembly checkpoint. *J Cell Biol* 153, 137-148 (2001).

Geng, Y., Eaton, E.N., Picon, M., Roberts, J.M., Lundberg, A.S., Gifford, A., Sardet, C. and Weinberg, R.A. Regulation of cyclin E transcription by E2Fs and retinoblastoma protein. *Oncogene* 12, 1173-1180 (1996).

Geng, Y., Whoriskey, W., Park, M.Y., Bronson, R.T., Medema, R.H., Li, T., Weinberg, R.A. and Sicinski, P. Rescue of cyclin D1 deficiency by knockin cyclin E. *Cell* 97, 767-777 (1999).

Geng, Y., Yu, Q., Sicinska, E., Das, M., Schneider, J.E., Bhattacharya, S., Rideout, W.M., Bronson, R.T., Gardner, H. and Sicinski, P. Cyclin E ablation in the mouse. *Cell* 114, 431-443 (2003).

Giambernardi, T.A., Grant, G.M., Taylor, G.P., Hay, R.J., Maher, V.M., McCormick, J.J. and Klebe, R.J. Overview of matrix metalloproteinase expression in cultured human cells. *Matrix Biol* 16, 483-496 (1998).

Gil, J., Kerai, P., Lleonart, M., Bernard, D., Cigudosa, J.C., Peters, G., Carnero, A. and Beach, D. Immortalization of primary human prostate epithelial cells by c-Myc. *Cancer Res* 65, 2179-2185 (2005).

Girard, F., Strausfeld, U., Fernandez, A. and Lamb, N.J. Cyclin A is required for the onset of DNA replication in mammalian fibroblasts. *Cell* 67, 1169-1179 (1991).

Gizard, F., Zhao, Y., Findeisen, H.M., Qing, H., Cohn, D., Heywood, E.B., Jones, K.L., Nomiyama, T. and Bruemmer, D. Transcriptional regulation of the S-Phase kinase-associated protein 2 by the NR4A orphan nuclear receptor NOR1 in vascular smooth muscle cells. *J Biol Chem* (2011).

Glozak, M.A., Sengupta, N., Zhang, X. and Seto, E. Acetylation and deacetylation of non-histone proteins. *Gene* 363, 15-23 (2005).

God, J.M. and Haque, A. Burkitt lymphoma: pathogenesis and immune evasion. *J Oncol* 2010 (2010).

Goldman, J.M. and Melo, J.V. Chronic myeloid leukemia--advances in biology and new approaches to treatment. *N Engl J Med* 349, 1451-1464 (2003).

Goldstein, G., Scheid, M., Hammerling, U., Schlesinger, D.H., Niall, H.D. and Boyse, E.A. Isolation of a polypeptide that has lymphocyte-differentiating properties and is probably represented universally in living cells. *Proc Natl Acad Sci U S A* 72, 11-15 (1975).

Gomez-Casares, M.T., Delgado, M.D., Lerga, A., Crespo, P., Quincoces, A.F., Richard, C. and Leon, J. Down-regulation of c-myc gene is not obligatory for growth inhibition and differentiation of human myeloid leukemia cells. *Leukemia* 7, 1824-1833 (1993).

Gomez-Casares, M.T., Garcia-Alegria, E., Lopez-Jorge, C.E., Ferrandiz, N., Blanco, R., Alvarez, S., Vaque, J.P., Bretones, G., Caraballo, J.M., Sanchez-Bailon, P.*, et al.* MYC antagonizes the differentiation induced by imatinib in chronic myeloid leukemia cells through downregulation of p27(KIP1). *Oncogene* (2012).

Gomez-Casares, M.T., Vaque, J.P., Lemes, A., Molero, T., Delgado, M.D. and Leon, J. C-myc expression in cell lines derived from chronic myeloid leukemia. *Haematologica* 89, 241-243 (2004).

Gomez-Roman, N., Grandori, C., Eisenman, R.N. and White, R.J. Direct activation of RNA polymerase III transcription by c-Myc. *Nature* 421, 290-294 (2003).

Gonda, T.J. and Metcalf, D. Expression of myb, myc and fos proto-oncogenes during the differentiation of a murine myeloid leukaemia. *Nature* 310, 249-251 (1984).

Goodliffe, J.M., Wieschaus, E. and Cole, M.D. Polycomb mediates Myc autorepression and its transcriptional control of many loci in Drosophila. *Genes Dev* 19, 2941-2946 (2005).

Goukassian, D., Diez-Juan, A., Asahara, T., Schratzberger, P., Silver, M., Murayama, T., Isner, J.M. and Andres, V. Overexpression of p27(Kip1) by doxycycline-regulated adenoviral vectors inhibits endothelial cell proliferation and migration and impairs angiogenesis. *Faseb J* 15, 1877-1885 (2001).

Gould, K.L. and Nurse, P. Tyrosine phosphorylation of the fission yeast cdc2+ protein kinase regulates entry into mitosis. *Nature* 342, 39-45 (1989).

Graff, J.R., Konicek, B.W., McNulty, A.M., Wang, Z., Houck, K., Allen, S., Paul, J.D., Hbaiu, A., Goode, R.G., Sandusky, G.E.*, et al.* Increased AKT activity contributes to prostate cancer progression by dramatically accelerating prostate tumor growth and diminishing p27Kip1 expression. *J Biol Chem* 275, 24500-24505 (2000).

Graham, F.L., Smiley, J., Russell, W.C. and Nairn, R. Characteristics of a human cell line transformed by DNA from human adenovirus type 5. *J Gen Virol* 36, 59-74 (1977).

Grandori, C., Cowley, S.M., James, L.P. and Eisenman, R.N. The Myc/Max/Mad network and the transcriptional control of cell behavior. *Annu Rev Cell Dev Biol* 16, 653-699 (2000).

Grandori, C., Mac, J., Siebelt, F., Ayer, D.E. and Eisenman, R.N. Myc-Max heterodimers activate a DEAD box gene and interact with multiple E box-related sites in vivo. *Embo J* 15, 4344-4357 (1996).

Grandori, C., Wu, K.J., Fernandez, P., Ngouenet, C., Grim, J., Clurman, B.E., Moser, M.J., Oshima, J., Russell, D.W., Swisshelm, K.*, et al.* Werner syndrome protein limits MYC-induced cellular senescence. *Genes Dev* 17, 1569-1574 (2003).

Gregory, M.A. and Hann, S.R. c-Myc proteolysis by the ubiquitin-proteasome pathway: stabilization of c-Myc in Burkitt's lymphoma cells. *Mol Cell Biol* 20, 2423-2435 (2000).

Grignani, F., Lombardi, L., Inghirami, G., Sternas, L., Cechova, K. and Dalla-Favera, R. Negative autoregulation of c-myc gene expression is inactivated in transformed cells. *Embo J* 9, 3913-3922 (1990).

Grimmler, M., Wang, Y., Mund, T., Cilensek, Z., Keidel, E.M., Waddell, M.B., Jakel, H., Kullmann, M., Kriwacki, R.W. and Hengst, L. Cdk-inhibitory activity and stability of p27Kip1 are directly regulated by oncogenic tyrosine kinases. *Cell* 128, 269-280 (2007).

Grosso, L.E. and Pitot, H.C. Transcriptional regulation of c-myc during chemically induced differentiation of HL-60 cultures. *Cancer Res* 45, 847-850 (1985).

Gstaiger, M., Jordan, R., Lim, M., Catzavelos, C., Mestan, J., Slingerland, J. and Krek, W. Skp2 is oncogenic and overexpressed in human cancers. *Proc Natl Acad Sci U S A* 98, 5043-5048 (2001).

Gu, W., Bhatia, K., Magrath, I.T., Dang, C.V. and Dalla-Favera, R. Binding and suppression of the Myc transcriptional activation domain by p107. *Science* 264, 251-254 (1994).

Guccione, E., Martinato, F., Finocchiaro, G., Luzi, L., Tizzoni, L., Dall' Olio, V., Zardo, G., Nervi, C., Bernard, L. and Amati, B. Myc-binding-site recognition in the human genome is determined by chromatin context. *Nat Cell Biol* 8, 764-770 (2006).

Guinez, C., Mir, A.M., Dehennaut, V., Cacan, R., Harduin-Lepers, A., Michalski, J.C. and Lefebvre, T. Protein ubiquitination is modulated by O-GlcNAc glycosylation. *Faseb J* 22, 2901-2911 (2008).

Guney, I., Wu, S. and Sedivy, J.M. Reduced c-Myc signaling triggers telomere-independent senescence by regulating Bmi-1 and p16(INK4a). *Proc Natl Acad Sci U S A* 103, 3645-3650 (2006).

Gutierrez, C., Guo, Z.S., Burhans, W., DePamphilis, M.L., Farrell-Towt, J. and Ju, G. Is c-myc protein directly involved in DNA replication? *Science* 240, 1202-1203 (1988).

Habib, T., Park, H., Tsang, M., de Alboran, I.M., Nicks, A., Wilson, L., Knoepfler, P.S., Andrews, S., Rawlings, D.J., Eisenman, R.N.*, et al.* Myc stimulates B lymphocyte differentiation and amplifies calcium signaling. *J Cell Biol* 179, 717-731 (2007).

Hanahan, D. and Weinberg, R.A. Hallmarks of cancer: the next generation. *Cell* 144, 646-674 (2011).

Hann, S.R. Role of post-translational modifications in regulating c-Myc proteolysis, transcriptional activity and biological function. *Semin Cancer Biol* 16, 288-302 (2006).

Hann, S.R. and Eisenman, R.N. Proteins encoded by the human c-myc oncogene: differential expression in neoplastic cells. *Mol Cell Biol* 4, 2486-2497 (1984).

Hann, S.R., King, M.W., Bentley, D.L., Anderson, C.W. and Eisenman, R.N. A non-AUG translational initiation in c-myc exon 1 generates an N- terminally distinct protein whose synthesis is disrupted in Burkitt's lymphomas. *Cell* 52, 185-195 (1988).

Hann, S.R., Thompson, C.B. and Eisenman, R.N. c-myc oncogene protein synthesis is independent of the cell cycle in human and avian cells. *Nature* 314, 366-369 (1985).

Hannon, G.J., Casso, D. and Beach, D. KAP: a dual specificity phosphatase that interacts with cyclin-dependent kinases. *Proc Natl Acad Sci U S A* 91, 1731-1735 (1994).

Hao, B., Zheng, N., Schulman, B.A., Wu, G., Miller, J.J., Pagano, M. and Pavletich, N.P. Structural basis of the Cks1-dependent recognition of p27(Kip1) by the SCF(Skp2) ubiquitin ligase. *Mol Cell* 20, 9-19 (2005).

Hara, T., Kamura, T., Kotoshiba, S., Takahashi, H., Fujiwara, K., Onoyama, I., Shirakawa, M., Mizushima, N. and Nakayama, K.I. Role of the UBL-UBA protein KPC2 in degradation of p27 at G1 phase of the cell cycle. *Mol Cell Biol* 25, 9292-9303 (2005).

Hara, T., Kamura, T., Nakayama, K., Oshikawa, K., Hatakeyama, S. and Nakayama, K. Degradation of p27(Kip1) at the G(0)-G(1) transition mediated by a Skp2-independent ubiquitination pathway. *J Biol Chem* 276, 48937-48943 (2001).

Harbour, J.W., Luo, R.X., Dei Santi, A., Postigo, A.A. and Dean, D.C. Cdk phosphorylation triggers sequential intramolecular interactions that progressively block Rb functions as cells move through G1. *Cell* 98, 859-869 (1999).

Harper, J.W., Adami, G.R., Wei, N., Keyomarsi, K. and Elledge, S.J. The p21 Cdk-interacting protein Cip1 is a potent inhibitor of G1 cyclin-dependent kinases. *Cell* 75, 805-816 (1993).

Harper, J.W., Burton, J.L. and Solomon, M.J. The anaphase-promoting complex: it's not just for mitosis any more. *Genes Dev* 16, 2179-2206 (2002).

Hartwell, L.H., Culotti, J., Pringle, J.R. and Reid, B.J. Genetic control of the cell division cycle in yeast. *Science* 183, 46-51 (1974).

Hartwell, L.H. and Weinert, T.A. Checkpoints: controls that ensure the order of cell cycle events. *Science* 246, 629-634 (1989).

Hateboer, G., Timmers, H.T., Rustgi, A.K., Billaud, M., van 't Veer, L.J. and Bernards, R. TATA-binding protein and the retinoblastoma gene product bind to overlapping epitopes on c-Myc and adenovirus E1A protein. *Proc Natl Acad Sci U S A* 90, 8489-8493 (1993).

Hatta, Y., Takeuchi, S., Yokota, J. and Koeffler, H.P. Ovarian cancer has frequent loss of heterozygosity at chromosome 12p12.3-13.1 (region of TEL and Kip1 loci) and chromosome 12q23-ter: evidence for two new tumour-suppressor genes. *Br J Cancer* 75, 1256-1262 (1997).

Hayashi, K., Makino, R., Kawamura, H., Arisawa, A. and Yoneda, K. Characterization of rat c-myc and adjacent regions. *Nucleic Acids Res* 15, 6419-6436 (1987).

He, C., Hu, H., Braren, R., Fong, S.Y., Trumpp, A., Carlson, T.R. and Wang, R.A. c-myc in the hematopoietic lineage is crucial for its angiogenic function in the mouse embryo. *Development* 135, 2467-2477 (2008).

He, L., Liu, J., Collins, I., Sanford, S., O'Connell, B., Benham, C.J. and Levens, D. Loss of FBP function arrests cellular proliferation and extinguishes c-myc expression. *Embo J* 19, 1034-1044 (2000).

Hengst, L., Dulic, V., Slingerland, J.M., Lees, E. and Reed, S.I. A cell cycle-regulated inhibitor of cyclin-dependent kinases. *Proc Natl Acad Sci U S A* 91, 5291-5295 (1994).

Hengst, L., Gopfert, U., Lashuel, H.A. and Reed, S.I. Complete inhibition of Cdk/cyclin by one molecule of p21(Cip1). *Genes Dev* 12, 3882-3888 (1998).

Hengst, L. and Reed, S.I. Translational control of p27Kip1 accumulation during the cell cycle. *Science* 271, 1861-1864 (1996).

Hengst, L. and Reed, S.I. Inhibitors of the Cip/Kip family. *Curr Top Microbiol Immunol* 227, 25-41 (1998).

Herbst, A., Hemann, M.T., Tworkowski, K.A., Salghetti, S.E., Lowe, S.W. and Tansey, W.P. A conserved element in Myc that negatively regulates its proapoptotic activity. *EMBO Rep* 6, 177-183 (2005).

Herkert, B. and Eilers, M. Transcriptional repression: the dark side of myc. *Genes Cancer* 1, 580-586 (2010).

Hermeking, H. and Eick, D. Mediation of c-Myc-induced apoptosis by p53. *Science* 265, 2091-2093 (1994).

Hermeking, H., Rago, C., Schuhmacher, M., Li, Q., Barrett, J.F., Obaya, A.J., O'Connell, B.C., Mateyak, M.K., Tam, W., Kohlhuber, F.*, et al.* Identification of CDK4 as a target of c-MYC. *Proc Natl Acad Sci U S A* 97, 2229-2234 (2000).

Hershko, D., Bornstein, G., Ben-Izhak, O., Carrano, A., Pagano, M., Krausz, M.M. and Hershko, A. Inverse relation between levels of p27(Kip1) and of its ubiquitin ligase subunit Skp2 in colorectal carcinomas. *Cancer* 91, 1745-1751 (2001).

Hershko, D.D. Oncogenic properties and prognostic implications of the ubiquitin ligase Skp2 in cancer. *Cancer* 112, 1415-1424 (2008).

Hicke, L., Schubert, H.L. and Hill, C.P. Ubiquitin-binding domains. *Nat Rev Mol Cell Biol* 6, 610-621 (2005).

Hiromura, K., Pippin, J.W., Fero, M.L., Roberts, J.M. and Shankland, S.J. Modulation of apoptosis by the cyclin-dependent kinase inhibitor p27(Kip1). *J Clin Invest* 103, 597-604 (1999).

Hoang, A.T., Cohen, K.J., Barrett, J.F., Bergstrom, D.A. and Dang, C.V. Participation of cyclin A in Myc-induced apoptosis. *Proc Natl Acad Sci U S A* 91, 6875-6879 (1994).

Hochegger, H., Takeda, S. and Hunt, T. Cyclin-dependent kinases and cell-cycle transitions: does one fit all? *Nat Rev Mol Cell Biol* 9, 910-916 (2008).

Holt, J.T., Redner, R.L. and Nienhuis, A.W. An oligomer complementary to c-myc mRNA inhibits proliferation of HL-60 promyelocytic cells and induces differentiation. *Mol Cell Biol* 8, 963-973 (1988).

Hong, F., Larrea, M.D., Doughty, C., Kwiatkowski, D.J., Squillace, R. and Slingerland, J.M. mTOR-raptor binds and activates SGK1 to regulate p27 phosphorylation. *Mol Cell* 30, 701-711 (2008).

Hu, S.S., Lai, M.M. and Vogt, P.K. Genome of avian myelocytomatosis virus MC29: analysis by heteroduplex mapping. *Proc Natl Acad Sci U S A* 76, 1265-1268 (1979).

Huang, H., Regan, K.M., Wang, F., Wang, D., Smith, D.I., van Deursen, J.M. and Tindall, D.J. Skp2 inhibits FOXO1 in tumor suppression through ubiquitin-mediated degradation. *Proc Natl Acad Sci U S A* 102, 1649-1654 (2005).

Huang, H.L., Weng, H.Y., Wang, L.Q., Yu, C.H., Huang, Q.J., Zhao, P.P., Wen, J.Z., Zhou, H. and Qu, L.H. Triggering Fbw7-mediated proteasomal degradation of c-Myc by oridonin induces cell growth inhibition and apoptosis. *Mol Cancer Ther* 11, 1155-1165 (2012).

Huang, Y.C., Chen, J.Y. and Hung, W.C. Vitamin D3 receptor/Sp1 complex is required for the induction of p27Kip1 expression by vitamin D3. *Oncogene* 23, 4856-4861 (2004).

Huang, Y.C. and Hung, W.C. 1,25-dihydroxyvitamin D3 transcriptionally represses p45Skp2 expression via the Sp1 sites in human prostate cancer cells. *J Cell Physiol* 209, 363-369 (2006).

Hummel, M., Bentink, S., Berger, H., Klapper, W., Wessendorf, S., Barth, T.F., Bernd, H.W., Cogliatti, S.B., Dierlamm, J., Feller, A.C.*, et al.* A biologic definition of Burkitt's lymphoma from transcriptional and genomic profiling. *N Engl J Med* 354, 2419-2430 (2006).

Hurley, L.H., Von Hoff, D.D., Siddiqui-Jain, A. and Yang, D. Drug targeting of the c-MYC promoter to repress gene expression via a G-quadruplex silencer element. *Semin Oncol* 33, 498-512 (2006).

Hwang, C.S., Shemorry, A. and Varshavsky, A. N-terminal acetylation of cellular proteins creates specific degradation signals. *Science* 327, 973-977 (2010).

Hydbring, P., Bahram, F., Su, Y., Tronnersjo, S., Hogstrand, K., von der Lehr, N., Sharifi, H.R., Lilischkis, R., Hein, N., Wu, S.*, et al.* Phosphorylation by Cdk2 is required for Myc to repress Ras-induced senescence in cotransformation. *Proc Natl Acad Sci U S A* 107, 58-63 (2010).

Iakova, P., Awad, S.S. and Timchenko, N.A. Aging reduces proliferative capacities of liver by switching pathways of C/EBPalpha growth arrest. *Cell* 113, 495-506 (2003).

Iguchi-Ariga, S.M., Itani, T., Kiji, Y. and Ariga, H. Possible function of the c-myc product: promotion of cellular DNA replication. *Embo J* 6, 2365-2371 (1987).

Imaki, H., Nakayama, K., Delehouzee, S., Handa, H., Kitagawa, M., Kamura, T. and Nakayama, K.I. Cell cycle-dependent regulation of the Skp2 promoter by GA-binding protein. *Cancer Res* 63, 4607-4613 (2003).

Inghirami, G., Grignani, F., Sternas, L., Lombardi, L., Knowles, D.M. and Dalla-Favera, R. Down-regulation of LFA-1 adhesion receptors by C-myc oncogene in human B lymphoblastoid cells. *Science* 250, 682-686 (1990).

Inoue, T., Kamiyama, J. and Sakai, T. Sp1 and NF-Y synergistically mediate the effect of vitamin D(3) in the p27(Kip1) gene promoter that lacks vitamin D response elements. *J Biol Chem* 274, 32309-32317 (1999).

Inuzuka, H., Gao, D., Finley, L.W., Yang, W., Wan, L., Fukushima, H., Chin, Y.R., Zhai, B., Shaik, S., Lau, A.W.*, et al.* Acetylation-dependent regulation of Skp2 function. *Cell* 150, 179-193 (2012).

Iritani, B.M. and Eisenman, R.N. c-Myc enhances protein synthesis and cell size during B lymphocyte development. *Proc Natl Acad Sci U S A* 96, 13180-13185 (1999).

Ishida, N., Hara, T., Kamura, T., Yoshida, M., Nakayama, K. and Nakayama, K.I. Phosphorylation of p27Kip1 on serine 10 is required for its binding to CRM1 and nuclear export. *J Biol Chem* 277, 14355-14358 (2002).

Jakel, H., Peschel, I., Kunze, C., Weinl, C. and Hengst, L. Regulation of p27 (Kip1) by mitogen-induced tyrosine phosphorylation. *Cell Cycle* 11 (2012).

Jakel, H., Weinl, C. and Hengst, L. Phosphorylation of p27Kip1 by JAK2 directly links cytokine receptor signaling to cell cycle control. *Oncogene* 30, 3502-3512 (2011).

James, M.K., Ray, A., Leznova, D. and Blain, S.W. Differential modification of p27Kip1 controls its cyclin D-cdk4 inhibitory activity. *Mol Cell Biol* 28, 498-510 (2008).

Jansen-Durr, P., Meichle, A., Steiner, P., Pagano, M., Finke, K., Botz, J., Wessbecher, J., Draetta, G. and Eilers, M. Differential modulation of cyclin gene expression by MYC. *Proc Natl Acad Sci U S A* 90, 3685-3689 (1993).

Jeffrey, P.D., Russo, A.A., Polyak, K., Gibbs, E., Hurwitz, J., Massague, J. and Pavletich, N.P. Mechanism of CDK activation revealed by the structure of a cyclinA-CDK2 complex. *Nature* 376, 313-320 (1995).

Ji, P., Goldin, L., Ren, H., Sun, D., Guardavaccaro, D., Pagano, M. and Zhu, L. Skp2 contains a novel cyclin A binding domain that directly protects cyclin A from inhibition by p27Kip1. *J Biol Chem* 281, 24058-24069 (2006).

Jia, L. and Sun, Y. SCF E3 ubiquitin ligases as anticancer targets. *Curr Cancer Drug Targets* 11, 347-356 (2011).

Jin, J., Cardozo, T., Lovering, R.C., Elledge, S.J., Pagano, M. and Harper, J.W. Systematic analysis and nomenclature of mammalian F-box proteins. *Genes Dev* 18, 2573-2580 (2004).

Jin, Q., Yu, L.R., Wang, L., Zhang, Z., Kasper, L.H., Lee, J.E., Wang, C., Brindle, P.K., Dent, S.Y. and Ge, K. Distinct roles of GCN5/PCAF-mediated H3K9ac and CBP/p300-mediated H3K18/27ac in nuclear receptor transactivation. *Embo J* 30, 249-262 (2011).

Johnston, L.A., Prober, D.A., Edgar, B.A., Eisenman, R.N. and Gallant, P. Drosophila myc regulates cellular growth during development. *Cell* 98, 779-790 (1999).

Jones, T.R. and Cole, M.D. Rapid cytoplasmic turnover of c-myc mRNA: requirement of the 3' untranslated sequences. *Mol Cell Biol* 7, 4513-4521 (1987).

Kalaszczynska, I., Geng, Y., Iino, T., Mizuno, S., Choi, Y., Kondratiuk, I., Silver, D.P., Wolgemuth, D.J., Akashi, K. and Sicinski, P. Cyclin A is redundant in fibroblasts but essential in hematopoietic and embryonic stem cells. *Cell* 138, 352-365 (2009).

Kamura, T., Hara, T., Kotoshiba, S., Yada, M., Ishida, N., Imaki, H., Hatakeyama, S., Nakayama, K. and Nakayama, K.I. Degradation of p57Kip2 mediated by SCFSkp2-dependent ubiquitylation. *Proc Natl Acad Sci U S A* 100, 10231-10236 (2003).

Kamura, T., Hara, T., Matsumoto, M., Ishida, N., Okumura, F., Hatakeyama, S., Yoshida, M., Nakayama, K. and Nakayama, K.I. Cytoplasmic ubiquitin ligase KPC regulates proteolysis of p27(Kip1) at G1 phase. *Nat Cell Biol* 6, 1229-1235 (2004).

Karlsson, A., Deb-Basu, D., Cherry, A., Turner, S., Ford, J. and Felsher, D.W. Defective double-strand DNA break repair and chromosomal translocations by MYC overexpression. *Proc Natl Acad Sci U S A* 100, 9974-9979 (2003).

Karn, J., Watson, J.V., Lowe, A.D., Green, S.M. and Vedeckis, W. Regulation of cell cycle duration by c-myc levels. *Oncogene* 4, 773-787 (1989).

Katayose, Y., Kim, M., Rakkar, A.N., Li, Z., Cowan, K.H. and Seth, P. Promoting apoptosis: a novel activity associated with the cyclin-dependent kinase inhibitor p27. *Cancer Res* 57, 5441-5445 (1997).

Kato, G.J., Barrett, J., Villa-Garcia, M. and Dang, C.V. An amino-terminal c-myc domain required for neoplastic transformation activates transcription. *Mol Cell Biol* 10, 5914-5920 (1990).

Kato, G.J., Lee, W.M., Chen, L.L. and Dang, C.V. Max: functional domains and interaction with c-Myc. *Genes Dev* 6, 81-92 (1992).

Keller, U.B., Old, J.B., Dorsey, F.C., Nilsson, J.A., Nilsson, L., MacLean, K.H., Chung, L., Yang, C., Spruck, C., Boyd, K.*, et al.* Myc targets Cks1 to provoke the suppression of p27Kip1, proliferation and lymphomagenesis. *Embo J* 26, 2562-2574 (2007).

Kelly, K., Cochran, B.H., Stiles, C.D. and Leder, P. Cell-specific regulation of the c-myc gene by lymphocyte mitogens and platelet-derived growth factor. *Cell* 35, 603-610 (1983).

Kenneth, N.S., Ramsbottom, B.A., Gomez-Roman, N., Marshall, L., Cole, P.A. and White, R.J. TRRAP and GCN5 are used by c-Myc to activate RNA polymerase III transcription. *Proc Natl Acad Sci U S A* 104, 14917-14922 (2007).

Kiessling, A., Sperl, B., Hollis, A., Eick, D. and Berg, T. Selective inhibition of c-Myc/Max dimerization and DNA binding by small molecules. *Chem Biol* 13, 745-751 (2006).

Kilpinen, S., Autio, R., Ojala, K., Iljin, K., Bucher, E., Sara, H., Pisto, T., Saarela, M., Skotheim, R.I., Bjorkman, M.*, et al.* Systematic bioinformatic analysis of expression levels of 17,330 human genes across 9,783 samples from 175 types of healthy and pathological tissues. *Genome Biol* 9, R139 (2008).

Kim, H.H., Kuwano, Y., Srikantan, S., Lee, E.K., Martindale, J.L. and Gorospe, M. HuR recruits let-7/RISC to repress c-Myc expression. *Genes Dev* 23, 1743-1748 (2009).

Kim, J., Lee, J.H. and Iyer, V.R. Global identification of Myc target genes reveals its direct role in mitochondrial biogenesis and its E-box usage in vivo. *PLoS One* 3, e1798 (2008).

Kim, J., Woo, A.J., Chu, J., Snow, J.W., Fujiwara, Y., Kim, C.G., Cantor, A.B. and Orkin, S.H. A Myc network accounts for similarities between embryonic stem and cancer cell transcription programs. *Cell* 143, 313-324 (2010).

Kim, J.W., Zeller, K.I., Wang, Y., Jegga, A.G., Aronow, B.J., O'Donnell, K.A. and Dang, C.V. Evaluation of myc E-box phylogenetic footprints in glycolytic genes by chromatin immunoprecipitation assays. *Mol Cell Biol* 24, 5923-5936 (2004).

Kim, S.Y., Herbst, A., Tworkowski, K.A., Salghetti, S.E. and Tansey, W.P. Skp2 regulates Myc protein stability and activity. *Mol Cell* 11, 1177-1188 (2003).

Kitagawa, M., Lee, S.H. and McCormick, F. Skp2 suppresses p53-dependent apoptosis by inhibiting p300. *Mol Cell* 29, 217-231 (2008).

Kiyokawa, H., Kineman, R.D., Manova-Todorova, K.O., Soares, V.C., Hoffman, E.S., Ono, M., Khanam, D., Hayday, A.C., Frohman, L.A. and Koff, A. Enhanced growth of mice lacking the cyclin-dependent kinase inhibitor function of p27(Kip1). *Cell* 85, 721-732 (1996).

Klapper, W., Szczepanowski, M., Burkhardt, B., Berger, H., Rosolowski, M., Bentink, S., Schwaenen, C., Wessendorf, S., Spang, R., Moller, P.*, et al.* Molecular profiling of pediatric mature B-cell lymphoma treated in population-based prospective clinical trials. *Blood* 112, 1374-1381 (2008).

Kleine-Kohlbrecher, D., Adhikary, S. and Eilers, M. Mechanisms of transcriptional repression by Myc. *Curr Top Microbiol Immunol* 302, 51-62 (2006).

Knoepfler, P.S. Myc goes global: new tricks for an old oncogene. *Cancer Res* 67, 5061-5063 (2007).

Knoepfler, P.S., Zhang, X.Y., Cheng, P.F., Gafken, P.R., McMahon, S.B. and Eisenman, R.N. Myc influences global chromatin structure. *Embo J* 25, 2723-2734 (2006).

Koepp, D.M., Schaefer, L.K., Ye, X., Keyomarsi, K., Chu, C., Harper, J.W. and Elledge, S.J. Phosphorylation-dependent ubiquitination of cyclin E by the SCFFbw7 ubiquitin ligase. *Science* 294, 173-177 (2001).

Koff, A., Ohtsuki, M., Polyak, K., Roberts, J.M. and Massague, J. Negative regulation of G1 in mammalian cells: inhibition of cyclin E-dependent kinase by TGF-beta. *Science* 260, 536-539 (1993).

Kohl, N.E., Kanda, N., Schreck, R.R., Bruns, G., Latt, S.A., Gilbert, F. and Alt, F.W. Transposition and amplification of oncogene-related sequences in human neuroblastomas. *Cell* 35, 359-367 (1983).

Kossatz, U., Vervoorts, J., Nickeleit, I., Sundberg, H.A., Arthur, J.S., Manns, M.P. and Malek, N.P. C-terminal phosphorylation controls the stability and function of p27kip1. *Embo J* 25, 5159-5170 (2006).

Kotake, Y., Nakayama, K., Ishida, N. and Nakayama, K.I. Role of serine 10 phosphorylation in p27 stabilization revealed by analysis of p27 knock-in mice harboring a serine 10 mutation. *J Biol Chem* 280, 1095-1102 (2005).

Kotoshiba, S., Kamura, T., Hara, T., Ishida, N. and Nakayama, K.I. Molecular dissection of the interaction between p27 and Kip1 ubiquitylation-promoting complex, the ubiquitin ligase that regulates proteolysis of p27 in G1 phase. *J Biol Chem* 280, 17694-17700 (2005).

Kozar, K., Ciemerych, M.A., Rebel, V.I., Shigematsu, H., Zagozdzon, A., Sicinska, E., Geng, Y., Yu, Q., Bhattacharya, S., Bronson, R.T.*, et al.* Mouse development and cell proliferation in the absence of D-cyclins. *Cell* 118, 477-491 (2004).

Krek, W. and Nigg, E.A. Differential phosphorylation of vertebrate p34cdc2 kinase at the G1/S and G2/M transitions of the cell cycle: identification of major phosphorylation sites. *Embo J* 10, 305-316 (1991).

Kretzner, L., Blackwood, E.M. and Eisenman, R.N. Myc and Max proteins possess distinct transcriptional activities. *Nature* 359, 426-429 (1992).

Kullmann, M., Gopfert, U., Siewe, B. and Hengst, L. ELAV/Hu proteins inhibit p27 translation via an IRES element in the p27 5'UTR. *Genes Dev* 16, 3087-3099 (2002).

Kurland, J.F. and Tansey, W.P. Crashing waves of destruction: the cell cycle and APC(Cdh1) regulation of SCF(Skp2). *Cancer Cell* 5, 305-306 (2004).

Kurland, J.F. and Tansey, W.P. Myc-mediated transcriptional repression by recruitment of histone deacetylase. *Cancer Res* 68, 3624-3629 (2008).

LaBaer, J., Garrett, M.D., Stevenson, L.F., Slingerland, J.M., Sandhu, C., Chou, H.S., Fattaey, A. and Harlow, E. New functional activities for the p21 family of CDK inhibitors. *Genes Dev* 11, 847-862 (1997).

Lacy, E.R., Filippov, I., Lewis, W.S., Otieno, S., Xiao, L., Weiss, S., Hengst, L. and Kriwacki, R.W. p27 binds cyclin-CDK complexes through a sequential mechanism involving binding-induced protein folding. *Nat Struct Mol Biol* 11, 358-364 (2004).

Lachman, H.M. and Skoultchi, A.I. Expression of c-myc changes during differentiation of mouse erythroleukaemia cells. *Nature* 310, 592-594 (1984).

Ladha, M.H., Lee, K.Y., Upton, T.M., Reed, M.F. and Ewen, M.E. Regulation of exit from quiescence by p27 and cyclin D1-CDK4. *Mol Cell Biol* 18, 6605-6615 (1998).

Landschulz, W.H., Johnson, P.F. and McKnight, S.L. The leucine zipper: a hypothetical structure common to a new class of DNA binding proteins. *Science* 240, 1759-1764 (1988).

Langdon, W.Y., Harris, A.W., Cory, S. and Adams, J.M. The c-myc oncogene perturbs B lymphocyte development in E-mu-myc transgenic mice. *Cell* 47, 11-18 (1986).

Larrea, M.D., Hong, F., Wander, S.A., da Silva, T.G., Helfman, D., Lannigan, D., Smith, J.A. and Slingerland, J.M. RSK1 drives p27Kip1 phosphorylation at T198 to promote RhoA inhibition and increase cell motility. *Proc Natl Acad Sci U S A* 106, 9268-9273 (2009a).

Larrea, M.D., Liang, J., Da Silva, T., Hong, F., Shao, S.H., Han, K., Dumont, D. and Slingerland, J.M. Phosphorylation of p27Kip1 regulates assembly and activation of cyclin D1-Cdk4. *Mol Cell Biol* 28, 6462-6472 (2008).

Larrea, M.D., Wander, S.A. and Slingerland, J.M. p27 as Jekyll and Hyde: regulation of cell cycle and cell motility. *Cell Cycle* 8, 3455-3461 (2009b).

Latres, E., Chiarle, R., Schulman, B.A., Pavletich, N.P., Pellicer, A., Inghirami, G. and Pagano, M. Role of the F-box protein Skp2 in lymphomagenesis. *Proc Natl Acad Sci U S A* 98, 2515-2520 (2001).

Laurenti, E., Varnum-Finney, B., Wilson, A., Ferrero, I., Blanco-Bose, W.E., Ehninger, A., Knoepfler, P.S., Cheng, P.F., MacDonald, H.R., Eisenman, R.N.*, et al.* Hematopoietic stem cell function and survival depend on c-Myc and N-Myc activity. *Cell Stem Cell* 3, 611-624 (2008).

Law, J.C., Ritke, M.K., Yalowich, J.C., Leder, G.H. and Ferrell, R.E. Mutational inactivation of the p53 gene in the human erythroid leukemic K562 cell line. *Leuk Res* 17, 1045-1050 (1993).

le Sage, C., Nagel, R., Egan, D.A., Schrier, M., Mesman, E., Mangiola, A., Anile, C., Maira, G., Mercatelli, N., Ciafre, S.A., *et al.* Regulation of the p27(Kip1) tumor suppressor by miR-221 and miR-222 promotes cancer cell proliferation. *Embo J* 26, 3699-3708 (2007).

Leon, J., Ferrandiz, N., Acosta, J.C. and Delgado, M.D. Inhibition of cell differentiation: a critical mechanism for MYC-mediated carcinogenesis? *Cell Cycle* 8, 1148-1157 (2009).

Lerga, A., Crespo, P., Berciano, M., Delgado, M.D., Canelles, M., Cales, C., Richard, C., Ceballos, E., Gutierrez, P., Ajenjo, N., *et al.* Regulation of c-Myc and Max in megakaryocytic and monocytic-macrophagic differentiation of K562 cells induced by protein kinase C modifiers: c-Myc is down-regulated but does not inhibit differentiation. *Cell Growth Differ* 10, 639-654 (1999).

Levens, D. You Don't Muck with MYC. *Genes Cancer* 1, 547-554 (2010).

Li, F., Wang, Y., Zeller, K.I., Potter, J.J., Wonsey, D.R., O'Donnell, K.A., Kim, J.W., Yustein, J.T., Lee, L.A. and Dang, C.V. Myc stimulates nuclearly encoded mitochondrial genes and mitochondrial biogenesis. *Mol Cell Biol* 25, 6225-6234 (2005).

Li, W., Bengtson, M.H., Ulbrich, A., Matsuda, A., Reddy, V.A., Orth, A., Chanda, S.K., Batalov, S. and Joazeiro, C.A. Genome-wide and functional annotation of human E3 ubiquitin ligases identifies MULAN, a mitochondrial E3 that regulates the organelle's dynamics and signaling. *PLoS One* 3, e1487 (2008).

Li, Z., Van Calcar, S., Qu, C., Cavenee, W.K., Zhang, M.Q. and Ren, B. A global transcriptional regulatory role for c-Myc in Burkitt's lymphoma cells. *Proc Natl Acad Sci U S A* 100, 8164-8169 (2003).

Liang, J., Shao, S.H., Xu, Z.X., Hennessy, B., Ding, Z., Larrea, M., Kondo, S., Dumont, D.J., Gutterman, J.U., Walker, C.L., *et al.* The energy sensing LKB1-AMPK pathway regulates p27(kip1) phosphorylation mediating the decision to enter autophagy or apoptosis. *Nat Cell Biol* 9, 218-224 (2007).

Liang, J., Zubovitz, J., Petrocelli, T., Kotchetkov, R., Connor, M.K., Han, K., Lee, J.H., Ciarallo, S., Catzavelos, C., Beniston, R., *et al.* PKB/Akt phosphorylates p27, impairs nuclear import of p27 and opposes p27-mediated G1 arrest. *Nat Med* 8, 1153-1160 (2002).

Lin, C.Y., Loven, J., Rahl, P.B., Paranal, R.M., Burge, C.B., Bradner, J.E., Lee, T.I. and Young, R.A. Transcriptional amplification in tumor cells with elevated c-Myc. *Cell* 151, 56-67 (2012).

Lin, H.K., Chen, Z., Wang, G., Nardella, C., Lee, S.W., Chan, C.H., Yang, W.L., Wang, J., Egia, A., Nakayama, K.I., *et al.* Skp2 targeting suppresses tumorigenesis by Arf-p53-independent cellular senescence. *Nature* 464, 374-379 (2010).

Lin, H.K., Wang, G., Chen, Z., Teruya-Feldstein, J., Liu, Y., Chan, C.H., Yang, W.L., Erdjument-Bromage, H., Nakayama, K.I., Nimer, S., *et al.* Phosphorylation-dependent regulation of cytosolic localization and oncogenic function of Skp2 by Akt/PKB. *Nat Cell Biol* 11, 420-432 (2009).

Lindstrom, M.S. and Wiman, K.G. Myc and E2F1 induce p53 through p14ARF-independent mechanisms in human fibroblasts. *Oncogene* 22, 4993-5005 (2003).

Lipkowitz, S. and Weissman, A.M. RINGs of good and evil: RING finger ubiquitin ligases at the crossroads of tumour suppression and oncogenesis. *Nat Rev Cancer* 11, 629-643 (2011).

Littlewood, T.D., Hancock, D.C., Danielian, P.S., Parker, M.G. and Evan, G.I. A modified oestrogen receptor ligand-binding domain as an improved switch for the regulation of heterologous proteins. *Nucleic Acids Res* 23, 1686-1690 (1995).

Liu, C., Fang, X., Ge, Z., Jalink, M., Kyo, S., Bjorkholm, M., Gruber, A., Sjoberg, J. and Xu, D. The telomerase reverse transcriptase (hTERT) gene is a direct target of the histone methyltransferase SMYD3. *Cancer Res* 67, 2626-2631 (2007).

Liu, D., Matzuk, M.M., Sung, W.K., Guo, Q., Wang, P. and Wolgemuth, D.J. Cyclin A1 is required for meiosis in the male mouse. *Nat Genet* 20, 377-380 (1998).

Liu, J., He, L., Collins, I., Ge, H., Libutti, D., Li, J., Egly, J.M. and Levens, D. The FBP interacting repressor targets TFIIH to inhibit activated transcription. *Mol Cell* 5, 331-341 (2000).

Liu, J., Kouzine, F., Nie, Z., Chung, H.J., Elisha-Feil, Z., Weber, A., Zhao, K. and Levens, D. The FUSE/FBP/FIR/TFIIH system is a molecular machine programming a pulse of c-myc expression. *Embo J* 25, 2119-2130 (2006).

Liu, J. and Levens, D. Making myc. *Curr Top Microbiol Immunol* 302, 1-32 (2006).

Liu, M., Lee, M.H., Cohen, M., Bommakanti, M. and Freedman, L.P. Transcriptional activation of the Cdk inhibitor p21 by vitamin D3 leads to the induced differentiation of the myelomonocytic cell line U937. *Genes Dev* 10, 142-153 (1996).

Liu, X., Tesfai, J., Evrard, Y.A., Dent, S.Y. and Martinez, E. c-Myc transformation domain recruits the human STAGA complex and requires TRRAP and GCN5 acetylase activity for transcription activation. *J Biol Chem* 278, 20405-20412 (2003).

Liu, Y.C., Li, F., Handler, J., Huang, C.R., Xiang, Y., Neretti, N., Sedivy, J.M., Zeller, K.I. and Dang, C.V. Global regulation of nucleotide biosynthetic genes by c-Myc. *PLoS One* 3, e2722 (2008).

Lolli, G. and Johnson, L.N. CAK-Cyclin-dependent Activating Kinase: a key kinase in cell cycle control and a target for drugs? *Cell Cycle* 4, 572-577 (2005).

Louis, S.F., Vermolen, B.J., Garini, Y., Young, I.T., Guffei, A., Lichtensztejn, Z., Kuttler, F., Chuang, T.C., Moshir, S., Mougey, V.*, et al.* c-Myc induces chromosomal rearrangements through telomere and chromosome remodeling in the interphase nucleus. *Proc Natl Acad Sci U S A* 102, 9613-9618 (2005).

Loyer, P., Trembley, J.H., Katona, R., Kidd, V.J. and Lahti, J.M. Role of CDK/cyclin complexes in transcription and RNA splicing. *Cell Signal* 17, 1033-1051 (2005).

Lozzio, C.B. and Lozzio, B.B. Human chronic myelogenous leukemia cell-line with positive Philadelphia chromosome. *Blood* 45, 321-334 (1975).

Lu, L., Schulz, H. and Wolf, D.A. The F-box protein SKP2 mediates androgen control of p27 stability in LNCaP human prostate cancer cells. *BMC Cell Biol* 3, 22 (2002).

Lu, Z. and Hunter, T. Ubiquitylation and proteasomal degradation of the p21(Cip1), p27(Kip1) and p57(Kip2) CDK inhibitors. *Cell Cycle* 9, 2342-2352 (2010).

Lundberg, A.S. and Weinberg, R.A. Functional inactivation of the retinoblastoma protein requires sequential modification by at least two distinct cyclin-cdk complexes. *Mol Cell Biol* 18, 753-761 (1998).

Luo, Q., Li, J., Cenkci, B. and Kretzner, L. Autorepression of c-myc requires both initiator and E2F-binding site elements and cooperation with the p107 gene product. *Oncogene* 23, 1088-1097 (2004).

Luscher-Firzlaff, J., Gawlista, I., Vervoorts, J., Kapelle, K., Braunschweig, T., Walsemann, G., Rodgarkia-Schamberger, C., Schuchlautz, H., Dreschers, S., Kremmer, E.*, et al.* The human trithorax protein hASH2 functions as an oncoprotein. *Cancer Res* 68, 749-758 (2008).

Luscher, B. and Vervoorts, J. Regulation of gene transcription by the oncoprotein MYC. *Gene* 494, 145-160 (2012).

Ma, L., Young, J., Prabhala, H., Pan, E., Mestdagh, P., Muth, D., Teruya-Feldstein, J., Reinhardt, F., Onder, T.T., Valastyan, S.*, et al.* miR-9, a MYC/MYCN-activated microRNA, regulates E-cadherin and cancer metastasis. *Nat Cell Biol* 12, 247-256 (2010).

Maheswaran, S., Lee, H. and Sonenshein, G.E. Intracellular association of the protein product of the c-myc oncogene with the TATA-binding protein. *Mol Cell Biol* 14, 1147-1152 (1994).

Mai, S., Fluri, M., Siwarski, D. and Huppi, K. Genomic instability in MycER-activated Rat1A-MycER cells. *Chromosome Res* 4, 365-371 (1996).

Makela, T.P., Koskinen, P.J., Vastrik, I. and Alitalo, K. Alternative forms of Max as enhancers or suppressors of Myc-ras cotransformation. *Science* 256, 373-377 (1992).

Makela, T.P., Tassan, J.P., Nigg, E.A., Frutiger, S., Hughes, G.J. and Weinberg, R.A. A cyclin associated with the CDK-activating kinase MO15. *Nature* 371, 254-257 (1994).

Malek, N.P., Sundberg, H., McGrew, S., Nakayama, K., Kyriakides, T.R. and Roberts, J.M. A mouse knock-in model exposes sequential proteolytic pathways that regulate p27Kip1 in G1 and S phase. *Nature* 413, 323-327 (2001).

Malumbres, M. and Barbacid, M. To cycle or not to cycle: a critical decision in cancer. *Nat Rev Cancer* 1, 222-231 (2001).

Malumbres, M. and Barbacid, M. Mammalian cyclin-dependent kinases. *Trends Biochem Sci* 30, 630-641 (2005).

Malumbres, M., Harlow, E., Hunt, T., Hunter, T., Lahti, J.M., Manning, G., Morgan, D.O., Tsai, L.H. and Wolgemuth, D.J. Cyclin-dependent kinases: a family portrait. *Nat Cell Biol* 11, 1275-1276 (2009).

Malumbres, M., Sotillo, R., Santamaria, D., Galan, J., Cerezo, A., Ortega, S., Dubus, P. and Barbacid, M. Mammalian cells cycle without the D-type cyclin-dependent kinases Cdk4 and Cdk6. *Cell* 118, 493-504 (2004).

Malynn, B.A., de Alboran, I.M., O'Hagan, R.C., Bronson, R., Davidson, L., DePinho, R.A. and Alt, F.W. N-myc can functionally replace c-myc in murine development, cellular growth, and differentiation. *Genes Dev* 14, 1390-1399 (2000).

Marhin, W.W., Chen, S., Facchini, L.M., Fornace, A.J., Jr. and Penn, L.Z. Myc represses the growth arrest gene gadd45. *Oncogene* 14, 2825-2834 (1997).

Marshall, N.F., Peng, J., Xie, Z. and Price, D.H. Control of RNA polymerase II elongation potential by a novel carboxyl-terminal domain kinase. *J Biol Chem* 271, 27176-27183 (1996).

Marti, A., Wirbelauer, C., Scheffner, M. and Krek, W. Interaction between ubiquitin-protein ligase SCFSKP2 and E2F-1 underlies the regulation of E2F-1 degradation. *Nat Cell Biol* 1, 14-19 (1999).

Martin, A., Odajima, J., Hunt, S.L., Dubus, P., Ortega, S., Malumbres, M. and Barbacid, M. Cdk2 is dispensable for cell cycle inhibition and tumor suppression mediated by p27(Kip1) and p21(Cip1). *Cancer Cell* 7, 591-598 (2005).

Martinato, F., Cesaroni, M., Amati, B. and Guccione, E. Analysis of Myc-induced histone modifications on target chromatin. *PLoS One* 3, e3650 (2008).

Martins, C.P. and Berns, A. Loss of p27(Kip1) but not p21(Cip1) decreases survival and synergizes with MYC in murine lymphomagenesis. *Embo J* 21, 3739-3748 (2002).

Maru, Y., Afar, D.E., Witte, O.N. and Shibuya, M. The dimerization property of glutathione S-transferase partially reactivates Bcr-Abl lacking the oligomerization domain. *J Biol Chem* 271, 15353-15357 (1996).

Mateyak, M.K., Obaya, A.J., Adachi, S. and Sedivy, J.M. Phenotypes of c-Myc-deficient rat fibroblasts isolated by targeted homologous recombination. *Cell Growth Differ* 8, 1039-1048 (1997).

Mateyak, M.K., Obaya, A.J. and Sedivy, J.M. c-Myc regulates cyclin D-Cdk4 and -Cdk6 activity but affects cell cycle progression at multiple independent points. *Mol Cell Biol* 19, 4672-4683 (1999).

Matsumura, I., Ishikawa, J., Nakajima, K., Oritani, K., Tomiyama, Y., Miyagawa, J., Kato, T., Miyazaki, H., Matsuzawa, Y. and Kanakura, Y. Thrombopoietin-induced differentiation of a human megakaryoblastic leukemia cell line, CMK, involves transcriptional activation of p21(WAF1/Cip1) by STAT5. *Mol Cell Biol* 17, 2933-2943 (1997).

Matsushime, H., Ewen, M.E., Strom, D.K., Kato, J.Y., Hanks, S.K., Roussel, M.F. and Sherr, C.J. Identification and properties of an atypical catalytic subunit (p34PSK-J3/cdk4) for mammalian D type G1 cyclins. *Cell* 71, 323-334 (1992).

Matsushime, H., Roussel, M.F., Ashmun, R.A. and Sherr, C.J. Colony-stimulating factor 1 regulates novel cyclins during the G1 phase of the cell cycle. *Cell* 65, 701-713 (1991).

Matushansky, I., Radparvar, F. and Skoultchi, A.I. Reprogramming leukemic cells to terminal differentiation by inhibiting specific cyclin-dependent kinases in G1. *Proc Natl Acad Sci U S A* 97, 14317-14322 (2000).

McAllister, S.S., Becker-Hapak, M., Pintucci, G., Pagano, M. and Dowdy, S.F. Novel p27(kip1) C-terminal scatter domain mediates Rac-dependent cell migration independent of cell cycle arrest functions. *Mol Cell Biol* 23, 216-228 (2003).

McEwan, I.J., Dahlman-Wright, K., Ford, J. and Wright, A.P. Functional interaction of the c-Myc transactivation domain with the TATA binding protein: evidence for an induced fit model of transactivation domain folding. *Biochemistry* 35, 9584-9593 (1996).

McGrath, C.F., Pattabiraman, N., Kellogg, G.E., Lemcke, T., Kunick, C., Sausville, E.A., Zaharevitz, D.W. and Gussio, R. Homology model of the CDK1/cyclin B complex. *J Biomol Struct Dyn* 22, 493-502 (2005).

McMahon, S.B., Van Buskirk, H.A., Dugan, K.A., Copeland, T.D. and Cole, M.D. The novel ATM-related protein TRRAP is an essential cofactor for the c-Myc and E2F oncoproteins. *Cell* 94, 363-374 (1998).

McMahon, S.B., Wood, M.A. and Cole, M.D. The essential cofactor TRRAP recruits the histone acetyltransferase hGCN5 to c-Myc. *Mol Cell Biol* 20, 556-562 (2000).

McMahon, S.B. Emerging Concepts in the Analysis of Transcriptional Targets of the MYC Oncoprotein: Are the Targets Targetable? *Genes Cancer* 1, 560-567 (2010).

Medema, R.H., Kops, G.J., Bos, J.L. and Burgering, B.M. AFX-like Forkhead transcription factors mediate cell-cycle regulation by Ras and PKB through p27kip1. *Nature* 404, 782-787 (2000).

Menssen, A. and Hermeking, H. Characterization of the c-MYC-regulated transcriptome by SAGE: identification and analysis of c-MYC target genes. *Proc Natl Acad Sci U S A* 99, 6274-6279 (2002).

Menssen, A., Hydbring, P., Kapelle, K., Vervoorts, J., Diebold, J., Luscher, B., Larsson, L.G. and Hermeking, H. The c-MYC oncoprotein, the NAMPT enzyme, the SIRT1-inhibitor DBC1, and the SIRT1 deacetylase form a positive feedback loop. *Proc Natl Acad Sci U S A* 109, E187-196 (2012).

Mertz, J.A., Conery, A.R., Bryant, B.M., Sandy, P., Balasubramanian, S., Mele, D.A., Bergeron, L. and Sims, R.J., 3rd Targeting MYC dependence in cancer by inhibiting BET bromodomains. *Proc Natl Acad Sci U S A* 108, 16669-16674 (2011).

Metzger, M.B., Hristova, V.A. and Weissman, A.M. HECT and RING finger families of E3 ubiquitin ligases at a glance. *J Cell Sci* 125, 531-537 (2012).

Mezquita, P., Parghi, S.S., Brandvold, K.A. and Ruddell, A. Myc regulates VEGF production in B cells by stimulating initiation of VEGF mRNA translation. *Oncogene* 24, 889-901 (2005).

Milne, T.A., Hughes, C.M., Lloyd, R., Yang, Z., Rozenblatt-Rosen, O., Dou, Y., Schnepp, R.W., Krankel, C., Livolsi, V.A., Gibbs, D.*, et al.* Menin and MLL cooperatively regulate expression of cyclin-dependent kinase inhibitors. *Proc Natl Acad Sci U S A* 102, 749-754 (2005).

Millard, S.S., Vidal, A., Markus, M. and Koff, A. A U-rich element in the 5' untranslated region is necessary for the translation of p27 mRNA. *Mol Cell Biol* 20, 5947-5959 (2000).

Millard, S.S., Yan, J.S., Nguyen, H., Pagano, M., Kiyokawa, H. and Koff, A. Enhanced ribosomal association of p27(Kip1) mRNA is a mechanism contributing to accumulation during growth arrest. *J Biol Chem* 272, 7093-7098 (1997).

Miller, M.E. and Cross, F.R. Cyclin specificity: how many wheels do you need on a unicycle? *J Cell Sci* 114, 1811-1820 (2001).

Min, Y.H., Cheong, J.W., Lee, M.H., Kim, J.Y., Lee, S.T., Hahn, J.S. and Ko, Y.W. Elevated S-phase kinase-associated protein 2 protein expression in acute myelogenous leukemia: its association with constitutive phosphorylation of phosphatase and tensin homologue protein and poor prognosis. *Clin Cancer Res* 10, 5123-5130 (2004).

Miroux, B. and Walker, J.E. Over-production of proteins in Escherichia coli: mutant hosts that allow synthesis of some membrane proteins and globular proteins at high levels. *J Mol Biol* 260, 289-298 (1996).

Miskimins, W.K., Wang, G., Hawkinson, M. and Miskimins, R. Control of cyclin-dependent kinase inhibitor p27 expression by cap-independent translation. *Mol Cell Biol* 21, 4960-4967 (2001).

Molatore, S., Marinoni, I., Lee, M., Pulz, E., Ambrosio, M.R., degli Uberti, E.C., Zatelli, M.C. and Pellegata, N.S. A novel germline CDKN1B mutation causing multiple endocrine tumors: clinical, genetic and functional characterization. *Hum Mutat* 31, E1825-1835 (2010).

Montagnoli, A., Fiore, F., Eytan, E., Carrano, A.C., Draetta, G.F., Hershko, A. and Pagano, M. Ubiquitination of p27 is regulated by Cdk-dependent phosphorylation and trimeric complex formation. *Genes Dev* 13, 1181-1189 (1999).

Morgan, D.O. Principles of CDK regulation. *Nature* 374, 131-134 (1995).

Morgan, D.O. Cyclin-dependent kinases: engines, clocks, and microprocessors. *Annu Rev Cell Dev Biol* 13, 261-291 (1997).

Morgan, D.O. *The cell cycle: Principles of Control.* London: New Science Press, 1st ed., (2007).

Morishita, D., Katayama, R., Sekimizu, K., Tsuruo, T. and Fujita, N. Pim kinases promote cell cycle progression by phosphorylating and down-regulating p27Kip1 at the transcriptional and posttranscriptional levels. *Cancer Res* 68, 5076-5085 (2008).

Mueller, P.R., Coleman, T.R., Kumagai, A. and Dunphy, W.G. Myt1: a membrane-associated inhibitory kinase that phosphorylates Cdc2 on both threonine-14 and tyrosine-15. *Science* 270, 86-90 (1995).

Muller, D., Bouchard, C., Rudolph, B., Steiner, P., Stuckmann, I., Saffrich, R., Ansorge, W., Huttner, W. and Eilers, M. Cdk2-dependent phosphorylation of p27 facilitates its Myc-induced release from cyclin E/cdk2 complexes. *Oncogene* 15, 2561-2576 (1997).

Muller, D., Thieke, K., Burgin, A., Dickmanns, A. and Eilers, M. Cyclin E-mediated elimination of p27 requires its interaction with the nuclear pore-associated protein mNPAP60. *Embo J* 19, 2168-2180 (2000).

Munoz-Alonso, M. and Leon, J. in G1 phase progression. (ed. Boonstra, J.) 1-29 (Landes Bioscience, New York; 2003).

Munoz-Alonso, M.J., Acosta, J.C., Richard, C., Delgado, M.D., Sedivy, J. and Leon, J. p21Cip1 and p27Kip1 induce distinct cell cycle effects and differentiation programs in myeloid leukemia cells. *J Biol Chem* 280, 18120-18129 (2005).

Murphy, M., Stinnakre, M.G., Senamaud-Beaufort, C., Winston, N.J., Sweeney, C., Kubelka, M., Carrington, M., Brechot, C. and Sobczak-Thepot, J. Delayed early embryonic lethality following disruption of the murine cyclin A2 gene. *Nat Genet* 15, 83-86 (1997).

Murphy, M.J., Wilson, A. and Trumpp, A. More than just proliferation: Myc function in stem cells. *Trends Cell Biol* 15, 128-137 (2005).

Murray, A.W. Recycling the cell cycle: cyclins revisited. *Cell* 116, 221-234 (2004).

Murray, A.W. and Hunt, T. The cell cycle: an introduction. *Oxford University Press* (1993).

Murre, C., McCaw, P.S. and Baltimore, D. A new DNA binding and dimerization motif in immunoglobulin enhancer binding, daughterless, MyoD, and myc proteins. *Cell* 56, 777-783 (1989).

Musat, M., Korbonits, M., Kola, B., Borboli, N., Hanson, M.R., Nanzer, A.M., Grigson, J., Jordan, S., Morris, D.G., Gueorguiev, M*., et al.* Enhanced protein kinase B/Akt signalling in pituitary tumours. *Endocr Relat Cancer* 12, 423-433 (2005).

Muto, A., Kizaki, M., Yamato, K., Kawai, Y., Kamata-Matsushita, M., Ueno, H., Ohguchi, M., Nishihara, T., Koeffler, H.P. and Ikeda, Y. 1,25-Dihydroxyvitamin D3 induces differentiation of a retinoic acid-resistant acute promyelocytic leukemia cell line (UF-1) associated with expression of p21(WAF1/CIP1) and p27(KIP1). *Blood* 93, 2225-2233 (1999).

Nagahara, H., Vocero-Akbani, A.M., Snyder, E.L., Ho, A., Latham, D.G., Lissy, N.A., Becker-Hapak, M., Ezhevsky, S.A. and Dowdy, S.F. Transduction of full-length TAT fusion proteins into mammalian cells: TAT-p27Kip1 induces cell migration. *Nat Med* 4, 1449-1452 (1998).

Nagano, Y., Fukushima, T., Okemoto, K., Tanaka, K., Bowtell, D.D., Ronai, Z., Reed, J.C. and Matsuzawa, S. Siah1/SIP regulates p27(kip1) stability and cell migration under metabolic stress. *Cell Cycle* 10, 2592-2602 (2011).

Nagl, N.G., Jr., Zweitzig, D.R., Thimmapaya, B., Beck, G.R., Jr. and Moran, E. The c-myc gene is a direct target of mammalian SWI/SNF-related complexes during differentiation-associated cell cycle arrest. *Cancer Res* 66, 1289-1293 (2006).

Nair, S.K. and Burley, S.K. X-ray structures of Myc-Max and Mad-Max recognizing DNA. Molecular bases of regulation by proto-oncogenic transcription factors. *Cell* 112, 193-205 (2003).

Nakayama, K., Ishida, N., Shirane, M., Inomata, A., Inoue, T., Shishido, N., Horii, I., Loh, D.Y. and Nakayama, K. Mice lacking p27(Kip1) display increased body size, multiple organ hyperplasia, retinal dysplasia, and pituitary tumors. *Cell* 85, 707-720 (1996).

Nakayama, K., Nagahama, H., Minamishima, Y.A., Matsumoto, M., Nakamichi, I., Kitagawa, K., Shirane, M., Tsunematsu, R., Tsukiyama, T., Ishida, N*., et al.* Targeted disruption of Skp2 results in accumulation of cyclin E and p27(Kip1), polyploidy and centrosome overduplication. *Embo J* 19, 2069-2081 (2000).

Nakayama, K., Nagahama, H., Minamishima, Y.A., Miyake, S., Ishida, N., Hatakeyama, S., Kitagawa, M., Iemura, S., Natsume, T. and Nakayama, K.I. Skp2-mediated degradation of p27 regulates progression into mitosis. *Dev Cell* 6, 661-672 (2004).

Nakayama, K.I., Hatakeyama, S. and Nakayama, K. Regulation of the cell cycle at the G1-S transition by proteolysis of cyclin E and p27Kip1. *Biochem Biophys Res Commun* 282, 853-860 (2001).

Nakayama, K.I. and Nakayama, K. Regulation of the cell cycle by SCF-type ubiquitin ligases. *Semin Cell Dev Biol* 16, 323-333 (2005).

Nakayama, K.I. and Nakayama, K. Ubiquitin ligases: cell-cycle control and cancer. *Nat Rev Cancer* 6, 369-381 (2006).

Nascimento, E.M., Cox, C.L., MacArthur, S., Hussain, S., Trotter, M., Blanco, S., Suraj, M., Nichols, J., Kubler, B., Benitah, S.A*., et al.* The opposing transcriptional functions of Sin3a and c-Myc are required to maintain tissue homeostasis. *Nat Cell Biol* 13, 1395-1405 (2011).

Nau, M.M., Brooks, B.J., Battey, J., Sausville, E., Gazdar, A.F., Kirsch, I.R., McBride, O.W., Bertness, V., Hollis, G.F. and Minna, J.D. L-myc, a new myc-related gene amplified and expressed in human small cell lung cancer. *Nature* 318, 69-73 (1985).

Nesbit, C.E., Tersak, J.M. and Prochownik, E.V. MYC oncogenes and human neoplastic disease. *Oncogene* 18, 3004-3016 (1999).

Ngo, C.V., Gee, M., Akhtar, N., Yu, D., Volpert, O., Auerbach, R. and Thomas-Tikhonenko, A. An in vivo function for the transforming Myc protein: elicitation of the angiogenic phenotype. *Cell Growth Differ* 11, 201-210 (2000).

Nguyen, L., Besson, A., Heng, J.I., Schuurmans, C., Teboul, L., Parras, C., Philpott, A., Roberts, J.M. and Guillemot, F. p27kip1 independently promotes neuronal differentiation and migration in the cerebral cortex. *Genes Dev* 20, 1511-1524 (2006).

Nickeleit, I., Zender, S., Sasse, F., Geffers, R., Brandes, G., Sorensen, I., Steinmetz, H., Kubicka, S., Carlomagno, T., Menche, D*., et al.* Argyrin a reveals a critical role for the tumor suppressor protein p27(kip1) in mediating antitumor activities in response to proteasome inhibition. *Cancer Cell* 14, 23-35 (2008).

Nie, Z., Hu, G., Wei, G., Cui, K., Yamane, A., Resch, W., Wang, R., Green, D.R., Tessarollo, L., Casellas, R*., et al.* c-Myc is a universal amplifier of expressed genes in lymphocytes and embryonic stem cells. *Cell* 151, 68-79 (2012).

Nurse, P. Genetic control of cell size at cell division in yeast. *Nature* 256, 547-551 (1975).

O'Donnell, K.A., Wentzel, E.A., Zeller, K.I., Dang, C.V. and Mendell, J.T. c-Myc-regulated microRNAs modulate E2F1 expression. *Nature* 435, 839-843 (2005).

O'Hagan, R.C., Ohh, M., David, G., de Alboran, I.M., Alt, F.W., Kaelin, W.G., Jr. and DePinho, R.A. Myc-enhanced expression of Cul1 promotes ubiquitin-dependent proteolysis and cell cycle progression. *Genes Dev* 14, 2185-2191 (2000).

Obaya, A.J., Kotenko, I., Cole, M.D. and Sedivy, J.M. The proto-oncogene c-myc acts through the cyclin-dependent kinase (Cdk) inhibitor p27(Kip1) to facilitate the activation of Cdk4/6 and early G(1) phase progression. *J Biol Chem* 277, 31263-31269 (2002).

Ogawa, H., Ishiguro, K., Gaubatz, S., Livingston, D.M. and Nakatani, Y. A complex with chromatin modifiers that occupies E2F- and Myc-responsive genes in G0 cells. *Science* 296, 1132-1136 (2002).

Ohtani, K., DeGregori, J. and Nevins, J.R. Regulation of the cyclin E gene by transcription factor E2F1. *Proc Natl Acad Sci U S A* 92, 12146-12150 (1995).

Old, J.B., Kratzat, S., Hoellein, A., Graf, S., Nilsson, J.A., Nilsson, L., Nakayama, K.I., Peschel, C., Cleveland, J.L. and Keller, U.B. Skp2 directs Myc-mediated suppression of p27Kip1 yet has modest effects on Myc-driven lymphomagenesis. *Mol Cancer Res* 8, 353-362 (2010).

Ortega, S., Prieto, I., Odajima, J., Martin, A., Dubus, P., Sotillo, R., Barbero, J.L., Malumbres, M. and Barbacid, M. Cyclin-dependent kinase 2 is essential for meiosis but not for mitotic cell division in mice. *Nat Genet* 35, 25-31 (2003).

Oster, S.K., Mao, D.Y., Kennedy, J. and Penn, L.Z. Functional analysis of the N-terminal domain of the Myc oncoprotein. *Oncogene* 22, 1998-2010 (2003).

Pagano, M., Tam, S.W., Theodoras, A.M., Beer-Romero, P., Del Sal, G., Chau, V., Yew, P.R., Draetta, G.F. and Rolfe, M. Role of the ubiquitin-proteasome pathway in regulating abundance of the cyclin-dependent kinase inhibitor p27. *Science* 269, 682-685 (1995).

Pajic, A., Spitkovsky, D., Christoph, B., Kempkes, B., Schuhmacher, M., Staege, M.S., Brielmeier, M., Ellwart, J., Kohlhuber, F., Bornkamm, G.W.*, et al.* Cell cycle activation by c-myc in a burkitt lymphoma model cell line. *Int J Cancer* 87, 787-793 (2000).

Palmieri, S., Kahn, P. and Graf, T. Quail embryo fibroblasts transformed by four v-myc-containing virus isolates show enhanced proliferation but are non tumorigenic. *Embo J* 2, 2385-2389 (1983).

Parisi, T., Beck, A.R., Rougier, N., McNeil, T., Lucian, L., Werb, Z. and Amati, B. Cyclins E1 and E2 are required for endoreplication in placental trophoblast giant cells. *Embo J* 22, 4794-4803 (2003).

Parker, L.L. and Piwnica-Worms, H. Inactivation of the p34cdc2-cyclin B complex by the human WEE1 tyrosine kinase. *Science* 257, 1955-1957 (1992).

Parker, M.W., Lo Bello, M. and Federici, G. Crystallization of glutathione S-transferase from human placenta. *J Mol Biol* 213, 221-222 (1990).

Patel, J.H., Du, Y., Ard, P.G., Phillips, C., Carella, B., Chen, C.J., Rakowski, C., Chatterjee, C., Lieberman, P.M., Lane, W.S.*, et al.* The c-MYC oncoprotein is a substrate of the acetyltransferases hGCN5/PCAF and TIP60. *Mol Cell Biol* 24, 10826-10834 (2004a).

Patel, J.H., Loboda, A.P., Showe, M.K., Showe, L.C. and McMahon, S.B. Analysis of genomic targets reveals complex functions of MYC. *Nat Rev Cancer* 4, 562-568 (2004b).

Pavletich, N.P. Mechanisms of cyclin-dependent kinase regulation: structures of Cdks, their cyclin activators, and Cip and INK4 inhibitors. *J Mol Biol* 287, 821-828 (1999).

Pear, W.S., Nolan, G.P., Scott, M.L. and Baltimore, D. Production of high-titer helper-free retroviruses by transient transfection. *Proc Natl Acad Sci U S A* 90, 8392-8396 (1993).

Pellegata, N.S., Quintanilla-Martinez, L., Siggelkow, H., Samson, E., Bink, K., Hofler, H., Fend, F., Graw, J. and Atkinson, M.J. Germ-line mutations in p27Kip1 cause a multiple endocrine neoplasia syndrome in rats and humans. *Proc Natl Acad Sci U S A* 103, 15558-15563 (2006).

Penn, L.J., Brooks, M.W., Laufer, E.M. and Land, H. Negative autoregulation of c-myc transcription. *Embo J* 9, 1113-1121 (1990).

Perez-Luna, M., Aguasca, M., Perearnau, A., Serratosa, J., Martinez-Balbas, M., Jesus Pujol, M. and Bachs, O. PCAF regulates the stability of the transcriptional regulator and cyclin-dependent kinase inhibitor p27Kip1. *Nucleic Acids Res* (2012).

Perez-Roger, I., Kim, S.H., Griffiths, B., Sewing, A. and Land, H. Cyclins D1 and D2 mediate myc-induced proliferation via sequestration of p27(Kip1) and p21(Cip1). *Embo J* 18, 5310-5320 (1999).

Perez-Roger, I., Solomon, D.L., Sewing, A. and Land, H. Myc activation of cyclin E/Cdk2 kinase involves induction of cyclin E gene transcription and inhibition of p27(Kip1) binding to newly formed complexes. *Oncogene* 14, 2373-2381 (1997).

Persson, H., Hennighausen, L., Taub, R., DeGrado, W. and Leder, P. Antibodies to human c-myc oncogene product: evidence of an evolutionarily conserved protein induced during cell proliferation. *Science* 225, 687-693 (1984).

Petroski, M.D. and Deshaies, R.J. Function and regulation of cullin-RING ubiquitin ligases. *Nat Rev Mol Cell Biol* 6, 9-20 (2005).

Philipp-Staheli, J., Payne, S.R. and Kemp, C.J. p27(Kip1): regulation and function of a haploinsufficient tumor suppressor and its misregulation in cancer. *Exp Cell Res* 264, 148-168 (2001).

Pickart, C.M. Mechanisms underlying ubiquitination. *Annu Rev Biochem* 70, 503-533 (2001).

Pickart, C.M. Back to the future with ubiquitin. *Cell* 116, 181-190 (2004).

Pickart, C.M. and Cohen, R.E. Proteasomes and their kin: proteases in the machine age. *Nat Rev Mol Cell Biol* 5, 177-187 (2004).

Pietenpol, J.A., Bohlander, S.K., Sato, Y., Papadopoulos, N., Liu, B., Friedman, C., Trask, B.J., Roberts, J.M., Kinzler, K.W., Rowley, J.D*., et al.* Assignment of the human p27Kip1 gene to 12p13 and its analysis in leukemias. *Cancer Res* 55, 1206-1210 (1995).

Pines, J. and Hunter, T. Isolation of a human cyclin cDNA: evidence for cyclin mRNA and protein regulation in the cell cycle and for interaction with p34cdc2. *Cell* 58, 833-846 (1989).

Pines, J. and Hunter, T. Human cyclin A is adenovirus E1A-associated protein p60 and behaves differently from cyclin B. *Nature* 346, 760-763 (1990).

Pippa, R., Espinosa, L., Gundem, G., Garcia-Escudero, R., Dominguez, A., Orlando, S., Gallastegui, E., Saiz, C., Besson, A., Pujol, M.J*., et al.* p27(Kip1) represses transcription by direct interaction with p130/E2F4 at the promoters of target genes. *Oncogene* (2011).

Planas-Silva, M.D. and Weinberg, R.A. The restriction point and control of cell proliferation. *Curr Opin Cell Biol* 9, 768-772 (1997).

Polyak, K., Kato, J.Y., Solomon, M.J., Sherr, C.J., Massague, J., Roberts, J.M. and Koff, A. p27Kip1, a cyclin-Cdk inhibitor, links transforming growth factor-beta and contact inhibition to cell cycle arrest. *Genes Dev* 8, 9-22 (1994a).

Polyak, K., Lee, M.H., Erdjument-Bromage, H., Koff, A., Roberts, J.M., Tempst, P. and Massague, J. Cloning of p27Kip1, a cyclin-dependent kinase inhibitor and a potential mediator of extracellular antimitogenic signals. *Cell* 78, 59-66 (1994b).

Pomerantz, M.M., Ahmadiyeh, N., Jia, L., Herman, P., Verzi, M.P., Doddapaneni, H., Beckwith, C.A., Chan, J.A., Hills, A., Davis, M*., et al.* The 8q24 cancer risk variant rs6983267 shows long-range interaction with MYC in colorectal cancer. *Nat Genet* 41, 882-884 (2009).

Ponce-Castaneda, M.V., Lee, M.H., Latres, E., Polyak, K., Lacombe, L., Montgomery, K., Mathew, S., Krauter, K., Sheinfeld, J., Massague, J*., et al.* p27Kip1: chromosomal mapping to 12p12-12p13.1 and absence of mutations in human tumors. *Cancer Res* 55, 1211-1214 (1995).

Poon, R.Y. and Hunter, T. Dephosphorylation of Cdk2 Thr160 by the cyclin-dependent kinase-interacting phosphatase KAP in the absence of cyclin. *Science* 270, 90-93 (1995).

Poon, R.Y., Toyoshima, H. and Hunter, T. Redistribution of the CDK inhibitor p27 between different cyclin.CDK complexes in the mouse fibroblast cell cycle and in cells arrested with lovastatin or ultraviolet irradiation. *Mol Biol Cell* 6, 1197-1213 (1995).

Popov, N., Schulein, C., Jaenicke, L.A. and Eilers, M. Ubiquitylation of the amino terminus of Myc by SCF(beta-TrCP) antagonizes SCF(Fbw7)-mediated turnover. *Nat Cell Biol* 12, 973-981 (2010).

Popov, N., Wanzel, M., Madiredjo, M., Zhang, D., Beijersbergen, R., Bernards, R., Moll, R., Elledge, S.J. and Eilers, M. The ubiquitin-specific protease USP28 is required for MYC stability. *Nat Cell Biol* 9, 765-774 (2007).

Post, S.M., Quintas-Cardama, A., Terzian, T., Smith, C., Eischen, C.M. and Lozano, G. p53-dependent senescence delays Emu-myc-induced B-cell lymphomagenesis. *Oncogene* 29, 1260-1269 (2010).

Prendergast, G.C., Lawe, D. and Ziff, E.B. Association of Myn, the murine homolog of max, with c-Myc stimulates methylation-sensitive DNA binding and ras cotransformation. *Cell* 65, 395-407 (1991).

Prendergast, G.C. and Ziff, E.B. DNA-binding motif. *Nature* 341, 392 (1989).

Price, D.H. Regulation of RNA polymerase II elongation by c-Myc. *Cell* 141, 399-400 (2010).

Prochownik, E.V. c-Myc: linking transformation and genomic instability. *Curr Mol Med* 8, 446-458 (2008).

Prochownik, E.V. and Kukowska, J. Deregulated expression of c-myc by murine erythroleukaemia cells prevents differentiation. *Nature* 322, 848-850 (1986).

Prouty, S.M., Hanson, K.D., Boyle, A.L., Brown, J.R., Shichiri, M., Follansbee, M.R., Kang, W. and Sedivy, J.M. A cell culture model system for genetic analyses of the cell cycle by targeted homologous recombination. *Oncogene* 8, 899-907 (1993).

Qi, Y., Tu, Y., Yang, D., Chen, Q., Xiao, J., Chen, Y., Fu, J., Xiao, X. and Zhou, Z. Cyclin A but not cyclin D1 is essential for c-myc-modulated cell-cycle progression. *J Cell Physiol* 210, 63-71 (2007).

Rabbitts, P.H., Watson, J.V., Lamond, A., Forster, A., Stinson, M.A., Evan, G., Fischer, W., Atherton, E., Sheppard, R. and Rabbitts, T.H. Metabolism of c-myc gene products: c-myc mRNA and protein expression in the cell cycle. *Embo J* 4, 2009-2015 (1985).

Rahl, P.B., Lin, C.Y., Seila, A.C., Flynn, R.A., McCuine, S., Burge, C.B., Sharp, P.A. and Young, R.A. c-Myc regulates transcriptional pause release. *Cell* 141, 432-445 (2010).

Rane, S.G., Dubus, P., Mettus, R.V., Galbreath, E.J., Boden, G., Reddy, E.P. and Barbacid, M. Loss of Cdk4 expression causes insulin-deficient diabetes and Cdk4 activation results in beta-islet cell hyperplasia. *Nat Genet* 22, 44-52 (1999).

Ravid, T. and Hochstrasser, M. Diversity of degradation signals in the ubiquitin-proteasome system. *Nat Rev Mol Cell Biol* 9, 679-690 (2008).

Ray, A., James, M.K., Larochelle, S., Fisher, R.P. and Blain, S.W. p27Kip1 inhibits cyclin D-cyclin-dependent kinase 4 by two independent modes. *Mol Cell Biol* 29, 986-999 (2009).

Reavie, L., Della Gatta, G., Crusio, K., Aranda-Orgilles, B., Buckley, S.M., Thompson, B., Lee, E., Gao, J., Bredemeyer, A.L., Helmink, B.A*., et al.* Regulation of hematopoietic stem cell differentiation by a single ubiquitin ligase-substrate complex. *Nat Immunol* 11, 207-215 (2010).

Reichert, M., Saur, D., Hamacher, R., Schmid, R.M. and Schneider, G. Phosphoinositide-3-kinase signaling controls S-phase kinase-associated protein 2 transcription via E2F1 in pancreatic ductal adenocarcinoma cells. *Cancer Res* 67, 4149-4156 (2007).

Reisman, D., Glaros, S. and Thompson, E.A. The SWI/SNF complex and cancer. *Oncogene* 28, 1653-1668 (2009).

Reynisdottir, I. and Massague, J. The subcellular locations of p15(Ink4b) and p27(Kip1) coordinate their inhibitory interactions with cdk4 and cdk2. *Genes Dev* 11, 492-503 (1997).

Riabowol, K., Draetta, G., Brizuela, L., Vandre, D. and Beach, D. The cdc2 kinase is a nuclear protein that is essential for mitosis in mammalian cells. *Cell* 57, 393-401 (1989).

Rodier, G., Coulombe, P., Tanguay, P.L., Boutonnet, C. and Meloche, S. Phosphorylation of Skp2 regulated by CDK2 and Cdc14B protects it from degradation by APC(Cdh1) in G1 phase. *Embo J* 27, 679-691 (2008).

Rodier, G., Montagnoli, A., Di Marcotullio, L., Coulombe, P., Draetta, G.F., Pagano, M. and Meloche, S. p27 cytoplasmic localization is regulated by phosphorylation on Ser10 and is not a prerequisite for its proteolysis. *Embo J* 20, 6672-6682 (2001).

Rotin, D. and Kumar, S. Physiological functions of the HECT family of ubiquitin ligases. *Nat Rev Mol Cell Biol* 10, 398-409 (2009).

Rots, N.Y., Iavarone, A., Bromleigh, V. and Freedman, L.P. Induced differentiation of U937 cells by 1,25-dihydroxyvitamin D3 involves cell cycle arrest in G1 that is preceded by a transient proliferative burst and an increase in cyclin expression. *Blood* 93, 2721-2729 (1999).

Ruddell, A., Mezquita, P., Brandvold, K.A., Farr, A. and Iritani, B.M. B lymphocyte-specific c-Myc expression stimulates early and functional expansion of the vasculature and lymphatics during lymphomagenesis. *Am J Pathol* 163, 2233-2245 (2003).

Russo, A.A., Jeffrey, P.D., Patten, A.K., Massague, J. and Pavletich, N.P. Crystal structure of the p27Kip1 cyclin-dependent-kinase inhibitor bound to the cyclin A-Cdk2 complex. *Nature* 382, 325-331 (1996a).

Russo, A.A., Jeffrey, P.D. and Pavletich, N.P. Structural basis of cyclin-dependent kinase activation by phosphorylation. *Nat Struct Biol* 3, 696-700 (1996b).

Sachdeva, M., Zhu, S., Wu, F., Wu, H., Walia, V., Kumar, S., Elble, R., Watabe, K. and Mo, Y.Y. p53 represses c-Myc through induction of the tumor suppressor miR-145. *Proc Natl Acad Sci U S A* 106, 3207-3212 (2009).

Saigusa, K., Hashimoto, N., Tsuda, H., Yokoi, S., Maruno, M., Yoshimine, T., Aoyagi, M., Ohno, K., Imoto, I. and Inazawa, J. Overexpressed Skp2 within 5p amplification detected by array-based comparative genomic hybridization is associated with poor prognosis of glioblastomas. *Cancer Sci* 96, 676-683 (2005).

Sakamuro, D., Eviner, V., Elliott, K.J., Showe, L., White, E. and Prendergast, G.C. c-Myc induces apoptosis in epithelial cells by both p53-dependent and p53-independent mechanisms. *Oncogene* 11, 2411-2418 (1995).

Samanta, A.K., Lin, H., Sun, T., Kantarjian, H. and Arlinghaus, R.B. Janus kinase 2: a critical target in chronic myelogenous leukemia. *Cancer Res* 66, 6468-6472 (2006).

Santamaria, D., Barriere, C., Cerqueira, A., Hunt, S., Tardy, C., Newton, K., Caceres, J.F., Dubus, P., Malumbres, M. and Barbacid, M. Cdk1 is sufficient to drive the mammalian cell cycle. *Nature* 448, 811-815 (2007).

Sarmento, L.M., Huang, H., Limon, A., Gordon, W., Fernandes, J., Tavares, M.J., Miele, L., Cardoso, A.A., Classon, M. and Carlesso, N. Notch1 modulates timing of G1-S progression by inducing SKP2 transcription and p27 Kip1 degradation. *J Exp Med* 202, 157-168 (2005).

Satyanarayana, A., Berthet, C., Lopez-Molina, J., Coppola, V., Tessarollo, L. and Kaldis, P. Genetic substitution of Cdk1 by Cdk2 leads to embryonic lethality and loss of meiotic function of Cdk2. *Development* 135, 3389-3400 (2008).

Satyanarayana, A. and Kaldis, P. Mammalian cell-cycle regulation: several Cdks, numerous cyclins and diverse compensatory mechanisms. *Oncogene* 28, 2925-2939 (2009).

Schlesinger, D.H. and Goldstein, G. Molecular conservation of 74 amino acid sequence of ubiquitin between cattle and man. *Nature* 255, 42304 (1975).

Schneider, G., Saur, D., Siveke, J.T., Fritsch, R., Greten, F.R. and Schmid, R.M. IKKalpha controls p52/RelB at the skp2 gene promoter to regulate G1- to S-phase progression. *Embo J* 25, 3801-3812 (2006).

Schuhmacher, M., Staege, M.S., Pajic, A., Polack, A., Weidle, U.H., Bornkamm, G.W., Eick, D. and Kohlhuber, F. Control of cell growth by c-Myc in the absence of cell division. *Curr Biol* 9, 1255-1258 (1999).

Schulman, B.A., Carrano, A.C., Jeffrey, P.D., Bowen, Z., Kinnucan, E.R., Finnin, M.S., Elledge, S.J., Harper, J.W., Pagano, M. and Pavletich, N.P. Insights into SCF ubiquitin ligases from the structure of the Skp1-Skp2 complex. *Nature* 408, 381-386 (2000).

Schwab, M., Alitalo, K., Klempnauer, K.H., Varmus, H.E., Bishop, J.M., Gilbert, F., Brodeur, G., Goldstein, M. and Trent, J. Amplified DNA with limited homology to myc cellular oncogene is shared by human neuroblastoma cell lines and a neuroblastoma tumour. *Nature* 305, 245-248. (1983).

Sears, R., Nuckolls, F., Haura, E., Taya, Y., Tamai, K. and Nevins, J.R. Multiple Ras-dependent phosphorylation pathways regulate Myc protein stability. *Genes Dev* 14, 2501-2514 (2000).

Sears, R., Ohtani, K. and Nevins, J.R. Identification of positively and negatively acting elements regulating expression of the E2F2 gene in response to cell growth signals. *Mol Cell Biol* 17, 5227-5235 (1997).

Sears, R.C. The life cycle of C-myc: from synthesis to degradation. *Cell Cycle* 3, 1133-1137 (2004).

Secombe, J. and Eisenman, R.N. The function and regulation of the JARID1 family of histone H3 lysine 4 demethylases: the Myc connection. *Cell Cycle* 6, 1324-1328 (2007).

Secombe, J., Li, L., Carlos, L. and Eisenman, R.N. The Trithorax group protein Lid is a trimethyl histone H3K4 demethylase required for dMyc-induced cell growth. *Genes Dev* 21, 537-551 (2007).

Sedivy, J.M. Can ends justify the means?: telomeres and the mechanisms of replicative senescence and immortalization in mammalian cells. *Proc Natl Acad Sci U S A* 95, 9078-9081 (1998).

Seitz, V., Butzhammer, P., Hirsch, B., Hecht, J., Gutgemann, I., Ehlers, A., Lenze, D., Oker, E., Sommerfeld, A., von der Wall, E*., et al.* Deep sequencing of MYC DNA-binding sites in Burkitt lymphoma. *PLoS One* 6, e26837 (2011).

Sekimoto, T., Fukumoto, M. and Yoneda, Y. 14-3-3 suppresses the nuclear localization of threonine 157-phosphorylated p27(Kip1). *Embo J* 23, 1934-1942 (2004).

Seoane, J., Pouponnot, C., Staller, P., Schader, M., Eilers, M. and Massague, J. TGFbeta influences Myc, Miz-1 and Smad to control the CDK inhibitor p15INK4b. *Nat Cell Biol* 3, 400-408 (2001).

Shao, Z., Zhang, Y., Yuan, G.C., Orkin, S.H. and Waxman, D.J. MAnorm: a robust model for quantitative comparison of ChIP-Seq data sets. *Genome Biol* 13, R16 (2012).

Shchors, K., Shchors, E., Rostker, F., Lawlor, E.R., Brown-Swigart, L. and Evan, G.I. The Myc-dependent angiogenic switch in tumors is mediated by interleukin 1beta. *Genes Dev* 20, 2527-2538 (2006).

Sheaff, R.J., Groudine, M., Gordon, M., Roberts, J.M. and Clurman, B.E. Cyclin E-CDK2 is a regulator of p27Kip1. *Genes Dev* 11, 1464-1478 (1997).

Sheiness, D. and Bishop, J.M. DNA and RNA from uninfected vertebrate cells contain nucleotide sequences related to the putative transforming gene of avian myelocytomatosis virus. *J Virol* 31, 514-521 (1979).

Sherr, C.J. D-type cyclins. *Trends Biochem Sci* 20, 187-190 (1995).

Sherr, C.J. and Roberts, J.M. CDK inhibitors: positive and negative regulators of G1-phase progression. *Genes Dev* 13, 1501-1512 (1999).

Sherr, C.J. and Roberts, J.M. Living with or without cyclins and cyclin-dependent kinases. *Genes Dev* 18, 2699-2711 (2004).

Shi, Y., Glynn, J.M., Guilbert, L.J., Cotter, T.G., Bissonnette, R.P. and Green, D.R. Role for c-myc in activation-induced apoptotic cell death in T cell hybridomas. *Science* 257, 212-214 (1992).

Shim, E.H., Johnson, L., Noh, H.L., Kim, Y.J., Sun, H., Zeiss, C. and Zhang, H. Expression of the F-box protein SKP2 induces hyperplasia, dysplasia, and low-grade carcinoma in the mouse prostate. *Cancer Res* 63, 1583-1588 (2003).

Shim, H., Dolde, C., Lewis, B.C., Wu, C.S., Dang, G., Jungmann, R.A., Dalla-Favera, R. and Dang, C.V. c-Myc transactivation of LDH-A: implications for tumor metabolism and growth. *Proc Natl Acad Sci U S A* 94, 6658-6663 (1997).

Shin, I., Yakes, F.M., Rojo, F., Shin, N.Y., Bakin, A.V., Baselga, J. and Arteaga, C.L. PKB/Akt mediates cell-cycle progression by phosphorylation of p27(Kip1) at threonine 157 and modulation of its cellular localization. *Nat Med* 8, 1145-1152 (2002).

Signoretti, S., Di Marcotullio, L., Richardson, A., Ramaswamy, S., Isaac, B., Rue, M., Monti, F., Loda, M. and Pagano, M. Oncogenic role of the ubiquitin ligase subunit Skp2 in human breast cancer. *J Clin Invest* 110, 633-641 (2002).

Sistrunk, C., Macias, E., Nakayama, K., Kim, Y. and Rodriguez-Puebla, M.L. Skp2 is necessary for Myc-induced keratinocyte proliferation but dispensable for Myc oncogenic activity in the oral epithelium. *Am J Pathol* 178, 2470-2477 (2011).

Sivakolundu, S.G., Bashford, D. and Kriwacki, R.W. Disordered p27Kip1 exhibits intrinsic structure resembling the Cdk2/cyclin A-bound conformation. *J Mol Biol* 353, 1118-1128 (2005).

Skaar, J.R., D'Angiolella, V., Pagan, J.K. and Pagano, M. SnapShot: F Box Proteins II. *Cell* 137, 1358, 1358 e1351 (2009).

Slingerland, J. and Pagano, M. Regulation of the cdk inhibitor p27 and its deregulation in cancer. *J Cell Physiol* 183, 10-17 (2000).

Slingerland, J.M., Hengst, L., Pan, C.H., Alexander, D., Stampfer, M.R. and Reed, S.I. A novel inhibitor of cyclin-Cdk activity detected in transforming growth factor beta-arrested epithelial cells. *Mol Cell Biol* 14, 3683-3694 (1994).

Solomon, M.J., Glotzer, M., Lee, T.H., Philippe, M. and Kirschner, M.W. Cyclin activation of p34cdc2. *Cell* 63, 1013-1024 (1990).

Song, L.B., Li, J., Liao, W.T., Feng, Y., Yu, C.P., Hu, L.J., Kong, Q.L., Xu, L.H., Zhang, X., Liu, W.L.*, et al.* The polycomb group protein Bmi-1 represses the tumor suppressor PTEN and induces epithelial-mesenchymal transition in human nasopharyngeal epithelial cells. *J Clin Invest* 119, 3626-3636 (2009).

Soos, T.J., Kiyokawa, H., Yan, J.S., Rubin, M.S., Giordano, A., DeBlasio, A., Bottega, S., Wong, B., Mendelsohn, J. and Koff, A. Formation of p27-CDK complexes during the human mitotic cell cycle. *Cell Growth Differ* 7, 135-146 (1996).

Sotelo, J., Esposito, D., Duhagon, M.A., Banfield, K., Mehalko, J., Liao, H., Stephens, R.M., Harris, T.J., Munroe, D.J. and Wu, X. Long-range enhancers on 8q24 regulate c-Myc. *Proc Natl Acad Sci U S A* 107, 3001-3005 (2010).

Spotts, G.D., Patel, S.V., Xiao, Q. and Hann, S.R. Identification of downstream-initiated c-Myc proteins which are dominant-negative inhibitors of transactivation by full-length c-Myc proteins. *Mol Cell Biol* 17, 1459-1468 (1997).

Spruck, C., Strohmaier, H., Watson, M., Smith, A.P., Ryan, A., Krek, T.W. and Reed, S.I. A CDK-independent function of mammalian Cks1: targeting of SCF(Skp2) to the CDK inhibitor p27Kip1. *Mol Cell* 7, 639-650 (2001).

Staege, M.S., Lee, S.P., Frisan, T., Mautner, J., Scholz, S., Pajic, A., Rickinson, A.B., Masucci, M.G., Polack, A. and Bornkamm, G.W. MYC overexpression imposes a nonimmunogenic phenotype on Epstein-Barr virus-infected B cells. *Proc Natl Acad Sci U S A* 99, 4550-4555 (2002).

Staller, P., Peukert, K., Kiermaier, A., Seoane, J., Lukas, J., Karsunky, H., Moroy, T., Bartek, J., Massague, J., Hanel, F.*, et al.* Repression of p15INK4b expression by Myc through association with Miz-1. *Nat Cell Biol* 3, 392-399 (2001).

Steiner, P., Philipp, A., Lukas, J., Godden-Kent, D., Pagano, M., Mittnacht, S., Bartek, J. and Eilers, M. Identification of a Myc-dependent step during the formation of active G1 cyclin-cdk complexes. *Embo J* 14, 4814-4826 (1995).

Steinman, R.A. Cell cycle regulators and hematopoiesis. *Oncogene* 21, 3403-3413 (2002).

Steward, M.M., Lee, J.S., O'Donovan, A., Wyatt, M., Bernstein, B.E. and Shilatifard, A. Molecular regulation of H3K4 trimethylation by ASH2L, a shared subunit of MLL complexes. *Nat Struct Mol Biol* 13, 852-854 (2006).

Stone, J., de Lange, T., Ramsay, G., Jakobovits, E., Bishop, J.M., Varmus, H. and Lee, W. Definition of regions in human c-myc that are involved in transformation and nuclear localization. *Mol Cell Biol* 7, 1697-1709 (1987).

Strausfeld, U., Labbe, J.C., Fesquet, D., Cavadore, J.C., Picard, A., Sadhu, K., Russell, P. and Doree, M. Dephosphorylation and activation of a p34cdc2/cyclin B complex in vitro by human CDC25 protein. *Nature* 351, 242-245 (1991).

Sun, J., Marx, S.O., Chen, H.J., Poon, M., Marks, A.R. and Rabbani, L.E. Role for p27(Kip1) in Vascular Smooth Muscle Cell Migration. *Circulation* 103, 2967-2972 (2001).

Sutterluty, H., Chatelain, E., Marti, A., Wirbelauer, C., Senften, M., Muller, U. and Krek, W. p45SKP2 promotes p27Kip1 degradation and induces S phase in quiescent cells. *Nat Cell Biol* 1, 207-214 (1999).

Sweeney, C., Murphy, M., Kubelka, M., Ravnik, S.E., Hawkins, C.F., Wolgemuth, D.J. and Carrington, M. A distinct cyclin A is expressed in germ cells in the mouse. *Development* 122, 53-64 (1996).

Takahashi, K. and Yamanaka, S. Induction of pluripotent stem cells from mouse embryonic and adult fibroblast cultures by defined factors. *Cell* 126, 663-676 (2006).

Takeuchi, S., Bartram, C.R., Wada, M., Reiter, A., Hatta, Y., Seriu, T., Lee, E., Miller, C.W., Miyoshi, I. and Koeffler, H.P. Allelotype analysis of childhood acute lymphoblastic leukemia. *Cancer Res* 55, 5377-5382 (1995).

Tamir, A., Petrocelli, T., Stetler, K., Chu, W., Howard, J., Croix, B.S., Slingerland, J. and Ben-David, Y. Stem cell factor inhibits erythroid differentiation by modulating the activity of G1-cyclin-dependent kinase complexes: a role for p27 in erythroid differentiation coupled G1 arrest. *Cell Growth Differ* 11, 269-277 (2000).

Taniguchi, T., Endo, H., Chikatsu, N., Uchimaru, K., Asano, S., Fujita, T., Nakahata, T. and Motokura, T. Expression of p21(Cip1/Waf1/Sdi1) and p27(Kip1) cyclin-dependent kinase inhibitors during human hematopoiesis. *Blood* 93, 4167-4178 (1999).

Tao, H. and Umek, R.M. Reciprocal regulation of gadd45 by C/EBP alpha and c-Myc. *DNA Cell Biol* 18, 75-84 (1999).

Taub, R., Kirsch, I., Morton, C., Lenoir, G., Swan, D., Tronick, S., Aaronson, S. and Leder, P. Translocation of the c-myc gene into the immunoglobulin heavy chain locus in human Burkitt lymphoma and murine plasmacytoma cells. *Proc Natl Acad Sci U S A* 79, 7837-7841 (1982).

Taules, M., Rodriguez-Vilarrupla, A., Rius, E., Estanyol, J.M., Casanovas, O., Sacks, D.B., Perez-Paya, E., Bachs, O. and Agell, N. Calmodulin binds to p21(Cip1) and is involved in the regulation of its nuclear localization. *J Biol Chem* 274, 24445-24448 (1999).

Tedesco, D., Lukas, J. and Reed, S.I. The pRb-related protein p130 is regulated by phosphorylation-dependent proteolysis via the protein-ubiquitin ligase SCF(Skp2). *Genes Dev* 16, 2946-2957 (2002).

Thompson, C.B., Challoner, P.B., Neiman, P.E. and Groudine, M. Levels of c-myc oncogene mRNA are invariant throughout the cell cycle. *Nature* 314, 363-366 (1985).

Tie, F., Banerjee, R., Conrad, P.A., Scacheri, P.C. and Harte, P.J. Histone demethylase UTX and chromatin remodeler BRM bind directly to CBP and modulate acetylation of histone H3 lysine 27. *Mol Cell Biol* 32, 2323-2334 (2012).

Tie, F., Banerjee, R., Stratton, C.A., Prasad-Sinha, J., Stepanik, V., Zlobin, A., Diaz, M.O., Scacheri, P.C. and Harte, P.J. CBP-mediated acetylation of histone H3 lysine 27 antagonizes Drosophila Polycomb silencing. *Development* 136, 3131-3141 (2009).

Tomoda, K., Kubota, Y., Arata, Y., Mori, S., Maeda, M., Tanaka, T., Yoshida, M., Yoneda-Kato, N. and Kato, J.Y. The cytoplasmic shuttling and subsequent degradation of p27Kip1 mediated by Jab1/CSN5 and the COP9 signalosome complex. *J Biol Chem* 277, 2302-2310 (2002).

Tomoda, K., Kubota, Y. and Kato, J. Degradation of the cyclin-dependent-kinase inhibitor p27Kip1 is instigated by Jab1. *Nature* 398, 160-165 (1999).

Torrano, V., Chernukhin, I., Docquier, F., D'Arcy, V., Leon, J., Klenova, E. and Delgado, M.D. CTCF regulates growth and erythroid differentiation of human myeloid leukemia cells. *J Biol Chem* 280, 28152-28161 (2005).

Toyoshima, H. and Hunter, T. p27, a novel inhibitor of G1 cyclin-Cdk protein kinase activity, is related to p21. *Cell* 78, 67-74 (1994).

Trotman, L.C., Alimonti, A., Scaglioni, P.P., Koutcher, J.A., Cordon-Cardo, C. and Pandolfi, P.P. Identification of a tumour suppressor network opposing nuclear Akt function. *Nature* 441, 523-527 (2006).

Tsai, L.H., Harlow, E. and Meyerson, M. Isolation of the human cdk2 gene that encodes the cyclin A- and adenovirus E1A-associated p33 kinase. *Nature* 353, 174-177 (1991).

Tsukiyama, T., Ishida, N., Shirane, M., Minamishima, Y.A., Hatakeyama, S., Kitagawa, M., Nakayama, K. and Nakayama, K. Down-regulation of p27Kip1 expression is required for development and function of T cells. *J Immunol* 166, 304-312 (2001).

Tsutsui, T., Hesabi, B., Moons, D.S., Pandolfi, P.P., Hansel, K.S., Koff, A. and Kiyokawa, H. Targeted disruption of CDK4 delays cell cycle entry with enhanced p27(Kip1) activity. *Mol Cell Biol* 19, 7011-7019 (1999).

Tsvetkov, L.M., Yeh, K.H., Lee, S.J., Sun, H. and Zhang, H. p27(Kip1) ubiquitination and degradation is regulated by the SCF(Skp2) complex through phosphorylated Thr187 in p27. *Curr Biol* 9, 661-664 (1999).

Tuupanen, S., Turunen, M., Lehtonen, R., Hallikas, O., Vanharanta, S., Kivioja, T., Bjorklund, M., Wei, G., Yan, J., Niittymaki, I.*, et al.* The common colorectal cancer predisposition SNP rs6983267 at chromosome 8q24 confers potential to enhanced Wnt signaling. *Nat Genet* 41, 885-890 (2009).

Vafa, O., Wade, M., Kern, S., Beeche, M., Pandita, T.K., Hampton, G.M. and Wahl, G.M. c-Myc can induce DNA damage, increase reactive oxygen species, and mitigate p53 function: a mechanism for oncogene-induced genetic instability. *Mol Cell* 9, 1031-1044 (2002).

van der Meer, T., Chan, W.Y., Palazon, L.S., Nieduszynski, C., Murphy, M., Sobczak-Thepot, J., Carrington, M. and Colledge, W.H. Cyclin A1 protein shows haplo-insufficiency for normal fertility in male mice. *Reproduction* 127, 503-511 (2004).

van Riggelen, J., Yetil, A. and Felsher, D.W. MYC as a regulator of ribosome biogenesis and protein synthesis. *Nat Rev Cancer* 10, 301-309 (2010).

Vennstrom, B., Sheiness, D., Zabielski, J. and Bishop, J.M. Isolation and characterization of c-myc, a cellular homolog of the oncogene (v-myc) of avian myelocytomatosis virus strain 29. *J Virol* 42, 773-779 (1982).

Vervoorts, J., Luscher-Firzlaff, J. and Luscher, B. The ins and outs of MYC regulation by posttranslational mechanisms. *J Biol Chem* 281, 34725-34729 (2006).

Vervoorts, J., Luscher-Firzlaff, J.M., Rottmann, S., Lilischkis, R., Walsemann, G., Dohmann, K., Austen, M. and Luscher, B. Stimulation of c-MYC transcriptional activity and acetylation by recruitment of the cofactor CBP. *EMBO Rep* 4, 484-490 (2003).

Viglietto, G., Motti, M.L., Bruni, P., Melillo, R.M., D'Alessio, A., Califano, D., Vinci, F., Chiappetta, G., Tsichlis, P., Bellacosa, A.*, et al.* Cytoplasmic relocalization and inhibition of the cyclin-dependent kinase inhibitor p27(Kip1) by PKB/Akt-mediated phosphorylation in breast cancer. *Nat Med* 8, 1136-1144 (2002).

Vlach, J., Hennecke, S., Alevizopoulos, K., Conti, D. and Amati, B. Growth arrest by the cyclin-dependent kinase inhibitor p27Kip1 is abrogated by c-Myc. *Embo J* 15, 6595-6604 (1996).

Vlach, J., Hennecke, S. and Amati, B. Phosphorylation-dependent degradation of the cyclin-dependent kinase inhibitor p27. *Embo J* 16, 5334-5344 (1997).

von der Lehr, N., Johansson, S., Wu, S., Bahram, F., Castell, A., Cetinkaya, C., Hydbring, P., Weidung, I., Nakayama, K., Nakayama, K.I.*, et al.* The F-box protein Skp2 participates in c-Myc proteosomal degradation and acts as a cofactor for c-Myc-regulated transcription. *Mol Cell* 11, 1189-1200 (2003).

Wagner, A.J., Kokontis, J.M. and Hay, N. Myc-mediated apoptosis requires wild-type p53 in a manner independent of cell cycle arrest and the ability of p53 to induce p21waf1/cip1. *Genes Dev* 8, 2817-2830 (1994).

Wang, C., Hou, X., Mohapatra, S., Ma, Y., Cress, W.D., Pledger, W.J. and Chen, J. Activation of p27Kip1 Expression by E2F1. A negative feedback mechanism. *J Biol Chem* 280, 12339-12343 (2005a).

Wang, G., Chan, C.H., Gao, Y. and Lin, H.K. Novel roles of Skp2 E3 ligase in cellular senescence, cancer progression, and metastasis. *Chin J Cancer* (2012a).

Wang, H., Bauzon, F., Ji, P., Xu, X., Sun, D., Locker, J., Sellers, R.S., Nakayama, K., Nakayama, K.I., Cobrinik, D.*, et al.* Skp2 is required for survival of aberrantly proliferating Rb1-deficient cells and for tumorigenesis in Rb1+/- mice. *Nat Genet* 42, 83-88 (2010a).

Wang, I.C., Chen, Y.J., Hughes, D., Petrovic, V., Major, M.L., Park, H.J., Tan, Y., Ackerson, T. and Costa, R.H. Forkhead box M1 regulates the transcriptional network of genes essential for mitotic progression and genes encoding the SCF (Skp2-Cks1) ubiquitin ligase. *Mol Cell Biol* 25, 10875-10894 (2005b).

Wang, R., Dillon, C.P., Shi, L.Z., Milasta, S., Carter, R., Finkelstein, D., McCormick, L.L., Fitzgerald, P., Chi, H., Munger, J.*, et al.* The transcription factor Myc controls metabolic reprogramming upon T lymphocyte activation. *Immunity* 35, 871-882 (2011a).

Wang, S., Raven, J.F. and Koromilas, A.E. STAT1 represses Skp2 gene transcription to promote p27Kip1 stabilization in Ras-transformed cells. *Mol Cancer Res* 8, 798-805 (2010b).

Wang, W., Ungermannova, D., Chen, L. and Liu, X. Molecular and biochemical characterization of the Skp2-Cks1 binding interface. *J Biol Chem* 279, 51362-51369 (2004).

Wang, X., Cunningham, M., Zhang, X., Tokarz, S., Laraway, B., Troxell, M. and Sears, R.C. Phosphorylation regulates c-Myc's oncogenic activity in the mammary gland. *Cancer Res* 71, 925-936 (2011b).

Wang, X., Gorospe, M., Huang, Y. and Holbrook, N.J. p27Kip1 overexpression causes apoptotic death of mammalian cells. *Oncogene* 15, 2991-2997 (1997).

Wang, Z., Fukushima, H., Inuzuka, H., Wan, L., Liu, P., Gao, D., Sarkar, F.H. and Wei, W. Skp2 is a promising therapeutic target in breast cancer. *Front Oncol* 1 (2012b).

Wang, Z., Zang, C., Rosenfeld, J.A., Schones, D.E., Barski, A., Cuddapah, S., Cui, K., Roh, T.Y., Peng, W., Zhang, M.Q.*, et al.* Combinatorial patterns of histone acetylations and methylations in the human genome. *Nat Genet* 40, 897-903 (2008).

Wanzel, M., Herold, S. and Eilers, M. Transcriptional repression by Myc. *Trends Cell Biol* 13, 146-150 (2003).

Warner, B.J., Blain, S.W., Seoane, J. and Massague, J. Myc downregulation by transforming growth factor beta required for activation of the p15(Ink4b) G(1) arrest pathway. *Mol Cell Biol* 19, 5913-5922 (1999).

Wasserman, N.F., Aneas, I. and Nobrega, M.A. An 8q24 gene desert variant associated with prostate cancer risk confers differential in vivo activity to a MYC enhancer. *Genome Res* 20, 1191-1197 (2010).

Watnick, R.S., Cheng, Y.N., Rangarajan, A., Ince, T.A. and Weinberg, R.A. Ras modulates Myc activity to repress thrombospondin-1 expression and increase tumor angiogenesis. *Cancer Cell* 3, 219-231 (2003).

Watson, J.D., Oster, S.K., Shago, M., Khosravi, F. and Penn, L.Z. Identifying genes regulated in a Myc-dependent manner. *J Biol Chem* 277, 36921-36930 (2002).

Wei, W., Ayad, N.G., Wan, Y., Zhang, G.J., Kirschner, M.W. and Kaelin, W.G., Jr. Degradation of the SCF component Skp2 in cell-cycle phase G1 by the anaphase-promoting complex. *Nature* 428, 194-198 (2004).

Weinberg, R.A. The retinoblastoma protein and cell cycle control. *Cell* 81, 323-330 (1995).

Welcker, M., Orian, A., Jin, J., Grim, J.E., Harper, J.W., Eisenman, R.N. and Clurman, B.E. The Fbw7 tumor suppressor regulates glycogen synthase kinase 3 phosphorylation-dependent c-Myc protein degradation. *Proc Natl Acad Sci U S A* 101, 9085-9090 (2004).

Wenzel, A., Cziepluch, C., Hamann, U., Schurmann, J. and Schwab, M. The N-Myc oncoprotein is associated in vivo with the phosphoprotein Max(p20/22) in human neuroblastoma cells. *Embo J* 10, 3703-3712 (1991).

Wierstra, I. and Alves, J. The c-myc promoter: still MysterY and challenge. *Adv Cancer Res* 99, 113-333 (2008).

Wilson, A., Murphy, M.J., Oskarsson, T., Kaloulis, K., Bettess, M.D., Oser, G.M., Pasche, A.C., Knabenhans, C., Macdonald, H.R. and Trumpp, A. c-Myc controls the balance between hematopoietic stem cell self-renewal and differentiation. *Genes Dev* 18, 2747-2763 (2004).

Wirbelauer, C., Sutterluty, H., Blondel, M., Gstaiger, M., Peter, M., Reymond, F. and Krek, W. The F-box protein Skp2 is a ubiquitylation target of a Cul1-based core ubiquitin ligase complex: evidence for a role of Cul1 in the suppression of Skp2 expression in quiescent fibroblasts. *Embo J* 19, 5362-5375 (2000).

Won, K.A., Xiong, Y., Beach, D. and Gilman, M.Z. Growth-regulated expression of D-type cyclin genes in human diploid fibroblasts. *Proc Natl Acad Sci U S A* 89, 9910-9914 (1992).

Wood, M.A., McMahon, S.B. and Cole, M.D. An ATPase/helicase complex is an essential cofactor for oncogenic transformation by c-Myc. *Mol Cell* 5, 321-330 (2000).

Wu, C.H., van Riggelen, J., Yetil, A., Fan, A.C., Bachireddy, P. and Felsher, D.W. Cellular senescence is an important mechanism of tumor regression upon c-Myc inactivation. *Proc Natl Acad Sci U S A* 104, 13028-13033 (2007).

Wu, F.Y., Wang, S.E., Sanders, M.E., Shin, I., Rojo, F., Baselga, J. and Arteaga, C.L. Reduction of cytosolic p27(Kip1) inhibits cancer cell motility, survival, and tumorigenicity. *Cancer Res* 66, 2162-2172 (2006).

Wu, K.J., Grandori, C., Amacker, M., Simon-Vermot, N., Polack, A., Lingner, J. and Dalla-Favera, R. Direct activation of TERT transcription by c-MYC. *Nat Genet* 21, 220-224 (1999).

Wu, S., Cetinkaya, C., Munoz-Alonso, M.J., von der Lehr, N., Bahram, F., Beuger, V., Eilers, M., Leon, J. and Larsson, L.G. Myc represses differentiation-induced p21CIP1 expression via Miz-1-dependent interaction with the p21 core promoter. *Oncogene* 22, 351-360 (2003).

Xiao, Q., Claassen, G., Shi, J., Adachi, S., Sedivy, J. and Hann, S.R. Transactivation-defective c-MycS retains the ability to regulate proliferation and apoptosis. *Genes Dev* 12, 3803-3808 (1998).

Xie, S., Lin, H., Sun, T. and Arlinghaus, R.B. Jak2 is involved in c-Myc induction by Bcr-Abl. *Oncogene* 21, 7137-7146 (2002).

Xiong, Y., Hannon, G.J., Zhang, H., Casso, D., Kobayashi, R. and Beach, D. p21 is a universal inhibitor of cyclin kinases. *Nature* 366, 701-704 (1993).

Xu, D., Popov, N., Hou, M., Wang, Q., Bjorkholm, M., Gruber, A., Menkel, A.R. and Henriksson, M. Switch from Myc/Max to Mad1/Max binding and decrease in histone acetylation at the telomerase reverse transcriptase promoter during differentiation of HL60 cells. *Proc Natl Acad Sci U S A* 98, 3826-3831 (2001).

Yada, M., Hatakeyama, S., Kamura, T., Nishiyama, M., Tsunematsu, R., Imaki, H., Ishida, N., Okumura, F., Nakayama, K. and Nakayama, K.I. Phosphorylation-dependent degradation of c-Myc is mediated by the F-box protein Fbw7. *Embo J* 23, 2116-2125 (2004).

Yang, R., Morosetti, R. and Koeffler, H.P. Characterization of a second human cyclin A that is highly expressed in testis and in several leukemic cell lines. *Cancer Res* 57, 913-920 (1997).

Yang, W., Shen, J., Wu, M., Arsura, M., FitzGerald, M., Suldan, Z., Kim, D.W., Hofmann, C.S., Pianetti, S., Romieu-Mourez, R.*, et al.* Repression of transcription of the p27(Kip1) cyclin-dependent kinase inhibitor gene by c-Myc. *Oncogene* 20, 1688-1702 (2001).

Yin, X.Y., Grove, L., Datta, N.S., Katula, K., Long, M.W. and Prochownik, E.V. Inverse regulation of cyclin B1 by c-Myc and p53 and induction of tetraploidy by cyclin B1 overexpression. *Cancer Res* 61, 6487-6493 (2001).

Yin, X.Y., Grove, L., Datta, N.S., Long, M.W. and Prochownik, E.V. C-myc overexpression and p53 loss cooperate to promote genomic instability. *Oncogene* 18, 1177-1184 (1999).

Yokoi, S., Yasui, K., Iizasa, T., Takahashi, T., Fujisawa, T. and Inazawa, J. Down-regulation of SKP2 induces apoptosis in lung-cancer cells. *Cancer Sci* 94, 344-349 (2003).

Yokoi, S., Yasui, K., Mori, M., Iizasa, T., Fujisawa, T. and Inazawa, J. Amplification and overexpression of SKP2 are associated with metastasis of non-small-cell lung cancers to lymph nodes. *Am J Pathol* 165, 175-180 (2004).

Yu, Z.K., Gervais, J.L. and Zhang, H. Human CUL-1 associates with the SKP1/SKP2 complex and regulates p21(CIP1/WAF1) and cyclin D proteins. *Proc Natl Acad Sci U S A* 95, 11324-11329 (1998).

Yung, Y., Walker, J.L., Roberts, J.M. and Assoian, R.K. A Skp2 autoinduction loop and restriction point control. *J Cell Biol* 178, 741-747 (2007).

Zeller, K.I., Haggerty, T.J., Barrett, J.F., Guo, Q., Wonsey, D.R. and Dang, C.V. Characterization of nucleophosmin (B23) as a Myc target by scanning chromatin immunoprecipitation. *J Biol Chem* 276, 48285-48291 (2001).

Zeller, K.I., Zhao, X., Lee, C.W., Chiu, K.P., Yao, F., Yustein, J.T., Ooi, H.S., Orlov, Y.L., Shahab, A., Yong, H.C.*, et al.* Global mapping of c-Myc binding sites and target gene networks in human B cells. *Proc Natl Acad Sci U S A* 103, 17834-17839 (2006).

Zeng, Y., Hirano, K., Hirano, M., Nishimura, J. and Kanaide, H. Minimal requirements for the nuclear localization of p27(Kip1), a cyclin-dependent kinase inhibitor. *Biochem Biophys Res Commun* 274, 37-42 (2000).

Zhang, H., Fan, S. and Prochownik, E.V. Distinct roles for MAX protein isoforms in proliferation and apoptosis. *J Biol Chem* 272, 17416-17424 (1997).

Zhang, H., Kobayashi, R., Galaktionov, K. and Beach, D. p19Skp1 and p45Skp2 are essential elements of the cyclin A-CDK2 S phase kinase. *Cell* 82, 915-925 (1995).

Zhang, L. and Wang, C. F-box protein Skp2: a novel transcriptional target of E2F. *Oncogene* 25, 2615-2627 (2006).

Zhang, P., Wong, C., DePinho, R.A., Harper, J.W. and Elledge, S.J. Cooperation between the Cdk inhibitors p27(KIP1) and p57(KIP2) in the control of tissue growth and development. *Genes Dev* 12, 3162-3167 (1998).

Zheng, N., Schulman, B.A., Song, L., Miller, J.J., Jeffrey, P.D., Wang, P., Chu, C., Koepp, D.M., Elledge, S.J., Pagano, M.*, et al.* Structure of the Cul1-Rbx1-Skp1-F boxSkp2 SCF ubiquitin ligase complex. *Nature* 416, 703-709 (2002).

Zhu, C.Q., Blackhall, F.H., Pintilie, M., Iyengar, P., Liu, N., Ho, J., Chomiak, T., Lau, D., Winton, T., Shepherd, F.A.*, et al.* Skp2 gene copy number aberrations are common in non-small cell lung carcinoma, and its overexpression in tumors with ras mutation is a poor prognostic marker. *Clin Cancer Res* 10, 1984-1991 (2004a).

Zhu, X.H., Nguyen, H., Halicka, H.D., Traganos, F. and Koff, A. Noncatalytic requirement for cyclin A-cdk2 in p27 turnover. *Mol Cell Biol* 24, 6058-6066 (2004b).

Zindy, F., Eischen, C.M., Randle, D.H., Kamijo, T., Cleveland, J.L., Sherr, C.J. and Roussel, M.F. Myc signaling via the ARF tumor suppressor regulates p53-dependent apoptosis and immortalization. *Genes Dev* 12, 2424-2433 (1998).

Zuo, T., Liu, R., Zhang, H., Chang, X., Liu, Y., Wang, L., Zheng, P. and Liu, Y. FOXP3 is a novel transcriptional repressor for the breast cancer oncogene SKP2. *J Clin Invest* 117, 3765-3773 (2007).

8. RESUMEN EN CASTELLANO

8. RESUMEN EN CASTELLANO

8.1 INTRODUCCIÓN

El ciclo celular es el proceso que permite a una célula eucariota duplicar su contenido genético y posteriormente dividirse en dos células hijas genéticamente idénticas. Este proceso se divide en cuatro fases: G1, S (en la cual la célula replica su genoma), G2 y M (en la cual la célula se divide en dos células hijas) (Morgan, 2007). La correcta progresión a través de las diferentes fases del ciclo celular está finamente regulada por la acción coordinada de diferentes complejos ciclina/CDK (Murray, 2004; Satyanarayana and Kaldis, 2009). Las CDKs o quinasas dependientes de ciclina son las subunidades catalíticas del complejo y forman parte de una gran familia de quinasas de residuos de serina y treonina, las cuales controlan la fosforilación de diferentes sustratos implicados en la progresión de las diferentes fases del ciclo celular (Malumbres*, et al.*, 2009). Las ciclinas, como su propio nombre indica, son proteínas que se sintetizan y se degradan específicamente durante las diferentes fases del ciclo y activan a las CDKs (Malumbres and Barbacid, 2005). La regulación de los complejos ciclina/CDK tiene lugar a varios niveles incluyendo, además de la unión de las ciclinas a sus respectivas CDKs, la activación o inhibición por fosforilación/defosforilación de determinados residuos en las CDKs, la unión a moléculas inhibidoras de CDKs (CKIs) o la degradación de los diferentes elementos (ciclinas y CKIs) por el sistema ubiquitina-proteosoma.

En esta Tesis nos hemos centrado en el inhibidor de CDKs de la familia Cip/Kip $p27^{Kip1}$ (p27 en adelante). Este inhibidor de CDKs se caracteriza por ser una proteína intrínsecamente desestructurada que interactúa con ambos componentes del complejo ciclina/CDK (Bienkiewicz*, et al.*, 2002; Lacy*, et al.*, 2004). p27 presenta en su dominio N-terminal una pequeña hélice $_3$10 que se inserta en el bolsillo catalítico de la CDK, mimetizando al ATP e inhibiendo su actividad quinasa (Russo*, et al.*, 1996; Pavletich, 1999). p27 puede unirse a una amplia variedad de complejos ciclina/CDK, siendo los complejos ciclina E-A/CDK2 su principal diana durante la transición entre las fases G1-S del ciclo celular (Polyak*, et al.*, 1994; Toyoshima and Hunter, 1994; Sherr and Roberts, 1999). p27 se regula principalmente a nivel de estabilidad proteica por el sistema ubiquitina-proteosoma, es decir, la degradación de p27 por el proteosoma está precedida de su ubiquitinación (Pagano*, et al.*, 1995). La ubiquitinación de p27 es mediada principalmente por el complejo ligasa de ubiquitinas SCF^{SKP2}, compuesto por la proteína de andamiaje CUL1 sobre la cual se ensamblan RBX1, que interacciona con la enzima conjugadora de ubiquitinas E2, y la proteína adaptadora SKP1. A la proteína adaptadora se le unen la proteína accesoria CKS1 y la proteína F-box SKP2. La función de las proteínas F-box es la de permitir el reconocimiento del sustrato de manera específica y por tanto, dentro del complejo SCF^{SKP2}, SKP2 se encarga del reconocimiento de p27 (Nakayama and Nakayama, 2005,2006).

SKP2, junto con SKP1 y CKS1, fue descubierta asociada a complejos ciclina A/CDK2, cuya actividad se asocia principalmente a fase S, de aquí su nombre “S-phase kinase associated protein” (Zhang*, et al.*, 1995). SKP2 presenta en su dominio N-terminal un motivo F-box que participa en la unión a SKP1 (Schulman*, et al.*, 2000; Zheng*, et al.*, 2002). En su dominio C-

terminal contiene una serie de repeticiones ricas en Leucina (LRR o "Leucine-rich repeats") que participan en su interacción con los sustratos como p27 (Wang*, et al.*, 2004), pero también con otros reguladores del ciclo celular como la ciclina E, p21, p57 y E2F1 (Nakayama and Nakayama, 2006; Frescas and Pagano, 2008). SKP2 se encuentra frecuentemente sobreexpresada en cáncer humano, en muchos casos asociada con la progresión tumoral. De hecho, SKP2 se comporta como un oncogén en ensayos de transformación (Frescas and Pagano, 2008; Hershko, 2008). La actividad oncogénica de SKP2 se atribuye principalmente a la degradación de p27 (Hershko, 2008). No obstante, el reconocimiento de p27 por parte del complejo SCF^{SKP2} requiere de la fosforilación previa de p27 en la treonina 187 y de su unión a complejos ciclina E-A/CDK2 (Carrano*, et al.*, 1999; Sutterluty*, et al.*, 1999; Tsvetkov*, et al.*, 1999). Son precisamente los complejos ciclina E/CDK2 los que fosforilan a p27 en la treonina 187 durante la transición entre las fases G1 y S, promoviendo su degradación por el sistema ubiquitina-proteosoma (Nakayama and Nakayama, 2006; Jakel*, et al.*, 2012). En consecuencia, los niveles de SKP2 y p27 correlacionan inversamente en muchos modelos celulares y en diversos tipos de cáncer humano, estando asociados los bajos niveles de p27 con un peor pronóstico de la enfermedad (Chu*, et al.*, 2008; Frescas and Pagano, 2008; Hershko, 2008).

c-MYC (MYC en adelante) es un factor de transcripción oncogénico de la familia de los factores de transcripción con dominio básico hélice-lazo-hélice cremallera de leucinas (b-HLH-LZ). A través de su actividad transcripcional, MYC ejerce una gran variedad de funciones biológicas en diferentes modelos celulares relacionadas con la proliferación celular, la inestabilidad genómica, metabolismo energético, la síntesis de proteínas y ribosomas, la comunicación intercelular y el control de la diferenciación celular (Eilers and Eisenman, 2008; Meyer and Penn, 2008; Leon*, et al.*, 2009; Luscher and Vervoorts, 2012). Para ello MYC forma heterodímeros con la proteína MAX, los cuales se unen a cajas E en las regiones reguladoras de los genes diana y recluta a diferentes coactivadores transcripcionales con actividad histona acetil-transferasa (como CBP/p300, GCN5, Tip60, etc.) o histona metil-transferasa (como MLL1) (Bres*, et al.*, 2009; Luscher and Vervoorts, 2012). A su vez MYC interacciona con diferentes elementos de la maquinaria de transcripción basal de la ARN polimerasa II y estimula la elongación del ARNm por esta enzima. De esta forma MYC regula cerca de 1000 genes y se une a un 15% de locis genómicos. La mayoría de genes diana (~60%) son activados por MYC de manera dependiente de cajas E, aunque una fracción importante de los genes diana (el ~40% restante) son reprimidos por MYC (Patel*, et al.*, 2004; Dang*, et al.*, 2006; Zeller*, et al.*, 2006). La expresión de MYC se encuentra desregulada en una amplia gama de cánceres humanos, en muchos casos asociada a la progresión tumoral y peor pronóstico (Nesbit*, et al.*, 1999; Lutz*, et al.*, 2002; Meyer and Penn, 2008).

Existe un antagonismo funcional entre MYC y p27 en la proliferación. Por un lado, MYC y la pérdida de p27 cooperan en modelos animales de carcinogénesis (Martins and Berns, 2002). Por otro lado, MYC inhibe la función de p27 en proliferación a través de diferentes mecanismos. En primer lugar, MYC reprime la expresión de p27 a nivel transcripcional (Yang*, et al.*, 2001; Chandramohan*, et al.*, 2004). En segundo lugar, MYC induce la expresión de ciclina E

directamente o a través de la inducción de E2F aumentando el número y la actividad de complejos ciclina E/CDK2 que fosforilan a p27 en la treonina 187 promoviendo la transición entre la fase G1 y S (Steiner*, et al.*, 1995; Vlach*, et al.*, 1996; Perez-Roger*, et al.*, 1997). Tercero, MYC induce la expresión de ciclina D1 y D2, y de sus parejas catalíticas CDK4 y CDK6, aumentando la cantidad de complejos ciclina D/CDK4-6 que a su vez secuestran a p27 de otros complejos ciclina E/CDK2 aumentando indirectamente la actividad de estos últimos (Soos*, et al.*, 1996; Bouchard*, et al.*, 1999; Perez-Roger*, et al.*, 1999; Obaya*, et al.*, 2002). En cuarto lugar, MYC induce la expresión de CUL1 (O'Hagan*, et al.*, 2000) y CKS1 (Keller*, et al.*, 2007) dos de las subunidades del complejo SCF^{SKP2}. Recientemente se ha observado una correlación entre MYC y la expresión de SKP2 en un modelo de linfoma murino, aunque con efectos modestos en linfomagénesis (Old*, et al.*, 2010). Sin embargo se desconoce el mecanismo de interacción entre MYC y SKP2.

En este trabajo hemos retomado el estudio de este antagonismo funcional entre MYC y p27 en proliferación. Para ello, hemos utilizado como modelo una sublínea celular estable derivada de la línea leucémica humana K562 (Lozzio and Lozzio, 1975) que expresa MYC y p27 de forma condicional (Kp27MER), obtenida en nuestro laboratorio por el Dr. Juan Carlos Acosta (Acosta*, et al.*, 2008). Estas células presentan una copia adicional del gen p27 controlado por el promotor de la metalotioneína de oveja que responde a diferentes concentraciones de Zinc (Zn^{2+}) en el medio de cultivo (entre 0 y 75 µM de $ZnSO_4$ en condiciones no tóxicas). Además las células Kp27MER expresan de forma constitutiva la proteína quimérica MYCER que puede ser activada en presencia de pequeñas dosis (100-200 nM) de 4-hidroxitamoxifeno (4HT) (Littlewood*, et al.*, 1995). La inducción ectópica de altos niveles de p27 mediante la adición de 75 µM $ZnSO_4$ al medio de cultivo (la dosis máxima permitida sin afectar a la viabilidad celular) se traduce en un bloqueo completo de la proliferación y en la acumulación de estas células en fase G1 del ciclo celular. Este fenómeno va acompañado de la inhibición de la actividad quinasa tanto de CDK2 como de CDK4 y CDK6 y de una diferenciación moderada y específica de estas células hacia el linaje eritroide (Acosta*, et al.*, 2008). La activación de MYC con 200 nM de 4HT en estas condiciones no es capaz de revertir la parada proliferativa mediada por los altos niveles de p27 (inducidos por 75 µM $ZnSO_4$), pero si es capaz de contrarrestar la diferenciación mediada por p27 reprimiendo la expresión de varios genes maestros de diferenciación eritroide (Acosta*, et al.*, 2008). Sin embargo, en presencia de niveles moderados de p27 (inducidos por la adición de 50 µM $ZnSO_4$ al medio de cultivo), MYC provoca un aumento en la fracción de células en fase S y un aumento consistente en la proliferación celular. Este efecto de MYC en la proliferación celular puede ser explicado, en parte, por la capacidad de MYC para inducir una reducción en los niveles de p27 a nivel de proteína (Acosta*, et al.*, 2008). En base a estas observaciones, hemos decidido utilizar este modelo como punto de partida para profundizar en el mecanismo molecular mediante el cual MYC induce dicha reducción en los niveles de p27, y que parece determinar su antagonismo en proliferación.

8.2 OBJETIVOS

Existe un antagonismo funcional entre el inhibidor de CDKs p27 y el factor de transcripción oncogénico MYC en proliferación celular y tumorogénesis. Aparte de ser un regulador positivo de ciclinas y CDKs, MYC posee la capacidad de contrarrestar los niveles de p27. Se han propuesto varios mecanismos para explicar la correlación inversa entre MYC y p27 tanto a nivel transcripcional como postranscripcional. Sin embargo algunos de estos mecanismos no han sido reproducidos en otros modelos experimentales o no han sido trasladados al contexto clínico. Por otro lado, en nuestro laboratorio hemos observado que este antagonismo entre MYC y p27 parece ser dependiente de los niveles de expresión de p27.

En el presente estudio nos hemos propuesto profundizar y en su caso encontrar mecanismos moleculares que puedan explicar el antagonismo entre MYC y p27 en diferentes contextos experimentales. Por tanto, nos hemos propuesto los siguientes objetivos:

1. Establecer el mecanismo molecular que determina el antagonismo entre MYC y p27 en proliferación; estudiar su funcionalidad en distintos sistemas celulares, en modelos animales y en cáncer humano.

2. Establecer por qué el efecto de MYC en la proliferación celular es dependiente de los niveles de p27.

8.3 RESULTADOS Y DISCUSIÓN

8.3.1. La interacción MYC-SKP2

Con el fin de determinar el mecanismo molecular que explicara la disminución de los niveles de p27 mediada por MYC en las células Kp27MER y por tanto el antagonismo funcional entre MYC y p27 en proliferación celular, en primer lugar decidimos analizar si alguno de los mecanismos previamente descritos en la literatura podía ser trasladado a nuestro modelo celular Kp27MER. La represión de p27 por MYC fue directamente descartada dado que, en las células Kp27MER, p27 estaba controlado por el promotor de la metalotioneína de oveja que respondía exclusivamente a metales pesados como el Zn^{2+}. Tampoco se encontraron cambios en los niveles proteicos de CUL1 y CKS1 que pudieran explicar la disminución p27. Por lo tanto, estas observaciones sugerían que en nuestro modelo estaba actuando un mecanismo alternativo a los previamente referidos.

Utilizando un estudio de expresión global de ARNm mediante microarrays en células Kp27MER (con el biochip de Affimetryx HG-U133A) llevado a cabo por el Dr. J.C. Acosta en su trabajo de Tesis encontramos que uno de los genes inducidos por MYC en presencia de altos niveles de p27 y por tanto en un contexto de parada proliferativa era SKP2, proteína estrechamente involucrada en la degradación de p27, generalmente asociada con la progresión a través de la fase S y con la proliferación celular. Los resultados fueron confirmados mediante RT-qPCR y Western Blot.

Con el fin de verificar que la inducción de SKP2 no se debía a un efecto indirecto de MYC sobre la proliferación, se estudiaron otros modelos en los cuales podíamos inducir MYC en un contexto de parada proliferativa. Para ello se utilizaron (i) células KMER (células K562 que expresan la proteína MYCER) (Albajar*, et al.*, 2011) tratadas con el inhibidor selectivo de BCR-ABL imatinib; (ii) células KMYCJ (células K562 con una copia adicional de MYC controlado por el promotor de la metalotioneína) tratadas con TPA (Delgado*, et al.*, 1995) y (iii), células KMYCBp53 (células K562 con una copia adicional de MYC controlado por el promotor de la metalotioneína y expresión constitutiva del mutante $p53^{Val35}$) en las cuales la activación de p53 a 32ºC detenía el ciclo celular e inducía apoptosis (Ceballos*, et al.*, 2000). En los tres modelos utilizados, la sobreexpresión o la activación de MYC fue capaz de inducir la expresión de SKP2 a nivel de ARN y de proteína cuando el ciclo celular se encontraba detenido, lo que indicaba que la inducción de SKP2 por MYC era independiente de la inducción de la proliferación mediada por MYC. Además, en base a los resultados del experimento en las células KMER en presencia y ausencia de imatinib, concluimos que la inducción de SKP2 podía considerarse independiente de la actividad de BCR-ABL, la cual había sido previamente relacionada con la activación transcripcional de SKP2 (Andreu*, et al.*, 2005; Chen*, et al.*, 2009).

Los resultados anteriores sugerían que *SKP2* podía ser un gen diana de MYC. Para confirmar esta posibilidad a continuación nos preguntamos si los niveles de SKP2 también respondían a la disminución de los niveles de MYC. Para ello utilizamos 3 aproximaciones diferentes. i) En primer lugar se silenció la expresión de MYC mediante siRNA en células K562.

El silenciamiento de MYC fue acompañado de una disminución en los niveles SKP2 a nivel de ARN y proteína. ii) Por otro lado, se analizó la expresión de SKP2 en dos modelos celulares que contenían el gen *MYC* controlado por un sistema *Tet-off* represible por tetraciclinas (Ej: doxiciclina): Las células linfoblastoides humanas P493.6 (Pajic*, et al.*, 2000) y las células epiteliales de pulmón de visón TM1 (Warner*, et al.*, 1999). En ambos modelos, la represión de *MYC* mediante doxiciclina fue acompañada por una reducción en los niveles de SKP2 a nivel de ARN y proteína. iii) Por último, se comparó la expresión SKP2 entre fibroblastos de rata deficientes en *Myc* (células HO15.19) y células parentales normales (células TGR-1) (Mateyak*, et al.*, 1997), observándose una menor expresión de SKP2 en las células $Myc^{-/-}$. Además en las células HO15.19, a diferencia de las células parentales TGR-1, la expresión de SKP2 no se vio prácticamente afectada por la ausencia de suero en el medio de cultivo, sugiriendo que MYC es el principal mediador de la expresión de SKP2 en respuesta a la estimulación con factores de crecimiento en estas células. En conjunto, todos los resultados anteriores sugerían que MYC no solo era un importante regulador de SKP2 en células humanas como K562 y P493.6, sino también en células de otras especies animales como visón y rata y por tanto que el efecto de MYC sobre SKP2 podía extrapolarse a diferentes modelos experimentales.

Para evaluar si el efecto de MYC sobre SKP2 era directo o indirecto, es decir, a través de otros factores de transcripción inducidos por MYC (como por ejemplo E2F1), se llevó a cabo un experimento de activación de MYCER en células Kp27MER en presencia de cicloheximida y por tanto, en ausencia de síntesis de nuevas proteínas. Los resultados mostraron que MYCER era capaz de inducir la expresión de SKP2 directamente sin necesidad de inducir la expresión de otros factores de transcripción intermediarios. De este forma concluimos que MYC inducia la expresión de SKP2 directamente en las células Kp27MER y por tanto que *SKP2* podía ser considerado un nuevo gen diana de MYC.

Para confirmarlo se realizaron ensayos de trans-activación con un vector que contenía el promotor de *SKP2* y el gen de la luciferasa como reportero (Huang and Hung, 2006). Para ello se utilizaron células KMYCJ tratadas con TPA (que como habíamos demostrado anteriormente, disminuía completamente los niveles endógenos de MYC) en presencia y ausencia de Zn^{2+} (para inducir el MYC exógeno). MYC no solo fue capaz de activar el promotor de *SKP2* sino que a la vez fue capaz de revertir el efecto del TPA sobre la actividad de dicho promotor.

Además, se realizó un análisis del promotor de *SKP2* humano para buscar posibles sitios de unión de MYC y se encontraron varias cajas E en el promotor y en el segundo exón del gen. Estudios de Inmunoprecipitación de cromatina (ChIP) demostraron que MYC se unía a una región que contenía dos cajas-E situadas a unas ~750 y ~400 pares de bases corriente arriba del inicio de transcripción respectivamente, controlando la expresión de *SKP2*. Nuestros resultados de ChIP fueron corroborados por otros resultados similares generados por el proyecto ENCODE (The Enciclopedia of DNA Elements), accesibles mediante la base de datos del UCSC (http://genome.ucsc.edu), que incluían diferentes estudios de ChIP-sequencing para varios factores de trascripción incluidos MYC y MAX en células K562, pero también otros reguladores o coactivadores transcripcionales como la histona acetiltransferasa p300 y la subunidad RBBP5 del

complejo histona metil transferasa MLL1 y diversas marcas de histonas asociadas a cromatina activa. Hay que destacar que los resultados de ChIP-seq para MYC y MAX también fueron observados en otras líneas celulares humanas como células de leucémia promielocítica aguda (NB4), células de carcinoma de pulmón (A549), hígado (HepG2) o cervix (HeLa). En base a todos estos resultados concluimos que *SKP2* puede ser considerado definitivamente un nuevo gen diana de MYC no solo en nuestro modelo K562, sino también en otros modelos celulares humanos. Además, a partir de los diversos estudios de ChIP-seq contenidos en esta base de datos proponemos un nuevo al mecanismo de activación del promotor de *SKP2* por MYC a través de los coactivadores p300 y MLL1, proteínas que ya se han visto interaccionar con MYC en otros modelos experimentales (ver Introducción).

Por otro lado, analizamos el posible efecto de SKP2 sobre la estabilidad de MYC y sobre su capacidad transcripcional en nuestro modelo celular, dado que había sido descrito que SKP2 participaba en la degradación de MYC (Kim*, et al.*, 2003; von der Lehr*, et al.*, 2003). Para ello se silenció *SKP2* en células K562 y se estudiaron los niveles de MYC a nivel de proteína sin encontrar diferencias significativas. Al mismo tiempo se estudió la actividad transcripcional de MYC en ausencia de SKP2 utilizando un vector reportero que contenía 4 cajas E canónicas en su promotor (Kiessling*, et al.*, 2006). Tampoco se encontraron diferencias significativas en la actividad transcripcional de MYC. Por tanto concluimos que SKP2 no afecta a la estabilidad y la actividad de MYC al menos en el modelo K562.

Finalmente, dado que la línea celular K562 provenía de un paciente de leucemia mieloide crónica (LMC), se estudiaron los niveles de SKP2 y MYC por RT-qPCR en muestras primarias de pacientes de LMC del Hospital Universitario Marqués de Valdecilla (Santander) y del Hospital Universitario Dr. Negrín (Las Palmas) encontrándose una correlación positiva en la expresión de ambos genes. También observamos que un grupo pequeño de pacientes que habían sido tratados con imatinib presentaban menores niveles de MYC y SKP2 a nivel de ARN, resultados similares a los obtenidos en el modelo celular KMER tratado con imatinib. Por otro lado, se utilizaron las bases de datos de Oncomine (www.oncomine.org) y GeneSapiens (www.genesapiens.org) para ver si existía correlación en la expresión de ambos genes en alguna otra patología neoplásica hematológica y se encontró una correlación positiva en leucemia mieloide aguda (LMA) y en linfoma, especialmente en linfoma de Burkitt, en el cual está demostrado que en el 98% de los casos *MYC* se encuentra translocado sobre el promotor de los genes que codifican para las cadenas ligera y pesada de las inmunoglobulinas (Delgado and Leon, 2010; Delgado*, et al.*, 2013). Estos resultados sugieren que MYC puede ser un regulador importante de SKP2 en todas estas patologías hematológicas pero probablemente también en muchos otros cánceres humanos en los que se han encontrado niveles elevados de SKP2.

8.3.2. El eje MYC-SKP2-p27

En la primera parte de esta Tesis habíamos demostrado convincentemente que la sobreexpresión de SKP2 era una consecuencia directa de la inducción de MYC, sugiriendo que MYC podía regular los niveles de p27 a través de la inducción de SKP2. En la segunda parte nos propusimos dilucidar si efectivamente la inducción de SKP2 por MYC realmente contribuía a la degradación de p27.

Para ello decidimos estudiar en primer lugar la fosforilación de p27 en la treonina 187 en respuesta a la activación de MYC en las células Kp27MER, ya que estaba descrito que esta fosforilación era un requisito indispensable para el reconocimiento de p27 por parte del complejo SCF^{SKP2} (Carrano*, et al.*, 1999; Sutterluty*, et al.*, 1999; Tsvetkov*, et al.*, 1999). Observamos que la activación de MYC promovía la fosforilación de p27 entre las 8-12 horas post-inducción e independientemente de los niveles de p27, sugiriendo que la quinasa involucrada en esta fosforilación no era inhibida por p27.

Estaba descrito que el principal complejo implicado en esta fosforilación era el complejo ciclina E/CDK2 (Muller*, et al.*, 1997; Sheaff*, et al.*, 1997; Vlach*, et al.*, 1997), que a su vez era el principal sustrato de p27, y que MYC inducía la expresión de ciclina E y la actividad de los complejos ciclina E/CDK2 (Jansen-Durr*, et al.*, 1993; Muller*, et al.*, 1997; Perez-Roger*, et al.*, 1997). Sin embargo, nosotros no observamos la inducción de ciclina E por MYC en las células Kp27MER. En cambio, vimos que la activación de MYC promovía un aumento en los niveles de ciclina A a nivel de proteína. En este sentido, también había sido descrito que MYC inducía la expresión de ciclina A (Jansen-Durr*, et al.*, 1993; Hoang*, et al.*, 1994; Muller*, et al.*, 1997) y que los complejos ciclina A/CDK2 también eran capaces de fosforilar a p27 en la treonina 187 (Muller*, et al.*, 1997; Zhu*, et al.*, 2004).

Mediante ensayos quinasa *in vitro* utilizando proteína p27 recombinante (His_6p27) como sustrato, observamos que los inmunocomplejos de ciclina A eran capaces de fosforilar a p27 y que, además, MYC era capaz de inducir actividad quinasa asociada a estos inmunocomplejos. Dado que CDK1 y CDK2 podían unirse a ciclina A, decidimos analizar la actividad quinasa de ambas CDKs para confirmar dicha fosforilación. Curiosamente, observamos que los inmunocomplejos de CDK2 estaban completamente inhibidos por el p27 endógeno (inducido por Zn^{2+}), incluso en presencia de MYC activo, excluyendo la posibilidad de que los complejos ciclina E-A/CDK2 fueran los responsables de la fosforilación de p27 inducida por MYC. Sin embargo observamos que los inmunocomplejos de CDK1 eran más refractarios a la inhibición por el p27 endógeno y además eran ligeramente activados en presencia de MYC activo. La unión de ciclina A a CDK1 y CDK2 en las células Kp27MER fue confirmada mediante coinmunoprecipitación. Estos datos sugerían que eran los complejos ciclina A/CDK1, y no los complejos ciclina E-A/CDK2, los responsables de la fosforilación de p27 en la treonina 187 mediada por MYC.

Para reforzar esta hipótesis, llevamos a cabo ensayos quinasa con inmunocomplejos de CDK1 y ciclina A procedentes de fibroblastos embrionarios de ratones deficientes en *Cdk2* y ciclinas E. De esta forma, demostramos, por un lado, que la ciclina E no era necesaria para activar a CDK2 y mediar la fosforilación de p27 en la treonina 187, sino que ciclina A podía

cumplir su función, y que, por otro lado, CDK2 tampoco era necesario para fosforilar a p27 y, por tanto, que CDK1 era capaz de suplir su función. Además, observamos que MYC era capaz de incrementar la actividad quinasa de los inmunocomplejos de ciclina A y CDK1 sobre el p27 recombinante, sugiriendo que los complejos ciclina A/CDK1 eran parcialmente responsables de esta fosforilación en respuesta a la activación de MYC. En base a todos estos resultados, proponemos que MYC induce la fosforilación de p27 en la treonina 187 a través de la activación de complejos ciclina A/CDK1 mediante la inducción de ciclina A, y no a través de la activación de complejos ciclina E/CDK2 como era anteriormente aceptado. Además, cabe destacar que este mecanismo es compatible con la inhibición total de complejos ciclina E/CDK2 por p27.

En segundo lugar nos quedaba por demostrar que la inducción de SKP2 por MYC era la responsable de la disminución de los niveles de p27 en células K562. Para ello utilizamos 3 aproximaciones:

i) Por un lado analizamos los niveles de MYC, SKP2 y p27 a nivel de proteína mediante inmunoblot en diferentes modelos celulares derivados de K562: células Kp27MER tratadas con Zn^{2+} y 4HT, células KMER paradas por alta densidad celular, células KMYC tratadas con imatinib o TPA y células K562 privadas de suero. En todos los casos observamos que la inducción de SKP2 por MYC se correlacionaba con la bajada de los niveles de p27 y viceversa. Estos resultados también fueron reproducidos en células TGR1 privadas de suero.

ii) A continuación decidimos estudiar la interacción entre SKP2 y p27 en células Kp27MER mediante inmunofluorescencia. Encontramos que SKP2 y p27 presentaban una localización nuclear en estas células, pero curiosamente ambos eran mutuamente excluyentes. Es decir, las células con altos niveles de SKP2 (Inducido por MYC, tras su activación con 4HT) no presentaban p27 y viceversa, las células con altos niveles de p27 (inducido por Zn^{2+}) no presentaban SKP2 en el núcleo. Este resultado reforzaba considerablemente la degradación de p27 por parte de SKP2 al menos en el modelo Kp27MER.

iii) Por último analizamos la expresión de p27 tras el silenciamiento de SKP2 mediante siRNA en células K562 y observamos que las células que expresaban bajos niveles de SKP2 presentaban mayores niveles de p27, lo cual se traducía en una reducción en su tasa proliferativa.

Por lo tanto, basándonos en estas 3 observaciones, proponemos que la inducción de SKP2 por MYC es la responsable de la disminución de los niveles de p27 y que el eje MYC-SKP2-p27 regula la proliferación en células de leucemia (K562) y sus derivadas. Es decir, podemos aseverar que la inducción de SKP2 por MYC y la posterior degradación de p27 es el mecanismo responsable del incremento de la proliferación observado en células Kp27MER tras la activación de MYC en presencia de unos niveles moderados de p27 (inducido con 50 µM de $ZnSO_4$).

Finalmente evaluamos la implicación del eje MYC-SKP2-p27 en tumorogénesis mediante ensayos de tumorogenicidad utilizando un modelo de xenotransplante subcutáneo de células K562 en ratones desnudos. Encontramos que las células K562 que presentaban bajos niveles de

SKP2 (por silenciamiento) desarrollaban tumores de menor tamaño. Estos resultados sugirieren que MYC, a través de la inducción de SKP2 y la degradación de p27, es, al menos en parte, responsable de la capacidad tumorogénica de estas células.

8.3.3. El efecto de MYC sobre los complejos proteicos de p27 y su relación con la proliferación

Por último, en la tercera parte de la Tesis, nos propusimos esclarecer porque MYC era capaz de contrarrestar la inhibición de ciclo celular en las células Kp27MER a niveles moderados de p27 (50 µM $ZnSO_4$) pero no a niveles elevados de p27 (75 µM $ZnSO_4$), a pesar de inducir en ambos casos su degradación a través de SKP2.

Para ello utilizamos la técnica de cromatografía de exclusión molecular, también conocida como gel filtración, que permitía separar complejos proteicos en condiciones nativas en función de su peso molecular. Mediante esta técnica, observamos que en células Kp27MER expuestas a altas dosis de Zn^{2+} (75 µM de $ZnSO_4$), p27 se distribuía entre dos tipos de complejos proteicos: uno de alto peso molecular (~200 kDa) asociado a complejos ciclina/CDK, y otro de bajo peso molecular (~50 kDa) en principio de naturaleza desconocida. La capacidad termorresistente de este segundo complejo y las características de elución similares a las de un p27 recombinante purificado de bacterias (His_6p27) nos permitió confirmar posteriormente que se trataba de p27 en forma libre (no unido a otras proteínas). Además, dada su movilidad en gel filtración como una proteína de ~50 kDa, nos llevó a sugerir en un primer momento que este se comportaba como un dímero en condiciones nativas. Sin embargo, mediante experimentos de mezcla entre dos p27 recombinantes (GST-p27 y His_6-p27) con el fin de encontrar heterodímeros, demostramos que el p27 libre no se comportaba como un dímero en condiciones nativas, sino que migraba anómalamente en gel filtración posiblemente debido a su forma alargada y su naturaleza intrínsecamente desestructurada. Esto fue confirmado mediante ultracentrifugación analítica en colaboración con el laboratorio de German Rivas, en el Centro de Investigaciones Biológicas (CSIC) en Madrid.

Por otro lado, los estudios de gel filtración también nos permitieron observar que las CDKs, a diferencia de las ciclinas, también eluían en dos picos mayoritariamente: uno asociado a ciclinas y p27 (230-150 kDa) y otro en forma libre al igual que p27 (~30 kDa). Esto sugería que las CDKs se encontraban en exceso dentro de las células y que, por tanto, las ciclinas eran las proteínas limitantes a la hora de formar los complejos ciclina/CDK. Asimismo, estos resultados también demostraban que p27 no se unía a CDKs libres, sino a complejos ciclina/CDK. Esta última observación y la presencia de p27 en forma libre sugerían que p27 podía estar excediendo los requerimientos para unirse a todos los complejos ciclina/CDK disponibles, y que el exceso de p27 podía ser a la vez el responsable del bloqueo total del ciclo celular.

Para estudiar esta posibilidad, decidimos realizar un estudio comparativo mediante gel filtración de la distribución de p27 en células Kp27MER a diferentes dosis de Zn^{2+}, en presencia y ausencia de MYC activo (+/- 4HT) y a diferentes tiempos (6,12 y 24 h). Este estudio reveló que:

i) La presencia de p27 libre era dependiente de los niveles de p27 sobre-expresados dentro de la célula, e independiente de la activación o no de MYC (al menos en las condiciones estudiadas). Es decir, solo observamos p27 libre cuando utilizamos altas dosis de Zn^{2+} (75 µM $ZnSO_4$) pero no a dosis moderadas (50 µM $ZnSO_4$).

ii) Que al inicio de la sobreexpresión de p27 (~6 horas post-inducción) con altas dosis de Zn^{2+} (75 µM $ZnSO_4$) no había acumulación de p27 en forma libre, sugiriendo que el p27 recién traducido se unía directamente a complejos ciclina/CDK, pero no se acumulaba inicialmente en forma libre. Estos datos apoyaban la observación de que p27 solo se unía a complejos ciclina/CDK y sugerían que la formación de nuevos complejos ciclina/CDK podían promover la unión de p27 libre.

iii) Que la activación de MYC promovía el desplazamiento del p27 libre hacia complejos de alto peso molecular. Esto podía ser debido, al menos en parte, a la inducción de ciclina A por MYC, como habíamos mencionado previamente, pero también a la inducción de ciclinas D2 o B1 (Acosta*, et al.*, 2008) y por tanto de nuevos complejos ciclina/CDK.

iv) Que a niveles moderados de p27 (inducidos con 50 µM $ZnSO_4$) no se observaba p27 en forma libre y por tanto, que la degradación de p27 solo podía tener lugar a partir de los complejos de alto peso molecular.

Esta última observación nos llevó a analizar la distribución de SKP2 en las cromatografías y encontramos que SKP2 coeluía con los complejos de alto peso molecular, sugiriendo la presencia de otros elementos del complejo SCF^{SKP2}, aunque experimentos adicionales son requeridos para su confirmación. Estos resultados concordaban con estudios previos que demostraban que el peso molecular estimado del complejo SCF^{SKP2} unido al complejo ciclina A/CDK2/p27 en gel filtración era de ~230 kDa (Hao*, et al.*, 2005)

En resumen, se concluye que el efecto de MYC en la proliferación de las células K562 (y probablemente en otros modelos celulares) depende de los niveles de proteína p27. A niveles bajos o moderados de p27, el eje MYC-SKP2 es capaz de contrarrestar el efecto de p27 como inhibidor del ciclo celular, promoviendo la proliferación celular. En esta situación, todo el p27 disponible estaría unido a complejos ciclina/CDK pero quedaría una parte de complejos ciclina/CDK libres (no inhibidos por p27). Sin embargo a niveles altos de p27, todos los complejos ciclina/CDK tendrían p27 unido (estando por tanto inhibidos) y habría una acumulación del exceso de p27 en forma libre. Este p27 libre actuaría como un reservorio de p27 capaz de inhibir nuevos complejos ciclina/CDK inducidos por MYC y al mismo tiempo sería capaz de contrarrestar la eliminación de p27 desde de los complejos ciclina/CDK/p27 por el eje MYC-SKP2. Esto explica por qué la proliferación de estas células permanece detenida a pesar de la degradación de p27 mediada por SKP2.

8.4. CONCLUSIONES

1. MYC regula la expresión de SKP2 en varias líneas celulares procedentes de diferentes especies y tejidos, y parece ser el principal mediador de la inducción de SKP2 en respuesta a los factores de crecimiento del suero. La inducción de SKP2 es independiente de la inducción de proliferación mediada por MYC.

2. MYC se une a la región promotora de *SKP2* e induce su expresión en ausencia de síntesis de proteínas, confirmando que SKP2 es un nuevo gen diana MYC.

3. SKP2 no afecta ni a la estabilidad ni a la actividad de MYC al menos en células K562.

4. La expresión de MYC y SKP2 correlacionan en diferentes neoplasias hematológicas incluyendo leucemia mieloide aguda, crónica y linfoma de Burkitt.

5. En las células K562, MYC promueve la fosforilación de p27 en la treonina 187 mediante inducción de la ciclina A y de la actividad quinasa asociada a dicha ciclina; fosforilación requerida para el reconocimiento de p27 por el complejo ligasa de ubiquitinas SCF^{SKP2}. Además, en células de ratón, MYC es capaz de promover dicha fosforilación independientemente de CDK2 o de las ciclinas E.

6. La inducción de SKP2 por MYC en células K562 se correlaciona con la disminución de p27; da lugar a un incremento en su tasa proliferativa y es, al menos en parte, responsable de su capacidad tumorogénica en xenotransplates en ratones desnudos.

7. Cuando p27 se expresa en niveles bajos o moderados en células K562, este se encuentra asociado a complejos de alto peso molecular junto con complejos ciclina/CDK y, posiblemente también, SCF^{SKP2}. A niveles altos de p27, este se acumula además en forma libre, lo cual se corresponde con un bloqueo total de la proliferación. MYC, mediante la inducción de ciclinas y CDKs, promueve el desplazamiento de p27 libre hacia los complejos de alto peso molecular. La desaparición de p27 en forma libre se relaciona con el estímulo proliferativo mediado por MYC.

9. PUBLICATIONS

THE JOURNAL OF BIOLOGICAL CHEMISTRY VOL. 286, NO. 11, pp. 9815–9825, March 18, 2011

SKP2 Oncogene Is a Direct MYC Target Gene and MYC Down-regulates p27^{KIP1} through SKP2 in Human Leukemia Cells*[S]

Received for publication, July 29, 2010, and in revised form, January 13, 2011 Published, JBC Papers in Press, January 18, 2011, DOI 10.1074/jbc.M110.165977

Gabriel Bretones[‡1], Juan C. Acosta[‡1,2], Juan M. Caraballo[‡1], Nuria Ferrándiz[‡1,2], M. Teresa Gómez-Casares[§], Marta Albajar[‡¶], Rosa Blanco[‡], Paula Ruiz[‡], Wen-Chun Hung[‖], M. Pilar Albero[**], Ignacio Perez-Roger[**], and Javier León[‡3]

From the [‡]Departamento de Biología Molecular, Instituto de Biomedicina y Biotecnología de Cantabria, Universidad de Cantabria, Consejo Superior de Investigaciones Científicas, SODERCAN (Sociedad para el Desarrollo de Cantabria), 39011 Santander, Spain, the [§]Servicio de Hematología, Hospital Dr. Negrín, 35020 Las Palmas de Gran Canaria, Spain, the [¶]Servicio de Hematología, Hospital Universitario Marqués de Valdecilla-Instituto de Investigación y Formación Marqués de Valdecilla, 39009 Santander, Spain, the [‖]Institute of Biomedical Sciences, National Sun Yat-Sen University, Kaohsiung 804, Republic of China, and the [**]Department of Chemistry, Biochemistry and Molecular Biology, Cardenal Herrera-CEU University, 46113 Moncada, Spain

SKP2 is the ubiquitin ligase subunit that targets p27^{KIP1} (p27) for degradation. SKP2 is induced in the G_1-S transit of the cell cycle, is frequently overexpressed in human cancer, and displays transformation activity in experimental models. Here we show that MYC induces SKP2 expression at the mRNA and protein levels in human myeloid leukemia K562 cells with conditional MYC expression. Importantly, in these systems, induction of MYC did not activate cell proliferation, ruling out SKP2 up-regulation as a consequence of cell cycle entry. MYC-dependent SKP2 expression was also detected in other cell types such as lymphoid, fibroblastic, and epithelial cell lines. MYC induced SKP2 mRNA expression in the absence of protein synthesis and activated the SKP2 promoter in luciferase reporter assays. With chromatin immunoprecipitation assays, MYC was detected bound to a region of human SKP2 gene promoter that includes E-boxes. The K562 cell line derives from human chronic myeloid leukemia. In a cohort of chronic myeloid leukemia bone marrow samples, we found a correlation between MYC and SKP2 mRNA levels. Analysis of cancer expression databases also indicated a correlation between MYC and SKP2 expression in lymphoma. Finally, MYC-induced SKP2 expression resulted in a decrease in p27 protein in K562 cells. Moreover, silencing of SKP2 abrogated the MYC-mediated down-regulation of p27. Our data show that SKP2 is a direct MYC target gene and that MYC-mediated SKP2 induction leads to reduced p27 levels. The results suggest the induction of SKP2 oncogene as a new mechanism for MYC-dependent transformation.

c-MYC (hereafter MYC) is an oncogenic transcription factor of the helix-loop-helix/leucine zipper protein family. MYC exerts a wide array of biological functions in different cellular models related to cell cycle control, genomic instability, energetic metabolism, protein synthesis, intercellular communication, and control of cell differentiation (for reviews see Refs. 1–3). MYC forms heterodimers with the protein MAX that bind to E-boxes in the regulatory regions of target genes. MYC regulates ~1000 genes and binds to 15% of genomic loci (4–7). Most target genes are activated by MYC in an E-box-dependent manner, although an important fraction of MYC target genes are repressed by MYC (reviewed in Refs. 8 and 9). Consistent with the biological activities of MYC, its expression is deregulated in a wide array of human solid tumors and in leukemia, often associated to tumor progression (10–12).

SKP2 is an oncogenic protein frequently overexpressed in human cancers. Moreover, *SKP2* behaves as an oncogene in transformation assays (13, 14). *SKP2* encodes the F-box protein of the ubiquitin ligase SCF^{SKP2} complex; this complex is comprised by three core subunits RBX1, CUL1, and SKP1, whereas the substrate is bound by SKP2 along with the small protein CKS1 (14, 15). More than 20 SKP2 substrates have been found, including several proteins involved in cell cycle control (*e.g.* cyclin E, p21, p57, and E2F1) (14), and SKP2 can suppress p53-mediated apoptosis (16). Nonetheless, the main oncogenic mechanism of SKP2 is attributed to degradation of the cyclin-dependent kinase (CDK)[4] inhibitor p27^{KIP1} (hereafter p27) (13).

p27 was originally described as a CDK inhibitor, with cyclin E-CDK2 complexes as its primary targets (17, 18). Low p27 levels are associated with a poor prognosis in most tumors (19, 20). p27 is regulated mainly at the protein stability level. The degradation of p27 by proteosomes is preceded by ubiquitylation (21), which is mediated by the SCF^{SKP2} complex, in which SKP2 is the p27-recognizing subunit (22–24). To be recognized

* This study was supported by Grant PN-SAF08-01581 from the Spanish Ministerio de Ciencia e Innovacion, Grant ISCIII-RETIC RD06/0020/0017 from the Spanish Ministerio de Sanidad y Consumo, a grant from University of Cantabria-IFIMAV (to J. L.), and Grants PI06-0285 and Proyecto Universidad Cardenal Herrera-Santander (to I. P.-R.).

[S] The on-line version of this article (available at http://www.jbc.org) contains supplemental Table S1 and Figs. S1–S3.

[1] Supported by fellowships from Spanish Ministerio de Ciencia e Innovacion.

[2] Present address: MRC Clinical Sciences Centre, Imperial College Faculty of Medicine, Hammersmith Hospital Campus, London, United Kingdom.

[3] To whom correspondence should be addressed: Departamento de Biología Molecular, Facultad de Medicina, IBBTEC, Cardenal Herrera Oria s/n, 39011 Santander, Spain. Tel.: 34-942-201952; E-mail: leonj@unican.es.

[4] The abbreviations used are: CDK, cyclin-dependent kinase; 4HT, 4-hydroxytamoxifen; CHX, cycloheximide; CML, chronic myeloid leukemia; TPA, phorbol-12-myristate-13-acetate; qPCR, quantitative PCR; sh, short hairpin.

by the SCF^{SKP2} complex, p27 must be bound to cyclin-CDK complexes and phosphorylated at Thr-187. p27 bound to cyclin E-CDK2 is a target for phosphorylation by the bound CDK2 or a second active cyclin E-CDK2 complex at Thr-187 (reviewed in Refs. 25 and 26). The oncogenic activity of SKP2 is attributed mainly to low p27 levels, and consistently, the levels of SKP2 and p27 inversely correlate in many tumors and cell models (13, 14).

MYC and p27 show functional antagonism in proliferation: MYC and the loss of p27 cooperate in animal carcinogenesis models (27), and MYC abrogates p27 function in proliferation. The antagonistic effect of MYC is mediated through several mechanisms (reviewed in Refs. 11). MYC down-regulates murine p27 at the transcriptional level (28, 29); in addition, it induces cyclin D2 and CDK4, which sequester p27 in CDK-cyclin complexes (30, 31); finally, MYC induces expression of CUL1 (32) and CKS1 (33), both components of the SCF^{SKP2} complex. A correlation between MYC and SKP2 expression was recently described in a murine lymphoma model, with only modest effects on p27 levels (34). The previous studies are nonetheless hampered by the fact that SKP2 is induced in cell cycle stimulation, which is also a well known MYC activity. This has made it difficult to distinguish whether SKP2 induction is a direct effect of MYC. Here we studied the MYC-SKP2-p27 axis in different cell models with conditional MYC expression in which MYC is induced in cell cycle-arrested cells. We show for here that SKP2 is a direct MYC target gene and that MYC-mediated SKP2 up-regulation contributes to p27 degradation.

EXPERIMENTAL PROCEDURES

Cell Lines and Cell Proliferation—K562 and K562-derived cell lines were cultured in RPMI 1640 medium with 8% fetal calf serum and antibiotics. Unless otherwise stated, the cells (2.5×10^5 cells/ml) were treated with 75 μM $ZnSO_4$, 200 nM 4-hydroxytamoxifen (4HT) (Sigma), 10 nM phorbol-12-myristate-13-acetate (TPA), and 1 μM imatinib. Transient transfections were performed in a nucleofector (Amaxa) following the manufacturer's instructions. Short hairpin expression vectors used were shMyc (35) and pSR-shSKP2 (36). KmycJ are K562 cells with a *MYC* gene inducible by $ZnSO_4$ (37). KMER4 are K562 cells stably transfected with a vector expressing the MycER construct.[5] MycER is activated by 4HT (38). Kp27-5 cells are K562 cells stably transfected with a *p27* gene inducible by Zn^{2+} (39). Kp27MER are Kp27-5 cells transduced with the MycER gene (40). KmycBp53 are KmycB cells expressing a p53 mutant that is activated at 32 °C (41). KMERshSKP2 are KMER4 cells infected with retrovirus expressing pSR-shSKP2 and selected with 1 μg/ml puromycin. pSR-shSKP2 was constructed by inserting the siRNA sequence AAGGGAGTGACAAAGACTTTGTTCAAGAGACAAAGTCTTTGTCACTCCCTT (36) into the BglII and HindIII sites of pSUPER-retro vector (the sequence of the hairpin loop is underlined). KMERpSR are KMER4 cells infected with the empty retroviral vector pSUPER-retro. TM1 are derived from the Mv1Lu lung epithelial cell line with a tetracyclin-repressible *MYC* gene (42). HO15.19 *Myc*-null rat fibroblasts were generated from parental TGR-1 by homologous recombination (43). TM1, HO15.19, and TGR1 cells were cultured in DMEM supplemented with 10% fetal calf serum and antibiotics. P493-6 cells are immortalized human B cells expressing a tetracyclin-repressible *MYC* gene (44) and were cultured in RPMI 1640 with 10% fetal calf serum and antibiotics. Cell proliferation was determined by cell counting in a hemocytometer.

Nude Mice Xenografts—KMERpSR or KMERshSKP2 cells (10^7) were resuspended in 0.2 ml of RPMI/Geltrex (Invitrogen) (1:1). The cell suspension was injected subcutaneously into the right and left flanks of 6-week-old female athymic nude mice (Hsd:Athymic Nude-Foxn1 *nu/nu*; Harlan Laboratories models); after 21–24 days, the mice were euthanized, and the tumors were weighed.

mRNA Analysis—Total RNA from cell lines and bone marrow cells was isolated using the RNeasy kit (Qiagen). RT was performed with i-Script reverse transcriptase (Bio-Rad). Quantitative PCR (qPCR) was performed with the SYBRGreen PCR kit (Bio-Rad). The sequences of primers used and amplicon sizes are shown in supplemental Table S1. The data were normalized to ribosomal protein S14 mRNA levels.

Immunoblots—Total cell lysates and immunoblots were carried out as described (39). The blots were developed with secondary antibodies conjugated to IRDye680 and IRDye800 (Li-Cor Biosciences) and visualized in an Odyssey scanner. The antibodies used were anti-actin (goat polyclonal, sc-1616), MYC (sc-764), SKP2 (sc-7164), p27 (sc-528), α-tubulin (sc-5546) (all rabbit polyclonals from Santa Cruz Biotechnology), p27 monoclonal antibody (K-25020; Transduction Labs), and Thr(P)-187-p27 (rabbit polyclonal, 71-7700; Invitrogen).

Chromatin Immunoprecipitation—The cells (5×10^7) were fixed in 1% formaldehyde, lysed with SDS, and sonicated, essentially as described (45). ChIP was performed using Dynabeads-Protein G (Dynal Biotech) coupled to anti-MYC antibody and rabbit IgG as specificity control. Quantitative PCR of eluted DNA was performed with the primers of SKP2 and lactate dehydrogenase genes indicated in supplemental Table S1.

Immunofluorescence Analysis—Kp27MER cells were treated with $ZnSO_4$ and/or 4HT for 24 h and immunostained with anti-SKP2 and -p27 antibodies as described and revealed with fluorescein- or rhodamine-conjugated secondary antibodies as described (40). The cells were mounted with Vectashield mounting medium (Vector Laboratories) with DAPI to visualize nuclei.

Luciferase Assays—The cells (3×10^6) were electroporated with an Amaxa electroporator and Mirus Ingenio (Mirus Bio LLC) transfection reagent. KmycJ cells were transfected with 3 μg of the −1148-SKP2 promoter (46) or pGL3basic vector (Promega) as control. K562 or KmycJ cells were nucleofected with 1.5 μg of 4×Ebox-Luc or the MYC-unresponsive 4×EboxMut-Luc reporter constructs (47). K562 cells were nucleofected with 1.5 μg of pSR-shSKP2 or pSUPER-retro vector. The cells were lysed, and luciferase activity was measured in duplicate in a dual luciferase reporter gene assay system (Promega). The data were normalized to *Renilla* luciferase values (0.5 μg of pRL-TK vector in each transfection).

[5] M. Albajar and J. Leon, submitted for publication.

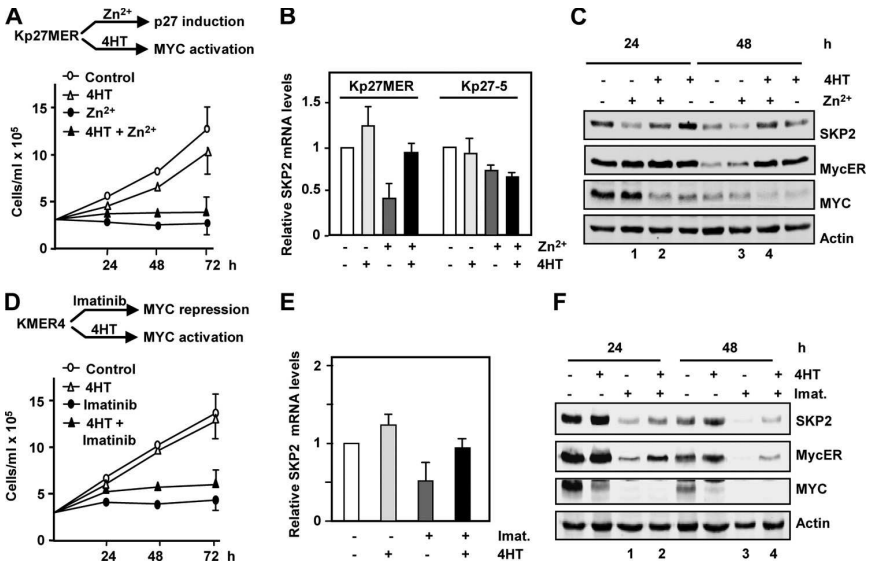

FIGURE 1. **SKP2 induction by MYC in Kp27MER and KMER cell lines.** *A*, the Kp27MER cell model (*top panel*). Proliferation rates of Kp27MER cells treated with 200 nM 4HT and 75 μM $ZnSO_4$ were measured by counting viable cells in a hemocytometer (*bottom panel*). *B*, SKP2 mRNA expression in Kp27MER cells and parental Kp27-5 cells. The cells were treated for 12 h with 200 nM 4HT and 50 μM ZnSO4, and mRNA expression was determined by RT-qPCR. The values are the means ± S.E. of three experiments. *C*, immunoblot showing SKP2 up-regulation in response to MYC in Kp27MER cells treated with 4HT and $ZnSO_4$ as indicated. *D*, the KMER4 cell model (*top panel*). Proliferation rates of KMER cells treated with 1 μM imatinib and 200 nM 4HT (*bottom panel*). *E*, KMER4 cells were treated with 1 μM imatinib and 200 nM 4HT (24 h), and SKP2 mRNA levels were determined by RT-qPCR. The values are the means ± S.E. of three experiments. *F*, KMER4 cells were treated with imatinib and 4HT as indicated, and the levels of SKP2, MYC, MycER, and actin (loading control) in total cell lysates were assayed by immunoblot.

Chronic Myeloid Leukemia (CML) Samples—Bone marrow mononuclear cells (prepared by Ficoll-Hypaque) from 4 healthy controls, 31 CML patients at diagnosis, and 8 patients that achieved the remission of the leukemia after treatment (Complete Molecular Response) (48) were studied. The patients were from the Hospital Universitario Marqués de Valdecilla (Santander) and Hospital Universitario Dr. Negrín (Las Palmas). The study was approved by the ethics committees of both hospitals.

RESULTS

Induction of MYC Is Associated to Induction of SKP2—We studied the MYC-SKP2 relationship in cell models in which (i) ectopic MYC expression is activated or induced and (ii) MYC induction does not stimulate cell proliferation, a critical condition to avoid SKP2 up-regulation subsequent to cell cycle progression. In the Kp27MER cell line, p27 can be induced with $ZnSO_4$, and MYC can be activated with 4HT (Fig. 1*A*, *top panel*). Large scale gene expression profiling in these cells showed that MYC activation provoked up-regulation of SKP2 mRNA (40). We set out to validate this microarray data. Induction of p27 resulted in rapid growth arrest (Fig. 1*A*) and SKP2 expression was down-regulated (Fig. 1*C*), as predicted. Importantly, MYC activation did not modify p27-mediated growth arrest in this model (Fig. 1*A*), confirming previous results (40). MYC activation (*i.e.* 4HT treatment) nonetheless resulted in a 2-fold increase in SKP2 mRNA in proliferation-arrested Kp27MER cells (Fig. 1*B*, *black bars*). Moreover, MYC activation induced robust up-regulation of SKP2 protein, as detected by immunoblot (Fig. 1*C*, compare *lanes 1* and *2* and *lanes 3* and *4*). The immunoblot also showed down-regulation of endogenous MYC following activation of ectopic MYC. This well known effect of ectopic MYC (49, 50) confirmed MycER activation by 4HT. In contrast to MycER-expressing cells, 4HT did not modify SKP2 expression in Kp27-5 cells, in which p27 is induced by Zn^{2+} but which do not carry the MycER allele (Fig. 1*B*).

We used KMER4 cells treated with 1 μM imatinib, a BCR-ABL inhibitor that causes rapid down-regulation of endogenous MYC in K562 cells (51). MYC activation with 4HT in KMER4 cells did not rescue the proliferation arrest mediated by imatinib (Fig. 1*D*). Treatment of KMER4 with imatinib led to down-regulation of SKP2 mRNA, as detected by RT-qPCR (Fig. 1*E*), and protein, as detected by immunoblot (Fig. 1*F*). Activation of MYC in the presence of imatinib resulted in a 2-fold induction of SKP2 mRNA after 24 h (Fig. 1*E*) and protein (Fig. 1*F*, compare *lanes 1* and *2* and *lanes 3* and *4*). Although BCR-ABL was previously reported to induce SKP2 (36, 52) and to induce MYC (51, 53), here we show that ectopic MYC up-regulates SKP2 in proliferation-arrested cells with inhibited BCR-ABL.

The KmycJ cell line is a K562 derivative that bears a $ZnSO_4$-inducible MYC allele (37). Treatment of K562 and KmycJ cells with 10 nM TPA resulted in growth arrest (Fig. 2*A*). TPA also induced a marked down-regulation of MYC, and as anticipated, SKP2 mRNA and protein expression were also repressed by TPA (supplemental Fig. S1). MYC induction did not rescue cells from TPA-induced growth arrest (Fig. 2*A*), confirming previous reports (54). We induced MYC in KmycJ cells pretreated (12 h) with 10 nM TPA, *i.e.* when the cells had very low endogenous MYC levels. In these TPA-arrested cells, MYC induction with Zn^{2+} resulted in a notable increase in SKP2 mRNA, as assessed by RT-qPCR (Fig. 2*B*), and in protein, as

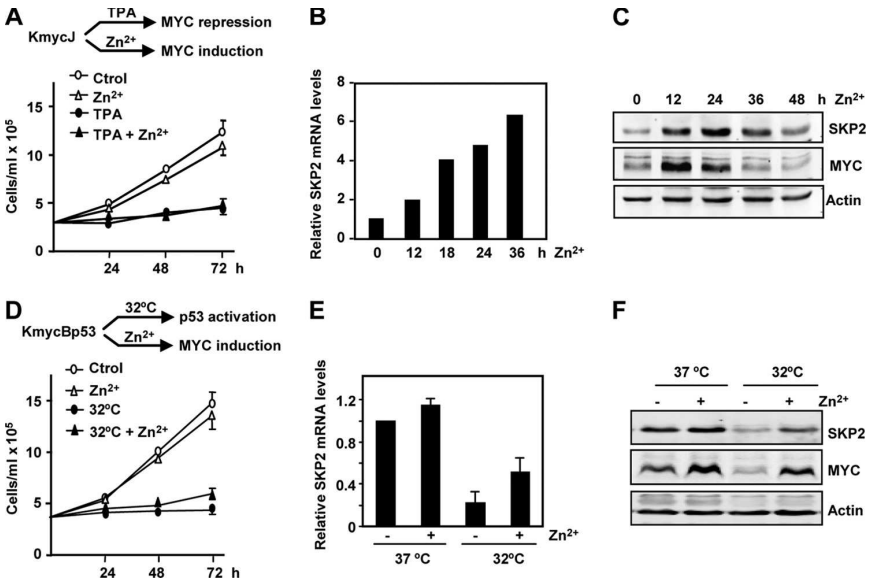

FIGURE 2. **SKP2 induction by MYC in KmycJ and KmycBp53 cell lines.** *A*, the KmycJ cell model (*top panel*). Proliferation rates of KMycJ cells treated with 10 nM TPA and 75 μM $ZnSO_4$ were measured by counting viable cells in a hemocytometer (*bottom panel*). *B*, KmycJ cells were treated with 10 nM TPA for 12 h and then induced with 75 μM $ZnSO_4$ as indicated. SKP2 mRNA levels were measured by RT-qPCR. *C*, KmycJ cells were treated as in *B*, and expression of SKP2, MYC, and actin (loading control) was assayed by immunoblot. *D*, the KmycBp53 cell model (*top panel*). Proliferation rates of KMycBp53 cells were treated with 75 μM $ZnSO_4$ and incubated at 37 or 32 °C (*bottom panel*). *E*, KmycBp53 cells were incubated (37 or 32 °C) alone or with $ZnSO_4$ for 24 h. SKP2 mRNA levels were determined by RT-qPCR. The values are the means ± S.E. of three experiments. *F*, KmycBp53 cells were treated as in *E*, and the levels of SKP2, MYC, and actin (loading control) in total cell lysates were assayed by immunoblot.

determined in immunoblot (Fig. 2*C*). The results were similar when we used a different MYC-inducible K562 cell line (KmycB) (not shown).

Finally, we assayed SKP2 induction by MYC in the KmycBp53 cell line. This is a K562-derived cell line bearing a p53 mutant that is activated at 32 °C and a Zn^{2+}-inducible MYC transgene (41). MYC induction did not antagonize the p53-mediated proliferation arrest at 32 °C (Fig. 2*D*). We found that MYC induction with Zn^{2+} resulted in the increase of SKP2 mRNA (Fig. 2*E*) and SKP2 protein (Fig. 2*F*), despite the fact that the cells were growth-arrested by p53 at 32 °C. We conclude that MYC induction provokes SKP2 induction independently of cell cycle activation.

Silencing of MYC Is Associated with Repression of SKP2 in Several Cell Types—To confirm the effects of MYC on SKP2 expression, we silenced MYC in K562 cells using siRNA. K562 cells were nucleofected with a short hairpin MYC vector (pRS-shMYC) (35). MYC silencing was confirmed by immunoblot and was accompanied by down-regulation of SKP2 protein (Fig. 3*A*) and mRNA (Fig. 3*B*). MYC silencing also resulted in down-regulation of B23/nucleophosmin mRNA (a MYC target gene used as positive control) but not of SKP1 mRNA, which encodes another component of the SCF^{SKP2} complex used here as negative control (Fig. 2*B*). To confirm the effect of MYC on SKP2 expression in cell models other than K562, we studied SKP2 expression in P493-6 cells, a human lymphoblastoid cell line carrying a tetracycline-repressible MYC transgene (55). In these cells, doxycycline treatment led to rapid MYC down-regulation accompanied by down-regulation of SKP2 protein (Fig. 3*C*) and mRNA (Fig. 3*D*). We also tested TM1 cells, a mink lung epithelial cell line also carrying a tet-off human MYC allele (42). In TM1 cells, doxycycline addition provoked MYC and SKP2 down-regulation (Fig. 3*E*), although the cells continued to grow (not shown).

Finally, we used the *Myc*-null rat cell line HO15.19, which does not express MYC (43). We analyzed MYC and SKP2 expression after serum deprivation in *Myc*-null and parental cells (TGR1). SKP2 levels were much lower but detectable in *Myc*-null cells. In contrast to parental cells, however, there was little decrease in SKP2 levels in response to serum deprivation (Fig. 3*F*). We conclude that MYC is a major regulator of SKP2 expression in cells from different tissues and species.

MYC Induces SKP2 mRNA in the Absence of Protein Synthesis—To assess whether MYC directly activated transcription of the *SKP2* gene, we performed the induction experiments in the presence of the protein synthesis inhibitor cycloheximide (CHX) using Kp27MER cells, in which MYC can be activated with 4HT and p27 can be induced by $ZnSO_4$. The cells were pretreated with 10 nM TPA (12 h) to down-regulate endogenous MYC and then treated with 10 μg/ml CHX for different periods. CHX effectiveness was confirmed by lack of induction of p27 protein in response to Zn^{2+} (Fig. 4*A*, compare p27 in *lanes 1* and *2 versus lanes 3* and *4* in the absence of 4HT and *lanes 5* and *6 versus lanes 7* and *8* in its presence). As predicted, endogenous MYC showed a high degradation rate. MycER was more stable in presence of 4HT (Fig. 4*A*, compare MycER levels in *lanes 9* and *10 versus lanes 11* and *12*), although the underlying molecular mechanism is unclear. In sharp contrast, we found that SKP2 was a long-lived protein (>6 h). SKP2 mRNA levels were determined by RT-qPCR. The results showed that 4HT activation of MycER led to increased SKP2 mRNA levels, even in the absence of synthesis of new proteins; this was prob-

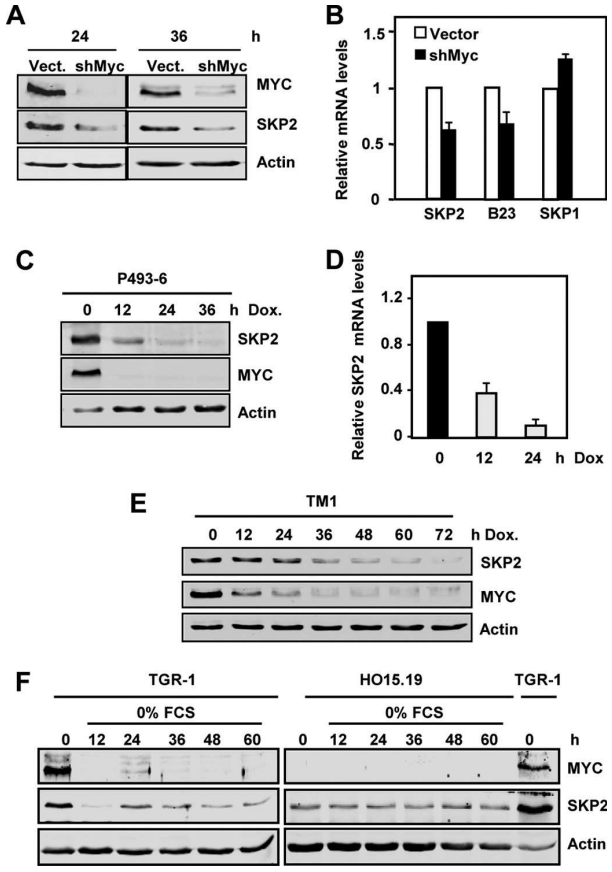

FIGURE 3. **SKP2 is down-regulated after MYC repression.** *A*, K562 cells were nucleofected with a short hairpin RNA vector for MYC (*shMYC*) or the empty vector (*Vect.*), and MYC, SKP2, and actin expression were assayed by immunoblot 24 and 36 h after nucleofection. *B*, K562 cells were transfected as in *A*; at 24 h after nucleofection, the levels of SKP2, B23/nucleophosmin (positive control), and SKP1 (negative control) mRNA were determined by RT-qPCR. The values are the means ± S.E. of three independent transfections. *C*, human lymphoid P493-6 cells were treated with 1 μg/ml doxycyclin (*Dox*), and SKP2, MYC, and actin expression were assayed by immunoblot. *D*, P493-6 cells were treated as in *C*, and SKP2 mRNA expression was determined by RT-qPCR. *E*, TM1 cells were treated with 2 μg/ml doxycyclin to repress MYC for the periods indicated, and SKP2, MYC, and actin expression were determined by immunoblot. *F*, *Myc*-null HO15.19 rat fibroblasts and parental TGR1 were serum-deprived for the indicated times, and SKP2, MYC, and actin expression analyzed by immunoblot.

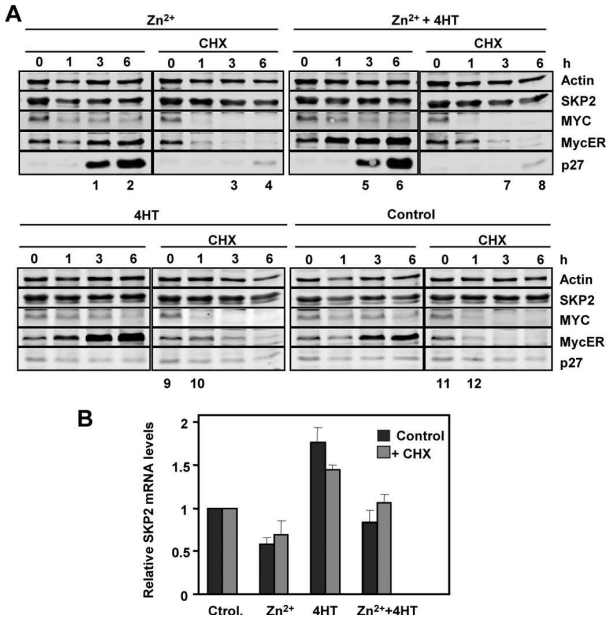

FIGURE 4. **MYC induces SKP2 in the absence of protein synthesis.** *A*, Kp27MER cells were pretreated for 12 h with 10 nM TPA and then treated with 10 μg/ml CHX, 4HT, and $ZnSO_4$ for 1–6 h. Expression of p27, SKP2, MYC, MycER, and actin were determined by immunoblot. *B*, SKP2 mRNA expression in Kp27MER was determined by RT-qPCR after 6 h of exposure to cycloheximide, $ZnSO_4$, and 4HT as indicated. The data show the means ± S.E. of three independent experiments. *Ctrol*, control.

ably dependent on the MycER activated by 4HT (Fig. 4*B*). Both MYC and MycER protein levels were very low after 6 h of CHX treatment, precluding analysis of SKP2 mRNA expression at longer treatment times.

MYC Activates and Binds to the Human SKP2 Promoter—We tested the ability of MYC to activate the human SKP2 promoter through promoter-luciferase assays. We transfected KmycJ cells with a luciferase reporter containing 1148 bp of SKP2 promoter (46). The results showed that the SKP2 promoter was activated by MYC (Fig. 5*A*, *top panel*). Consistent with MYC repression by TPA, MYC transactivation activity was reduced in TPA-treated cells after transfection and was elevated when MYC was induced by Zn^{2+}. As a positive control, we used a luciferase reporter bearing four E-boxes (4×Ebox-Luc), which was also activated by MYC (Fig. 5*A*, *bottom panel*). The empty luciferase construct and the reporter with four mutated E-boxes (4×EboxMut-Luc) were used for normalization. These results suggested that SKP2 could be a direct MYC target gene.

Sequence analysis of the human *SKP2* gene revealed several E-boxes in the promoter and in the second exon. We thus used ChIP to analyze promoter occupancy by MYC. The localization of E-boxes in the human *SKP2* gene and the amplicons analyzed in the ChIP experiments are shown in Fig. 5*B*. ChIP demonstrated MYC binding to a region with two E-boxes (CATGCG and CACGCG), mapping at −756 and −389 upstream of the transcription start site (Fig. 5*C*); both sequences are described as high affinity E-boxes for MYC *in vivo* (56, 57). As negative controls, we used K562 cells treated with imatinib and TPA, which inhibit MYC expression (Fig. 1, *E* and *F*, and supplemental Fig. S1). MYC binding was dramatically reduced after both treatments (Fig. 5*C*). This MYC-binding region was also detected in K562 and HeLa cells in the ENCODE genome-wide ChIP sequencing project, published by the UCSC genome browser (assembly NCBI36/hg18, Yale/UC Davis/Harvard study). MYC binding to the E-box of the lactate dehydrogenase A (58) was used as positive control (Fig. 5*C*). Taken collectively, our results indicate that human *SKP2* is a direct MYC target gene, at least in human cells.

MYC and SKP2 Expression Correlated in Chronic Myeloid Leukemia Cells—The K562 cell line is derived from a human CML patient in blast crisis. To confirm the correlation between SKP2 and MYC expression *in vivo*, we used RT-qPCR to determine mRNA levels of SKP2 and MYC in the bone marrow of 31

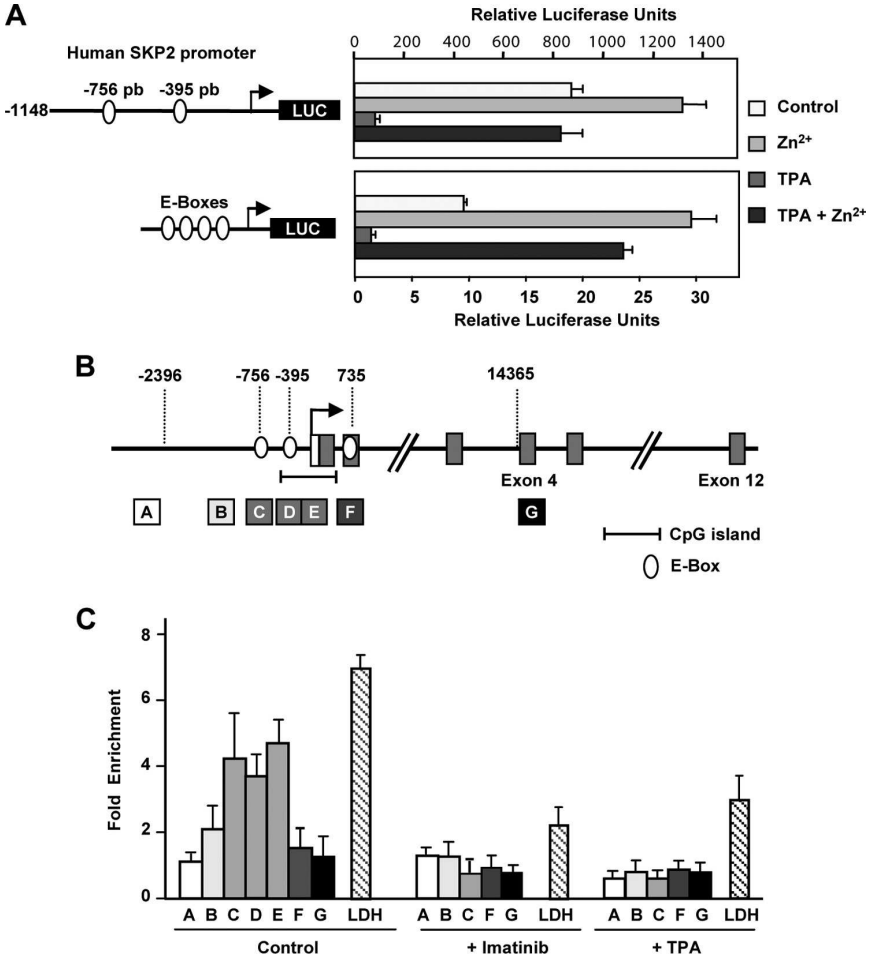

FIGURE 5. **MYC activates and binds to the human SKP2 promoter.** *A*, MYC activation of the human SKP2 promoter. KmycJ cells were electroporated with a luciferase construct of the human SKP2 promoter and a 4xE-Box luciferase reporter. At 12 h post-transfection, the cells were divided into four aliquots and treated with 10 nM TPA to repress endogenous MYC and 75 μM $ZnSO_4$ to induce exogenous MYC. At 36 h post-transfection, the cell lysates were prepared, and firefly and *Renilla* luciferase activities were determined. SKP2-luciferase data were normalized to the value of cells transfected with the empty vector (pGL3basic-Luc); 4×Ebox-Luc data were normalized to the mutated 4×EboxMut-Luc construct. The data were normalized to *Renilla* luciferase activity for transfection efficiency. The data show the means ± S.E. of three measurements in two duplicate experiments. *B*, scheme of the human *SKP2* gene. Amplicons (*boxes A–E*) used for ChIP assays are indicated; *ovals* indicate E-boxes. Coordinates and CpG island are as in the UCSC Genome Browser. *C*, chromatin was immunoprecipitated with anti-MYC antibody and rabbit IgG and measured in quantitative PCR for amplicons A–E. Kp27MER cells were treated for 12 h with 1 μM imatinib or 10 nM TPA to down-regulate endogenous MYC. Lactate dehydrogenase (*LDH*) E-box amplicon was used as positive control (58). The results are expressed as enrichment of DNA in chromatin immunoprecipitated with anti-MYC (with respect the signal with anti-rabbit IgG) and normalized to the amplicon A signal. The values are the means ± S.E. of three determinations from two (TPA and imatinib) or three (plus control) independent ChIP experiments.

CML patients at diagnosis, 8 CML patients that responded to the treatment, and 4 healthy controls (Fig. 6*A*). Although the cohort is small, the correlation between MYC and SKP2 expression was statistically significant (Fig. 6*B*). To determine whether this correlation between MYC and SKP2 at the mRNA level also occurred at the protein level, we analyzed protein extracts by immunoblot; the results confirmed the MYC/SKP2 correlation in seven of eight patients tested (Fig. 6*C*). We used the Oncomine database to examine a possible correlation between MYC and SKP2 mRNA levels in other hematopoietic neoplasias. Three expression profiling studies showed that Burkitt lymphoma cells, in which MYC expression is deregulated as a consequence of a chromosomal translocation, also expressed higher SKP2 levels (supplemental Fig. S2). We also queried the correlation between MYC and SKP2 expression in tumor samples with the *in silico* transcriptomics database of the GeneSapiens system (59). CML is not included in these databases, but analyses showed a correlation between MYC and SKP2 expression in human lymphoma (supplemental Figs. S2 and S3).

MYC Induces SKP2 Accumulation in the Cell Nucleus and p27 Phosphorylation—Previous studies firmly established that SKP2 participates in p27 degradation, and our results so far demonstrated that SKP2 is a MYC target gene in K562 cells. We thus evaluated whether MYC-induced SKP2 also resulted in p27 down-regulation in our models. p27 can be degraded in cytoplasm by a SKP2-independent pathway (60, 61), but SKP2-dependent ubiquitylation of p27 takes place in the cell nucleus (15). We thus performed immunofluorescence studies to explore the localization of both proteins in the K562 model. The results in Kp27MER cells showed that MYC acti-

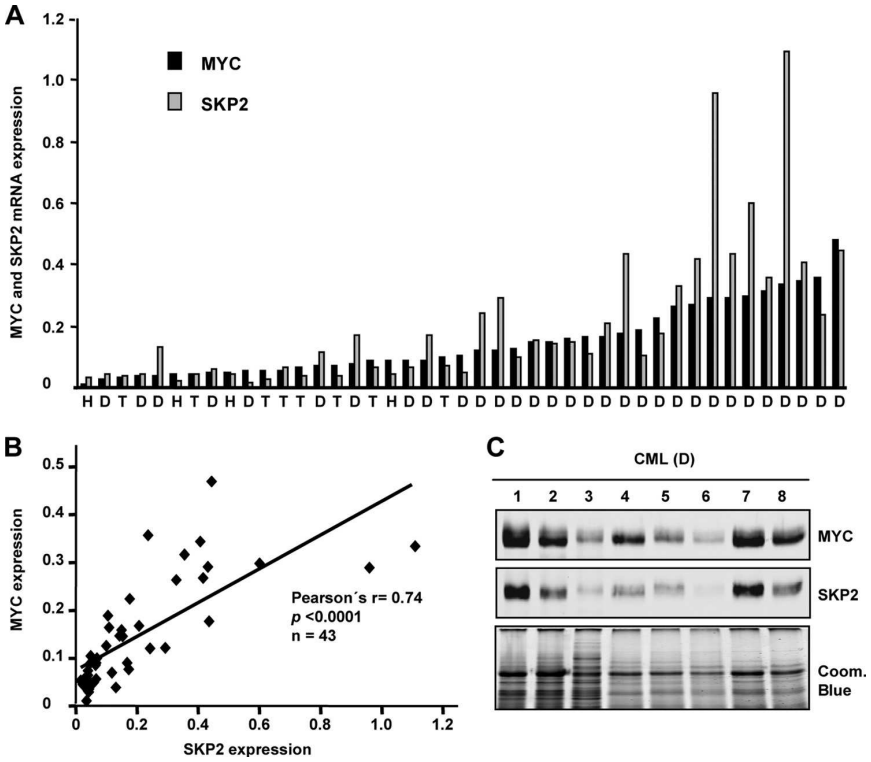

FIGURE 6. **MYC and SKP2 expression in CML patients.** *A*, RT-qPCR analysis of MYC and SKP2 mRNA expression in 31 samples from CML patients at diagnosis in chronic phase (*D*), 8 patients in complete molecular response under imatinib treatment (*T*), and 4 healthy donors (*H*). The data are the means of three determinations, arranged from low to high MYC expression. mRNA values were normalized to the levels of ribosomal protein small 14 in each case. *B*, correlation between MYC and SKP2 levels in CML patients. The *solid line* indicates the linear prediction. The Pearson's *r*, and *p* values are indicated. *C*, immunoblot showing SKP2 and MYC expression in samples of CML patients at diagnosis. A picture of the gel stained with Coomassie (*Coom.*) Blue is shown to assess protein loading.

vation resulted in increased nuclear SKP2 and decreased nuclear p27 levels in most cells. It is of note that some cells showing higher nuclear SKP2 levels also showed lower p27 (Fig. 7*A*).

The actual substrate of the SCF^{SKP2} complex is p27 phosphorylated in threonine 187 (26). For MYC-mediated degradation of p27 via SKP2 up-regulation, it is thus necessary that a substantial fraction of p27 be in the form of Thr(P)-187-p27. In a kinetic study to determine total p27 and Thr(P)-187-p27 in Kp27MER cells treated with Zn^{2+} and 4HT (4–24 h), MYC initially provoked an increase in the phosphorylated p27 fraction (10-fold after 8 h compared with control cells; Fig. 7*B*). At longer treatment times, the phospho-p27 fraction and the total p27 levels were reduced, as anticipated. We performed a dose-response study to analyze total p27 and Thr(P)-187-p27 levels in cells treated with 50 or 75 μM Zn^{2+} and 4HT (12 h). The results again showed that MYC activation resulted in a significant increase in the Thr(P)-187-p27 fraction (Fig. 7*C*). This increased p27 phosphorylation can be explained in part by the MYC-induced up-regulation of CDK2 and cyclins in these cells (40).

MYC Reduces p27 Protein Levels in K562—The previous results indicated that SKP2 and p27 colocalize in the nucleus and that a significant fraction of p27 is phosphorylated in Thr-187, a prerequisite to acting as a SKP2 substrate. We assayed the MYC effect on ectopic p27 levels after p27 induction with 50 μM $ZnSO_4$. At this $ZnSO_4$ concentration, p27 levels were not high enough to titrate out the SCF^{SKP2} system, as occurs with higher $ZnSO_4$ doses (Fig. 7*B* and data not shown). Immunoblot analysis showed that MYC activation with 4HT resulted in a significant decrease in p27 levels when p27 was induced with Zn^{2+} (Fig. 8*A*, compare *lanes 1* and *2* and *lanes 3* and *4*). Consistent with the reduction in p27, the proliferation rate was augmented by MYC in Kp27MER cells treated with 50 μM $ZnSO_4$ (data not shown and Ref. 40). In contrast, 4HT did not reduce p27 levels in parental Kp27-5 cells, which bear a Zn^{2+}-inducible p27 but not the *MycER* construct (Fig. 8*B*). We also tested the MYC effect on the endogenous p27 that is up-regulated when the KMER4 cells reach quiescence by culture saturation ($\sim 1.5 \times 10^6$ cells/ml after 3 days of culture). Immunoblot results demonstrated that SKP2 levels were higher and p27 was lower in cells with activated MYC (Fig. 8*C*).

As a second approach to testing the MYC-SKP-p27 axis in our model, we infected KMER4 cells with retrovirus expressing a short hairpin SKP2 (shSKP2) vector to generate the cell line KMERshSKP2. Immunoblot results confirmed that SKP2 levels were reduced by shSKP2 and that p27 levels were concomitantly increased (Fig. 9*A*) compared with the KMERpSR cell line expressing the empty vector. In agreement with the increased p27 abundance, shSKP2-expressing cells grew at a

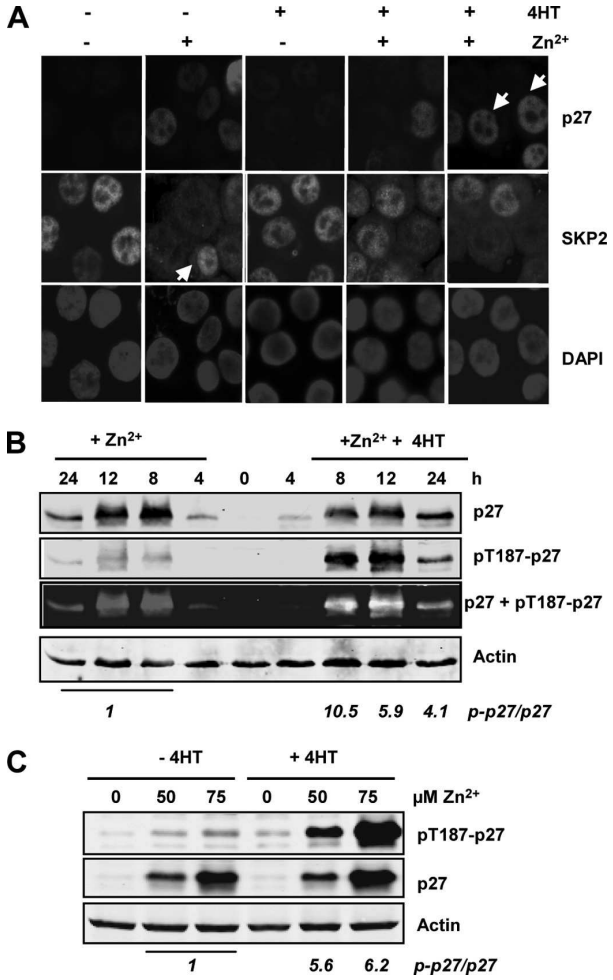

FIGURE 7. **SKP2 colocalizes with p27 in the cell nucleus and Myc induces p27 phosphorylation.** *A*, immunofluorescence of p27 and SKP2 proteins in Kp27MER cells exposed for 24 h to $ZnSO_4$ and 4HT. Most 4HT-treated cells expressed nuclear SKP2, but two fields were selected to show cells with low SKP2 and high p27 levels (*arrows*). Most cells exposed to $ZnSO_4$ showed high p27 levels and low SKP2 in the nuclei, but a field was selected showing a cell with high SKP2 and low p27 (*arrow*). The nuclei were DAPI-stained. *B*, Kp27MER cells were treated for 4–24 h with 75 μM $ZnSO_4$. Total p27, Thr(P)-187-p27 (*pT187-p27*), and actin (as loading control) were assayed by immunoblotting. The *third panel* shows the signal of total p27 (*red*) and phospho-p27 (*green*) to show the coexpression of both forms (*yellow*). Total p27 and Thr(P)-187-p27 ratios as determined by densitometry are shown (*bottom panel*). *C*, Kp27MER cells were treated for 12 h with 200 nM 4HT and 50 or 75 μM $ZnSO_4$, as indicated. Total p27, Thr(P)-187-p27 (*pT187-p27*), and actin (loading control) were assayed by immunoblot. Total p27:Thr(P)-187-p27 signal ratios, as determined by densitometry, are shown (*bottom panel*).

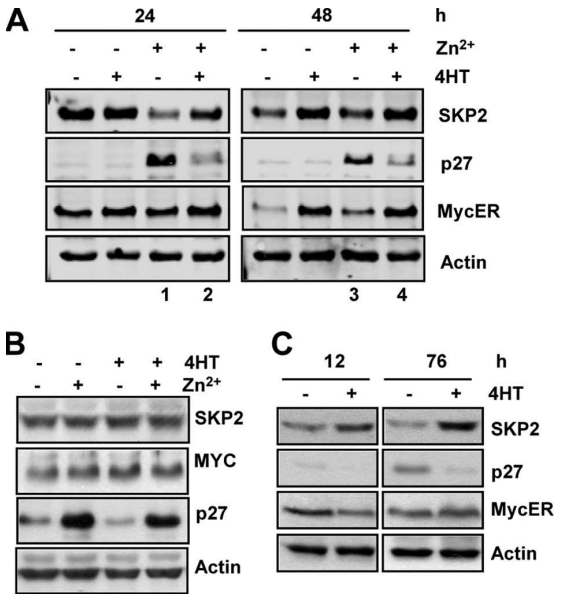

FIGURE 8. **MYC-induced SKP2 correlates with p27 down-regulation.** *A*, expression of p27 in Kp27MER after MYC activation. The cells were treated with 200 nM 4HT and 50 μM $ZnSO_4$ for 24 and 48 h. p27, SKP2, and MYC protein levels were determined by immunoblot. *B*, Kp27-5 cells were treated for 48 h with $ZnSO_4$ and 4HT, and protein levels of SKP2, MYC, p27 and actin (loading control) were determined by immunoblot. *C*, KMER4 cells were cultured for 76 h to reach quiescence caused by cell density, alone or with 200 nM 4HT to activate MYC. SKP2, p27, and MycER protein levels were determined by immunoblot.

reduced rate (Fig. 9*B*) and showed cell accumulation in the G_1 phase (not shown). This difference in growth rates was reproduced *in vivo*; whereas KMERpSR xenografts readily formed tumors in nude mice, KMERshSKP2 cells did not form tumors, or they were much smaller (Fig. 9, *C* and *D*). Consistent with the lack of SKP2, p27 levels were not reduced by MYC in cells expressing shSKP2 (not shown). Previous reports describe a positive effect of SKP2 on MYC stability and transcriptional activity (62, 63). Nonetheless, we found no significant changes in MYC levels after SKP2 silencing in K562 cells (Fig. 9*A*). We also tested MYC transcriptional activity after SKP2 silencing by the shSKP2 expression vector. SKP2 silencing was confirmed by immunoblot (Fig. 9*E*), but luciferase assays failed to show a significant SKP2 effect on MYC-dependent transcriptional activity (Fig. 9*F*). Collectively, our results show that MYC induces SKP2 and that this induction is responsible, at least in part, for p27 down-regulation.

DISCUSSION

MYC stimulates proliferation, and SKP2 expression is associated with cell cycle progression (actually, SKP2 stands for S phase kinase-associated protein 2). This has made it difficult to date to distinguish whether SKP2 induction is a direct or an indirect effect of MYC. Here we used four K562 cell-based models in which MYC can be induced or activated in cell cycle-arrested cells. Proliferation arrest was achieved by several approaches: ectopic p27 overexpression, p53 activation, TPA, and imatinib treatments. In all cases, MYC induction resulted in SKP2 up-regulation. In TM1 epithelial cells, MYC repression similarly provoked SKP2 down-regulation although cells continued to proliferate. SKP2 regulation by MYC was therefore not an indirect effect of MYC-induced cell cycle progression. Moreover, our data strongly suggest that SKP2 is a direct MYC target gene based on three additional observations: (i) MYC up-regulates SKP2 mRNA expression when protein synthesis is inhibited, (ii) MYC activates the SKP2 promoter in luciferase reporter assays, and (iii) MYC binds to an E-box in the 5′ regulatory region of human SKP2 in ChIP assays. Up-regulation of SKP2 was also recently reported in MYC-induced murine lym-

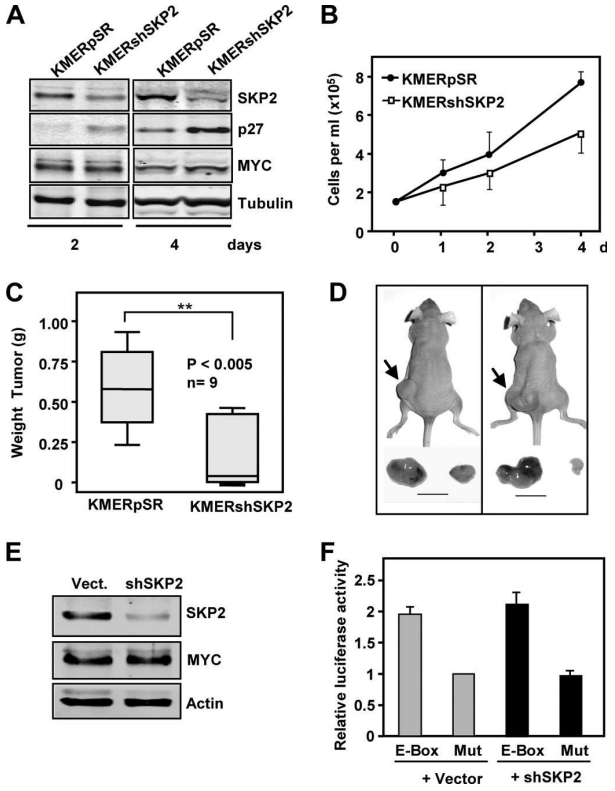

FIGURE 9. **SKP2 silencing results in increased p27 without modifying MYC levels or activity.** *A*, KMERshSKP2 and KMERpSR cells were cultured for 2 and 4 days, and the protein levels of SKP2, p27, MYC, and α-tubulin (loading control) in cell lysates were assessed by immunoblot. *B*, proliferation rates of KMERpSR and KMERshSKP2 cells were measured by counting viable cells in a hemocytometer. The values are the means ± S.E. of three independent experiments. *C*, KMERpSR and KMERshSKP2 cells were injected into the left and right flanks, respectively, of nude mice. Tumor weight was scored after 15–20 days and is shown in the box plot (covering from 25 to 75% percentiles). The *line* represents the median. *D*, representative tumors induced in nude mice. *Bar*, 1 cm. *E*, immunoblot analysis of transfected cell lysates to assess down-regulation of SKP2 protein in cells expressing the shSKP2 vector (*Vect.*). *F*, transactivation of a MYC-responsive reporter in cells with silenced SKP2. K562 cells were cotransfected with the shSKP2 vector or the corresponding empty vector and the 4×Ebox-Luc or 4xE-boxMut-Luc luciferase reporters (*Mut*). At 36 h post-transfection, the cell lysates were prepared, and luciferase activity was determined. The data were normalized to *Renilla* luciferase activity for transfection efficiency. The data show the means ± S.E. of three measurements in two duplicate experiments.

phoma, although in contrast to our results, SKP2 was not described as a direct target of MYC and had no effect on p27 degradation (34). The reason for this discrepancy could lie in the different cell types and species involved, although MYC binding to the SKP2 promoter of mouse embryonic stem cells has recently been reported (64).

Our K562 cell model is derived from CML, and in a cohort of CML patient bone marrow samples, we found a correlation between SKP2 and MYC expression. Expression of the tyrosine kinase BCR-ABL is the hallmark of CML (65). SKP2 is reported to be a mediator of BCR-ABL-induced myeloid leukemia in mice (66), stressing the importance of MYC-mediated induction of SKP2 in CML cells. Cancer gene expression databases such as Oncomine and GeneSapiens also show a MYC-SKP2 correlation in human lymphomas with activated MYC. Our data are consistent with recent reports that SKP2 is among the MYC-induced genes in transcriptional profiling analysis in murine hematopoietic stem cells (67) and in genome-wide transcriptional response to MYC silencing in human breast carcinoma cells (68). SKP2 is nonetheless subject to complex regulation by several transcription factors besides MYC, and SKP2 expression should thus not be expected to correlate to MYC in all cell types or tumors. However, our results show that MYC is required for serum-dependent SKP2 expression in rat fibroblasts.

p27 can be degraded via SKP2-dependent and -independent systems (61, 69). The phenotype of *Skp2*$^{-/-}$ mice and cells is rescued by the concomitant knock-out of the p27 (*Cdkn1B*) gene, however, indicating that the main transformation mechanism of SKP2 is linked to p27 degradation (70, 71). In our K562 model, SKP2 induction by MYC also results in reduced p27 levels. Moreover, Thr-187 phosphorylation is a prerequisite for SKP2 binding, and MYC promotes p27 phosphorylation at Thr-187. Although other unknown mechanisms may also operate, Thr-187 phosphorylation is likely related to the MYC-induced up-regulation of CDK2 and cyclins A and E reported in many systems (8, 11). A MYC-induced up-regulation of p27-bound CDK2 has also been reported in K562 cells (40). Thus, MYC would drive p27 degradation by increasing both the levels of SKP2 and of its substrate Thr(P)-187-p27. In other models, MYC is reported to induce other SCF complex members such as CKS1 (33) or CUL1 (32), reinforcing the idea that control of p27 levels is an important MYC function.

SKP2 is reported to participate in MYC degradation and, at the same time, to activate MYC transcriptional activity (62, 63). However, in our model, the SKP2 effect on MYC levels was marginal, in contrast to the decrease observed in p27. In addition, we detected no effect on MYC transcriptional activity as measured with luciferase reporters. This discrepancy might be due to the different cell types used in our study. A recent report showed that MYC degradation in hematopoietic cells is only dependent on FBW7 ubiquitin ligase and not on SKP2 (67). Another possible explanation is exhaustion of the SKP2-dependent degradation machinery for MYC in our system (63), because the K562 cell line expresses high basal MYC levels compared with other human leukemia cell lines (72).

The demonstration of *SKP2* as a MYC target gene reveals a previously unreported mechanism for the transforming activity, because SKP2 is itself an oncogenic protein. It is widely accepted that abrogation of p27 activity is one of the MYC transforming mechanisms. Here we propose another mechanism, that of p27 degradation through SKP2 induction. Our data strongly suggest that the MYC deregulation/SKP2 induction/p27 degradation axis contributes to the carcinogenic mechanism of MYC.

Acknowledgments—We thank Jesus Gil for shMyc vector, Novartis for imatinib mesylate, John Sedivy for Myc-null cells, Pilar Frade and Carmen E. López-Jorge for technical assistance, and the staff of the Departments of Hematology of Hospital Universitario Marqués de Valdecilla (Santander) and Hospital Universitario Dr. Negrín (Las Palmas) for providing patient samples. We are grateful to M. Dolores Delgado for comments on the manuscript.

REFERENCES

1. Eilers, M., and Eisenman, R. N. (2008) *Genes Dev.* **22,** 2755–2766
2. Meyer, N., and Penn, L. Z. (2008) *Nat. Rev. Cancer* **8,** 976–990
3. Leon, J., Ferrandiz, N., Acosta, J. C., and Delgado, M. D. (2009) *Cell Cycle* **8,** 1148–1157
4. Zeller, K. I., Zhao, X., Lee, C. W., Chiu, K. P., Yao, F., Yustein, J. T., Ooi, H. S., Orlov, Y. L., Shahab, A., Yong, H. C., Fu, Y., Weng, Z., Kuznetsov, V. A., Sung, W. K., Ruan, Y., Dang, C. V., and Wei, C. L. (2006) *Proc. Natl. Acad. Sci. U.S.A.* **103,** 17834–17839
5. Orian, A., van Steensel, B., Delrow, J., Bussemaker, H. J., Li, L., Sawado, T., Williams, E., Loo, L. W., Cowley, S. M., Yost, C., Pierce, S., Edgar, B. A., Parkhurst, S. M., and Eisenman, R. N. (2003) *Genes Dev.* **17,** 1101–1114
6. Li, Z., Van Calcar, S., Qu, C., Cavenee, W. K., Zhang, M. Q., and Ren, B. (2003) *Proc. Natl. Acad. Sci. U.S.A.* **100,** 8164–8169
7. Fernandez, P. C., Frank, S. R., Wang, L., Schroeder, M., Liu, S., Greene, J., Cocito, A., and Amati, B. (2003) *Genes Dev.* **17,** 1115–1129
8. Dang, C. V., O'Donnell, K. A., Zeller, K. I., Nguyen, T., Osthus, R. C., and Li, F. (2006) *Semin. Cancer Biol* **16,** 253–264
9. Patel, J. H., Loboda, A. P., Showe, M. K., Showe, L. C., and McMahon, S. B. (2004) *Nat. Rev. Cancer* **4,** 562–568
10. Nesbit, C. E., Tersak, J. M., and Prochownik, E. V. (1999) *Oncogene* **18,** 3004–3016
11. Lutz, W., Leon, J., and Eilers, M. (2002) *Biochim. Biophys. Acta* **1602,** 61–71
12. Delgado, M. D., and Leon, J. (2010) *Genes Cancer* **1,** 605–616
13. Hershko, D. D. (2008) *Cancer* **112,** 1415–1424
14. Frescas, D., and Pagano, M. (2008) *Nat. Rev. Cancer* **8,** 438–449
15. Nakayama, K. I., and Nakayama, K. (2006) *Nat. Rev. Cancer* **6,** 369–381
16. Kitagawa, K., Kotake, Y., and Kitagawa, M. (2009) *Cancer Sci.* **100,** 1374–1381
17. Polyak, K., Lee, M. H., Erdjument-Bromage, H., Koff, A., Roberts, J. M., Tempst, P., and Massagué, J. (1994) *Cell* **78,** 59–66
18. Coats, S., Flanagan, W. M., Nourse, J., and Roberts, J. M. (1996) *Science* **272,** 877–880
19. Chu, I. M., Hengst, L., and Slingerland, J. M. (2008) *Nat. Rev. Cancer* **8,** 253–267
20. Slingerland, J., and Pagano, M. (2000) *J. Cell. Physiol.* **183,** 10–17
21. Pagano, M., Tam, S. W., Theodoras, A. M., Beer-Romero, P., Del Sal, G., Chau, V., Yew, P. R., Draetta, G. F., and Rolfe, M. (1995) *Science* **269,** 682–685
22. Carrano, A. C., Eytan, E., Hershko, A., and Pagano, M. (1999) *Nat. Cell Biol.* **1,** 193–199
23. Sutterlüty, H., Chatelain, E., Marti, A., Wirbelauer, C., Senften, M., Müller, U., and Krek, W. (1999) *Nat. Cell Biol.* **1,** 207–214
24. Tsvetkov, L. M., Yeh, K. H., Lee, S. J., Sun, H., and Zhang, H. (1999) *Curr. Biol.* **9,** 661–664
25. Galea, C. A., Wang, Y., Sivakolundu, S. G., and Kriwacki, R. W. (2008) *Biochemistry* **47,** 7598–7609
26. Lu, Z., and Hunter, T. (2010) *Cell Cycle* **9,** 2342–2352
27. Martins, C. P., and Berns, A. (2002) *EMBO J.* **21,** 3739–3748
28. Yang, W., Shen, J., Wu, M., Arsura, M., FitzGerald, M., Suldan, Z., Kim, D. W., Hofmann, C. S., Pianetti, S., Romieu-Mourez, R., Freedman, L. P., and Sonenshein, G. E. (2001) *Oncogene* **20,** 1688–1702
29. Chandramohan, V., Jeay, S., Pianetti, S., and Sonenshein, G. E. (2004) *J. Immunol.* **172,** 5522–5527
30. Perez-Roger, I., Kim, S. H., Griffiths, B., Sewing, A., and Land, H. (1999) *EMBO J.* **18,** 5310–5320
31. Bouchard, C., Thieke, K., Maier, A., Saffrich, R., Hanley-Hyde, J., Ansorge, W., Reed, S., Sicinski, P., Bartek, J., and Eilers, M. (1999) *EMBO J.* **18,** 5321–5333
32. O'Hagan, R. C., Ohh, M., David, G., de Alboran, I. M., Alt, F. W., Kaelin, W. G., Jr., and DePinho, R. A. (2000) *Genes Dev.* **14,** 2185–2191
33. Keller, U. B., Old, J. B., Dorsey, F. C., Nilsson, J. A., Nilsson, L., MacLean, K. H., Chung, L., Yang, C., Spruck, C., Boyd, K., Reed, S. I., and Cleveland, J. L. (2007) *EMBO J.* **26,** 2562–2574
34. Old, J. B., Kratzat, S., Hoellein, A., Graf, S., Nilsson, J. A., Nilsson, L., Nakayama, K. I., Peschel, C., Cleveland, J. L., and Keller, U. B. (2010) *Mol Cancer Res.* **8,** 353–362
35. Bernard, D., Pourtier-Manzanedo, A., Gil, J., and Beach, D. H. (2003) *J. Clin. Invest.* **112,** 1724–1731
36. Andreu, E. J., Lledó, E., Poch, E., Ivorra, C., Albero, M. P., Martínez-Climent, J. A., Montiel-Duarte, C., Rifón, J., Pérez-Calvo, J., Arbona, C., Prósper, F., and Pérez-Roger, I. (2005) *Cancer Res.* **65,** 3264–3272
37. Delgado, M. D., Lerga, A., Cañelles, M., Gómez-Casares, M. T., and León, J. (1995) *Oncogene* **10,** 1659–1665
38. Littlewood, T. D., Hancock, D. C., Danielian, P. S., Parker, M. G., and Evan, G. I. (1995) *Nucleic Acid Res.* **23,** 1686–1690
39. Muñoz-Alonso, M. J., Acosta, J. C., Richard, C., Delgado, M. D., Sedivy, J., and León, J. (2005) *J. Biol. Chem.* **280,** 18120–18129
40. Acosta, J. C., Ferrándiz, N., Bretones, G., Torrano, V., Blanco, R., Richard, C., O'Connell, B., Sedivy, J., Delgado, M. D., and León, J. (2008) *Mol. Cell. Biol.* **28,** 7286–7295
41. Ceballos, E., Delgado, M. D., Gutierrez, P., Richard, C., Müller, D., Eilers, M., Ehinger, M., Gullberg, U., and León, J. (2000) *Oncogene* **19,** 2194–2204
42. Warner, B. J., Blain, S. W., Seoane, J., and Massagué, J. (1999) *Mol. Cell. Biol.* **19,** 5913–5922
43. Mateyak, M. K., Obaya, A. J., Adachi, S., and Sedivy, J. M. (1997) *Cell Growth Differ.* **8,** 1039–1048
44. Schuhmacher, M., Staege, M. S., Pajic, A., Polack, A., Weidle, U. H., Bornkamm, G. W., Eick, D., and Kohlhuber, F. (1999) *Curr. Biol.* **9,** 1255–1258
45. Shang, Y., Hu, X., DiRenzo, J., Lazar, M. A., and Brown, M. (2000) *Cell* **103,** 843–852
46. Huang, Y. C., and Hung, W. C. (2006) *J. Cell. Physiol.* **209,** 363–369
47. Kiessling, A., Sperl, B., Hollis, A., Eick, D., and Berg, T. (2006) *Chem. Biol.* **13,** 745–751
48. Baccarani, M., Cortes, J., Pane, F., Niederwieser, D., Saglio, G., Apperley, J., Cervantes, F., Deininger, M., Gratwohl, A., Guilhot, F., Hochhaus, A., Horowitz, M., Hughes, T., Kantarjian, H., Larson, R., Radich, J., Simonsson, B., Silver, R. T., Goldman, J., and Hehlmann, R. (2009) *J. Clin. Oncol.* **27,** 6041–6051
49. Penn, L. J., Brooks, M. W., Laufer, E. M., and Land, H. (1990) *EMBO J.* **9,** 1113–1121
50. Grignani, F., Lombardi, L., Inghirami, G., Sternas, L., Cechova, K., and Dalla-Favera, R. (1990) *EMBO J.* **9,** 3913–3922
51. Gómez-Casares, M. T., Vaqué, J. P., Lemes, A., Molero, T., Delgado, M. D., and León, J. (2004) *Haematologica* **89,** 241–243
52. Chen, J. Y., Wang, M. C., and Hung, W. C. (2009) *Leuk. Res.* **33,** 1520–1524
53. Xie, S., Lin, H., Sun, T., and Arlinghaus, R. B. (2002) *Oncogene* **21,** 7137–7146
54. Lerga, A., Crespo, P., Berciano, M., Delgado, M. D., Cañelles, M., Calés, C., Richard, C., Ceballos, E., Gutierrez, P., Ajenjo, N., Gutkind, S., and León, J. (1999) *Cell Growth Differ.* **10,** 639–654
55. Pajic, A., Spitkovsky, D., Christoph, B., Kempkes, B., Schuhmacher, M., Staege, M. S., Brielmeier, M., Ellwart, J., Kohlhuber, F., Bornkamm, G. W., Polack, A., and Eick, D. (2000) *Int. J. Cancer* **87,** 787–793
56. Grandori, C., Mac, J., Siëbelt, F., Ayer, D. E., and Eisenman, R. N. (1996) *EMBO J.* **15,** 4344–4357
57. Kim, J., Lee, J. H., and Iyer, V. R. (2008) *Plos One* **3,** e1798
58. Kim, J. W., Zeller, K. I., Wang, Y., Jegga, A. G., Aronow, B. J., O'Donnell, K. A., and Dang, C. V. (2004) *Mol. Cell. Biol.* **24,** 5923–5936
59. Kilpinen, S., Autio, R., Ojala, K., Iljin, K., Bucher, E., Sara, H., Pisto, T., Saarela, M., Skotheim, R. I., Björkman, M., Mpindi, J. P., Haapa-Paananen, S., Vainio, P., Edgren, H., Wolf, M., Astola, J., Nees, M., Hautaniemi, S., and Kallioniemi, O. (2008) *Genome Biol.* **9,** R139
60. Hara, T., Kamura, T., Nakayama, K., Oshikawa, K., Hatakeyama, S., and Nakayama, K. (2001) *J. Biol. Chem.* **276,** 48937–48943
61. Kamura, T., Hara, T., Matsumoto, M., Ishida, N., Okumura, F., Hatakeyama, S., Yoshida, M., Nakayama, K., and Nakayama, K. I. (2004) *Nat. Cell Biol.* **6,** 1229–1235
62. Kim, S. Y., Herbst, A., Tworkowski, K. A., Salghetti, S. E., and Tansey, W. P. (2003) *Mol. Cell* **11,** 1177–1188
63. von der Lehr, N., Johansson, S., Wu, S., Bahram, F., Castell, A., Cetinkaya,

C., Hydbring, P., Weidung, I., Nakayama, K., Nakayama, K. I., Söderberg, O., Kerppola, T. K., and Larsson, L. G. (2003) *Mol. Cell* **11,** 1189–1200
64. Kim, J., Woo, A. J., Chu, J., Snow, J. W., Fujiwara, Y., Kim, C. G., Cantor, A. B., and Orkin, S. H. (2010) *Cell* **143,** 313–324
65. Melo, J. V., and Barnes, D. J. (2007) *Nat. Rev Cancer* **7,** 441–453
66. Agarwal, A., Bumm, T. G., Corbin, A. S., O'Hare, T., Loriaux, M., VanDyke, J., Willis, S. G., Deininger, J., Nakayama, K. I., Druker, B. J., and Deininger, M. W. (2008) *Blood* **112,** 1960–1970
67. Reavie, L., Della Gatta, G., Crusio, K., Aranda-Orgilles, B., Buckley, S. M., Thompson, B., Lee, E., Gao, J., Bredemeyer, A. L., Helmink, B. A., Zavadil, J., Sleckman, B. P., Palomero, T., Ferrando, A., and Aifantis, I. (2010) *Nat. Immunol.* **11,** 207–215
68. Cappellen, D., Schlange, T., Bauer, M., Maurer, F., and Hynes, N. E. (2007) *EMBO Rep.* **8,** 70–76
69. Miranda-Carboni, G. A., Krum, S. A., Yee, K., Nava, M., Deng, Q. E., Pervin, S., Collado-Hidalgo, A., Galic, Z., Zack, J. A., Nakayama, K., Nakayama, K. I., and Lane, T. F. (2008) *Genes Dev.* **22,** 3121–3134
70. Nakayama, K., Nagahama, H., Minamishima, Y. A., Miyake, S., Ishida, N., Hatakeyama, S., Kitagawa, M., Iemura, S., Natsume, T., and Nakayama, K. I. (2004) *Dev. Cell* **6,** 661–672
71. Kossatz, U., Dietrich, N., Zender, L., Buer, J., Manns, M. P., and Malek, N. P. (2004) *Genes Dev.* **18,** 2602–2607
72. Delgado, M. D., Chernukhin, I. V., Bigas, A., Klenova, E. M., and León, J. (1999) *FEBS Lett.* **444,** 5–10

MOLECULAR AND CELLULAR BIOLOGY, Dec. 2008, p. 7286–7295 Vol. 28, No. 24
0270-7306/08/$08.00+0 doi:10.1128/MCB.00752-08

Myc Inhibits p27-Induced Erythroid Differentiation of Leukemia Cells by Repressing Erythroid Master Genes without Reversing p27-Mediated Cell Cycle Arrest▽‡

Juan C. Acosta,[1]†§ Nuria Ferrándiz,[1]† Gabriel Bretones,[1] Verónica Torrano,[1] Rosa Blanco,[1] Carlos Richard,[2] Brenda O'Connell,[3] John Sedivy,[3] M. Dolores Delgado,[1] and Javier León[1]*

Cancer Molecular Biology Group, Department of Molecular Biology, Instituto de Biomedicina y Biotecnología de Cantabria, Universidad de Cantabria-CSIC-IDICAN, Santander, Spain[1]; Department of Hematology, Hospital Universitario Marqués de Valdecilla-IFIMAV, Santander, Spain[2]; and Department of Molecular Biology, Cell Biology, and Biochemistry and Center for Genomics and Proteomics, Brown University, Providence, Rhode Island[3]

Received 9 May 2008/Returned for modification 13 June 2008/Accepted 28 September 2008

Inhibition of differentiation has been proposed as an important mechanism for Myc-induced tumorigenesis, but the mechanisms involved are unclear. We have established a genetically defined differentiation model in human leukemia K562 cells by conditional expression of the cyclin-dependent kinase (Cdk) inhibitor p27 (inducible by Zn^{2+}) and Myc (activatable by 4-hydroxy-tamoxifen). Induction of p27 resulted in erythroid differentiation, accompanied by Cdk inhibition and G_1 arrest. Interestingly, activation of Myc inhibited p27-mediated erythroid differentiation without affecting p27-mediated proliferation arrest. Microarray-based gene expression indicated that, in the presence of p27, Myc blocked the upregulation of several erythroid-cell-specific genes, including NFE2, JUNB, and GATA1 (transcription factors with a pivotal role in erythropoiesis). Moreover, Myc also blocked the upregulation of Mad1, a transcriptional antagonist of Myc that is able to induce erythroid differentiation. Cotransfection experiments demonstrated that Myc-mediated inhibition of differentiation is partly dependent on the repression of Mad1 and GATA1. In conclusion, this model demonstrates that Myc-mediated inhibition of differentiation depends on the regulation of a specific gene program, whereas it is independent of p27-mediated cell cycle arrest. Our results support the hypothesis that differentiation inhibition is an important Myc tumorigenic mechanism that is independent of cell proliferation.

c-Myc (Myc herein after) is an oncogenic transcription factor of the helix-loop-helix/leucine zipper (HLH-LZ) protein family that elicits a variety of biological responses related to cell cycle control, genomic instability, immortalization, energetic metabolism, ribosome biogenesis, apoptosis, intercellular communication, and control of cell differentiation (for reviews, see references 5, 17, 21, and 40). Myc forms heterodimers with the protein Max and the Myc-Max dimers bind to E-boxes in regulatory regions to transactivate genes. Also, an important number of Myc target genes (30 to 50% across different studies) are repressed by Myc-Max in an E-box-independent manner (18, 27, 39, 58; see also the Myc target gene database [www.myccancergene.org]). The mechanism for Myc-mediated transactivation involves chromatin acetylation, whereas the mechanisms for Myc-mediated transrepression remain poorly defined, with the exception of a few genes (1, 9, 11, 41). On the other hand, Max form dimers with proteins of the Mad family. Mad proteins are also HLH-LZ proteins that function as Myc antagonists, since Mad-Max dimers repress transcription upon binding to E-boxes (5, 21). Consistent with the Myc effects on cultured cells and transgenic models, deregulated expression of Myc is found in a wide array of human cancers, in many cases associated with disease progression (30, 36).

Work in different mouse models has demonstrated that Myc promotes differentiation in some tissues by expanding the stem cell population (53, 56) or by promoting both proliferation and differentiation of immature precursors (22). However, enforced Myc expression blocks differentiation of a wide variety of cell types both in vitro and in vivo (for reviews, see references 21 and 40). Actually, inhibition of differentiation was one of the first biological effects described for Myc (8, 16, 44). However, in contrast to the extensive research carried out on the mechanisms by which Myc enhances proliferation, the mechanisms for the Myc-mediated suppression of differentiation are much less known. Since proliferation and differentiation are usually mutually exclusive and Myc drives cells into proliferation, it has been argued that Myc prevents terminal differentiation by blocking the cell cycle exit (21, 40). Consistently, Myc induces the expression of genes that promote cell cycle progression (cyclins D2 and E1, Cdk4) and represses cell cycle inhibitors as $p21^{Waf1}$ and $p27^{Kip1}$ (referred to as p27 hereafter) (30).

p27 was originally described as a negative regulator of cell-cycle progression through the inhibition of cyclin-dependent kinases (Cdks) (37, 46). However, p27 has also been involved in biological functions unrelated to cell cycle, including the differentiation of erythroid precursors (14, 48). Regarding he-

* Corresponding author. Mailing address: Dpto. de Biología Molecular, Facultad de Medicina, Avda. Cardenal Herrera Oria s/n, 39011 Santander, Spain. Phone: 34-942-201952. Fax: 34-942-201945. E-mail: leonj@unican.es.

† J.C.A. and N.F. contributed equally to this study.

‡ Supplemental material for this article may be found at http://mcb.asm.org/.

§ Present address: MRC Clinical Sciences Centre, Faculty of Medicine, Imperial College, Hammersmith Campus, London, United Kingdom.

▽ Published ahead of print on 6 October 2008.

matopoiesis, p27 is expressed in $CD34^+$ progenitor cells and in the primitive erythroid precursors (48, 55), but p27-deficient mice do not show gross abnormalities in the hematopoietic lineages (reviewed in reference 34).

A functional antagonism between Myc and p27 in proliferation has been well established: Myc and p27 loss cooperates in animal carcinogenesis models (31), and several reports demonstrate the ability of Myc to abrogate p27 function (7, 43, 51, 54) and expression (54). However, in sharp contrast to the information on the antagonism between Myc and p27 in proliferation, the possible Myc-p27 cross talk in differentiation has not been investigated.

The study of Myc effects on differentiation has been impaired by the complex array of pathways activated by cytokines and chemicals used as differentiation inducers in most model systems. We previously showed that induction of p27 results in erythroid differentiation of K562 (35), and here we have investigated the role of Myc in this genetically defined differentiation model. We found that Myc blocks p27-mediated differentiation but that it cannot rescue the p27-dependent proliferation arrest and Cdk inhibition. We also report that Myc blocks the upregulation of Mad1 and of a set of erythroid-differentiation-determining genes such as the transcription factor GATA1.

MATERIALS AND METHODS

Cell culture, differentiation assays, and transfections. K562 cells were grown in RPMI 1640 medium supplemented with 8% fetal calf serum and antibiotics. Kp27MER and KMER4 sublines were generated electroporating the pBABE-MycER plasmid (28) into Kp27-5 and KMT sublines, which have been described previously (35). The Kp27pBP and KMTpBP sublines were generated by electroporating Kp27-5 and KMT with pBABE-puro vector. A total of 10^7 cells were electroporated with 20 μg of DNA (260 V and 1 mFa in a Bio-Rad gene pulser) and selected with 1 μg of puromycin (Sigma)/ml. Cells (2.5×10^5 cells/ml) were treated with $ZnSO_4$ to induce p27 expression, and 4-hydroxy-tamoxifen (4HT; Sigma) to activate MycER. Unless otherwise stated, $ZnSO_4$ and 4HT were used at 75 μM and 100 nM, respectively. Transient transfection of Kp27MER (80,000 cells) was carried out with Lipofectamine 2000 (Invitrogen) with 1.2 μg of pEF-GATA1 (50) and pEF-NFE2 (29) vectors or empty vector. Nucleofections of K562 cells were performed in a Nucleofector (Amaxa) according to the manufacturer's indications with pCEFL-Myc (32), pCEFL-Mad1 (constructed by inserting human Mad1cDNA into the pCEFL vector), pCEFL-p27 (35), pCEFL-MycV394D, pME-MycD106-143 (49), CMV-MadMyc (6), pEF-GATA1, pEF-NFE2, and 0.25 μg of a green fluorescent protein (GFP) vector (pmaxGFP; Amaxa) to assess transfection efficiency.

Proliferation and cell cycle assays. Cell counting was performed in hemacytometer. For DNA synthesis assay, cells were pulsed with 30 μM bromodeoxyuridine (BrdU; Roche Applied Science) for 1 h, fixed in 90% ethanol, treated with RNase and HCl, and incubated with fluorescein isothiocyanate-conjugated anti-BrdU monoclonal antibody (Roche Applied Science) for 30 min as described previously (34). Cells were analyzed by flow cytometry (Excalibur; BD Biosciences). For cell cycle analysis, cells were resuspended in phosphate-buffered saline (PBS)-sodium citrate buffer containing 10 μg of bovine serum albumin/ml, 200 μg of RNase/ml, and 50 μg of propidium iodide (Sigma Chemical Co.)/ml. The cells were incubated at 37°C in darkness for 30 min and then analyzed by flow cytometry using CellQuest software.

RNA analysis. Total RNA was isolated by using an RNeasy kit (Qiagen). For reverse transcription-PCR (RT-PCR), first-strand cDNA was synthesized from 1 μg of total RNA by using SuperScript II RNase reverse transcriptase (Invitrogen) with random primers. Quantitative PCR (qPCR) was performed with a QuantiTect Sybr green PCR kit (Qiagen). The sequences of the primers used and amplicon sizes are shown in the Table S1 in the supplemental material. The data were normalized to ribosomal protein S14 (RPS14) mRNA levels. RPS14 has not been described as the Myc target gene (www.myccancergene.org).

Luciferase reporter assays. Three million of Kp27MER cells were electroporated at 260 V and 1 mFa in a Bio-Rad electroporator with 3 μg of pGL2-M4-Luc reporter (24) and 1 μg of pRL-TK (Promega). After 24 h of incubation, cultures were split into aliquots and further incubated for 24 h with $ZnSO_4$ and/or 4HT. Cells were lysed, and the luciferase activity was measured in duplicate by a dual-luciferase reporter gene assay system (Promega). The data were normalized against the *Renilla* luciferase activity.

Gene expression profiling. Biotinylated cRNA was obtained from total RNA and hybridized to Affymetrix HG-U133A chip in the Genomic Facility of Centro de Investigación del Cancer (Salamanca, Spain). The data analysis and hierarchical tree clusters were generated by using the dChip software (26; see also http://biosun1.harvard.edu/complab/dchip/). The expression data was filtered so as to include genes with expression changes ≥2.3-fold and with a signal difference ≥50 between compared samples. The analysis was performed with data from two independent experiments and RNA preparations of each treatment (control, $ZnSO_4$, 4HT, and $ZnSO_4$ + 4HT) in Kp27MER and K562. The interaction network for differentially expressed genes was generated by using Ingenuity Pathways Analysis software.

Immunofluorescence and immunoblotting. For immunofluorescence, Kp27MER cells were treated with $ZnSO_4$ and/or 4HT for 12 and 24 h and immunostained with the anti-Myc and anti-p27 antibodies, as well as with DAPI (4′,6′-diamidino-2-phenylindole) to stain nuclei. A total of 2×10^4 to 5×10^4 Kp27MER cells were centrifuged at 1,500 rpm for 5 min, resuspended in 8 μl of PBS, and dried on microslides. Cells were fixed for 15 min in 3.7% paraformaldehyde in PBS at room temperature and permeabilized with 0.5% Triton X-100 for 30 min. The cells were then incubated with primary (16 h at 4°C), washed, and incubated with secondary antibodies (1 h at room temperature). The primary antibodies used were anti-Myc rabbit polyclonal antibody and anti-p27 mouse monoclonal antibody (both diluted 1:25). Secondary antibodies were conjugated with Texas Red or FITC (Jackson Laboratories). Cells were mounted with antifading mounting medium Vectashield (Vector Laboratories) with DAPI to visualize the nuclei. Images were recorded by using a Bio-Rad MRC 1024 confocal laser microscope. Immunoblots were performed as previously described (35). Blots were revealed with an ECL system (Amersham). The antibodies used are described in Table S2 in the supplemental material.

Immunoprecipitations and kinase activity assays. Protein extracts (500 μg per assay) were immunoprecipitated with 1 μg of anti-cyclin D2, cyclin D3, and Cdk2 and p27 antibodies (see Table S2 in the supplemental material). Immunoprecipitation and kinase activity assays were performed as described previously (35).

Microarray data were deposited in the ArrayExpress database under accession number E-MEXP-1772.

RESULTS

Generation of K562 sublines with conditional expression of p27 and Myc. We previously reported that induction of p27 in K562 human myeloid cells resulted in G_1 arrest and erythroid differentiation (35). We took advantage of this differentiation system to ask whether Myc interferes with p27-mediated differentiation and to study the possible mechanisms involved. For this purpose, we first generated cells with conditional expression of both p27 and Myc. Kp27-5 cells (which carry a Zn^{2+}-inducible p27 allele) were stably transfected with an expression vector for the fusion protein MycER, where Myc activity is activated by 4HT (28). One of the transfectants, termed Kp27MER, was selected, and immunoblot analysis confirmed that the cells expressed MycER and retained p27 induction by Zn^{2+}. The activation of MycER by 4HT was assessed, first, by the Myc downregulation of endogenous Myc (Fig. 1A), an effect observed in many cell lines, including K562 (12, 42). We further confirmed the activation of MycER by transactivation assays with a luciferase reporter carrying E-boxes (Fig. 1B). Immunofluorescence studies demonstrated that, in Kp27MER cells, $ZnSO_4$ induced a dramatic accumulation of p27 in cell nucleus and that the concomitant activation of Myc by 4HT did not modify this p27 localization (Fig. 1C). Altogether, the results demonstrated the activation of MycER in response to 4HT in Kp27MER cells.

Myc inhibits p27-induced erythroid differentiation. We next sought to determine whether Myc could antagonize the ery-

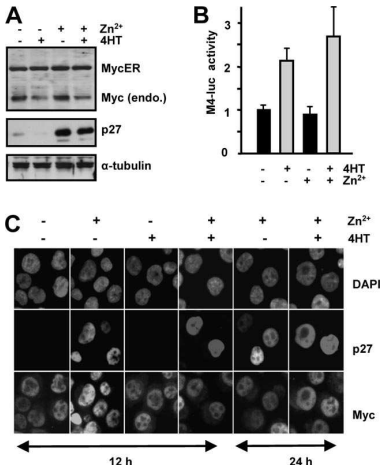

FIG. 1. Myc activation and p27 induction in Kp27MER cells. (A) Kp27MER cells were incubated with 100 nM 4HT and/or 75 μM $ZnSO_4$ during 24 h, and protein extracts were analyzed by Western blotting with antibodies to Myc, p27, and α-tubulin as a loading control. (B) Induction of Myc transactivation activity in Kp27MER in response to 4HT. Cells were electroporated with a Myc-responsive luciferase construct, and after 24 h the cultures were split into aliquots and further incubated for 24 h with $ZnSO_4$ and/or 4HT as indicated. The data represent promoter activity normalized against the *Renilla* luciferase activity. (C) Double immunofluorescence showing p27 and Myc subcellular localization. Kp27MER cells were treated for 12 and 24 h with $ZnSO_4$ and/or 4HT as indicated. Cytospin preparations were subjected to immunofluorescence with anti-Myc and anti-p27 antibodies and stained with DAPI to visualize the nuclei.

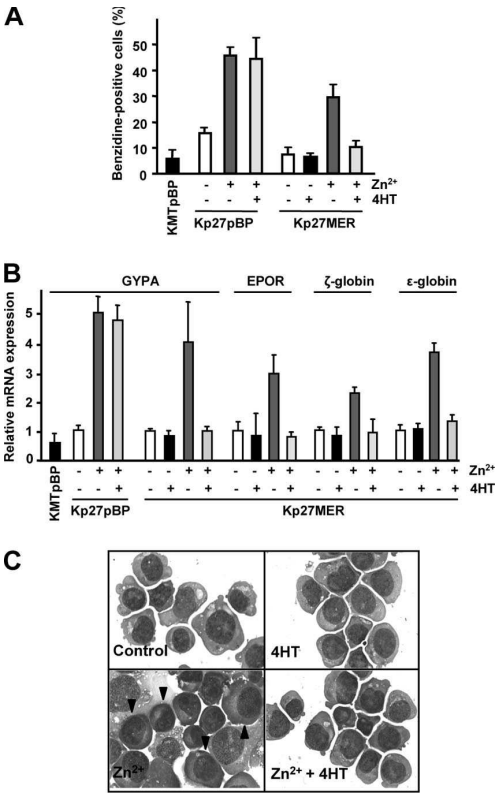

FIG. 2. Myc inhibits the erythroid differentiation induced by p27. (A) Cells were treated for 72 h with $ZnSO_4$ and 4HT, and the fraction of hemoglobinized cells was assayed by the benzidine test. Values are means ± the standard deviations (SD) of three experiments. (B) Downregulation of erythroid genes by Myc. Kp27MER as well as control Kp27pBP cells were treated with $ZnSO_4$ and 4HT as indicated. The expression of the GYPA, EPOR, ζ-globin, and ε-globin expression was determined by RT-qPCR. Cells were incubated with $ZnSO_4$ and/or 4HT for 24 h except GYPA (72 h). Expression levels were graphed relative to untreated Kp27MER cells. The data are means ± the standard errors of the mean (SEM) of three independent experiments. (C) Kp27MER cells were treated for 96 h with 75 μM $ZnSO_4$ and 200 nM 4HT as indicated, and cytospin preparations were stained by the May-Grünwald-Giemsa method. Micrographs of representative fields are shown. Arrows indicate cells with morphological features of erythroid differentiation resembling basophilic erythroblasts.

throid differentiation mediated by p27. Kp27MER cells were treated with $ZnSO_4$ to induce p27 and 4HT to activate Myc, and the erythroid differentiation was analyzed first by the fraction of cells containing hemoglobin as determined by the benzidine test. This fraction was reduced by 4HT in Kp27MER cells but not in control Kp27pBP cells (Fig. 2A). Myc effect was further confirmed by the expression of erythroid-cell-specific genes as glycophorin A (GYPA), erythropoietin receptor (EPOR), ζ-globin, and ε-globin. mRNA levels of these genes were induced by p27, and this induction was blocked by 4HT (Fig. 2B). Finally, Myc also reversed the morphological differentiation into erythroid phenotype induced by p27, as shown by the dramatic reduction in the number of basophilic erythroblast-like cells (Fig. 2C). Altogether, the results show that Myc inhibited p27-induced differentiation.

Myc does not antagonize the proliferation arrest mediated by p27. As proposed for other models, we explored the possibility that Myc could inhibit erythroid differentiation by maintaining the cells in a proliferative state. When p27 was induced with 75 μM Zn^{2+}, Kp27MER cells underwent a rapid growth arrest, similar to that induced by p27 in control cells (Kp27pBP) (Fig. 3A). In agreement with the growth determinations, p27 induction was accompanied by S-phase depletion and G_1-phase arrest (Fig. 3B). Surprisingly, the activation of Myc by 4HT in these conditions did not reverse this arrest (Fig. 3A), and cell cycle analysis revealed the G_1-phase arrest provoked by p27 upon treatment with 75 μM Zn^{2+} was not modified by Myc (i.e., by 4HT treatment) (Fig. 3B). Treatment with lower Zn^{2+} concentrations (50 μM) resulted in moderate p27 levels (Fig. 3C) and a less severe proliferation arrest than with higher p27 levels (i.e., with 75 μM Zn^{2+}) (Fig. 3A). Consistently, moderate p27 levels (i.e., with 50 μM Zn^{2+}) induced a weaker differentiation, which was also blunted by Myc (not shown). In the presence of moderate p27 levels, however, Myc provoked a slight but consistent increase in proliferation (Fig. 3A). This effect depended on Myc since 4HT did not modify the proliferation rate of control Kp27pBP cells (Fig. 3A). Consistently, Myc provoked an increase in the fraction of cells in S phase when the cell cycle was analyzed (Fig. 3B). In agreement with this result, Myc reversed the moderate repression of the mitotic cyclin B1 in cells treated with 50 μM Zn^{2+}, as determined by immunoblot analysis (Fig. 3D). In contrast, the ex-

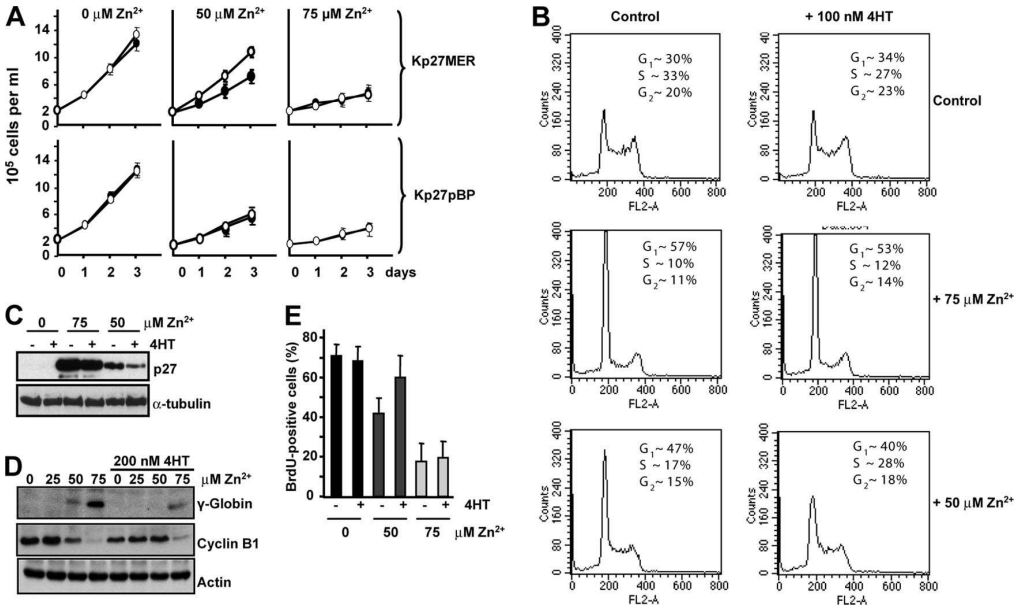

FIG. 3. Myc induced proliferation in p27-arrested cells is p27 dose dependent. (A) Growth curves of Kp27MER and Kp27pBP cells treated with (○) or without (●) 4HT and 75 or 50 μM $ZnSO_4$. Values are means ± the SD of three experiments. (B) Cell cycle analysis of Kp27MER treated for 24 h with 100 nM 4HT and 50 or 75 μM $ZnSO_4$ as indicated. The percentages of the cells in each cell cycle phase are indicated. (C) Dose-dependent expression of p27. Kp27MER cells were treated with 50 and 75 μM $ZnSO_4$ and 4HT for 24 h, and the expression of p27 and α-tubulin (as loading control) was assayed by immunoblotting. (D) Kp27MER cells were treated with the indicated concentrations of $ZnSO_4$ and 4HT, and the expression of cyclin B1 (to assay proliferation), γ-globin (to assay differentiation), and actin (as loading control) was assayed by immunoblotting. (E) DNA synthesis in Kp27MER cells assayed by BrdU incorporation. Cells were incubated during 24 h with or without 4HT and 75 or 50 μM $ZnSO_4$ and pulsed for 1 h with BrdU, and the incorporation of the nucleoside was determined by flow cytometry. The graph shows the percentages of BrdU-positive cells. The data are means ± the SD from three independent experiments.

pression of the erythroid gene γ-globin was similarly blunted by Myc in the presence of 75 or 50 μM Zn^{2+}. The results were confirmed by measurements of DNA synthesis by BrdU incorporation assays. As expected, DNA synthesis was halted in Kp27MER cells treated with 75 μM Zn^{2+} (i.e., high p27 levels). Activation of Myc did not relieve this inhibition (Fig. 3E). However, DNA synthesis was not totally inhibited in cells treated with 50 μM Zn^{2+} (moderate p27 levels), and Myc induced a moderate increase in DNA synthesis (Fig. 3E). We conclude that Myc inhibits p27-induced erythroid differentiation without reversing the p27-mediated cell cycle arrest.

Myc does not reverse p27-mediated inhibition of Cdks. The best-defined biochemical activity of p27 is the inhibition of Cdk activity. Thus, we sought to determine whether Myc impaired this activity in the K562 model in conditions where Myc is blocking differentiation. We first compared the expression of cyclins D and Cdk4, Cdk6, and Cdk2 in cells arrested and differentiated by p27 (i.e., treated with $ZnSO_4$) and in cells with the differentiation blocked after Myc activation (i.e., treated with $ZnSO_4$ and 4HT) (Fig. 4A). p27 induced the accumulation of cyclins D, an effect likely due to protein stabilization since there was no upregulation of cyclins D mRNA (data not shown). Myc also induced a small increase in cyclin A, cyclin D2, Cdk4, and Cdk2. No significant changes were observed in parental K562 cells treated with $ZnSO_4$ or 4HT (results not shown).

In most models, the G_1-phase arrest by p27 is associated with retinoblastoma (RB) hypophosphorylation. Immunoblot experiments show that this was also the case in Kp27MER treated with $ZnSO_4$. Interestingly, in the presence of p27, most of the RB remained hypophosphorylated upon 4HT addition (Fig. 4B). We next analyzed the levels of RB phosphorylated in Ser780 and Thr821 using phospho-specific antibodies. Phosphorylation in Ser780 and Thr821 have been reported as specific for Cdk4/6 and Cdk2, respectively (25, 57). Immunoblot results confirmed that p27 profoundly repressed RB phosphorylation and that Myc could reverse none of them.

We next studied the kinase activity in cyclin D2 and cyclin D3 complexes, the most prevalent cyclin D forms in K562 (Fig. 4A and data not shown) using RB protein as substrate. In this setting, the kinase activity assayed is mostly due to Cdk2, Cdk4, and Cdk6. The kinase activity was dramatically inhibited by p27, and Myc only slightly reversed this inhibition (Fig. 4C), which is consistent with the small increase in phospho-RB observed in 4HT-treated cells (Fig. 4B). K562 cells are deficient in $p15^{INK4B}$ and $p16^{INK4A}$ (13), and thus these proteins cannot contribute to Cdk4/6 inhibition in this system. Since RB is also the substrate for Cdk2 kinase activity, we assayed the kinase activity after immunoprecipitation with anti-Cdk2 antibody and in the presence or absence of Myc (i.e., with or without 4HT treatment). The results showed a dramatic inhibition of Cdk2 activity in p27-expressing cells, which was unchanged by Myc (Fig. 4C). Thus, Myc cannot reverse the inhibition of Cdk4/6 and Cdk2 elicited by p27. The possibility still

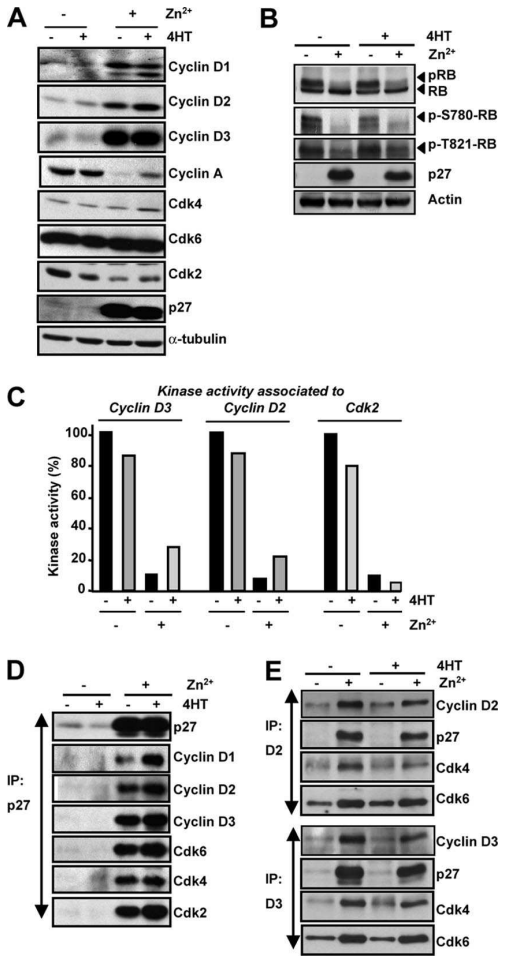

FIG. 4. Myc does not reverse Cdk inhibition by p27. (A) Expression of G_1-phase cyclins and Cdks. Protein extracts of Kp27MER cells treated for 24 h with or without 4HT and $ZnSO_4$ were assayed by immunoblotting for the indicated cyclins and Cdks. (B) Myc does not reverse RB hypohosphorylation. Total RB levels and phospho-specific RB levels were determined by immunoblotting in Kp27MER cells. See Table S2 in the supplemental material for antibody details. The position of hypophosphorylated RB and hyperphosphorylated RB (pRB) are marked by arrowheads. (C) Cdk activity determination. Lysates were immunoprecipitated with antibodies to cyclin D2, cyclin D3, and Cdk2 and assayed for kinase activity using RB (for cyclins) or histone H1 (For Cdk2) as a substrate. The kinase activity was normalized against the amounts of cyclin D2, D3, and Cdk2 pulled down in the immunoprecipitates. (D) Composition of p27 complexes. Lysates from Kp27MER cells treated with $ZnSO_4$ and/or 4HT were immunoprecipitated with anti-p27 antibodies, and the levels of p27, cyclin D1, D2, D3, Cdk6, Cdk4, and Cdk2 in the immunoprecipitates were assayed by immunoblotting. The corresponding nonimmunoprecipitated samples are shown in panel A. (E) Cyclin D2 and D3 immunoprecipitations. Cells were treated with $ZnSO_4$ and/or 4HT, lysates were immunoprecipitated with cyclin D2 or cyclin D3 antibodies, and the levels of p27, Cdk4, and Cdk6 in the immunoprecipitates were assayed by immunoblotting.

existed that Cdk inhibition was a secondary effect of the p27-induced differentiation rather than the inhibitory interaction of p27 with cyclin-Cdk complexes. Thus, we studied the proteins associated with p27 by immunoprecipitation experiments. Cdk2, Cdk4, and Cdk6 were found in p27 immunoprecipitates, and Myc did not modify their levels (Fig. 4D). However, Myc activation also resulted in greater amounts of cyclins D. Thus, we also tested the possibility that Myc modified the affinity of p27 for cyclin D-Cdk4/6 complexes. However, Myc activation did not change the relative amounts of p27, Cdk4, and Cdk6 present in cyclin D2 and D3 immunoprecipitates (Fig. 4E) and correlated to the amounts present in total extracts (Fig. 4A and data not shown). The results are again consistent with the lack of recovery in Cdk activity (Fig. 4C). Taken together, the data demonstrate that Myc inhibited p27-induced erythroid differentiation without reversing the p27-dependent inhibition of Cdks, a result that is consistent with the inability of Myc to reverse p27-mediated proliferation arrest.

Myc antagonizes the upregulation of erythroid-cell-specific genes mediated by p27. Since Myc inhibited Kp27MER differentiation without rescuing the cells from the G_1 arrest imposed by p27, this model provided an ideal opportunity to identify proliferation-independent targets of Myc that may explain its activity as a differentiation inhibitor. We therefore carried out microarray analysis with the Affymetrix platform testing RNA from Kp27MER cells either untreated or treated for 12 h with $ZnSO_4$, 4HT, or both. The experimental conditions and associated phenotypes, as well as the number of regulated genes, are schematized in Fig. 5A. We focused in the genes regulated by Myc in the presence of p27, comparing the transcriptomes of Kp27MER treated with $ZnSO_4$ with cells treated with $ZnSO_4$ plus 4HT. After subtracting the genes changed in control samples, filtering, and statistical analysis, we found that Myc regulated 200 genes with $\geq$2.3-fold change, being 121 genes downregulated (see Table S3 in the supplemental material). The clustering analysis of these genes showed that all Myc-expressing cells cluster together (Fig. 5B). This data set was further analyzed with the Ingenuity Pathways software to reveal the network of interactions between differentially regulated genes in the Kp27MER cells after induction of Myc and thus assaying the possible relevance of Myc activation in this model. The results revealed that the top-ranked network had Myc at the most significant node of interactions among proteins whose expression levels (at the mRNA level) changed between cells treated with $ZnSO_4$ and cells treated with $ZnSO_4$ plus 4HT (Fig. 5C). This result argues that Myc is responsible for the phenotypic change of Kp27MER cells upon addition of 4HT.

Myc downregulates erythroid genes. Microarray analysis revealed that a significant fraction of the genes downregulated by Myc in the presence of p27 were erythroid cell related (see Table S4 in the supplemental material), and the same result was observed for other erythroid genes (e.g., ε-globin and ζ-globin). Interestingly, some of these genes downregulated by Myc encode transcription factors able to drive erythroid differentiation in cell culture, as well as in in vivo models, such as GATA1, NFE2, STAT5A, STAT3, LMO2, LYL1, and JUNB. Moreover, Myc upregulated genes that block erythroid differentiation, such as the NOTCH ligand JAG2 and the transcription factor MAFK. Myc-mediated regulation of GATA1, NFE2, JUNB, and MAFK mRNA levels was confirmed by RT-qPCR (Fig. 6A). In contrast, Myc did not antagonize the p27-mediated downregulation of genes involved in DNA replication and mitosis, in agreement with the inability of Myc to

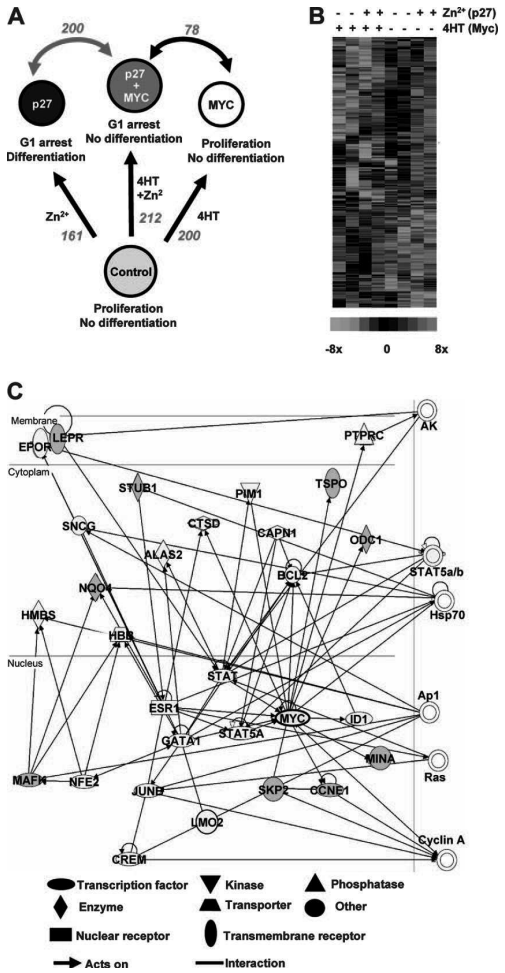

FIG. 5. Myc-regulated genes in the Kp27MER system. (A) Scheme of the Kp27MER samples subjected to microarray analysis and the resulting phenotypes. Cells were treated for 12 h with $ZnSO_4$ and 4HT. The numbers of genes regulated (≥2.3-fold) are indicated in red. Gene expression changes between samples separated by the red line are subjected to clustering analysis in panel B. (B) Heat map of clustered samples and genes of expression data of duplicated samples of Kp27MER treated with $ZnSO_4$ (i.e., p27) in the presence or absence of 4HT (i.e., Myc). The hierarchical clustering was performed for genes with expression variation ≥2.3-fold between cells expressing p27 and cells expressing p27 and Myc ($P < 0.005$), after subtraction of the corresponding controls in parental K562 cells. The genes are listed in the Table S3 in the supplemental material. The scale at the bottom shows the relationship between color saturation and the expression ratios. (C) Interaction network for differentially expressed genes in the presence of Myc and p27. A knowledge-based database (Ingenuity Pathways Analysis) was seeded with the differentially expressed genes between cells expressing p27 and cells expressing p27+Myc shown in panel B. Genes in red were upregulated and those in gray were downregulated in the samples treated with 4HT (i.e., Myc). The figure represents the network with the highest score identified by the program and shows Myc (in blue) at a central node of the network. The meanings of node shape and lines are indicated at the bottom.

reverse p27-mediated growth arrest as cyclins E, Cdk1, Cdc6, Cdc25A, PCNA, RFCs, and MCMs (results not shown). We sought to confirm the effect of Myc on p27-induced differentiation observed in the Kp27MER cell line in the parental K562 cells. For this, K562 cells were transiently transfected by nucleofection with expression vectors for p27 and Myc. In agreement with the results obtained with the Kp27MER line, p27-transfected K562 cells overexpressed erythroid-cell-specific genes such as GYPA and EPOR, and transfection of Myc vector inhibited this effect (Fig. 6B). It has been described that Myc represses genes through the interaction with the zinc finger protein Miz1, forming a complex that binds to the region of the transcription initiation site (reviewed in reference 52). To test the possibility that Miz1 could be involved in the repression of erythroid genes and to confirm the effects of Myc on p27-induced differentiation, we transiently transfected K562 cells with expression vectors for p27, Myc, and MycV394D, a mutant unable to bind Miz1 (23). MycV394D was as efficient as wild-type Myc in antagonizing the upregulation of GATA1 and NFE2 induced by p27 (Fig. 6B). Consistently, we did not detect binding of Myc to the region of GATA1 gene that contains the transcription initiation site by chromatin immunoprecipitation (data not shown). This result suggests that Myc repress GATA1 and NFE2 through a Miz1-independent mechanism. We also sought to determine whether the Myc effect is dependent on Myc box II. This region is required for transactivation, for transformation, and also for gene repression activities of Myc (reviewed in references 21 and 40). The results showed that MycD106-143 (carrying a deletion that encompasses Myc box II) was much less efficient at antagonizing p27-mediated upregulation of GATA1 and NFE2 (Fig. 6B) and other erythroid markers as ε-globin and EPOR (data not shown).

GATA1 antagonizes the effect of Myc as an inhibitor of erythroid differentiation. Of the genes regulated by Myc, we focused on GATA1 and NFE2, two transcription factors essential for erythroid lineage commitment (19). In erythroid differentiation, GATA1 nucleates the subsequent binding (2). Thus, we sought to determine whether GATA1 and NFE2 were partly responsible for the p27-induced differentiation by transiently transfecting Kp27MER cells. We first confirmed by immunoblot analysis that GATA1 transfection and overexpression did not modify the induction of p27 by $ZnSO_4$ (Fig. 6C). Activation of Myc (i.e., by 4HT treatment) impaired erythroid differentiation, as assessed by the diminished upregulation of GYPA (Fig. 6D), ε-globin (Fig. 6E), and the fraction of hemoglobinized cells (data not shown). However, differentiation was increased to some extent by GATA1 coexpression (Fig. 6D,E). We also transfected Kp27MER cells with NFE2 expression vector (Fig. 6F). In contrast to GATA1, NFE2, at the levels achieved in the transfections, did not rescue the differentiation inhibitory effect of Myc as assayed by ε-globin expression (Fig. 6G) and benzidine staining (not shown). When both GATA1 and NFE2 were cotransfected, the effect was similar to that achieved by GATA1 alone (data not shown). Thus, downregulation of GATA1 is involved in the differentiation inhibition by Myc, but other additional mechanisms seem to be operative.

Myc antagonizes Mad1 upregulation mediated by p27. It has been shown that Mad1, which forms dimers with Max that repress transcription, antagonizes Myc functions. In addition,

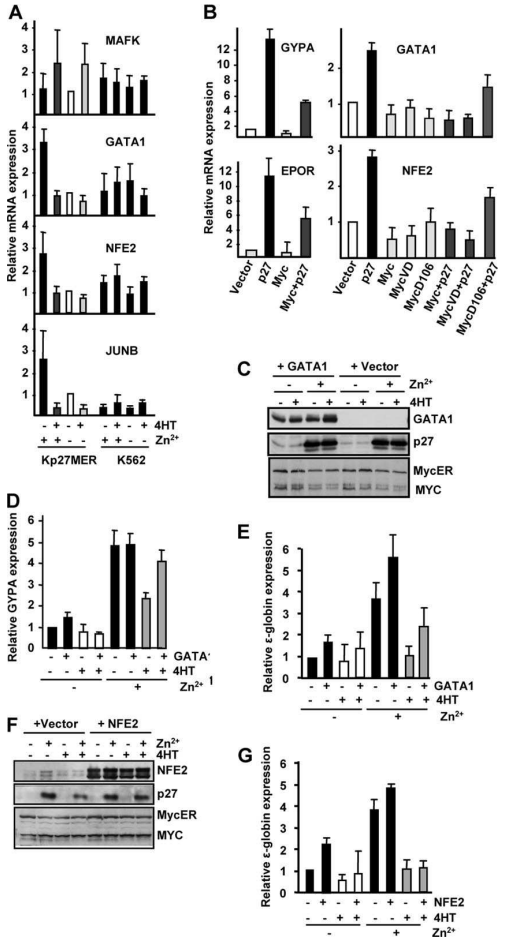

FIG. 6. Erythroid genes downregulated by Myc. (A) Kp27MER and K562 cells were incubated for 12 h with $ZnSO_4$ and/or 4HT, and mRNA levels of the indicated erythroid transcription factor genes were determined by RT-qPCR. Values represent means ± the SEM of three independent experiments. (B) Expression of erythroid genes in K562 cells after transient transfection of vectors for p27, Myc, Myc-V394D (MycVD), and Myc D106-143 (MycD106). The plasmids were nucleofected, and the mRNA levels of GYPA, EPOR (24 h after transfection), or GATA1 and NFE2 (48 h after transfection) were determined by RT-qPCR. An expression vector for GFP was cotransfected in each case, and the data were normalized to the expression of GFP. Values are means ± the SEM from four independent experiments. (C) Enforced expression of GATA1 in Kp27MER. Cells were transfected by lipofection with GATA1 or empty vector. At 12 h after transfection, cells were treated with $ZnSO_4$ and/or 4HT. After 24 h of incubation, the expression of GATA1, p27, and Myc was analyzed by immunoblotting. The anti-GATA1 antibody used recognizes the N-terminal domain of mouse protein. (D) GYPA mRNA levels assayed by RT-qPCR in Kp27MER cells transiently transfected with GATA1. At 12 h after transfection the cells were treated for 72 h with $ZnSO_4$ and 4HT, and the mRNA level was determined by RT-qPCR. Values are means ± the SEM of two independent experiments. (E) ε-Globin mRNA levels of Kp27MER transfected with GATA1, assayed as in panel D. (F) Enforced expression of NFE2 in Kp27MER. Cells were transfected with an NFE2 expression vector or empty vector and analyzed by immunoblotting as in panel C. (G) ε-Globin mRNA levels of Kp27MER transfected with NFE2, assayed as in panel D. The data are means ± the SEM of two independent experiments.

it has been reported that Mad1 induces erythroid differentiation in Friend murine erythroleukemia cells (10). Thus, we sought to determine whether the functional antagonism between Myc and Mad1 could also contribute to explain the Myc-mediated inhibition of differentiation in the K562 system. We assayed the expression of Mad proteins in the Kp27MER system and found that Mad1 protein (Fig. 7A) and mRNA (Fig. 7B) was upregulated upon p27-induced differentiation. Interestingly, Mad1 upregulation was reduced when Myc was activated by 4HT (Fig. 7A and B). In contrast, other members of the Mad family such as Mnt and Mxi1 were not upregulated by p27 (Fig. 7A). Moreover, transient transfection of p27 in K562 resulted in an increase in Mad1 mRNA (not shown). We next sought to determine whether Mad1 could contribute to p27-induced differentiation in this model. Cells were transiently transfected with expression vectors for Mad1 and Myc, and the erythroid differentiation was assayed by the benzidine test and the expression of ε-globin and EPOR. The results showed that Mad1 increased the expression of differentiation markers (Fig. 7D and E). We also transfected the MadMyc construct, which carries the transrepression domain of Mad1 linked to the HLH-LZ domain of Myc and acts as a strong repressor of Myc-responsive transcription (6). MadMyc was transfected into K562, and its expression demonstrated by immunoblotting (Fig. 7C). We found that MadMyc efficiently induced differentiation as assessed by the upregulation of EPOR and ε-globin genes (Fig. 7E). Finally, coexpression of Myc blunted the differentiation induced by Mad1 and by Mad-Myc in transient-transfection experiments (Fig. 7C and D). We conclude that Mad1 upregulation is part of the differentiation response and that Myc also functions as a Mad1 antagonist in this system.

DISCUSSION

One of the first biological activities described for Myc was differentiation inhibition, namely, the chemically induced erythroid differentiation of FMEL cells (8, 16, 44). This effect is consistent with the erythroleukemia induced in transgenic mice with enforced Myc expression in erythroid precursors (47). However, the mechanisms by which Myc blocks differentiation are poorly understood. Proliferation stimulation can certainly contribute to Myc-mediated inhibition of differentiation, but the hypothesis that Myc exerts proliferation-independent mechanisms to block differentiation has received little attention. Several studies have shown that Myc antagonizes the cell cycle arrest effect of p27, and the prevalent mechanism proposed is the sequestration of p27 in type D cyclins complexes (7, 43, 51). In contrast, there is little information on whether and how Myc impairs p27-induced differentiation. In this context, it has been shown that the monocytic differentiation induced by retinoic acid in U937 myeloid cells is mediated by p27 and inhibited by Myc (15) and that inactivation of p27 gene rescues the cerebellar development otherwise impaired in N-*Myc*-deficient mice (59).

We have established a genetically defined model system where differentiation can be induced in K562 human myeloid leukemia cells by p27 induction and Myc can be conditionally activated. The molecular mechanisms by which p27 induces differentiation in this model are unknown. However, they do

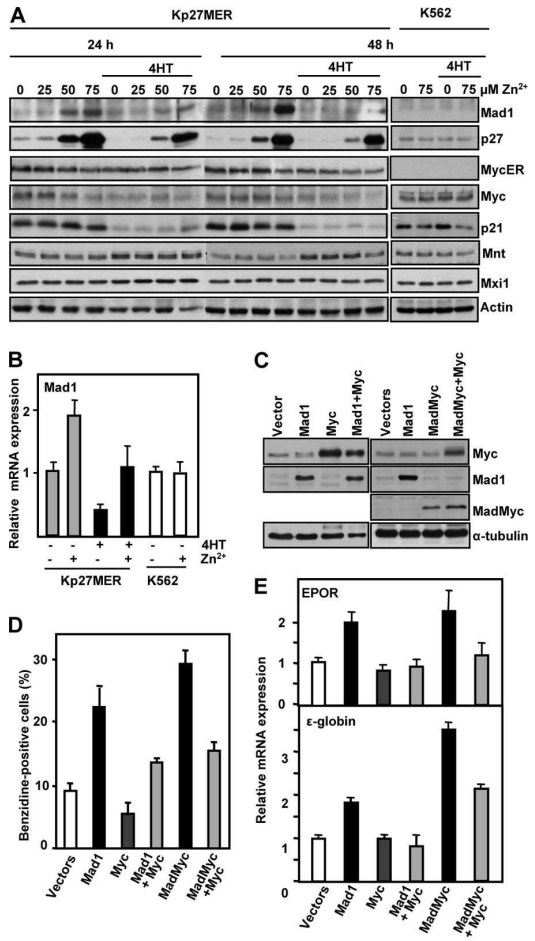

FIG. 7. Mad1 induction by p27 and repression by Myc. (A) Immunoblot showing Mad1 expression in Kp27MER cells treated with 200 nM 4HT and the indicated concentrations of $ZnSO_4$. The expression of p27, Mnt, and Mxi1 (members of the Mad family) was also determined. The levels of p21 and endogenous Myc are also shown to confirm the activation of Myc by 4HT. (B) Expression of Mad1 mRNA in Kp27MER and K562 cells. Cells were treated for 12 h with 4HT and $ZnSO_4$, and mRNA expression was determined by RT-qPCR. The data are means ± the SEM of three experiments. (C) Mad1 induces the expression of erythroid markers in K562, and Myc impairs the Mad1-induced differentiation. K562 cells were nucleofected with expression vectors for Mad1, Myc, the MadMyc hybrid construct, and a mixture of Mad1+Myc and MadMyc+Myc vectors. At 24 h after transfection, the expression of the ectopic proteins was analyzed by immunoblotting. (D) K562 cells were transfected as in panel C, and the benzidine-positive cells were scored 72 h after transfection to assess erythroid differentiation. The data are means ± the SEM of two independent experiments. (E) EPOR and ε-globin mRNA levels were assayed by RT-qPCR in K562 cells transiently transfected as described in panel C. The data are means ± the SEM of two independent experiments.

not entirely depend on cell cycle arrest since p21 also arrests proliferation of K562 while inducing a different type of differentiation (34). In the present study we show that Myc impairs the erythroid differentiation through a mechanism that is independent of the proliferation arrest and Cdk inhibition imposed by p27. Thus, the Myc effect on differentiation inhibition is uncoupled from its effects on proliferation. Microarray analysis showed that Myc antagonizes the p27-mediated upregulation of genes of transcription factors that direct erythroid differentiation (GATA1, NFE2, JUNB, LMO2, and STAT5A). Myc also antagonizes the p27-mediated downregulation of genes that oppose erythroid differentiation (MAFK and JAG2). Moreover, enforced expression of GATA1, a "master gene" of erythropoiesis (19), partially rescues the differentiation inhibition induced by Myc, indicating that Myc effect is mediated, in part, by antagonizing GATA1 induction. However, GATA1 is only partly rescuing the anti-differentiation effect of Myc, since Myc is likely impairing differentiation by repressing several erythroid-determining genes.

The molecular mechanism by which Myc represses GATA1 is unclear. Actually, about half of Myc target genes are repressed, but the mechanism of repression is unknown for the vast majority of the genes. In a small subset of genes, Myc-mediated repression depends on the interaction with Miz1 (52). In the case of GATA1 in the K562 model, this effect seems to be Miz1 independent, since a Myc mutant unable to bind Miz1 antagonized the upregulation of GATA1 and erythroid differentiation as efficiently as did wild-type Myc. In contrast, a Myc mutant lacking Myc box II (a conserved region required for transformation, transactivation, and repression activities of Myc) cannot efficiently antagonize p27-induced differentiation in our model. This result has also been observed for other differentiation models (4, 20) and suggests that Myc is using a common molecular mechanism to transform and to abrogate differentiation. On the other hand, it has been reported that GATA1 represses Myc and induces p27 in murine embryonic cells (45), suggesting the possibility of a regulatory p27-GATA1 loop. However, GATA1 does not repress Myc in our K562 model (data not shown).

Myc and Mad1 have antagonist activities in transcription upon binding to the same E-boxes and in cell proliferation (5, 21). We found that p27-induced differentiation of K562 is accompanied by Mad1 upregulation and that Mad1 is able to promote K562 erythroid differentiation, although less efficiently than p27. Moreover, MadMyc, a chimeric protein that represses gene expression upon binding to Myc-binding sites (6), is a potent differentiation inducer. Thus, Myc would antagonize this Mad1 effect at the transcriptional level. Furthermore, Myc activation in our model provokes Mad1 downregulation in K562 cells and Myc coexpression impairs Mad1 and MadMyc-induced differentiation. This suggests that the impairment of Mad1 function by Myc is contributing to differentiation inhibition in the K562p27MER model. These results are consistent with Mad1 inducing erythroid differentiation of murine erythroleukemia cells (10). Moreover, it has been shown that Mad1 and p27 cooperate for a correct development of the myeloid compartment in vivo (33). Similar scenery seems to operate in K562 differentiation, and our data suggest that Myc might impair the Mad1-p27 functional interaction.

In summary, the results in the K562 model demonstrate that the differentiation-inhibitory effect of Myc depends on its gene regulatory activity and is uncoupled from its effect as proliferation stimulator. Importantly, tumor cell redifferentiation is the mechanism for the tumor regression after Myc deactivation in some transgenic mice models (reviewed in reference 3).

Moreover, Myc is one of the four transcription factor set capable of conferring pluripotent stem cell properties to differentiated adult cells, and Myc is reactivated in the tumors arising in the chimeric mice derived from such cells (38). Thus, it is conceivable that Myc displays common pathways as a "stem cell-ness" keeper and as an oncogene, preventing differentiation in both cases. Our results in the K562 model support the hypothesis that inhibition of cell differentiation is a Myc tumorigenic mechanism independent of Myc effects in cell proliferation.

ACKNOWLEDGMENTS

We thank Xose Bustelo for help with the Ingenuity Systems software; Jerry Adams, Yaacob Ben-David, Rene Bernards, Martin Eilers, Robert Eisenman, Trevor Littlewood, and Itsaso Mauleon for vectors; and Pilar Frade for technical assistance.

This study was supported by grants CICYT SAF05-00461 from the Spanish Ministerio de Educacion y Ciencia (MEC), ISCIII-RETIC RD06/0020 from the Spanish Ministerio de Sanidad y Consumo, API-17-05 from the Fundación Marques de Valdecilla (to J.L), and FIS04/1083 (to M.D.D). J.C.A., G.B., and N.F. were supported by fellowships from the MEC, and V.T. was supported by a Lady Tata Memorial Trust award.

REFERENCES

1. **Adhikary, S., and M. Eilers.** 2005. Transcriptional regulation and transformation by Myc proteins. Nat. Rev. Mol. Cell. Biol. **6:**635–645.
2. **Anguita, E., J. Hughes, C. Heyworth, G. A. Blobel, W. G. Wood, and D. R. Higgs.** 2004. Globin gene activation during haemopoiesis is driven by protein complexes nucleated by GATA-1 and GATA-2. EMBO J. **23:**2841–2852.
3. **Arvanitis, C., and D. W. Felsher.** 2005. Conditionally MYC: insights from novel transgenic models. Cancer Lett. **226:**95–99.
4. **Bar-Ner, M., L. T. Messing, C. M. Cultraro, M. J. Birrer, and S. Segal.** 1992. Regions within the c-Myc protein that are necessary for transformation are also required for inhibition of differentiation of murine erythroleukemia cells. Cell Growth Differ. **3:**183–190.
5. **Baudino, T. A., and J. L. Cleveland.** 2001. The Max network gone mad. Mol. Cell. Biol. **21:**691–702.
6. **Berns, K., E. M. Hijmans, and R. Bernards.** 1997. Repression of c-Myc responsive genes in cycling cells causes G_1 arrest through reduction of cyclin E/CDK2 kinase activity. Oncogene **15:**1347–1356.
7. **Bouchard, C., K. Thieke, A. Maier, R. Saffrich, J. Hanley-Hyde, W. Ansorge, S. Reed, P. Sicinski, J. Bartek, and M. Eilers.** 1999. Direct induction of cyclin D2 by Myc contributes to cell cycle progression and sequestration of p27. EMBO J. **18:**5321–5333.
8. **Coppola, J. A., and M. D. Cole.** 1986. Constitutive c-myc oncogene expression blocks mouse erythroleukaemia cell differentiation but not commitment. Nature **320:**760–763.
9. **Cowling, V. H., and M. D. Cole.** 2006. Mechanism of transcriptional activation by the Myc oncoproteins. Semin. Cancer Biol. **16:**242–252.
10. **Cultraro, C. M., T. Bino, and S. Segal.** 1997. Function of the c-Myc antagonist Mad1 during a molecular switch from proliferation to differentiation. Mol. Cell. Biol. **17:**2353–2359.
11. **Dang, C. V., A. O'Donnell, K., K. I. Zeller, T. Nguyen, R. C. Osthus, and F. Li.** 2006. The c-Myc target gene network. Semin. Cancer Biol. **16:**253–264.
12. **Delgado, M. D., A. Lerga, M. Canelles, M. T. Gomez-Casares, and J. Leon.** 1995. Differential regulation of Max and role of c-Myc during erythroid and myelomonocytic differentiation of K562 cells. Oncogene **10:**1659–1665.
13. **Delgado, M. D., J. P. Vaque, I. Arozarena, M. A. Lopez-Ilasaca, C. Martinez, P. Crespo, and J. Leon.** 2000. H-, K-, and N-Ras inhibit myeloid leukemia cell proliferation by a $p21^{WAF1}$-dependent mechanism. Oncogene **19:**783–790.
14. **Denicourt, C., and S. F. Dowdy.** 2004. Cip/Kip proteins: more than just CDKs inhibitors. Genes Dev. **18:**851–855.
15. **Dimberg, A., F. Bahram, I. Karlberg, L. G. Larsson, K. Nilsson, and F. Oberg.** 2002. Retinoic acid-induced cell cycle arrest of human myeloid cell lines is associated with sequential down-regulation of c-Myc and cyclin E and posttranscriptional up-regulation of $p27^{Kip1}$. Blood **99:**2199–2206.
16. **Dmitrovsky, E., W. M. Kuehl, G. F. Hollis, I. R. Kirsch, T. P. Bender, and S. Segal.** 1986. Expression of a transfected human c-myc oncogene inhibits differentiation of a mouse erythroleukaemia cell line. Nature **322:**748–750.
17. **Eisenman, R. N.** 2001. Deconstructing myc. Genes Dev. **15:**2023–2030.
18. **Fernandez, P. C., S. R. Frank, L. Wang, M. Schroeder, S. Liu, J. Greene, A. Cocito, and B. Amati.** 2003. Genomic targets of the human c-Myc protein. Genes Dev. **17:**1115–1129.
19. **Ferreira, R., K. Ohneda, M. Yamamoto, and S. Philipsen.** 2005. GATA1 function, a paradigm for transcription factors in hematopoiesis. Mol. Cell. Biol. **25:**1215–1227.
20. **Freytag, S. O., C. V. Dang, and W. M. Lee.** 1990. Definition of the activities and properties of c-myc required to inhibit cell differentiation. Cell Growth Differ. **1:**339–343.
21. **Grandori, C., S. M. Cowley, L. P. James, and R. N. Eisenman.** 2000. The Myc/Max/Mad network and the transcriptional control of cell behavior. Annu. Rev. Cell Dev. Biol. **16:**653–699.
22. **Habib, T., H. Park, M. Tsang, I. M. de Alboran, A. Nicks, L. Wilson, P. S. Knoepfler, S. Andrews, D. J. Rawlings, R. N. Eisenman, and B. M. Iritani.** 2007. Myc stimulates B lymphocyte differentiation and amplifies calcium signaling. J. Cell Biol. **179:**717–731.
23. **Herold, S., M. Wanzel, V. Beuger, C. Frohme, D. Beul, T. Hillukkala, J. Syvaoja, H. P. Saluz, F. Haenel, and M. Eilers.** 2002. Negative regulation of the mammalian UV response by Myc through association with Miz-1. Mol. Cell **10:**509–521.
24. **Hurlin, P. J., C. Queva, and R. N. Eisenman.** 1997. Mnt, a novel Max-interacting protein is coexpressed with Myc in proliferating cells and mediates repression at Myc binding sites. Genes Dev. **11:**44–58.
25. **Kitagawa, M., H. Higashi, H. K. Jung, I. Suzuki-Takahashi, M. Ikeda, K. Tamai, J. Kato, K. Segawa, E. Yoshida, S. Nishimura, and Y. Taya.** 1996. The consensus motif for phosphorylation by cyclin D1-Cdk4 is different from that for phosphorylation by cyclin A/E-Cdk2. EMBO J. **15:**7060–7069.
26. **Li, C., and W. H. Wong.** 2001. Model-based analysis of oligonucleotide arrays: expression index computation and outlier detection. Proc. Natl. Acad. Sci. USA **98:**31–36.
27. **Li, Z., S. Van Calcar, C. Qu, W. K. Cavenee, M. Q. Zhang, and B. Ren.** 2003. A global transcriptional regulatory role for c-Myc in Burkitt's lymphoma cells. Proc. Natl. Acad. Sci. USA **100:**8164–8169.
28. **Littlewood, T. D., D. C. Hancock, P. S. Danielian, M. G. Parker, and G. I. Evan.** 1995. A modified estrogen receptor ligand-binding domain as an improved switch for the regulation of heterologous proteins. Nucleic Acids Res. **23:**1686–1690.
29. **Lu, S. J., S. Rowan, M. R. Bani, and Y. Ben-David.** 1994. Retroviral integration within the Fli-2 locus results in inactivation of the erythroid transcription factor NF-E2 in Friend erythroleukemias: evidence that NF-E2 is essential for globin expression. Proc. Natl. Acad. Sci. USA **91:**8398–8402.
30. **Lutz, W., J. Leon, and M. Eilers.** 2002. Contributions of Myc to tumorigenesis. Biochim. Biophys. Acta **1602:**61–71.
31. **Martins, C. P., and A. Berns.** 2002. Loss of $p27^{Kip1}$ but not $p21^{Cip1}$ decreases survival and synergizes with MYC in murine lymphomagenesis. EMBO J. **21:**3739–3748.
32. **Mauleon, I., M. N. Lombard, M. J. Munoz-Alonso, M. Canelles, and J. Leon.** 2004. Kinetics of myc-max-mad gene expression during hepatocyte proliferation in vivo: differential regulation of mad family and stress-mediated induction of c-myc. Mol. Carcinog. **39:**85–90.
33. **McArthur, G. A., K. P. Foley, M. L. Fero, C. R. Walkley, A. J. Deans, J. M. Roberts, and R. N. Eisenman.** 2002. MAD1 and $p27^{KIP1}$ cooperate to promote terminal differentiation of granulocytes and to inhibit Myc expression and cyclin E-CDK2 activity. Mol. Cell. Biol. **22:**3014–3023.
34. **Munoz-Alonso, M., and J. Leon.** 2003. G_1 phase control and cell differentiation, p. 1–29. *In* J. Boonstra (ed.), G_1 phase progression. Landes Bioscience, New York, NY.
35. **Munoz-Alonso, M. J., J. C. Acosta, C. Richard, M. D. Delgado, J. Sedivy, and J. Leon.** 2005. $p21^{Cip1}$ and $p27^{Kip1}$ induce distinct cell cycle effects and differentiation programs in myeloid leukemia cells. J. Biol. Chem. **280:**18120–18129.
36. **Nesbit, C. E., J. M. Tersak, and E. V. Prochownik.** 1999. MYC oncogenes and human neoplastic disease. Oncogene **18:**3004–3016.
37. **Obaya, A. J., and J. M. Sedivy.** 2002. Regulation of cyclin-Cdk activity in mammalian cells. Cell Mol. Life Sci. **59:**126–142.
38. **Okita, K., T. Ichisaka, and S. Yamanaka.** 2007. Generation of germline-competent induced pluripotent stem cells. Nature **448:**313–317.
39. **Orian, A., B. van Steensel, J. Delrow, H. J. Bussemaker, L. Li, T. Sawado, E. Williams, L. W. Loo, S. M. Cowley, C. Yost, S. Pierce, B. A. Edgar, S. M. Parkhurst, and R. N. Eisenman.** 2003. Genomic binding by the *Drosophila* Myc, Max, Mad/Mnt transcription factor network. Genes Dev. **17:**1101–1114.
40. **Oster, S. K., C. S. Ho, E. L. Soucie, and L. Z. Penn.** 2002. The myc oncogene: MarvelouslY Complex. Adv. Cancer Res. **84:**81–154.
41. **Patel, J. H., A. P. Loboda, M. K. Showe, L. C. Showe, and S. B. McMahon.** 2004. Analysis of genomic targets reveals complex functions of MYC. Nat. Rev. Cancer **4:**562–568.
42. **Penn, L. J., M. W. Brooks, E. M. Laufer, and H. Land.** 1990. Negative autoregulation of c-myc transcription. EMBO J. **9:**1113–1121.
43. **Perez-Roger, I., S. H. Kim, B. Griffiths, A. Sewing, and H. Land.** 1999. Cyclins D1 and D2 mediate myc-induced proliferation via sequestration of $p27^{Kip1}$ and $p21^{Cip1}$. EMBO J. **18:**5310–5320.
44. **Prochownik, E. V., and J. Kukowska.** 1986. Deregulated expression of c-myc by murine erythroleukaemia cells prevents differentiation. Nature **322:**848–850.
45. **Rylski, M., J. J. Welch, Y. Y. Chen, D. L. Letting, J. A. Diehl, L. A. Chodosh,**

G. A. Blobel, and M. J. Weiss. 2003. GATA-1-mediated proliferation arrest during erythroid maturation. Mol. Cell. Biol. **23:**5031–5042.
46. **Sherr, C. J., and J. M. Roberts.** 1999. CDK inhibitors: positive and negative regulators of G_1-phase progression. Genes Dev. **13:**1501–1512.
47. **Skoda, R. C., S. F. Tsai, S. H. Orkin, and P. Leder.** 1995. Expression of c-MYC under the control of GATA-1 regulatory sequences causes erythroleukemia in transgenic mice. J. Exp. Med. **181:**1603–1613.
48. **Taniguchi, T., H. Endo, N. Chikatsu, K. Uchimaru, S. Asano, T. Fujita, T. Nakahata, and T. Motokura.** 1999. Expression of $p21^{Cip1/Waf1/Sdi1}$ and $p27^{Kip1}$ cyclin-dependent kinase inhibitors during human hematopoiesis. Blood **93:**4167–4178.
49. **Vaque, J. P., J. Navascues, Y. Shiio, M. Laiho, N. Ajenjo, I. Mauleon, D. Matallanas, P. Crespo, and J. Leon.** 2005. Myc antagonizes Ras-mediated growth arrest in leukemia cells through the inhibition of the Ras-ERK-$p21^{Cip1}$ pathway. J. Biol. Chem. **280:**1112–1122.
50. **Visvader, J. E., A. G. Elefanty, A. Strasser, and J. M. Adams.** 1992. GATA-1 but not SCL induces megakaryocytic differentiation in an early myeloid line. EMBO J. **11:**4557–4564.
51. **Vlach, J., S. Hennecke, K. Alevizopoulos, D. Conti, and B. Amati.** 1996. Growth arrest by the cyclin-dependent kinase inhibitor $p27^{Kip1}$ is abrogated by c-Myc. EMBO J. **15:**6595–6604.
52. **Wanzel, M., S. Herold, and M. Eilers.** 2003. Transcriptional repression by Myc. Trends Cell Biol. **13:**146–150.
53. **Wilson, A., M. J. Murphy, T. Oskarsson, K. Kaloulis, M. D. Bettess, G. M. Oser, A. C. Pasche, C. Knabenhans, H. R. Macdonald, and A. Trumpp.** 2004. c-Myc controls the balance between hematopoietic stem cell self-renewal and differentiation. Genes Dev. **18:**2747–2763.
54. **Yang, W., J. Shen, M. Wu, M. Arsura, M. FitzGerald, Z. Suldan, D. W. Kim, C. S. Hofmann, S. Pianetti, R. Romieu-Mourez, L. P. Freedman, and G. E. Sonenshein.** 2001. Repression of transcription of the $p27^{Kip1}$ cyclin-dependent kinase inhibitor gene by c-Myc. Oncogene **20:**1688–1702.
55. **Yaroslavskiy, B., S. Watkins, A. D. Donnenberg, T. J. Patton, and R. A. Steinman.** 1999. Subcellular and cell-cycle expression profiles of CDK-inhibitors in normal differentiating myeloid cells. Blood **93:**2907–2917.
56. **Zanet, J., S. Pibre, C. Jacquet, A. Ramirez, I. M. de Alboran, and A. Gandarillas.** 2005. Endogenous Myc controls mammalian epidermal cell size, hyperproliferation, endoreplication, and stem cell amplification. J. Cell Sci. **118:**1693–1704.
57. **Zarkowska, T., and S. Mittnacht.** 1997. Differential phosphorylation of the retinoblastoma protein by G_1/S cyclin-dependent kinases. J. Biol. Chem. **272:**12738–12746.
58. **Zeller, K. I., X. Zhao, C. W. Lee, K. P. Chiu, F. Yao, J. T. Yustein, H. S. Ooi, Y. L. Orlov, A. Shahab, H. C. Yong, Y. Fu, Z. Weng, V. A. Kuznetsov, W. K. Sung, Y. Ruan, C. V. Dang, and C. L. Wei.** 2006. Global mapping of c-Myc binding sites and target gene networks in human B cells. Proc. Natl. Acad. Sci. USA **103:**17834–17839.
59. **Zindy, F., P. S. Knoepfler, S. Xie, C. J. Sherr, R. N. Eisenman, and M. F. Roussel.** 2006. N-Myc and the cyclin-dependent kinase inhibitors $p18^{Ink4c}$ and $p27^{Kip1}$ coordinately regulate cerebellar development. Proc. Natl. Acad. Sci. USA **103:**11579–11583.

Oncogene (2012), 1–8

www.nature.com/onc

SHORT COMMUNICATION

MYC antagonizes the differentiation induced by imatinib in chronic myeloid leukemia cells through downregulation of $p27^{KIP1}$

MT Gómez-Casares[1], E García-Alegria[2], CE López-Jorge[1], N Ferrándiz[2,5], R Blanco[2], S Alvarez[3], JP Vaqué[2,6], G Bretones[2], JM Caraballo[2], P Sánchez-Bailón[4], MD Delgado[2], J Martín-Perez[4], JC Cigudosa[3] and J León[2]

Chronic myeloid leukemia (CML) progresses from a chronic to a blastic phase where the leukemic cells are proliferative and undifferentiated. The CML is nowadays successfully treated with BCR-ABL kinase inhibitors as imatinib and dasatinib. In the CML-derived K562 cell line, low concentrations of imatinib induce proliferative arrest and erythroid differentiation. We found that imatinib upregulated the cell cycle inhibitor $p27^{KIP1}$ (p27) in a time- and -concentration dependent manner, and that the extent of imatinib-mediated differentiation was severely decreased in cells with depleted p27. MYC (c-Myc) is a transcription factor frequently deregulated in human cancer. MYC is overexpressed in untreated CML and is associated to poor response to imatinib. Using K562 sublines with conditional MYC expression (induced by Zn^{2+} or activated by 4-hydroxy-tamoxifen) we show that MYC prevented the erythroid differentiation induced by imatinib and dasatinib. The differentiation inhibition is not due to increased proliferation of MYC-expressing clones or enhanced apoptosis of differentiated cells. As p27 overexpression is reported to induce erythroid differentiation in K562, we explored the effect of MYC on imatinib-dependent induction of p27. We show that MYC abrogated the imatinib-induced upregulation of p27 concomitantly with the differentiation inhibition, suggesting that MYC inhibits differentiation by antagonizing the imatinib-mediated upregulation of p27. This effect occurs mainly by p27 protein destabilization. This was in part due to MYC-dependent induction of SKP2, a component of the ubiquitin ligase complex that targets p27 for degradation. The results suggest that, although MYC deregulation does not directly confer resistance to imatinib, it might be a factor that contributes to progression of CML through the inhibition of differentiation.

Oncogene advance online publication, 18 June 2012; doi:10.1038/onc.2012.246

Keywords: Myc; imatinib; dasatinib; p27; chronic myeloid leukemia; differentiation

INTRODUCTION

c-Myc (MYC herein after) is an oncogenic transcription factor of the helix–loop–helix/leucine zipper protein family. MYC is a widespread regulator of transcription that regulates about one thousand genes.[1,2] MYC is found deregulated in around half of human tumors and appears frequently associated with tumor progression in solid tumors and leukemia.[3,4] MYC activities include increased proliferative potential, enhanced protein synthesis and energetic metabolism and genomic instability.[2,5] One of the most relevant activities of MYC in carcinogenesis is the impairment of cell differentiation[6].

p27 was originally described as a cyclin-dependent kinases inhibitor, with cyclin E-cyclin-dependent kinases 2 complexes as its primary targets.[7,8] p27 is regulated mainly at the protein stability level and low p27 levels are associated with a poor prognosis in most tumors.[9,10] The degradation of p27 in proteasoma is preceded by ubiquitylation by the SCF^{SKP2} complex, where SKP2 is the p27-recognizing subunit.[11–13] Recently it has been shown that *SKP2* is a MYC target gene, which may explain the inverse correlation between MYC and p27 levels found in many systems.[14]

Chronic myeloid leukemia (CML) is a myeloproliferative malignancy that progresses from a relatively benign chronic phase to a blastic crisis phase.[15] The molecular hallmark of all CML phases is the expression of the BCR-ABL kinase. CML is a hematopoietic stem cell malignancy where BCR-ABL would lead to a progressive block of differentiation and increased genetic instability.[16–18] However, the molecular mechanisms underlying CML progression into the blastic phase are still uncertain. We recently showed that MYC expression was higher in CML patients at diagnosis and that correlated with a poor response to imatinib.[19] Moreover MYC antagonizes the erythroid differentiation of the CML-derived cell line K562 induced by cytosine arabinoside[20] and by p27.[21] Imatinib, a BCR-ABL inhibitor, is the frontline drug in CML therapy.[22–24] Given that differentiation inhibition is a hallmark of the CML progression we explored a possible effect of MYC on imatinib-dependent differentiation. We show here that MYC impairs the imatinib-induced erythroid

[1]Servicio de Hematología and Unidad de Investigación, Hospital Universitario Dr Negrín, Las Palmas, Spain; [2]Group of Transcriptional Control and Cancer, Departamento de Biología Molecular, Facultad de Medicina, Instituto de Biomedicina y Biotecnología de Cantabria (IBBTEC), Universidad de Cantabria-CSIC-SODERCAN, Santander, Spain; [3]Human Cancer Genetics Program, Centro Nacional de Investigaciones Oncológicas (CNIO), Madrid, Spain and [4]Instituto de Investigaciones Biomédicas Alberto Sols, CSIC, Madrid, Spain. Correspondence: Professor J León, Group of Transcriptional Control and Cancer, Departamento de Biología Molecular, Facultad de Medicina, Instituto de Biomedicina y Biotecnología de Cantabria (IBBTEC), Universidad de Cantabria-CSIC-SODERCAN, Avda Cardenal Herrera Oria s/n, Santander, Cantabria 39011, Spain.
E-mail: leonj@unican.es
[5]Current address: MRC Clinical Sciences Centre, Imperial College Faculty of Medicine Hammersmith Hospital Campus, London, UK
[6]Current address: IFIMAV, Santander, Spain
Received 8 February 2012; revised and accepted 4 May 2012

differentiation of CML-derived cells. This inhibition is mediated by destabilization of p27, which is achieved in part by the induction of SKP2. Our data suggests that the block in differentiation is a mechanism by which MYC contributes to CML progression.

RESULTS AND DISCUSSION

Treatment of K562 cells with low imatinib concentrations (0.5 μM) abolished cell proliferation as shown by cell counting (Figure 1a) and by [^{3}H]thymidine incorporation (Figure 1b). We examined the imatinib-induced erythroid differentiation in cells treated with 0.5 μM imatinib. The fraction of benzidine-positive (assessed by benzidine cytochemical assay, which detects cells containing hemoglobin) augmented in a dose and time-dependent manner (Figure 1c). The erythroid differentiation was also confirmed by the increased mRNA levels of ε-globin, transferring receptor 2 and erythropoietin receptor (Figure 1d) and glycophorin A as measured by flow cytometry (not shown). Higher imatinib concentrations (2.5 μM) also induced erythroid differentiation but provoked significant apoptosis (Shah *et al*.,[25] Albajar *et al*.[26] and data not shown).

We next investigated the mechanism for imatinib-induced erythroid differentiation. It was reported that p27 induces erythroid differentiation in K562 cells[27] and that BCR-ABL activity decreases p27 levels.[28,29] Thus, we tested the hypothesis that differentiation depended on imatinib-mediated upregulation of p27. Imatinib induced the expression of p27 protein in K562 cells in a time- and concentration-dependent manner (Figure 1e). Importantly, there was a correlation between p27 levels and erythroid differentiation as assessed by the expression of γ-globin (Figure 1e). To confirm p27 involvement we analyzed the imatinib effect in p27 depleted cells. A short-hairpin vector for p27 was transiently transfected into K562, resulting in lower p27 levels in cells treated with imatinib, as compared with empty vector-transfected cells (Figure 1f). Consistently, these cells showed a lower level of differentiation in response to imatinib as assessed by the elevated γ-globin expression (Figure 1f, compare lanes 2 versus 4) and by the increase in the fraction of benzidine-positive cells (Figure 1f, bottom panel).

To investigate whether the imatinib-induced p27 was sufficient to differentiate the cells, we compared the levels of p27 and differentiation obtained by imatinib in K562 with those achieved by Zn^{2+} in Kp27-5 cells. These are K562 cells carrying a zinc-inducible *p27* gene that undergoes erythroid differentiation upon p27 induction.[27] The proliferative arrest induced by p27 in Kp27-5 cells was similar to that achieved by imatinib and the antiproliferative effects of p27 and imatinib were not additive (Figure 1g). Also, p27 did not potentiate the imatinib-induced apoptosis (not shown). The levels of p27 achieved after 24 h of imatinib treatment were similar to those of Kp27-5 treated with Zn^{2+} for the same period of time (Figure 1h) and the concomitant treatment with Zn^{2+} and imatinib did not significantly increase the levels of p27 (Figure 1h, upper panel). Consistently, the extent of differentiation was similar to the differentiation achieved with Zn^{2+} or imatinib alone (Figure 1h, lower panel). In a second approach to elevate p27 levels we used the proteasome inhibitor bortezomib. Bortezomib provoked the accumulation of p27 in a concentration- and time-dependent manner (Supplementary Figure 1a) and induced erythroid differentiation of K562, as shown by the accumulation of hemoglobinized cells and ε-globin expression (Supplementary Figures 1b and c). We conclude that the upregulation of p27 is, at least in part, responsible of the differentiation elicited by imatinib.

As p27 is described as a cyclin-dependent kinases inhibitor, we asked whether differentiation was linked to proliferation arrest using K562-R cell line, a K562 derivative resistant to imatinib mainly due to LYN kinase overexpression.[30] In K562-R imatinib did not provoke growth arrest (Figure 2a) and erythroid differentiation (Figures 2b and c). Consistently, p27 expression was not induced in K562-R cells treated with imatinib concentrations high enough (2.5 μM) to inhibit BCR-ABL, as assessed by CRK-L phosphorylation (Figure 2c). Similar results were observed in KmycBT315I, a imatinib-resistant cell line expressing the BCR-ABL-T315I mutant[19] (not shown). However, imatinib-induced erythroid differentiation is not a mere consequence of the growth arrest because other drugs that provoke growth arrest of K562 (interferon-α, busulfan, TPA, staurosporin) do not induce erythroid differentiation.[20,31,32]

It has been reported that MYC is involved in CML progression.[19] Thus, we investigated whether MYC also impaired the imatinib-induced differentiation. We first showed that the low concentrations of imatinib capable of inducing differentiation also caused MYC downregulation in K562 after 24–72 h of treatment (Figure 2d). This downregulation was also demonstrated at the mRNA level, as shown by northern analysis (Figure 2e). It was noteworthy the correlation between the imatinib-mediated MYC repression and erythroid differentiation, as assessed by globin expression (Figures 2d and e). The decrease in MYC mRNA suggested that imatinib repressed MYC at the transcriptional level. This was confirmed by luciferase assays using a luciferase reporter harboring the human MYC promoter which was inactivated by imatinib (Figure 2f).

The former results prompted us to study whether MYC impaired the differentiation triggered by imatinib. To explore this we used two K562 sublines with conditional MYC expression. KMER4 cells expresses the MycER fusion protein,[19] which is activated by 4-hydroxy-tamoxifen (4HT).[33] The expression of MycER in KMER4 cells treated with imatinib was confirmed by immunoblot (Figure 3a). The benzidine assay indicated that MYC antagonized the imatinib-dependent differentiation in KMER4 cells (Figure 3b). We also demonstrated that the imatinib-mediated induction of ε-globin and transferring receptor 2 mRNA was blunted by MYC (Figure 3c). We sought to confirm the former results in a different system of conditional MYC expression. KmycB cells carry a Zn^{2+}-inducible MYC.[20] KmycB treated with Zn^{2+} in the presence of imatinib expressed significant levels of MYC (Figure 3d). Importantly, the addition of $ZnSO_4$ did not result in supra-physiological levels of MYC but rather restores the levels of control cells. MYC expression in KmycB resulted in a dramatic decrease in the fraction of hemoglobin-containing cells (Figure 3e). We also found that MYC decreased the levels of erythroid markers as ε-globin and transferring receptor 2 mRNA which were induced by imatinib (Figure 3f). Treatment with 4HT or Zn^{2+} did not modify the differentiation of parental K562 (not shown). To further confirm the effect of MYC on imatinib-dependent differentiation we hybridized complementary DNA microarrays containing probes of 4466 genes with labeled complementary DNA from KmycB cells treated with imatinib in the presence or absence of MYC. Out of 30 genes that were downregulated by MYC in imatinib-treated cells, 15 genes are associated to erythroid lineage or erythrocyte markers, including embryonic globins, heme synthesis genes, erythrocyte membrane proteins and erythroid-specific enzyme isoforms (Supplementary Table 1). Altogether, the results demonstrate that MYC impairs the erythroid differentiation mediated by imatinib in K562 cells.

We also tested the effect of dasatinib, a more potent BCR-ABL inhibitor also active against SRC kinase and recently introduced in CML therapy.[34,35] Dasatinib induced differentiation of K562 (Figure 3g), as well as downregulation of MYC and upregulation of p27 (Figure 3h). Next, we asked whether MYC impaired the dasatinib-mediated differentiation. For this purpose we used KMER4 cells, which expressed the MycER protein in the presence of dasatinib and 4HT (Figure 3i). We found that the activation of MYC impaired the dasatinib-induced differentiation of KMER4, as shown by the benzidine test (Figure 3j) and the expression of γ-globin (Figure 3k). We conclude that MYC impairs the differentiation induced by the anti-CML drugs imatinib and dasatinib.

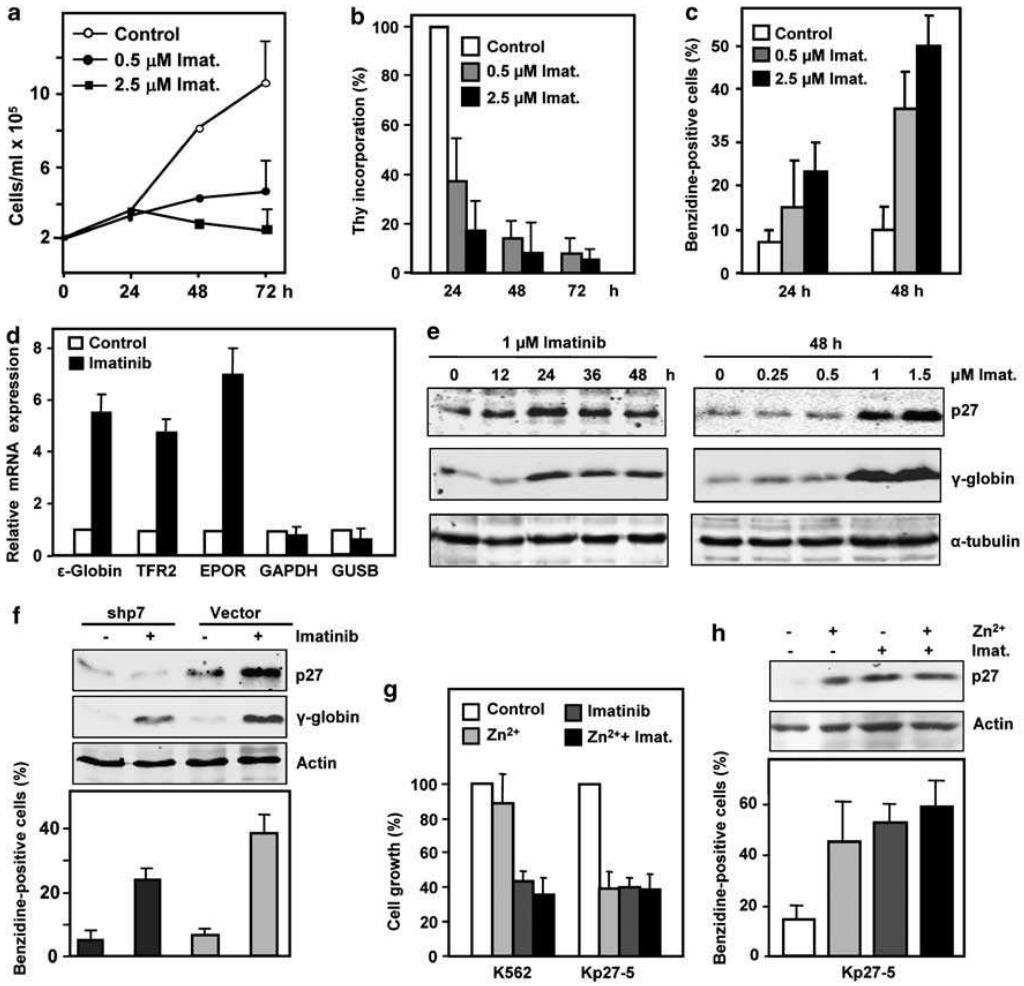

Figure 1. Erythroid differentiation induced by imatinib in K562 cells. (**a**) Inhibition of proliferation mediated by imatinib. Cells were treated with the indicated concentrations of imatinib and proliferation was determined by cell counting, using a hemocytometer. (**b**) DNA synthesis arrest mediated by imatinib. Cells were treated for 24–72 h with imatinib and DNA synthesis was determined by ^{3}H-thymidine incorporation as described.[19] Data are mean values of ^{3}H-thymidine incorporation from three experiments, relative to the thymidine incorporation in untreated cells at each time point; bars, s.e.m. (**c**) Erythroid differentiation induced by imatinib. The fraction of hemoglobinized (benzidine-positive) cells was determined after treatment with 0.5 μM and 2.5 μM imatinib for 24 and 48 h. Benzidine assays were performed essentially as described.[44] At least 300 cells were counted in each determination. Data are mean values from three independent experiments; bars, s.e.m. (**d**) Expression of ε-globin, transferring receptor 2 (TFR2) and erythropoietin receptor (EPOR) mRNA measured by reverse transcription-quantitative PCR (RT–qPCR) in K562 cells treated with 0.5 μM imatinib for 48 h. Expression of the housekeeping genes *GAPDH* (glyceraldehyde 3-phosphate dehydrogenase) and *GUSB* (β-glucuronidase) were also measured as controls of non-erythroid genes. Total RNA extraction was carried out with the Trizol reagent (Life Technologies, Carlsbad, CA, USA). For RT–qPCR, the first-strand complementary DNA was synthesized from 1 μg of total RNA using SuperScript II RNase reverse transcriptase (Invitrogen, Carlsbad, CA, USA) and random primers as described.[26] The data were normalized against the levels of ribosomal protein small 14 (RPS14) mRNA. qPCR were carried out in a MyCycler apparatus (BioRad, Hercules, CA, USA). Primer sequences are available upon request. Data are mean values from three mRNA determinations from two independent experiments; bars, s.e.m. (**e**) Induction of p27 by imatinib in K562. Cells were treated with 1 μM imatinib for 0–48 h (left panel), and for 48 h with 0–1.5 μM imatinib (right panel). The levels of p27 and γ-globin were determined by immunoblot. Tubulin expression was determined to assess protein loading. Cell lysis and protein immunoblotting were performed as described.[21] The antibodies used were: anti-α-tubulin (H-300, rabbit polyclonal), γ-globin (51-7, mouse monoclonal) and p27 (C19, rabbit polyclonal). All antibodies were from Santa Cruz Biotech (Santa Cruz, CA, USA). (**f**) Upper panel: siRNA-mediated depletion of p27 impairs the imatinib-dependent differentiation. A p27 short-hairpin vector[45] was transiently transfected by nucleofection (kit V, Amaxa, Koln, Germany) into K562 cells and 12 h later imatinib (1 μM) was added. After 48 h of imatinib treatment the cells were lysed and the protein levels of p27, γ-globin and actin (as loading control) were determined by immunoblot (upper panel). Anti-actin antibody was I-19, goat polyclonal from Santa Cruz Biotech. The transfection was repeated three times with essentially the same result. Lower panel: fraction of hemoglobinized (benzidine-positive) cells determined after 48 h treatment with 1 μM imatinib and 60 h post-transfection. Data are mean values from two independent experiments; bars, s.e.m. (**g**) Imatinib and p27 do not cooperate in the proliferation arrest of K562 cells. Kp27-5 cells were treated for 72 h with 0.5 μM imatinib or/and 75 μM $ZnSO_4$ as indicated and proliferation was determined by cell counting. (**h**) Upper panel, Kp27-5 cells were treated for 24 h with 75 μM $ZnSO_4$ or 1 μM imatinib and the levels of actin and p27 were determined by immunoblot. Lower panel, the fraction of benzidine-positive cells was also determined in the same samples and data (mean ± s.e.m.) is indicated at the bottom of each lane.

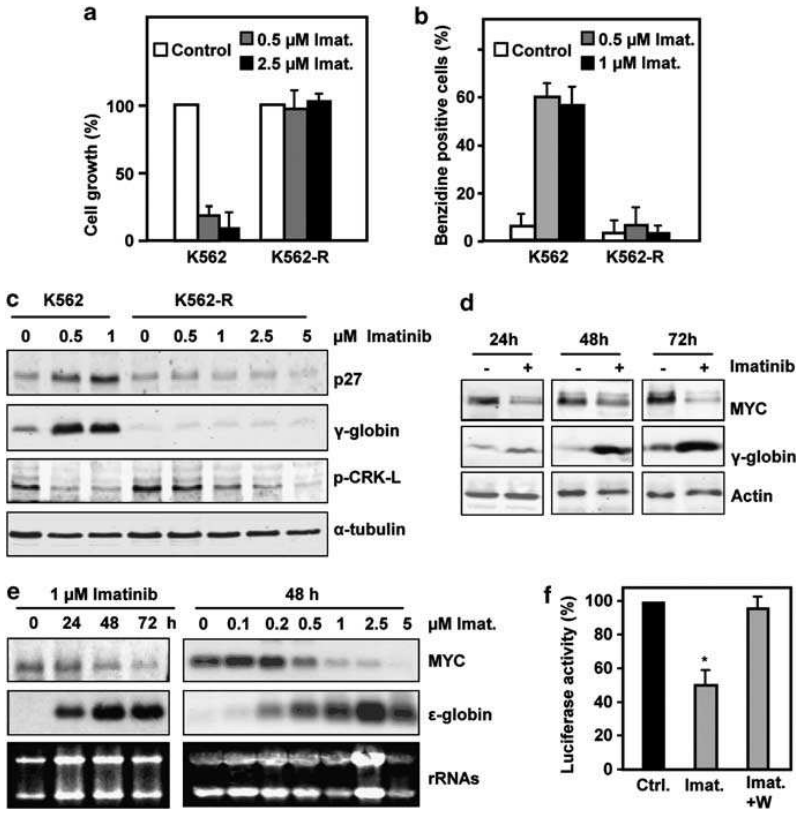

Figure 2. Imatinib-dependent differentiation is associated to proliferative arrest and MYC downregulation. (**a**) K562 and K562-R cells were seeded at a density of 2×10^5 cells/ml and treated for 48 h with the indicated imatinib concentrations and the cells were counted after 72 h. (**b**) K562 and K562-R cells were treated for 48 h with the indicated imatinib concentrations and subjected to the benzidine cytochemical test to count hemoglobin-producing cells. Data are mean values ± s.e.m. of three independent experiments. (**c**) K562-R cells and parental K562 cells were treated for 48 h with the indicated imatinib concentrations and the levels of p27, γ-globin (to assess erythroid differentiation) and phospho-CRK-L (to assess BCR-ABL activity) (anti-phosho-Tyr207-Crk-L, from Cell Signalling, Danvers, MA, USA) determined by immunoblot. α-tubulin levels were also measured to assess the protein loading. (**d**) Concomitant MYC downregulation and γ-globin upregulation induced by imatinib. K562 cells were treated with 0.5 μM imatinib for the indicated periods of time and the MYC and γ-globin protein levels were determined by immunoblot. Levels of actin were determined as a control of protein loading. MYC antibody (N-262, rabbit polyclonal from Santa Cruz Biotech). (**e**) Downregulation of MYC mRNA by imatinib in K562. Cells were treated with the indicated concentrations of imatinib for 48 h and the MYC and ε-globin mRNA levels were determined by Northern analysis. Probe labeling with (α-^{32}P)dCTP and filter hybridization were carried out according to standard procedures. Probes for human MYC and ε-globin were as described.[46] A picture of the filter after transfer showing the ribosomal RNAs stained with ethidium bromide is shown in each case to assess the loading and integrity of the RNAs. (**f**) Imatinib represses the MYC promoter in K562 cells. The activity of a MYC luciferase construct carrying 2.4 kb of human MYC promoter[47] was assayed after 24 h of treatment with 0.5 μM imatinib ('Imat.'), washed and further incubated 24 h without drug ('Imat + W'). Transfections (2×10^6 cells per transfection) were performed at 260 v and 1 mFa in a Bio-Rad electroporator (BioRad). As an internal control, cells were co-transfected with pRL-null plasmid encoding for Renilla luciferase (Promega) and the luciferase activity was normalized to Renilla luciferase. Data are mean values of three independent experiments; bars, s.e.m.; *$P < 0.05$ versus control and washed cells.

So far we showed that (a) imatinib-mediated differentiation depends on the upregulation of p27 and, (b) MYC inhibits this differentiation. As MYC impairs p27-mediated differentiation of K562[21] we determined p27 expression in KMER4 cells treated with 4HT and 0.5 μM imatinib, that is, under conditions where erythroid differentiation was inhibited by MYC. The results of the immunoblot showed that MYC activation blunted the upregulation of p27 by imatinib after 24h and 48 h of treatment (Figure 4a). To assess the erythroid differentiation we determined γ-globin expression levels which correlated with those of p27 (Figure 4a). We confirmed this effect of MYC using the KmycB cells. The induction of MYC antagonized the upregulation of p27 and γ-globin by imatinib in KmycB (Figure 4b). Although MYC decreased p27 protein levels, MYC did not significantly reduced p27 mRNA levels in the presence of imatinib (not shown). Therefore, we concluded that MYC should control p27 stability. To test this hypothesis, we first ruled out that MYC interferes with the inhibition of BCR-ABL activity by imatinib (Supplementary Figure 2a). As BCR-ABL activates SRC kinase[36] and SRC stimulates p27 degradation[37] we asked whether MYC impaired SRC inactivation by imatinib. Imatinib partially inhibited the activity of SRC, as expected (Supplementary Figure 2c) and the specific SRC inhibitor SU6656 induced erythroid differentiation at non-cytotoxic concentrations (Supplementary Figure 2b). Interestingly, MYC activation antagonized the differentiation provoked by SU6656 (Supplementary Figure 2b), in agreement with the inhibition of dasatinib-mediated differentiation shown above. However, MYC did not revert SRC inactivation, either in KmycB cells upon induction of MYC by Zn^{2+} or in KMER4 cells upon activation of MYC by 4HT (Supplementary Figures 2c and d

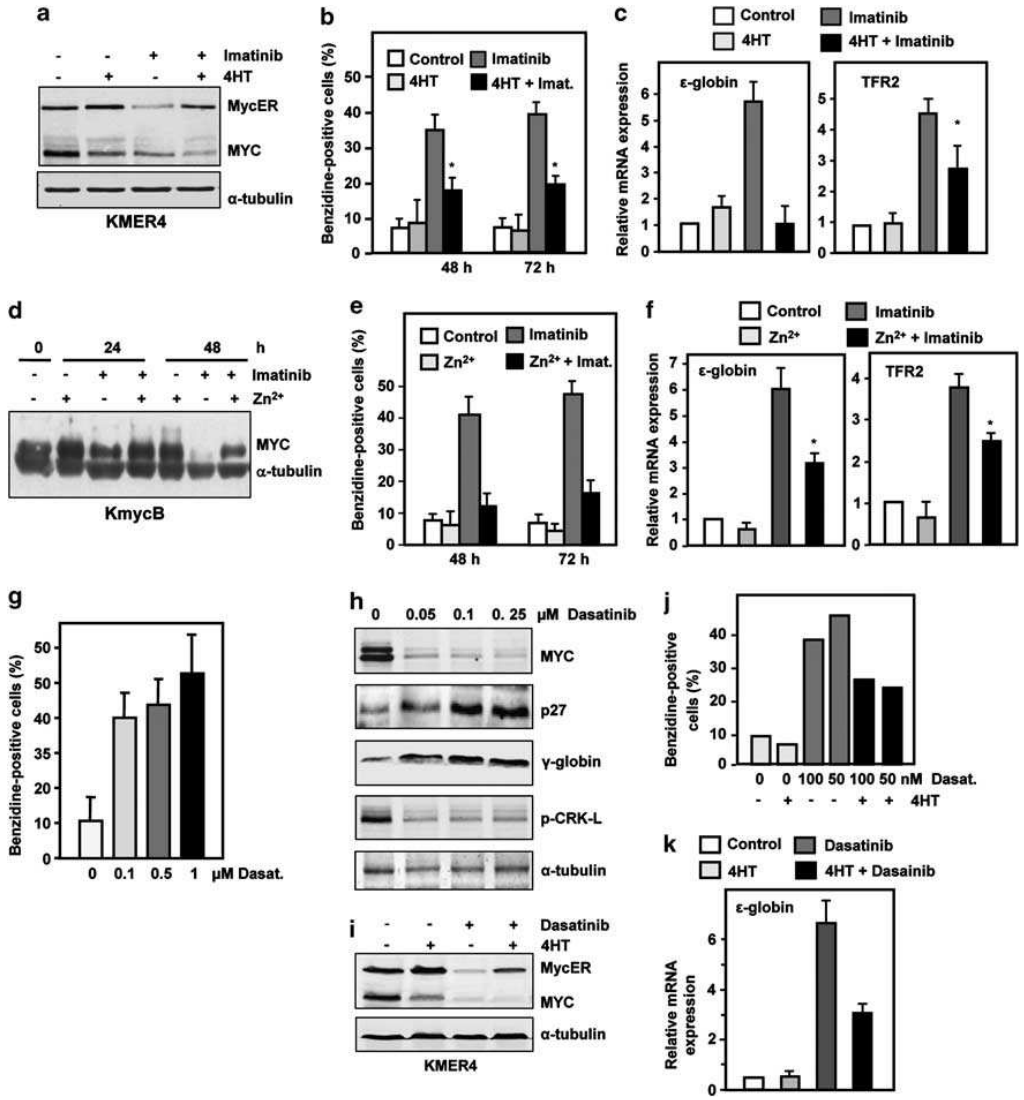

Figure 3. MYC impairs the erythroid differentiation induced by imatinib. (**a**) Immunoblot showing MYC protein levels in KMER4 cells treated for 48 h with 0.5 μM imatinib and 200 nM 4HT. The upper and lower band corresponds to the ectopic MycER and endogenous MYC protein, respectively. Alpha-tubulin levels are shown to assess the protein loading. (**b**) KMER4 cells were treated with 0.5 μM imatinib and 200 nM 4HT for 48–72 h and subjected to the benzidine test to score hemoglobin-producing cells. Data are mean values ± s.e.m. of three independent experiments. *$P<0.05$ versus imatinib. (**c**) KMER4 cells treated for 48 h with 0.5 μM imatinib and/or 200 nM 4HT. The erythroid differentiation was assessed by ε-globin and transferring receptor 2 (TFR2) mRNA expression. Data are mean values ± s.e.m. of two independent experiments. *$P<0.05$ versus imatinib treatment. (**d**) Immunoblot showing the MYC protein levels in KmycB cells treated with 0.5 μM imatinib and 75 μM $ZnSO_4$ (to induce MYC) for the indicated periods of time. α-tubulin levels were also determined to assess the protein loading. (**e**) KmycB were treated as in (**b**) and subjected to the benzidine test to score hemoglobin-producing cells. Data are mean values ± s.e.m. of three independent experiments. *$P<0.05$ versus imatinib. (**f**) KmycB cells were for 48 h with 0.5 μM imatinib and 75 μM $ZnSO_4$ and the erythroid differentiation was assessed by ε-globin and TFR2 mRNA expression. Data are mean values ± s.e.m. of three independent experiments. *$P<0.05$ versus imatinib treatment. (**g**) Erythroid differentiation induced by dasatinib (purchased from LC Laboratories, Woburn, MA, USA) in K562 cells. The fraction of benzidine-positive cells was determined after treatment with the indicated dasatinib concentrations for 48 h. Data are mean values ± s.e.m. from three independent experiments. (**h**) Immunoblot showing the downregulation of MYC and upregulation of p27 in response to dasatinib. K562 cells were treated for 48 h with the indicated concentrations of dasatinib and the levels of the proteins shown at the right were determined by immunoblot. Globin was determined to assess erythroid differentiation, p-CRK-L to assess the inhibition of BCR-ABL by dasatinib and α-tubulin to assess protein loading. (**i**) Immunoblot showing the levels of MYC protein in KMER4 cells treated for 48 h with 100 nM dasatinib and 200 nM 4HT. The upper and lower band corresponds to the ectopic MycER and endogenous MYC protein, respectively. Alpha-tubulin levels are shown to assess the protein loading. (**j**) KMER4 cells were treated with 50 or 100 nM dasatinib and 200 nM 4HT for 48 h and subjected to the benzidine test to score hemoglobin-producing cells. One representative experiment is shown. (**k**) KMER4 cells were treated for 24 h with 100 nM dasatinib and the erythroid differentiation was assessed by ε-globin mRNA expression. Data are mean values ± s.e.m. of two independent experiments.

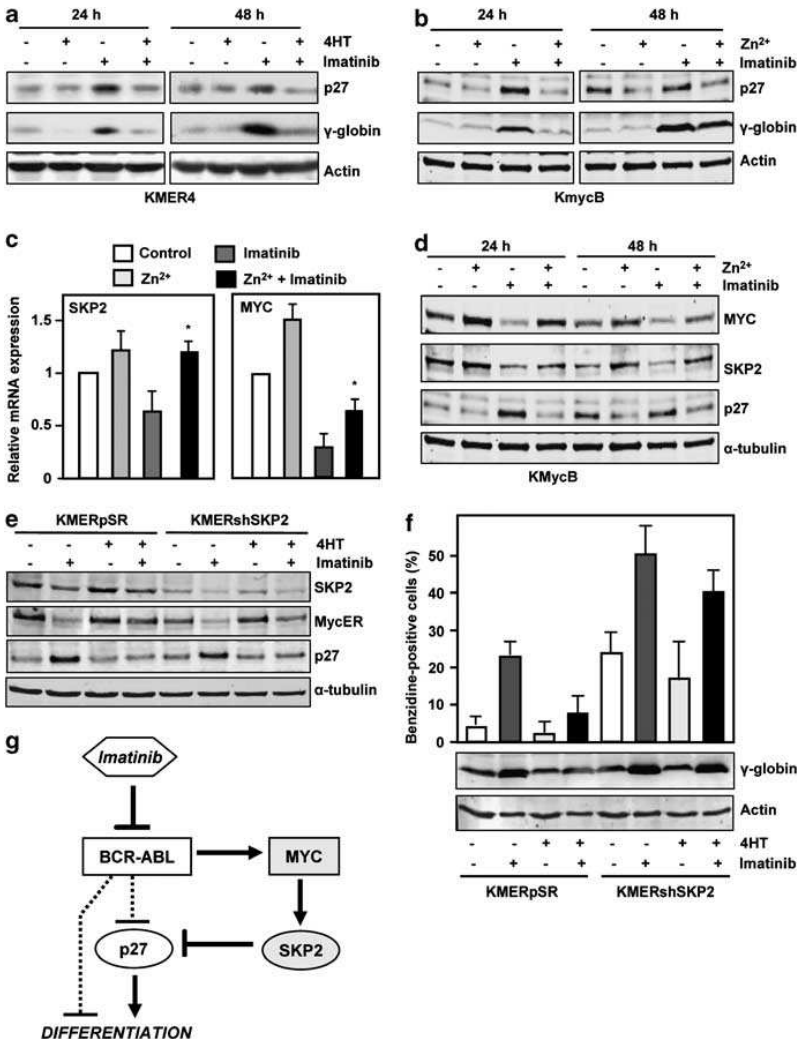

Figure 4. Myc antagonizes the upregulation of p27 induced by imatinib. (**a**) KMER4 cells were treated for 24–48 h with 0.5 μM imatinib and 4HT as indicated. The levels of p27 and γ-globin (as a marker of erythroid differentiation) were determined by immunoblot. Levels of actin were determined as a control of protein loading. (**b**) KmycB cells were treated for 24–48 h with 0.5 μM imatinib and 75 μM $ZnSO_4$ as indicated. The levels of the proteins indicated at the right were determined by immunoblot. (**c**) KmycB cells were treated for 48 h with 0.5 μM imatinib and 75 μM $ZnSO_4$ as indicated and mRNA expression of MYC and SKP2 determined by RT–qPCR. Data are mean values ± s.e.m. of three independent experiments. (**d**) MYC-mediated induction of SKP2 in the presence of imatinib correlates with decreased p27 levels. KmycB cells were treated for 24–48 h with 75 μM $ZnSO_4$ and 0.5 μM imatinib as indicated, and the levels of MYC, SKP2, p27 and α-tubulin (as protein loading control) were assayed by immunoblot. (**e**) KMERshSKP2 and the control cells (KMERpSR) were treated with 1 μM imatinib and 200 nM 4HT for 24 h as indicated, and the levels of SKP2, MycER and p27 were determined by immunoblot, using α-tubulin as protein loading control. (**f**) Enhanced erythroid differentiation in cells with silenced SKP2. KMERshSKP2 cells and control cells (KMERpSR) were treated with 1 μM imatinib and 200 nM 4HT for 72 h and the fraction of differentiated cells was determined by the benzidine assay. Data are mean values from three independent experiments; bars, s.e.m. (upper graph). The levels of γ-globin were determined by immunoblot, using actin as protein loading control (lower panel). (**g**) Model for MYC-mediated inhibition of the differentiation induced by imatinib in CML cells. The model proposes that, in the presence of imatinib, MYC can provoke the downregulation of p27 through the induction of SKP2. Other alternative pathways leading to the downregulation of p27 or the cell differentiation by BCR-ABL cannot be ruled out and are shown in dotted lines.

respectively). Therefore we ruled out SRC activity as a major mechanism for p27 degradation in response to MYC.

SKP2 is the p27-recognizing component of the SCF^{SKP2} ubiquitilation complex and the main regulator of p27 levels *in vivo*.[38,39] In addition, SKP2 is upregulated by BCR-ABL[40,41] and *SKP2* is a MYC target gene.[14] Therefore, we tested the hypothesis that, in the presence of imatinib, MYC downregulates p27 through the induction of SKP2. We first confirmed that the zinc-mediated induction of MYC in the presence of imatinib results in SKP2 mRNA increase in KmycB cells (Figure 4c). The immunoblot of Figure 4d shows that p27 protein levels are decreased upon MYC and SKP2 upregulation. To confirm the SKP2 involvement we next used KMERshSKP2 cells, which are a K562 derivative carrying the MycER construct and in which SKP2 has been partially silenced.[14] The expression of MycER and the reduced levels of SKP2 in KMERshSKP2 were confirmed by immunoblot (Figure 4e). The

extent of differentiation was significantly higher in shSKP2-expressing cells, as assessed by the benzidine assay and the expression of γ-globin (Figure 4f), as well as by the increased ε-globin and erythropoietin receptor mRNA (not shown). As expected, the anti-differentiation effect of MYC was also reduced in SKP2-depleted cells, as compared with control cells (Figure 4f). Therefore, it is likely that the reported induction of SKP2 expression by BCR-ABL is indeed mediated by MYC. Altogether, these results suggest that the induction of SKP2 is at least one mechanism by which MYC antagonizes the differentiation mediated by imatinib.

In summary, we have demonstrated that MYC impairs the differentiation of K562 induced by anti-CML drugs as imatinib and dasatinib. The relevance of our work is based in that (a) the loss of myeloid differentiation is a critical hallmark of CML progression into blastic phase and (b) that MYC has been involved in CML progression. The inhibition of differentiation is not due to overgrowth of MYC-expressing undifferentiated clones or to apoptosis of differentiated clones, as we previously showed that MYC induction does not stimulate cell proliferation and does not enhance the apoptosis due to imatinib ([19] and data not shown). In contrast, our data show that MYC impairs differentiation by blocking p27 upregulation induced by imatinib. We cannot rule out additional mechanisms by which BCR-ABL downregulate p27 (for example, PI3 kinase activation,[28]) or that MYC blocks differentiation through SKP2-independent mechanisms, but the results suggest that MYC opposes imatinib-dependent differentiation through the MYC-SKP2-p27 axis. The model is depicted in Figure 4g. It is reasonable to speculate that p27 upregulation is one of the mechanisms by which imatinib contributes not only to limit the proliferation of leukemic cells but also to prevent the loss of differentiation control. Interestingly, ablation of SKP2 in hematopoietic progenitors attenuates BCR-ABL-induced myeloproliferative disease[42] and erythroid differentiation in bone marrow is associated with accumulation of p27.[43] In conclusion, MYC deregulation may contribute to CML progression through different mechanisms including inhibition of cell differentiation.

CONFLICT OF INTEREST

The authors declare no conflict of interest.

ACKNOWLEDGEMENTS

We thank Pilar Frade, María Aramburu and Guillermo Santana for technical assistance, Robert Eisenman, Theodore Lee and Robert Sclafani for constructs, and M Teresa Molero and Carlos Richard for useful comments on the manuscript. Funding for this work was provided by grants SAF11-23796 and ISCIII-RETIC RD06/0020/0017 to JL, FIS 11/00397 to MDD, SAF09-09254 and Fundación Mutua Madrileña to JMP, FIS08-0878 to SA and FIS08-0440 to JCC.

REFERENCES

1 Dang CV, O'Donnell KA, Zeller KI, Nguyen T, Osthus RC, Li F. The c-Myc target gene network. *Semin Cancer Biol* 2006; **16**: 253–264.
2 Eilers M, Eisenman RN. Myc's broad reach. *Genes Dev* 2008; **22**: 2755–2766.
3 Nesbit CE, Tersak JM, Prochownik EV. MYC oncogenes and human neoplastic disease. *Oncogene* 1999; **18**: 3004–3016.
4 Vita M, Henriksson M. The Myc oncoprotein as a therapeutic target for human cancer. *Semin Cancer Biol* 2006; **16**: 318–330.
5 Meyer N, Penn LZ. Reflecting on 25 years with MYC. *Nat Rev Cancer* 2008; **8**: 976–990.
6 Leon J, Ferrandiz N, Acosta JC, Delgado MD. Inhibition of cell differentiation: a critical mechanism for MYC-mediated carcinogenesis? *Cell Cycle* 2009; **8**: 1148–1157.
7 Polyak K, Lee MH, Erdjument-Bromage H, Koff A, Roberts JM, Tempst P *et al.* Cloning of p27Kip1, a cyclin-dependent kinase inhibitor and a potential mediator of extracellular antimitogenic signals. *Cell* 1994; **78**: 59–66.
8 Coats S, Flanagan WM, Nourse J, Roberts JM. Requirement of p27Kip1 for restriction point control of the fibroblast cell cycle. *Science* 1996; **272**: 877–880.
9 Chu IM, Hengst L, Slingerland JM. The Cdk inhibitor p27 in human cancer: prognostic potential and relevance to anticancer therapy. *Nat Rev Cancer* 2008; **8**: 253–267.
10 Slingerland J, Pagano M. Regulation of the cdk inhibitor p27 and its deregulation in cancer. *J Cell Physiol* 2000; **183**: 10–17.
11 Carrano AC, Eytan E, Hershko A, Pagano M. SKP2 is required for ubiquitin-mediated degradation of the CDK inhibitor p27. *Nat Cell Biol* 1999; **1**: 193–199.
12 Sutterluty H, Chatelain E, Marti A, Wirbelauer C, Senften M, Muller U *et al.* p45SKP2 promotes p27Kip1 degradation and induces S phase in quiescent cells. *Nat Cell Biol* 1999; **1**: 207–214.
13 Tsvetkov LM, Yeh KH, Lee SJ, Sun H, Zhang H. p27(Kip1) ubiquitination and degradation is regulated by the SCF(Skp2) complex through phosphorylated Thr187 in p27. *Curr Biol* 1999; **9**: 661–664.
14 Bretones G, Acosta JC, Caraballo JM, Ferrandiz N, Gomez-Casares MT, Albajar M *et al.* SKP2 oncogene is a direct MYC target gene and MYC down-regulates p27(KIP1) through SKP2 in human leukemia cells. *J Biol Chem* 2011; **286**: 9815–9825.
15 Faderl S, Talpaz M, Estrov Z, O'Brien S, Kurzrock R, Kantarjian HM. The biology of chronic myeloid leukemia. *N Engl J Med* 1999; **341**: 164–172.
16 Melo JV, Barnes DJ. Chronic myeloid leukaemia as a model of disease evolution in human cancer. *Nat Rev Cancer* 2007; **7**: 441–453.
17 Savona M, Talpaz M. Getting to the stem of chronic myeloid leukaemia. *Nat Rev Cancer* 2008; **8**: 341–350.
18 Kavalerchik E, Goff D, Jamieson CH. Chronic myeloid leukemia stem cells. *J Clin Oncol* 2008; **26**: 2911–2915.
19 Albajar M, Gomez-Casares MT, Llorca J, Mauleon I, Vaque JP, Acosta JC *et al.* MYC in chronic myeloid leukemia: induction of aberrant DNA synthesis and association with poor response to imatinib. *Mol Cancer Res* 2011; **9**: 564–576.
20 Delgado MD, Lerga A, Canelles M, Gomez-Casares MT, Leon J. Differential regulation of Max and role of c-Myc during erythroid and myelomonocytic differentiation of K562 cells. *Oncogene* 1995; **10**: 1659–1665.
21 Acosta JC, Ferrandiz N, Bretones G, Torrano V, Blanco R, Richard C *et al.* Myc inhibits p27-induced erythroid differentiation of leukemia cells by repressing erythroid master genes without reversing p27-mediated cell cycle arrest. *Mol Cell Biol* 2008; **28**: 7286–7295.
22 O'Dwyer ME, Mauro MJ, Druker BJ. Recent advancements in the treatment of chronic myelogenous leukemia. *Annu Rev Med* 2002; **53**: 369–381.
23 Ren R. Mechanisms of BCR-ABL in the pathogenesis of chronic myelogenous leukaemia. *Nat Rev Cancer* 2005; **5**: 172–183.
24 Quintas-Cardama A, Cortes J. Molecular biology of bcr-abl1-positive chronic myeloid leukemia. *Blood* 2009; **113**: 1619–1630.
25 Shah NP, Kasap C, Weier C, Balbas M, Nicoll JM, Bleickardt E *et al.* Transient potent BCR-ABL inhibition is sufficient to commit chronic myeloid leukemia cells irreversibly to apoptosis. *Cancer Cell* 2008; **14**: 485–493.
26 Albajar M, Gutierrez P, Richard C, Rosa-Garrido M, Gomez-Casares MT, Steegmann JL *et al.* PU.1 expression is restored upon treatment of chronic myeloid leukemia patients. *Cancer Lett* 2008; **270**: 328–336.
27 Munoz-Alonso MJ, Acosta JC, Richard C, Delgado MD, Sedivy J, Leon J. p21Cip1 and p27Kip1 induce distinct cell cycle effects and differentiation programs in myeloid leukemia cells. *J Biol Chem* 2005; **280**: 18120–18129.
28 Gesbert F, Sellers WR, Signoretti S, Loda M, Griffin JD. BCR/ABL regulates expression of the cyclin-dependent kinase inhibitor p27Kip1 through the phosphatidylinositol 3-Kinase/AKT pathway. *J Biol Chem* 2000; **275**: 39223–39230.
29 Jonuleit T, van der Kuip H, Miething C, Michels H, Hallek M, Duyster J *et al.* Bcr-Abl kinase down-regulates cyclin-dependent kinase inhibitor p27 in human and murine cell lines. *Blood* 2000; **96**: 1933–1939.
30 Wu J, Meng F, Kong LY, Peng Z, Ying Y, Bornmann WG *et al.* Association between imatinib-resistant BCR-ABL mutation-negative leukemia and persistent activation of LYN kinase. *J Natl Cancer Inst* 2008; **100**: 926–939.
31 Gomez-Casares MT, Delgado MD, Lerga A, Crespo P, Quincoces AF, Richard C *et al.* Down-regulation of c-myc gene is not obligatory for growth inhibition and differentiation of human myeloid leukemia cells. *Leukemia* 1993; **7**: 1824–1833.
32 Lerga A, Crespo P, Berciano M, Delgado MD, Canelles M, Cales C *et al.* Regulation of c-Myc and Max in megakaryocytic and monocytic-macrophagic differentiation of K562 cells induced by protein kinase C modifiers: c- Myc is down-regulated but does not inhibit differentiation. *Cell Growth Differ* 1999; **10**: 639–654.
33 Littlewood TD, Hancock DC, Danielian PS, Parker MG, Evan GI. A modified oestrogen receptor ligand-binding domain as an improved switch for the regulation of heterologous proteins. *Nucleic Acids Res* 1995; **23**: 1686–1690.
34 Schenone S, Brullo C, Musumeci F, Botta M. Novel dual Src/Abl inhibitors for hematologic and solid malignancies. *Expert Opin Investig Drugs* 2011; **19**: 931–945.
35 Kantarjian HM, Baccarani M, Jabbour E, Saglio G, Cortes JE. Second-generation tyrosine kinase inhibitors: the future of frontline CML therapy. *Clin Cancer Res* 2011; **17**: 1674–1683.

36 Rubbi L, Titz B, Brown L, Galvan E, Komisopoulou E, Chen SS *et al.* Global phosphoproteomics reveals crosstalk between Bcr-Abl and negative feedback mechanisms controlling Src signaling. *Sci Signal* 2011; **4**: ra18.
37 Chu I, Sun J, Arnaout A, Kahn H, Hanna W, Narod S *et al.* p27 phosphorylation by Src regulates inhibition of cyclin E-Cdk2. *Cell* 2007; **128**: 281–294.
38 Nakayama K, Nagahama H, Minamishima YA, Miyake S, Ishida N, Hatakeyama S *et al.* Skp2-mediated degradation of p27 regulates progression into mitosis. *Dev Cell* 2004; **6**: 661–672.
39 Kossatz U, Dietrich N, Zender L, Buer J, Manns MP, Malek NP. Skp2-dependent degradation of p27kip1 is essential for cell cycle progression. *Genes Dev* 2004; **18**: 2602–2607.
40 Andreu EJ, Lledo E, Poch E, Ivorra C, Albero MP, Martinez-Climent JA *et al.* BCR-ABL induces the expression of Skp2 through the PI3K pathway to promote p27Kip1 degradation and proliferation of chronic myelogenous leukemia cells. *Cancer Res* 2005; **65**: 3264–3272.
41 Chen JY, Wang MC, Hung WC. Transcriptional activation of Skp2 by BCR-ABL in K562 chronic myeloid leukemia cells. *Leuk Res* 2009; **33**: 1520–1524.
42 Agarwal A, Bumm TG, Corbin AS, O'Hare T, Loriaux M, VanDyke J *et al.* Absence of SKP2 expression attenuates BCR-ABL-induced myeloproliferative disease. *Blood* 2008; **112**: 1960–1970.
43 Hsieh FF, Barnett LA, Green WF, Freedman K, Matushansky I, Skoultchi AI *et al.* Cell cycle exit during terminal erythroid differentiation is associated with accumulation of p27(Kip1) and inactivation of cdk2 kinase. *Blood* 2000; **96**: 2746–2754.
44 Rowley PT, Ohlsson-Wilhelm BM, Farley BA, LaBella S. Inducers of erythroid differentiation in K562 human leukemia cells. *Exp Hematol* 1981; **9**: 32–37.
45 Roy S, Singh RP, Agarwal C, Siriwardana S, Sclafani R, Agarwal R. Downregulation of both p21/Cip1 and p27/Kip1 produces a more aggressive prostate cancer phenotype. *Cell Cycle* 2008; **7**: 1828–1835.
46 Gomez-Casares MT, Vaque JP, Lemes A, Molero T, Delgado MD, Leon J. C-myc expression in cell lines derived from chronic myeloid leukemia. *Haematologica* 2004; **89**: 241–243.
47 Lee TC, Ziff EB. Mxi1 is a repressor of the c-Myc promoter and reverses activation by USF. *J Biol Chem* 1999; **274**: 595–606.

Supplementary Information accompanies the paper on the Oncogene website (http://www.nature.com/onc)

Journal of Cellular Physiology

MYC Accelerates p21^{CIP}-Induced Megakaryocytic Differentiation Involving Early Mitosis Arrest in Leukemia Cells

MARÍA J. MUÑOZ-ALONSO,[1,2] LAURA CEBALLOS,[1,3] GABRIEL BRETONES,[1,4] PILAR FRADE,[1] JAVIER LEÓN,[1,4]* AND ALBERTO GANDARILLAS[1,3,5]*

[1] *Departamento de Biología Molecular, Universidad de Cantabria, Santander, Spain*

[2] *Instituto de Investigaciones Biomédicas Alberto Sols, CSIC, Madrid*

[3] *Fundación Marqués de Valdecilla-Instituto de Formación e Investigación Marqués de Valdecilla (IFIMAV), Santander, Spain*

[4] *Instituto de Biomedicina y Biotecnología de Cantabria (IBBTEC), Universidad de Cantabria-CSIC-SODERCAN, Santander, Spain*

[5] *Dermatologie Moléculaire-IURC/UMI, Languedoc-Roussillon, INSERM, Montpellier, France*

p21^{CIP} is a potent cell cycle inhibitor often up-regulated in differentiation. Protooncogene MYC induces cell growth and proliferation, inhibits differentiation and represses p21^{CIP}. However, both molecules are involved in processes of polyploidisation, cell size increase, differentiation and senescence. It is unclear why MYC has a dual role in differentiation. We have previously shown that overexpression of p21^{CIP} in K562 myeloid cells induces megakaryocytic differentiation with polyploidy. We have now investigated the requirements for p21^{CIP} to block mitosis and induce differentiation in the presence of overactivated MYC. Silencing and over-expression studies showed that p21^{CIP} is required to induce differentiation. However, the expression of p21^{CIP} needs to be transient to irreversibly inhibit mitosis but not DNA replication, what leads to polyploidy. Transient overexpression of p21^{CIP} caused early down-regulation of mitotic Cyclins and up-regulation of G1/S Cyclins D and E, changes typical of endoreplication. Interestingly, over-activation of MYC did not release the proliferative block imposed by p21^{CIP} and instead, accelerated cell size increase, megakaryocytic differentiation and polyploidisation. Our data suggests that in some systems p21^{CIP} takes part in a mitosis control driving MYC-induced cellular growth into differentiation.
J. Cell. Physiol. 227: 2069–2078, 2012. © 2011 Wiley Periodicals, Inc.

Transcription factor MYC is a central regulator of cellular growth, with wide implications in cellular processes from proliferation to apoptosis (Eilers and Eisenman, 2008; Meyer and Penn, 2008). MYC is amplified in a variety of malignancies and it often inhibits cell differentiation (Nesbit et al., 1999; Vita and Henriksson, 2006; Leon et al., 2009). However, MYC has been found to stimulate differentiation in systems where it is closely associated with cell growth (Eilers and Eisenman, 2008). It is unclear why MYC has this dual effect on differentiation and it has been proposed that it might depend on the cell context and whether it has or not a direct effect on mitosis (Johnston et al., 1999; Gandarillas et al., 2000; Beer et al., 2004). In some systems, overactivation of MYC causes cell hypertrophy with polyploidy due to a mitosis block (e.g., Schmidt, 1999; Felsher et al., 2000; Gandarillas et al., 2000; Maines et al., 2004; Pierce et al., 2004; Zanet et al., 2005). The capacity of MYC to drive the cell cycle is in part due to its ability to repress cell cycle inhibitors (Lutz et al., 2002; Wu et al., 2003).

Small cell cycle inhibitors of the CIP and KIP families are often induced during cellular differentiation or apoptosis and lost in human cancer (Besson et al., 2008). In particular, p21^{CIP} (hereafter p21) is involved in a variety of differentiation systems (Weiss, 2003; Abbas and Dutta, 2009). p21 binds and inhibits the Cyclin dependent kinases (CDKs) that control the different cell cycle phases. The initially established function of p21 was cell cycle arrest in G1 by inhibiting the DNA replication phase CDK2. Consistently, p21 is repressed by the cell cycle inducer MYC (reviewed in Jung and Hermeking, 2009; Leon et al., 2009). However, a growing body of data has shown that p21 is also able to block mitosis through binding CDK1 and yet allow DNA replication and cellular growth (e.g., Bates et al., 1998; Medema et al., 1998; reviewed in Ullah et al., 2009). Re-replication and polyploidy are often found in cancer but also in normal cells undergoing terminal differentiation and cellular growth (referred to as endoreplication; reviewed in Edgar and Orr-Weaver, 2001; Ullah et al., 2009). One of such systems is the megakaryocyte, which grows in size and ploidy prior to fragment into platelets (Ravid et al., 2002a). Megakaryocytic differentiation associates with p21 induction (Kikuchi et al., 1997; Matsumura et al., 1997; Baccini et al., 2001). Interestingly,

María J. Muñoz-Alonso and Laura Ceballos contributed equally to this work.

Additional Supporting Information may be found in the online version of this article.

Contract grant sponsor: Plan Nacional I+D, MICINN;
Contract grant number: SAF08-01581.
Contract grant sponsor: ISCIII, MICINN;
Contract grant number: RTICC-RD06/0020/0017.
Contract grant sponsor: La Ligue Contre le Cancer de l'Herault.
Contract grant sponsor: Société Française de Dermatologie.
Contract grant sponsor: SCIII-FIS, Programa Regiones Emergentes;
Contract grant number: SCIII-FIS PI08/0890.
Contract grant sponsor: Universidad de Cantabria-FMV/IFIMAV.

*Correspondence to: Javier León and Alberto Gandarillas, Facultad de Medicina, Departamento de Biología Molecular, IBBTEC, Cardenal Herrera Oria s/n, 39011 Santander, Spain.
E-mail: leonj@unican.es and gandarillasa@unican.es

Received 6 July 2011; Accepted 7 July 2011

Published online in Wiley Online Library (wileyonlinelibrary.com), 18 July 2011.
DOI: 10.1002/jcp.22935

we have shown that over-expression of p21 in human K562 myeloid leukemia cells, induces megakaryocytic differentiation with polyploidy. In contrast, over-expression of another CDK2 inhibitor, $p27^{KIP}$, induced erythroid differentiation without polyploidy (Muñoz-Alonso et al., 2005) and this process is inhibited by MYC (Acosta et al., 2008). The mechanisms by which p21 blocks mitosis and triggers megakaryocytic differentiation, as well as the role of MYC in this process, are unclear.

We have taken advantage of a p21-inducible expression system due to a Zinc-regulatable promotor, to investigate the crosstalk between MYC overactivation and a mitosis block in K562 cells. We have made use of various DNA constructs to (i) to knock-down endogenous p21 by antisense sequences or (ii) to express p21 or MYC constitutively or conditionally. The results show that a transient expression of p21 is necessary and sufficient to early and irreversibly block mitosis in the concurrence of DNA replication, leading to polyploidy. Remarkably, overactivation of MYC not only was unable to abrogate the mitosis arrest caused by p21, but it amplified and accelerated megakaryocytic differentiation. The evidence provides novel clues into the mechanisms by which p21 in some instances provokes increased cell volume and polyploidy and into the dual role of MYC in mitosis control and differentiation.

Material and Methods

DNA constructs and antibodies

The entire coding sequence of human p21 was subcloned in the sense orientation into pLPCX to generate pLPCXp21 and in the antisense orientation into pCEFL to construct pCEFLASp21. In the pCEFL vector the expression of the cloned genes is directed by the translation EF-1α promoter. The pMTp21 vector that contains the sheep metallothionein promoter for Zn^{2+}-inducible expression was described previously (Muñoz-Alonso et al., 2005). This promoter, due to its regulatory features, achieves a transient expression of the genes it controls upon addition of Zn^{2+} likely due to promoter transcriptional deactivation (Delgado et al., 1995; Muñoz-Alonso et al., 2005). pBabe and pBabeMycER are described in Littlewood et al. (1995). The following primary antibodies were used in this study from Santa Cruz Biotech (Santa Cruz, CA): anti- p21 (C-19), CDK2 (M2), CDK4 (C-22), CDK6 (C-21; M2), total-Rb (C-15), Cyclin E (HE12), Cyclin A (BF683), Cyclin B1 (GNS1), p(Y15)-CDK1, MYC (N-262), Actin (I-19), Cyclin D2, Cyclin D3 and phospho-histone H3 (p-Ser10, sc-8656-R). pRb-Ser780 (phospho-Rb; P-Rb) was from Cell Signaling (Beverly, MA); α-tubulin (a gift from N. Cowan, New York University, New York); p21 (P1484) and cdk1 (p34cdc2) from Sigma Chemical Co. (St. Louis, MO) CD61 (VI-PL2) from BD Pharmingen (San Diego, CA).

Cell culture, transfections and retroviral infections

K562 cell line was derived from a human chronic myeloid leukemia in blast crisis (Klein et al., 1976). K562 cells retain the capacity to undergo erythroid or megakaryocytic differentiation depending on the stimulus (Delgado et al., 1995; Lerga et al., 1999). Treatment of K562 cells by staurosporin (STA) induces polyploidisation, large cell size and markers specific of megaryocytes and platelets (Lerga et al., 1999). Kp21-3 and Kp21-4 lines (hereafter, Kp21) are K562 cells stably containing a Zn^{2+}-inducible p21 expression construct (Muñoz-Alonso et al., 2005); Kas21A, Kas21B and Kas21C K562 stably expressing a p21 anti-sense construct (pCEFL-AS-p21) and Kpc1 and Kpc2 are K562 stably containing the empty vector (pCEFL) as controls. K21A, K21B ad Kp21C are K562 stably transfected with a vector for p21 (pLPCX-p21) and Kplx are K562 transfected with the empty vector (pLPCX). All lines were generated by electroporation (260 V and 1 mFa in a Bio-Rad electroporator, Hercules, CA), subsequently selected by 0.5 mg/ml G418 (Invitrogen, Carlsbad, CA) and cloned by limiting dilution. To generate K562 cells expressing conditional p21 and pBabe-MycER (Littlewood et al., 1995), Kp21 cells were infected with pBabeMycER-carrying retrovirus produced by AM12 amphotrophic cells and selected with 1 μg/ml puromycin as previously described (Morgenstern and Land, 1991). pBabe-puro empty vector was used to make control cells. To generate K562 expressing conditional p21 and constitutive MYC, K562 were nucleofected (Kit V, Amaxa) with pMTp21 and pBabe-Myc. Empty vectors were transfected in parallel samples as controls to generate the Kp21pb cell line. To make stable pools, cells were selected from 48 h after the transfection with 0.5 mg/ml G418 and 1 μg/ml puromycin (pBabe-puro). Cells were grown in RPMI 1640 medium (Lonza, Cologne, Germany) supplemented with 10% fetal calf serum and antibiotics in a 37°C incubator with 5% CO_2. All experiments were performed on exponentially growing cultures and repeated at least twice with duplicate samples with similar results. Cells were plated at 2.5×10^5 cells/ml in fresh medium and 6 h later treated with 100 nM STA (Sigma) to induce megakaryocytic differentiation, 50–75 μM $ZnSO_4$ to induce p21 or 200 nM 4-hydroxy-tamoxifen (OHT) to activate MycER. For 3 days treatments, the culture medium was replaced by fresh medium after 48 h by centrifugation.

Flow-cytometry

Cells treated or untreated with STA, $ZnSO_4$ and/or 4-hydroxy-tamoxifen for the indicated periods of time were stained with propidium iodide as described previously (Zanet et al., 2005) and analysed by flow cytometry on FACScan™ or a BD FACSCanto™ (BD Biosciences, San Diego, CA). One million cells were stained per sample. Ten thousand events were gated and acquired in list mode for every sample and analysed using CellQuest or BDFACSDiva software (BD Biosciences). For double staining for the megakaryocytic marker CD61 and DNA, 1 million cells were fixed in 70% ethanol and stained as described in Zanet et al. (2005). Double and single blank cell samples were always included for cross-filters fluorescence compensation Negative isotope control immunoglobulins were always used to control the staining on parallel samples (mouse IgGs; Sigma). The secondary antibody was goat anti mouse-Dylight (Jackson ImmunoResearch Inc. West Grove, PA). Large cells were defined as those with a size bigger than 90% of the control cells in each analysis (see Supplementary Figs. 2, 3 and 5).

mRNA expression

Total RNA was isolated using RNeasy Kit (Qiagen, Valencia, CA) according to the manufacturer's instructions, separated by electrophoresis through agarosa-formaldehyde gel and transferred to nitrocellulose. Northern blots were hybridised to ^{32}P-labelled probes as described (Muñoz-Alonso et al., 2005). Probes were fragments of human integrin β_3, vimentin, Cdc25A and Cdc25B cDNAs (provided by A. Corbí, C.I.B, Madrid, Spain).

Western blotting

Cell pellets were lysed in a buffer containing 50 mM Tris (pH 8.0), 150 mM NaCl, 1% Nonidet P-40, phosphatase inhibitors and protease inhibitors. Insoluble debris was removed by centrifugation at 12,000 rpm for 30 min at 4°C. Protein concentration was determined using a Bio-Rad protein assay. Equal amounts (40–80 μg) of extracts were resolved on 12–7% by SDS-PAGE and transferred to nitrocellulose membranes using standard techniques. The membranes were blocked with 5% dry milk in 0.05% Tween-Tris buffered saline (TTBS), probed with primary antibodies followed by incubation with horseradish peroxidase-conjugated secondary antibodies

(Bio-Rad) and analysed by ECL (GE Healthcare Biosciences, Piscataway, NJ), or with IRdye800 secondary antibody (Lincoln, NE) and analysed with an Odyssey scanner (Li-Cor). Densitometric analyses were performed with a ChemiDoc (Bio-Rad).

Immunoprecipitation and kinase activity assays

CDK2- or Cyclin B1-associated kinase activities assay were performed as described previously (Mateyak et al., 1999). Briefly, cells were washed with PBS and lysed at 4°C in a buffer containing 50 mM Hepes (pH 7.5), 150 mM NaCl, 2.5 mM EGTA, 1 mM EDTA, 1 mM dithriothreitol (DTT), 10% glycerol, 0.25% tween20, 10 mM β-gycerophosphate and phosphatase and protease inhibitors. Five hundred micrograms of cellular protein extract were immunoprecipitated with 1 μg of anti-CDK2 (M2; Santa Cruz) or anti-Cyclin B antibodies (GNSI; Santa Cruz), and collected on Gammabind Sepharose (Pharmacia) beads. After extensive washed, kinase activity was assayed by transfer ^{32}P to Histone H1 as substrate at 30°C for

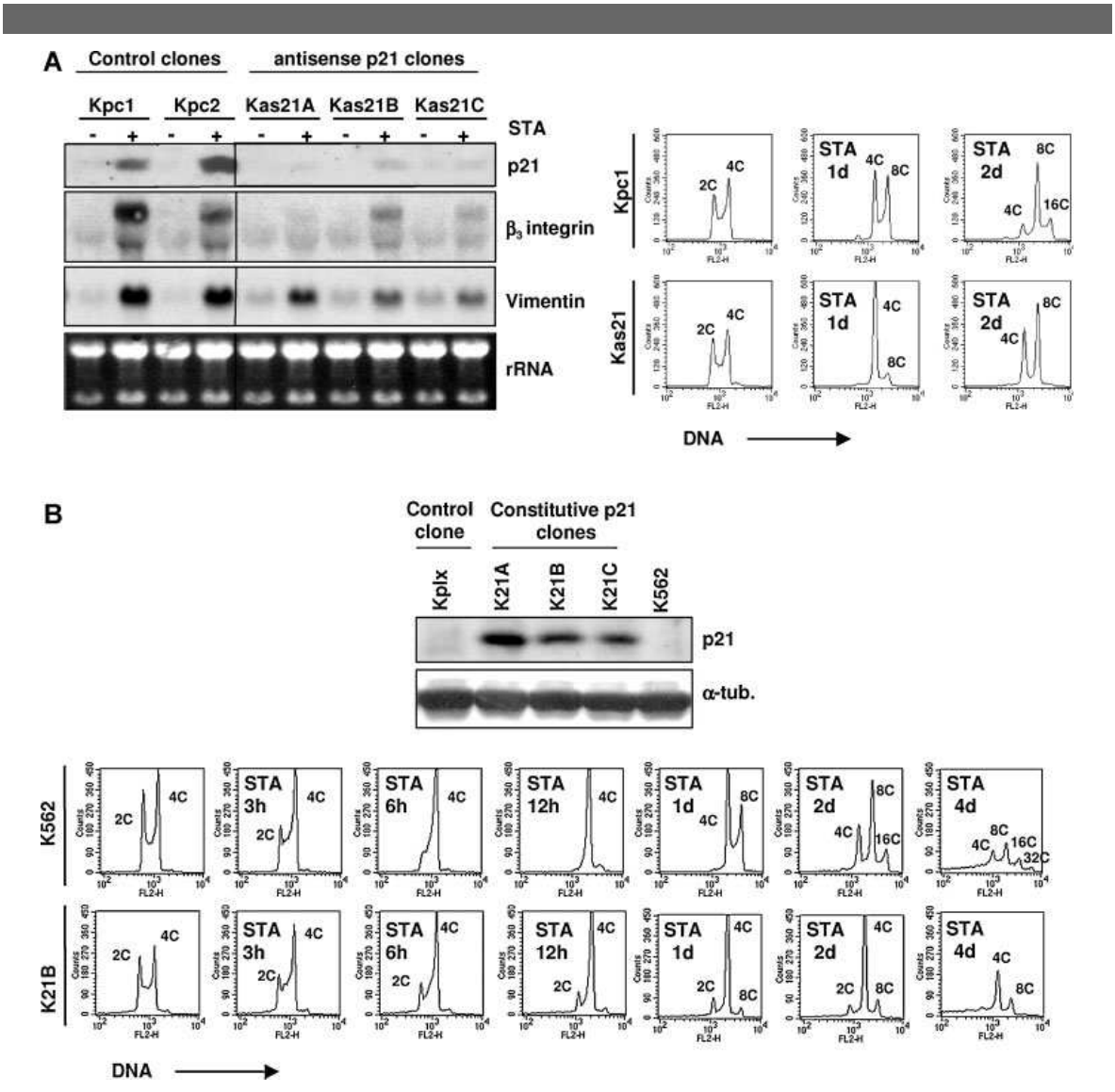

Fig. 1. Transient expression of p21 is required to induce megakaryocytic differentiation. A: left panel: K562 clones expressing antisense p21 (Kas21A, Kas21B, Kas21C) or control clones (Kpc1, Kpc2) were treated with STA to induce megakaryocytic differentiation. mRNA expression of p21 (after 3 h of treatment) and differentiation markers β3 integrin, and vimentin (after 72 h of treatment) were analysed by northen blotting. rRNA (stained with ethidium bromide) is shown as loading control. Right panel: DNA content as analysed by flow-cytometry of the cells indicated, untreated, or treated with STA for the lengths of time indicated. B: upper panel: Western blotting showing protein levels of p21 and α-tubulin (as loading control) in K562 and clones constitutively expressing p21 (K21A, K21B, K21C) or the empty vector (Kplx). Lower panel: DNA content of K562 and Kp21B cells analysed by propidium iodide staining and flow-cytometry after treatment with STA as indicated. Data are representative of three independent experiments.

30 min with 10 μCi [γ-^{32}P] ATP (6,000 Ci/mmol; Amersham Pharmacia) and 5 μg of histone H1 (Roche, Mannheim, Germany). The reaction products were separated by SDS-PAGE, transferred to immobilon P membranes (Millipore), exposed to X-ray film and quantified with a PhosphorImager (Bio-Rad). To detect the immunoprecipitated proteins, the complexes were subject to western blotting as above.

Results

Transient expression of p21 is required to induce megakaryocytic differentiation

K562 human myeloid leukaemia cells retain the capacity to undergo erythroid or megakaryocytic differentiation depending on the stimulus (Delgado et al., 1995; Lerga et al., 1999). Treatment of K562 cells by STA induces polyploidisation, large

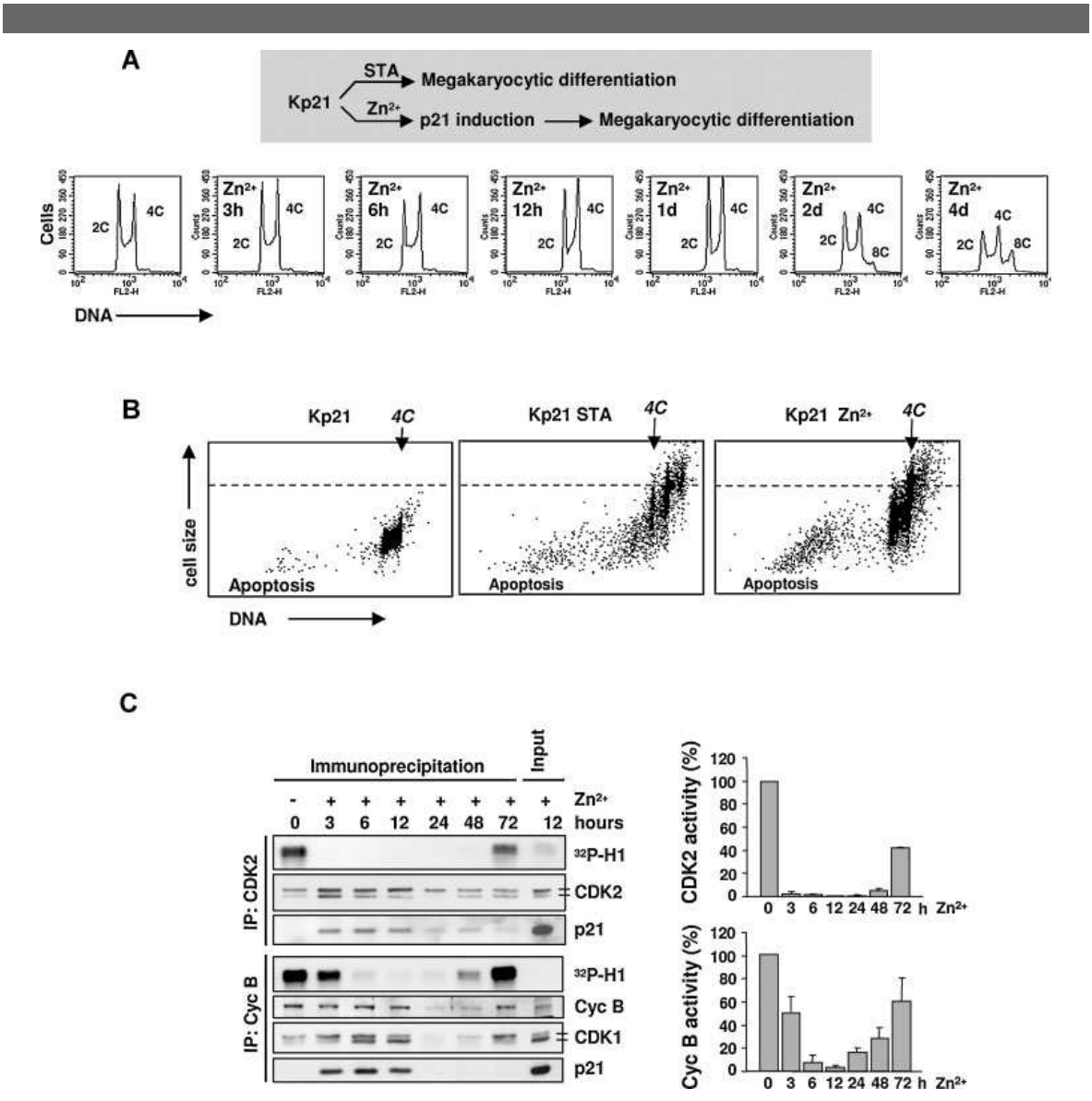

Fig. 2. Transient expression of p21 blocks mitosis and slows down cell cycle progression but not cellular growth. A: upper panel: scheme of the p21 and differentiation induction in the Kp21 cell line. Lower panel: DNA content of Kp21 cells as determined by propidium iodide staining and flow-cytometry after addition of Zn^{2+} for the lengths of time indicated; peaks of cells with 2, 4 or 8 DNA contents (C) are indicated. B: Flow-cytometry dot plot representing cell size (forward light scatter, Y-axis) and DNA content (X-axis) of Kp21 cells untreated, or after addition of stauroporin (STA) or Zn^{2+} for 4 days; note that p21 provokes a higher size increase than STA for the same level of ploidy (e.g., 4C). Data are representative of two independent experiments. C: left panel: kinase assays (on histone H1 as substrate) after immunoprecipitation (IP) with anti-CDK2 and anti-cyclin B. The levels of CDK1, CDK2 and p21 in the immunoprecipitates were determined by western. Right panel: Bar histograms show the quantification of the kinase assays indicated in (C), relative to the activity of the untreated control cells (100%); small bars are s.e.m.

cell size and markers specific of megaryocytes and platelets (Lerga et al., 1999). Therefore STA induces mechanisms of megakaryocytic differentiation in these malignant cells. In addition, the megakaryocytic programme induced by STA is associated by an early and transient induction of endogenous p21 (Muñoz-Alonso et al., 2005) and this also mimics natural megakaryocytic differentiation (Taniguchi et al., 1999; Yaroslavskiy et al., 1999). Consistently, when transient expression of p21 is achieved by a Zn^{2+}-conditional transgene in K562 cells, they undergo a similar megakaryocytic programme (Muñoz-Alonso et al., 2005). The metallothionein promoter utilised, due to its regulatory features, achieves a transient expression of the genes it controls upon addition of Zn^{2+} as described previously (see Materials and Methods section, Delgado et al., 1995; Muñoz-Alonso et al., 2005). The transient expression of p21 induced by Zn^{2+} mimics the induction of the endogenous gene by STA (Muñoz-Alonso et al., 2005) and during normal megakaryocytic differentiation (Taniguchi et al., 1999; Yaroslavskiy et al., 1999). In order to investigate whether endogenous p21 is involved in the signal to differentiation of K562 upon Zn^{2+}, we generated K562 sublines constitutively overexpressing antisense mRNA (Kas21A, Kas21B and Kas21C). Antisense p21 blunted the up-regulation of endogenous p21 and the capacity of the cells to differentiate towards megakaryocytes in response to STA, as measured by the expression of β3-integrin and vimentin and polyploidy (Fig. 1A). We next investigated the effect of constitutive p21 expression on STA-induced differentiation. In addition, we generated K562 cell lines with constitutive overexpression of p21 (K21A, K21B, K21C; Fig. 1B). As expected, these cells proliferated more slowly as compared to the parental K562 (Supplementary Fig. 1A–C). As shown in Figure 1B, high constitutive expression of p21 also inhibited the acquisition of polyploidy characteristic of megakaryocytic differentiation induced by STA.

Transient p21 causes early mitosis arrest

Forced transient induction of p21 provoked K562 cells to accumulate in G2/M, re-replicate and become polyploid (Fig. 2A; Muñoz-Alonso et al., 2005). In addition, p21 induction produced a dramatic increase in cell size (forward light scatter, FSC; Fig. 2B). This increase was even stronger than that observed in cells undergoing megakaryocytic differentiation in response to STA for the same level of ploidy (for e.g., 4C in Fig. 2B). The smaller increase in ploidy produced by p21 as compared with the increase produced by STA might be due to the transient inhibition of the DNA replication kinase CDK2. Consistently, p21 bound to CDK2 as well as to the mitosis complex Cyclin B/CDK1 (Fig. 2C). This inhibited the kinase activity of the different forms of both CDKs, whose expression subsequently decreased. However, their associated activities started to recover by 48 h, as p21 became undetectable (Figs. 2C).

In order to explore how transient over-expression of p21 affected the cell cycle regulation in the onset of megakaryocytic differentiation, we examined the dynamics of Cyclins and CDKs, key regulators of the different phases of the cell cycle (Murray, 2004). As shown in Figure 3, the induction of p21 provoked an up-regulation of Cyclins D2, D3 and E that peaked by 2 days, whereas they decreased in control cells due to culture saturation (see also Supplementary Fig. 2). Cyclins D and E have both been involved in the endoreplication that accompanies megakaryocytic differentiation and polyploidisation (Wang et al., 1995; Garcia et al., 2000; Geng et al., 2003). In contrast, CDK1, Cyclins A and B, which are required for completion of mitosis, were transiently suppressed by 24 h (Figs. 2C and 3 and Supplementary Fig. 2). The detection of p21 in the immunoprecipitates of mitotic

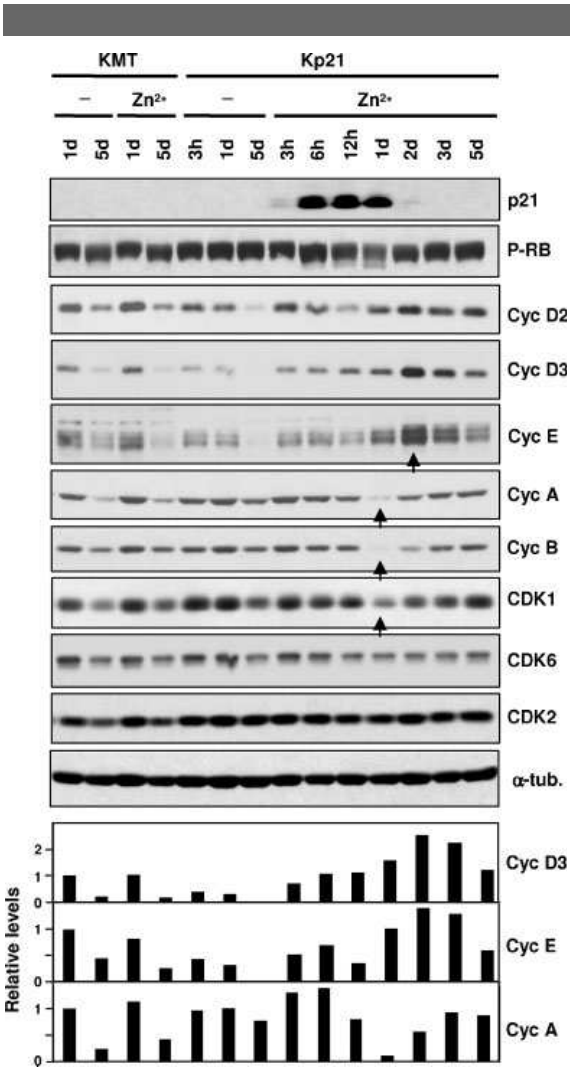

Fig. 3. Transient p21 causes early inhibition of mitotic regulators. Expression of the cell cycle regulators indicated on the right, analysed by western blotting after induction of p21 by addition of Zn^{2+} for the lengths of time indicated. Cyc: Cyclin; α-tubulin (α-tub.) as a loading control. Note that Cyclins A and B and CDK1 are down-regulated whereas Cyclins D and E accumulate, after the addition of Zn^{2+} (arrows). Bar histograms: densitometry of signals for Cyclins D3, E and A, normalised to the levels of α-tubulin.

Cyclins decreased by 24 h as the Cyclins did, anticipating the decline of total p21 (Figs. 2C and 3). CDC25A and B, phosphatases involved in CDK2 and CDK1 activation, were also down-regulated concomitantly with the induction of p21 (not shown). No significant changes were observed in the expression of CDK6 or CDK2 (Fig. 3) and CDK4 (not shown). Although the effects exerted by transient p21 over the cell cycle regulators were also transient, they caused an irreversibly block of mitosis exit (Fig. 2A,B). Therefore, p21 provoked a transient S phase arrest but an irreversible mitosis block. In fact, a 6h Zn^{2+} treatment of Kp21 cells to induce p21 was sufficient to irreversibly trigger megakaryocyte differentiation and polyploidy (Muñoz-Alonso et al., 2005; León et al., unpublished).

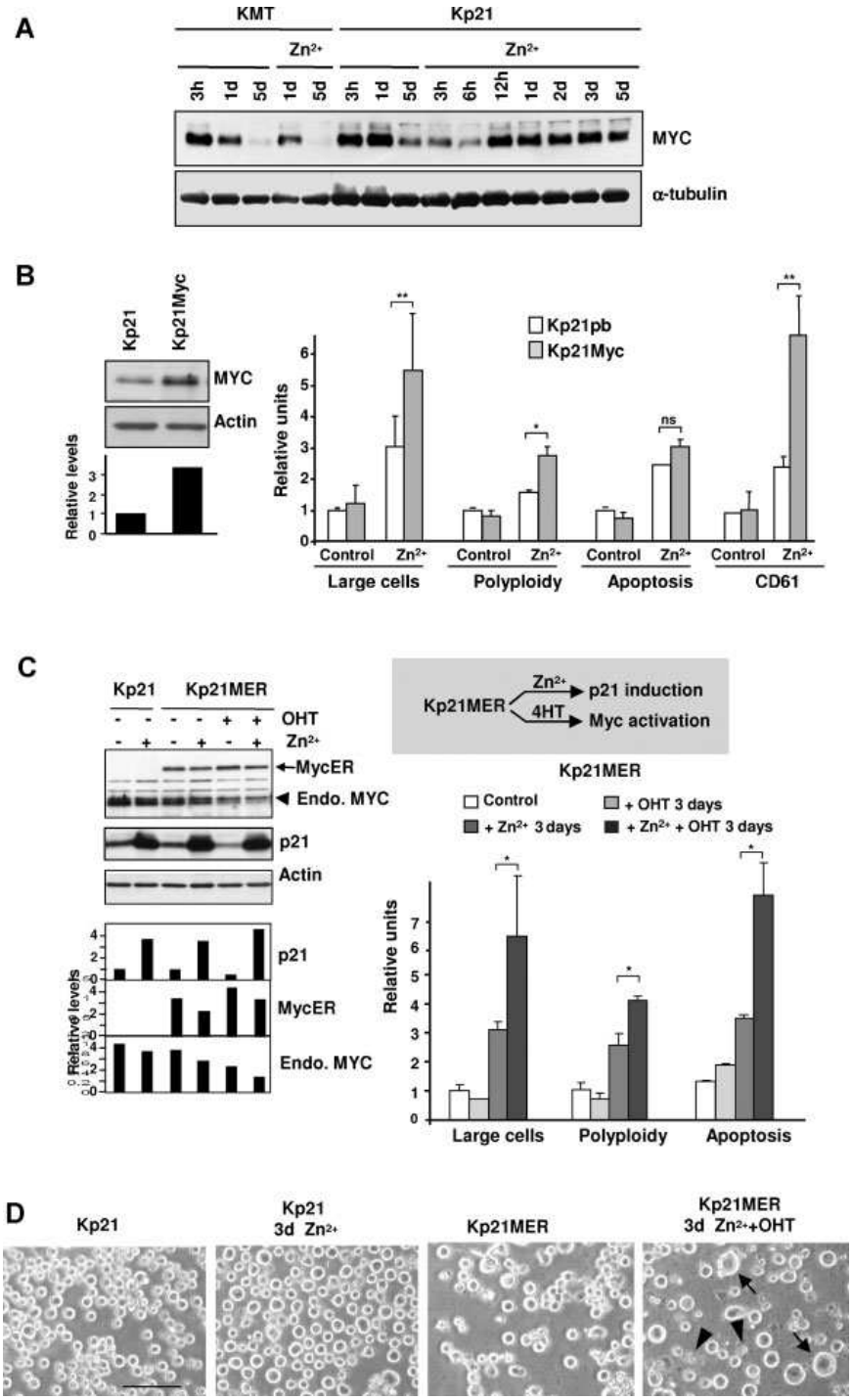
A
KMT
Kp21
Zn2+
Zn2+
3h 1d 5d 1d 5d 3h 1d 5d 3h 6h 12h 1d 2d 3d 5d
MYC
α-tubulin
B
Kp21
Kp21Myc
MYC
Actin
Relative levels
Kp21pb
Kp21Myc
Relative units
Control Zn2+
Large cells
Polyploidy
Apoptosis
CD61
ns
C
Kp21
Kp21MER
OHT
Zn2+
←MycER
◀ Endo. MYC
p21
Actin
MycER
Kp21MER
Zn2+ p21 induction
4HT Myc activation
Control
+ OHT 3 days
+ Zn2+ 3 days
+ Zn2+ + OHT 3 days
Large cells
Polyploidy
Apoptosis
D
Kp21
Kp21 3d Zn2+
Kp21MER
Kp21MER 3d Zn2++OHT

Fig. 4.

MYC enhances p21 effects in differentiation and polyploidisation

Proto-oncogene MYC is a potent cell cycle activator and has the ability to repress p21 but also to cause increased cell size and ploidy (see Introduction section). Moreover, MYC has been involved in mouse megakaryocytic differentiation in vivo (Guo et al., 2009), but had no effect per se on the differentiation capacity of K562 cells. We first examined the expression of endogenous MYC after the induction of p21 by Zn^{2+}. Transient induction of p21 in K562 caused down-regulation of MYC by 6 h, which recovered by 12 h and was sustained during differentiation whereas it became undetectable in control cells due to culture saturation (Fig. 4A). We questioned whether constitutive overactivation of the cell cycle by MYC would release the early cell cycle block imposed by p21 in K562 and affect megakaryocyte differentiation.

We generated Kp21 cells stably expressing wild type MYC, termed Kp21Myc. These cells constitutively express ectopic MYC to levels threefold above those of endogenous MYC (Fig. 4B). Overexpression of MYC by itself in Kp21cells did not cause detectable effects on polyploidy and differentiation (Fig. 4B and Supplementary Fig. 3). However, when p21 was also induced by addition of Zn^{2+} in Kp21Myc cells, there was a significant increase of cell size and polyploidy and a slight increase in apoptosis with respect to Kp21 cells (on basis of the proportion of large, polyploid or apoptotic cells; Fig. 4B and Supplementary Fig. 3). More strikingly, ectopic MYC in cells overexpressing p21 led to an increase of CD61 expression, a specific marker of megakaryocytes and platelets, that was by 3 days markedly higher than the effect caused by the mere induction of p21 (Fig. 4B and Supplementary Fig. 3).

To monitor the effects of MYC overactivation, we generated Kp21 cells expressing OHT-activatable MycER (Kp21MER; Fig. 4C–D). The use of conditional MycER (activatable by 4-hydroxytamoxifen (OHT); Littlewood et al., 1995) allows an acute activation of MYC, avoiding cell culture selection effects. Activation of MycER by OHT in Kp21 cells down-regulated endogenous MYC and p21 as previously described (Fig. 4C and Supplementary Fig. 5; Facchini et al., 1997). The mere activation of MycER had no significant effect on polyploidy or differentiation (Fig. 4C and S4). Interestingly, concomitant induction of p21 (by Zn^{2+}) and MycER (by OHT) for 3 days led to a striking increase of cell size and polyploidy (Fig. 4C–D and Supplementary Fig. 4). The ectopic overactivation of MycER also resulted in a significant fraction of apoptosis (Fig. 4C), as described in other systems (reviewed in Hoffman and Liebermann, 1998). After 5 days a fraction of cells underwent mitotic catastrophe and fragmented and the remaining cells culminated terminal differentiation (Supplementary Fig. 4B). Altogether the results show that MYC was unable to release the mitotic block imposed by p21. Consistently, the combination of p21 induction and MYC overactivation produced frequent aberrant giant cell structures typical of mitosis failure (Supplementary Fig. 4B, arrows).

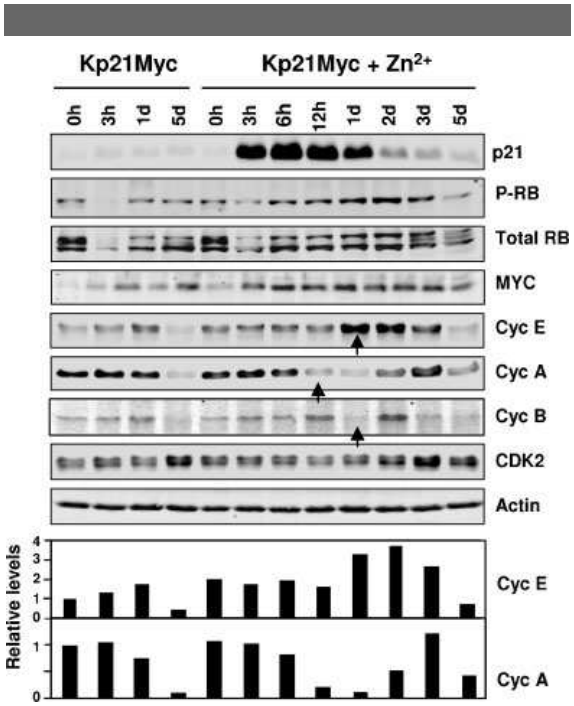

Fig. 5. MYC accelerates the changes in the cell cycle regulation caused by p21. Expression of the cell cycle regulators indicated on the right, analysed by western blotting after induction of p21 untreated, or after for the indicated periods of time after addition of Zn^{2+} in the presence of constitutive MYC. Actin was used as a protein loading control. Cyc: Cyclin. Data are representative of two independent experiments. Note that Cyclin A is down-regulated already by 12 h and Cyclin E accumulates by 24 h after addition of Zn^{2+} (arrows). Histograms: densitometric analysis of signals for Cyclins E and A, normalised to the levels of actin.

Analyses of cell cycle regulators showed that overexpression of MYC accelerated by 24h the up-regulation of Cyclin E observed in Kp21 + Zn^{2+} (compare Figs. 3 and 5). MYC also potentiated the inactivation of tumour suppressor Rb by phosphorylation (P-Rb; Fig. 5). In addition, the activation of MycER in Kp21 cells enhanced the up-regulation of Cyclin D2 (Supplementary Fig. 5). Altogether, MYC attenuated the early inhibition of cell cycle entry imposed by the transient expression of p21 but permitted and accelerated the down-regulation of mitotic Cyclins A and B caused by p21 (compare Figs. 5 and 3). Phosphorylation of histone H3, a marker of chromosome condensation, indicated a slight accumulation of

Fig. 4. MYC enhances p21-induced megakaryocytic differentiation. A: Expression of MYC in Kp21 cells as analysed by western blotting after addition of Zn^{2+} for the lengths of time indicated; α-tubulin was used as protein loading control; KMT are control cells expressing the empty vector. B: left panel: MYC protein expression in Kp21Myc cells as compared with parental Kp21 cells. Actin was a loading control. The histogram below shows the densitometric quantification of MYC signal normalised to the actin levels. Right panel: Bar histogram showing quantitations of the flow-cytometry analyses of Kp21Myc and Kp21pb (empty vector control cells) 3 days after addition of Zn^{2+}. Cell size, polyploidy, apoptosis and expression of CD61 marker were determined by the gates shown in Supplementary Fig. 3 (M1, M2). Small bars are SD. $^{*}P < 0.05$; n.s., non-significant difference ($P > 0.05$) C, left panel: Expression of MycER, endogenous MYC and p21 in Kp21MER cells untreated or after the treatments indicated. Protein levels were determined by western blotting; the histogram shows the densitometric analysis of the signal for endogenous MYC (endo., arrowhead) or MycER (arrow), normalised to the actin levels. Right panel: cell size, polyploidy and apoptosis in Kp21MER cells untreated, or upon activation of MycER with OHT and/or induction of p21 for 3 days as indicated; quantitations by flow-cytometry as in B and Supplementary Fig. 3. $^{*}P < 0.05$ D: Representative microphotographs of Kp21 and Kp21MER cells after the treatments indicated from experiments in (E). Bar: 150 μm. Arrows mark big cells in cultures after induction of p21 and activation of MYC. Small apoptotic-like cells are also observed in these cultures (arrowheads).

mitotic nuclei concomitant with p21 induction (Supplementary Fig. 6).

Altogether the results indicate that MYC stimulated S phase progression independently on the mitosis block produced by p21 and augmented the polyploidisation induced by p21. We therefore questioned whether overactivation of MYC would rescue these cells from the block imposed by p21 to the polyploidisation induced by STA (Fig. 1B). As expected, endogenous MYC was markedly down-regulated by 6 h after addition of STA (Fig. 6A). In these conditions p21 expression is sustained by Zn^{2+} and STA along the assay (Figs. 3 and 1A). Sustained expression of p21 blocked STA-induced polyploidisation (Fig. 6B and Supplementary Fig. 7). Interestingly however, p21 did not inhibit the expression of the megakaryocytic marker CD61 induced by STA (Fig. 6B and Supplementary Fig. 6), indicating that polyploidisation and differentiation are uncoupled megakaryocytic features (see also, Kikuchi et al., 1997). Overexpression of wild type MYC was unable to release the block imposed by p21 to STA-induced polyploidisation, or to suppress the induction of the megakaryocytic marker CD61 (Fig. 6B and Supplementary Fig. 7).

Discussion

Proto-oncogene MYC induces cell cycle progression and inhibits differentiation in part by repressing cell cycle inhibitors such as p21 (reviewed in Jung and Hermeking, 2009; Leon et al., 2009). We have here provided evidence that both molecules synergise to drive post-mitotic megakaryocytic differentiation and polyploidy. The studies show that transient p21 caused an irreversible mitosis block that was independent on and dominant over, MYC potential to induce proliferation.

K562 myeloid leukemia cells can be induced to undergo erythroid or megakaryocytic differentiation depending on the stimulus (Leon et al., 2009). Both treatment with STA or ectopic transient expression of p21 in these cells induces megakaryocytic features that mimic the natural differentiation process (Lerga et al., 1999; Muñoz-Alonso et al., 2005). Natural megakaryocytic differentiation also involves induction of p21 (Yaroslavskiy et al., 1999; Taniguchi et al., 1999). The role of p21 in this process is however unclear, since constitutive overexpression of the inhibitor in cultured megakaryocytes inhibited polyploidisation (Baccini et al., 2001). p21 is capable to

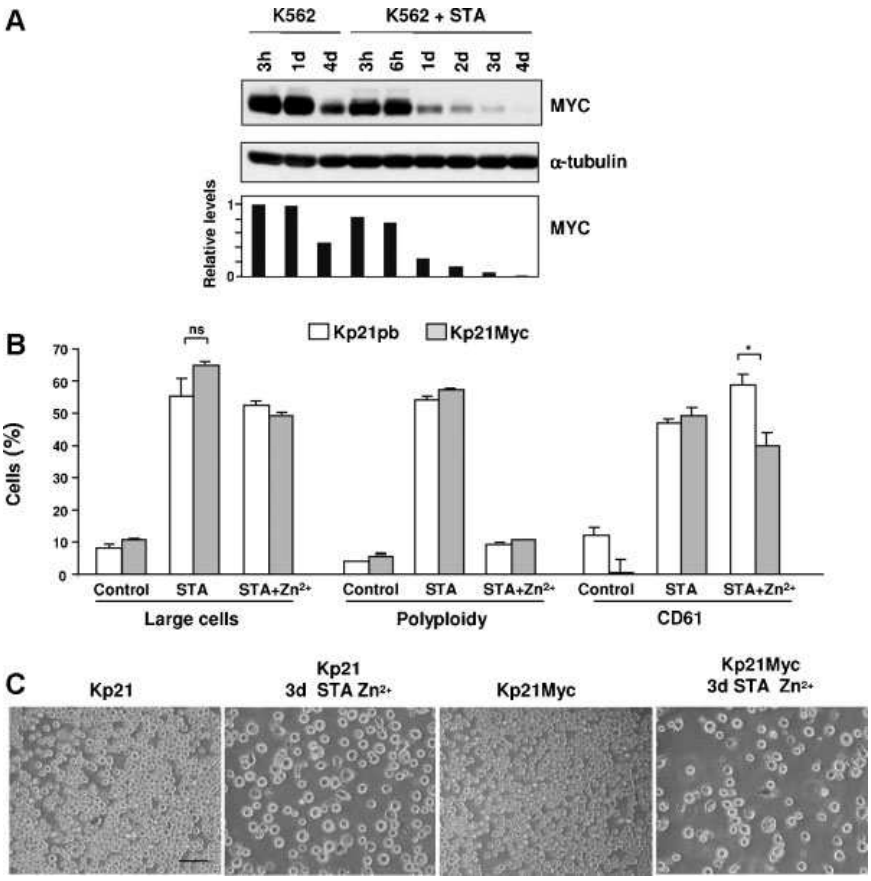

Fig. 6. MYC is unable to inhibit the block imposed by sustained p21 to polyploidisation. A: Western blotting of MYC in K562 cells untreated or treated with STA for the periods of time indicated. Bar histogram: densitometry of signal for MYC, normalised to the levels of α-tubulin (α-tub). B: Kp21Myc and Kp21pb were untreated or treated for 72 h with STA, or STA and Zn^{2+} as indicated and the cell size, polyploidy, apoptosis and expression of CD61 were determined by flow-cytometry as in Fig. 4. Data are mean of three independent experiments with duplicate samples ± SD. *$P < 0.05$; n.s., non-significant difference ($P > 0.05$). C: Representative microphotographs of cells treated as indicated from experiments in (B). Bar: 150 μm.

block either cell cycle entry and DNA replication by inhibiting CDK2, or the execution of mitosis by inhibiting mitotic CDK1. In the latter case the cell cycle block allows DNA replication (reviewed in Ullah et al., 2009). Our p21 knock-down studies showed that the endogenous protein is required to drive K562 cells towards megakaryocytic differentiation. However, sustained expression of p21 rendered these cells resistant to undergo megakaryocytic differentiation.

There is a good rationale for the need of p21 expression to be transient to induce megakaryocytic polyploidy. In our experiments, p21 induction sequentially inhibited mitotic CDK1 and S phase kinase CDK2. Subsequently, p21 must be down regulated to allow cell cycle progression, since constitutive inhibition of CDK2 by p21 did not allow cell cycle progression and DNA re-replication. After the initial inhibition of CDKs their activities recovered and Cyclins D2, D3 and E accumulated. D-type Cyclins have been associated with endoreplication (see Wang et al., 1995; Datar et al., 2000). Elevated Cyclin E accompanies endoreplication in a variety of biological systems (Edgar and Orr-Weaver, 2001; Larkins et al., 2001; Ravid et al., 2002b; Guidotti et al., 2003; Zanet et al., 2010). More specifically, ectopic Cyclin E is able to drive endoreplication in K562 cells (Garcia et al., 2000) and it is required in vivo for polyploidisation of mouse megakaryocytes (Geng et al., 2003). Therefore the inhibition of the S phase of DNA replication by transient induction of p21 in K562 was also transient, whereas the block of mitosis was irreversible. Consistently, cumulative evidence shows that the levels of CDK2 activity required to drive DNA replication are lower than the levels of CDK1 activity required to drive mitosis (Krasinska et al., 2008; Coudreuse and Nurse, 2010). In addition, recent evidence indicates that deregulated Cyclin E impairs mitosis through CDC25 (Bagheri-Yarmand et al., 2010) and we detected accumulation of Cyclin E and down-regulation of CDC25A and B in our experiments after induction of p21. Finally, p21 might block mitosis in K562 cells by mechanisms added to CDK1 inhibition, since it down-regulates the transcription of other mitotic regulators (Chang et al., 2000; León et al., unpublished).

The mitotic block imposed by transient expression of p21 was irreversible even in the presence of overactivated MYC. This is intriguing because MYC has been shown to repress p21 expression (Seoane et al., 2002; Wu et al., 2003). However in some cases MYC and p21 coexist. For instance, MYC stimulates epidermal differentiation involving cellular growth (Gandarillas and Watt, 1997; Gandarillas et al., 2000) and induction of p21 (Harvat et al., 1998; Dazard et al., 2000; Dotto, 2000; Gandarillas et al., 2000). Recently, up-regulation of p21 has also been found in MYC-induced senescence in the absence of CDK2 (Campaner et al., 2010). Although MYC has more often been shown to promote proliferation, it drives post-mitotic differentiation in some cell systems (Leon et al., 2009). It is unclear why MYC has a dual effect on cell differentiation, but two lines of argument might provide clues to this issue: (i) MYC promotes differentiation in systems where differentiation is closely associated to cell growth (Zanet et al., 2005; Eilers and Eisenman, 2008). (ii) MYC might promote mitosis or not depending on the cellular context and other activated molecular pathways (Gandarillas, 2000; Beer et al., 2004).

The cooperation between MYC and p21 in megakaryocytic differentiation here shown is in contrast with the inhibition of p27-induced erythroid differentiation in the same cells (Acosta et al., 2008). $p27^{KIP}$ is another CDK inhibitor of the CIP/KIP family (Besson et al., 2008). However and unlike p21, it has not been clearly shown to bind mitotic CDK1 and it might thus be more specific of CDK2 (Besson et al., 2008; Abbas and Dutta, 2009; Ullah et al., 2009). Interestingly, p27 induced erythroid differentiation and arrested K562 cells in G1. In contrast, p21 provoked polyploidisation and increased cell volume. Polyploidisation or endoreplication significantly simulates cell size increase (e.g., Edgar and Orr-Weaver, 2001). Consistently, inactivation of MYC in mouse bone marrow progenitors in vivo led to a lesser level of ploidy and smaller megakaryocytes and platelets (Guo et al., 2009). Similar observations have been made in MYC-deficient flies and MYC-deficient mouse epidermis (Maines et al., 2004; Pierce et al., 2004; Zanet et al., 2005; Steiger et al., 2008). Therefore, MYC might promote differentiation processes that are associated with cellular growth and inhibit differentiation processes that are associated with cell cycle arrest.

In our studies MYC function was independent of mitosis control. The effect of p21 in blocking mitosis was dominant over MYC-activation of the cell cycle. MYC is not required for megakaryocytic differentiation (Guo et al., 2009) and in our studies it had no effect per se on the megakaryocytic differentiation capacity (Lerga et al., 1999). However, by establishing an irreversible block on mitosis via p21, the stimulation of cell cycle progression and cellular growth by MYC in our experiments accelerated and enhanced cell size increase and poliploidisation (see Fig. 7). Therefore, the p21-block of mitosis drove MYC cell cycle activation into cellular growth and differentiation.

Apoptosis often acts to limit MYC oncogenic potential. For instance, overexpression of MYC in mouse bone marrow progenitors provoked acute myeloid leukemia due to their intrinsic resistance to apoptosis (Luo et al., 2005). MYC also contributes to progression of human leukemia (Delgado and Leon, 2010). The mitosis control by p21 leading to differentiation in the presence of overactivated MYC might constitute an anti-oncogenic mechanism alternative to apoptosis.

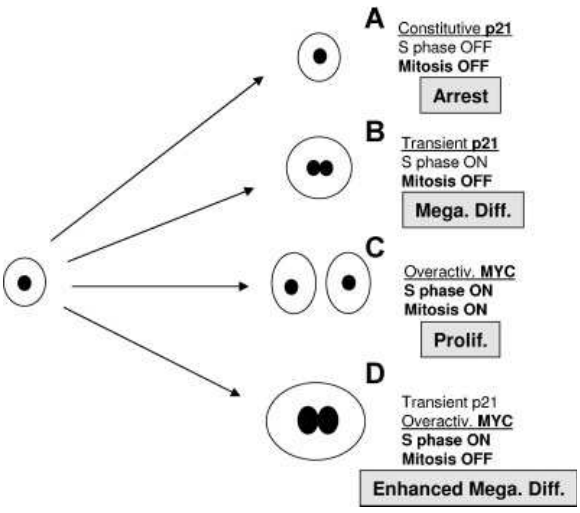

Fig. 7. Model for the combined action of MYC and p21 in K562 cells. A: Constitutive p21 inhibits S phase and mitotic CDKs thus inhibiting cell cycle progression. B: Transient p21 blocks mitosis but allows cell size increase and DNA polyploidisation, resulting in megakaryocytic differentiation (Mega. Diff.). C: Overactivation of MYC drives cellular growth and proliferation. D: The combined action of transient p21 and overactivation of MYC on the one hand irreversibly blocks mitosis and on the other hand it stimulates the S phase of the cell cycle and enhances cell size increase and polyploidy, resulting in accelerated megakaryocytic differentiation.

Acknowledgments

AG is grateful to the INSERM (France) and to the Laboratoire de Dermatologie Moléculaire for allowing him to take this work over during a sabbatical stay abroad. We are grateful to Angel Corbí (CIB, Madrid) and Manuel Serrano (CNIO, Madrid) for providing plasmids, María Aramburu and Rosa Blanco for technical assistance, Dolores Delgado and Ana Freije for critical reading of the manuscript and Anna Solinís for revising the English writing. MJMA was supported by Asociación Española Contra el Cáncer (AECC; Spain), GB by the FPI Program from Ministerio de Ciencia e Innovación (MICINN), LC and AG by Instituto de Salud Carlos III (ISCIII; Spain). The work was funded by grants SAF08-01581 from Plan Nacional I + D, MICINN (Spain; JL), RTICC-RD06/0020/0017 from ISCIII, MICINN (Spain; JL), La Ligue Contre le Cancer de l'Herault (France; AG), the Société Française de Dermatologie (France; AG), the SCIII-FIS, Programa Regiones Emergentes and SCIII-FIS PI08/0890 (Spain; AG) and a co-operative grant from Universidad de Cantabria-Sistema Cántabro de Salud (Cantabria, Spain; JL and AG).

Literature Cited

Abbas T, Dutta A. 2009. p21 in cancer: Intricate networks and multiple activities. Nat Rev Cancer 9:400–414.

Acosta JC, Ferrandiz N, Bretones G, Torrano V, Blanco R, Richard C, O'Connell B, Sedivy J, Delgado MD, Leon J. 2008. Myc inhibits p27-induced erythroid differentiation of leukemia cells by repressing erythroid master genes without reversing p27-mediated cell cycle arrest. Mol Cell Biol 28:7286–7295.

Baccini V, Roy L, Vitrat N, Chagraoui H, Sabri S, Le Couedic JP, Debili N, Wendling F, Vainchenker W. 2001. Role of p21(Cip1/Waf1) in cell-cycle exit of endomitotic megakaryocytes. Blood 98:3274–3282.

Bagheri-Yarmand R, Nanos-Webb A, Biernacka A, Bui T, Keyomarsi K. 2010. Cyclin E deregulation impairs mitotic progression through premature activation of Cdc25C. Cancer Res 70:5085–5095.

Bates S, Ryan KM, Phillips AC, Vousden KH. 1998. Cell cycle arrest and DNA endoreduplication following p21Waf1/Cip1 expression. Oncogene 17:1691–1703.

Beer S, Zetterberg A, Ihrie RA, McTaggart RA, Yang Q, Bradon N, Arvanitis C, Attardi LD, Feng S, Ruebner B, Cardiff RD, Felsher DW. 2004. Developmental context determines latency of MYC-induced tumorigenesis. PLoS Biol 2:e332.

Besson A, Dowdy SF, Roberts JM. 2008. CDK inhibitors: Cell cycle regulators and beyond. Dev Cell 14:159–169.

Campaner S, Doni M, Hydbring P, Verrecchia A, Bianchi L, Sardella D, Schleker T, Perna D, Tronnersjo S, Murga M, Fernandez-Capetillo O, Barbacid M, Larsson LG, Amati B. 2010. Cdk2 suppresses cellular senescence induced by the c-myc oncogene. Nat Cell Biol 12:54–59, sup pp. 51–14.

Chang BD, Watanabe K, Broude EV, Fang J, Poole JC, Kalinichenko TV, Roninson IB. 2000. Effects of p21Waf1/Cip1/Sdi1 on cellular gene expression: Implications for carcinogenesis, senescence, and age-related diseases. Proc Natl Acad Sci USA 97:4291–4296.

Coudreuse D, Nurse P. 2010. Driving the cell cycle with a minimal CDK control network. Nature 468:1074–1079.

Datar SA, Jacobs HW, de la Cruz AF, Lehner CF, Edgar BA. 2000. The Drosophila cyclin D-Cdk4 complex promotes cellular growth. EMBO J 19:4543–4554.

Dazard JE, Piette J, Basset-Seguin N, Blanchard JM, Gandarillas A. 2000. Switch from p53 to MDM2 as differentiating human keratinocytes lose their proliferative potential and increase in cellular size. Oncogene 19:3693–3705.

Delgado MD, Leon J. 2010. Myc roles in hematopoiesis and leukemia. Genes Cancer 1:605–616.

Delgado MD, Lerga A, Canelles M, Gomez-Casares MT, Leon J. 1995. Differential regulation of Max and role of c-Myc during erythroid and myelomonocytic differentiation of K562cells. Oncogene 10:1659–1665.

Dotto GP. 2000. p21(WAF1/Cip1): More than a break to the cell cycle? Biochim Biophys Acta 1471:M43–M56.

Edgar BA, Orr-Weaver TL. 2001. Endoreplication cell cycles: More for less. Cell 105:297–306.

Eilers M, Eisenman RN. 2008. Myc's broad reach. Genes Dev 22:2755–2766.

Facchini LM, Chen S, Marhin WW, Lear JN, Penn LZ. 1997. The Myc negative autoregulation mechanism requires Myc-Max association and involves the c-myc P2 minimal promoter. Mol Cell Biol 17:100–114.

Felsher DW, Zetterberg A, Zhu J, Tlsty T, Bishop JM. 2000. Overexpression of MYC causes p53-dependent G2 arrest of normal fibroblasts. Proc Natl Acad Sci USA 97:10544–10548.

Gandarillas A. 2000. Epidermal differentiation, apoptosis, and senescence: Common pathways? Exp Gerontol 35:53–62.

Gandarillas A, Watt FM. 1997. c-Myc promotes differentiation of human epidermal stem cells. Genes Dev 11:2869–2882.

Gandarillas A, Davies D, Blanchard JM. 2000. Normal and c-Myc-promoted human keratinocyte differentiation both occur via a novel cell cycle involving cellular growth and endoreplication. Oncogene 19:3278–3289.

Garcia P, Frampton J, Ballester A, Cales C. 2000. Ectopic expression of cyclin E allows non-endomitotic megakaryoblastic K562cells to establish re-replication cycles. Oncogene 19:1820–1833.

Geng Y, Yu Q, Sicinska E, Das M, Schneider JE, Bhattacharya S, Rideout WM, Bronson RT, Gardner H, Sicinski P. 2003. Cyclin E ablation in the mouse. Cell 114:431–443.

Guidotti JE, Bregerie O, Robert A, Debey P, Brechot C, Desdouets C. 2003. Liver cell polyploidization: A pivotal role for binuclear hepatocytes. J Biol Chem 278:19095–19101.

Guo Y, Niu C, Breslin P, Tang M, Zhang S, Wei W, Kini AR, Paner GP, Alkan S, Morris SW, Diaz M, Stiff PJ, Zhang J. 2009. c-Myc-mediated control of cell fate in megakaryocyte-erythrocyte progenitors. Blood 114:2097–2106.

Harvat BL, Wang A, Seth P, Jetten AM. 1998. Up-regulation of p27Kip1, p21WAF1/Cip1 and p16Ink4a is associated with, but not sufficient for, induction of squamous differentiation. J Cell Sci 111:1185–1196.

Hoffman B, Liebermann DA. 1998. The proto-oncogene c-myc and apoptosis. Oncogene 17:3351–3357.

Johnston LA, Prober DA, Edgar BA, Eisenman RN, Gallant P. 1999. Drosophila myc regulates cellular growth during development. Cell 98:779–790.

Jung P, Hermeking H. 2009. The c-MYC-AP4-p21 cascade. Cell Cycle 8:982–989.

Kikuchi J, Furukawa Y, Iwase S, Terui Y, Nakamura M, Kitagawa S, Kitagawa M, Komatsu N, Miura Y. 1997. Polyploidization and functional maturation are two distinct processes during megakaryocytic differentiation: Involvement of cyclin-dependent kinase inhibitor p21 in polyploidization. Blood 89:3980–3990.

Klein E, Ben-Bassat H, Neumann H, Ralph P, Zeuthen J, Polliack A, Vanky F. 1976. Properties of the K562 cell line, derived from a patient with chronic myeloid leukemia. Int J Cancer 18:421–431.

Krasinska L, Cot E, Fisher D. 2008. Selective chemical inhibition as a tool to study Cdk1 and Cdk2 functions in the cell cycle. Cell Cycle 7:1702–1708.

Larkins BA, Dilkes BP, Dante RA, Coelho CM, Woo YM, Liu Y. 2001. Investigating the hows and whys of DNA endoreduplication. J Exp Bot 52:183–192.

Leon J, Ferrandiz N, Acosta JC, Delgado MD. 2009. Inhibition of cell differentiation: A critical mechanism for MYC-mediated carcinogenesis? Cell Cycle 8:1148–1157.

Lerga A, Crespo P, Berciano M, Delgado MD, Canelles M, Cales C, Richard C, Ceballos E, Gutierrez P, Ajenjo N, Gutkind S, Leon J. 1999. Regulation of c-Myc and Max in megakaryocytic and monocytic-macrophagic differentiation of K562cells induced by protein kinase C modifiers: c-Myc is down-regulated but does not inhibit differentiation. Cell Growth Differ 10:639–654.

Littlewood TD, Hancock DC, Danielian PS, Parker MG, Evan GI. 1995. A modified oestrogen receptor ligand-binding domain as an improved switch for the regulation of heterologous proteins. Nucleic Acids Res 23:1686–1690.

Luo H, Li Q, O'Neal J, Kreisel F, Le Beau MM, Tomasson MH. 2005. c-Myc rapidly induces acute myeloid leukemia in mice without evidence of lymphoma-associated antiapoptotic mutations. Blood 106:2452–2461.

Lutz W, Leon J, Eilers M. 2002. Contributions of Myc to tumorigenesis. Biochim Biophys Acta 1602:61–71.

Maines JZ, Stevens LM, Tong X, Stein D. 2004. Drosophila dMyc is required for ovary cell growth and endoreplication. Development 131:775–786.

Mateyak MK, Obaya AJ, Sedivy JM. 1999. c-Myc regulates cyclin D-Cdk4 and -Cdk6 activity but affects cell cycle progression at multiple independent points. Mol Cell Biol 19:4672–4683.

Matsumura I, Ishikawa J, Nakajima K, Oritani K, Tomiyama Y, Miyagawa J, Kato T, Miyazaki H, Matsuzawa Y, Kanakura Y. 1997. Thrombopoietin-induced differentiation of a human megakaryoblastic leukemia cell line, CMK, involves transcriptional activation of p21(WAF1/Cip1) by STAT5. Mol Cell Biol 17:2933–2943.

Medema RH, Klompmaker R, Smits VA, Rijksen G. 1998. p21waf1 can block cells at two points in the cell cycle, but does not interfere with processive DNA-replication or stress-activated kinases. Oncogene 16:431–441.

Meyer N, Penn LZ. 2008. Reflecting on 25 years with MYC. Nat Rev Cancer 8:976–990.

Morgenstern JP, Land H. 1991. Choice and manipulation of retroviral vectors. Methods Mol Biol 7:181–206.

Muñoz-Alonso MJ, Acosta JC, Richard C, Delgado MD, Sedivy J, Leon J. 2005. p21Cip1 and p27Kip1 induce distinct cell cycle effects and differentiation programs in myeloid leukemia cells. J Biol Chem 280:18120–18129.

Murray AW. 2004. Recycling the cell cycle: Cyclins revisited. Cell 116:221–234.

Nesbit CE, Tersak JM, Prochownik EV. 1999. MYC oncogenes and human neoplastic disease. Oncogene 18:3004–3016.

Pierce SB, Yost C, Britton JS, Loo LW, Flynn EM, Edgar BA, Eisenman RN. 2004. dMyc is required for larval growth and endoreplication in Drosophila. Development 131:2317–2327.

Ravid A, Rubinstein E, Gamady A, Rotem C, Liberman UA, Koren R. 2002a. Vitamin D inhibits the activation of stress-activated protein kinases by physiological and environmental stresses in keratinocytes. J Endocrinol 173:525–532.

Ravid K, Lu J, Zimmet JM, Jones MR. 2002b. Roads to polyploidy: The megakaryocyte example. J Cell Physiol 190:7–20.

Schmidt EV. 1999. The role of c-myc in cellular growth control. Oncogene 18:2988–2996.

Seoane J, Le HV, Massague J. 2002. Myc suppression of the p21(Cip1) Cdk inhibitor influences the outcome of the p53 response to DNA damage. Nature 419:729–734.

Steiger D, Furrer M, Schwinkendorf D, Gallant P. 2008. Max-independent functions of Myc in Drosophila melanogaster. Nat Genet 40:1084–1091.

Taniguchi T, Endo H, Chikatsu N, Uchimaru K, Asano S, Fujita T, Nakahata T, Motokura T. 1999. Expression of p21(Cip1/Waf1/Sdi1) and p27(Kip1) cyclin-dependent kinase inhibitors during human hematopoiesis. Blood 93:4167–4178.

Ullah Z, Lee CY, Depamphilis ML. 2009. Cip/Kip cyclin-dependent protein kinase inhibitors and the road to polyploidy. Cell division 4:10.

Vita M, Henriksson M. 2006. The Myc oncoprotein as a therapeutic target for human cancer. Semin Cancer Biol 16:318–330.

Wang Z, Zhang Y, Kamen D, Lees E, Ravid K. 1995. Cyclin D3 is essential for megakaryocytopoiesis. Blood 86:3783–3788.

Weiss RH. 2003. p21Waf1/Cip1 as a therapeutic target in breast and other cancers. Cancer Cell 4:425–429.

Wu S, Cetinkaya C, Munoz-Alonso MJ, von der Lehr N, Bahram F, Beuger V, Eilers M, Leon J, Larsson LG. 2003. Myc represses differentiation-induced p21CIP1 expression via Miz-1-dependent interaction with the p21 core promoter. Oncogene 22:351–360.

Yaroslavskiy B, Watkins S, Donnenberg AD, Patton TJ, Steinman RA. 1999. Subcellular and cell-cycle expression profiles of CDK-inhibitors in normal differentiating myeloid cells. Blood 93:2907–2917.

Zanet J, Pibre S, Jacquet C, Ramirez A, de Alboran IM, Gandarillas A. 2005. Endogenous Myc controls mammalian epidermal cell size, hyperproliferation, endoreplication and stem cell amplification. J Cell Sci 118:1693–1704.

Zanet J, Freije A, Ruiz M, Coulon V, Sanz JR, Chiesa J, Gandarillas A. 2010. A mitosis block links active cell cycle with human epidermal differentiation and results in endoreplication. PLoS One 5:e15701.

c-Myc Inhibits Ras-Mediated Differentiation of Pheochromocytoma Cells by Blocking c-Jun Up-Regulation

José P. Vaqué,[1] Belén Fernández-García,[3] Pablo García-Sanz,[1] Nuria Ferrandiz,[1] Gabriel Bretones,[1] Fernando Calvo,[2] Piero Crespo,[2] María C. Marín,[3] and Javier León[1]

[1]Grupo de Biología Molecular del Cáncer, Dpto. de Biología Molecular and Instituto de Biomedicina y Biotecnología de Cantabria, Universidad de Cantabria-CSIC-IDICAN and [2]Instituto de Investigaciones Biomédicas, Unidad de Biomedicina de la Universidad de Cantabria-CSIC, Universidad de Cantabria, Santander, Spain; and [3]Instituto de Biomedicina, Universidad de León, León, Spain

Abstract

Although mutant Ras proteins were originally described as transforming oncoproteins, they induce growth arrest, senescence, and/or differentiation in many cell types. c-Myc is an oncogenic transcription factor that cooperates with Ras in cellular transformation and oncogenesis. However, the Myc-Ras relationship in cellular differentiation is largely unknown. Here, we have analyzed the effects of c-Myc on PC12-derived cells (UR61 cell line), harboring an inducible *N-Ras* oncogene. In these cells, Ras activation induces neuronal-like differentiation by a process involving c-Jun activation. We found that c-Myc inhibited Ras-mediated differentiation by a mechanism that involves the blockade of c-Jun induction in response to Ras signal. Accordingly, ectopically expressed c-Jun could bypass c-Myc impediment of Ras-induced differentiation and activator protein 1 activation. Interestingly, it did not rescue the proliferative arrest elicited by Ras and did not enhance the differentiation-associated apoptosis. The blockade of Ras-mediated induction of c-Jun takes place at the level of *c-Jun* proximal promoter. Mutational analysis revealed that c-Myc regions involved in DNA binding and transactivation are required to block differentiation and c-Jun induction. c-Myc does not seem to require Miz-1 to inhibit differentiation and block c-Jun induction. Furthermore, Max is not required for c-Myc activity, as UR61 cells lack a functional *Max* gene. c-Myc–inhibitory effect on the Ras/c-Jun connection is not restricted to UR61 cells as it can occur in other cell types as K562 or HEK293. In conclusion, we describe a novel interplay between c-Myc and c-Jun that controls the ability of Ras to trigger the differentiation program of pheochromocytoma cells. (Mol Cancer Res 2008;6(2):325–39)

Introduction

c-Myc (Myc hereafter) is an oncogenic transcription factor of the basic-helix-loop-helix protein family. Myc forms heterodimers with the protein Max. Myc-Max dimers bind to specific DNA sequences (E-boxes) in the regulatory regions of target genes. Genes up-regulated by Myc include genes involved in carbohydrate metabolism, protein biosynthesis, cell cycle regulation, and other less represented functions. Also, an important fraction of the genes targeted by Myc (30-50% in different studies) are repressed by it (reviewed in refs. 1-3; a list of regulated genes can be found online[4]). Consistent with its effects on cultured cells and transgenic *in vivo* models, deregulated expression of Myc is found in a wide array of human cancers, in many cases associated to disease progression (4, 5).

Myc activity on its genomic targets translates into multiple biological effects. Importantly, Myc activity drives cells into proliferation by mechanisms impinging on G_1 cell cycle phase control (6, 7). Myc is also known to block differentiation in a number of model systems (5, 8). The mechanism(s) whereby Myc inhibits differentiation are unclear, but, as terminal differentiation is usually associated with cell cycle arrest, it has been proposed that Myc inhibits differentiation by stimulating cell cycle progression. Indeed, a significant number of Myc-induced genes encode positive regulators of the cell cycle (e.g., *cyclin D2, cyclin E1*, and *CDK4*), whereas cell cycle inhibitors such as $p15^{INK4B}$, $p21^{WAF1}$, and $p27^{KIP1}$ are repressed by Myc (7).

The Ras family of small GTPases includes three closely related proteins in mammals (H-, K-, and N-Ras). Ras proteins are activated by signals originated in surface receptors, acting as key components of signaling pathways by relaying signals downstream through diverse routes. Activated Ras interacts with diverse signaling effectors. One of the most relevant is the Raf kinase that signals through activation of mitogen-activated

Received 4/18/07; revised 9/3/07; accepted 10/9/07.
Grant support: Spanish Ministerio de Educación y Ciencia grant SAF05-0461, Fundación Marqués de Valdecilla AP05-17, and ISCIII-RETIC RD06/0020 (J. León) and Ministerio de Educación y Ciencia SAF05-0461CO2 (M.C. Marín). The costs of publication of this article were defrayed in part by the payment of page charges. This article must therefore be hereby marked *advertisement* in accordance with 18 U.S.C. Section 1734 solely to indicate this fact.
Requests for reprints: Javier León, Dpto. de Biología Molecular, Facultad de Medicina, Avda. Cardenal Herrera Oria s/n, 39011 Santander, Spain. Phone: 34-942-201952; Fax: 34-942-201945. E-mail: leonj@unican.es

doi:10.1158/1541-7786.MCR-07-0180

[4] http://www.myccancergene.org

protein/extracellular signal-regulated kinase (ERK) kinase and ERK kinases (9, 10). *Ras* has been classically regarded as a transforming oncogene. In fact, activating point mutations in *Ras* genes that render a constitutively active protein have been found in 30% of all human cancers (11). However, the proliferative and transforming activity of Ras is cell context dependent. Thus, Ras exerts proliferation arrest and senescence in primary fibroblasts (12) and also exerts antiproliferative effects in some tumor cell lines as leukemia-derived K562 (13, 14). Also, Ras can induce differentiation of pheochromocytoma cells (15-17) and adipocytic precursors (18). Moreover, a systematic survey of the literature reveals that the most common response to Ras ectopic expression in cell lines derived from distinct tissues with differentiation potential is differentiation (19).

One of the earliest examples of oncogene cooperation was described for Myc and Ras in the transformation of rodent primary fibroblasts (20). However, to date, all the studies on Myc and Ras cross-talk have been undertaken in murine or human fibroblasts (21, 22) and in murine models (23-25), where Myc-Ras cooperation results in cellular transformation and oncogenesis (23-25). In sharp contrast, the Myc-Ras cross-talk in differentiation models has not been studied.

PC12 cells is a rat pheochromocytoma-derived cell line that, in response to nerve growth factor (NGF), differentiates into a sympathetic neuron-like phenotype, characterized by neurite outgrowth and induction of neuronal specific genes (26). NGF activates Ras and NGF-induced differentiation is dependent on Ras-ERK activation (27, 28). Consistently, *H-Ras* (15, 17), *K-Ras* (17), and *N-Ras* (16) oncogenes induce neuronal-like differentiation in PC12 cells.

c-Jun is a transcription factor of the leucine zipper family that dimerizes with another leucine zipper partner protein (c-Jun itself, ATF2 and members of the Fos and Fra families) to form active activator protein 1 (AP-1) complexes (29, 30). c-Jun expression is subjected to positive autoregulation, which depends on two AP-1 sites in the proximal promoter (30). In PC12, it has been shown that NGF induces c-Jun expression (31, 32) and that the concerted signaling through ERK and Jun NH_2-terminal kinase converge at the expression and phosphorylation of c-Jun, an essential event for NGF-induced differentiation (33-35). Consistently, ectopic expression of constitutively active c-Jun is sufficient to induce neuronal-like differentiation of these cells (33).

Here, we investigated the effect of Myc constitutive expression in Ras-mediated differentiation. For this purpose, we used the UR61 cell line, a PC12-derived cell line with inducible expression of the *N-Ras* oncogene. Surprisingly, we found that Myc impairs the neuronal-like differentiation induced by Ras through a mechanism involving the repression of c-Jun up-regulation.

Results

Myc Inhibits Ras-Mediated Differentiation of UR61 Cells

Treatment of UR61 cells with dexamethasone led to a progressive increase in N-Ras mRNA (Fig. 1A) and protein expression (Fig. 1B). This resulted in neuronal-like differentiation, as shown by morphologic changes, including the extension of neurites (Fig. 1C, *bottom*) as well as nuclear reorganization and expression of neuronal markers (not shown). Differentiation of UR61cells was maximal and irreversible after 24 h of exposure to dexamethasone (Fig. 1C).

To study Ras-Myc interaction in UR61 differentiation, we generated by retroviral infection a polyclonal cell line (termed UR61Myc) with constitutive expression of human Myc protein. As a control for potential Ras-independent effects of Myc, we also infected U7 cells (UR61 parental cells) with Myc viruses and obtained the cell line U7Myc. To assess the activity of Myc in these cells, we determined the transactivation of a reporter containing four Myc-responsive E-boxes directing the expression of the luciferase gene. The results (Fig. 2A) showed the transactivation of the E-box–containing promoter in UR61Myc. We also tested the expression of *PDK2* (pyruvate dehydrogenase kinase 2) and *LDHB* (lactate dehydrogenase B), two genes previously described as Myc target genes.[4] We chose these genes because they appeared up-regulated in UR61Myc cells in our preliminary microarray analysis. The mRNA levels was determined by quantitative reverse transcription-PCR (RT-PCR), and the results showed that both genes were up-regulated in UR61Myc cells compared with control cells in the absence or presence of Ras (i.e., dexamethasone; Fig. 2B).

We next asked whether constitutive expression of Myc modified the Ras-induced neuronal differentiation in these cells. Most of the UR61V cells (75-85% in our culture conditions) extended neurites upon Ras induction. In sharp contrast, the majority of UR61Myc cells (around 90%) either lacked neurites or these were much shorter (Fig. 2C), suggesting that Myc can inhibit the activation of the differentiation program activated by Ras in these cells. We sought to confirm the inhibition of differentiation by analyzing the expression of two neuronal differentiation markers known to be up-regulated by NGF in PC12 cells, namely GAP43 (neuromodulin, a neuronal plasticity-related protein; refs. 36, 37) and SNAP25 (synaptosomal-associated protein 25 kDa, a protein involved in synaptic exocytosis; ref. 38). Real-time RT-PCR revealed that Myc inhibited Ras mediated up-regulation of both markers (Fig. 2D). In contrast, treatment of U7V or U7Myc cells with dexamethasone did not result in morphologic differentiation (not shown) and did not induce the expression of these genes (Fig. 2D). The absence of up-regulation of GAP43 protein in UR61Myc cells by Ras was also confirmed by immunoblot (Fig. 2E).

To confirm that Myc overexpression was the cause for the block in differentiation of UR61Myc cells, we asked whether the suppression of Myc expression restored the differentiation-competent phenotype. To this purpose, we used a vector expressing a short hairpin RNA for human Myc (shMyc) previously shown to suppress human Myc expression (39). The ability of this vector to reduce Myc levels in UR61Myc cells was confirmed by immunoblot analysis (Fig. 3A). To test shMyc effect on differentiation, UR61 cells were cotransfected with a green fluorescent protein (GFP) vector together with the shMyc vector or the empty vector and the fraction of GFP-expressing differentiated cells was then scored. The result indicated that shMyc transfection significantly increased the fraction of differentiated cells upon treatment with dexamethasone (Fig. 3B). These data show that Myc antagonizes Ras-mediated differentiation.

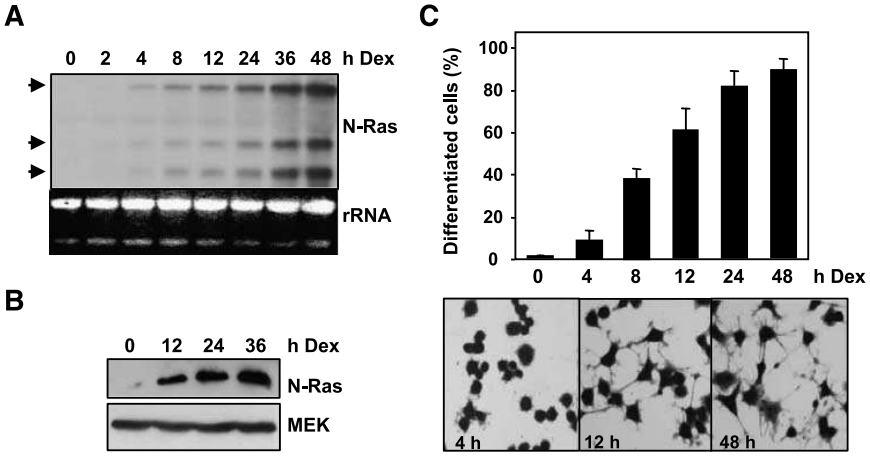

FIGURE 1. Ras induces differentiation in UR61 cells. **A.** Northern analysis showing the induction of N-Ras in UR61 cells upon treatment with 200 nmol/L dexamethasone (*Dex*). Arrows, the three transcripts of the murine transgene. A picture of the filter stained with ethidium bromide is shown to assess RNA loading and integrity. **B.** N-Ras protein induction in UR61 cells. Cells were treated with 200 nmol/L dexamethasone for 12 to 36 h as indicated and whole-cell extracts were subjected to immunoblotting for N-Ras and (as protein loading control) MEK. **C.** Irreversibility of Ras-induced differentiation. UR61 cells were treated with 200 nmol/L dexamethasone for the indicated periods, washed twice with PBS, and the morphologically differentiated cells were scored after 48 h. Columns, mean of two independent experiments; bars, SE. Bottom, representative micrographs of cells corresponding to the indicated time points stained with crystal violet.

Myc Does Not Inhibit Ras Induction and Activation

We next explored possible mechanisms by which Myc could impair Ras-induced differentiation. First, we wanted to rule out the possibility that Myc could hinder directly or indirectly the activity of mouse mammary tumor virus promoter, so as to inhibit the induction of Ras expression by dexamethasone. Northern blot analysis showed that N-Ras mRNA induction was similar in the parental UR61, UR61V, and the Myc-expressing UR61Myc cells (Fig. 4A). We also confirmed by immunoblot that N-Ras protein induction was similar in UR61V and in UR61Myc cells (Fig. 4B). In the immunoblot shown in Fig. 4B, as well in others described below (Figs. 5E and 7A), it is apparent that Myc protein levels were dramatically elevated in response to Ras. This effect is dependent on Ras, and not on the hormone, as shown by Myc immunoblot analysis of the U7Myc cells (which lack Ras ectopic expression; Fig. 4B). The Ras-dependent increase in protein levels is likely due to Myc stabilization, an effect previously reported in other systems (40), although concomitant increase in mRNA levels cannot be ruled out. Next, we tested the possibility that Myc impaired not the expression, but the activation of N-Ras oncoprotein in this system. Activation of Ras was analyzed by a Ras-GTP pull-down assay with the Ras-binding domain of Raf, which only binds GTP-bound Ras. The results showed that the fraction of active N-Ras was unchanged in UR61Myc cells compared with UR61V cells (Fig. 4C). We concluded that Ras activation was not impaired by Myc expression in this model, and thus Myc is acting at a level downstream of Ras activation.

Myc Does Not Inhibit Proliferation Arrest of UR61 Cells Induced by Ras

In view of the well-known effects of Myc as a stimulator of cell cycle progression and the growth arrest associated to Ras-mediated differentiation in UR61 cells, it was conceivable that Myc would inhibit differentiation by maintaining the cells in a proliferative state. As such, we asked whether Myc-expressing cells continued proliferating despite the induction of Ras. To test this, we seeded similar numbers of UR61V and UR61Myc cells, and after 48 and 72 h the attached cells were counted. The results (Fig. 5A) showed that cells expressing Myc, despite their undifferentiated phenotype, remained growth arrested, similarly to differentiating UR61. To analyze the cell cycle distribution, DNA content was determined by flow cytometry. Ras induction resulted in a depletion of S-phase cells in both differentiating UR61V and nondifferentiated UR61Myc cells (Fig. 5B). In conclusion, Myc impaired Ras-mediated differentiation but did not reverse the proliferation arrest elicited by Ras. It has been previously reported that Myc sensitizes different cell types in response to growth factor deprivation and other stress stimuli (41). Myc-dependent apoptosis have also been reported in serum-deprived PC12 cells (42). Thus, we analyzed the effect of Myc on apoptosis of UR61 cells. Similarly to parental PC12 cells, serum deprivation resulted in higher rate of cell death in UR61Myc than UR61 cells (Fig. 5C). The results also confirmed the previous results (Fig. 5A and B) that Myc expression does not induce cell proliferation in Ras-induced cells.

It was conceivable that proliferation of UR61Myc cells in the presence of dexamethasone was limited by concomitant enhanced apoptosis mediated by Myc. We studied the apoptosis in response to Ras induction in both cell lines. The results showed that differentiation was accompanied with apoptosis, which increased after 24 h (i.e., once morphologic differentiation was already at its maximum levels). However, the extent of apoptosis was similar in UR61Myc cells and in control UR61V cells. This result was assessed by measuring apoptosis through the binding of Annexin V

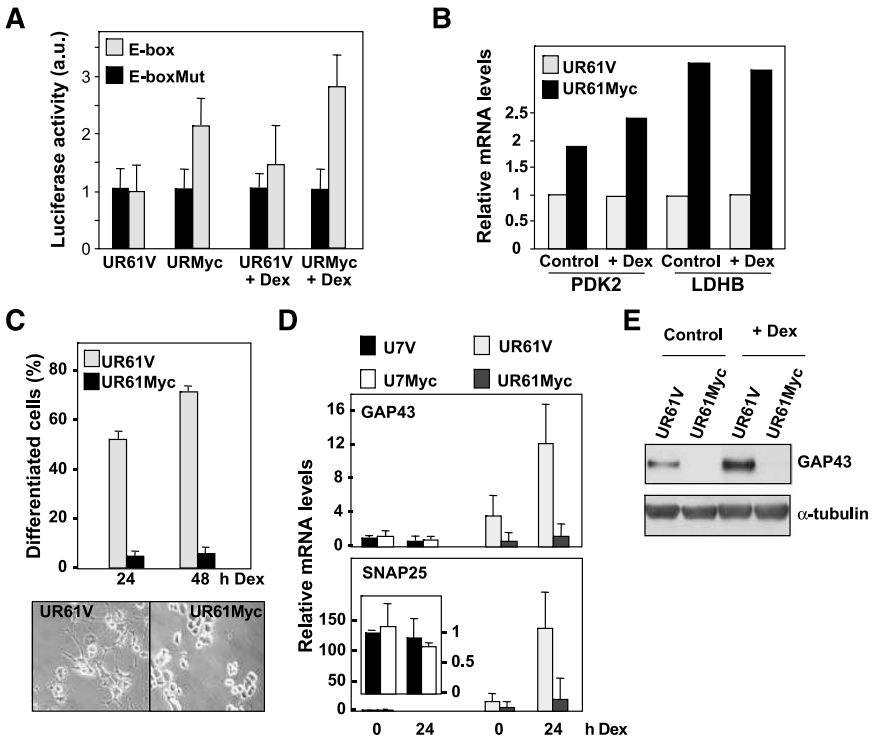

FIGURE 2. Myc inhibits Ras-induced differentiation of UR61 cells. **A.** Transactivation of a Myc-responsive promoter by UR61V and UR61Myc cells. Cells were transiently transfected with a luciferase reporter containing four E-boxes or four mutated E-boxes (*E-boxMut*). Data are relative to the activity in cells transfected with the mutated E-box. Columns, mean of two independent experiments; bars, SE. **B.** mRNA expression of *PDK2* and *LDHB*. Cells were treated for 24 h with 200 nmol/L dexamethasone as indicated, total RNA was prepared, and relative mRNA levels were determined by quantitative RT-PCR with normalization against levels of RPS14 mRNA. **C.** Right graph, fraction of cells with neurites of the indicated cell lines was measured after 24 and 48 h of treatment with 200 nmol/L dexamethasone. Columns, mean of three independent experiments; bars, SE. Left, representative images from UR61V or UR61Myc cells treated for 24 h with 200 nmol/L dexamethasone. **D.** mRNA expression of the neuronal-specific genes *GAP43* and *SNAP25*. Cells were treated with 200 nmol/L dexamethasone as indicated and total RNA was prepared. Relative levels of *GAP43* and *SNAP25* transcripts were measured as in **A**. Inset, *SNAP25* expression in U7V and U7Myc cells. Data are relative to the mRNA levels of untreated U7V cells. Columns, mean of two measurements; bars, SE. **E.** UR61V and UR61Myc cells were treated with 200 nmol/L dexamethasone for 36 h as indicated and whole-cell extracts were subjected to immunoblotting for GAP43 and (as protein loading control) α-tubulin.

(Fig. 5D) and the fraction of cells with sub-G_1 content of DNA (Fig. 5E). In aggregate, the results indicate that in this model Myc is impairing differentiation without inducing cell proliferation.

Myc Inhibits Ras-Mediated AP-1 Activity and c-Jun Expression in UR61 Cells

It is well established that in PC12 cells, sustained Ras-ERK activity induces c-Jun expression and that c-Jun up-regulation is critical for NGF-mediated differentiation (33). Thus, we asked whether this was also the case in the UR61 model. Similarly to PC12, the expression of c-Jun mRNA and protein increased upon Ras activation in UR61 cells (Fig. 6A and C). To assess the relevance of c-Jun in UR61 differentiation, we used a constitutively activated form of c-Jun (v-Jun). Cells were co-transfected with v-Jun expression vector (or the empty vector) and a GFP expression vector in a 10:1 ratio. The cells were treated with dexamethasone and the fraction of morphologically differentiated GFP-positive cells was scored 24 h later. It was found that ~55% of the v-Jun transfected cells appeared differentiated 24 h after transfection, versus <5% in cells transfected with the empty vector. Thus, v-Jun was sufficient to induce differentiation in UR61 cells in the absence of Ras induction (Fig. 6B). The above results suggested that the Ras-Jun signal was sufficient for the differentiation of UR61 cells, similarly to what is described for NGF-induced differentiation in PC12 cells (33, 43, 44).

Given this relationship between c-Jun and differentiation in UR61 cells, we next sought to investigate whether Myc could affect the Ras-mediated up-regulation of *c-Jun* gene expression. To address this, we first analyzed c-Jun expression in UR61V and UR61Myc cells after Ras induction. In UR61V cells, c-Jun levels dramatically increased upon dexamethasone addition but this induction was abrogated in UR61Myc cells after 24 h of treatment, when differentiation is irreversible (Fig. 6C, *left*). It has been described that the protein ATF2 dimerizes with c-Jun to form the AP-1 factor that binds the c-Jun promoter (45) and that ATF2 is also activated during differentiation of PC12 cells (43). Thus, we studied ATF2 levels and phosphorylation in the UR61 model. We observed ATF2 phosphorylation in UR61 after Ras induction, but Myc did not modify the levels of phospho-ATF2 (Fig. 6C, *right*).

We next analyzed whether Myc overexpression also antagonized c-Jun binding to DNA in the UR61 model. We did electrophoretic mobility shift assays using as the probe an oligonucleotide encompassing the AP-1 (*jun1*) site of the rat *c-Jun* promoter mapping at −133/−126, conserved in human, mouse, and rat genes (46, 47). We tested nuclear extracts from UR61V and UR61Myc cells untreated or treated for 24 h with dexamethasone to induce Ras. The results (Fig. 6D) showed that Ras activation resulted in a dramatic retardation in control cells, but Myc completely inhibited this effect. We sought to confirm this result by testing the binding of c-Jun to its own promoter by chromatin immunoprecipitation (ChIP). c-Jun autoregulates its transcription via two conserved AP-1 binding sites (termed *jun1* and *jun2*, mapping at −124 and −243 from transcription start site), conserved in rat, mouse, and human promoters (46, 47). These sites are also critical for c-Jun induction during PC12 differentiation (48). The results of ChIP analysis (Fig. 6E) showed a dramatic increase in the amount of c-Jun bound to a promoter fragment containing *jun1* and *jun2* sites after Ras induction in control UR61V cells. In contrast, such binding was not observed in UR61Myc cells.

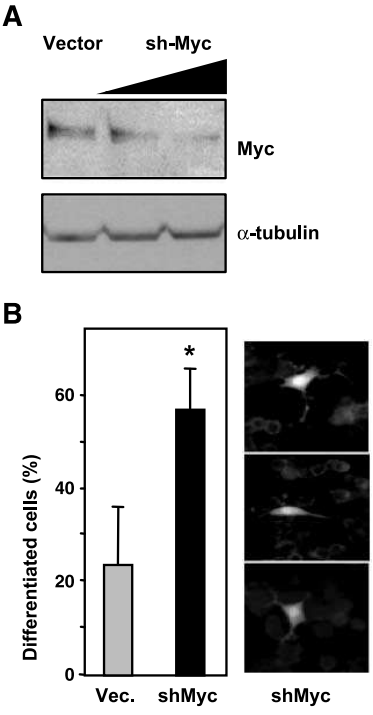

FIGURE 3. Silencing of Myc expression in UR61Myc cells restores the differentiation response to Ras. **A.** Reduction of Myc protein levels in UR61Myc transfected with a shMyc expression vector (pRS/myc). Cells were transfected with 8 μg of vector and 4 and 8 μg of pRS/myc. Twenty-four hours after transfection, Myc levels were determined by immunoblot. Levels of α-tubulin were also determined as protein loading control. **B.** Cells were cotransfected with vectors for GFP and shMyc (or the empty vector) in a 1:10 proportion (GFP/Myc) and incubated for 12 h. Dexamethasone was then added (200 nmol/L) and after 24 h the fraction of differentiated cells among those expressing GFP were counted. Columns, mean of two independent experiments; bars, SE. *, $P < 0.01$, statistically significant difference from control. Right, three representative images of cells expressing Myc/GFP.

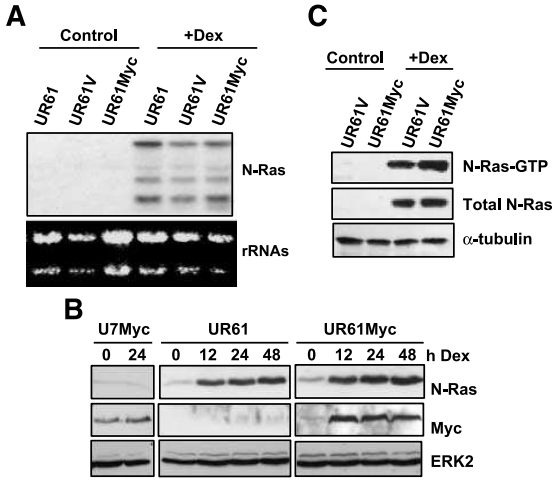

FIGURE 4. Myc does not impair N-Ras induction and activity in UR61Myc cells. **A.** Northern blot demonstrating N-Ras mRNA induction in the indicated cell lines untreated or treated for 24 h with 200 nmol/L dexamethasone. A picture of the filter stained with ethidium bromide is shown to assess RNA loading and integrity. **B.** Immunoblots showing the induction of N-Ras protein by 200 nmol/L dexamethasone. The same blot was successively incubated with antibodies against N-Ras, Myc, and (as loading control) ERK2. **C.** Rasf-RBD pull-down analysis showing the fraction of active Ras (Ras-GTP) in UR61V and UR61Myc cells. Pulled-down material was subjected to immunoblot incubated with anti–N-Ras and (as protein loading control) anti–α-tubulin antibodies.

Although UR61Myc is a polyclonal cell line generated by viral transduction, to rule out the possibility that the inhibition of c-Jun expression was due to an artifact during the selection of the cell line, we followed two experimental approaches. First, we generated a UR61-derived cell line with conditional Myc activation. UR61 cells were infected with a retrovirus expressing the MycER fusion protein, which can be activated by 4-hydroxytamoxifen. The resultant polyclonal cell line was termed UR61MER. The functionality of the MycER chimera was confirmed by the transactivation assays using a luciferase reporter carrying four Myc-responsive E-boxes in the promoter. The results show that the treatment with 4-hydroxytamoxifen resulted in increased transactivation of the promoter (Fig. 7A). As expected, treatment with 4-hydroxytamoxifen partially inhibited the morphologic differentiation induced with dexamethasone (not shown). Immunoblot analysis revealed that Ras-mediated up-regulation of c-Jun decreased upon addition of 4-hydroxytamoxifen in a dose-dependent manner (Fig. 7B). The immunoblot also showed that Ras also dramatically stabilized the MycER protein, as already observed for Myc protein in UR61Myc cells (Fig. 4B). Overall, the results obtained with both cell lines (UR61Myc and UR61MER) show that Myc ablates Ras-mediated up-regulation of c-Jun.

The second approach to elucidate the effect of Myc on c-Jun regulation was to transiently express Myc in UR61 and analyze the expression of c-Jun, after Ras induction, in the transfected (GFP expressing) cells. The results indicated that in almost every Myc-expressing cell under observation, c-Jun was

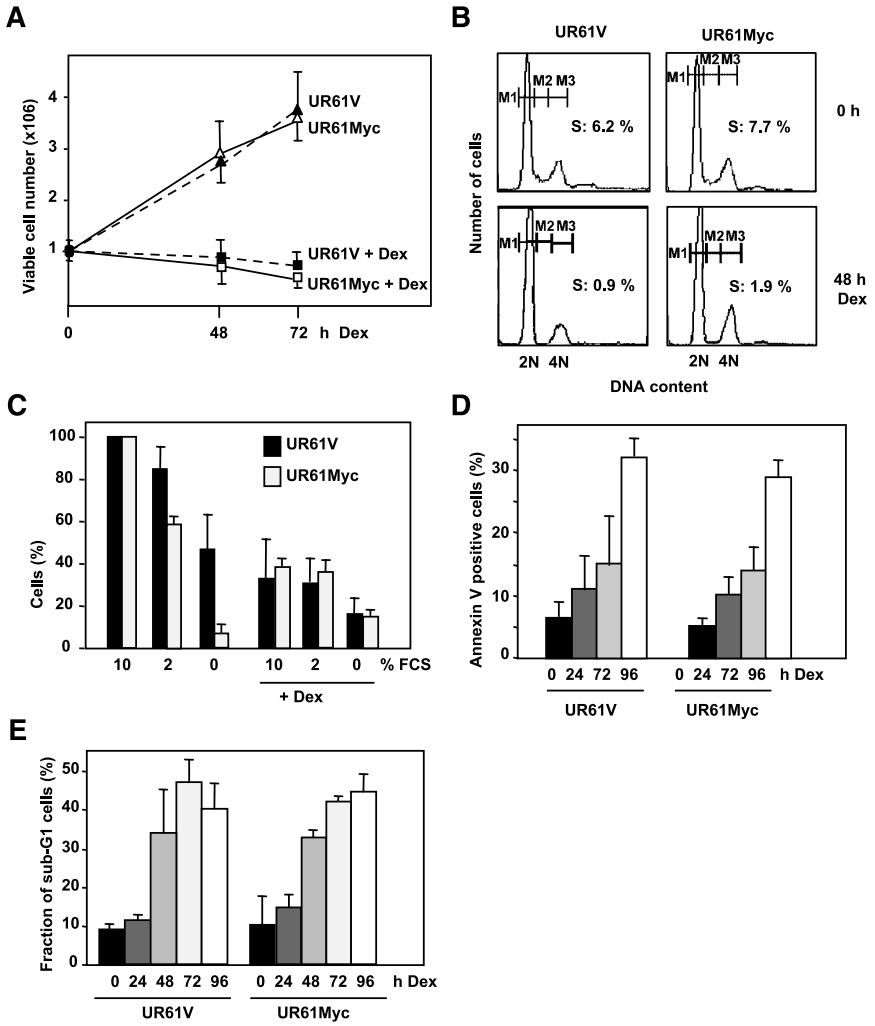

FIGURE 5. Myc does not rescue Ras-mediated proliferation arrest of UR61 cells. **A.** Growth curves of UR61Myc and UR61V (control cells) treated with 200 nmol/L dexamethasone to induce Ras. At the indicated times, the number of viable cells was determined by trypan blue method. Points, mean of four independent experiments; bars, SE. **B.** Cell cycle distribution of UR61Myc and UR61V cells after 48 h of Ras induction. Cell nuclei were stained with propidium iodide and the cell cycle distribution was analyzed by flow cytometry. The fraction of cells in S phase is indicated in each case. **C.** Cells were seeded in six-well plates at a density of 150,000 per well. Twenty-four hours later, the medium was replaced with fresh medium containing 0%, 2%, and 10% FCS and 100 nmol/L dexamethasone and further incubated for up to 72 h. Cells were stained with crystal violet and the cell amount was measured as indicated in Materials and Methods. Columns, mean from two independent experiments; bars, SE. **D.** Apoptosis of UR61V and UR61Myc cells assessed by Annexin V binding. Cells were treated with 200 nmol/L dexamethasone for the indicated periods and the fraction of cells bound to Annexin V was analyzed by flow cytometry. Columns, mean of two independent experiments; bars, SE. **E.** Apoptosis of UR61V and UR61Myc cells analyzed by the fraction of subdiploid cells. Cells were stained with bromodeoxyuridine and analyzed by flow cytometry. Columns, mean of two independent experiments; bars, SE.

undetectable or very low when compared with neighboring untransfected cells (Fig. 7C). In turn, if the mechanism responsible for the inhibition of differentiation elicited by Myc was the down-regulation of c-Jun expression, it would be expected that c-Jun overexpression should counteract the Myc effect. We addressed this point by transfecting a c-Jun expression vector into UR61Myc cells and quantifying the morphologically differentiated cells upon Ras induction. The results showed that c-Jun expression resulted in a 3-fold increase on UR61Myc cells undergoing differentiation compared with cells transfected with the empty vector (Fig. 7D). Altogether, these data argue that Myc inhibits differentiation of UR61 via the down-regulation of c-Jun expression and activity.

Myc Inhibits Ras-Mediated Transcriptional Activation of c-Jun Promoter

The aforementioned results indicated that Myc blocked the up-regulation of c-Jun expression induced by Ras. We next asked whether Myc exerted this effect at a transcriptional level. To this end, we first analyzed c-Jun mRNA levels by quantitative RT-PCR. The results showed that 24 h after the induction of Ras by dexamethasone addition, c-Jun mRNA dramatically increased in control UR61V cells but not in UR61Myc cells (Fig. 8A). This result suggested that, in the UR61 system, Myc was impairing c-Jun expression at the transcriptional level. Thus, we next tested whether Myc inhibited the activity of the Jun promoter. We carried out luciferase reporter assays in UR61 cells with a luciferase reporter carrying the murine c-Jun proximal promoter. We found that Myc partially inhibited Ras-mediated activation of c-Jun promoter (Fig. 8B). However, Myc had no effect on the transactivation exerted by an activated c-Jun isoform (i.e., v-Jun), suggesting that Myc did not affect the transcriptional activity of c-Jun and its effect is likely limited to inhibit its induction in response to Ras.

As noted above, two AP-1 response elements (*jun1* and *jun2*) in *c-Jun* promoter are critical for c-Jun autoregulation

and bound by c-Jun in UR61 cells (Fig. 6E). To investigate whether Myc effects on c-Jun transcription depended on these AP-1 sites, we analyzed the effect of the transient coexpression of H-RasG12V and Myc on the transcriptional activity of AP-1 using a luciferase reporter containing four AP-1 response elements (4×AP-1-Luc). The results (Fig. 8C) showed that Ras activated this promoter, but the coexpression of Myc inhibited the activation of AP-1. In contrast, a Myc mutant carrying a deletion of a conserved region required for transactivation and transformation (MycD106-143) was unable to block Ras-mediated activation of c-Jun promoter (Fig. 8B) and to antagonize c-Jun transcriptional activity in UR61 cells using the 4×AP-Luc reporter (Fig. 8C). Similarly, a Myc mutant carrying and insertion in the basic region and unable to bind DNA (MycIn373; ref. 49) did not repress the Ras-induced activation of the AP-1 reporter (Fig. 8C). However, Myc did not impair the activation of the AP-1-Luc reporter induced by a constitutively activated c-Jun form as v-Jun

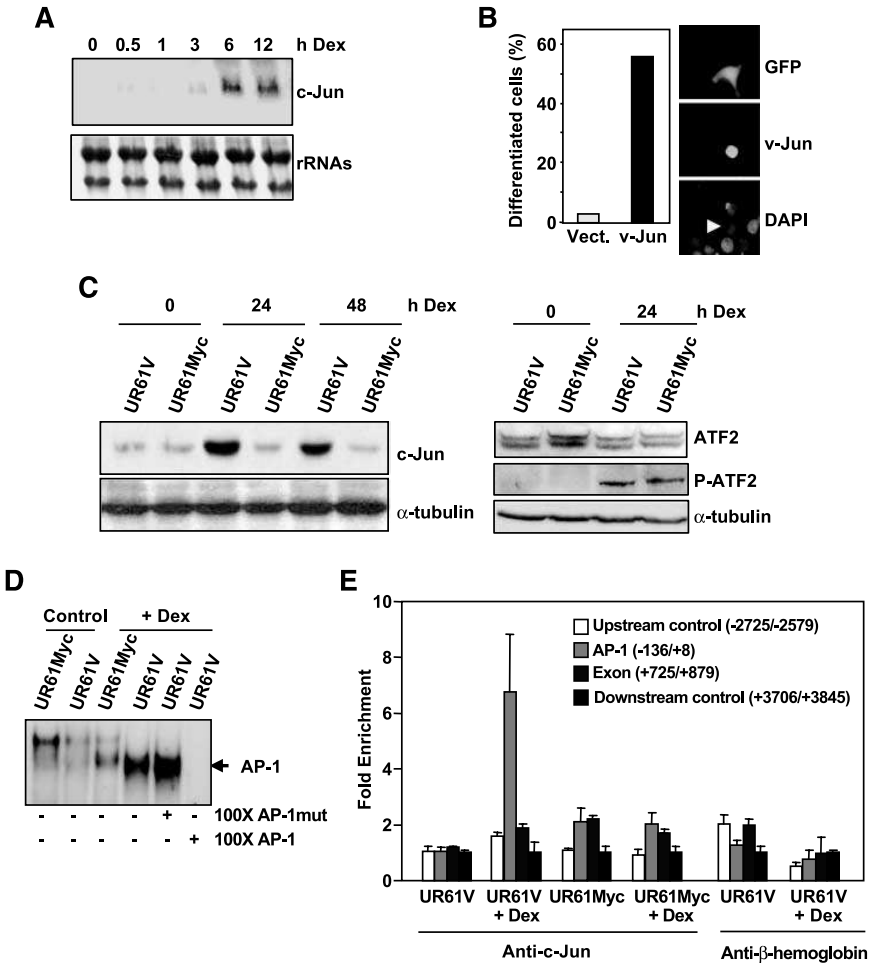

FIGURE 6. Myc impairs Ras-induced up-regulation of c-Jun. **A.** Expression of c-Jun mRNA during Ras-induced differentiation of UR61 cells. Cells were treated with 200 nmol/L dexamethasone for the indicated periods, and total RNA was analyzed by Northern blot. **B.** v-Jun induces differentiation of UR61 cells. Cells were transiently cotransfected with expression vectors for v-Jun and GFP in a proportion 1:10 (GFP/Jun). Twenty-four hours after the transfection, the fraction of morphologically differentiated cells was determined. The graph shows the results from 300 GFP-expressing cells. A representative image with a GFP/Jun–expressing differentiated cell is shown at the right. **C.** c-Jun up-regulation induced by Ras is impaired in UR61Myc cells. Cells were treated with dexamethasone for the indicated periods and whole-cell extracts were subjected to immunoblotting for c-Jun (*left*), ATF2, and phosphorylated ATF2 (*P-ATF2*; *right*). α-Tubulin levels were also determined as loading control. **D.** Electrophoretic mobility shift assay showing the inhibition of protein bound to a Jun/ATF2-binding site in UR61Myc cells in response to Ras-mediated differentiation. UR61V extracts were incubated with the labeled probe plus a 100-fold excess of unlabeled probe or unlabeled mutated probe as specificity controls. **E.** ChIP of c-Jun on the promoter of rat c-Jun, showing that Myc inhibits binding of c-Jun to its promoter in UR61Myc cells upon induction of Ras. Cells were treated with 200 nmol/L dexamethasone for 24 h to induce Ras and the chromatin was immunoprecipitated with anti–c-Jun and (as a specificity control) anti–β-hemoglobin antibodies. The immunoprecipitated DNA was analyzed by quantitative PCR was carried out with primers encompassing the *jun1* and *jun2* sites of rat c-Jun promoter (AP-1 amplicon) and other three control amplicons as indicated. Data are normalized to the corresponding inputs of chromatin before immunoprecipitation and are expressed as relative to the value of the downstream control amplicon. Columns, mean of two independent ChIP experiments; bars, SE.

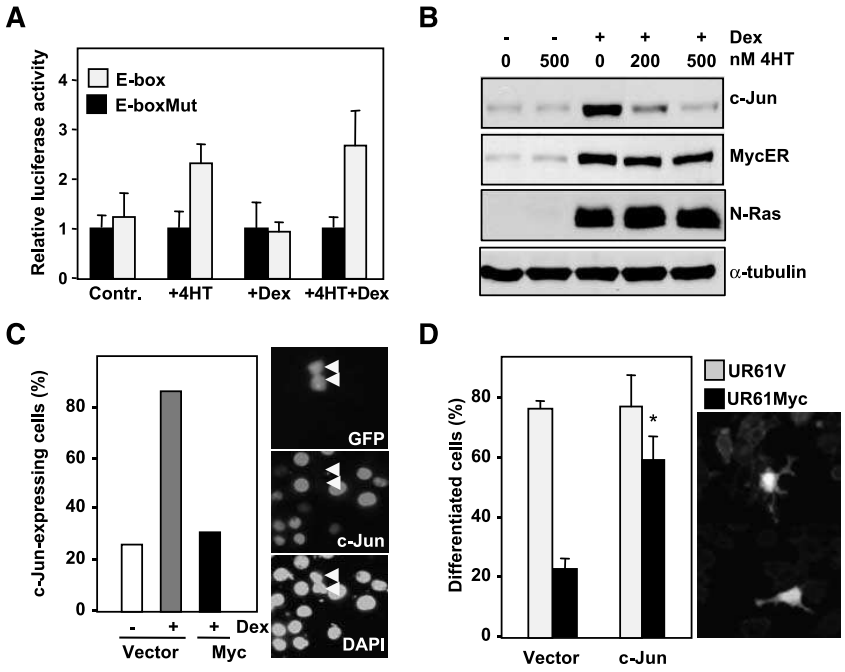

FIGURE 7. Myc-dependent inhibition of c-Jun up-regulation by Ras. **A.** Transactivation of a Myc-responsive promoter in UR61MER cells. Cells were transiently transfected with a luciferase reporter containing four E-boxes or four mutated E-boxes (*E-boxMut*). Following 24 h of transfection, 4-hydroxytamoxifen (*4HT*) was added to 500 nmol/L, and 1 h later dexamethasone was added to 200 nmol/L. The cells were further incubated for 24 h and the luciferase activity was measured in duplicates. Luciferase activity is expressed relative to the activity in cells transfected with the mutated E-box. Columns, mean of two independent transfection experiments; bars, SE. **B.** Myc down-regulated c-Jun in UR61MER cells. 4-Hydroxytamoxifen was added to the indicated concentrations 1 h before dexamethasone (final concentration, 100 nmol/L). Lysates were prepared 12 h later and analyzed by immunoblot with antibodies against c-Jun, Myc (detecting the MycER protein), N-Ras, and α-tubulin. **C.** UR61 cells were cotransfected with an expression vector for human Myc and GFP in a 10:1 proportion. Twelve hours after transfection, the cells were treated with dexamethasone and 24 h later the expression of c-Jun was assayed by immunofluorescence. The results from 500 GFP-expressing cells are shown in the graph and a representative field is shown at the right. Arrowheads, two cells expressing Myc/GFP and lacking c-Jun. **D.** Ectopic c-Jun rescues the Myc-mediated inhibition of differentiation. Left graph, UR61V and UR61Myc were cotransfected with mixtures of expression vectors for GFP and c-Jun (or its empty vector) in a 1:10 proportion. Twelve hours after transfection, the cells were treated with dexamethasone, and 24 h later the fraction of differentiated cells was determined. The results from 400 GFP-expressing cells are shown in the graph. Columns, mean of three independent transfections; bars, SE. The difference between UR61Myc cells transfected with the empty vector and the c-Jun vector was significant (*, $P < 0.01$). Right, images of UR61Myc cells transfected with c-Jun and GFP and treated with dexamethasone showing two differentiating cells.

(Fig. 8C). Thus, although Myc antagonizes Ras-mediated induction of c-Jun, it did not impair c-Jun transcriptional activity once it is activated.

Myc represses some promoters through the interaction with the zinc finger protein Miz-1 (reviewed in ref. 50). We explored the possibility of Miz-1 involvement in the UR61 model by using the MycV394D mutant, which is unable to bind Miz-1 (51). The results showed that MycV394D abolished Ras-mediated activation of the AP-1 reporter as efficiently as wild-type Myc (Fig. 8C), suggesting that the repression that Myc exerts on c-Jun promoter does not depend on its interaction with Miz-1. We also addressed the possible involvement of Miz-1 by ectopically expressing Miz-1 in UR61V and UR61Myc and asking whether the differentiation and/or c-Jun expression were affected in UR61Myc cells. Cells were transiently transfected by nucleofection with a Miz-1 expression vector, resulting in ≥40% efficiency of transfection. Morphologic differentiation, expression of the differentiation marker GAP43/Neuromodulin, and expression of c-Jun protein were determined in the transfected cells. The results indicated that Miz-1 overexpression did not modify the block in c-Jun expression of UR61Myc cells (Fig. 8D, *top*) and in morphologic differentiation (Fig. 8D, *bottom*). Finally, we asked whether the repression of Miz-1 blunted the effect of Myc on c-Jun regulation. For this purpose, we infected the UR61Myc cells with a retrovirus expressing a short-hairpin RNA for rat *Miz-1* gene (shMiz-1). This retroviral construct has been previously validated in rat cells (52). As we could not detect endogenous Miz-1 protein, we confirmed the repression of Miz-1 at the mRNA level, comparing the UR61Myc-shMiz1 with the cells transduced with the empty vector (UR61Myc-pRS). The results showed 40% to 50% reduction in Miz-1 expression (Fig. 8E). The results also show a down-regulation of Miz-1 by dexamethasone, a result also observed in parental UR61V and UR61Myc cells (not shown). We next asked whether the reduction in Miz-1 affected the block in Ras-mediated induction of c-Jun. The results showed that c-Jun was not induced by Ras in cells expressing shMiz-1. On the contrary, a modest decrease in c-Jun mRNA levels was detected, which was similar in control cells and shMiz-1 cells (Fig. 8E). Also, no induction of the

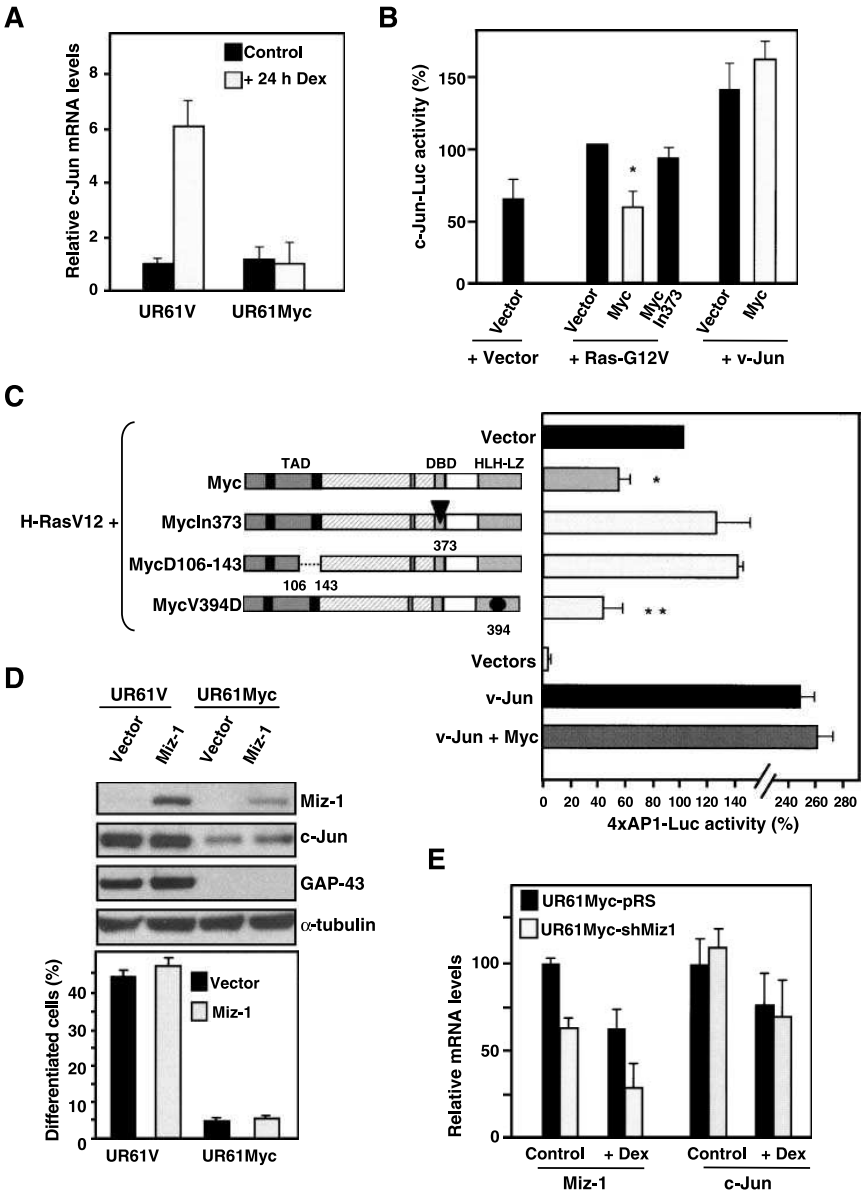

FIGURE 8. Myc impairs Ras-mediated activation of c-Jun promoter in UR61 cells. **A.** Inhibition of c-Jun mRNA up-regulation in UR61Myc cells after 24 h of treatment with dexamethasone. Levels of c-Jun transcripts in UR61Myc and UR61V cells were determined by quantitative RT-PCR. Columns, mean of four independent experiments (six measurements); bars, SE. **B.** Activity of murine c-Jun promoter. UR61 cells were cotransfected with the c-Jun-luc reporter and H-Ras-G12V or v-Jun (2 μg) and the Myc or its vector (4 μg) as indicated. Luciferase activity was measured 24 h after transfection and normalized against the activity detected with RasG12V. Columns, mean of three independent transfections; bars, SE. The difference between values of cells transfected with wild-type Myc and vector were statistically significant ($P < 0.01$). **C.** Activity of the 4×AP-1-luciferase reporter. UR61 cells were cotransfected with the reporter and expression vectors for Ras-G12V or v-Jun (5 μg) and Myc wild-type or mutants (5 μg) as indicated at the right of the graph. Luciferase activity was measured 24 h after transfection and normalized against the RasG12V+vector value. Columns, mean of three independent transfections; bars, SE. Differences in luciferase activity between samples transfected with wild-type Myc, MycV394D, and vector were statistically significant (*, $P < 0.05$; **, $P < 0.01$), whereas the difference between MycIn373 and vector was not significant. **D.** Top, cells were nucleofected with an expression vector for Miz-1 or the corresponding empty vector. Following 12 h of transfection, dexamethasone was added to 200 nmol/L, and 24 h later whole-cell extracts were subjected to immunoblotting for Miz-1, c-Jun, GAP-43 (as a control for differentiation), and α-tubulin (as protein loading control). Bottom, fraction of morphologically differentiated cells from the above described transfections. Columns, mean of two independent transfections; bars, SE. **E.** Expression of Miz-1 and c-Jun mRNA in UR61Myc-shMiz1 and the control cell line UR61Myc-pRS (transduced with the empty vector). Cells were treated for 24 h with 200 nmol/L dexamethasone as indicated and RNA was prepared and analyzed by quantitative RT-PCR using RPS14 mRNA levels as internal control. The expression in untreated UR61Myc-pRS cells was defined as 100% for each gene and the other values were normalized accordingly.

neuronal marker SNAP25 and no morphologic differentiation was detected in cells expressing shMiz-1 treated with dexamethasone (not shown). Taken together, the results suggest that Myc blocks c-Jun induction by a mechanism independent from Miz-1.

As UR61 are deficient in Max, we considered the possibility that Myc impairs c-Jun induction through mechanisms unrelated to DNA binding activity of Myc. We first showed that a Myc mutant defective for DNA binding, MycIn373, failed to block Ras-mediated activation of c-Jun promoter-luciferase reporter (Fig. 8B) and the 4×AP-1-Luc reporter (Fig. 8C). Thus, we assayed the ability of MycIn373 to inhibit differentiation in transient transfection experiments. The results showed that MycIn373 was not able to inhibit Ras-mediated differentiation compared with wild-type Myc (Fig. 9A). These results suggest that Myc must bind to DNA targets to exert its effect as differentiation inhibitor in this model. Thus, we asked whether Myc could bind the promoter of rat c-Jun. Bioinformatic analysis revealed the presence of a noncanonical E-box (CATGCG) in the 5′ region of rat *c-Jun* gene, mapping at −805/−799. ChIP analysis showed that Myc bound this E-box, and some binding was also detected to the amplicon containing the AP-1 sites. This could mean a low-affinity binding or, more likely, a residual binding to the proximity of the E-box–containing amplicon.

Myc Inhibits Ras-Mediated Transcriptional Activation of c-Jun Promoter in Different Cell Types

Finally, to address whether Myc repression of the Ras-mediated c-Jun induction is unique to the UR61 model, either because of its species or neuronal origin or its deficiency in Max (ref. 53; and data not shown), we analyzed four human cell lines derived from different tissues: HEK293T (kidney embryo cells), HeLa (cervical carcinoma cells), MEG05, and K562 (both myeloid leukemia cells). In these cell lines, Ras did not induce differentiation; however, in K562 and HeLa, Ras provokes proliferation arrest (14). Expression vectors for oncogenic H-Ras and Myc were cotransfected in these cell lines along with the 4×AP-1-Luc reporter. The results showed that Ras activated this promoter and Myc antagonized this effect in all the cell types (Fig. 10A), confirming our previous results in UR61 cells. In K562 cells, similar results were obtained using a luciferase reporter for the proximal promoter of collagenase II, a typical AP-1–responsive promoter (not shown). We also tested the MycIn373 and MycD106-143 mutants in the K562 and we found that both were incapable of inhibiting AP-1 reporter (Fig. 10A), thus reproducing the results observed in UR61. Finally, we asked whether this effect correlated with down-regulation of c-Jun protein in HEK293T cells (which shows higher transfection efficiency). The immunoblot results revealed that Myc antagonized the up-regulation of c-Jun brought about by oncogenic Ras (Fig. 10B), thus confirming that impairment of c-Jun up-regulation by Myc was not unique to the UR61 model.

Discussion

Whereas the cooperation between Myc and Ras in transformation has been explored in numerous studies, their functional interaction during cellular differentiation has been poorly investigated. This is surprising considering that the induction of differentiation is one of the most prominent effects of Ras (19) and that differentiation inhibition is one of the main and first biological effects described for Myc (reviewed in refs. 5, 8). In the present study, we show that Myc abrogates Ras-mediated neuronal differentiation of pheochromocytoma UR61 cells without reversing the proliferation arrest, and that the differentiation inhibition is mediated, at least in part, by blocking c-Jun up-regulation.

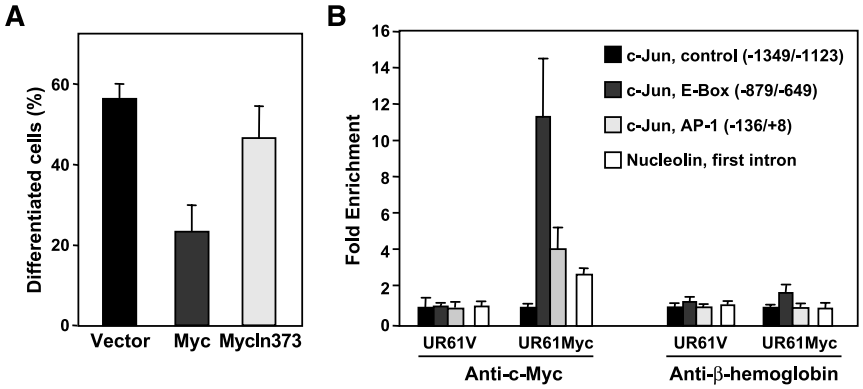

FIGURE 9. A. DNA binding domain of Myc is required for differentiation inhibition. UR61 cells were transiently transfected with expression vectors for GFP and wild-type Myc, MycIn373, and the empty vector (pMLV). Twelve hours after transfection, dexamethasone was added and the fraction of differentiated cells was determined after 48 h. Columns, means from two independent experiments; bars, SD. **B.** ChIP of Myc on the promoter of rat c-Jun. Cells were treated with 200 nmol/L dexamethasone for 24 h to induce Ras and the chromatin was immunoprecipitated with anti–c-Myc and (as a specificity control) anti–β-hemoglobin antibodies. The immunoprecipitated DNA was analyzed by quantitative PCR, which was carried out with primers encompassing the three amplicons of the rat c-Jun promoter and, as a control for Myc binding, the first intron of rat nucleolin. Data are normalized to the corresponding inputs of chromatin before immunoprecipitation and are expressed as relative to the value of the *c-Jun* gene upstream amplicon. Columns, mean of two independent ChIP experiments; bars, SE.

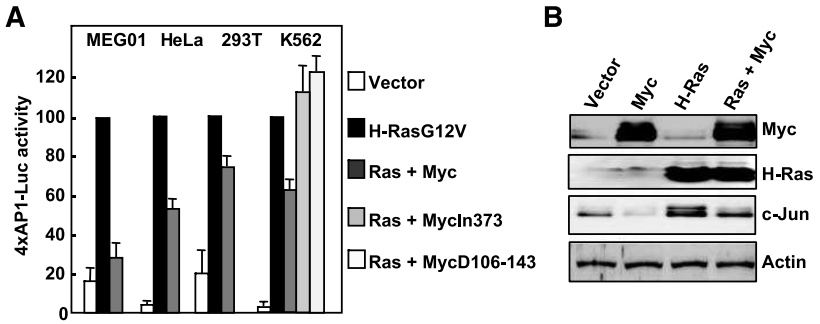

FIGURE 10. Myc impairs Ras-mediated activation of c-Jun in different cell lines. **A.** Luciferase assays with 4×AP-1-luciferase reporter in the indicated cell lines. Cells were electroporated with the reporter (2 μg), Ras expression vector (pCEFL-H-RasG12V, 2 μg), and Myc (pMLV-Myc wild-type, pMLV-MycIn373, and pMLV-MycD106-143, 5 μg). Luciferase activity was measured 36 h after transfection and normalized against the H-RasG12V value. Columns, mean of three independent transfections; bars, SE. **B.** Myc-mediated inhibition of c-Jun up-regulation in HEK293T cells. Cells were grown for 5 h in medium with 1% FCS and transfected with 1.5 μg of H-RasG12V expression vector and 4.5 μg of Myc expression vector (or 6 μg of empty vector) and 36 h later protein extracts were prepared and analyzed by immunoblot for the indicated proteins.

In the classic experiments on Ras and Myc cooperation in transformation of primary fibroblasts (20), Myc seems to antagonize Ras-mediated growth arrest and senescence, switching Ras into a growth-promoting protein (12). In contrast, in the UR61 model, Myc inhibits Ras-induced differentiation without affecting the growth inhibition associated to differentiation. Apoptosis ensues once the cells have achieved differentiation, but Myc does not enhance this apoptosis. Thus, the observed growth arrest is not due to apoptosis concomitant with increased-Myc induced proliferation. Inhibition of cell differentiation by Myc has been explained in some models as the result of the stimulation of cellular proliferation, thus antagonizing the cell cycle arrest associated to terminal differentiation (5, 6). However, our results in the UR61 system argue that unabated proliferation is not the only mechanism by which Myc can inhibit differentiation.

One of the first identified biochemical effects of Ras was the up-regulation of c-Jun, not only in fibroblasts (54, 55) but also in PC12 cells (31). However, the effect of Myc on the Ras-Jun interaction had not been explored thus far. This is probably because Ras cooperates with either c-Jun or Myc to induce transformation of fibroblasts, and therefore a major effect of Myc on the Ras-Jun pathway during transformation was not to be expected. However, in those models where the Ras-Jun signal results in cell differentiation, Myc could block the Ras-Jun effect. In UR61 cells, we found that Ras up-regulates c-Jun and that constitutively active c-Jun (i.e., v-Jun) is sufficient to induce differentiation, as previously described in parental PC12 cells (33, 56). Interestingly, Myc impairs this Ras-induced up-regulation of c-Jun in UR61 cells, and coexpression of Myc with c-Jun decreases the antagonistic effect of Myc on Ras-induced differentiation. Although alternative mechanisms could also contribute to Myc-mediated inhibition of differentiation (e.g., regulation of genes other than *c-Jun*), our results indicate that c-Jun suppression mediated by Myc plays an essential role for the inhibition of Ras-induced differentiation.

The data suggest that Myc antagonizes c-Jun up-regulation at the transcriptional level, as shown by the drop of c-Jun mRNA and the diminished c-Jun promoter activity. However, Myc could not reverse the transactivation activity of the constitutively activated v-Jun and did not impair Jun NH_2-terminal kinase activity as assessed by Jun NH_2-terminal kinase phosphorylation.[5] These findings are consistent with a model in which Myc blunts Ras-mediated transcriptional activation of c-Jun by interfering with its positive autoregulation, but does not impair the transactivation activity of c-Jun once it is expressed and active.

The mechanism underlying this unexpected activity of Myc is unclear, but Myc impairment of Ras-mediated activation of c-Jun is not exclusive of PC12-derived cells, as it is also observed in other cell lines derived from different tissues. The mechanism seems to be independent of Miz-1, as (*a*) it is reproduced by a Myc mutant (MycV394D) unable to bind Miz-1, and (*b*) enforced Miz-1 expression and partial Miz-1 silencing do not modify the Myc-mediated inhibition of differentiation and the block in c-Jun up-regulation. Our observations are consistent with a recent report in human lymphoid cells that identifies *c-Jun* as a gene down-regulated by Myc (57). Interestingly, UR61 cells are deficient for Max,[5] like their parental cell line, PC12 (53). Max independence for Myc-mediated apoptosis of PC12 (upon serum deprivation) has already been described (42). We now show that Myc blocks c-Jun induction and neuronal differentiation in a Max-independent manner. However, Max deficiency is not required for inhibition of AP-1–dependent transcription by Myc, because such inhibition is not unique to UR61 but also occurs in Max-expressing cells (e.g., HeLa, HEK293T, and K562).

Interestingly, a DNA-binding defective Myc mutant is unable to block differentiation and to inhibit c-Jun induction, suggesting that DNA binding is required for Myc activity in this system. Also, Myc mutant lacking the conserved Myc box II region (amino acids 106-143, required for transactivation and transformation) failed to inhibit c-Jun promoter activity. ChIP assays show that Myc binds an E-box in the rat c-Jun promoter in UR61Myc cells, although further work is required to elucidate whether Myc binding is directly involved in the

[5] Unpublished results.

block of the promoter activation and which are the dimerization partners of Myc, if any, when bound to the E-box. Thus, the mechanism for the Myc effect may be indirect, that is, mediated through the up-regulation or repression of other Myc target genes. Further work in our laboratories is aimed to dissect the mechanism(s) by which Myc interferes with c-Jun autoregulation in UR61 without Max intervention.

Regardless of the molecular mechanisms involved, our results support the hypothesis that inhibition of differentiation by Myc occurs independently of its effects on proliferation and this may represent an important mechanism by which Myc exerts its oncogenic function. It is noteworthy that recent observations in conditional Myc-expressing mice indicate that redifferentiation upon discontinued expression of Myc is the mechanism responsible for tumor regression in some models (58).

In summary, our findings identified a novel activity of Myc, which is its ability to prevent cell differentiation provoked by Ras by inhibiting the expression of c-Jun. In turn, these observations suggest that the proproliferative and the differentiation inhibitory activities of Myc can both contribute to promote the unregulated growth of Myc-induced neoplasias.

Materials and Methods

Cell Culture and Retroviral Infections

U7 cell line is a derivative of PC12 characterized by faster growth and a diminished differentiation capacity (16, 59). The UR61 cell line was generated by the stable transfection of U7 cells with an *N-ras* oncogene (N-*rasQ61K*) under the control of the dexamethasone-inducible mouse mammary tumor virus promoter (60). Ecotropic retroviruses were generated in Phoenix-E cells. To generated U7 and UR61 cells with constitutive expression of Myc, cells were infected with pBSH2-h-Myc and pBSH2 retrovirus, in the presence of polybrene (4 μg/mL). Retroviral pBSH2 and pBSH2-h-c-Myc vectors have been described (61). Infected cells were selected with 100 μg/mL hygromycin-B (Roche Applied Science). To generate U7 and UR61 cells expressing the Myc-ER fusion protein, cells were infected with the pBabePuro and pBabePuro-MycER retroviruses (62) and selected with puromycin (1 μg/mL). To generate UR61Myc-pRS and UR61Myc-shMiz1, UR61Myc cells were infected with pRetroSuper and pRetroSuper-shMiz1 retroviruses (52) and selected with puromycin (1 μg/mL).

U7 and UR61 and their derivatives were grown in DMEM supplemented with 8% FCS, gentamicin (80 μg/mL), and ciprofloxacin (2 μg/mL). The media for UR61 and its derivatives were also supplemented with G418 (250 μg/mL). HeLa and HEK293T cells were grown in DMEM with 8% FCS; K562 and MEG01 (both derived from human chronic myeloid leukemia) were grown in RPMI 1640 with 8% FCS. Unless otherwise stated, Ras was induced with 200 nmol/L dexamethasone (Sigma Chemical Co.) and MycER was activated with 200 or 500 nmol/L 4-hydroxytamoxifen (Sigma Chemical).

Cell Growth, Apoptosis, and Differentiation

Cell proliferation was assessed by counting trypsinized cell suspensions in hemocytometer and by crystal violet staining. For this, cells were washed with PBS, stained with 1% crystal violet in methanol for 15 min, dry, destained with 10% acetic acid for 2 h, and the color was measured in a colorimeter at $A_{590\ nm}$. For apoptosis determination by Annexin V binding, cells were trypsinized, washed with PBS, and the Annexin V binding was determined by flow cytometry and Annexin V-phycoerythrin (BD PharMingen) following the manufacturer's instructions. For determination of subdiploid cells, the cells were stained with propidium iodide and analyzed as described below. Cell morphology was assessed by phase-contrast microscopy. Cells forming at least one neurite as long as the diameter of the cell soma was scored as differentiated. At least 300 cells were scored in each differentiation experiment.

Cell Cycle Analysis

Cells (1×10^6) were collected and suspended in PBS, then fixed in ethanol 90% 4°C for 30 min. Cells were resuspended in PBS-sodium citrate buffer containing 10 μg/mL bovine serum albumin, 200 μg/mL RNase, 50 μg/mL propidium iodide (Sigma Chemical); incubated at 37°C in the darkness for 30 min; and analyzed by flow cytometry in an Excalibur cytometer (Becton Dickinson) and with the CellQuest software.

Expression Vectors and Transient Transfections

The vectors used in transient transfections were as follows: pCEFL-H-RasG12V (14), pRS/myc (expressing short-hairpin RNA for human Myc; ref. 39), pMLV-Myc, pMLV-MycIn373 (49, 63), pCEFL-Myc (64), pCEFL-MycV394D (65), pRSV-v-Jun and pRSV-c-Jun (66), pcDNA3-Miz1 (provided by Martin Eilers, Marburg University, Marburg, Germany), pEGFP-N2 (expressing GFP; Clontech Laboratories), and the corresponding empty vectors (pCEFL, pMLV, pcDNA3, and pRetroSuper). For transient transfections for immunofluorescence or protein expression analysis, plasmids were transfected into UR61 and HEK293T cells with FuGene-6 transfection reagent (Roche Applied Science). Nucleofection was carried out in an Amaxa nucleofector using the kit V (Amaxa AG). Two million cells were transfected with 2.5 μg of the Miz-1 expression vector or the corresponding empty vector and 0.5 μg of the GFP-encoding vector pmaxGFP (Amaxa). At least 40% of the cells expressed GFP 24 h after each nucleofection.

Immunoblots

Cells were lysed in cold NP40 buffer and 50 μg of protein per lane were electrophoresed on SDS-10% polyacrylamide gels and transferred onto nitrocellulose membranes by standard procedures. The primary antibodies used were anti–c-Jun (Santa Cruz Biotechnology), anti–c-Myc (Santa Cruz Biotechnology), anti-MEK1/2 (Cell Signalling), anti–N-Ras (Santa Cruz Biotechnology), anti-ATF2 (Cell Signalling), anti–phospho-Thr$^{69/71}$-ATF2 (Cell Signalling), anti-ERK2 (Santa Cruz Biotechnology), anti-GAP43 (BD Transduction Laboratories), anti–Miz-1 (Santa Cruz Biotechnology), anti-actin (Santa Cruz Biotechnology), and anti–α-tubulin (provided by Nicholas Cowan, New York University, New York, NY). Immunoblots were revealed with the enhanced chemiluminescence system (Amersham Pharmacia Biotech).

Immunofluorescence

Cells (grown at 50% of confluence on coverslips) were transfected with a mixture of the GFP vector pEGFP-N2 (Clontech) and the indicated expression vector (Myc, shMyc, v-Jun, c-Jun) in a 1:10 proportion and 2 μg of total DNA. After transfection, cells were incubated for 12 h, treated with 200 nmol/L dexamethasone for 24 h, and then fixed in 3.7% paraformaldehyde-PBS. Immunofluorescence was done as described (13) using the anti–c-Jun antibody and Texas red–conjugated goat anti-rabbit IgG (The Jackson Laboratory). The statistical significance was determined using Student's *t* test.

Electrophoretic Mobility Shift Assays

Nuclear extracts from UR61 cells were prepared as described (67). Gel retardation assays were done at room temperature in 20 μL reactions containing 15 μg of protein of nuclear extract and annealed oligonucleotides previously labeled with [α-^{32}P]dCTP using Klenow fragment. DNA-protein and free complexes were resolved in 4% nondenaturating polyacrylamide gels. The oligonucleotides were 5′-GGAAGGCCTTGGGGTGACATCATGGGCTATTTTTAG-3′ and its complementary 5′-CTTCCGGAACCCCACTGTAGTACCCGATAAAAATGGG-3′. The AP-1 site at −133 of rat promoter (Genbank accession no. NM021835) is underlined (46, 47). As specificity controls, we incubated extracts with the labeled probe and a 100-fold excess of cold probe and of a mutated probe with the underlined nucleotides (AP-1 binding site) mutated to ATCAGCAT.

Chromatin Immunoprecipitation

Cells (5×10^7) were used for each ChIP assay. Cells were fixed in 1% formaldehyde, lysed, and sonicated essentially as described (68). The ChIP was done by using Dynabeads-Protein G (Dynal Biotech) coupled to anti–c-Myc, anti–c-Jun, and (as specificity control) anti–β-hemoglobin antibodies (all rabbit polyclonal antibodies were from Santa Cruz Biotechnology). Dynabeads were incubated with lysates for 12 h at 4°C and washed several times with 50 mmol/L HEPES (pH 7.6), 1 mmol/L EDTA, 0.7% sodium deoxycholate, 1% NP40, and 0.5 mol/L LiCl. Chromatin was eluted with 500 μL elution buffer [50 mmol/L Tris (pH 8), 10 mmol/L EDTA, 1% SDS], decrosslinked (8h at 65°C), and purified through Qiaquick columns (Qiagen). Real-time PCRs of the eluted DNA were done at 56°C as annealing temperature in a Bio-Rad iCycler apparatus. The PCR primers (in 5′-3′ sense) are listed below. The sites of the rat c-*Jun* gene where the corresponding amplicons map (with respect to the transcription start site as in the NM021835 sequence) are indicated. For the distal upstream sequence (negative control), TTGGAAGACTGAGGGCAAAC and TGAAAGCTCGGTTGGTAAGG, which amplify between −2725 and −2579; for the proximal upstream sequence (negative control), CAAGCTCGCCACCTCTTTAG and CTGGGAAAACAAGCCTTGAG, which amplify between −879 and −649; for E-box (−879/−799 from rat c-Jun transcription start site), ATTCCGAGCACAGCAAATCT and AATGATCTGGGCGATTGAAG, amplifying between −879 and −648; for the AP-1 sites (*jun1* and *jun2*), CATTACCTCATCCCGTGAGC and AGGCAGTCTCTGCACACTCA, amplifying between −136 and +8; for the c-*jun* exon (negative control), CGCACGCTCCTAAACAAACT and CGTTTCCATCTTTGCAGTCA, amplifying between +725 and +3845; for the downstream sequence (negative control), GAGCCTGTGGTGGTAAATCC and GTGCCTCCACTCCCAGTAAC, amplifying between +3706 and +3845; for nucleolin first intron (positive control for Myc binding; ref. 69), CGCGTCCGAGGCA GTG and TCCATCTACCGTCACGGTCAG.

RNA Analysis

Total RNA was isolated using Tri Reagent (Ambion, Inc.). For Northern blot analysis, total RNA (15 μg per lane) was separated by electrophoresis through agarose-formaldehyde gel and transferred to nitrocellulose. Probe labeling with [α-^{32}P]dCTP and filter hybridization were carried out according to standard procedures. Probe for mouse N-*Ras* and c-*Jun* have been described (70, 71). The amount and integrity of the rRNAs were assessed by staining of the filter with ethidium bromide. cDNAs were obtained by reverse transcription using ScriptTM Kit (Bio-Rad Laboratories). For quantitative RT-PCR, cDNAs were amplified with SYBR-fluorescein PCR mix (ABgene) using an iCycler Bio-Rad apparatus. The primers for the indicated rat genes, written in the 5′ to 3′ sense, were as follows: for *c-Jun*, CGCACGCTCCTAAACAAACT and CGTTTCCATCTTTGCAGTCA; for *GAP43*, GTCAAACCGGAGGATAAGG and CTTCTCCACACCA-TCAGCAA; for *SNAP25*, GAATCGCCAGATTGACAGG and CCATGAGAGAAGCATGAAGGA; for *Miz-1*, ACCATCTCCTCCCATTCCTC and CCGCTGAATACTGCTTTGAAC-3′; for *LDHB*, TCTGGATTCTGCTCGGTTTC and GACTCCTGCCACATTCACC; for *PDK2*, AGGAAGTCAATGCCACCAAC and TTGATGGGAGGGAGAGTGAG; for *ribosomal protein 14* (*RPS14*), 5′-CAAGGGGAAGGAA-AAGAAGG-3′ and 5′-GAGGACTCATCTCG-GTCAGc-3′. The expression of the different genes was normalized against levels of *RPS14* mRNA.

Luciferase Assays

The luciferase reporters used were as follows: 4×AP-1-Luc, carrying four concatamers of a consensus AP-1–binding site (72); pJun-luc, carrying the mouse proximal promoter and part of the first exon (73); pGL3-E-box, carrying four E-box elements in the pGL3 vector; and pGL3-E-BoxMut, carrying four mutated E-boxes (74). For the assays with 4×AP-1-Luc and pJun-Luc, cells (2×10^6) were electroporated at 260 V and 1 mFa (Bio-Rad Gene pulser). Luciferase assays were done using 2 μg of the firefly luciferase reporter and 1 μg of the plasmid for *Renilla* luciferase (pRL-Null, Promega), and, when indicated, 5 μg of the expression vectors. Thirty-six hours after electroporation, the cells were lysed and luciferase activity was measured with the Dual Luciferase Assay kit (Promega). For the assays with pGL3-E-box and pGL3-E-boxMut, the cells were incubated for 24 h after transfection and further incubated for other 24 h in the presence or absence of 200 nmol/L dexamethasone and/or 500 nmol/L 4-hydroxytamoxifen. The cells were lysed and luciferase activity was measured as above.

The activity of firefly luciferase was normalized to that of *Renilla* luciferase used as internal control. Statistical significance of the differences between luciferase values was based on *P* values calculated using the Student's *t* test.

Ras Activation Assay

Ras-GTP was determined by the glutathione *S*-transferase-Ras–binding domain of Raf (amino acids 1-149) pull-down assay as described previously (75). Total and pulled-down proteins were analyzed by immunoblot antibodies.

Acknowledgments

We thank Angel Pellicer for U7 and UR61 cell lines; Bruno Amati (European Institute of Oncology, Milan, Italy), Thorsten Berg, (Department of Molecular Biology, Max Planck Institute, Martinsried, Germany), Carme Caelles (Institute for Biomedical Research, Barcelona, Spain), Angel Corbí (Centro de Investigaciones Biológicas, Madrid, Spain), Dirk Eick (Institute of Clinical Molecular Biological and Tumor Genetics, Munich, Germany), Jesus Gil (MRC Clinical Sciences, Imperial College, London, United Kingdom), Carla Grandori (Fred Hutchinson Cancer Research Center, Seattle, WA), Silvio Gutkind (National Institute of Dental and Craniofacial Research, NIH, Bethesda, MD), Martin Eilers (Institute of Molecular Biology and Tumor Research, University of Marburg, Marburg, Germany), Trevor Littlewood (Nuffield Department of Clinical Laboratory Sciences, University of Oxford, Oxford, United Kingdom), and Steven McMahon (The Wistar Institute, Philadelphia, PA) for luciferase reporters, retroviral constructs, and expression vectors; Nicholas Cowan for anti-tubulin antibody; Miguel Lafarga and M. Teresa Berciano (Dpto. de Bilogia Celular, Universidad de Cantabria, Santander, Spain) for help with confocal microscopy; Rosa Blanco, Pilar Frade, and Silvia Gonzalez for technical assistance; and M. Dolores Delgado and Carme Caelles for helpful discussions.

References

1. Dang CV, O'Donnell KA, Zeller KI, Nguyen T, Osthus RC, Li F. The c-Myc target gene network. Semin Cancer Biol 2006;16:253–64.

2. Patel JH, Loboda AP, Showe MK, Showe LC, McMahon SB. Analysis of genomic targets reveals complex functions of MYC. Nat Rev Cancer 2004;4:562–8.

3. Adhikary S, Eilers M. Transcriptional regulation and transformation by Myc proteins. Nat Rev Mol Cell Biol 2005;6:635–45.

4. Nesbit CE, Tersak JM, Prochownik EV. MYC oncogenes and human neoplastic disease. Oncogene 1999;18:3004–16.

5. Oster SK, Ho CS, Soucie EL, Penn LZ. The myc oncogene: MarvelouslY complex. Adv Cancer Res 2002;84:81–154.

6. Grandori C, Cowley SM, James LP, Eisenman RN. The Myc/Max/Mad network and the transcriptional control of cell behavior. Annu Rev Cell Dev Biol 2000;16:653–99.

7. Lutz W, Leon J, Eilers M. Contributions of Myc to tumorigenesis. Biochim Biophys Acta 2002;1602:61–71.

8. Henriksson M, Luscher B. Proteins of the Myc network: essential regulators of cell growth and differentiation. Adv Cancer Res 1996;68:109–82.

9. Campbell SL, Khosravi-Far R, Rossman KL, Clark GJ, Der CJ. Increasing complexity of Ras signaling. Oncogene 1998;17:1395–413.

10. Bos JL. Ras-like GTPases. Biochim Biophys Acta 1997;1333:M19–31.

11. Midgley RS, Kerr DJ. Ras as a target in cancer therapy. Crit Rev Oncol Hematol 2002;44:109–20.

12. Serrano M, Lin AW, McCurrach ME, Beach D, Lowe SW. Oncogenic ras provokes premature cell senescence associated with accumulation of p53 and p16INK4a. Cell 1997;88:593–602.

13. Vaque JP, Navascues J, Shiio Y, et al. Myc antagonizes Ras-mediated growth arrest in leukemia cells through the inhibition of the Ras-ERK-p21Cip1 pathway. J Biol Chem 2005;280:1112–22.

14. Delgado MD, Vaque JP, Arozarena I, et al. H-, K- and N-Ras inhibit myeloid leukemia cell proliferation by a p21WAF1-dependent mechanism. Oncogene 2000;19:783–90.

15. Bar-Sagi D, Feramisco JR. Microinjection of the ras oncogene protein into PC12 cells induces morphological differentiation. Cell 1985;42:841–8.

16. Guerrero I, Wong H, Pellicer A, Burstein DE. Activated N-ras gene induces neuronal differentiation of PC12 rat pheochromocytoma cells. J Cell Physiol 1986;129:71–6.

17. Noda M, Ko M, Ogura A, et al. Sarcoma viruses carrying ras oncogenes induce differentiation-associated properties in a neuronal cell line. Nature 1985;318:73–5.

18. Benito M, Porras A, Nebreda AR, Santos E. Differentiation of 3T3–1 fibroblasts to adipocytes induced by transfection of ras oncogenes. Science 1991;253:565–8.

19. Crespo P, Leon J. Ras proteins in the control of the cell cycle and cell differentiation. Cell Mol Life Sci 2000;57:1613–36.

20. Land H, Parada LF, Weinberg RA. Tumorigenic conversion of primary embryo fibroblasts requires at least two cooperating oncogenes. Nature 1983;304:596–602.

21. Sears R, Leone G, DeGregori J, Nevins JR. Ras enhances Myc protein stability. Mol Cell 1999;3:169–79.

22. Leone G, DeGregori J, Sears R, Jakoi L, Nevins JR. Myc and Ras collaborate in inducing accumulation of active cyclin E/Cdk2 and E2F. Nature 1997;387:422–6.

23. Compere SJ, Baldacci P, Sharpe AH, Thompson T, Land H, Jaenisch R. The ras and myc oncogenes cooperate in tumor induction in many tissues when introduced into midgestation mouse embryos by retroviral vectors. Proc Natl Acad Sci U S A 1989;86:2224–8.

24. Sinn E, Muller W, Pattengale P, Tepler I, Wallace R, Leder P. Coexpression of MMTV/v-Ha-ras and MMTV/c-myc genes in transgenic mice: synergistic action of oncogenes *in vivo*. Cell 1987;49:465–75.

25. D'Cruz CM, Gunther EJ, Boxer RB, et al. c-MYC induces mammary tumorigenesis by means of a preferred pathway involving spontaneous Kras2 mutations. Nat Med 2001;7:235–9.

26. Greene LA, Tischler AS. Establishment of a noradrenergic clonal line of rat adrenal pheochromocytoma cells which respond to nerve growth factor. Proc Natl Acad Sci U S A 1976;73:2424–8.

27. Cowley S, Paterson H, Kemp P, Marshall CJ. Activation of MAP kinase kinase is necessary and sufficient for PC12 differentiation and for transformation of NIH 3T3 cells. Cell 1994;77:841–52.

28. Muroya K, Hattori S, Nakamura S. Nerve growth factor induces rapid accumulation of the GTP-bound form of p21ras in rat pheochromocytoma PC12 cells. Oncogene 1992;7:277–81.

29. Eferl R, Wagner EF. AP-1: a double-edged sword in tumorigenesis. Nat Rev Cancer 2003;3:859–68.

30. Mechta-Grigoriou F, Gerald D, Yaniv M. The mammalian Jun proteins: redundancy and specificity. Oncogene 2001;20:2378–89.

31. Sassone-Corsi P, Der CJ, Verma IM. ras-induced neuronal differentiation of PC12 cells: possible involvement of fos and jun. Mol Cell Biol 1989;9:3174–83.

32. Wu BY, Fodor EJ, Edwards RH, Rutter WJ. Nerve growth factor induces the proto-oncogene c-jun in PC12 cells. J Biol Chem 1989;264:9000–3.

33. Leppa S, Saffrich R, Ansorge W, Bohmann D. Differential regulation of c-Jun by ERK and JNK during PC12 cell differentiation. EMBO J 1998;17:4404–13.

34. Waetzig V, Herdegen T. MEKK1 controls neurite regrowth after experimental injury by balancing ERK1/2 and JNK2 signaling. Mol Cell Neurosci 2005;30:67–78.

35. Eriksson M, Taskinen M, Leppa S. Mitogen activated protein kinase-dependent activation of c-Jun and c-Fos is required for neuronal differentiation but not for growth and stress response in PC12 cells. J Cell Physiol 2007;210:538–48.

36. Munoz A, Wrighton C, Seliger B, Bernal J, Beug H. Thyroid hormone receptor/c-erbA: control of commitment and differentiation in the neuronal/chromaffin progenitor line PC12. J Cell Biol 1993;121:423–38.

37. Hans A, Syan S, Crosio C, Sassone-Corsi P, Brahic M, Gonzalez-Dunia D. Borna disease virus persistent infection activates mitogen-activated protein kinase and blocks neuronal differentiation of PC12 cells. J Biol Chem 2001;276:7258–65.

38. Verderio C, Pozzi D, Pravettoni E, et al. SNAP-25 modulation of calcium dynamics underlies differences in GABAergic and glutamatergic responsiveness to depolarization. Neuron 2004;41:599–610.

39. Bernard D, Pourtier-Manzanedo A, Gil J, Beach DH. Myc confers androgen-independent prostate cancer cell growth. J Clin Invest 2003;112:1724–31.

40. Sears RC. The life cycle of C-myc: from synthesis to degradation. Cell Cycle 2004;3:1133–7.

41. Nilsson JA, Cleveland JL. Myc pathways provoking cell suicide and cancer. Oncogene 2003;22:9007–21.

42. Wert M, Kennedy S, Palfrey HC, Hay N. Myc drives apoptosis in PC12 cells in the absence of Max. Oncogene 2001;20:3746–50.

43. Leppa S, Eriksson M, Saffrich R, Ansorge W, Bohmann D. Complex functions of AP-1 transcription factors in differentiation and survival of PC12 cells. Mol Cell Biol 2001;21:4369–78.

44. Xia Z, Dickens M, Raingeaud J, Davis RJ, Greenberg ME. Opposing effects of ERK and JNK-p38 MAP kinases on apoptosis. Science 1995;270: 1326–31.

45. Shaulian E, Karin M. AP-1 as a regulator of cell life and death. Nat Cell Biol 2002;4:E131–6.

46. Angel P, Hattori K, Smeal T, Karin M. The jun proto-oncogene is positively autoregulated by its product, Jun/AP-1. Cell 1988;55:875–85.

47. Kitabayashi I, Saka F, Gachelin G, Yokoyama K. Nucleotide sequence of rat c-jun protooncogene. Nucleic Acids Res 1990;18:3400.

48. Groot M, Boxer LM, Thiel G. Nerve growth factor- and epidermal growth factor-regulated gene transcription in PC12 pheochromocytoma and INS-1 insulinoma cells. Eur J Cell Biol 2000;79:924–35.

49. Canelles M, Delgado MD, Hyland KM, et al. Max and inhibitory c-Myc mutants induce erythroid differentiation and resistance to apoptosis in human myeloid leukemia cells. Oncogene 1997;14:1315–27.

50. Wanzel M, Herold S, Eilers M. Transcriptional repression by Myc. Trends Cell Biol 2003;13:146–50.

51. Herold S, Wanzel M, Beuger V, et al. Negative regulation of the mammalian UV response by Myc through association with Miz-1. Mol Cell 2002;10:509–21.

52. Patel JH, McMahon SB. Targeting of Miz-1 is essential for Myc mediated apoptosis. J Biol Chem 2006;281:3283–9.

53. Hopewell R, Ziff EB. The nerve growth factor-responsive PC12 cell line does not express the Myc dimerization partner Max. Mol Cell Biol 1995;15:3470–8.

54. Alani R, Brown P, Binetruy B, et al. The transactivating domain of the c-Jun proto-oncoprotein is required for cotransformation of rat embryo cells. Mol Cell Biol 1991;11:6286–95.

55. Binetruy B, Smeal T, Karin M. Ha-Ras augments c-Jun activity and stimulates phosphorylation of its activation domain. Nature 1991;351:122–7.

56. Dragunow M, Xu R, Walton M, et al. c-Jun promotes neurite outgrowth and survival in PC12 cells. Brain Res Mol Brain Res 2000;83:20–33.

57. Zeller KI, Zhao X, Lee CW, et al. Global mapping of c-Myc binding sites and target gene networks in human B cells. Proc Natl Acad Sci U S A 2006;103: 17834–9.

58. Arvanitis C, Felsher DW. Conditionally MYC: insights from novel transgenic models. Cancer Lett 2005;226:95–9.

59. Greene LA, Rukenstein A. Regulation of acetylcholinesterase activity by nerve growth factor. Role of transcription and dissociation from effects on proliferation and neurite outgrowth. J Biol Chem 1981;256:6363–7.

60. Guerrero I, Pellicer A, Burstein DE. Dissociation of c-fos from ODC expression and neuronal differentiation in a PC12 subline stably transfected with an inducible N-ras oncogene. Biochem Biophys Res Commun 1988;150: 1185–92.

61. Vlach J, Hennecke S, Alevizopoulos K, Conti D, Amati B. Growth arrest by the cyclin-dependent kinase inhibitor p27Kip1 is abrogated by c-Myc. EMBO J 1996;15:6595–604.

62. Littlewood TD, Hancock DC, Danielian PS, Parker MG, Evan GI. A modified oestrogen receptor ligand-binding domain as an improved switch for the regulation of heterologous proteins. Nucleic Acids Res 1995;23:1686–90.

63. Stone J, De Lange T, Ramsay G, et al. Definition of regions in human c myc that are involved in transformation and nuclear localization. Mol Cell Biol 1987; 7:1697–709.

64. Mauleon I, Lombard MN, Munoz-Alonso MJ, Canelles M, Leon J. Kinetics of myc-max-mad gene expression during hepatocyte proliferation *in vivo*: differential regulation of mad family and stress-mediated induction of c-myc. Mol Carcinog 2004;39:85–90.

65. Ceballos E, Munoz-Alonso MJ, Berwanger B, et al. Inhibitory effect of c-Myc on p53-induced apoptosis in leukemia cells. Microarray analysis reveals defective induction of p53 target genes and upregulation of chaperone genes. Oncogene 2005;24:4559–71.

66. Angel P, Baumann I, Stein B, Delius H, Rahmsdorf HJ, Herrlich P. 12-*O*-tetradecanoyl-phorbol-13- acetate induction of the human collagenase gene is mediated by an inducible enhancer element located in the 5′-flanking region. Mol Cell Biol 1987;7:2256–66.

67. Caelles C, Gonzalez-Sancho JM, Munoz A. Nuclear hormone receptor antagonism with AP-1 by inhibition of the JNK pathway. Genes Dev 1997;11: 3351–64.

68. Shang Y, Hu X, DiRenzo J, Lazar MA, Brown M. Cofactor dynamics and sufficiency in estrogen receptor-regulated transcription. Cell 2000;103:843–52.

69. Frank SR, Schroeder M, Fernandez P, Taubert S, Amati B. Binding of c-Myc to chromatin mediates mitogen-induced acetylation of histone H4 and gene activation. Genes Dev 2001;15:2069–82.

70. Quincoces AF, Leon J. Serum growth factors up-regulate H-ras, K-ras, and N-ras proto-oncogenes in fibroblasts. Cell Growth Differ 1995;6:271–9.

71. Palmer HG, Sanchez-Carbayo M, Ordonez-Moran P, Larriba MJ, Cordon-Cardo C, Munoz A. Genetic signatures of differentiation induced by 1α,25-dihydroxyvitamin D3 in human colon cancer cells. Cancer Res 2003;63: 7799–806.

72. Rincon M, Flavell RA. AP-1 transcriptional activity requires both T-cell receptor-mediated and co-stimulatory signals in primary T lymphocytes. EMBO J 1994;13:4370–81.

73. Marinissen MJ, Chiariello M, Tanos T, Bernard O, Narumiya S, Gutkind JS. The small GTP-binding protein RhoA regulates c-jun by a ROCK-JNK signaling axis. Mol Cell 2004;14:29–41.

74. Kiessling A, Sperl B, Hollis A, Eick D, Berg T. Selective inhibition of c-Myc/Max dimerization and DNA binding by small molecules. Chem Biol 2006; 13:745–51.

75. Taylor SJ, Shalloway D. Cell cycle-dependent activation of Ras. Curr Biol 1996;6:1621–7.